# Effects of Storage on the Linear Viscoelastic Response of Polymer-Modified Asphalt at Intermediate to High Temperatures

by
Stacey D. Reubush

Thesis submitted to the Faculty of the
Virginia Polytechnic Institute and State University
in partial fulfillment of the requirements for the degree of

**Master of Science**
**In**
**Civil Engineering**

**APPROVED**

Dr. Imad L. Al-Qadi, Chair
Professor of Civil Engineering

Dr. Thomas C. Ward
Professor of Chemistry

Dr. Gerardo W. Flintsch
Assistant Professor of Civil Engineering

November 1999

# Effects of Storage on the Linear Viscoelastic Response of Polymer-Modified Asphalt at Intermediate to High Temperatures

Stacey D. Reubush

Chair: Dr. Imad L. Al-Qadi

The Via Department of Civil and Environmental Engineering

**Abstract**

The design and construction of roads with longer service lives is a priority of civil engineers. The selection of appropriate highway materials with respect to climatic and loading conditions may significantly increase the lifespan of pavements. One material receiving interest in the area of improved roadway performance is polymer-modified binder. The complex behavior of polymer-modified binders, particularly over time, is not yet well-understood by engineers. Therefore, an experimental study was performed to determine the effects of four years of storage at room temperatures (23°C) on the dynamic mechanical properties of polymer-modified binders at intermediate and high temperatures. A typical paving grade (AC-20) and three elastomeric modifiers, each at three concentrations were used. Initial tests were performed in 1995 to evaluate the effects of short-term aging as simulated by the Rolling Thin Film Oven Test (RTFOT) procedure. This study encompasses a second phase of testing occurring after the modified binders were stored at ambient room temperature (23°C) for four years. The study found that significant changes affecting the dynamic response of binders occur during long term storage at a temperature of 23°C. These changes are dependent on the type and concentration of modifier and may be beneficial. Additionally, four mathematical models describing the dynamic response of binders were evaluated and found to be variable in their ability to accurately predict response of modified binders. Most of these models are not well suited for prediction of the response of stored binders.

# ACKNOWLEDGEMENT

The author expresses appreciation to her advisor, Dr. Imad L. Al-Qadi for contributing to this opportunity to conduct research and providing guidance throughout the project. In addition, thanks are given to the committee members, Drs. Gerardo W. Flintsch and Thomas C. Ward, for the granting of their time and expertise to help in the completion of this work.

The author extends deep appreciation to her family for their support and understanding throughout her studies. Additionally, the assistance of the author's colleagues, Amara, Salman, Walid, Alex, Erin, James, Kiran, Ramzi, Mostafa, Samer and Brian greatly contributed to the author's knowledge as well as the progress of this research.

# TABLE OF CONTENTS

# LIST OF FIGURES

# LIST OF TABLES

# CHAPTER 1 INTRODUCTION

The economy of modern industrialized nations is directly related to their ability to efficiently move people, goods, and services on demand. Without an effective transportation system, a nation cannot hope to compete in the rapidly changing global economy. The United States is no exception to this rule. As of 1996, there were over four million miles of highways and streets in the United States. Unfortunately, 59% of these roads are judged to be in poor, mediocre, or fair condition (FHWA, 1996). Most of today's roadways were designed for less than half the current demands placed upon them. Additionally, increases in percentages of truck traffic and the greater hauling capacity of those trucks have overstressed some roadways to the point where they are simply crumbling. A solution to deteriorating roadways lies in the choice of better construction materials, which requires greater understanding of their fundamental behavior and properties.

The design and construction of roads with longer service lives has always drawn the attention of engineers. Selection of appropriate highway materials with respect to climatic and loading conditions can significantly contribute to the fulfillment of this goal and can lead to significant long-term national savings. One material that has received interest in the area of improved roadway performance is polymer-modified asphalt.

## 1.1 Background

Bituminous mixtures, commonly called hot-mix asphalt or HMA, are complex mixtures composed of a bituminous binder and mineral aggregate. The binder acts as an adhesive, gluing the aggregate into a dense mass and waterproofing the aggregate particles. The aggregate, when bound together, acts as a stone framework to give strength and toughness to the composite system. Mixture performance is affected by both the aggregate and binder individual properties and interactions. However, the binder requires special attention as its characteristics may change dramatically with changing temperature, loading, and/or stage of aging.

For several decades, blending different types of asphalt was the only way to obtain improvements in binder properties. In recent years, however, advances in

asphalt technology and a greater understanding of the behavior of asphalt binder have led researchers to examine the benefits of introducing modifiers into the binder to enhance their performance. Advances in polymer technology have made the use of some polymers as a binder modifier an attractive alternative.

Such modification has been found to change the dynamic response of binders in many ways, depending on the concentration and type of modifier and composition of the binder. A complete understanding of the mechanisms involved in the response and performance of these modified binders has not yet been reached. The theories set forth in the area of viscoelasticity are thought to be valid, for the most part, in describing the responses of asphalt binders, both unmodified and modified. These theories have been utilized in the description of the binder responses to temperature and loading rates.

Several models have been introduced within the last decade to predict the dynamic response of binders. The model introduced by Christensen and Anderson (1992) was evaluated for several binders in the Strategic Highway Research Program (SHRP) and found to be suitable for characterizing unmodified binders at intermediate to high ranges of the dynamic shear modulus. Stastna *et al*. (1996) introduced a model to evaluate dynamic responses of modified or unmodified binders. Previous research at Virginia Tech (Gahvari, 1996) resulted in the proposal of a model to more accurately describe the dynamic response of polymer-modified binders before and after aging in the Rolling Thin Film Oven. More recently, Marasteanu and Anderson (1999) introduced a model modified from the Christensen–Anderson model that improved the fit of response predictions for unmodified and modified binders.

## 1.2 Problem Statement

Bituminous binders are complex materials exhibiting elastic, viscoelastic, and viscous behaviors as their temperature and/or loading rate changes. The incorporation of polymers into binders may enhance the properties of the base binder, yet also adds complexity to the binder behavior. Recently, polymer-modified binder testing has begun to draw more interest as engineers realize the potential of these materials and begin to understand the relationships between laboratory analysis and field performance of the binder system. However, little testing has been performed to evaluate the effects of intermediate temperature storage on binder aging and the related changes in response. Testing is necessary to determine the effects of such storage. In addition, current

models of viscoelastic properties are not proven to remain accurate in their predictions when binders are exposed to intermediate temperature aging conditions. Therefore, a need exists for the validation of such models to allow the accurate prediction of binder properties after the binder is subjected to varying types of aging, including intermediate temperature aging.

## 1.3 Objectives of Research

It is the objective of this research to evaluate samples of polymer-modified asphalt using dynamic mechanical testing to determine if the binder response has changed after four years of storage at a temperature of 23°C. Mechanical analysis was performed on the samples at Virginia Tech (Gahvari, 1996) when originally produced and these results will serve as a basis for comparison. Results of all tests will be compared using statistical analysis to determine if significant differences due to aging are present. Additionally, the results will be used to verify the accuracy of previously developed models describing dynamic mechanical response when applied to aged binders.

## 1.4 Scope of Research

To accomplish the objectives of this study, dynamic mechanical analysis was performed on stored specimens of unmodified and polymer-modified binder at specific temperatures and over a specified range of frequencies. Three polymer modifiers were evaluated at three percentages (by weight). Control samples of the unmodified binder were evaluated to provide a basis for comparison. All samples were tested after four years of storage at a temperature of approximately 23°C. The effects of aging in the Rolling Thin Film Oven prior to storage were investigated by testing unaged specimens as well as specimens subjected to aging in the Rolling Thin Film Oven. Comparisons were made between specimens to evaluate the effects of each modifier on the base binder after storage. Non-linear regression techniques were utilized to evaluate the effectiveness of four response models to estimate the response of each binder type before and after storage.

Chapter 2 describes the properties of asphalt binder and polymer modifiers, discusses basic viscoelastic theory, and explains the evolution and meaning of the

viscoelastic models evaluated as part of this study. Chapter 3 describes the experimental procedures utilized in this investigation. Chapter 4 presents the data obtained from the experimentation and discusses the results acquired through analysis. Chapter 5 yields the summary, findings, and conclusions of the research experiment, and Chapter 6 offers recommendations for further analysis.

# CHAPTER 2 BACKGROUND

Asphalt binder has been used as a construction material since approximately 3200 BC when it was first used in Mesopotamia as a cement and waterproofing medium (Asphalt Institute, 1993). It is appealing as a construction material because it is durable, waterproof, a strong adhesive, and resistant to most acids, alkalis, and salts. The most common usage today is in flexible pavements as a binder.

Bituminous mixtures, commonly called hot-mix asphalt or HMA, are complex mixtures composed of a asphalt binder and mineral aggregate. The binder acts as an adhesive, gluing the aggregate into a dense mass and waterproofing the aggregate particles. The aggregate, when bound together, acts as a stone framework to give strength and toughness to the composite system. Mixture performance is affected by both the aggregate and binder individual properties and their interactions. However, the binder often requires special attention as its characteristics may change dramatically with changing temperature, loading rate, and/or stage of aging.

For several decades, blending different types of asphalt was the only way to obtain improvements in binder properties. In recent years, however, advances in asphalt technology and a greater understanding of the behavior of asphalt have led researchers to examine the benefits of introducing modifiers into binders to enhance their performance. Advances in polymer technology have caused polymers to become an attractive alternative for modification of asphalt cements. Some authors have suggested as many as twenty-two specific benefits associated with polymer modification of asphalts (Bouldin *et al*., 1991; Collins *et al*., 1991; Khattak and Baladi, 1998; King and King, 1986; Lewandowski, 1994; Schuler *et al*., 1987). However, other researchers have seen no benefits (Al Dhaleen *et al*., 1992) or have even noted adverse effects in performance (Brown *et al*., 1992). Much of the difficulty in conclusively determining benefits or drawbacks to the use of polymer modified asphalts lies in the lack of complete understanding of their behavior.

During the last fifteen years, studies have been conducted to better understand the behavior, application, and performance-related problems of modified binders. Several of these have addressed the microstructure of asphalt-polymer blends including

compatibility and asphalt-polymer interactions (Collins *et al*., 1991; King and King, 1986; Krause and Hall, 1983; Schuler *et al*., 1987; Shin *et al*., 1996). The effects of accelerated aging on the rheological behavior and temperature susceptibility of polymer-modified binders has been investigated by Chiu *et al*. (1994), Collins and Bouldin (1992), and Goodrich (1988). However, there have been limited studies involving testing at intermediate to high temperatures to examine the complex shear modulus of modified asphalt binders after several years of storage. Only one study found noted the possibility of effects of storage on unmodified binders. Thenoux *et al*. (1988) investigated the effects of twelve years of intermediate temperature storage on the physical properties of unmodified binders and determined that there were no significant effects. This was not verified for polymer modified binders. The first step in the investigation of polymer modified asphalt binders is to understand the fundamental properties and behaviors of asphalt binder and polymers and to appreciate the rheological theory that applies to these materials.

## 2.1 Asphalt Cement

Asphalt is a natural constituent of most petroleum. There are two sources of asphalt: natural deposits and refined petroleum. In natural sources, the asphalt is a product of long-term natural distillation of petroleum. Manufactured asphalt is a product of the fractional distillation of petroleum. The primary source of asphalt used in paving today is that obtained from petroleum refining.

### *2.1.1 Chemistry*

Asphalt is a complex organic mixture, composed of hydrocarbons with small percentages of sulfur, nitrogen, and oxygen. The chemical composition varies, as shown in Table 2.1. Sulfur, nitrogen, and oxygen are called heteroatoms, and their presence may have significant effects on asphalt properties.

Many molecular structures are found in asphalts, however, the commonly used classification separates asphalt into three generic fractions based on polarity and solubility: asphaltenes, resins, and oils. This model is based on the colloidal (micellular) model first introduced by Nellensteyn (1924). Figure 2.1 demonstrates a basic schematic of the colloidal model constituents. *Asphaltenes* are high polarity, high molecular weight hydrocarbons. They are found in aromatic rings with few side chains.

Table 2.1 Chemical composition of asphalt (after SHRP, 1993).

| Chemical Constituent | Percentage of Composition |
|---|---|
| Carbon | 70-85% |
| Hydrogen | 7-12% |
| Nitrogen | 0-1% |
| Sulfur | 1-7% |
| Oxygen | 0-5% |
| Small amounts of dispersed metals (as oxides, salts, or in metal-containing organic compounds) | |

*Resins* are an intermediate weight, semi-solid fraction formed of aromatic rings with side chains. Resins are polar molecules that act as peptizing agents to prevent asphaltene molecules from coagulating. The lightest molecular weight materials are the non-polar oils. *Oils* generally have a high proportion of chains as compared to the number of rings. In some literature, the resins and oils are referred to collectively as maltenes. In general, asphaltenes produce the bulk of the asphalt, resins contribute to adhesion and ductility, and oils influence flow and viscosity properties (Krebs and Walker, 1971).

According to the colloidal model, the rheology of the asphalt is highly affected by the degree to which the resins are effective in keeping the asphaltene fraction dispersed in the oil (Traxler, 1961). Asphalts which have well-dispersed asphaltenes, due to sufficient amounts of peptizing agents, are considered *sol-type* asphalts and exhibit high temperature susceptibilities, high ductility, low rates of age hardening, little thixotropy, and Newtonian behavior. *Gel-type* asphalts have poorly dispersed asphaltenes and show low temperature susceptibilities, low ductility, rapid age-hardening, significant

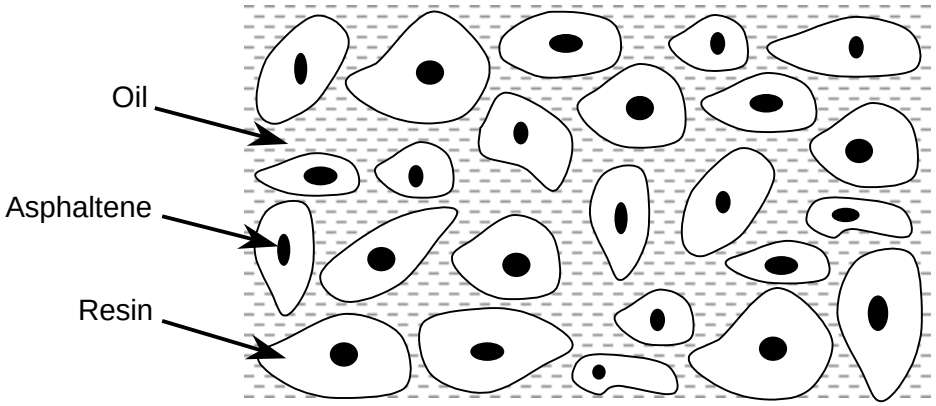


Figure 2.1 Constituents of asphalt.

thixotropy, and non-Newtonian behavior.

A second model, proposed by Anderson *et al.* (1991), is the dispersed polar fluid model. This model addresses the viscoelastic nature of asphalt more accurately than the colloidal model. The dispersed polar fluid model considers asphalt as having molecules of varying size and polar functionality continuously distributed in a fluid, as shown in Figure 2.2. The molecules in this model can be classified under three general categories of molecular structure: *aliphatics*, *cyclics*, and *aromatics* (Asphalt Institute, 1997). The general structures are shown in Figure 2.3. *Aliphatic* molecules, which are also called paraffinics, are three-dimensional, linear, chain-like molecules that are "oily" or "waxy" in nature. *Cyclic* molecules, known also as naphthenic molecules, have three-dimensional saturated carbon ring structures. *Aromatic* molecules have flat, stable carbon rings that may be stacked together. Bonding between constituent molecules at various levels is responsible for the delayed elasticity and viscous flow characteristics of asphalt. Branthaver *et al.* (1996) reported success in verifying this model and suggested that unusual rheological properties of some asphalts may be related to molecular weight distributions in the polar molecules.

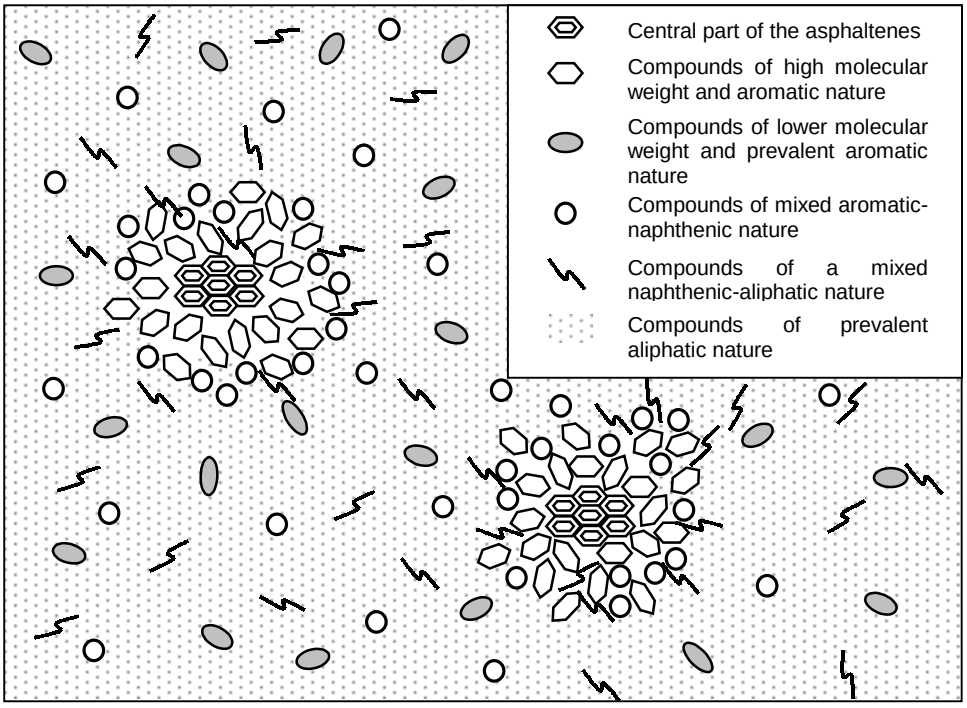


Figure 2.2 Colloidal model for asphalt cement (after Kennedy *et al.*, 1990).

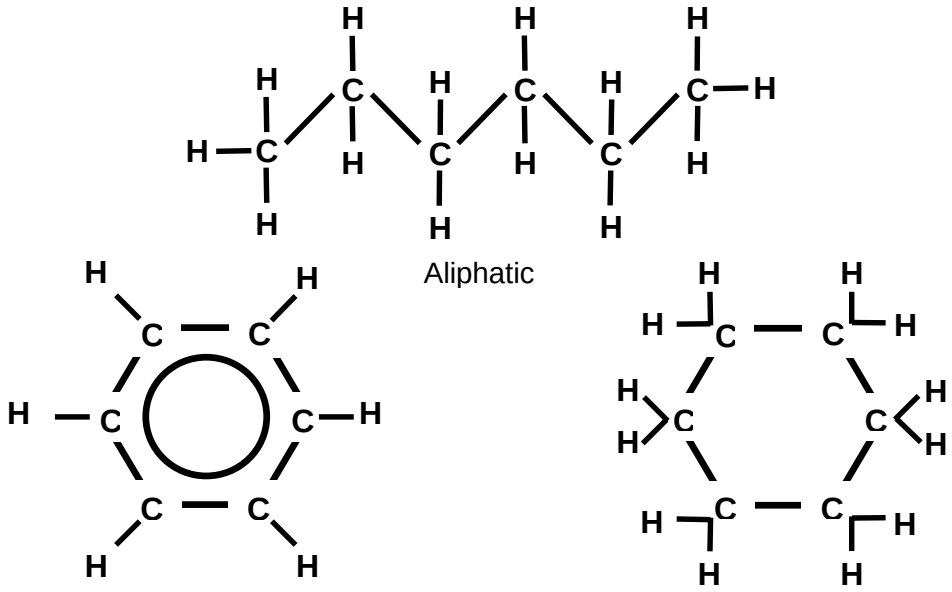


Figure 2.3 Types of asphalt molecules.

### *2.1.2 Rheology*

Asphalts behave in a unique manner depending upon the load applied and the rate of loading. Temperature is also a factor; however, it can be correlated with the rate of loading. At slow rates of loading, or high temperatures, asphalt behaves in a viscous manner. At low temperatures, or higher rates of loading, asphalt behaves in an increasingly elastic manner. At intermediate temperatures, asphalt has the characteristics of both an elastic solid and a viscous fluid.

Elastic materials show proportionality between applied stress and deformation. This response can be compared to the action of a spring. When a stress is applied to an elastic material, there is instantaneous deformation, much as when a tension load is applied to a spring. When the stress is held constant, the deformation is constant. This would correspond to holding the spring at a constant tension. Upon release of the stress, the elastic material will completely recover from the applied deformation, as does the spring when the tension is released. This behavior is governed by Hooke's law and expressed as follows:

$$\sigma = E \cdot \varepsilon \qquad (2.1)$$

or

$$\tau = G \cdot \gamma \qquad (2.2)$$

where

$\sigma$ = applied normal stress, kPa;

E = modulus of elasticity, kPa;

$\varepsilon$ = axial strain;

$\tau$ = applied shear stress, kPa;

G = shear modulus, kPa; and

$\gamma$ = shear strain.

Viscous materials flow when exposed to stress and will continue to flow under constant levels of stress. Deformations are not recovered by the material. The response of viscous materials may be explained by using a dashpot (assuming the stress is proportional to the time rate of deformation) as an analogy. When the rate of loading is varied, the resulting level of stress will differ. As a load is applied to the dashpot, it will deform gradually with time. When the load is released, no deformation is recovered by the dashpot. Mathematically, viscous response is expressed as follows:

$$\tau = \eta \cdot d\gamma / dt \qquad (2.3)$$

where

$\tau$ = shear stress, kPa;

$\eta$ = coefficient of viscosity; and

$d\gamma / dt$ = rate of application of shear strain (or rate of shear).

The relationships between shear stress and rate of shear are used to classify viscous materials into two basic categories: Newtonian and non-Newtonian. Newtonian materials show a linear relationship between shear stress and the rate of shear. In this case, $\eta$, the viscosity coefficient, is a constant and is the slope of the line. Non-Newtonian materials exhibit a non-linear relationship between shear stress and rate of shear. These materials are said to be in states of shear thinning or shear thickening

depending upon the particular shape of the shear stress vs. rate of shear curve (see Figure 2.4).

Certain materials show both viscous and elastic components depending upon the rate of loading; such materials are classified as viscoelastic materials. Under rapid loading rates, viscoelastic materials behave in an elastic manner. When loaded slowly, a viscous response is observed. At intermediate loading rates, a combination of elastic and viscous response is seen. Asphalts behave as viscoelastic materials. Additionally, different asphalts may display Newtonian or non-Newtonian traits during their viscous responses.

The exhibition of Newtonian or non-Newtonian traits by asphalt binder is a function of the degree of dissolution of the asphaltenes in the oil resin phase. If the asphaltenes are well dissolved, or there is only a small proportion of asphaltenes, the asphalt will show Newtonian behavior at low shear rates. Non-Newtonian behavior is observed when the asphaltenes are less well dissolved or constitute a greater proportion of the asphalt.

A general model was developed by van der Poel (1954) to describe the viscoelastic response of asphalt. The linear relationship between stress and strain for small deformations is used as a basis for the stiffness modulus and is described as follows:

$$S = \sigma / \varepsilon \qquad (2.4)$$

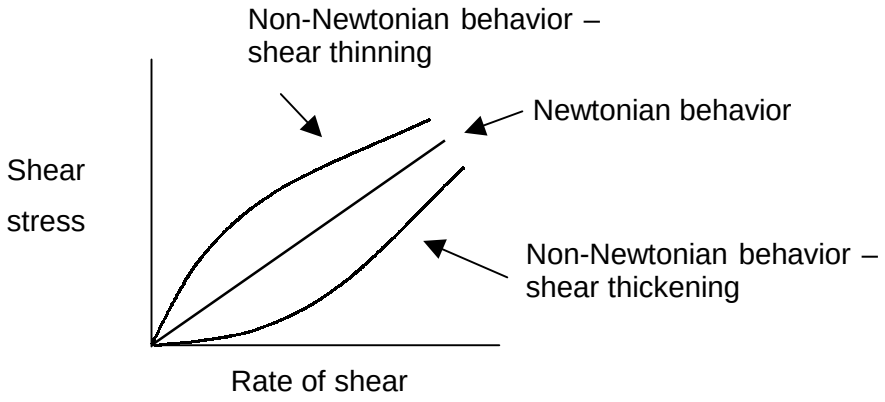


Figure 2.4 Shear stress vs. rate of shear for viscous materials.

where

S = stiffness modulus;

$\sigma$ = stress; and

$\varepsilon$ = strain.

Since the stiffness modulus can be determined over a wide range of loading conditions and times (from creep behavior to dynamic loading), it is possible to investigate the effects of temperature on response.

### *2.1.3 Aging*

Another factor influencing the performance and characteristics of asphalt binder is a phenomenon known as *aging*. Several factors may contribute to this hardening of the asphalt such as oxidation, volatilization, polymerization, and thixotropy. Because asphalt is an organic compound, it is able to react with oxygen in the environment. As the oxidation reaction occurs, it changes the composition of the asphalt, creating a more brittle structure. This occurrence is called *age hardening* or *oxidative hardening*. *Volatilization* occurs when the lighter constituents of the asphalt evaporate. Generally, this is attributed to elevated temperatures that are found primarily during the HMA production process. *Polymerization* is the means by which resins are thought to combine into asphaltenes, causing an increase in the brittleness of the asphalt along with a tendency toward non-Newtonian behavior. Finally, *thixotropy*, or an increase in viscosity over time, also contributes to the aging phenomenon in asphalt. However, the most important factors in the aging process of asphalt appear to be oxidation and volatilization.

The occurrence of *steric hardening*, a time-dependent reversible molecular association, also effects binder properties but is not considered a means of aging. Steric hardening is only a factor at intermediate temperatures; at high temperatures excess kinetic energy in the system prevents the association, and at low temperatures the rate of association is considered slowed due to the binder's high viscosity (Peterson, 1984).

### *2.1.4 Physical Hardening*

Bahia and Anderson (1993) reported a mechanism by which binder properties may change at low temperatures. This mechanism, called *physical hardening*, occurs at

temperatures close to or below the glass transition temperature ($T_g$) and causes significant hardening of the binder. The rate and magnitude of the hardening phenomena has been observed to increase with decreasing temperature and is believed to be similar to the phenomena called physical aging on amorphous solids (Struik, 1978).

Physical hardening can be explained using the free volume theory, introduced by Doolittle (1951), and relationships between temperature and molecular mobility. The free volume theory considers molecular mobility dependent on the relative volume of molecules present per unit of free space, or free volume. Based on the free volume theory, when an amorphous material is cooled from a temperature above its glass transition temperature, molecular adjustments and the collapse of free volume are rapid and of the same order of magnitude as the temperature drop. The molecular adjustments become slower as the temperature reaches $T_g$ and, if crystallization does not occur, a temperature is reached at which the collapse of free volume cannot occur within the experimental cooling time. At that temperature, the structural state of the material is frozen-in and deviates from thermal equilibrium due to the continuous drop in kinetic energy. For many amorphous solids, this state results in a slow, time-dependent structural relaxation process, driven by the bias in internal energy. Recently, there has been postulation that physical hardening may occur in binders at temperatures well above the glass transition temperature (Marasteanu and Anderson, 1999). This is postulated to occur because asphalt binder, when cooled, reaches a non-equilibrium glassy state that continues to approach equilibrium as the temperature is kept constant.

## 2.2 Asphalt Cement Tests

A number of traditional tests are usually performed to characterize the physical properties, consistency, and aging of asphalt. Penetration and viscosity are measured to determine temperature susceptibility and serve as the basis for some grading systems. In Europe, the softening point is used for specification purposes as a measure of consistency. The traditional tests are also performed on aged asphalt to examine the affects of aging. More recently, several tests have been adopted that measure dynamic rheological properties of aged and unaged asphalts to offer a more practical and accurate prediction of properties and performance.

### *2.2.1 Consistency Tests*

*Penetration test*

The penetration test (ASTM Test Method D5 (ASTM, 1997)) is an empirical test used to measure consistency. The test is performed by bringing a container of asphalt to the standard test temperature of 25°C. A 100g weighted needle of specified dimensions is allowed to penetrate the sample for 5 seconds. The depth of penetration, expressed in units of 0.1mm, is considered the "penetration" of the asphalt binder.

*Softening point (ring and ball) test*

The softening point test (ASTM Test Method D36 (ASTM, 1997)) is also used to measure asphalt consistency. The test is performed by confining asphalt samples in brass rings and loading the samples with steel balls. The samples are placed in a beaker of water at a specified height above a metal plate. They are then heated at a specified rate. As the asphalt heats, the weight of the steel ball pulls the sample down toward the plate. When the sample and ball touch the plate, the water temperature is measured and designated as the ring and ball softening point of the asphalt.

*Kinematic viscosity test*

The kinematic viscosity test (ASTM Test Method D2170 (ASTM, 1997)) measures the viscosity of asphalt binder at 135°C using a cross-arm viscometer. The asphalt flows through the viscometer and is timed. The viscosity is found by multiplying the time interval by a calibration factor and is expressed in centistokes. In this measurement of viscosity, gravitational flow is used; therefore, the density of the material affects the rate of flow.

*Absolute viscosity test*

The absolute viscosity test (ASTM Test Method D2171 (ASTM, 1997)) measures the viscosity of asphalt at 60°C. Because the asphalt at this temperature is too viscous to flow readily through the capillary viscometer, a partial vacuum is used to induce flow. As in the kinematic viscosity test, the time interval of the flow is multiplied by a calibration factor for the viscometer to determine the viscosity. However, results of this test are expressed in poises. Since the flow is induced by a partial vacuum, gravitational effects are negligible, unlike the kinematic viscosity test. The absolute viscosity may

also be calculated from the kinematic viscosity by multiplying the latter by the density of the asphalt at the test temperature.

### *2.2.2 Aging Methods*

*Thin film oven test (TFOT)*

The thin film oven test (ASTM Test Method D1754 (ASTM, 1998)) is a method of aging asphalt by subjecting it to conditions approximating those that occur during normal hot-mix plant operations. Samples of the asphalt are placed in pans on a rotating shelf in an oven at a temperature of 163°C for five hours. The aged residue may be tested to determine the effects of hardening due to aging.

*Rolling thin film oven test (RTFOT)*

The rolling thin film oven test (ASTM Test Method D2872 (ASTM, 1998)) is a modification of the thin film oven test. Instead of the sample being placed in pans on a rotating shelf, the samples are poured into specially designed bottles. The bottles are placed horizontally into a vertically rotating rack in an oven maintained at 163°C. As the bottles are rotated, fresh films of asphalt are exposed. Additionally, once during each rotation, the bottle opening passes before an air jet that purges accumulated vapors from the bottle and exposes the asphalt to additional air to intensify the aging effect. The residue from the rolling thin film oven test is subsequently tested to determine the effects of aging. A schematic of the rolling thin film oven is seen in Figure 2.5.

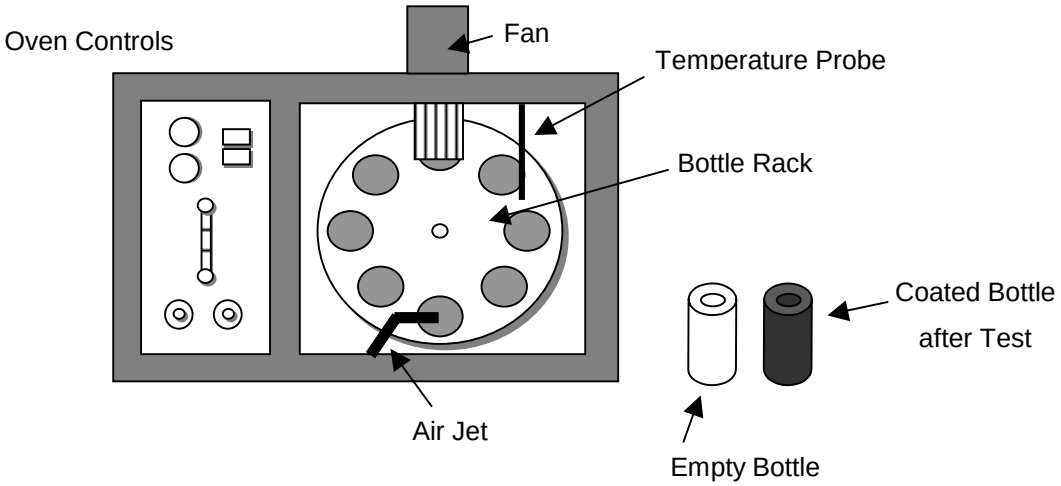


Figure 2.5 A schematic of the rolling thin film oven.

### *2.2.3 New Methods and Tests*

*Pressure aging vessel (PAV)*

The pressure aging vessel is a method of aging the asphalt to simulate the effects of long term aging in the field. After the asphalt has first been aged in the rolling thin film oven, it may be aged in the pressure aging vessel. Asphalt samples are placed in sample tins and loaded into the vessel (see Figure 2.6). Once inside the vessel, the samples are maintained at a temperature of 90, 100, or 110°C and subjected to 2070 kPa pressure for 20 hours. The differences in temperature correspond to differing climates expected in field applications. After removal from the pressure aging vessel, the samples may be tested in the dynamic shear rheometer and bending beam rheometer (discussed below) to determine the effects of long term aging.

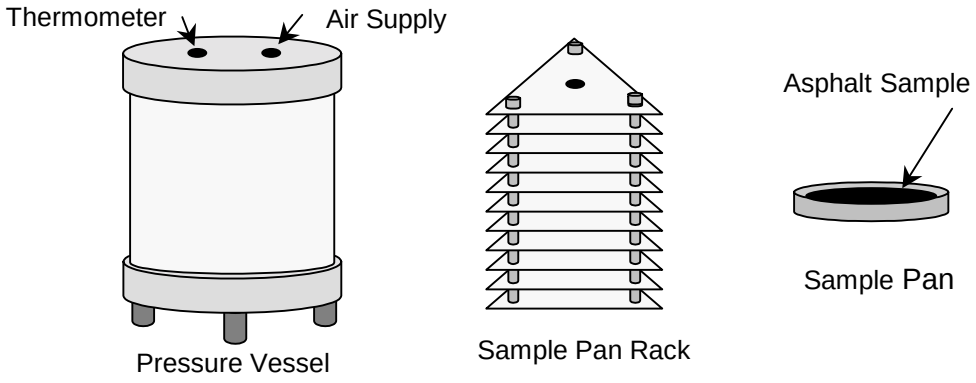


Figure 2.6 Pressure aging vessel.

*Rotational viscometer*

The rotational viscosity test is used to evaluate the high temperature workability of binders. The test is only performed on unaged binder. The viscometer measures binder viscosity at high temperatures to evaluate the fluidity of asphalt during pumping and mixing. A specific mass of sample is poured into a cylindrical testing chamber. The torque applied to a rotating spindle is measured and used to evaluate the binders relative resistance to rotation, yielding the binder viscosity. A schematic of the rotational viscometer is shown in Figure 2.7.

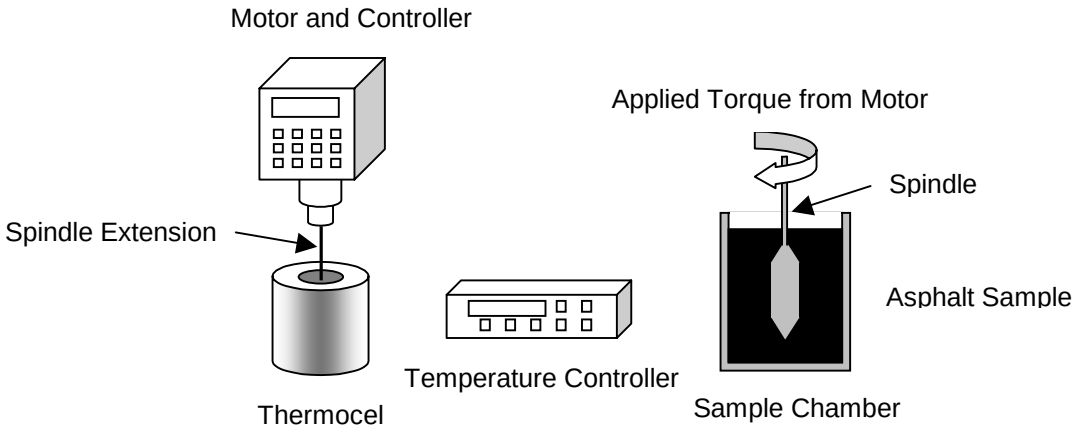


Figure 2.7 The rotational viscometer.

*Dynamic shear rheometer (DSR)*

The dynamic shear rheometer is used to evaluate the complex shear modulus of binders. The rheometer uses an oscillating plate to exert a torque on an asphalt sample. The rheometer characterizes viscous and elastic behavior of the binder by measuring the complex modulus (G*) and phase angle (δ). To measure these quantities, a 1mm thick by 25mm diameter or 2mm thick by 8mm diameter specimen is sandwiched between the two plates of the rheometer, as seen in Figure 2.8. The rheometer then applies a shear stress on the sample and uses the resulting strain and time lag to determine the response of the binder. Testing temperatures range from 5 to 75°C. For performance grading (a binder classification method), the test is performed in 3°

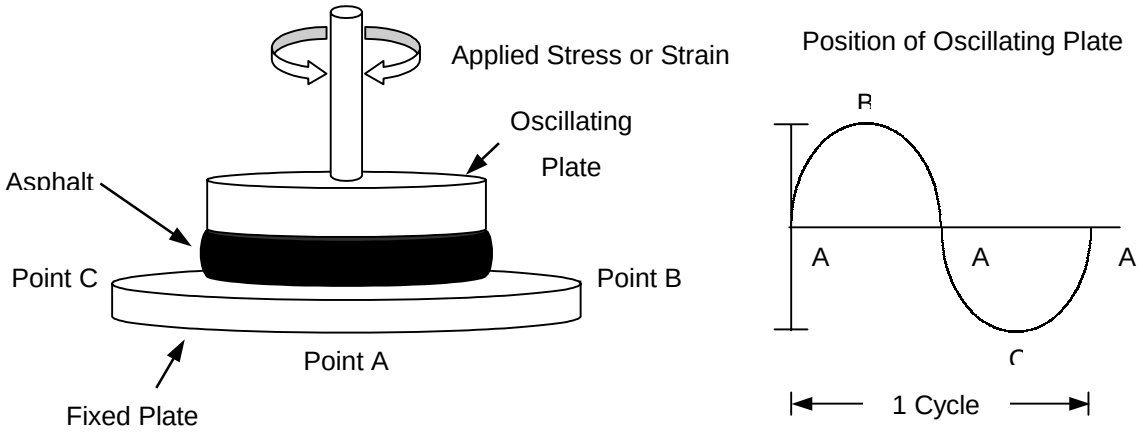


Figure 2.8 Dynamic shear rheometer plate setup.

increments from 5 to 40°C, and in 6° increments from 40 to 75°C. Lower temperature testing is used for fatigue cracking characterization and high temperature testing is used to characterize rutting performance. Unaged samples, as well as RTFO and PAV aged samples, are tested to characterize the binder at all ages.

*Bending beam rheometer (BBR)*

The bending beam rheometer is used to evaluate binder stiffness properties at low temperatures. The test is performed on samples that have been aged in both the RTFO and PAV to simulate binder performance after mixing and exposure to field aging. The values measured are the creep stiffness and the m-value, an indication of the change in stiffness as a load is applied. The test applies a load to the center of a simply supported asphalt beam specimen, as observed in Figure 2.9. The amount of deflection, or creep, over 240 seconds is measured and the stiffness and m-value (the slope of creep stiffness versus the log time at 60 sec) are calculated.

*Direct tension test*

The direct tension test is used in conjunction with the bending beam rheometer to characterize the low temperature performance of high stiffness binders. The test is used to determine the amount of ductility that binders exhibit before failure at very low temperatures and is performed on samples that have been aged in the rolling thin film

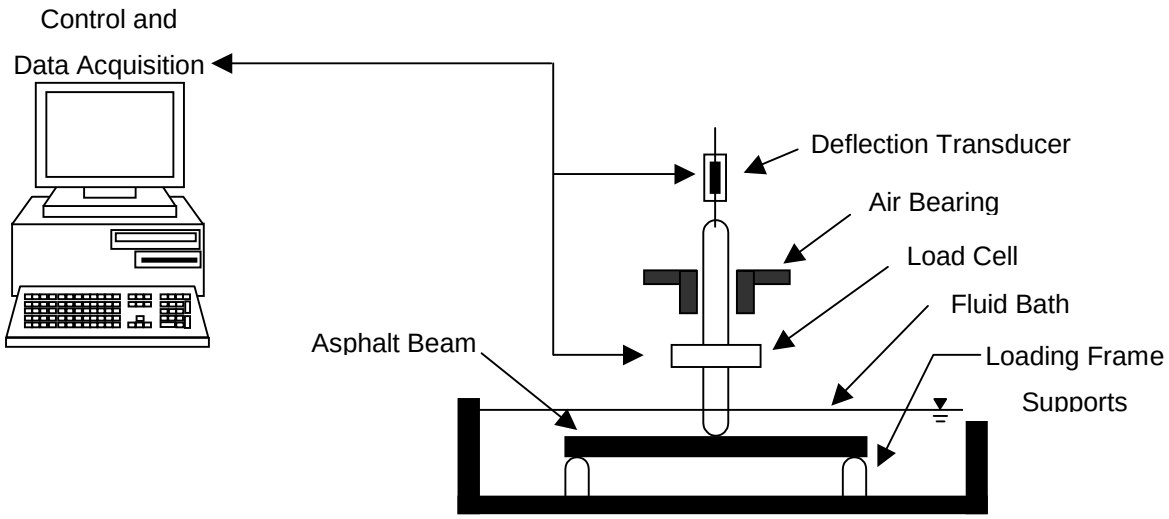


Figure 2.9 Bending beam rheometer.

oven and pressure aging vessel. "Dog-bone" shaped specimens are pulled under tension until failure occurs. The sample failure strain is calculated from the elongation at the maximum stress.

## 2.3 Polymers

Polymers are complex chain molecules formed from the combination of smaller simple molecules called monomers. Polymers are widely used in various applications, including asphalt binder modification. There are several classification methods used to categorize polymers. These include classification by reaction to temperature, chemistry of synthesis, structure, and area of application. The subcategories of each classification system are shown in Table 2.2.

Polymers used in the asphalt industry are often classified as elastomers or plastomers, with the most commonly used being the elastomers (King and King, 1986; Lewandowski, 1994). These classifications are based on the polymers' resistance to deformation. Elastomers exhibit increased tensile strength with elongation and have the ability to recover to the initial condition after an applied load is removed. Plastomers have high early strength under deformation, but are less flexible than elastomers and tend to fracture under large strains (King and King, 1986). Additionally, plastomers deform more slowly than elastomers under an equivalent load.

Examples of elastomeric modifiers include styrene-butadiene-styrene (SBS), styrene-isoprene-styrene (SIS), styrene-ethylene/butylene-styrene (SEBS), and styrene-butadiene rubber (SBR). Ethylene-vinyl-acetate (EVA), polyvinylchloride (PVC), and polyethylene/polypropylene are examples of plastomers.

Table 2.2 Classification schemes for polymers (after Losen, 1993).

| **Classification** | Reaction to Temperature | Chemistry of Synthesis | Structure | Area of Application |
|---|---|---|---|---|
| **Sub-Category** | Thermoset<br>Thermoplastic | Condensation<br>Addition | Linear Random<br>Linear Block<br>Branched<br>Graft<br>Crosslinked | Elastomer<br>Plastic<br>Fiber<br>Adhesive<br>Sealant<br>Cellular Material |

### *2.3.1 Thermoplastic Block Copolymers*

Block copolymers are produced by reacting monomers or repeat units together using specific processes. In general, three basic architectural structures of block copolymers may be formed (Noshay and McGrath, 1977). The simplest arrangement is a diblock structure, commonly called an A-B block copolymer, which is composed of a segment of "A" repeat units and a segment of "B" repeat units. Examples of diblock structures are seen in styrene-butadiene (SB), styrene-ethylene-propylene (SEP), and styrene-ethylene-butadiene (SEB). The second and most common architecture is the triblock structure, considered as an A-B-A structure. This structure consists of a single "B" repeat unit segment located between two "A" repeat unit segments. Styrene-butadiene-styrene (SBS) and styrene-isoprene-styrene (SIS) are two examples. The multiblock structure is the third basic type of block copolymer. Considered as $-(A\text{-}B)-_n$, multiblock structures contain many alternating "A" and "B" blocks. Examples include styrene-butadiene $(SB)_n$ and styrene-isoprene $(SI)_n$. Representations of the three architectures can be seen in Figure 2.10.

Block copolymers are synthesized using complicated processes. The most common techniques are living addition polymerization and step-growth condensation (Noshay and McGrath, 1977). Living addition polymerization techniques are generally used to produce diblock and triblock structures, while step-growth condensation procedures are used to synthesize multiblock structures. In the case of producing a diblock or triblock structure, first anionic polymerization is used to create a polystyrene of desired molecular weight. Next, a rubbery mid-block (usually isoprene or butadiene) is polymerized on the existing polystyrene block to create a diblock unit. The diblock units are linked together to form triblock copolymers using various coupling agents (Collins and Mikols, 1985). A-B-A and $-(A\text{-}B)-_n$ block copolymers exhibit unique elastomeric behavior that is characterized by thermoplasticity along with rubber-like behavior. This is caused by the development of a two-phase system within the polymer composed of a hard block having a glass transition or melt temperature above room temperature and a soft block having a glass transition temperature below room temperature. Above the hard block glass transition temperature, the hard blocks are associated in rigid domains that serve as physical cross-links connected by rubbery springs or reinforcement sites. For the most common block copolymers, styrene acts as the hard block, having a glass transition temperature above 100°C, and the rubbery mid-block acts as the soft block.

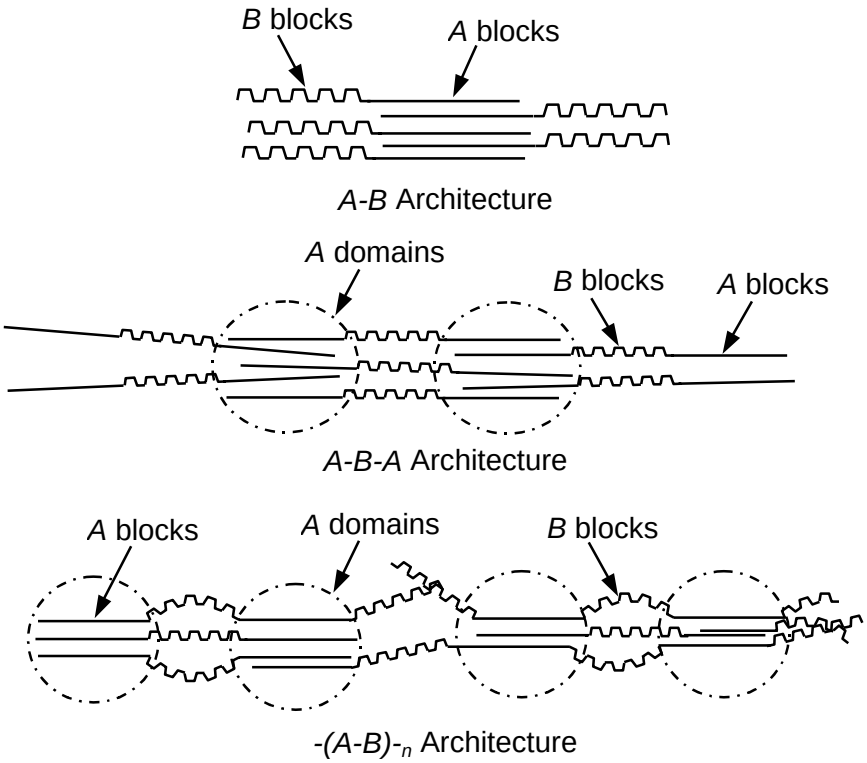


Figure 2.10 Schematic representation of various block copolymer architectures (after Noshay and McGrath, 1977).

At temperatures below the glass transition temperature of the hard block, the block copolymer acts as a three-dimensional rubbery system; at temperatures below the glass transition temperature of the soft block, the rigid domains soften.

The mechanical properties and performance of block copolymers are significantly affected by the block lengths and weight fractions of the hard and soft blocks. For example, in the case of styrene-rubber block copolymers, an increase in the styrene/rubber ratio results in increasing moduli and ultimate tensile strength and decreased flexibility (Holden *et al*., 1969). Bishop and Davison (1969) found that at high styrene contents, polystyrene formed a continuous matrix and rubber became the dispersed phase, resulting in a copolymer showing neither the thermoplasticity of polystyrene nor the elastomeric properties of rubber.

### *2.3.2 Random Copolymers*

Random copolymers are characterized by a statistical placement of comonomer repeat units along a backbone chain (Noshay and McGrath, 1977). They are easily synthesized using free radical and ionic addition, ring-opening polymerization, and many

types of step-growth. Random copolymers act as homogeneous systems that exhibit single-phase morphology and do not create a network. In addition, they demonstrate characteristics between the extremes of the reacting monomers.

An example of a random copolymer is styrene-butadiene rubber (SBR), formed by randomly reacting styrene and butadiene together. The behavior of SBR is between the flexibility of butadiene and the stiffness of styrene and is a function of the relative proportions of the two components.

## 2.4 Linear Viscoelastic Theory

Linear viscoelastic theory addresses the performance of materials that exhibit properties of both linear elasticity and linear viscosity. Linear elastic materials exhibit strain responses that are not time dependent and that are in phase with the applied stress. In general terms, an elastic material, when subjected to an impulsive constant load, will deform instantly, maintain a constant deformation, and then return to the original configuration upon removal of the load. Linear viscoelastic materials show strain responses that are time dependent and out of phase with the applied stress. When viscous materials are subjected to instantaneous constant loading, they do not show immediate responses. Instead, their deformation increases with a constant rate and the deformation remains after the load is removed.

Linear viscoelastic materials, as the name suggests, display properties in between those of linear elastic and linear viscous materials. Their behavior is time dependent and includes both elastic and viscous behavioral components. Upon application of an instantaneous load that is kept constant over time, a viscoelastic material may or may not show instantaneous deformation, but will show an increasing deformation over time. The deformation may approach a finite limit or continue infinitely depending on the material, but upon removal of the load, there will be partial to nearly full recovery of the deformation. This behavior can be characterized by transient or dynamic responses. Some of the parameters that explain linear viscoelastic behavior are described in the following subsections.

### *2.4.1 Relaxation Response*

Relaxation is the time dependent stress response to a sudden constant strain that is seen in viscoelastic materials. The applied strain can be described as follows:

$$\varepsilon_a(t) = \hat{\varepsilon}\, H(t) \tag{2.5}$$

where

$\varepsilon_a(t)$ = uniaxial applied strain;

$\hat{\varepsilon}$ = strain magnitude; and

H(t) = unit step function.

The unit step function, H(t), describes the application of the load and is defined as:

$$H(t) = \begin{cases} 1 & t \geq 0 \\ 0 & t \leq 0 \end{cases} \tag{2.6}$$

The stress resulting from the applied strain is the following:

$$\sigma_r(t) = \hat{\varepsilon}\, E(t) \tag{2.7}$$

where

$\sigma_r(t)$ = uniaxial stress response, Pa; and

E(t) = relaxation modulus.

In the nonlinear response range, generally occurring at large strain magnitudes, the relaxation modulus is a function of both time and stress magnitude ($E = E(t, \hat{\sigma})$).

Under conditions of shear strain, the relaxation modulus, G(t), is used to represent the response as follows:

$$G(t) = \frac{\tau(t)}{\gamma} \tag{2.8}$$

where

G(t) = shear relaxation modulus; and

$\tau(t)$ = resulting shear stress;

$\gamma$ = applied shear strain.

### *2.4.2 Creep Response*

To measure creep response, a material is subjected to a suddenly-applied constant load and the resulting strain is measured over time. The load, or stress, is defined as follows:

$$\sigma_a(t) = \hat{\sigma} H(t) \tag{2.9}$$

where

$\sigma_a(t)$ = uniaxial applied stress, Pa; and

$\hat{\sigma}$ = stress magnitude, Pa.

The resulting strain can be defined as:

$$\varepsilon_r(t) = \hat{\sigma} D(t) \tag{2.10}$$

where

$\varepsilon_r(t)$ = uniaxial stress response; and

$D(t)$ = creep compliance, $Pa^{-1}$.

When shear stresses are applied, the shear creep compliance, J(t), is used as follows:

$$J(t) = \frac{\gamma(t)}{\tau} \tag{2.11}$$

where

$J(t)$ = shear creep compliance, $Pa^{-1}$;

$\gamma(t)$ = resulting shear strain; and

$\tau$ = applied shear stress, Pa.

The stiffness modulus, S(t), is often used when testing asphalt binders and is expressed as follows:

$$S(t) = \frac{1}{D(t)} \tag{2.12}$$

where S(t) is the stiffness modulus in Pa.

For very short loading times and at equilibrium ($t \rightarrow 0$ and $t \rightarrow \infty$), the binder stiffness and modulus are equivalent:

$$S(t) = E(t) \tag{2.13}$$

However, the two functions are not equivalent at intermediate loading times.

### *2.4.3 Dynamic Response*

The most accurate characterization of viscoelastic behavior is achieved with dynamic mechanical analysis. Dynamic testing is performed using either a stress or strain controlled mode. For stress controlled tests, sinusoidal stresses are applied and the resulting strains are monitored over time. For strain controlled tests, sinusoidal strains are applied and the stress outputs are monitored over time.

Stain controlled testing is related to the previous discussion of the relaxation response. For this testing mode, the applied strain is considered the real part (mathematically) of the complex strain. The complex strain is expressed as:

$$\varepsilon^* = \hat{\varepsilon}\, e^{i\omega t} = \hat{\varepsilon}\,(\cos \omega t + i \sin \omega t) \tag{2.14}$$

where

$\varepsilon^*$ = complex strain;

t = time, s; and

$\omega$ = frequency, rad.

The applied strain is, therefore:

$$\varepsilon_a(t) = \hat{\varepsilon} \cos \omega t \tag{2.15}$$

Using a similar approach, the stress output is expressed as the real part of the complex stress. The complex stress and stress output are shown in equations 2.16 and 2.17, respectively:

$$\sigma^* = \hat{\sigma}\, e^{i(\omega t + \delta)} = \hat{\sigma}\,[\cos (\omega t + \delta) + i \sin (\omega t + \delta)] \tag{2.16}$$

$$\sigma_r(t) = \hat{\sigma} \cos (\omega t + \delta) \tag{2.17}$$

where

$\sigma^*$ = complex stress; and

$\delta$ = phase angle, rad.

For elastic materials, the applied stress and resulting strain are always in phase, meaning that the phase angle, $\delta$, is equal to zero. In viscous materials, the resulting strain will lag behind the applied stress by $^{\pi}/_{2}$ rad, meaning that $\delta = {}^{\pi}/_{2}$. Therefore, the phase angle of a viscoelastic material is always between 0 and $^{\pi}/_{2}$, or $0 < \delta < {}^{\pi}/_{2}$.

The dynamic complex modulus is defined as the ratio of complex stress to complex strain:

$$E^*(i\omega) = \frac{\sigma^*}{\varepsilon^*} = \frac{\hat{\sigma}}{\hat{\varepsilon}} e^{i\delta} \tag{2.18}$$

where

$E^*(i\omega)$ = dynamic complex modulus, Pa.

The dynamic complex modulus can be resolved into a storage modulus and loss modulus, representing the in phase and out of phase components of the complex modulus:

$$E^*(i\omega) = E'(\omega) + i\,E''(\omega) \tag{2.19}$$

where

$E'(i\omega)$ = dynamic storage modulus, Pa; and

$E''(i\omega)$ = dynamic loss modulus, Pa.

The absolute value of the complex modulus may be calculated:

$$\left|E^*(i\omega)\right| = \sqrt{\left[E'(\omega)\right]^2 + \left[E'(\omega)\right]^2} = \frac{\hat{\sigma}}{\hat{\varepsilon}} \tag{2.20}$$

Through mathematical manipulation of equations 2.19 and 2.20, the following relationships may be derived:

$$E' = \left|E^*\right| \cos\delta \tag{2.21}$$

$$E'' = \left|E^*\right| \sin\delta \tag{2.22}$$

$$\tan\delta = \frac{E''}{E'} \tag{2.23}$$

where tan $\delta$ is the loss tangent, a measure of relative energy dissipation.

For testing in stress controlled mode, similar equations are derived for the dynamic complex compliance:

$$D^*(i\omega) = \frac{\varepsilon^*}{\sigma^*} = \frac{\hat{\varepsilon}}{\hat{\sigma}} e^{-i\delta} \tag{2.24}$$

$$D^*(i\omega) = D'(\omega) - iD''(\omega) \tag{2.25}$$

$$\tan\delta = \frac{D''}{D'} \tag{2.26}$$

where:

$D^*(i\omega)$ = dynamic complex compliance;

$D'(\omega)$ = dynamic storage compliance, $Pa^{-1}$; and

$D''(\omega)$ = dynamic loss compliance, $Pa^{-1}$.

When performing dynamic mechanical testing in the shear mode, the moduli G* (comprised of G′ and G″) and the compliance J* (comprised of J′ and J″) represent the response.

### *2.4.4 Relaxation Spectrum*

The relaxation spectrum can be considered a density function that represents the moduli over time. All viscoelastic functions can be derived from the relaxation spectrum. The relaxation spectrum can also be used as a fundamental approach to mathematical modeling of viscoelastic response (Jongepier and Kuilman, 1970). As extremely complicated solutions result from the derivation of relaxation spectra from dynamic viscoelastic functions, use is made of approximate interrelations between the linear viscoelastic functions to obtain expressions for relaxation spectra. Ninomiya and Ferry (1959) presented an example of this type of approximation:

$$H(\tau) = \frac{G'(a\omega) - G'\left(\frac{\omega}{a}\right)}{2\ln a} - \frac{a^2}{(a^2-1)^2} \frac{G'(a^2\omega) - G'\left(\frac{\omega}{a^2}\right) - 2G'(a\omega) - G'\left(\frac{\omega}{a}\right)}{2\ln a}\Bigg|_{\omega=\frac{1}{\tau}} \tag{2.27}$$

where

$H(\tau)$ = relaxation spectra; and

$a$ = constant greater than one, selected such that $0.2 \leq \log a \leq 0.4$.

A similar equation was presented to calculate the spectrum from the loss modulus:

$$H(\tau) = \frac{2}{\pi}\left\{G''(\omega) - \frac{a}{(a-1)^2}\left[G''(a\omega) + G''\left(\frac{\omega}{a}\right) - 2G''(\omega)\right]\right\}\Bigg|_{\omega=\frac{1}{\tau}} \tag{2.28}$$

Second order approximations based on the slope of the storage modulus were presented by Tschoegl (1989):

$$H(\tau) = \frac{dG'(\omega)}{d\ln\omega} + \frac{1}{2}\frac{d^2G'(\omega)}{d(\ln\omega)^2}\Bigg|_{\omega=\frac{1}{\sqrt{2\tau}}} \tag{2.29}$$

$$H(\tau) = \frac{dG'(\omega)}{d\ln\omega} - \frac{1}{2}\frac{d^2G'(\omega)}{d(\ln\omega)^2}\Bigg|_{\omega=\frac{\sqrt{2}}{\tau}} \tag{2.30}$$

Equations 2.29 and 2.30 are representative of the positive and negative slopes of $H(\tau)$, respectively. First order equations based on the slope of the loss modulus are also presented. These can be applied to the positive and negative slope areas of the $H(\tau)$ curves, respectively, and are expressed as follows:

$$H(\tau) = \frac{2}{\pi}\left[G''(\omega) + \frac{dG''(\omega)}{d\ln\omega}\right]\Bigg|_{\omega=\frac{1}{\sqrt{3\tau}}} \tag{2.31}$$

$$H(\tau) = \frac{2}{\pi}\left[G''(\omega) - \frac{dG''(\omega)}{d\ln\omega}\right]\Bigg|_{\omega=\frac{\sqrt{3}}{\tau}} \tag{2.32}$$

Other approximations may be found in literature and have varying degrees of accuracy. The approach of Ninomiya and Ferry (1959) is preferred for practicality, as it utilizes the values of the moduli obtained in experiments, rather than the time derivatives.

### *2.4.5 Time-Temperature Superposition*

Viscoelastic material responses are both time and temperature dependent. This means that the moduli values found through dynamic mechanical analysis are simultaneously functions of frequency and of temperature. Since performing tests over

large frequency ranges is impractical, it is necessary to use methods that extend the frequency scale of measurements taken over a limited frequency range.

Tobolosky and Eyring (1943) observed the similarities in response curves obtained at different temperatures. Differences between these curves were seen to be their location along the time (or frequency) axis. This led to the conclusion that time dependency and frequency dependency are separable, and the introduction of the time-temperature superposition principle (Schwartzel and Sraverman, 1952; Tobolosky, 1956). The principle states that viscoelastic data taken at any temperature may be translated to other temperatures by multiplicative translation along the time scale. This asserts that a change in temperature is equivalent to a shift in the logarithmic time scale.

The principle of time-temperature superposition, also called the method of reduced variables (Ferry, 1980), is relevant for materials considered thermorheologically simple (Schwarzl and Sraverman, 1952). Such materials are defined by their ability to conform to the time-temperature superposition principle. Many noncrystalline homopolymers and homogeneous copolymers fall into the classification of thermorheologically simple. Several researchers (Brodnyn *et al*., 1960 and Dickinson and Witt, 1974) have determined that asphalt cements can be considered thermorheologically simple materials.

The mathematical description of time-temperature superposition is as follows:

$$F(T_1, \omega) = F\left(T_2, \frac{\omega}{a_T}\right) \tag{2.33}$$

where

$F(T_1, \omega)$ = value of viscoelastic function at temperature $T_1$ and frequency $\omega$;

$F(T_2, \frac{\omega}{a_T})$ = value of viscoelastic function at temperature $T_2$ and frequency $\omega/\alpha_T$;

and

$a_T$ = horizontal shift factor, a function of $T_1$ and $T_2$.

Dynamic mechanical tests are performed at several selected temperatures over a limited range of frequency. The test results for one viscoelastic function are plotted versus frequency. A curve corresponding to one temperature is selected as the reference curve. All other curves are shifted along the frequency axis to partially overlap the

reference curve and form a continuous smooth curve, extending across a wide range of frequency, referred to as the master curve. The shift factor, $a_T$, is the amount of shift required for each individual curve to fit the master curve and is a measure of the temperature dependency of the response. A graphical explanation is presented in Figure 2.11.

The use of time-temperature superposition requires three conditions to be met according to Ferry (1980).

- Shapes of adjacent response curves should exactly match;
- The shift factor for each function must be unique; and
- The variations in the shift factor with temperature should follow a rational pattern, compatible with experience.

*Thermorheological Complexity and Thermorheological Simplicity*

The validity of time-temperature superposition principle for thermorheologically simple materials is based on the underlying assumption that all relaxation times are equally affected by a change in temperature. This means that the ratio of the relaxation time at a certain temperature to the same relaxation time at another temperature is constant for the entire range of relaxation times:

$$\frac{\tau_i(T)}{\tau_i(T_r)} = a_T \tag{2.34}$$

where

$\tau_i$ = $i^{th}$ relaxation time at temperature T or reference temperature $T_r$; and

$a_T$ = shift factor from temperature T to reference temperature $T_r$.

From a chemical point of view, thermorheological simplicity is expected only from noncrystalline polymers having no strongly polarized groups. This is because changes in crystalline structures and interactions with polar groups tend to depend on temperature in a different way than viscous flow in amorphous nonpolar materials. Additionally, the structure of thermorheologically simple materials causes them to experience the same sequence of molecular processes at different temperatures, with temperature affecting only the speed of the process (Schwarzl and Sraverman, 1952).

Thermorheologically complex materials have different sequencing of molecular processes at different temperatures. As noted above, this is partially because crystalline structures and polar groups are more temperature dependent than amorphous structures and nonpolar groups in their responses. Therefore, the coincidence of mechanical response curves is not possible along the time or frequency axis by a simple translation. For these materials, the shift factor is a function of time or frequency in addition to temperature, hence equation 2.34 presented above is not applicable (Fesko and Tschoegl, 1971). Superposition must be performed on a point by point basis as

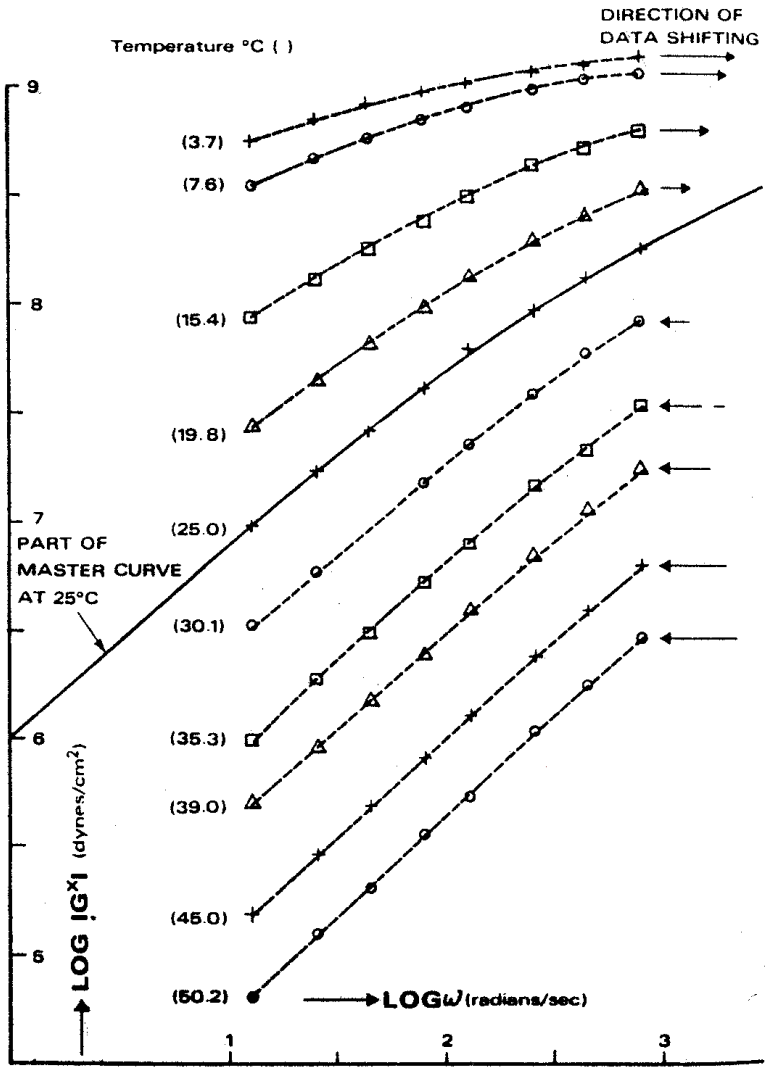


Figure 2.11 Graphical presentation of the time-temperature superposition principle (after Dickenson and Witt, 1974).

shown in Figure 2.12. This demonstrates the dependence of the shift factor on both temperature and time.

Thermorheological simplicity is exhibited in single-phase systems, such as homopolymers. Random copolymers, such as SBR, have a single transition phase between those of styrene and butadiene and can be categorized as thermorheologically simple. However, heterophase systems incorporate constituents having different temperature dependencies. This causes the material to exhibit multiple transitions that correspond to the phase transitions of the constituents, making the temperature dependence of the material extremely complex. In these systems, the relaxation mechanism of each phase is associated with a distinct distribution of relaxation times. Therefore, the systems are thermorheologically complex. Examples of heterophase systems can be seen in block copolymers, polymer blends, and asphalt-polymer mixtures.

Extensive research has been performed by Tschoegl and colleagues (Fesko and Tschoegl, 1971; Lim *et al*., 1971; Cohen and Tschoegl, 1973; Fesko and Tschoegl, 1974; Kaplan and Tschoegl, 1974; Cohen and Tschoegl, 1976) to evaluate the application of time-temperature superposition to hetero-phase systems. The studies resulted in the development of models for the shift factors of two-phase materials, given

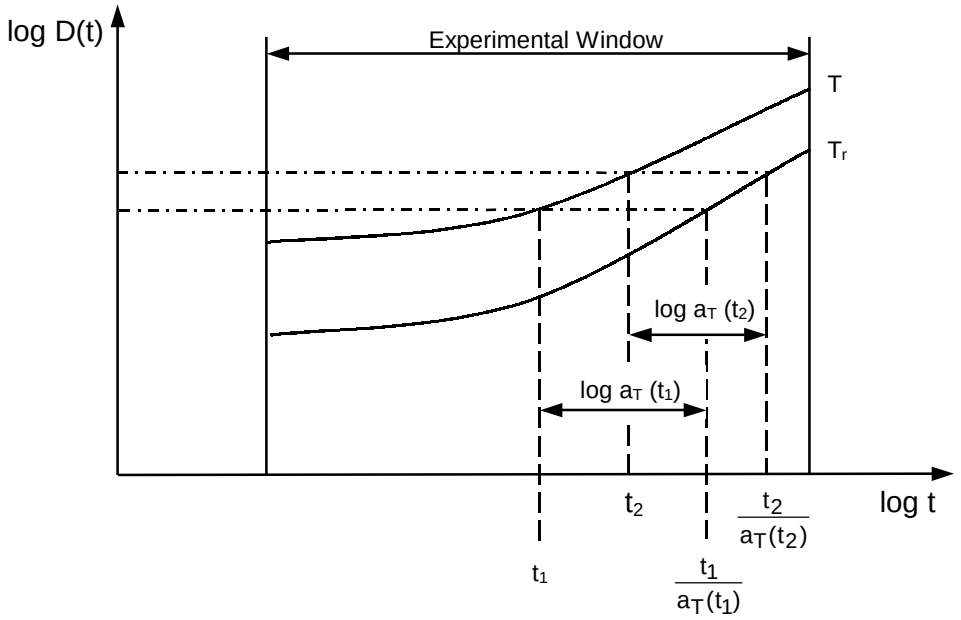


Figure 2.12 Example of superposition along the time axis for thermorheologically complex materials (after Fesko and Tschoegl, 1971).

that the dynamic mechanical properties and temperature dependence of the constituent phases were known. In addition, the contour map method for representation of time and temperature dependence of mechanical response functions was proposed.

Fesko and Tschoegl (1971) showed that, for a thermorheologically complex material, the following was evident:

$$\left(\frac{\partial \log F(t)}{\partial \log t}\right)_T = \left(\frac{\partial \log F(t/a_T(t))}{\partial \log t/a_T(t)}\right)_{T_r}\left[1-\left(\frac{\partial \log a_T(t)}{\partial \log t}\right)_T\right] \tag{2.35}$$

where

F = viscoelastic function, such as modulus, compliance, etc.; and

$a_T$ = time-dependent shift factor.

This expresses that, on a log-log scale, the slope of an isothermal segment of the response curve at any loading time equals the slope of the shifted curve to the reference temperature multiplied by a factor representing the effect of time on the shift factor. Since, for a thermorheologically simple material the shift factor is not time dependent, equation 2.35 can be reduced to the following:

$$\left(\frac{\partial \log F(t)}{\partial \log t}\right)_T = \left(\frac{\partial \log F(t/a_T(t))}{\partial \log t/a_T(t)}\right)_{T_r} \tag{2.36}$$

This shows the equality of slopes of the isothermal segments of the response curve and the master curve at corresponding loading times.

In addition to equation 2.35, Fesko and Tschoegl (1971) developed another equation to express the slope of F(t) with respect to T at a constant time:

$$\left(\frac{\partial \log a_T(t)}{\partial T}\right)_t = \left(\frac{\partial \log F(T)}{\partial T}\right)_t\left[\left(\frac{\partial F[t/a_T(t)]}{\partial \log t/a_T(t)}\right)^{-1}\right]_{T_r} \tag{2.37}$$

As equation 2.37 cannot be integrated, it is not practical to use. Instead, a model proposed by Takayanagi (1965) was used to predict the shift function of a two-phase system based on the temperature shift factors of each constituent phase (assuming that the constituent phases are individually thermorheologically simple). This model assumes the two phases to be connected partly in series and partly in parallel. The series connection assumption results in additive compliances, while the parallel

connection results in additive moduli. The shift factors may be decomposed and expressed as follows (Fesko and Tschoegl, 1974):

$$\log a_T = n_1(t)\log a_{T1} + n_2(t)\log a_{T2} \tag{2.38}$$

with

$$n_1(t) + n_2(t) = 1 \tag{2.39}$$

where

$a_1$ and $a_2$ = shift factors corresponding to phases 1 and 2, respectively; and

$n_1(t)$ and $n_2(t)$ = time dependent weighting factors.

The factors $n_1(t)$ and $n_2(t)$ are complicated functions of relaxation or retardation spectra of the respective phases and are proportional to the weight fraction of each phase. Based on the viscoelastic function under consideration, these factors have different functions. In the case of storage compliance, D'(ω), the factors are expressed as follows (Fesko and Tschoegl, 1971):

$$n_1(\omega) = \left.\frac{w_1 L_1(\tau)}{w_1 L_1[\tau / a_T(\omega)] + w_2 L_2[\tau / a_T(\omega)]}\right|_{\tau=\frac{1}{\omega}} \tag{2.40}$$

$$n_2(\omega) = \left.\frac{w_2 L_2(\tau)}{w_1 L_1[\tau / a_T(\omega)] + w_2 L_2[\tau / a_T(\omega)]}\right|_{\tau=\frac{1}{\omega}} \tag{2.41}$$

where

$L_1$ and $L_2$ = first approximation to the retardation spectrum for phases 1 and 2, respectively; and

$w_1$ and $w_2$ = weight fractions of phases 1 and 2, respectively.

Therefore, equation 2.38 yields different composite shift factors for D(t), D'(ω), D"(ω), etc.

If the values of viscoelastic functions and the temperature dependencies are known for individual phases, equations 2.38 through 2.41 may be used to evaluate the temperature dependence of a two-phase system. This allows the master curve for the thermorheologically complex two-phase material to be constructed.

Although the time or temperature dependence of thermorheologically simple materials is usually presented by isothermal or isochronal measurements, this method of presentation may result in misleading information if used for thermorheologically complex materials. Therefore, an additional method of presentation was proposed that offers simultaneous presentation of time and temperature dependency of thermorheologically complex materials (Cohen and Tschoegl, 1976; Tschoegl and Cohen, 1978). This method utilizes a contour map that traces the loci of points of the constant response as a function of logarithmic time and temperature. The contour map provides insight into the complexity of the time-temperature relations of the material. An example contour map developed for the loss compliance of an SBS triblock copolymer is shown in Figure 2.13.

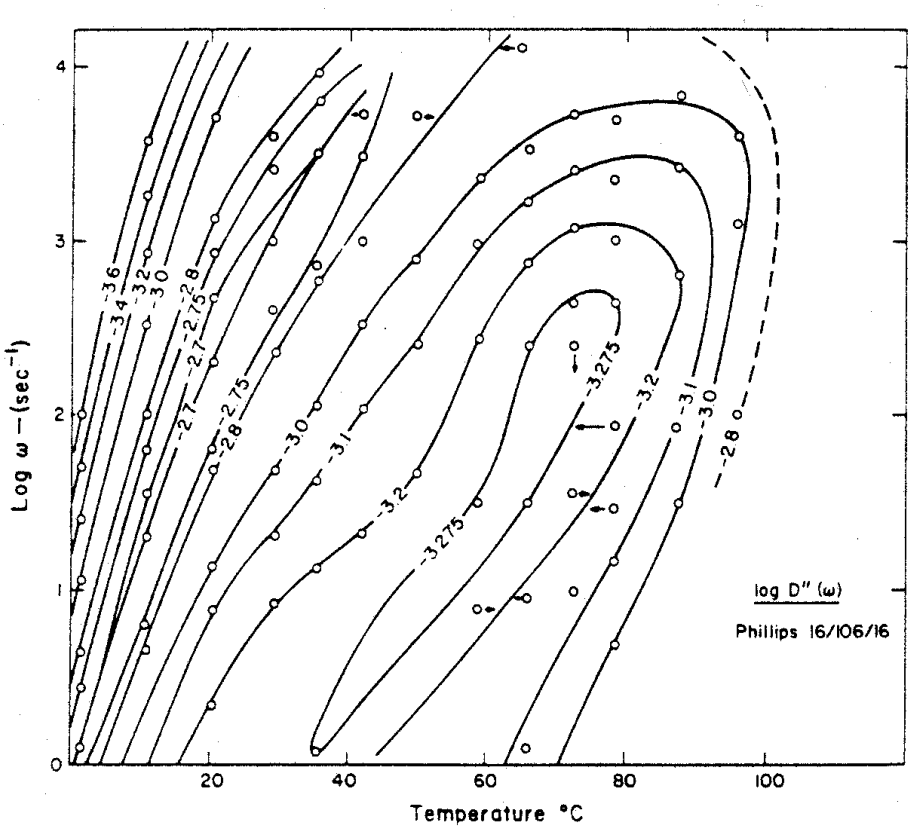


Figure 2.13 Example of a contour map of the logarithmic loss compliance as a function of temperature and logarithmic frequency for a styrene-butadiene-styrene (SBS) sample (after Cohen and Tschoegl, 1976).

## 2.5 Current Research

Research has generated analytical expressions that characterize the viscoelastic response of asphalt cement as related to the frequency dependence and temperature dependence, particularly since the late 1960's. The most notable of these models include those developed by Dobson (1969), Jongepier and Kuilman (1969, 1970), Dickenson and Witt (1974), Christensen and Anderson (1992), Stasta *et al*. (1996), Gahvari (1996), and Marasteanu and Anderson (1999). While the results of these studies have advanced the understanding of asphalt cement response, most studies were performed using unmodified asphalts. This leads to discrepancies when the models are used in the analysis of modified binder response. However, in order to understand the basis for models describing the behavior of modified asphalts, descriptions of these models are presented.

### *2.5.1 Jongepier - Kuilman Model*

Jongepier and Kuilman (1969, 1970) performed dynamic analysis of sixteen asphalt cements. The analysis was performed across a temperature range of –20 to 160°C, with measurements above 40°C being made in terms of viscosity. The test frequency range extended from 0.003 to 314.159 rad/s. The mathematical model for frequency dependency was based on an assumption of a log normal relaxation time distribution:

$$H(\tau) = \frac{G_g}{\beta\sqrt{\pi}} e^{-\left[\frac{\ln\tau/\tau_m}{\beta}\right]^2} \qquad (2.42)$$

where

$H(\tau)$ = logarithmic relaxation spectrum;

$G_g$ = glassy modulus, Pa;

$\beta$ = width of the distribution function;

$\tau$ = time, s; and

$\tau_m$ = time constant, s.

The glassy modulus is the limiting value of the storage modulus at very high frequencies and is expressed as follows:

$$G_g = \int_{-\infty}^{+\infty} H(\tau) d \ln \tau \quad (2.43)$$

The time constant, $\tau_m$, is defined as:

$$\tau_m = \frac{\eta}{G_g} e^{-\frac{\beta^2}{4}} \quad (2.44)$$

where $\eta$ is the zero shear viscosity.

Using the approach given by Ninomiya and Ferry (1959), the equations for the storage and loss moduli were developed and are as follows, respectively:

$$G'(x) = \frac{G_g}{\beta\sqrt{\pi}} \exp - \left[\frac{\beta(x - 1/2)}{2}\right]^2 \times \int_0^{\infty} \exp - \left(\frac{u}{\beta}\right)^2 \frac{\cosh(x + 1/2)u}{\cosh u} du \quad (2.45)$$

$$G''(x) = \frac{G_g}{\beta\sqrt{\pi}} \exp - \left[\frac{\beta(x - 1/2)}{2}\right]^2 \times \int_0^{\infty} \exp - \left(\frac{u}{\beta}\right)^2 \frac{\cosh(x - 1/2)u}{\cosh u} du \quad (2.46)$$

where the transformations u and x are defined as:

$$u = \ln \omega\tau \quad (2.47)$$

$$x = \frac{2}{\beta^2} \ln \omega_r \quad (2.48)$$

and $\omega_r$ is a dimensionless reduced frequency given as follows:

$$\omega_r = \frac{\omega\eta_0}{G_g} \quad (2.49)$$

where $G_g$ is the glassy modulus.

After performing dynamic mechanical analysis, the factor $\beta$ was found to characterize the shape of the relaxation spectrum, and was thus determined to be a rational parameter for characterizing binders. Additionally, $\beta$ was observed to be strongly correlated with the composition of asphalt binder.

### *2.5.2 Dobson Model*

The model developed by Dobson (1969) evaluates the frequency dependence of asphalt based on the master curves of the complex modulus and loss tangent. These

are described as functions of frequency. The resulting model determines the relative frequency in terms of the relative modulus, $G_r$:

$$\log \omega_r = \log G_r - \frac{1}{b}\left[\log(1-G_r^b) + \frac{20.5-G_r^b}{230.3}\right] \tag{2.50}$$

where

$\omega_r$ = relative frequency;

$G_r$ = relative modulus; and

b = parameter describing the width of the relaxation spectrum.

No further explanation detailing the type of distribution function that comprises b is made. However, Dobson noted that b can be considered a shear susceptibility parameter and is related to the penetration index. The relative frequency, $\omega_r$, is expressed as follows:

$$\omega_r = \frac{\eta_0\, \omega\, \alpha_T}{G_g} \tag{2.51}$$

where

$G_g$ = glassy modulus, Pa;

$\eta_0$ = the limiting low frequency viscosity at the reference temperature;

$\omega$ = frequency, rad/s; and

$\alpha_T$ = shift factor describing the temperature variation of Newtonian viscosity.

The relative modulus is defined as follows:

$$G_r = \frac{\left|G^*\right|}{G_g} \tag{2.52}$$

where $|G^*|$ is the ratio of peak stress to peak strain.

Dobson based the following relationship between complex modulus and loss tangent on experimental observations:

$$\frac{d \log \left|G^*\right|}{d \log \omega} = \frac{\tan \delta}{(1+\tan \delta)(1-0.01 \tan \delta)} \tag{2.53}$$

where $\delta$ is the phase angle.

The expression shown in Equation 2.53 is valid only for values of tan $\delta < 9.5$.

To consider the temperature dependence of the asphalt response, the Williams-Landel-Ferry (WLF) equation was implemented by Dobson to describe the shift factors. Brodnyn *et al*. (1960) found that for temperatures such that $T\text{-}T_s > (-20)$, the WLF equation with universal constants fit shift factor data. This was confirmed and verified that at lower temperatures the equation overestimates shift factors. Therefore, the WLF equation as determined by Dobson has two pairs of constants to account for temperatures above and below the reference temperature. The first of the equations is as follows:

$$\log \alpha_T = \frac{-12.5(T - T_s)}{142.5 + (T - T_s)} \tag{2.54}$$

where $T_s$ is the reference temperature.

Equation 2.54 is valid for temperatures in the range $T - T_s < 0$. For temperatures in the range of $T - T_s > 0$, the following equation applies:

$$\log \alpha_T = \frac{-8.86\,(T - T_g)}{101.6 + (T - T_s)} \tag{2.55}$$

where $T_g$ is the glass transition temperature. The reference temperature $T_s$ is not specified, however, it should be an equi-viscous temperature for asphalts.

### *2.5.3 Dickenson - Witt Model*

Dickenson and Witt (1974) performed dynamic mechanical testing on fourteen different asphalt cements and developed analytical expressions for the complex modulus and phase angle in terms of frequency. Testing was performed at temperatures of 2 to 52°C and frequencies of 12.56 to 753.98 rad/s. They proposed the following modulus equation:

$$\log G_r = \frac{1}{2}\left[\log \omega_r - \sqrt{(\log \omega_r)^2 + (2\beta)^2}\right] \tag{2.56}$$

where

$G_r$ = relative modulus;

$\omega_r$ = relative angular frequency; and

$\beta$ = shear susceptibility parameter.

The relative modulus is defined as the ratio of the measured modulus to the shear modulus at an infinitely high rate of shear. The relative angular frequency, as explained by Dobson (1969), is expressed in equation 2.51. The shear susceptibility parameter varies based on the composition and aging of the binder. The equation for the modulus describes a hyperbola whose asymptotes, log $G_r$ = log $\omega_r$ and log $G_r$ = 0, indicate the viscous and elastic response extremes, respectively. The phase angle was expressed mathematically:

$$\delta = \delta' + \frac{\pi - 2\delta'}{4}\left[1 - \frac{\log \omega_r}{\sqrt{(\log \omega_r)^2 + (2\beta)^2}}\right] \qquad (2.57)$$

where $\delta$' is a small angle (0 to 3°) assigned based on the glassy modulus.

Based on equations 2.56 and 2.57, the values of the storage and loss moduli were computed and used to develop the relaxation spectra. The coincidence of the relaxation spectra confirmed the validity of the developed equations. Additionally, Dickinson and Witt observed that the spectra were not symmetrical with respect to the maximum value and disputed Jongepier and Kuilman's assumption of a log Gaussian distribution of relaxation times.

Dickinson and Witt described the temperature dependency of their experimental data using Dobson's version of the WLF equation. Based on two sets of constants proposed by Dobson, the reference temperature for the range of studied asphalts was estimated.

### *2.5.4 Christensen - Anderson Model*

Christensen and Anderson (1992) performed dynamic mechanical analysis on eight Strategic Highway Research Program (SHRP) core asphalts for the purpose of developing and verifying mathematical models describing the viscoelastic behavior of asphalt cement. The analysis was performed at temperatures from –35 to 60°C and at frequencies of 0.1 to 100 rad/s. Mathematical models were derived based on a logistic distribution function used to describe the relaxation spectra. The complex modulus is described as follows:

$$|G^*(\omega)| = G_g\left[1+\left(\frac{\omega_c}{\omega}\right)^{\frac{\log 2}{R}}\right]^{-\frac{R}{\log 2}} \quad (2.58)$$

where

$|G^*(\omega)|$ = complex shear modulus, Pa;

$\omega_c$ = crossover frequency, rad/s; and

R = rheological index.

The rheological index is determined as:

$$R = \log\left(\frac{G_g}{|G^*(\omega)|}\right)_{\omega=\omega_c} \quad (2.59)$$

The phase angle is described by:

$$\delta(\omega) = \frac{90}{1+\left(\frac{\omega}{\omega_c}\right)^{\frac{\log 2}{R}}} \quad (2.60)$$

The parameters $\omega_c$ and R have considerable physical significance. The crossover frequency, $\omega_c$, is the frequency at which the phase angle, $\delta$, is equal to 45°. This frequency has been found in several empirical observations to coincide with the intersection of the glassy and viscous asymptotes of the modulus master curve. Therefore, the crossover frequency is considered a location parameter of the master curve. The rheological index represents the width of the relaxation spectrum and is considered a shape parameter for the master curve. Asphalts having larger R values exhibit wider relaxation spectra.

The temperature dependency of shift factors was determined using both the WLF equation and the Arrhenious function. A defining temperature, $T_d$, was defined as the limit below which an Arrhenious function was used and above which the WLF equation was used to determine shift factor temperature dependency. It was suggested that there was a strong correlation between the defining temperature, $T_d$, and the glassy transition temperature, $T_g$, although no explicit relationship was established. It was observed that, at temperatures above $T_d$, the WLF equation yielded reasonable values for the shift

factors. Below the $T_d$, an Arrhenious function was defined to determine the shift factors and characterize the temperature dependency of the binder as follows:

$$\log a_T = \frac{H_a}{2.303R}\left(\frac{1}{T} - \frac{1}{T_d}\right) \tag{2.61}$$

where

$T_d$ = defining temperature, °K;

$H_a$ = activation energy for flow below $T_d$, J/mol; and

R = ideal gas constant, 8.314 J/mol·°K.

The model proposed by Christiansen and Anderson is relatively simple in shape, as compared to previous models, however, some discrepancies were observed by the authors for moduli below $10^5$ Pa when comparisons were made between the model generated data and experimental data. They determined that the model was strictly suitable for characterizing response at intermediate to high ranges of the modulus, though limited in application at the asymptotes of response.

### *2.5.5 Stastna – Zanzotto - Kennepohl Model*

Stastna *et al.* (1996) proposed a simple model of the complex modulus and phase angle based on a generalization of the Maxwell model. This model was derived from the generalized viscoelastic model. The equation for complex modulus is given as follows:

$$\left|G^*(\omega)\right| = i\eta_0\,\omega\left\{\frac{\prod_1^m [1+(\omega\mu_k)^2]}{\prod_1^n [1+(\omega\lambda_k)^2]}\right\}^{1/2(n-m)} \tag{2.62}$$

where

m and n = the numbers of relaxation times, with m being less than n;

$\mu_k$ and $\lambda_k$ = relaxation times; and

$\eta_0$ = zero-shear viscosity.

The phase shift, $\delta(\omega)$, can be expressed as follows:

$$\delta(\omega) = \frac{\pi}{2} + \frac{1}{n-m}\left[\sum_{1}^{m} a\tan(\mu_k \omega) - \sum_{1}^{n} a\tan(\lambda_k \omega)\right] \quad (2.63)$$

To verify the proposed equations, dynamic mechanical analysis was performed on five modified and nineteen unmodified asphalt binders. Equations 2.62 and 2.63 were found to accurately model the responses of both unmodified and modified asphalts. However, Marasteanu and Anderson (1999) determined that the model lacks statistical validity when applied to a typical experimental data set, because the number of unknown parameters approaches the degrees of freedom found in the data.

### *2.5.6 Gahvari Model*

Gahvari (1996) performed dynamic mechanical testing on several modified binders. Experimental complex modulus results were compared with results based on the models of Christensen and Anderson and significant discrepancies between results were observed, leading to the conclusion that previously proposed models were insufficient for use with modified binders. Therefore, additional mathematical models were determined to characterize the responses of modified binders.

The model for storage modulus was developed based on a modified Mitcherlich equation:

$$\frac{d\log G'(\omega)}{d\log \omega} = p(\log G_g - \log G') \quad (2.64)$$

where

G' ($\omega$) = storage modulus, Pa;

$\omega$ = reduced frequency, rad/s;

$G_g$ = glassy modulus, Pa; and

p = proportionality factor.

Equation 2.62 is solved to determine the storage modulus as follows:

$$\log G'(\omega) = \log G_g\left[1 - \left(\frac{e^{-l}}{\omega^{\log e}}\right)^{p}\right] \quad (2.65)$$

where l is location parameter for the master curve and determined as follows:

$$l = \log \frac{1}{\omega}\Big|_{G'=1} \tag{2.66}$$

Alternatively, equation 2.65 may be written as:

$$\log G'(\omega) = \log G_g\left[1 - \exp(-p(\log \omega + l))\right] \tag{2.67}$$

The location parameter, l, marks the point of intersection of the plot of storage modulus curve with the reciprocal frequency axis on a log-log scale. The location parameter was seen to be a function of the polymer type, polymer concentration level and aging condition of the binder. The proportionality factor, p, determines the rate at which the storage modulus curve approaches the glassy asymptote.

The expression for the loss factor is based on a hyperbolic function and is determined as follows:

$$\log G''(\omega) = (\log G''_{max} + d) - \sqrt{(\log \omega - \log \omega_d)^2 + d^2} \tag{2.68}$$

where

G”(ω) = loss modulus, Pa;

$G''_{max}$ = peak value of the loss modulus, Pa;

d = half length of the transverse axis, Pa; and

$\omega_d$ = location parameter for the master curve radius, rad/s.

The location parameter, $\omega_d$, is expressed as:

$$\omega_d = \omega\Big|_{G''=G''_{max}} \tag{2.69}$$

The location parameter indicates the frequency at which the loss modulus reaches the peak value.

The loss factor equation represents one arm of a hyperbola centered at (log $\omega_d$, log $G''_{max}$ + d) on the log ω - log G” coordinate system. The hyperbola approaches an asymptote at low frequencies that is described by the following:

$$\log G''(\omega) = (\log \omega - \log \omega_d) + (\log G''_{max} + d) \tag{2.70}$$

The asymptote represents the viscous asymptote of response.

In determining the master curves, the WLF equation was found to adequately describe the temperature dependence of the binders. The shift factors were found to conform to the following:

$$\log a_T = \frac{-8.86(T - T_s)}{101.6 + (T - T_s)} - \log b \qquad (2.71)$$

where

$a_T$ = experimentally measured shift factor;

$T_s$ = reference temperature, °C; and

b = vertical translation factor.

Using the observed shift factors, non-linear least squares analysis determined the values for the reference temperature, $T_s$, and the vertical translation factor, b.

Gahvari's model may be criticized as it does not conform to the prerequisites for complex measurements that force the storage and loss modulus models to be related.

### *2.5.7 Marasteanu - Anderson Model*

Marasteanu and Anderson (1999) modified the model developed by Christensen and Anderson (1992) to improve the fit for both unmodified and modified binders. The revised model shows significant improvement in fit when modeling the extreme regions of the frequency range. The researchers applied the Havriliak and Negami model (Havriliak and Negami, 1966) to the initial Christensen-Anderson model, resulting in the following equation for the complex modulus:

$$|G^*(\omega)| = G_g\left[1 + \left(\frac{\omega_c}{\omega}\right)^v\right]^{-\frac{w}{v}} \qquad (2.72)$$

The parameter v is described by the following equation:

$$v = \frac{\log 2}{R} \qquad (2.73)$$

The parameter w addresses the issue of how fast or slow the phase angle converges to the ninety and zero degree asymptotes as the frequency goes to zero or infinity, respectively. It can best be interpreted from the expression for the phase angle, $\delta(\omega)$:

$$\delta(\omega) = \frac{90\,w}{1+\left(\frac{\omega}{\omega_c}\right)^v} \tag{2.74}$$

This model was applied to thirty-eight unmodified and modified binders, and the degree of precision in modeling the complex modulus was greater than the original Christensen-Anderson model. However, anomalies were still seen in the construction of a smooth master curve for the phase angle when testing binders that did not behave as thermorheologically simple materials.

# CHAPTER 3 RESEARCH APPROACH

The research in this study is a continuation of previous experimentation performed by Gahvari (1996) at Virginia Tech. The previous experiment consisted of measuring the complex moduli of asphalt-polymer blends at frequencies between 0.16 to 30 Hz and temperatures ranging from 5 to 75°C. The mixes were prepared by Gahvari using a conventional AC-20 paving grade asphalt binder and several different elastomeric polymer modifiers. Each polymeric additive was blended with asphalt binder at three different concentrations. The modifiers used were thermoplastic block copolymers. These polymers represent a wide range of chemical structures, and mechanical and physical properties. The study also investigated the effect of short-term aging on the rheological properties of the polymer-modified asphalt blends.

The current study consists of dynamic mechanical analysis on the base asphalt and three of the polymer modified asphalt blends. The collected data were processed, analyzed, and compared with the data gathered previously. Additionally, the data were used to validate several analytical models used to describe the response of polymer modified asphalt blends to dynamic mechanical testing.

## 3.1 Selection of Materials

All samples tested were prepared more than four years ago (Gahvari, 1996). The base asphalt used was AC-20 asphalt supplied by the Amoco Oil Company. Table 3.1 shows the results of conventional testing and Corbett analysis of the base asphalt.

Several elastomeric polymers were utilized in the original study for asphalt modification. These included two SBR random copolymers, two SBS linear block copolymers, two SEBS linear block copolymers, and one $(SB)_n$ branched copolymer. The block copolymers were supplied by the Shell Chemical Company. The random copolymers were manufactured by the Goodyear Company and supplied by the Shell Chemical Company. In this study, three of the modified sample types were selected for evaluation. The three samples were selected based on two criteria:

Table 3.1 Results of conventional testing and Corbett analysis on AC-20 base asphalt.

| Conventional Test Property | Unaged Binder | Binder Residue from Thin Film Oven Test |
|---|---|---|
| Specific Gravity | 1.037 | |
| Penetration @ 25°C, 0.1mm | 66 | 40 |
| Absolute Viscosity @ 60°C, poise | 2054 | 4232 |
| Kinematic Viscosity @ 135°C, cSt | 437 | |
| Corbett Analysis Results | | |
| Asphaltenes | 14.0 – 14.3% | |
| Polar Aromatics | 13.2 – 19.0% | |
| Naphthene Aromatics | 51.2 – 53.4% | |
| Saturates | 14.5 – 18.0% | |
| Unrecovered | 1.1 – 1.3% | |

1. Significant differences in response at varying polymer concentrations, and
2. Significant differences in response after aging in the rolling thin film oven.

The combination of these criteria led to the selection of modified samples which were judged most likely to show significant changes in dynamic response after four years of ambient temperature aging. In addition, the samples were chosen to reflect variety among the modifiers. The samples selected included one SBS linear block copolymer, one SEBS linear block copolymer, and one $(SB)_n$ radial block copolymer, all supplied by the Shell Chemical Company. Table 3.2 shows the typical properties of the three selected block copolymer modifiers.

## 3.2 Binder Designations

Each binder-polymer combination was given a four-character code. The first character, A, referred to the binder type used, Amoco AC-20. The second character, U or R, referred to the aging condition of the binder, U designated unaged binder, while R

Table 3.2 Properties of thermoplastic block copolymers used in this study at 23°C (Shell, 1992).

| Trade Name | Kraton D-1101* | Kraton G-1652* | Kraton D-1184* |
|---|---|---|---|
| Designation | S | G | N |
| Structure | Linear SBS | Linear SEBS | Radial $(SB)_n$ |
| Physical Form | Porous Pellet | Powder | Porous Pellet |
| Plasticizer Oil Content, %w | 0 | 0 | 0 |
| Specific Gravity | 0.94 | 0.91 | 0.94 |
| Brookfield Viscosity @ 25°C, cps | 4000 | 1350 | 20000 |
| Tensile Strength, Pa (ASTM D412) | 31700 | 31050 | 27600 |
| 300% Modulus, Pa (ASTM D412) | 2760 | 4830 | 5520 |
| Elongation, % (ASTM D412) | 880 | 500 | 820 |
| Styrene/Butadiene Ratio | 31/69 | 29/71 | 30/70 |

* Supplied by the Shell Chemical Company.

was indicative of rolling thin film oven residue. The third character designated the polymer additive as seen in Table 3.2. The fourth character denoted the concentration, by weight of binder, of the polymer. For example, AUS3 denotes an unaged blend of binder with polymer S (linear SBS) having 3% polymer (by weight of the binder). The sample designated ARS3 is the rolling thin film oven residue of the same binder. AU00 and AR00 designate the unmodified samples in unaged and aged conditions, respectively.

## 3.3 Testing Instruments

Dynamic mechanical tests were performed using a Bohlin stress-controlled dynamic shear rheometer (DSR) with a parallel plate configuration (Bohlin, 1990) as

shown in Figure 3.1. Sample temperatures were controlled by immersing the sample and parallel plates in a temperature controlled water bath. The water temperature was controlled to an accuracy of 0.1°C by a pump-equipped bath that circulates the water and regulates the temperature. The parallel plate configuration utilized plates of two sizes. For testing at temperatures between 45 and 75°C, 25mm diameter plates were used with samples having a thickness of 1mm. At lower test temperatures, from 5 to 35°C, 8mm diameter plates were used with samples having a thickness of 2mm. The smaller diameter plates were used at temperatures below 35°C, because, due to the high stiffness of the binder, high shear stresses were required to reach the desired test strains.

The dynamic shear rheometer operates under the general theory of dynamic mechanical analysis. A circular specimen is mounted between two circular plates. In general, the lower plate is fixed and the upper plate is free to rotate about a vertical axis. Specimens are subjected to specific shear stresses at designated frequencies by the application of torque to the upper plate. The response is measured as the angular deflection of the sample. The following equations have been developed to compute the storage and loss moduli (Bohlin, 1990):

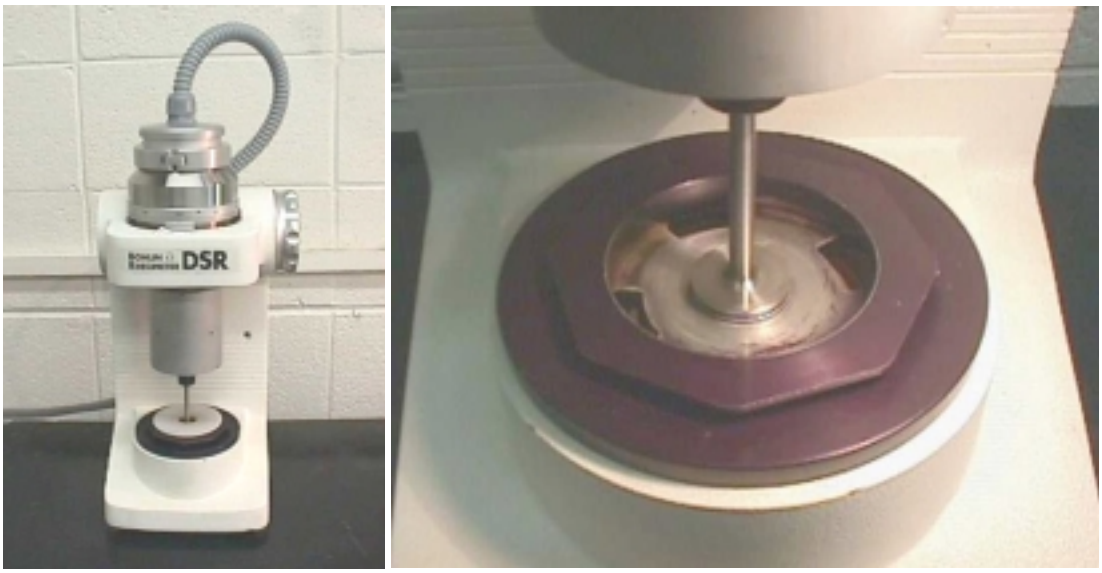


(a) (b)

Figure 3.1 (a) Dynamic shear rheometer used in this study and (b) close-up of the parallel plate configuration in place.

$$G' = \frac{2h}{\pi R^4} \frac{\left| T_D^* \right| \cos\phi + I\omega^2 \left| \theta^* \right|}{\left| \theta^* \right|} \tag{3.1}$$

$$G'' = \frac{2h}{\pi R^4} \frac{\left| T_D^* \right| \sin\phi}{\left| \theta^* \right|} \tag{3.2}$$

where

h = sample thickness, m;

R = sample radius, m;

$T^*_D$ = complex output torque, N·m;

$\theta^*$ = complex angular deflection of the sample, rad;

I = system inertia, kg·m;

$\omega$ = angular frequency, rad/s, and;

$\phi$ = raw phase angle, rad, composed of the actual phase angle and the phase angle between the output and sample torque.

The calculation of $|G^*|$ and tan $\delta$ are then possible utilizing the following identities:

$$\left| G^* \right| = \sqrt{[G']^2 + [G'']^2} \tag{3.3}$$

$$\tan\ \delta = \frac{G'}{G''} \tag{3.4}$$

## 3.4 Sample Preparation

Samples were prepared for initial testing and analysis by Gahvari (1996). The Amoco Company supplied the base binder, AC-20, in a 19L container. This was placed in an oven maintained at 140 ± 5°C for approximately five hours before being poured into several one liter cans. During the heating process, the binder was periodically stirred to ensure uniformity. The one liter cans of binder were sealed and stored at room temperature until the blends were prepared for this research.

The manufacturer supplied polymer G as a fine uniform powder. This was deemed suitable for mixing with the binder due to the high surface area of the particles. Polymers S and N were supplied as approximately 3mm particles. These polymers were reduced in size using a laboratory granulator then passed through a 1.18mm sieve to obtain fine, uniform particles. Polymers were blended with the base binder at three concentration levels. These were two, three, and four percent by weight of the binder.

Mixing of the polymer and binder was performed using a Lightnin Labmaster model L1UO3 laboratory mixer. The mixer was capable of operating at speeds of 50 to 1800 rpm. Additionally, quantitative measurement of mixing parameters such as speed, power input, and pumping capacity as measured by the impeller generated flow was possible. A three-blade propeller-paddle having a 50mm blade diameter was used for mixing.

The blends were prepared by first heating a one liter can of the base binder in a preheated oven at 140°C until sufficiently fluid such that 400g might be transferred into a 1000mL glass beaker. The beaker was placed in a heating mantle to maintain a constant temperature during the blending process. The mixing temperature ranged from 163 to 177°C depending on the type of polymer being blended with the binder. The temperature was monitored with two thermocouples. One thermocouple was placed between the beaker and heating mantle to monitor the power input. The second thermocouple was placed inside the beaker to directly measure the binder temperature.

After placing the mixer shaft directly at the center of the beaker, with the propeller one third of the depth from the bottom, the binder was heated to the desired temperature while the mixer operated at 100 rpm. Once the target temperature was reached inside the beaker, the polymer was added over a period of 30 min, during which the mixer speed was increased by three consecutive steps to a speed of 400 rpm. The polymer was added at a slow rate to prevent aggregation of the polymer particles.

After the entire amount of polymer was added to the base binder, the mixing speed was increased to 800 and then to 1000 rpm and the mixing was continued for three to 10 hrs until a uniform blend was obtained. After mixing was complete, the beaker was transferred to an oven maintained at a temperature of 163°C. After one hr, if no obvious signs of phase separation were observed, the blend was poured into 30mL cans. The cans were sealed and stored at room temperature.

Immediately after the preparation of a blend, four 35g samples were poured into bottles for the Rolling Thin Film Oven Test. These samples were aged in accordance with the procedures for the RTFOT established in ASTM D2872 (ASTM, 1998). After aging, the samples were transferred into 30mL cans that were sealed and stored at room temperature for further testing.

Samples were prepared for dynamic mechanical analysis following strict procedures. For each replicate tested, a 30mL can of binder was placed in an oven preheated to a temperature of 163°C. The binder was heated until sufficiently fluid to pour two specimens for use in analysis. During the heating process the binder was stirred often to ensure uniformity in the specimens. Specimens were formed using two procedures.

During the initial testing by Gahvari (1996), difficulty was encountered when premolded 8mm diameter specimens were used for testing at temperatures below 35°C. At these temperatures, slippage between the specimen and plates is a concern and was found to occur. Therefore, those specimens were poured directly on the upper plate of the rheometer and trimmed to the required dimensions. These difficulties were not seen when using the premolded 25mm diameter specimens; thus the use of premolded specimens was continued at temperatures above 35°C. During testing performed in this study, it was found that low temperature slippage could be avoided by allowing the 8mm premolded specimens to reach equilibrium at a temperature of 45°C while in place in the rheometer prior to testing the specimen at temperatures of 35°C or lower. Therefore, it was decided to use premolded 8mm and 25mm specimens to lower the variability often seen in poured and trimmed specimens.

After a specimen was poured into a mold, it was allowed to cool at room temperature for approximately 20 min, until the specimen could be removed from the mold without damage. As both an 8mm and 25mm specimen were formed from one can of heated binder, it was necessary to store one specimen until it could be tested in the rheometer. The stored specimen was placed in a freezer kept at a temperature of approximately –14°C, to prevent changes in the molded shape. Additionally, the low temperatures prevented the specimens from undergoing additional aging that may have introduced differences in results between replicates. The stored specimens were allowed to return to room temperature for approximately one-half hr prior to placement in the rheometer for testing.

The dynamic shear rheometer was preheated to a temperature of 45°C prior to insertion of the test specimens. This applied to both the 8mm and 25mm diameter specimens. The preheat temperature was the initial test temperature for the 25mm diameter specimen and was found to eliminate the possibility of slippage at low temperature testing for 8mm diameter specimens. The specimens were placed on the upper plate of the rheometer as it was lowered into place at the specified height above the bottom plate. The plate spacing specified by AASHTO TP5 (AASHTO, 1994) was used for dynamic mechanical analysis with the dynamic shear rheometer. For testing at temperatures above 40°C, a specimen with a height of 1mm and a diameter of 25mm was used. For testing at temperatures below 40°C, a specimen having a height of 2mm and a diameter of 8mm was used. Specimens were placed in the rheometer and the plates were adjusted to a height 0.05mm above the required height. The specimen was trimmed with a hot spatula such that the sides of the specimen were the required diameter and were perpendicular to the plate surfaces. The plate spacing was then reduced by 0.05mm to the required specimen height. This created a slight bulge of the specimen sides, seen in Figure 3.2, as required by AASHTO TP5 (AASHTO, 1994). Following this preparation, the specimens were subjected to testing.

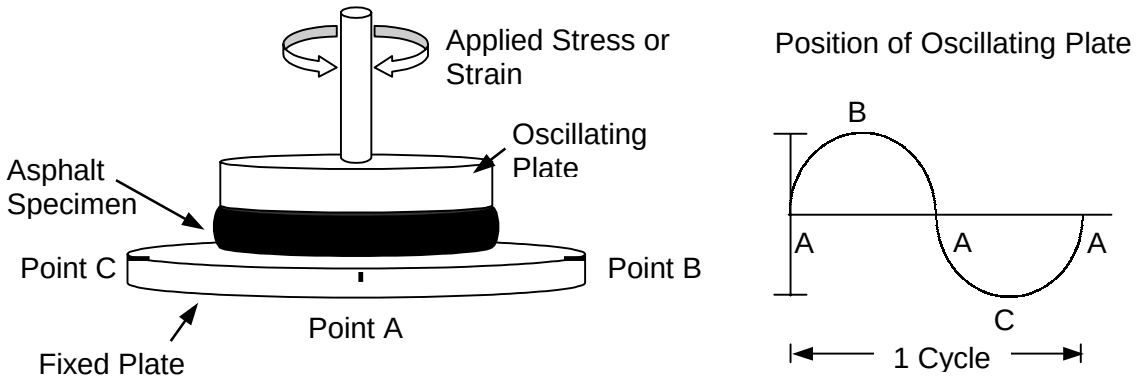


Figure 3.2 Parallel plate setup for dynamic shear rheometer with specimen in place.

## 3.5 Dynamic Mechanical Analysis

### *3.5.1 Stress Sweeps*

Dynamic mechanical testing was preformed at eight temperatures ranging from 5 to 75°C, in 10°C increments. Gahvari (1996) performed stress sweeps at all temperatures and selected frequencies and strains to insure that measurements would be taken in the linear viscoelastic range of response. At 15°C and higher temperatures, frequencies of 3.142, 6.283, and 9.425 rad/s were used in the stress sweeps. A frequency of 0.063 rad/s was used for stress sweeps performed at 5°C. Within the linear viscoelastic range of response, the values of viscoelastic functions are independent of the applied stress amplitude. However, in the non-linear region of response, the moduli will decrease with increasing stress. Due to gradual variations in the measured moduli during the stress sweeps, an exact line between the linear and non-linear regions of response was difficult to determine; therefore the division was arbitrarily determined as the strain at which the moduli dropped to 95% of the initial value. This is seen in Figure 3.3. Based on the results of the stress sweeps, a uniform set of target strains were established and used for testing. For the testing performed in this study, the values determined previously were applied. These values were found to produce results in the linear range of response and allowed comparisons with the results obtained by Gahvari. The target strains used in the frequency sweeps are shown in Table 3.3.

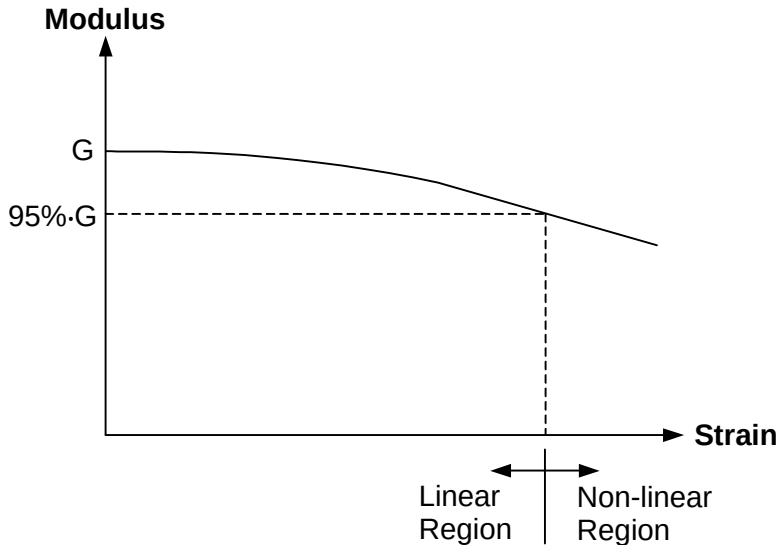


Figure 3.3 Defining the linear and non-linear regions of response.

Table 3.3 Target strains for frequency sweeps.

| Test Temperature, °C | Target Strain, % |
|---|---|
| 5 | 0.8 |
| 15 | 1 |
| 25 | 2 |
| 35 | 3 |
| 45 | 6.5 |
| 55-75 | 9 |

### *3.5.2 Frequency Sweeps*

Frequency sweeps were performed on all samples in the unaged and aged state and over the entire range of temperatures. At temperatures 35°C and below thirty-two frequencies were used, ranging from 0.063 to 94.248 rad/s. At temperatures 45°C and above, 34 frequencies ranging from 0.063 to 188.496 rad/s were used.

Before starting measurements, the rheometer was preheated to a temperature of 45°C. The apparatus with the specimen in place was allowed to reach equilibrium for approximately 30 min. This assured the bond between the specimen and the rheometer plates, and improved the repeatability of the measurements.

In the case of the 8mm sample, the temperature was then lowered in 10°C increments, the sample was allowed to reach equilibrium for at least thirty min, and a frequency sweep was performed in ascending order of frequencies. The procedure continued until data was obtained at all desired temperatures.

In the case of the 25mm sample, measurements began at 45°C after the sample reached equilibrium. Similar to the procedure for the 8mm sample, the test temperature was increased by 10°C increments. The sample was allowed to reach equilibrium for at least 30 min then a frequency sweep was performed in ascending order of frequencies. The procedure continued until a sweep was performed at the 75°C test temperature.

All tests were performed in replicate. To ensure representative sampling, replicate samples were poured from different sample cans. As previously noted, each replicate consisted of an 8mm and 25mm diameter specimen, which were poured from the same sample can.

Frequency sweeps resulted in the measurement of the dynamic shear storage and loss moduli over the entire range of frequencies tested. Additionally, the rheometer

calculated the complex dynamic shear modulus and phase angle over the range of frequencies. These parameters may be plotted to form isothermal curves describing the binder response at each temperature and frequency. Furthermore, the data may be manipulated to form mastercurves indicating the response referenced to a specific temperature over a wider range of frequencies than was actually tested. The use and application of this data will be further discussed in chapter four.

### *3.5.3 Repeatability of Dynamic Mechanical Tests*

Dynamic mechanical testing of binders, and particularly polymer-modified binders, often results in data having significant variability between replicates. Several factors are known to contribute to this problem. Temperature variations are a main cause of variability between replicates. It has been found (Gahvari, 1996) that temperature variations as small as ±0.5°C may cause up to 15% change in the values of the complex modulus. During this testing, the rheometer was able to maintain temperatures to an accuracy of ±0.1°C, which is sufficient to minimize errors. In addition to maintaining a constant temperature, it is important to be certain that specimens are at thermal equilibrium. To ensure this, the specimen was allowed to equilibrate at the test temperature for no less than 30 min prior to performing a test. The equilibrium time was considered long enough to eliminate the possibility of temperature gradients within the specimen.

Specimen preparation was determined to be a major factor affecting variability. Parallel plate geometry specimens may be prepared by two different methods, as mentioned previously. The first is by prefabricating the specimen to the desired geometry using silicon rubber molds. This is a preferred method because the specimen geometry may be tightly controlled and is easily reproducible. However, slippage may occur during testing at low temperatures due to a lack of bonding between the specimen and the parallel plates. The occurrence of this slippage may be eliminated by heating the specimen in place for at least 30 minutes at a temperature of 45°C to allow the specimen to adhere to the plates. The second method of specimen preparation eliminates the possibility of slippage, as the liquid binder is poured directly on the testing plate and trimmed to specification after the plate is in place. However, this method introduces errors through the trimming process. As noted in equations 3.1 and 3.2, the measured moduli are inversely proportional to the radius of the specimen taken to the

fourth power. Thus, deviations in the diameter of the specimen can lead to significant errors in measurements of the moduli.

Another factor that may affect repeatability is the compliance error. This is a result of transferring angular deflection generated by the equipment motor into the force transducer instead of into the specimen. This tends to occur at extremely low temperatures when the binder stiffness is relatively high as compared to the system stiffness. As no tests were performed below 5°C, it was not expected that compliance errors would be a source of variability.

The effects of steric hardening were a concern of this study. The storage of binders, particularly polymer modified binders, at ambient temperatures for extended periods of time may lead to the formation of molecular associations causing new structures within the binder. The formations of molecular associations within the binder causes an increase in the complex modulus over time; however, the associations may be reversed and the asphalt returned to the initial structure by heating to temperatures of 160 to 170°C. To reduce the effects of steric hardening, the containers of binder were placed in an oven and heated to a temperature of 163°C for at least 15 min. The samples were rigorously stirred prior to fabricating the specimens. Additionally, the samples were cooled immediately in a freezer when not tested immediately after fabrication to prevent steric hardening from affecting test results.

Another factor that may affect repeatability is testing procedure. Uniform guidelines were developed and followed for every aspect of specimen fabrication, insertion into the parallel plates and trimming, sequencing of frequency sweeps, and other elements of the testing procedures.

A final factor affecting repeatability of measurements was the calibration of the rheometer. As the calibration may change over time, the rheometer was periodically checked on a monthly basis by testing polybutene, a viscosity standard produced by the Cannon Company. Polybutene is commonly used as a certified viscosity standard to check calibration of capillary viscometers at 60°C, but may also be used in checking the calibration of dynamic shear rheometers. At 60°C, the dynamic viscosity of polybutene is highly independent of frequency and approaches steady state viscosity. The monthly checks of the rheometer calibration were performed by comparing the rheometer-measured dynamic viscosity of the oil at 60°C with the Newtonian viscosity stated by the manufacturer.

# CHAPTER 4 DATA PRESENTATION AND ANALYSIS

Two sets of data were utilized in this study. The first was gathered during previous work conducted by Gahvari (1996) at Virginia Tech and consists of the original sample results. The second set was gathered after samples prepared by Gahvari were stored at ambient room temperature (23°C) for four years and are denoted as the stored sample results. Each set of data is comprised of duplicate results of dynamic mechanical testing of 20 binder-polymer samples. The principle of time-temperature superposition was applied to the data to generate mastercurves of the shear storage and loss moduli. The mastercurves for the original samples and stored samples are presented in Appendices A and C, respectively. The shift factors used in the generation of the mastercurves for the original and stored samples are presented in Appendices B and D, respectively. Examples of G' and G" isothermal curves and mastercurves and corresponding shift factors are given in Figures 4.1 and 4.2 for the original specimen AU00.

A statistical analysis was performed to determine if significant differences existed between independent replicates of each sample. A Studentized t-test with a level of significance of 0.05 was used to determine if significant differences were present. No significant differences were found between any two replicates.

The averages of the replicate measurements of the shear storage and loss moduli mastercurves for each sample were used to determine if significant differences were seen in the shear storage and loss moduli before and after storage. The graphical comparisons of the mastercurves for the original and stored samples are presented in Appendix E.

Four dynamic shear response prediction models were evaluated utilizing the data collected before and after storage. These models were introduced by Christensen and Anderson (1992), Gahvari (1996), Stastna *et al*. (1996), and Marasteanu and Anderson (1999).

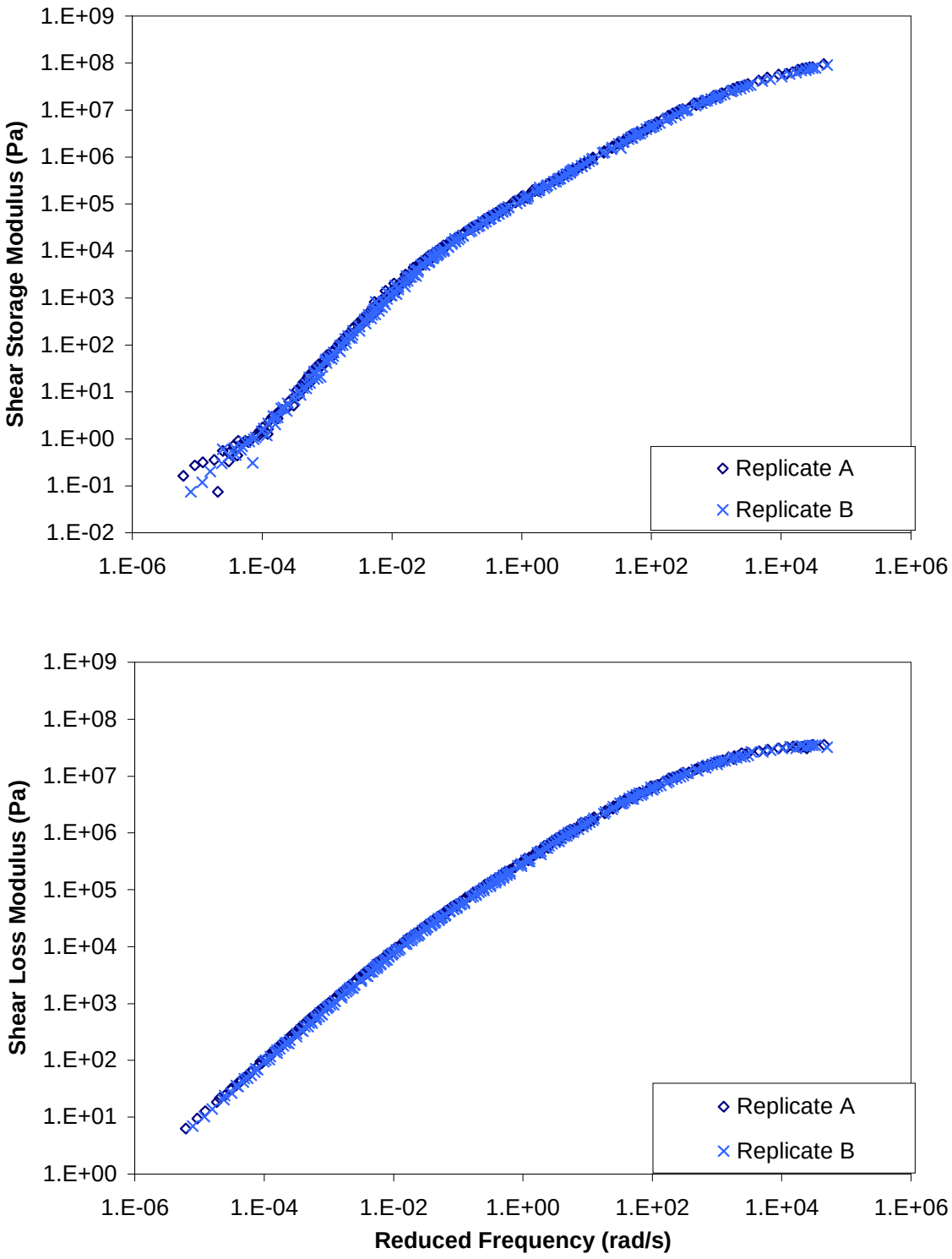


Figure 4.1 Example of G' and G" mastercurves for original specimen AUG3.

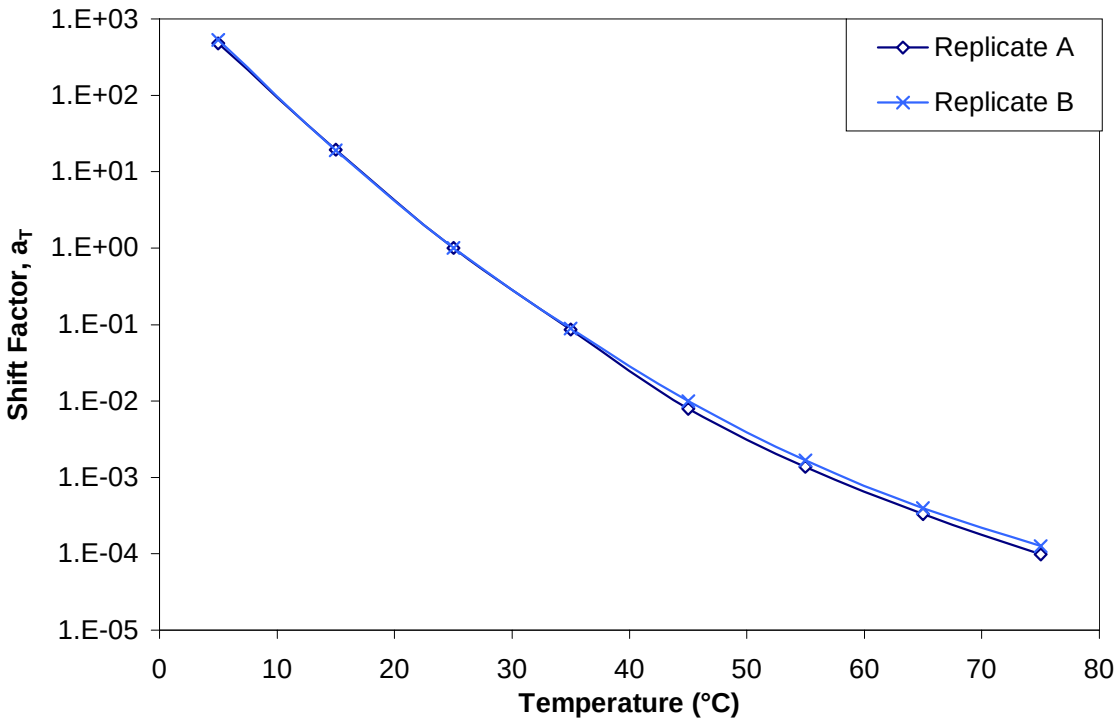


Figure 4.2 Shift factors for original specimen AUG3.

## 4.1 Effect of Storage

As can be seen from the graphs presented in Appendix E, the rheological behavior of modified binders after the four-year storage period did not follow a specific trend. However, for most specimens evaluated, the prominent changes in moduli due to storage were seen at low frequencies (corresponding to high temperatures). Increases in the moduli at low frequencies are indicative of increased viscosity. This is beneficial, as the binder tends to resist permanent deformations and this reduces the tendency to flow. Intermediate to high frequency responses were also affected, although generally to a lesser degree.

To better explain the trends seen in the polymer-modified binder shear moduli, it is important to understand the changes that shear moduli exhibit over the frequency sweep studied. Ferry (1980) reported that modulus versus frequency plots may have four zones. These are the terminal (or flow) zone, rubbery plateau, glassy transition, and glassy zone. Sperling (1992) reports the presence of five zones in modulus versus frequency plots. These include the four zones proposed by Ferry and the rubbery flow

zone, which occurs between the rubbery plateau and the flow zone. The five zones can be seen in Figure 4.3a for an amorphous polymer. Not all zones may be seen in the responses of unmodified or modified binders at the frequencies and temperatures utilized in this study. A mastercurve of G' for specimen AUS4, seen in Figure 4.3b, shows the regions noticed in this study: the rubbery flow and glassy transition regions of response. Although typically located between the rubbery flow and glassy transition regions, the plateau region was not observed in the binders tested.

The importance of changes in the zones is evident when examining the molecular behavior of a material in these areas. In the flow zone, molecular motion is in the form of reptation, or movement of chains. When discussing a binder, this movement controls the viscosity and enhances properties such as resistance to flow and ability of the binder to “heal” (Kim *et al*., 1990). As the temperature decreases, molecular motion causes the material to behave in a manner characterized by rubber elasticity and flow responses; this is identified as the rubber flow region. The rubber plateau region corresponds to “rubbery” response, which may be considered somewhat independent of frequency, as evidenced by the horizontal slope of the mastercurve over several decades of frequency seen in Figure 4.3a. In this region, molecular motion is considerably less, as the viscosity is greatly increased over that noted in the flow zone. This area has been attributed to the formation of a polymeric network within modified binders (Bouldin *et al*., 1991). However, at polymer contents below 7%, the polymer tends to be dispersed within the binder phase of the system (Brule, 1997) and thus an extensive network may not be formed. The glassy transition region occurs at higher frequencies as molecular motion begins to slow prior to the material entering the glassy zone. The glassy zone is seen at very high frequencies (low temperatures) and is due to the decrease in molecular motion as the material approaches its glass transition. A summary of the characteristics of each region is presented in Table 4.1.

As noted above, the most noticeable changes in moduli due to storage were noted at low frequencies as the binder was in the rubbery flow region. Figure 4.4 shows both G' and G" increasing at low frequencies for specimen AUG3. In general, binder modification was found to insignificantly change G' and G" of most binders in the glassy transition region. However, a significant improvement was noticed at low frequencies. Figure 4.5 is an example of the magnitude of change seen after storage in the rubbery flow and glassy transition regions of G' and G" when 5% of polymer S is added to the

a)

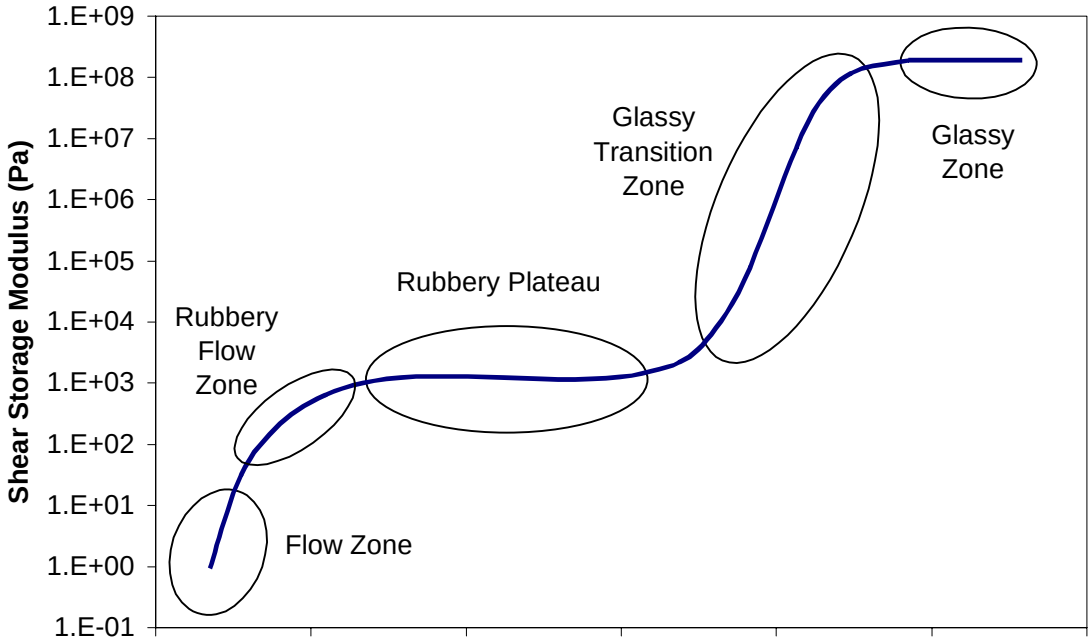


b)

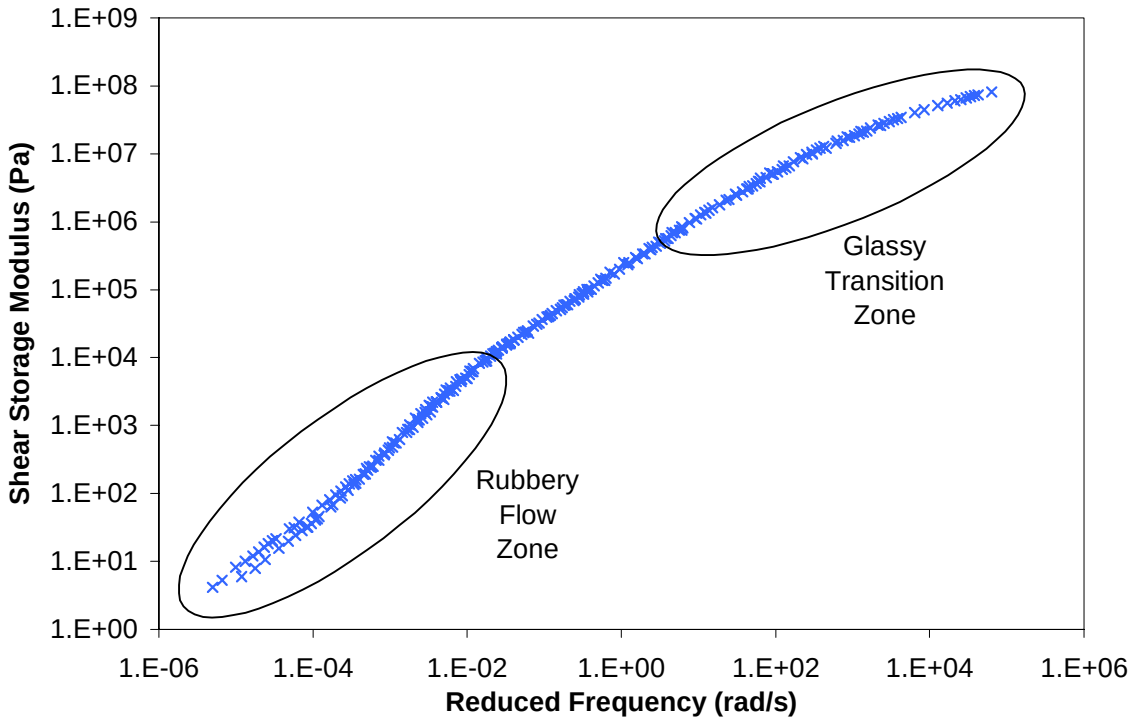


Figure 4.3 Examples of a) the five rheological zones seen in the response of an amorphous polymer (after Sperling, 1992); and b) the rheological zones seen in the shear mastercurve of a typical binder in this study, stored sample AUS4.

Table 4.1 Characteristics of the five rheological zones usually appearing in shear storage mastercurves.

| Zone | Characteristics |
|---|---|
| Flow | Molecular motion is in form of reptation. Modulus values change rapidly with changes in frequency. |
| Rubbery Flow | Material experiences both rubber elasticity and flow characteristics. Modulus values change less rapidly with frequency than in the flow zone. |
| Rubbery Plateau | Material behaves in a "rubbery" fashion. Molecular motion is in the forms of reptation and diffusion. Modulus values are somewhat independent of frequency, and become constant over as much as several decades of frequency. |
| Glassy Transtion | Molecular motion is slowed as material enters glassy zone. Modulus values change rapidly over a short temperature span. |
| Glassy | Material is glassy and often brittle. Molecular motion is restricted to vibrations and short-range rotational motions. Modulus values are relatively constant. |

base binder. Similar magnitudes of change are seen between the unmodified and modified binders prior to storage.

Comparisons were made between the mastercurves created from original test results and those created from results of testing after four years of storage for the unmodified binder and each of the three polymer types: SEBS linear block copolymer (Polymer G), $(SB)_n$ radial block copolymer (Polymer N), and SBS linear block copolymer (Polymer S). The results of testing before and after the storage period were compared for each polymer at each concentration and each aging state.

Comparisons between original and stored samples and the base binder are summarized in Tables 4.2 through 4.5. Each sample was evaluated over the regions presented in Figure 4.3b. It appears that the rubbery plateau region is absent in the obtained results. However, results between the rubbery flow zone and glassy transition are referred to as the "intermediate area". The ranges of frequency assumed to be covered by each zone is as follows: rubbery flow zone, $1.0 \times 10^{-6}$ to $1.5 \times 10^{-2}$ rad; intermediate area, $1.5 \times 10^{-2}$ to $2.5 \times 10$ rad; and glassy transition zone, $2.5 \times 10$ to $1.0 \times 10^{5}$ rad. These frequency ranges were based on the areas of the dynamic shear mastercurves where each behavior was observed. The comparisons consider the average value of the shear storage or loss moduli of the sample over the frequency

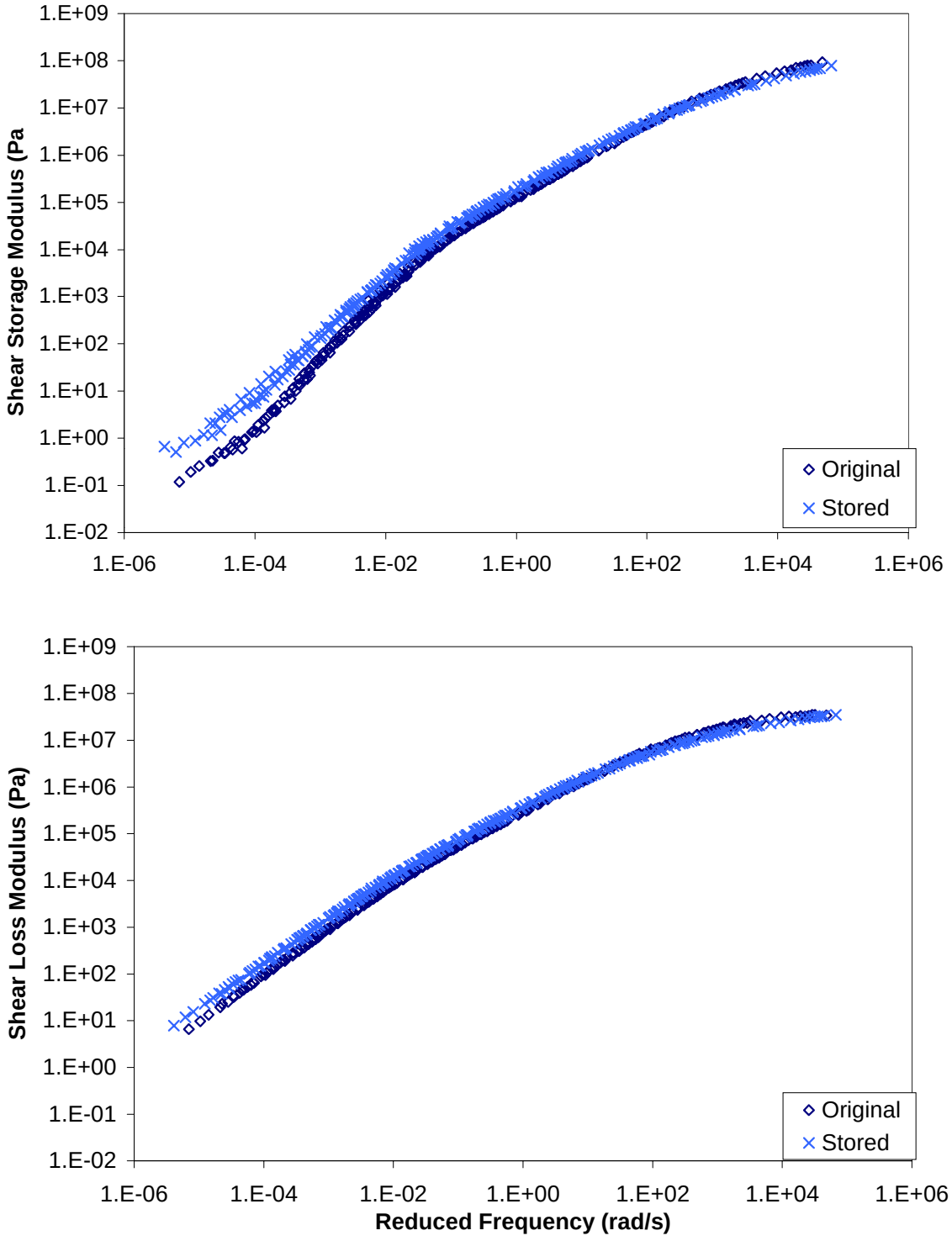


Figure 4.4 Mastercurves for specimen AUG3 showing an increase in the rubbery flow region of the storage and loss shear moduli after storage.

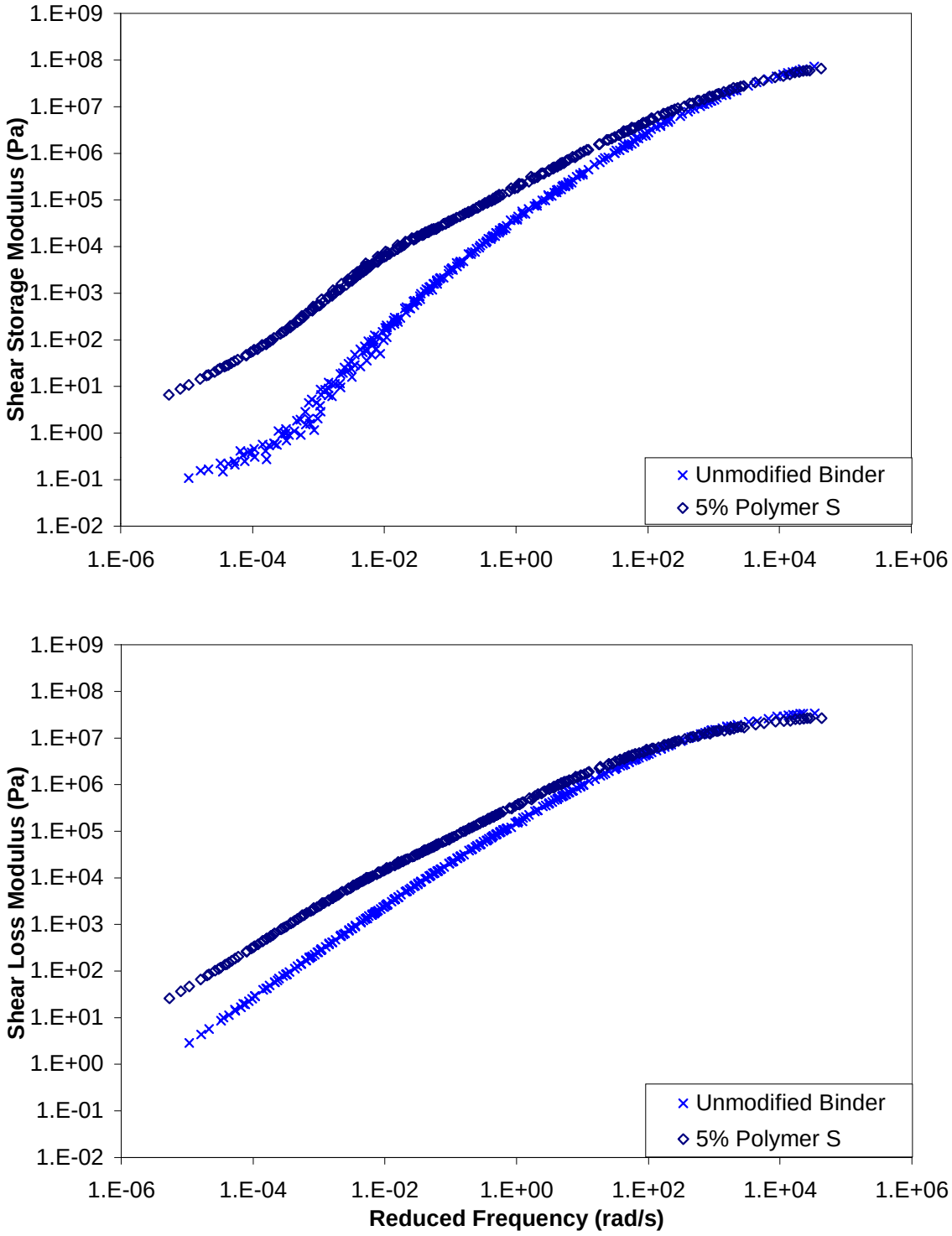


Figure 4.5a Mastercurves for specimens AU00 and AUS5 before storage showing the typical magnitude of change of the response in the rubbery flow and glassy transition regions due to modification.

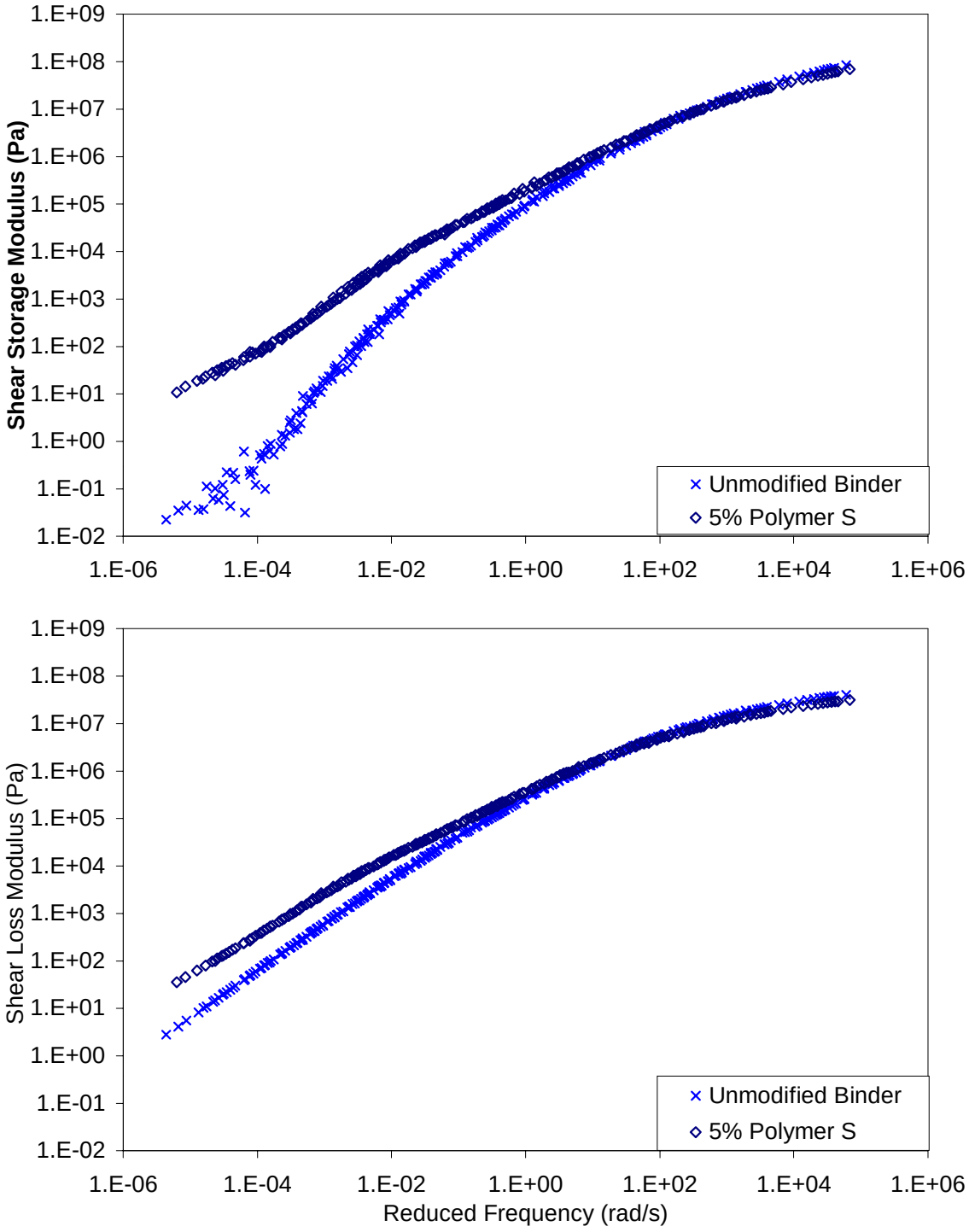


Figure 4.5b Mastercurves for specimens AU00 and AUS5 after storage showing the typical magnitude of change of the response in the rubbery flow and glassy transition regions due to modification.

Table 4.2 Results of shear storage and loss moduli compared to original unaged modified samples.

| | | G' | | G" | |
|---|---|---|---|---|---|
| Sample | zone | Original AU00 | Original AR00 | Original AU00 | Original AR00 |
| aug3 | rubbery flow | higher | lower | higher | lower |
| | intermediate area | higher | lower | higher | lower |
| | glassy transition | higher | lower | higher | lower |
| aug4 | rubbery flow | higher | higher | higher | higher |
| | intermediate area | higher | higher | higher | ~ equal |
| | glassy transition | higher | lower | ~ equal | lower |
| aug5 | rubbery flow | higher | higher | higher | higher |
| | intermediate area | higher | higher | higher | higher |
| | glassy transition | higher | ~ equal | higher | ~ equal |
| aun3 | rubbery flow | higher | higher | higher | ~ equal |
| | intermediate area | higher | lower | higher | lower |
| | glassy transition | higher | lower | ~ equal | lower |
| aun4 | rubbery flow | higher | higher | higher | higher |
| | intermediate area | higher | ~ equal | higher | ~ equal |
| | glassy transition | higher | lower | ~ equal | lower |
| aun5 | rubbery flow | higher | higher | higher | higher |
| | intermediate area | higher | higher | higher | higher |
| | glassy transition | higher | lower | ~ equal | lower |
| aus3 | rubbery flow | higher | higher | higher | ~ equal |
| | intermediate area | higher | lower | higher | higher |
| | glassy transition | higher | lower | ~ equal | higher |
| aus4 | rubbery flow | higher | higher | higher | higher |
| | intermediate area | higher | ~ equal | higher | lower |
| | glassy transition | higher | lower | ~ equal | lower |
| aus5 | rubbery flow | higher | higher | higher | higher |
| | intermediate area | higher | higher | higher | ~ equal |
| | glassy transition | higher | lower | ~ equal | lower |

interval. The original samples were compared only with the original base binders, AU00 and AR00. The stored samples were compared with the AU00 and AR00 base binder test results both before and after storage.

*Unmodified Specimens*

Results for the unmodified base binder indicated that after storage, specimen AU00 showed an increase in both G' and G" below the glassy transition region. In the glassy transition region, G' and G" were unchanged. As expected, no significant change occurred in the glassy region due to storage. This indicates that the response of the binder will not change at low temperatures after storage. The increase in G' and G" below this region, however, may be due to aging. The RTFO-aged unmodified binder, AR00, showed decreases in G' and G" after storage across the entire tested frequency

Table 4.3 Results of shear storage and loss moduli compared to original RTFO-aged modified samples.

| | | G' | | G" | |
|---|---|---|---|---|---|
| Sample | zone | Original AU00 | Original AR00 | Original AU00 | Original AR00 |
| arg3 | rubbery flow | higher | higher | higher | higher |
| | intermediate area | higher | higher | higher | higher |
| | glassy transition | higher | ~ equal | higher | ~ equal |
| arg4 | rubbery flow | higher | higher | higher | higher |
| | intermediate area | higher | higher | higher | higher |
| | glassy transition | higher | higher | higher | ~ equal |
| arg5 | rubbery flow | higher | higher | higher | higher |
| | intermediate area | higher | higher | higher | higher |
| | glassy transition | higher | ~ equal | higher | lower |
| arn3 | rubbery flow | higher | higher | higher | higher |
| | intermediate area | higher | higher | higher | higher |
| | glassy transition | higher | ~ equal | higher | ~ equal |
| arn4 | rubbery flow | higher | higher | higher | higher |
| | intermediate area | higher | higher | higher | higher |
| | glassy transition | higher | ~ equal | higher | ~ equal |
| arn5 | rubbery flow | higher | higher | higher | higher |
| | intermediate area | higher | higher | higher | higher |
| | glassy transition | higher | ~ equal | lower | ~ equal |
| ars3 | rubbery flow | higher | higher | higher | higher |
| | intermediate area | higher | higher | higher | higher |
| | glassy transition | higher | ~ equal | higher | ~ equal |
| ars4 | rubbery flow | higher | higher | higher | higher |
| | intermediate area | higher | higher | higher | higher |
| | glassy transition | higher | ~ equal | higher | ~ equal |
| ars5 | rubbery flow | higher | higher | higher | higher |
| | intermediate area | higher | higher | higher | higher |
| | glassy transition | higher | lower | ~ equal | lower |

range. This suggests that the effects of RTFO aging are reduced over time for unmodified binders and a "healing" may occur.

*Polymer G-Modified Specimens*

Binder modified with Polymer G showed different trends of behavior at different polymer contents when unaged. Specimen AUG3 exhibited a slight reduction in G' in the glassy transition region and an increase in the intermediate and rubbery flow regions. The loss shear modulus (G") was found to show similar behavior, with increases in value in the intermediate and rubbery flow regions. The areas showing the greatest increase in G' and G" lie within the rubbery flow zone. This is indicative of enhanced performance at low frequencies (corresponding to high temperatures) and reduction of the moduli at high frequencies, which may reduce the binder brittleness at low temperatures.

Table 4.4 Results of shear storage and loss moduli compared to stored unaged modified samples.

| | | G' | | | | G'' | | | |
|---|---|---|---|---|---|---|---|---|---|
| Sample | zone | Original AU00 | Original AR00 | Stored AU00 | Stored AR00 | Original AU00 | Original AR00 | Stored AU00 | Stored AR00 |
| aug3 | rubbery flow | higher | higher | higher | higher | higher | higher | higher | higher |
| | intermediate area | higher | ~ equal | higher | higher | higher | lower | higher | higher |
| | glassy transition | ~ equal | lower | ~ equal | ~ equal | higher | lower | ~ equal | ~ equal |
| aug4 | rubbery flow | higher | higher | higher | higher | higher | ~ equal | higher | higher |
| | intermediate area | higher | ~ equal | higher | higher | higher | lower | ~ equal | ~ equal |
| | glassy transition | lower | lower | lower | lower | lower | lower | lower | lower |
| aug5 | rubbery flow | higher | higher | higher | higher | higher | higher | higher | higher |
| | intermediate area | higher | higher | higher | higher | higher | lower | higher | higher |
| | glassy transition | lower | lower | lower | lower | lower | lower | lower | lower |
| aun3 | rubbery flow | higher | higher | higher | higher | higher | higher | higher | higher |
| | intermediate area | higher | ~ equal | higher | ~ equal | higher | lower | lower | ~ equal |
| | glassy transition | ~ equal | lower | ~ equal | lower | lower | lower | lower | lower |
| aun4 | rubbery flow | higher | higher | higher | higher | higher | higher | higher | higher |
| | intermediate area | higher | ~ equal | higher | higher | higher | lower | higher | ~ equal |
| | glassy transition | ~ equal | lower | lower | lower | ~ equal | lower | lower | lower |
| aun5 | rubbery flow | higher | higher | higher | higher | higher | higher | higher | higher |
| | intermediate area | higher | higher | higher | higher | higher | higher | higher | higher |
| | glassy transition | higher | lower | ~ equal | ~ equal | lower | lower | lower | lower |
| aus3 | rubbery flow | higher | higher | higher | higher | higher | higher | higher | higher |
| | intermediate area | higher | ~ equal | higher | ~ equal | higher | lower | higher | ~ equal |
| | glassy transition | ~ equal | lower | ~ equal | ~ equal | ~ equal | lower | lower | ~ equal |
| aus4 | rubbery flow | higher | higher | higher | higher | higher | higher | higher | higher |
| | intermediate area | higher | higher | higher | higher | higher | ~ equal | higher | higher |
| | glassy transition | higher | lower | higher | higher | ~ equal | lower | ~ equal | ~ equal |
| aus5 | rubbery flow | higher | higher | higher | higher | higher | higher | higher | higher |
| | intermediate area | higher | higher | higher | higher | higher | ~ equal | higher | higher |
| | glassy transition | higher | lower | ~ equal | ~ equal | lower | lower | lower | ~ equal |

Table 4.5 Results of shear storage and loss moduli compared to stored RTFO-aged modified samples.

| | | G' | | | | G" | | | |
|---|---|---|---|---|---|---|---|---|---|
| Sample | zone | Original AU00 | Original AR00 | Stored AU00 | Stored AR00 | Original AU00 | Original AR00 | Stored AU00 | Stored AR00 |
| arg3 | rubbery flow | higher | higher | higher | higher | higher | higher | higher | higher |
| | intermediate area | higher | higher | higher | higher | higher | higher | higher | higher |
| | glassy transition | higher | lower | higher | higher | ~ equal | lower | ~ equal | ~ equal |
| arg4 | rubbery flow | higher | higher | higher | higher | higher | higher | higher | higher |
| | intermediate area | higher | higher | higher | higher | higher | higher | higher | higher |
| | glassy transition | higher | lower | higher | higher | ~ equal | lower | ~ equal | ~ equal |
| arg5 | rubbery flow | higher | higher | higher | higher | higher | higher | higher | higher |
| | intermediate area | higher | higher | higher | higher | higher | higher | higher | higher |
| | glassy transition | higher | higher | higher | higher | higher | ~ equal | higher | higher |
| arn3 | rubbery flow | higher | higher | higher | higher | higher | higher | higher | higher |
| | intermediate area | higher | higher | higher | higher | higher | higher | higher | higher |
| | glassy transition | ~ equal | lower | ~ equal | ~ equal | lower | lower | lower | lower |
| arn4 | rubbery flow | higher | higher | higher | higher | higher | higher | higher | higher |
| | intermediate area | higher | higher | higher | higher | higher | higher | higher | higher |
| | glassy transition | higher | ~ equal | higher | higher | ~ equal | lower | ~ equal | ~ equal |
| arn5 | rubbery flow | higher | higher | higher | higher | higher | higher | higher | higher |
| | intermediate area | higher | higher | higher | higher | higher | higher | higher | higher |
| | glassy transition | higher | ~ equal | higher | higher | lower | lower | lower | lower |
| ars3 | rubbery flow | higher | higher | higher | higher | higher | higher | higher | higher |
| | intermediate area | higher | higher | higher | higher | higher | higher | higher | higher |
| | glassy transition | higher | lower | higher | higher | higher | lower | higher | higher |
| ars4 | rubbery flow | higher | higher | higher | higher | higher | higher | higher | higher |
| | intermediate area | higher | higher | higher | higher | higher | ~ equal | higher | higher |
| | glassy transition | ~ equal | lower | lower | lower | ~ equal | lower | ~ equal | higher |
| ars5 | rubbery flow | higher | higher | higher | higher | higher | higher | higher | higher |
| | intermediate area | higher | higher | higher | higher | higher | higher | higher | higher |
| | glassy transition | higher | lower | higher | higher | ~ equal | lower | ~ equal | ~ equal |

Specimens AUG4 and AUG5 both exhibited similar behavior at certain frequency ranges after storage. In both cases, G' decreased at intermediate to high frequencies above the rubbery flow region and increased within that region. However, the loss shear modulus (G") decreased across the entire range of frequencies of the mastercurve.

The real and imaginary parts of the complex modulus of Polymer G-modified specimens exposed to RTFO-aging showed similar trends. RTFO-aged specimens ARG3 and ARG4 exhibited a reduction in G' values above 1 rad/s and increased values below 1 rad/s.

The loss shear modulus (G") for the two samples showed a reduction above a frequency of approximately 1 rad/s and no change below that frequency. The effects seemed to be greater for both G' and G" as the polymer content increased to 4%. Specimen ARG5 showed a different response, however. Both G' and G" tended to increase across the frequency range. The increase appeared greater at frequencies below 100 rad/s, however. In general, the response of ARG3 and ARG4 was more favorable at both low and high frequencies than ARG5, which shows an improvement at low frequencies only. RTFO-aged specimens showed more consistent performance trends compared to the unaged specimens. The trends appeared to correlate with the increase in polymer additive in a predictable manner.

*Polymer N-Modified Specimens*

Evaluation of unaged specimens modified with polymer N showed similar trends in G' and G" behavior for different polymer concentrations. Specimen AUN3 showed a decrease in G' in the intermediate and glassy transition regions and an increase below thoseregions. The loss shear modulus (G") exhibited a similar trend. Specimen AUN4 exhibited a decrease in G' values at test frequencies above the rubbery flow region and showed a very slight increase in that region. The loss shear moduli (G") exhibited a slight decrease over the entire frequency range tested. Specimen AUN5 exhibited a constant decrease across all frequencies for G' and G". The increase in G' and G" at lower test frequencies in the rubbery flow region is indicative of improved high temperature performance. The decrease in G' and G" at high frequencies in the glassy transition region denotes better performance at low temperatures (considering low temperature cracking).

It appeared that polymer modification, in this case, was desired. Results for this polymer after four years of storage are in agreement with the explanation given by Brule (1997). Brule reports that at polymer contents below 4%, the polymer is dispersed in the binder and enhances both high and low temperature properties of the system. However, at contents around 5%, the mixture may form microstructures consisting of two phases that may cause instability in the response, which may be detrimental to performance.

RTFO-aged specimens modified with polymer N were assessed for changes in G' and G" due to storage. The storage and loss shear moduli (G' and G") for specimens ARN3, ARN4, and ARN5 showed interesting trends with increasing polymer content. All specimens showed a decrease in G' at high frequencies in the glassy transition region; however, the reduction magnitude became less with increasing polymer content. At intermediate frequencies, G' was unchanged for specimen ARN3 and began to increase with increasing polymer content. The response at low frequencies, in the rubbery flow region, was greater than the response prior to storage, but the difference became less with increasing polymer content. The overall trend generally indicated that G' was less affected by storage as the polymer content increased. The loss shear moduli (G") showed a trend covering the entire frequency range. Specimen ARN3 showed a slightly lowered G" after storage. Specimens ARN4 and ARN5 showed an increase in G" after storage that increased with higher polymer content. Such a change in G' and G" is considered favorable for binder performance.

*Polymer S-Modified Specimens*

Unaged specimens modified with polymer S were found to have no trends across the three polymer contents. Specimens AUS3 and AUS4 exhibited slight changes in G' and G" at high frequencies in the glassy transition region. However, both specimens showed an increase that became greater with increasing polymer content in G' and G" at intermediate to low frequencies. The increases in both G' and G" indicate enhanced elasticity at intermediate to high temperatures and therefore enhanced performance. Specimen AUS5 showed no change in G' above the rubbery flow region and only a slight increase at frequencies within the rubbery flow region. No change was seen in G" across the range of test frequencies. In addition, no significant change was observed across polymer contents for either the storage or loss shear moduli for RTFO-aged specimens modified with polymer S after four years of storage.

## 4.2 Model Evaluations

Four models were evaluated to determine their predictive abilities for binders before and after RTFO-aging and before and after storage for base binder and polymer-modified binders. The models evaluated included those proposed by Christensen and Anderson (1992), Gahvari (1996), Stastna *et al*. (1996), and Marasteanu and Anderson (1999). The models were validated using the mean square error of prediction (MSEP). This method evaluates the bias and variance of the prediction and yields a single measure of model predictive capability (Rawlings, 1988). The MSEP is defined as the average squared difference between an actual data point and the predicted data point from a given model and its equation can be written as follows:

$$MSEP = \frac{\sum (y_i - \hat{y}_i)^2}{n} \qquad (4.1)$$

where

$y_i$ = actual data point;

$\hat{y}_i$ = predicted data point; and

n = number of data points in the analysis.

The analysis of MSEP method was used on the log transformed actual and predicted data points to determine the ability of each model to predict the behavior of the tested specimens. The log transformed points were used to allow for a consistent comparison between all models. Model constants were determined from the first replicate of each sample, with the second replicate considered as an independent validation data set. For each sample, using the model developed from the first replicate, the moduli and/or phase angle data were predicted for each frequency in the second replica. The differences between the predicted and actual values for the second replica were calculated, and the average of the square differences yielded the MSEP for the model.

### *4.2.1 Christensen-Anderson Model*

The Christensen-Anderson model was derived based on a logistic distribution function used to describe the relaxation spectra of binders. The model has been tested with unmodified and modified binders and was found to show good approximation of rheological behavior (Marasteanu and Anderson, 1999) with the exception of extreme

values of the modulus. The complex modulus and phase angle are described as follows (Christensen and Anderson, 1992):

$$\left|G^*(\omega)\right| = G_g\left[1+\left(\frac{\omega_c}{\omega}\right)^{\frac{\log 2}{R}}\right]^{-\frac{R}{\log 2}} \tag{4.2}$$

$$\delta(\omega) = \frac{90}{1+\left(\frac{\omega}{\omega_c}\right)^{\frac{\log 2}{R}}} \tag{4.3}$$

The definitions of the parameters are presented in Chapter 2.

Two methods have been proposed to determine the characteristic parameters of the model. These include a graphical method and nonlinear regression.

Graphical methods of determining the glassy modulus ($G_g$), crossover frequency ($\omega_c$), and rheological index (R) were reported by Anderson *et al*. (1994) and were utilized to determine the characteristic parameters for each sample. Appendices F and G present the graphs used to estimate the characteristic parameters of the original and stored binder samples, respectively.

The glassy modulus may be estimated by plotting the measured complex modulus as a function of the phase angle for phase angles less than 10°. As the measured data in this study did not extend to this phase angle, the glassy modulus was assumed to be 1 GPa for all samples. This value is reported in the literature (Anderson *et al*., 1994) as an appropriate estimate.

The crossover frequency may be estimated by plotting the log of the reduced frequency versus the log of the tangent of the phase angle (log tan $\delta$). The crossover frequency occurs at a phase angle of 45°, when the value of log tan $\delta$ is zero. It was observed that the plot was nearly linear for values of tan $\delta$ between 0.5 and 2; therefore, a linear trendline was used to assist in the determination of the crossover frequency. Figure 4.6 is an example of the graph used to find the crossover frequency for stored specimen AUG3.

The rheological index may be estimated by plotting log (log G*) versus log tan $\delta$, similarly to the procedure for determining the crossover frequency. The value of the log

of the crossover modulus, log G*($\omega_c$), is found by taking the antilog of the value of log (log G*) found at a phase angle of 45° (when log tan $\delta$ is equivalent to zero). The rheological index is the difference between the log of the glassy modulus (in this study assumed to be 9.0) and the log of the crossover modulus. When determining the value of log (log G*), it was seen that the plot of log (log G*) versus log tan $\delta$ behaved as a second order function for values of tan $\delta$ between 0.5 and 2; therefore a parabolic trendline was fitted to the data to assist in the estimation of log (log G*($\omega_c$)). Figure 4.7 is an example of the graph used in the determination of the rheological index for stored specimen AUG3.

Following the graphical determination of the model parameters for each sample, the model was compared with the data collected from the second sample replicate. The model parameters are reported in Tables 4.6 and 4.7 for the original and stored binders, respectively. The MSEP results for the model are reported in Table 4.8 for all specimens.

Additionally, the values and prediction errors of the characteristic parameters were calculated by applying nonlinear least-squares regression to the data utilizing SAS, a statistical analysis program. An example of the input used to generate the model parameters and resulting output is given in Appendix H for the original specimen AUG3. Tables 4.9 and 4.10 summarize the results of the nonlinear least square analysis for the original and stored specimens, respectively.

As with the graphical determination of parameters, the regression analysis was performed to determine the model parameters using the first sample replicate values. Following this, the predicted results from the model using these parameters were compared with the data obtained from the second sample replicate. The MSEP results were calculated for the regressed model and are summarized for all samples in Table 4.11. The MSEP results for both the regressed model and the graphically determined model are quite good. The MSEP values for the graphically determined model are lower than those of the regressed model, and thus indicate better binder behavior predictions than does the regressed model. Although found using a subjective method, the graphically determined model is more representative of physical trends seen in the binder response.

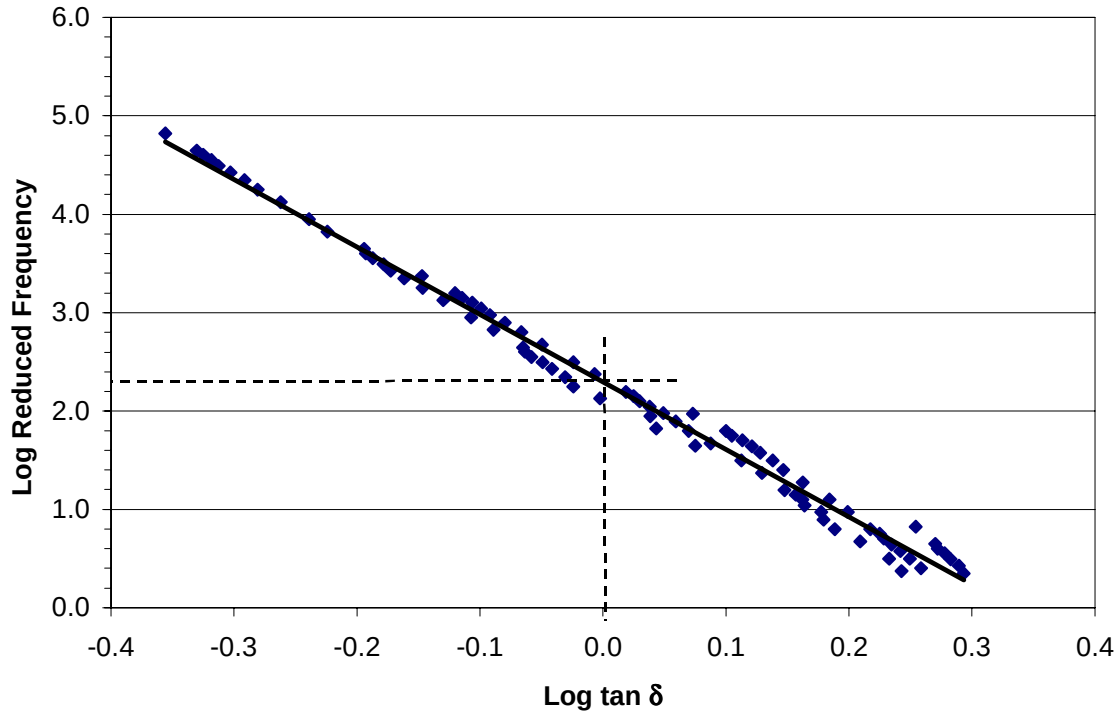


Figure 4.6 Example of method used to graphically interpret crossover frequency for stored specimen AUG3.

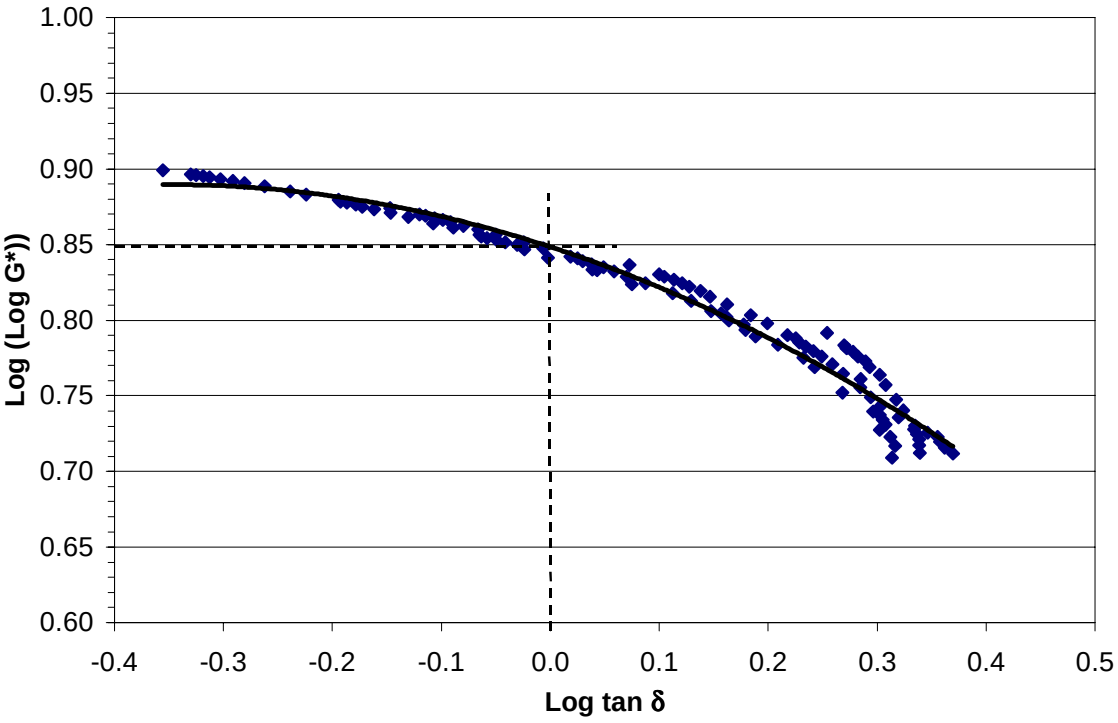


Figure 4.7 Example of method used to graphically determine rheological index for stored specimen AUG3.

Table 4.6 Christensen-Anderson model parameters determined graphically for original specimens.

| Sample | $\omega_c$, rad/s | Log ($G^*(\omega_c)$) | R |
|---|---|---|---|
| AU00 | 1584.89 | 7.34514 | 1.65486 |
| AR00 | 251.19 | 7.21107 | 1.78893 |
| AUG3 | 446.68 | 7.2778 | 1.7222 |
| AUG4 | 223.87 | 7.11214 | 1.88786 |
| AUG5 | 158.49 | 7.01455 | 1.98545 |
| ARG3 | 123.03 | 7.14496 | 1.85504 |
| ARG4 | 79.43 | 7.04693 | 1.95307 |
| ARG5 | 50.12 | 6.91035 | 2.08965 |
| AUN3 | 478.63 | 7.19449 | 1.80551 |
| AUN4 | 281.84 | 7.09578 | 1.90422 |
| AUN5 | 131.83 | 6.98232 | 2.01768 |
| ARN3 | 154.88 | 7.07946 | 1.92054 |
| ARN4 | 60.26 | 6.96627 | 2.03373 |
| ARN5 | 89.13 | 6.99842 | 2.00158 |
| AUS3 | 426.53 | 7.17794 | 1.82206 |
| AUS4 | 338.84 | 7.16143 | 1.83857 |
| AUS5 | 199.53 | 7.01455 | 1.98545 |
| ARS3 | 120.23 | 6.98232 | 2.01768 |
| ARS4 | 109.65 | 6.99842 | 2.00158 |
| ARS5 | 79.43 | 6.95024 | 2.04976 |

Comparison of the graphically determined and regressed parameter values indicated several differences in results between the methods of determining the parameters. Rheological index and crossover frequency values were found to be higher when graphically determined as compared to the regression method. It was observed that the values of the crossover frequency tend to follow two trends regardless of the method of determination: values found for stored specimens were approximately half of those found for original specimens, and increasing polymer contents tended to have decreasing crossover frequencies. During the regression analysis, the glassy modulus was evaluated from the presented equation, and was found to be considerably lower than the value recommended for use when data was not experimentally available. The regressed values averaged $2.81 \times 10^8$ and $3.40 \times 10^8$ for the original and stored samples, respectively. It is believed that this may have affected the accuracy of the regression results. Additionally, the model has been found to have errors at high values of G' (Marasteanu and Anderson, 1999).

Table 4.7 Christensen-Anderson model parameters determined graphically for stored specimens.

| Sample | $\omega_c$, rad/s | Log ($G^*(\omega_c)$) | R |
|---|---|---|---|
| AU00 | 602.56 | 7.0795 | 1.92054 |
| AR00 | 354.81 | 6.9984 | 2.00158 |
| AUG3 | 199.53 | 6.9502 | 2.04976 |
| AUG4 | 131.83 | 6.6834 | 2.31656 |
| AUG5 | 52.48 | 6.63743 | 2.36257 |
| ARG3 | 77.62 | 6.92628 | 2.07372 |
| ARG4 | 35.48 | 6.65273 | 2.34727 |
| ARG5 | 25.7 | 6.8897 | 2.1103 |
| AUN3 | 158.49 | 6.91831 | 2.08169 |
| AUN4 | 141.25 | 6.69885 | 2.30115 |
| AUN5 | 52.48 | 6.60693 | 2.39307 |
| ARN3 | 66.07 | 6.91831 | 2.08169 |
| ARN4 | 26.3 | 6.79986 | 2.20014 |
| ARN5 | 25.12 | 6.82339 | 2.17661 |
| AUS3 | 251.19 | 7.01455 | 1.98545 |
| AUS4 | 177.83 | 6.98232 | 2.01768 |
| AUS5 | 223.87 | 6.95024 | 2.04976 |
| ARS3 | 89.13 | 6.45654 | 2.54346 |
| ARS4 | 56.23 | 6.87068 | 2.12932 |
| ARS5 | 31.62 | 6.76862 | 2.23138 |

### *4.2.2 Stastna-Zanzotto-Kennpohl Model*

The model proposed by Stastna *et al*. (1996) is reported to be well suited for the characterization of unmodified and modified binders. The expressions for the phase angle and complex modulus are as follows (Stastna *et al*., 1996):

$$\left| G^*(\omega) \right| = i\eta_0\ \omega \left\{ \frac{\prod_1^m [1+(\omega\mu_k)^2]}{\prod_1^n [1+(\omega\lambda_k)^2]} \right\}^{1/2(n-m)} \tag{4.4}$$

$$\delta(\omega) = \frac{\pi}{2} + \frac{1}{n-m}\left[ \sum_1^m a\tan(\mu_k\omega) - \sum_1^n a\tan(\lambda_k\omega) \right] \tag{4.5}$$

The definitions of the parameters were discussed in Chapter 2.

Table 4.8 MSEP values for the Christensen-Anderson model using graphical determination of parameters.

| Sample | Original Specimens | | Stored Specimens | |
|---|---|---|---|---|
| | G* | δ | G* | δ |
| AU00 | 0.1366 | 0.0010 | 0.0207 | 0.0013 |
| AR00 | 0.0282 | 0.0013 | 0.0136 | 0.0014 |
| AUG3 | 0.0169 | 0.0007 | 0.0071 | 0.0008 |
| AUG4 | 0.0024 | 0.0009 | 0.0120 | 0.0016 |
| AUG5 | 0.0355 | 0.0015 | 0.0187 | 0.0009 |
| ARG3 | 0.0085 | 0.0009 | 0.0131 | 0.0006 |
| ARG4 | 0.0029 | 0.0009 | 0.0316 | 0.0004 |
| ARG5 | 0.0203 | 0.0014 | 0.0782 | 0.0244 |
| AUN3 | 0.0015 | 0.0005 | 0.0070 | 0.0007 |
| AUN4 | 0.0167 | 0.0014 | 0.0562 | 0.0015 |
| AUN5 | 0.0326 | 0.0029 | 0.0641 | 0.0064 |
| ARN3 | 0.0024 | 0.0010 | 0.0098 | 0.0006 |
| ARN4 | 0.0019 | 0.0011 | 0.0110 | 0.0005 |
| ARN5 | 0.0649 | 0.0028 | 0.0171 | 0.0009 |
| AUS3 | 0.0026 | 0.0006 | 0.0090 | 0.0005 |
| AUS4 | 0.0022 | 0.0007 | 0.0030 | 0.0008 |
| AUS5 | 0.0035 | 0.0010 | 0.0322 | 0.0012 |
| ARS3 | 0.0135 | 0.0010 | 0.1850 | 0.0017 |
| ARS4 | 0.0075 | 0.0009 | 0.1697 | 0.0011 |
| ARS5 | 0.0134 | 0.0011 | 0.0013 | 0.0005 |

This model was deemed not feasible for evaluation due to its impracticality and the great number of parameters that were not readily ascertainable. It is the opinion of the author that the number of parameters necessary for characterization cause the model to be impractical for applications beyond research.

### *4.2.3 Gahvari Model*

The model introduced by Gahvari (1996) was developed for use with modified binders when he concluded that existing models were not accurate in their predictions of binder response. The shear storage and loss moduli equations are as follows (Gahvari, 1996):

$$\log G'(\omega) = \log G_g\left[1 - \exp(-p(\log \omega + l))\right] \tag{4.6}$$

$$\log G''(\omega) = (\log G''_{max} + d) - \sqrt{(\log \omega - \log \omega_d)^2 + d^2} \tag{4.7}$$

Table 4.9 Christensen-Anderson model parameters determined using nonlinear least squares regression for original specimens.

| Sample | $\omega_c$ | s ($\omega_c$) | R | s (R) | $G_g$ | s (Gg) | $R^2$ | RMSE | DoF |
|---|---|---|---|---|---|---|---|---|---|
| AU00 | 1115.5 | 23.9981 | 1.1 | 0.0169 | 2.80E+08 | 8.38E+06 | 0.9997 | 2.19E+05 | 255 |
| AR00 | 254.0 | 7.9806 | 1.2 | 0.0149 | 2.69E+08 | 5.69E+06 | 0.9997 | 2.82E+05 | 263 |
| AUG3 | 509.8 | 20.4468 | 1.2 | 0.2170 | 2.92E+08 | 9.59E+06 | 0.9995 | 3.88E+05 | 263 |
| AUG4 | 232.9 | 8.3153 | 1.3 | 0.0169 | 2.46E+08 | 5.86E+06 | 0.9997 | 2.47E+05 | 263 |
| AUG5 | 193.4 | 7.7662 | 1.3 | 0.0170 | 2.50E+08 | 5.62E+06 | 0.9997 | 3.08E+05 | 263 |
| ARG3 | 145.8 | 8.2234 | 1.3 | 0.0237 | 2.92E+08 | 9.13E+06 | 0.9994 | 4.97E+05 | 263 |
| ARG4 | 97.9 | 6.2363 | 1.3 | 0.0242 | 2.45E+08 | 7.32E+06 | 0.9993 | 5.04E+05 | 263 |
| ARG5 | 81.7 | 5.3744 | 1.4 | 0.0233 | 2.63E+08 | 7.18E+06 | 0.9994 | 4.70E+05 | 263 |
| AUN3 | 460.2 | 13.2464 | 1.3 | 0.0165 | 2.81E+08 | 7.25E+06 | 0.9998 | 2.04E+05 | 255 |
| AUN4 | 229.0 | 10.3170 | 1.4 | 0.0223 | 2.90E+08 | 9.39E+06 | 0.9997 | 2.57E+05 | 255 |
| AUN5 | 99.0 | 4.9480 | 1.5 | 0.2150 | 2.70E+08 | 7.76E+06 | 0.9997 | 2.40E+05 | 255 |
| ARN3 | 104.1 | 5.2899 | 1.5 | 0.0213 | 3.15E+08 | 8.82E+06 | 0.9997 | 3.01E+05 | 255 |
| ARN4 | 59.3 | 4.4010 | 1.6 | 0.3000 | 3.17E+08 | 1.20E+07 | 0.9995 | 3.65E+05 | 255 |
| ARN5 | 34.4 | 3.1530 | 1.7 | 0.3400 | 3.28E+08 | 1.38E+07 | 0.9993 | 4.39E+05 | 255 |
| AUS3 | 391.6 | 15.5465 | 1.3 | 0.0208 | 2.84E+08 | 8.81E+06 | 0.9996 | 2.68E+05 | 263 |
| AUS4 | 328.4 | 10.4691 | 1.3 | 0.0173 | 3.09E+08 | 8.12E+06 | 0.9998 | 2.12E+05 | 263 |
| AUS5 | 210.6 | 9.7560 | 1.3 | 0.2140 | 2.23E+08 | 6.68E+06 | 0.9996 | 2.55E+05 | 263 |
| ARS3 | 95.7 | 5.6300 | 1.5 | 0.0250 | 3.20E+08 | 1.05E+07 | 0.9995 | 3.57E+05 | 263 |
| ARS4 | 87.0 | 4.6367 | 1.5 | 0.2230 | 3.12E+08 | 9.13E+06 | 0.9997 | 2.88E+05 | 263 |
| ARS5 | 75.1 | 5.5389 | 1.4 | 0.2770 | 2.39E+08 | 8.10E+06 | 0.9993 | 4.08E+05 | 263 |

Table 4.10 Christensen-Anderson model parameters determined using nonlinear least squares regression for stored specimens.

| Sample | $\omega_c$ | s ($\omega_c$) | R | s (R) | $G_g$ | s (Gg) | $R^2$ | RMSE | DoF |
|---|---|---|---|---|---|---|---|---|---|
| AU00 | 431.5 | 9.2819 | 1.5 | 0.0123 | 4.10E+08 | 7.78E+06 | 0.9999 | 1.18E+05 | 263 |
| AR00 | 161.8 | 9.4960 | 1.7 | 0.0280 | 4.57E+08 | 1.83E+07 | 0.9997 | 2.59E+05 | 263 |
| AUG3 | 148.1 | 4.1028 | 1.6 | 0.0128 | 3.79E+08 | 6.79E+06 | 0.9999 | 1.27E+05 | 263 |
| AUG4 | 100.8 | 1.3526 | 1.6 | 0.0057 | 1.88E+08 | 1.44E+06 | 0.9999 | 3.16E+04 | 263 |
| AUG5 | 45.8 | 0.8231 | 1.7 | 0.0068 | 1.75E+08 | 1.49E+06 | 0.9999 | 4.41E+04 | 263 |
| ARG3 | 52.0 | 1.1837 | 1.7 | 0.0089 | 3.89E+08 | 4.38E+06 | 0.9999 | 1.01E+05 | 263 |
| ARG4 | 23.8 | 1.1147 | 1.7 | 0.0159 | 1.92E+08 | 3.46E+06 | 0.9998 | 1.31E+05 | 263 |
| ARG5 | 23.7 | 0.7868 | 1.7 | 0.0114 | 3.75E+08 | 4.88E+06 | 0.9999 | 1.79E+05 | 263 |
| AUN3 | 138.7 | 2.4212 | 1.6 | 0.0097 | 3.04E+08 | 4.50E+06 | 0.9999 | 6.02E+04 | 262 |
| AUN4 | 95.8 | 5.3291 | 1.7 | 0.0257 | 2.00E+08 | 7.19E+06 | 0.9997 | 1.17E+05 | 262 |
| AUN5 | 40.5 | 0.9553 | 1.7 | 0.0095 | 1.96E+08 | 2.37E+06 | 0.9999 | 5.25E+04 | 262 |
| ARN3 | 45.4 | 0.9376 | 1.8 | 0.0079 | 4.02E+08 | 3.99E+06 | 0.9999 | 9.20E+04 | 263 |
| ARN4 | 18.4 | 0.3581 | 1.9 | 0.0070 | 3.68E+08 | 3.06E+06 | 0.9999 | 1.17E+05 | 263 |
| ARN5 | 16.1 | 0.9780 | 1.9 | 0.0220 | 4.19E+08 | 1.07E+07 | 0.9998 | 2.30E+05 | 263 |
| AUS3 | 194.0 | 2.1394 | 1.6 | 0.0056 | 3.74E+08 | 3.11E+06 | 0.9999 | 5.03E+04 | 263 |
| AUS4 | 135.7 | 1.6163 | 1.6 | 0.0055 | 3.88E+08 | 2.99E+06 | 0.9999 | 5.54E+04 | 263 |
| AUS5 | 137.0 | 5.5960 | 1.7 | 0.0190 | 3.98E+08 | 1.05E+07 | 0.9999 | 1.58E+05 | 262 |
| ARS3 | 51.3 | 2.2550 | 1.8 | 0.0174 | 4.26E+08 | 9.45E+06 | 0.9999 | 6.21E+04 | 263 |
| ARS4 | 30.9 | 1.8124 | 1.8 | 0.0212 | 3.76E+08 | 9.52E+06 | 0.9998 | 2.29E+05 | 263 |
| ARS5 | 29.2 | 0.8912 | 1.8 | 0.0112 | 3.74E+08 | 5.07E+06 | 0.9999 | 1.15E+05 | 263 |

Table 4.11 MSEP values for the Christensen-Anderson model using nonlinear least squares regression for determination of parameters.

| Sample | Original Specimens | | Stored Specimens | |
|---|---|---|---|---|
| | G* | δ | G* | δ |
| AU00 | 0.0040 | 0.0001 | 0.0088 | 0.0003 |
| AR00 | 0.0066 | 0.0003 | 0.0034 | 0.0009 |
| AUG3 | 0.0295 | 0.0008 | 0.0010 | 0.0004 |
| AUG4 | 0.0874 | 0.0015 | 0.0018 | 0.0003 |
| AUG5 | 0.1919 | 0.0039 | 0.0043 | 0.0004 |
| ARG3 | 0.0332 | 0.0011 | 0.0103 | 0.0005 |
| ARG4 | 0.0786 | 0.0022 | 0.0658 | 0.0080 |
| ARG5 | 0.1696 | 0.0035 | 0.1387 | 0.0021 |
| AUN3 | 0.0502 | 0.0010 | 0.0060 | 0.0004 |
| AUN4 | 0.0791 | 0.0028 | 0.1313 | 0.0022 |
| AUN5 | 0.0960 | 0.0045 | 0.3470 | 0.0076 |
| ARN3 | 0.0161 | 0.0009 | 0.0834 | 0.0003 |
| ARN4 | 0.0306 | 0.0013 | 0.0016 | 0.0027 |
| ARN5 | 0.0496 | 0.0021 | 0.0231 | 0.0057 |
| AUS3 | 0.0321 | 0.0008 | 0.0010 | 0.0003 |
| AUS4 | 0.0375 | 0.0017 | 0.0120 | 0.0012 |
| AUS5 | 0.0878 | 0.0031 | 0.0355 | 0.0016 |
| ARS3 | 0.0286 | 0.0007 | 0.0037 | 0.0003 |
| ARS4 | 0.0319 | 0.0011 | 0.1844 | 0.0011 |
| ARS5 | 0.0835 | 0.0034 | 0.0080 | 0.0009 |

The parameters for the equations include proportionality factor, p, a location parameter, l, a distance parameter, d, and a mastercurve radius location parameter, $\omega_d$. These parameters are described fully in Chapter 2. The values and prediction errors for the parameters were determined by a nonlinear least squares regression method utilizing SAS. An example of the input used to generate the model parameters and resulting output is given in Appendix I for original specimen AUG3. Tables 4.12 and 4.13 summarize the values and errors found for the parameters using nonlinear least squares analysis for the original and stored samples, respectively.

It is of interest to note that the regressed values for the glassy modulus found from the shear storage equation are much closer to the values suggested by Anderson et al. (1991) than those found from regression utilizing the Christensen-Anderson model. This suggests that the Gahvari model is optimized for regression of all parameters and does not require the assumption of any values. In examining the parameters found from

Table 4.12a. Estimated parameters for original specimens for shear storage modulus using model proposed by Gahvari.

| Original Samples | P | s(P) | L | s(L) | Log $G_g$ | s (Log $G_g$) |
|---|---|---|---|---|---|---|
| AU00 | 0.1198 | 0.0040 | 3.5078 | 0.0149 | 13.1851 | 0.3039 |
| AR00 | 0.1558 | 0.0023 | 4.1425 | 0.0097 | 10.9948 | 0.0941 |
| AUG3 | 0.1675 | 0.0020 | 4.1003 | 0.0082 | 10.4187 | 0.0694 |
| AUG4 | 0.1512 | 0.0021 | 4.7749 | 0.0121 | 10.4778 | 0.0778 |
| AUG5 | 0.1531 | 0.0027 | 5.1748 | 0.0194 | 10.1994 | 0.0907 |
| ARG3 | 0.1345 | 0.0021 | 6.1380 | 0.0200 | 10.3126 | 0.0798 |
| ARG4 | 0.1752 | 0.0016 | 4.9701 | 0.0093 | 9.8415 | 0.0443 |
| ARG5 | 0.1549 | 0.0017 | 5.8250 | 0.0143 | 9.8936 | 0.0509 |
| AUN3 | 0.1254 | 0.0019 | 4.6621 | 0.0119 | 11.5827 | 0.1058 |
| AUN4 | 0.0812 | 0.0018 | 5.6973 | 0.0195 | 14.2073 | 0.2027 |
| AUN5 | 0.0743 | 0.0024 | 6.3555 | 0.0332 | 14.4678 | 0.2996 |
| ARN3 | 0.1652 | 0.0029 | 4.9944 | 0.0174 | 9.9457 | 0.0884 |
| ARN4 | 0.1468 | 0.0025 | 5.4443 | 0.0189 | 10.2776 | 0.0861 |
| ARN5 | 0.1044 | 0.0016 | 6.3100 | 0.0186 | 11.8616 | 0.0978 |
| AUS3 | 0.1428 | 0.0018 | 4.4612 | 0.0098 | 10.9171 | 0.0776 |
| AUS4 | 0.1368 | 0.0019 | 4.7478 | 0.0117 | 11.0097 | 0.0863 |
| AUS5 | 0.1034 | 0.0020 | 5.5456 | 0.0189 | 12.2217 | 0.1378 |
| ARS3 | 0.1615 | 0.0016 | 4.9718 | 0.0100 | 10.1312 | 0.0524 |
| ARS4 | 0.1533 | 0.0021 | 5.2043 | 0.0146 | 10.1949 | 0.0568 |
| ARS5 | 0.1335 | 0.0022 | 5.6670 | 0.0198 | 10.6319 | 0.0895 |

Table 4.12b Estimated parameters for original specimens for loss shear modulus using model proposed by Gahvari.

| Original Samples | D | s (D) | Log $\omega_D$ | s (Log $\omega_D$) | Log $G_{max}$ | s (Log $G_{max}$) |
|---|---|---|---|---|---|---|
| AU00 | 2.4783 | 0.0303 | 4.0979 | 0.0276 | 7.4599 | 0.0106 |
| AR00 | 3.1934 | 0.0398 | 3.8919 | 0.0313 | 7.4583 | 0.0107 |
| AUG3 | 3.6195 | 0.0514 | 4.2569 | 0.0416 | 7.4806 | 0.0141 |
| AUG4 | 4.8083 | 0.0671 | 4.5261 | 0.0507 | 7.4325 | 0.0160 |
| AUG5 | 5.9333 | 0.0950 | 4.8920 | 0.0668 | 7.5029 | 0.0198 |
| ARG3 | 1.8890 | 0.1602 | 3.8379 | 0.1359 | 7.8151 | 0.0561 |
| ARG4 | 4.8674 | 0.0605 | 4.1615 | 0.0416 | 7.4288 | 0.0122 |
| ARG5 | 7.0536 | 0.1138 | 4.7946 | 0.0700 | 7.4613 | 0.0203 |
| AUN3 | 4.6548 | 0.0503 | 4.8097 | 0.0410 | 7.4956 | 0.0138 |
| AUN4 | 5.8674 | 0.0504 | 5.1985 | 0.0381 | 7.5363 | 0.0121 |
| AUN5 | 6.9622 | 0.0860 | 5.4089 | 0.0603 | 7.5363 | 0.0180 |
| ARN3 | 5.3522 | 0.0637 | 4.5728 | 0.0453 | 7.4560 | 0.0135 |
| ARN4 | 6.0053 | 0.0707 | 4.6916 | 0.0478 | 7.4334 | 0.0136 |
| ARN5 | 6.8877 | 0.0544 | 4.9102 | 0.0352 | 7.4734 | 0.0096 |
| AUS3 | 4.2847 | 0.0442 | 4.5744 | 0.0350 | 7.4497 | 0.0116 |
| AUS4 | 4.8261 | 0.0530 | 4.7354 | 0.0417 | 7.4833 | 0.0136 |
| AUS5 | 6.0900 | 0.0613 | 5.1369 | 0.0448 | 7.4675 | 0.0137 |
| ARS3 | 4.8860 | 0.0523 | 4.3107 | 0.0371 | 7.4286 | 0.0111 |
| ARS4 | 5.5348 | 0.0396 | 4.5939 | 0.0396 | 7.4397 | 0.0117 |
| ARS5 | 6.2438 | 0.0651 | 4.7885 | 0.0433 | 7.4348 | 0.0122 |

Table 4.13a Estimated parameters for stored specimens for storage shear modulus using model proposed by Gahvari.

| Stored Samples | P | s(P) | L | s(L) | Log $G_g$ | s (Log $G_g$) |
|---|---|---|---|---|---|---|
| AU00 | 0.1806 | 0.0035 | 3.6257 | 0.0112 | 10.2108 | 0.1161 |
| AR00 | 0.1835 | 0.0029 | 3.9056 | 0.0107 | 10.0072 | 0.0893 |
| AUG3 | 0.1529 | 0.0024 | 4.6183 | 0.0131 | 10.4746 | 0.0905 |
| AUG4 | 0.1379 | 0.0025 | 4.8332 | 0.0178 | 10.5271 | 0.1030 |
| AUG5 | 0.1455 | 0.0026 | 5.1236 | 0.0203 | 10.1795 | 0.0918 |
| ARG3 | 0.1635 | 0.0016 | 4.9735 | 0.0100 | 10.0320 | 0.0507 |
| ARG4 | 0.1659 | 0.0022 | 5.0293 | 0.0144 | 9.7342 | 0.0612 |
| ARG5 | 0.1360 | 0.0017 | 6.0157 | 0.0155 | 10.5352 | 0.0633 |
| AUN3 | 0.1335 | 0.0030 | 4.8650 | 0.0189 | 10.9563 | 0.1409 |
| AUN4 | 0.0880 | 0.0031 | 5.4502 | 0.0325 | 13.2152 | 0.2923 |
| AUN5 | 0.1276 | 0.0023 | 5.5126 | 0.0206 | 10.6343 | 0.0997 |
| ARN3 | 0.1181 | 0.0017 | 5.6787 | 0.0155 | 11.4226 | 0.0920 |
| ARN4 | 0.1555 | 0.0022 | 5.6546 | 0.0175 | 9.9051 | 0.0680 |
| ARN5 | 0.1085 | 0.0016 | 6.4964 | 0.0200 | 11.4386 | 0.0925 |
| AUS3 | 0.1281 | 0.0018 | 4.8927 | 0.0111 | 11.2693 | 0.0938 |
| AUS4 | 0.1160 | 0.0020 | 5.3006 | 0.0162 | 11.6797 | 0.1187 |
| AUS5 | 0.0977 | 0.0019 | 5.6513 | 0.0194 | 12.4949 | 0.1428 |
| ARS3 | 0.1552 | 0.0016 | 5.0919 | 0.0107 | 10.2115 | 0.0545 |
| ARS4 | 0.1577 | 0.0016 | 5.2873 | 0.0114 | 9.9798 | 0.0502 |
| ARS5 | 0.1325 | 0.0015 | 5.8774 | 0.0141 | 10.5368 | 0.0589 |

Table 4.13b Estimated parameters for stored specimens for loss shear modulus using model proposed by Gahvari.

| Stored Samples | D | s (D) | Log $\omega_D$ | s (Log $\omega_D$) | Log $G_{max}$ | s (Log $G_{max}$) |
|---|---|---|---|---|---|---|
| AU00 | 3.2382 | 0.0534 | 4.2345 | 0.0432 | 7.4158 | 0.0150 |
| AR00 | 3.5253 | 0.0598 | 4.1800 | 0.0457 | 7.4067 | 0.0153 |
| AUG3 | 4.4584 | 0.0661 | 4.3978 | 0.0489 | 7.3874 | 0.0152 |
| AUG4 | 5.0983 | 0.0573 | 4.5677 | 0.0396 | 7.1237 | 0.0117 |
| AUG5 | 5.3993 | 0.0613 | 4.4239 | 0.0400 | 7.1236 | 0.0113 |
| ARG3 | 5.0073 | 0.0692 | 4.3409 | 0.0473 | 7.4033 | 0.0138 |
| ARG4 | 5.1434 | 0.0691 | 4.1577 | 0.0435 | 7.1645 | 0.0120 |
| ARG5 | 6.5490 | 0.0675 | 4.6004 | 0.0423 | 7.4795 | 0.0112 |
| AUN3 | 5.2780 | 0.1875 | 4.8745 | 0.1489 | 7.3905 | 0.0484 |
| AUN4 | 5.3004 | 0.0670 | 4.7408 | 0.0480 | 7.1450 | 0.0146 |
| AUN5 | 6.0229 | 0.0825 | 4.6583 | 0.0543 | 7.1493 | 0.0152 |
| ARN3 | 5.7614 | 0.0540 | 4.6297 | 0.0366 | 7.4462 | 0.0104 |
| ARN4 | 6.2778 | 0.0769 | 4.5303 | 0.0488 | 7.3796 | 0.0132 |
| ARN5 | 7.3104 | 0.0770 | 4.9636 | 0.0481 | 7.4659 | 0.0127 |
| AUS3 | 4.7428 | 0.0529 | 4.6214 | 0.0411 | 7.4127 | 0.0132 |
| AUS4 | 5.3849 | 0.0492 | 4.7892 | 0.0361 | 7.4536 | 0.0110 |
| AUS5 | 5.9063 | 0.1450 | 5.0609 | 0.1036 | 7.4413 | 0.0310 |
| ARS3 | 5.2436 | 0.0586 | 4.5011 | 0.0404 | 7.4440 | 0.0118 |
| ARS4 | 5.8030 | 0.0634 | 4.5751 | 0.0414 | 7.3986 | 0.0115 |
| ARS5 | 6.6133 | 0.0657 | 4.7651 | 0.0414 | 7.3885 | 0.0111 |

the regression, no specific trends were seen between aged and unaged specimens, between original and stored specimens, or among the percentages of polymer added.

The Gahvari models do, however, have drawbacks: the lack of relationship between the storage and loss shear moduli. Based on the physical meaning of these quantities, the equations should be related through the complex shear modulus and phase angle. However, the given equations are not related. The loss modulus equation particularly, is not physically significant in its development with respect to the binder.

The parameters determined from the first replicate were used to predict the results of the second replicate for each sample. The accuracy of the model was evaluated using the MSEP; results are presented in Table 4.14. The values obtained from the MSEP indicate that the model exhibits reasonable accuracy in predicting binder response for both unmodified and modified binders. The opposition to the acceptance of the Gahvari as the best available model for prediction lies in the lack of relationship between the storage and loss shear moduli equations.

Table 4.14 MSEP values for the Gahvari model.

| Sample | Original Specimens | | Stored Specimens | |
|---|---|---|---|---|
| | G' | G" | G' | G" |
| AU00 | 0.0462 | 0.0030 | 0.0541 | 0.0230 |
| AR00 | 0.0216 | 0.0030 | 0.0357 | 0.0046 |
| AUG3 | 0.0164 | 0.0039 | 0.0269 | 0.0047 |
| AUG4 | 0.0098 | 0.0027 | 0.0191 | 0.0036 |
| AUG5 | 0.0082 | 0.0035 | 0.0194 | 0.0019 |
| ARG3 | 0.6516 | 0.3744 | 0.0188 | 0.0105 |
| ARG4 | 0.0082 | 0.0035 | 0.1676 | 0.0727 |
| ARG5 | 0.0540 | 0.0144 | 0.0578 | 0.0451 |
| AUN3 | 0.0064 | 0.0021 | 0.0078 | 0.0033 |
| AUN4 | 0.0157 | 0.0015 | 0.1453 | 0.1046 |
| AUN5 | 0.0124 | 0.0022 | 0.1742 | 0.0780 |
| ARN3 | 0.0206 | 0.0074 | 0.2288 | 0.1369 |
| ARN4 | 0.0153 | 0.0028 | 0.0218 | 0.0104 |
| ARN5 | 0.0040 | 0.0014 | 0.0048 | 0.0022 |
| AUS3 | 0.0112 | 0.0023 | 0.0354 | 0.0095 |
| AUS4 | 0.0116 | 0.0025 | 0.0178 | 0.0013 |
| AUS5 | 0.0073 | 0.0032 | 0.0092 | 0.0036 |
| ARS3 | 0.0071 | 0.0017 | 0.0103 | 0.0050 |
| ARS4 | 0.0062 | 0.0024 | 0.2412 | 0.1725 |
| ARS5 | 0.0045 | 0.0024 | 0.0082 | 0.0028 |

### *4.2.4 Marasteanu-Anderson Model*

This model was introduced as modification of the Christensen-Anderson model that improved the fit for both unmodified and modified binders. The model equations are as follows (Marasteanu and Anderson, 1999):

$$|G^*(\omega)| = G_g\left[1+\left(\frac{\omega_c}{\omega}\right)^v\right]^{-\frac{w}{v}} \tag{4.8}$$

$$\delta(\omega) = \frac{90\,w}{1+\left(\frac{\omega}{\omega_c}\right)^v} \tag{4.9}$$

Explanation of the model parameters can be found in Chapter 2. The values of the model parameters were determined using nonlinear regression techniques in the SAS statistical analysis program similar to those utilized to determine the parameters for the Christensen-Anderson model. An example of the input used to generate the parameters and the resulting output is given in Appendix J for original specimen AUG3. The values and prediction errors of these parameters are presented in Tables 4.15 and 4.16 for the original and stored samples, respectively.

The model parameters were indeterminate for half of the stored specimens. The regression values found for the parameters did not converge to a finite value. The configuration of the specimens showed no trends that could be concluded to cause this lack of convergence. Of the parameters that were determined, no clear trends could be seen when comparing results before and after storage due to the limited number of regression results for stored samples. In general, it was concluded that there were not enough results of regression from the stored specimens to evaluate the model with respect to stored binders.

After evaluating the original samples, it was found that the values of the crossover frequency increased with increasing polymer content. For the unmodified specimens and those modified with polymer G, the crossover frequency increased after RTFO aging. For the specimens modified with polymer N or S, the crossover frequency decreased after RTFO aging. The values of v, a parameter indicative of the rheological index as introduced in the Marasteneau-Anderson model, were consistently in the range of 0.2 to 0.3 for all original specimens. The values found for w, a parameter indicating

Table 4.15 Estimated parameters for original specimens for Marasteanu-Anderson model.

| Sample | $\omega_c$ | s ($\omega_c$) | v | s (v) | w | s (w) | $G_g$ | s ($G_g$) | $R^2$ | RMSE | DoF |
|---|---|---|---|---|---|---|---|---|---|---|---|
| AU00 | 436.0 | 349.24 | 0.2 | 0.0180 | 1.1 | 0.1110 | 3.15E+08 | 3.02E+07 | 0.9997 | 2.18E+05 | 255 |
| AR00 | 462.6 | 238.92 | 0.3 | 0.0140 | 0.9 | 0.0620 | 2.54E+08 | 1.43E+07 | 0.9997 | 2.82E+05 | 263 |
| AUG3 | 483.8 | 423.01 | 0.3 | 0.0220 | 1.0 | 0.1110 | 2.93E+08 | 2.76E+07 | 0.9995 | 3.88E+05 | 263 |
| AUG4 | 1931.7 | 599.59 | 0.3 | 0.0154 | 0.8 | 0.0335 | 1.93E+08 | 9.69E+06 | 0.9997 | 2.39E+05 | 263 |
| AUG5 | 3792.7 | 696.66 | 0.3 | 0.0149 | 0.7 | 0.0200 | 1.78E+08 | 6.28E+06 | 0.9997 | 2.77E+05 | 263 |
| ARG3 | 838.2 | 496.36 | 0.3 | 0.0210 | 0.8 | 0.0630 | 2.48E+08 | 1.79E+07 | 0.9994 | 4.94E+05 | 263 |
| ARG4 | 2427.0 | 729.05 | 0.3 | 0.0218 | 0.7 | 0.0309 | 1.78E+08 | 8.90E+06 | 0.9993 | 4.81E+05 | 263 |
| ARG5 | 4607.9 | 1006.31 | 0.3 | 0.0181 | 0.6 | 0.0208 | 1.78E+08 | 7.03E+06 | 0.9995 | 4.22E+05 | 263 |
| AUN3 | 907.6 | 489.21 | 0.3 | 0.0150 | 0.9 | 0.0610 | 2.60E+08 | 1.85E+07 | 0.9998 | 2.04E+05 | 255 |
| AUN4 | 90.2 | 121.46 | 0.2 | 0.0170 | 1.1 | 0.1550 | 3.13E+08 | 3.40E+07 | 0.9997 | 2.57E+05 | 255 |
| AUN5 | 160.1 | 160.18 | 0.2 | 0.0150 | 1.0 | 0.0990 | 2.60E+08 | 2.27E+07 | 0.9997 | 2.40E+05 | 255 |
| ARN3 | 41.4 | 57.38 | 0.2 | 0.0150 | 1.1 | 0.1550 | 3.35E+08 | 3.12E+07 | 0.9997 | 3.01E+05 | 255 |
| ARN4 | 1.8 | 5.89 | 0.2 | 0.0180 | 1.4 | 0.4110 | 3.82E+08 | 5.56E+07 | 0.9995 | 3.64E+05 | 255 |
| ARN5 | 0.1 | 2.50 | 0.2 | 0.0190 | 1.5 | 0.5440 | 3.99E+08 | 6.58E+07 | 0.9993 | 4.40E+05 | 255 |
| AUS3 | 211.2 | 227.20 | 0.2 | 0.0170 | 1.1 | 0.1280 | 3.01E+08 | 2.93E+07 | 0.9996 | 2.68E+05 | 263 |
| AUS4 | 796.5 | 452.77 | 0.2 | 0.0150 | 0.9 | 0.0610 | 2.80E+08 | 2.05E+07 | 0.9998 | 2.12E+05 | 263 |
| AUS5 | 3370.2 | 989.20 | 0.3 | 0.0186 | 0.8 | 0.0307 | 1.60E+08 | 8.98E+06 | 0.9996 | 2.44E+05 | 263 |
| ARS3 | 218.2 | 225.91 | 0.2 | 0.0180 | 0.9 | 0.1020 | 2.99E+08 | 2.83E+07 | 0.9996 | 2.44E+05 | 263 |
| ARS4 | 527.7 | 372.35 | 0.2 | 0.0150 | 0.8 | 0.0640 | 2.67E+08 | 2.05E+07 | 0.9997 | 2.44E+05 | 263 |
| ARS5 | 599.6 | 466.50 | 0.2 | 0.0200 | 0.8 | 0.0730 | 2.03E+08 | 1.63E+07 | 0.9993 | 2.44E+05 | 263 |

Table 4.16 Estimated parameters for stored specimens for Marasteanu-Anderson model.

| Sample | $\omega_c$ | s ($\omega_c$) | v | s (v) | w | s (w) | $G_g$ | s ($G_g$) | $R^2$ | RMSE | DoF |
|---|---|---|---|---|---|---|---|---|---|---|---|
| AU00 | 349.0 | 214.88 | 0.2 | 0.0090 | 1.0 | 0.0620 | 4.19E+08 | 2.64E+07 | 0.9999 | 1.19E+05 | 263 |
| AR00 | | | | | | | | | | | |
| AUG3 | | | | | | | | | | | |
| AUG4 | 176.0 | 48.09 | 0.2 | 0.0034 | 0.9 | 0.0247 | 1.80E+08 | 4.24E+06 | 0.9999 | 3.14E+04 | 263 |
| AUG5 | | | | | | | | | | | |
| ARG3 | 1.2 | 1.13 | 0.1 | 0.0040 | 1.4 | 0.1160 | 4.75E+08 | 2.02E+07 | 0.9999 | 9.61E+04 | 263 |
| ARG4 | 0.2 | 0.34 | 0.1 | 0.0080 | 1.6 | 0.2920 | 2.35E+08 | 1.59E+07 | 0.9999 | 1.28E+05 | 263 |
| ARG5 | 21.9 | 15.89 | 0.2 | 0.0060 | 1.0 | 0.0680 | 3.77E+08 | 1.57E+07 | 0.9999 | 1.79E+05 | 263 |
| AUN3 | | | | | | | | | | | |
| AUN4 | | | | | | | | | | | |
| AUN5 | | | | | | | | | | | |
| ARN3 | 7.6 | 5.06 | 0.2 | 0.0040 | 1.2 | 0.0680 | 4.46E+08 | 1.60E+07 | 0.9999 | 9.05E+04 | 263 |
| ARN4 | 2.6 | 1.63 | 0.1 | 0.0030 | 1.2 | 0.0610 | 4.08E+08 | 1.23E+07 | 0.9999 | 7.09E+04 | 263 |
| ARN5 | 0.2 | 0.51 | 0.1 | 0.0100 | 1.4 | 0.3290 | 5.13E+08 | 5.41E+07 | 0.9998 | 2.28E+05 | 263 |
| AUS3 | 141.7 | 45.25 | 0.2 | 0.0040 | 1.0 | 0.0310 | 3.85E+08 | 1.11E+07 | 0.9999 | 5.03E+04 | 263 |
| AUS4 | | | | | | | | | | | |
| AUS5 | | | | | | | | | | | |
| ARS3 | | | | | | | | | | | |
| ARS4 | | | | | | | | | | | |
| ARS5 | 625.9 | 203.19 | 0.2 | 0.0054 | 0.8 | 0.0237 | 2.95E+08 | 9.90E+06 | 0.9999 | 1.06E+05 | 263 |

the rate of convergence of the phase angle to the zero or 90° asymptote, were found to decrease after RTFO aging for the unmodified specimens and those modified with polymer G or S. The values of w increased after RTFO aging for specimens modified with polymer N. An increasing w value indicates a binder that tends to approach the 90° asymptote at an increasing rate. A decreasing w value indicates that the binder approaches the 0° asymptote, or rubbery flow region, at an increased rate.

After determining the model parameters from the first replicate of each specimen, the model was fitted to the second replicate and the accuracy of the model was evaluated; see Table 4.17. The MSEP values found for the model using the regression techniques of this study indicate that the model is not a good predictor of binder response. As noted above, there were not enough results to evaluate the models performance with respect to stored binders. In general, for the regression procedure utilized, the model was found highly sensitive to starting parameters, and therefore is not considered to produce an accurate prediction of binder response under this method. It should be noted that this conclusion is drawn based on utilization of a single nonlinear

Table 4.17 MSEP values for the Marasteanu-Anderson model.

| Sample | Original Specimens | | Stored Specimens | |
|---|---|---|---|---|
| | G* | δ | G* | δ |
| AU00 | 0.0844 | 0.0010 | 0.0026 | 0.0003 |
| AR00 | 0.0363 | 0.0010 | | |
| AUG3 | 0.0257 | 0.0017 | | |
| AUG4 | 0.0193 | 0.0022 | 0.0181 | 0.0007 |
| AUG5 | 0.0252 | 0.0045 | | |
| ARG3 | 0.0343 | 0.0024 | 1.9098 | 0.0246 |
| ARG4 | 0.0397 | 0.0056 | 4.5052 | 0.0156 |
| ARG5 | 0.1034 | 0.0118 | 0.0978 | 0.0035 |
| AUN3 | 0.0130 | 0.0008 | | |
| AUN4 | 0.1554 | 0.0053 | | |
| AUN5 | 0.2188 | 0.0052 | | |
| ARN3 | 0.0407 | 0.0023 | 0.3237 | 0.0040 |
| ARN4 | 0.1582 | 0.0116 | 1.3884 | 0.0013 |
| ARN5 | 0.6226 | 0.0224 | 1.4992 | 0.0045 |
| AUS3 | 0.2032 | 0.0019 | 0.0396 | 0.0007 |
| AUS4 | 0.0307 | 0.0006 | | |
| AUS5 | 0.1146 | 0.0224 | | |
| ARS3 | 0.0065 | 0.0007 | | |
| ARS4 | 0.0230 | 0.0026 | | |
| ARS5 | 0.0325 | 0.0012 | 0.0090 | 0.0011 |

regression method; if differing methods of regression are used the results may be very different.

## 4.3 Results of Model Evaluations

The MSEP values found for the Christensen-Anderson and Marasteanu-Anderson models were compared to evaluate the effectiveness of each model in accurately predicting the behavior of the second replicate of each specimen. Both methods of determining the parameters for the Christensen-Anderson model were evaluated in this comparison. The values of the MSEP are presented in Tables 4.8, 4.11, and 4.17.

Analysis of the MSEP indicated that for original modified binder specimens the graphical determination of parameters for the Christensen-Anderson model resulted in the most accurate prediction of response. For the unmodified original specimens, the regressed parameters utilized in the Christensen-Anderson model provided a better prediction of behavior. Fixing the values of the glassy modulus during the regression of the Christensen-Anderson model is likely to increase the predictive accuracy of the model, as the behavior of the data will depend only on parameters that may be graphically verified. The values of the glassy modulus should then be determined experimentally, or set at the value recommended in the literature (Anderson *et al*., 1991). The Marasteanu-Anderson model was found to produce results that were highly dependent on the initial values of the regression procedure. It is postulated that the Marasteanu-Anderson model would be found to have better accuracy if different procedures for regression were used. The methods utilized in this study were but one method; there are many other nonlinear regression techniques that may be used with greater success to evaluate the parameters of this model. In particular, utilizing log transformed data has the potential to lessen errors found in the regression procedure. Additionally, as for the Christensen-Anderson model, the values of the glassy modulus should be fixed. This reduces the number of parameters that must be determined through regression and should increase the predictive accuracy of the model for modified and unmodified binders.

The MSEP results from the Gahvari model were evaluated individually and were found to indicate very good accuracy for most specimens. Values of the MSEP were slightly higher than those observed for the Christensen-Anderson model, and appear to

fit the data well. The difficulty in accepting the Gahvari model lies in its lack of physical significance. The model is a mathematical description of the binder response that does not take into account the relationship between the shear storage and loss moduli. In addition to the comparisons of model accuracy made through use of the MSEP, all models were evaluated visually. Fitted data were plotted versus the experimentally determined data. Figure 4.8 is an example of the plots used to visually evaluate the models. Figure 4.8a shows the response of the second replicate of original specimen AU00 as compared to the Marasteanu-Anderson model and the two methods of the Christensen-Anderson model. Figure 4.8b shows the response of the second replicate of original specimen AU00 as compared to the Gahvari model. A complete compilation of all plots can be found in Appendices K and L for the original and stored specimens, respectively.

The visual observations substantiated the conclusions drawn from the analysis of MSEP. However, the differences between the models are made more obvious than those expressed by error values. It can be seen in many cases that the Marasteanu-Anderson model is unstable regarding its predictive ability as compared to the Christensen-Anderson model and the Gahvari model. The regressed parameter and graphically determined parameter forms of the Christensen-Anderson model are found to exhibit similar fits of the data in most cases. The Gahvari model is seen to have good predictive ability of the data for most specimens, although deviations are seen at extreme values of the storage and loss shear moduli - a shortcoming caused by the geometrical properties of the model.

a)

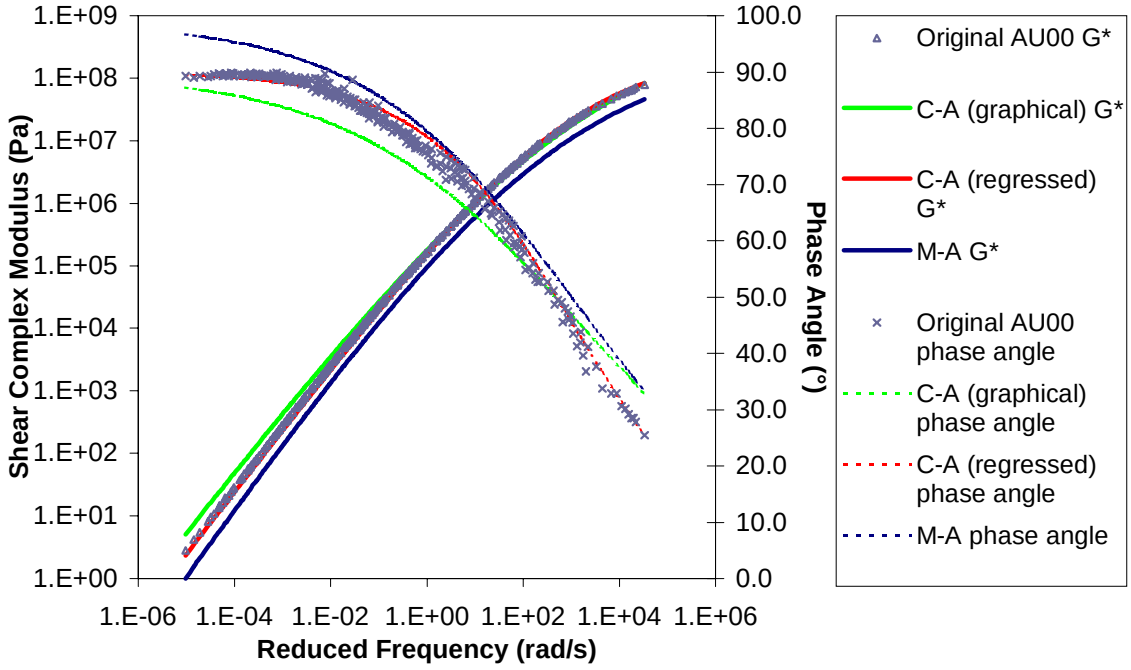


b)

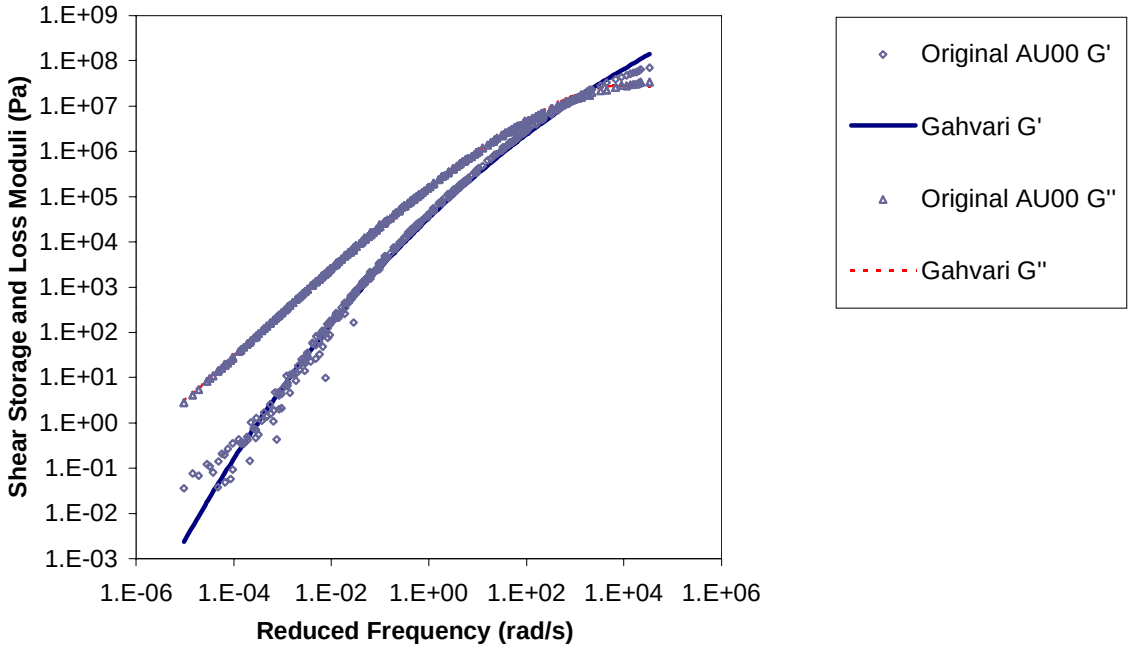


Figure 4.8 Graphs of original specimen AU00 response versus responses predicted by a) the Christensen-Anderson (C-A) model with graphically determined parameters, Christensen-Anderson (C-A) model with regressed parameters, and Marasteanu-Anderson (M-A) model; and b) Gahvari models.

# CHAPTER 5 SUMMARY, FINDINGS AND CONCLUSIONS

This study was performed to evaluate samples of polymer-modified asphalt using dynamic mechanical testing to determine if the binder response changed after four years of storage at a temperature of 23°C. Testing indicated that significant changes occurred in the storage and loss shear moduli of unmodified and modified binders during four years of storage. The most notable changes in response of binders were found to occur at low frequencies. The effects of storage on modified binders were found to be dependent on polymer type and concentration. Additionally, test results were used to verify the accuracy of previously developed models describing dynamic mechanical response when applied to polymer-modified binders and aged binders. The models evaluated included those introduced by Christensen-Anderson, Stastna, Gahvari, and Marasteanu-Anderson. The mean square error of prediction was used to evaluate each model's ability to predict binder response. Additionally a visual evaluation of the fit was performed. The Christensen-Anderson model formulated with graphically determined parameters was found to have the best ability to predict the dynamic response of unmodified and modified binders before and after storage. The next preferred model was the Christensen-Anderson model formulated with regressed parameters.

## 5.1 Findings

The following findings were noted during this study:

- Significant increases in storage and loss shear moduli were noted in the rubbery flow region in the unmodified binder when stored for four years at room temperature (23°C).
- Effects of long-term intermediate temperature storage are dependent on the polymer type and polymer content.
- Tested polymer-modified binders, after four years of storage, showed improvements in high-temperature (low frequency) performance as indicated by storage and loss shear moduli mastercurves constructed from dynamic mechanical data. However, the effect at high frequencies was insignificant.

- Increases in shear moduli measurements due to aging applied by the Rolling Thin Film Oven Test were still seen in measurements taken after four years of storage at room temperature (23°C).
- The parameter values of the Christensen-Anderson model were found to depend upon the method of parameter determination. These differences significantly affected the accuracy of the model in predicting binder responses.
- The Stastna model was found unfeasible for use due to the large number of defining parameters necessary for model formulation.
- The Gahvari model was found to be readily used and relatively accurate in response predictions for both original and stored binders; however, the model failed to relate G' and G'' through $\delta$.
- Parameters of the Marasteanu-Anderson model were difficult to find through nonlinear regression and were dependent on the initial values of the regression procedure. The model was unsuitable for use with stored binders and did not predict the response of original modified binders well.

## 5.2 Conclusions

Aged and unaged asphalt binder specimens modified with three different polymers, each at three percentages, were tested before and after four years of storage at a temperature of 23°C and compared with unmodified specimens subjected to the same aging, storage, and testing conditions. The following conclusions were drawn:

- Significant changes affecting the dynamic response of asphalt binders occur during long term storage at a temperature of 23°C. These changes are least apparent at intermediate and high frequencies. In modified binders, these changes are dependent on the type and concentration of modifier and may be beneficial.
- Four mathematical models describing the dynamic response of binders were evaluated and were found to be variable in their ability to accurately predict response of modified binders. Most of these models were found to be less accurate in predicting the response of unmodified and polymer-modified binders after storage.

# CHAPTER 6 RECOMMENDATIONS

Based on the results of this study, the following recommendations may be made:

- Further testing on additional binder and polymer types and concentrations should be performed before and after storage to determine trends in the dynamic response due to polymer type, concentration level, and binder-polymer interactions.
- An evaluation of the effects of accelerated long term aging on the dynamic response of modified binders should be performed using the pressure aging vessel.
- It appears that further investigations need to be conducted to develop a suitable model to predict the storage and loss shear moduli of polymer-modified and unmodified binder.

# REFERENCES

Al Dhalaan, M., F. Balghuniam, I. Al Dhubaib, and A. S. Noureldin. (1992) “Field Trials with Polymer Modified Asphalts in Saudi Arabia.” *Polymer Modified Asphalt Binders*, STP 1108, K. R. Woodlaw and S. Shuler, Eds., ASTM, Philadelphia, PA, 203-223.

Anderson, D. A., D. W. Christensen, and H. Bahia. (1991) "Physical Properties of Asphalt Cement and the Development of Performance Related Specifications." *Journal of the Association of Asphalt Paving Technologists*, Vol. 60, 437-475.

Anderson, D. A., D. W. Christensen, H. U. Bahia, R. Dongre, M. G. Sharma, C. E. Antle, and J. Button. (1994) "Binder Characterization and Evaluation Volume 3: Physical Characterization." Report No. SHRP-A-369, Strategic Highway Research Program, National Research Council, Washington, DC, 475 p.

*Annual Book of ASTM Standards*. (1997a) Vol. 04.03, Philadelphia, PA.

*Annual Book of ASTM Standards*. (1997b) Vol. 04.04, Philadelphia, PA.

Asphalt Institute. (1993) Introduction to Asphalt, 8th Edition, Asphalt Institute, Lexington, KY.

Asphalt Institute. (1997) SUPERPAVE: Performance Graded Asphalt Binder Specification and Testing, Asphalt Institute, Lexington, KY.

*AASHTO Provisional Standards*. (1994) “AASHTO TP5, Standard Test Method for Determining the Rheological Properties of Asphalt Binder Using a Dynamic Shear

Rheometer (DSR).” American Association of State Highway and Transportation Officials, Washington, DC.

Bahia, H. U. and D. A. Anderson. (1993) “Glass Transition Behavior and Physical Hardening of Asphalt Binders.” *Journal of the Association of Asphalt Paving Technologists*, Vol. 62, 93-129.

Bishop, E. T. and S. Davison. (1969) "Network Characteristics of the Thermoplastic Elastomers." *Journal of Polymer Science*, Part C, No. 26, 59-79.

Bouldin, M. G., J. H. Collins, and A. Berker. (1991) "Rheology and Microstructure of Polymer/Asphalt Blends." *Rubber Chemistry and Technology*, Vol. 64, No. 4, 577-600.

Branthaver, J. F., R. E. Robertson, and J. J. Duvall. (1996) “Relationships between Molecular Weights and Rheological Properties of Asphalts.” *Transportation Research Record*, No. 1534, Transportation Research Board, Washington, DC, 10-14.

Brodnyan, J. G., F. H. Gaskins, W. Philippoff, and E. Thelen. (1960) "The Rheology of Asphalt, III. Dynamic Mechanical Properties of Asphalt." *Transactions of the Society of Rheology*, Vol. 4, 279-296.

Brown, E. R., F. Parker, and M. R. Smith. (1992) “Study of the Effectiveness of Styrene-Butadiene Rubber Latex in Hot Mix Asphalt Mixes.” *Transportation Research Record*, No. 1342, Transportation Research Board, Washington, DC, 85-91.

Brule, B. (1997) “Polymer-Modified Asphalt Cement Used in the Road Construction Industry: Basic Principles.” *Asphalt Science and Technology*, A. M. Usmani, Ed., Marcel Dekker Inc., New York, NY, 463-477.

Chiu, C., M. Tia, B. E. Ruth, and G. C. Page. (1994) "Investigation of Laboratory Aging Processes of Apshalt Binders Used in Florida." *Transportation Research Record*, No. 1436, Transportation Research Board, Washington, DC, 60-70.

Christensen, D. W. and D. A. Anderson. (1992) "Interpretation of Dynamic Mechanical Test Data for Paving Grade Asphalt Cements." *Journal of the Association of Asphalt Paving Technologists*, Vol. 61, 67-116.

Cohen, R. E. and N. W. Tschoegl. (1973) "Dynamic Mechanical Properties of Block Copolymer Blends - A Study of the Effects of Terminal Chains in Elastomeric Materials." *International Journal of Polymeric Materials*, Vol. 2, No. 3, 205-223.

Cohen R.E. and N. W. Tschoegl. (1976) "Comparison of the Dynamic Mechanical Properties of Two Styrene-Butadiene-Styrene Triblock Copolymers with 1,2- and 1,4-Polybutadiene Center Blocks." *Transactions of the Society of Rheology*, Vol. 20, Issue 1, 153-169.

Collins, J. H., M. G. Bouldin, R. Gelles, and A. Berker. (1991) "Improved Performance of Paving Asphalts by Polymer Modification." *Journal of the Association of Asphalt Paving Technologists*, Vol. 60, 43-79.

Collins, J. H. and W. J. Mikols. (1985) "Block Copolymer Modification of Asphalt Intended for Surface Dressing Applications." *Journal of the Association of Asphalt Paving Technologists*, Vol. 54, 1-17.

Collins, J. H. and M. G. Bouldin. (1992) “Stability of Straight and Polymer Modified Asphalts.” *Transportation Research Record*, No. 1342, Transportation Research Board, Washington, DC, 92-100.

Dickinson, E. J., and H. P. Witt. (1974) "The Dynamic Shear Modulus of Paving Asphalts as a Function of Frequency." *Transactions of the Society of Rheology*, Vol. 18, No. 4, 591-606.

Dobson, G. R. (1969) "The Dynamic Mechanical Properties of Bitumen." *Proceedings of the Association of Asphalt Paving Technologists*, Vol. 38, 123-139.

Doolittle, A. K. (1951) “Studies in Newtonian Flow. II The Dependence of Viscosity of Liquids on Free-Space.” *Journal of Applied Physics*, Vol. 22, No. 12, 1471.

Ferry, J. D. (1980) *Viscoelastic Properties of Polymers*. 3rd Edition, John Wiley & Sons, Inc., New York, NY.

Fesko, D. J., and N. W. Tschoegl. (1971) "Time-Temperature Superposition in Thermorheologically Complex Materials." *Journal of Polymer Science*, Part C, No. 35, Viscoelastic Relaxation on Polymers, 51-69.

Fesko, D. J., and N. W. Tschoegl. (1974) "Time-Temperature Superposition in Styrene/Butadiene/Styrene Block Copolymers." *International Journal of Polymeric Materials*, Vol. 31, No. 1, 51-79.

Gahvari, F. (1996) “Modeling of the Linear Viscoelastic Response of Polymer Modified Asphalt Binders at Intermediate and High Temperatures.” Ph.D. Dissertation, Virginia Polytechnic Institute and State University, Blacksburg, VA.

Goodrich, J. L. (1988) "Asphalt and Polymer Modified Asphalt Properties Related to the Performance of Asphalt Concrete Mixes." *Proceedings of the Association of Asphalt Paving Technologists*, Vol. 57, 116-175.

Havriliak, S. and S. Negami. (1966) "A Complex Plane Analysis of α-Dispersions in Some Polymer Systems." *Journal of Polymer Science*, Part C, No. 14.

Holden, G., E. T. Bishop, and E. R. Legge. (1969) "Thermoplastic Elastomers." *Journal of Polymer Science*, Part C, No. 26, 37-57.

Jongepier, R. and B. Kuilman. (1969) "Characteristics of the Rheology of Bitumen." *Proceedings of the Association of Asphalt Paving Technologists*, Vol. 38, 99-122.

Jongepier, R. and B. Kuilman. (1970) "The Dynamic Shear Modulus of Bitumens as a Function of Frequency and Temperature." *Rheologica Acta*, Vol. 9, No. 1, 102-111.

Kaplan, D. and N. W. Tschoegl. (1974) "Time-Temperature Superposition in Two-Phase Blends." *Polymer Science and Technology*, Vol. 4, Recent Advances in Polymer Blends, Grafts, and Blocks, 415-430.

Kennedy, T. W., R. J. Cominsky, E. T. Harrington, and R. B. Leahy. (1990) “Hypotheses and Models Employed in the SHRP Asphalt Research Program.” Report No. SHRP-A/WP-90-008, Strategic Highway Research Program, National Research Council, Washington, DC, 63 p.

Khattak, M. J. and G. Y. Baladi. (1998) "Engineering Properties of Polymer Modified Asphalt Mixtures." Paper presented at the Transportation Research Board 77th Annual Meeting, Paper No. 980573, Washington, DC.

Kim, Y., D. Little, and F. Benson. (1990) “Chemical and Mechanical Evaluation on Healing Mechanism of Asphalt Concrete.” *Proceedings of the Association of Asphalt Paving Technologists*, Vol. 59, 240-272.

King, G. N. and H. W. King. (1986) "Polymer Modified Asphalts, an Overview." *Solutions for Pavement Rehabilitation Problems*, S. P. Lahue, Ed., ASCE, New York, NY, 240-254.

Krause, G. and D. S. Hall. (1983) "Applications of Elastomeric Diene-Styrene Block Copolymers." *Block Copolymers: Science and Technology*, MMI Press Symposium Series, Vol. 3, D. J. Meier, Ed., Harwood Academic Publishers, New York, NY, 167-195.

Krebs, R. D. and R. D. Walker. (1971) *Highway Materials*. McGraw-Hill, New York, NY.

Lewandowski, L. H. (1994) "Polymer Modification of Paving Asphalt Binders." *Rubber Chemistry and Technology*, Vol. 67, No. 3, 447-480.

Lim, C. K., R. E. Cohen, and N. W. Tschoegl. (1971) "Time-Temperature Superposition in Block Copolymers." *Multicomponent Polymer Systems*, Advances in Chemistry Series, No. 99, American Chemical Society Publications, Washington, DC, 397-417.

Marasteanu, M. O. and D. A. Anderson. (1999) “Improved Model for Bitumens Rheological Characterization.” Paper submitted to the Eurobitume Workshop on Performance-Related Properties for Bituminous Binders, Luxembourg, Sweden.

Nellensteyn, F. J. (1924) “The Constitution of Asphalt.” *Institute of Petroleum Technology*, Vol. 10, 311-325.

Ninomiya, K. and J. D. Ferry. (1959) "Some Approximate Equations Useful in the Phenomenological Treatment of Linear Viscoelastic Data." *Journal of Colloid Science*, Vol. 14, 36-48.

Noshay, A. and J. E. McGrath. (1977) *Block Coploymers, Overview and Critical Survey*. Academic Press, Inc., New York, NY.

Peterson, J. C. (1984) “Chemical Composition of Asphalt as Related to Asphalt Durability – State of the Art.” *Transportation Research Record*, No. 999, Transportation Research Board, Washington, DC, 13-30.

Rawlings, J. O. (1988) *Applied Regression Analysis: A Research Tool*. Wadsworth and Brooks / Cole Advanced Books & Software, Pacific Grove, CA.

Schuler, T. S., J. H. Collins, and J. P. Kirkpatrick. (1987) “Polymer-Modification Asphalt Properties as Related to Asphalt Concrete Performance.” *Asphalt Rheology: Relationship to Mixture*, STP 941, O. E. Briscoe, Ed., ASTM, Philadelphia, PA, 179-193.

Schwartzl, F. and A. J. Sraverman. (1952) "Time-Temperature Dependence of Linear Viscoelastic Behavior." *Journal of Applied Physics*, Vol. 23, No. 8, 838-843.

Shin, E. E., A. Bhurke, E. Scott, S. Rozeveld, and L. T. Drzal. (1996) "Microstructure, Morphology, and Failure Modes of Polymer-Modified Asphalt." *Transportation Research Record*, No. 1535, Transportation Research Board, Washington, DC, 61-73.

Sperling, L. (1992) *Introduction to Physical Polymer Science*. John Wiley and Sons, Inc., New York, NY.

Stastna, J., L. Zanzotto, and G. Kennepohl. (1996) “Dynamic Material Functions and the Structure of Asphalts.” *Transportation Research Record*, No. 1535, Transportation Research Board, Washington, DC, 3-9.

Struik, L. C. E. (1978) Physical Aging in Amorphous Polymers and Other Materials. Elsevier Scientific, New York, NY.

Takayanagi, M. (1965) *Proceedings of the 4th International Congress on Rheology*, Part 1, Interscience, 161.

Thenoux, G., C. A. Bell, and J. E. Wilson. (1988) “Evaluation of Physical and Fractional Properties of Asphalt and Their Interrelationship.” *Transportation Research Record*, No. 1171, Transportation Research Board, Washington, DC, 82-97.

Tobolosky, A. V. (1956) "Stress Relaxation Studies of the Viscoelastic Properties of Polymers." *Journal of Applied Physics*, Vol. 27, No. 7, 673-685.

Tobolosky, A. V. and H. Eyring. (1943) "Mechanical Properties of Polymeric Materials." *Journal of Chemical Physics*, Vol. 11, No. 3, 125-134.

Traxler, R. N. (1961) *Asphalt: Its Composition, Properties, and Uses*. Reinhold, NY.

Tschoegl, N. W. (1989) *The Phenomenological Theory of Linear Viscoelastic Behavior, An Introduction*. Springer-Verlag, New York, NY.

Tschoegl, N. W. and R. E. Cohen. (1978) “The Representation of the Time-Dependent Properties of Heterophase Polymers.” *Polymer Reprints*, Vol. 19, No. 1, American Chemical Society, Division of Polymer Chemistry, 49-52.

van der Poel, C. (1954) “A General System Describing the Viscoelastic Properties of Bitumens and Its Relation to Routine Test Data.” *Journal of Applied Chemistry*, Vol. 4, 221-236.

# APPENDIX A

- This appendix includes the storage and loss shear modulus mastercurves for all original specimens.

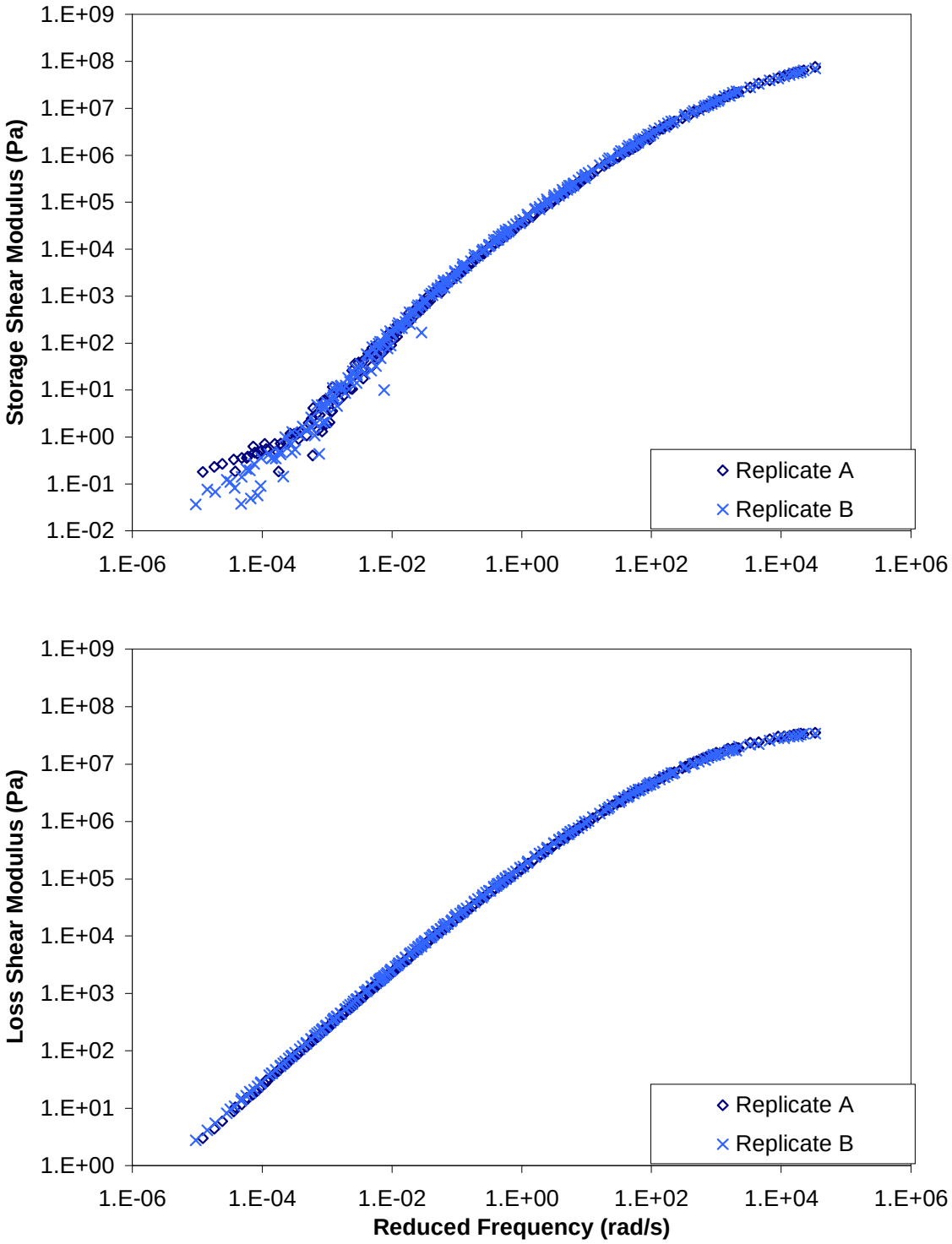


Figure A.1 Storage and loss shear moduli mastercurves for specimen AU00.

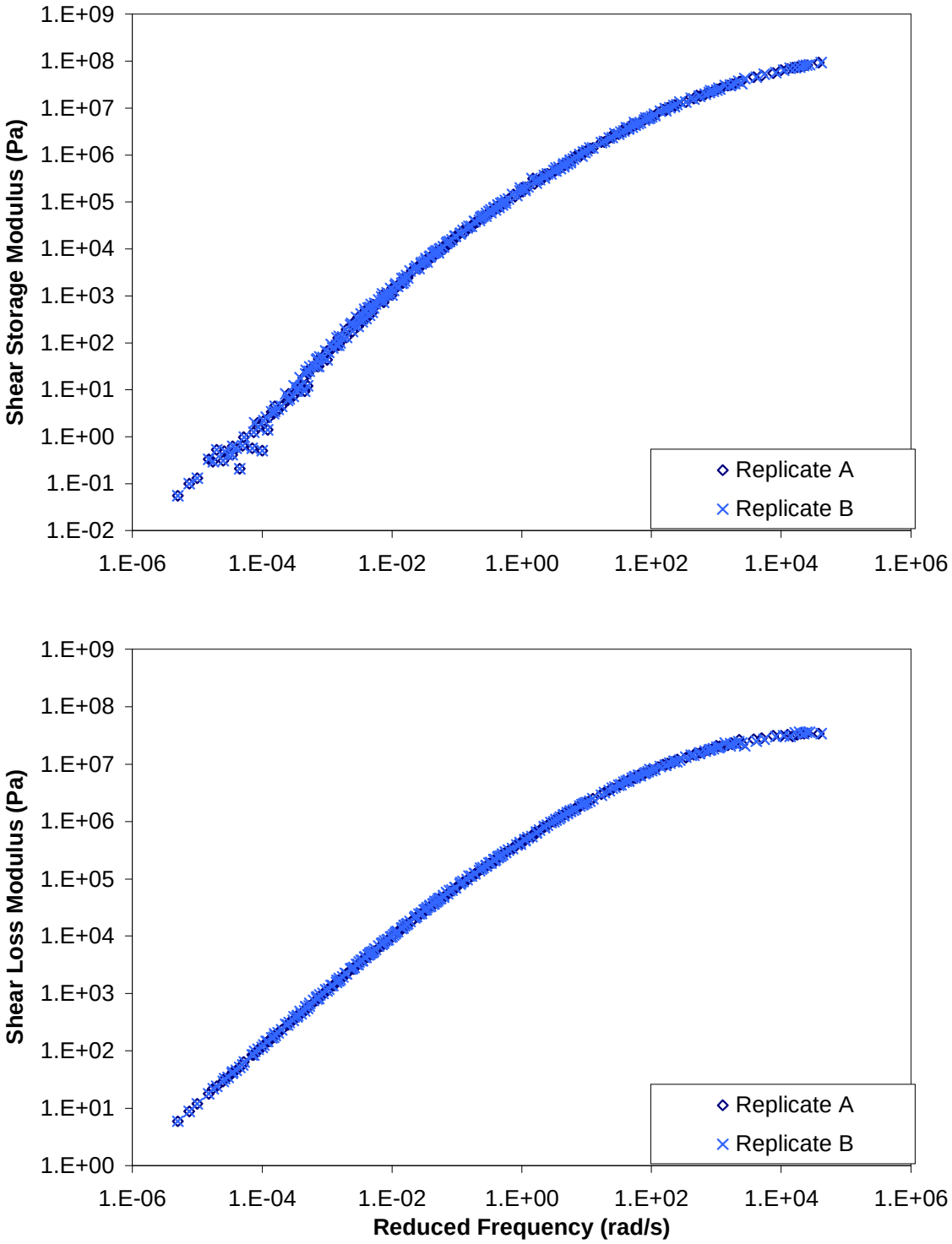


Figure A.2 Storage and loss shear moduli mastercurves for specimen AR00.

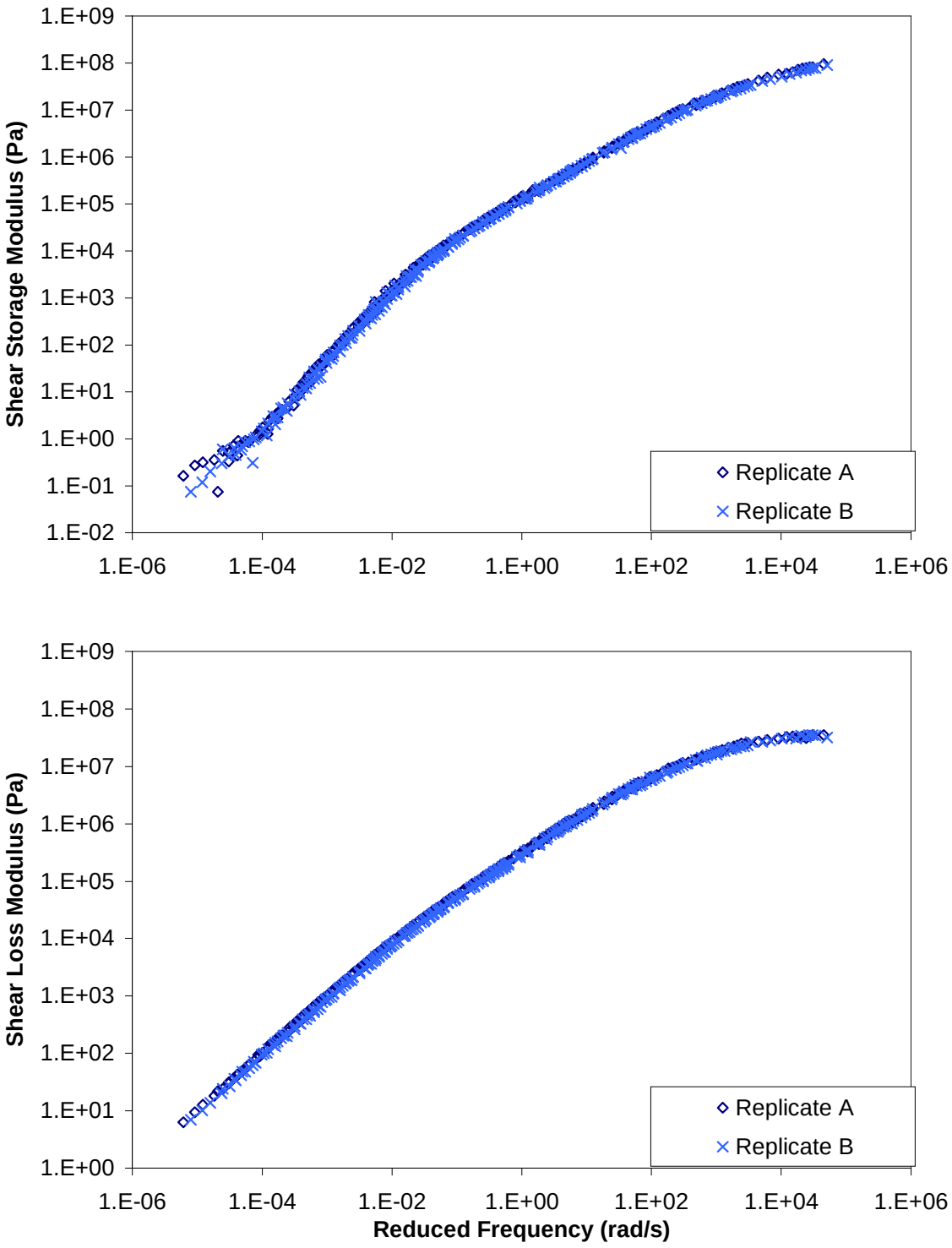


Figure A.3 Storage and loss shear moduli mastercurves for specimen AUG3.

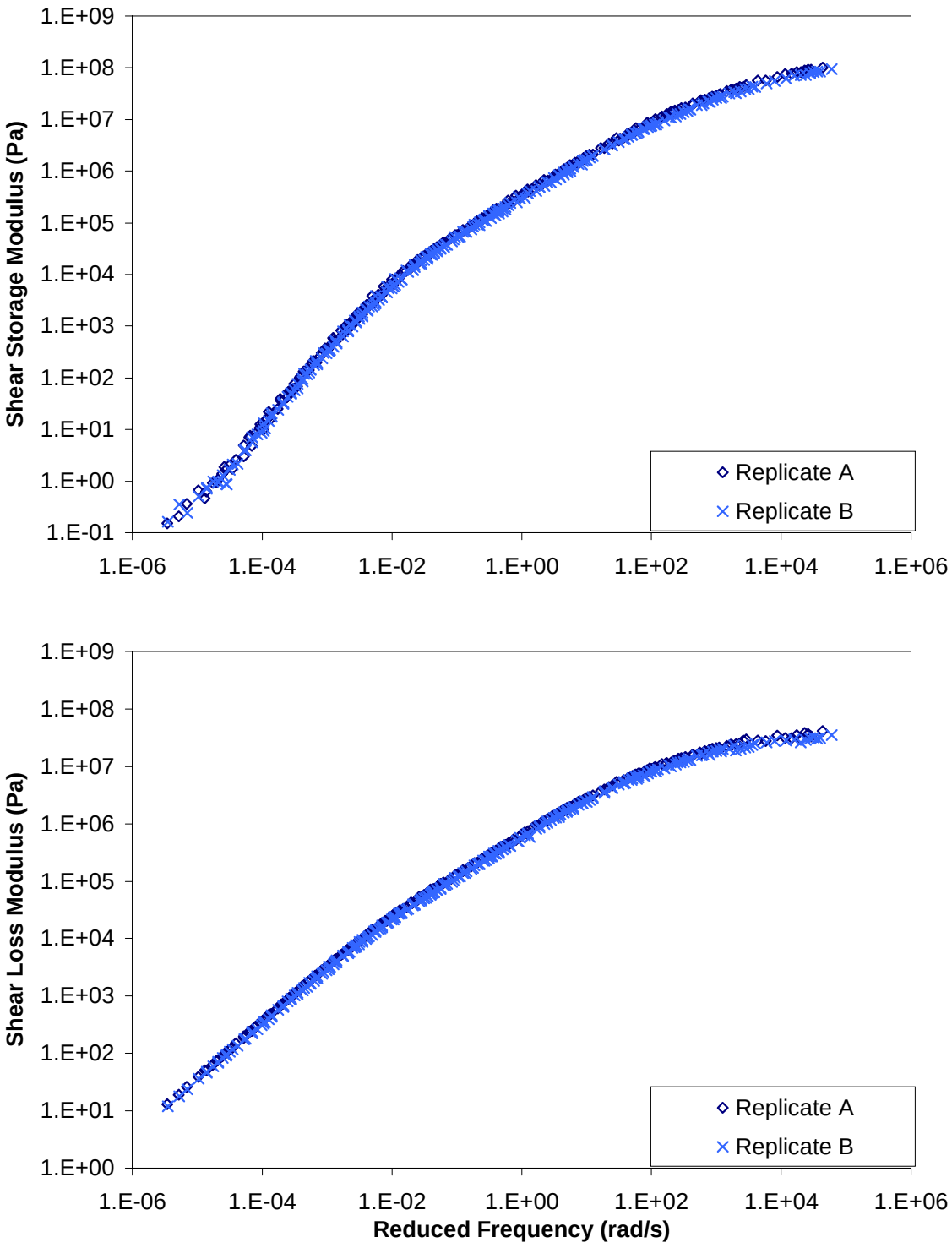


Figure A.4 Storage and loss shear moduli mastercurves for specimen ARG3.

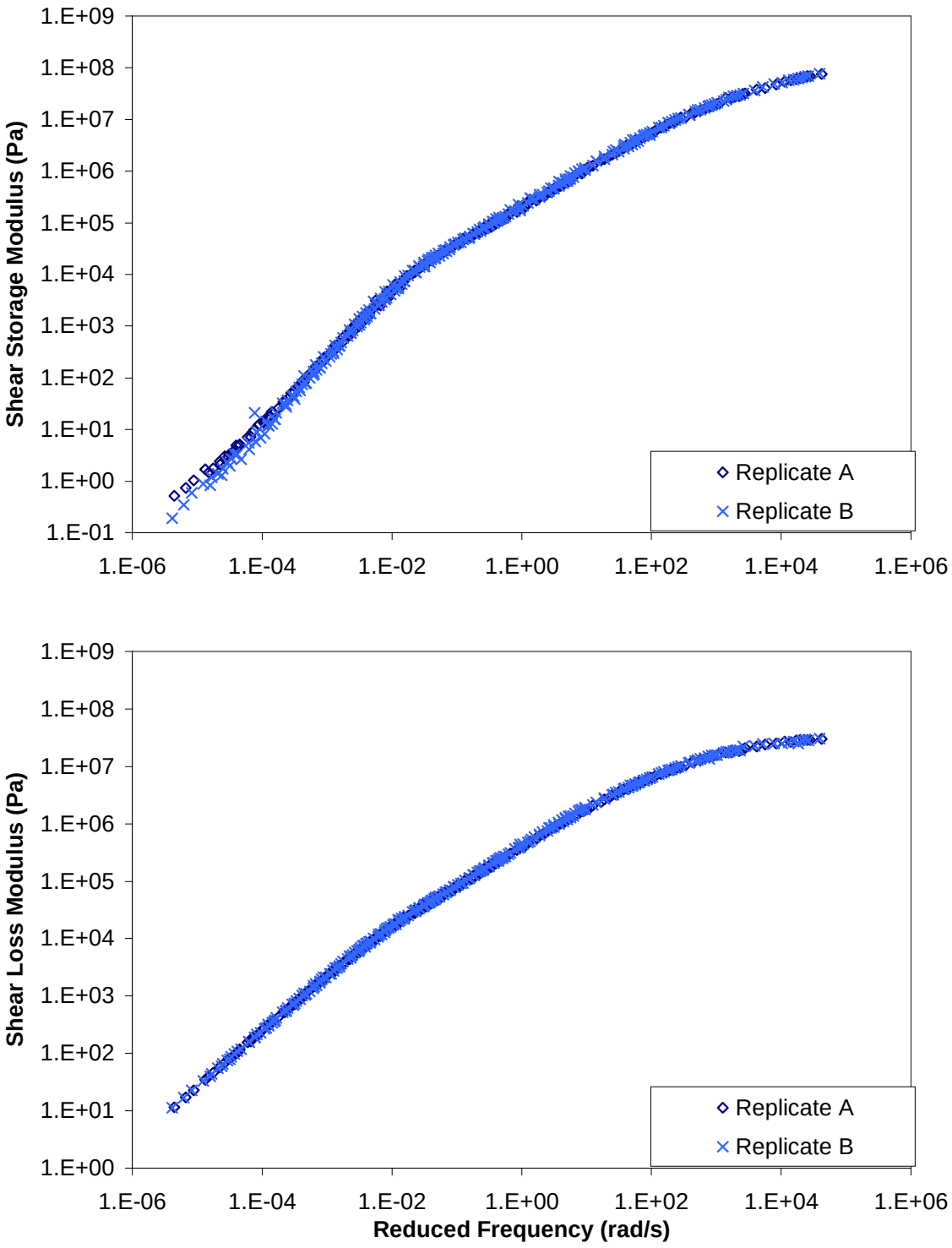


Figure A.5 Storage and loss shear moduli mastercurves for specimen AUG4.

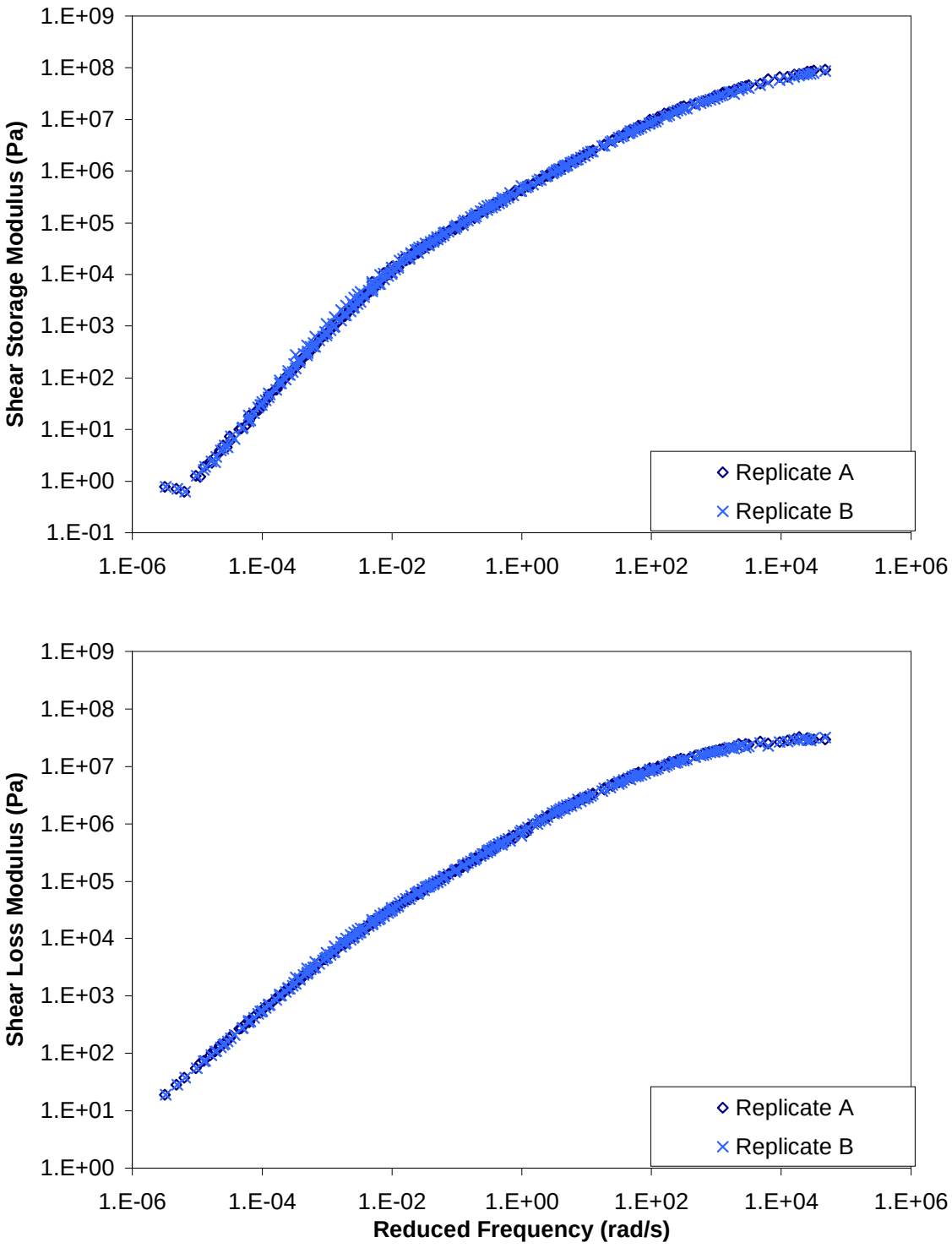


Figure A.6 Storage and loss shear moduli mastercurves for specimen ARG4.

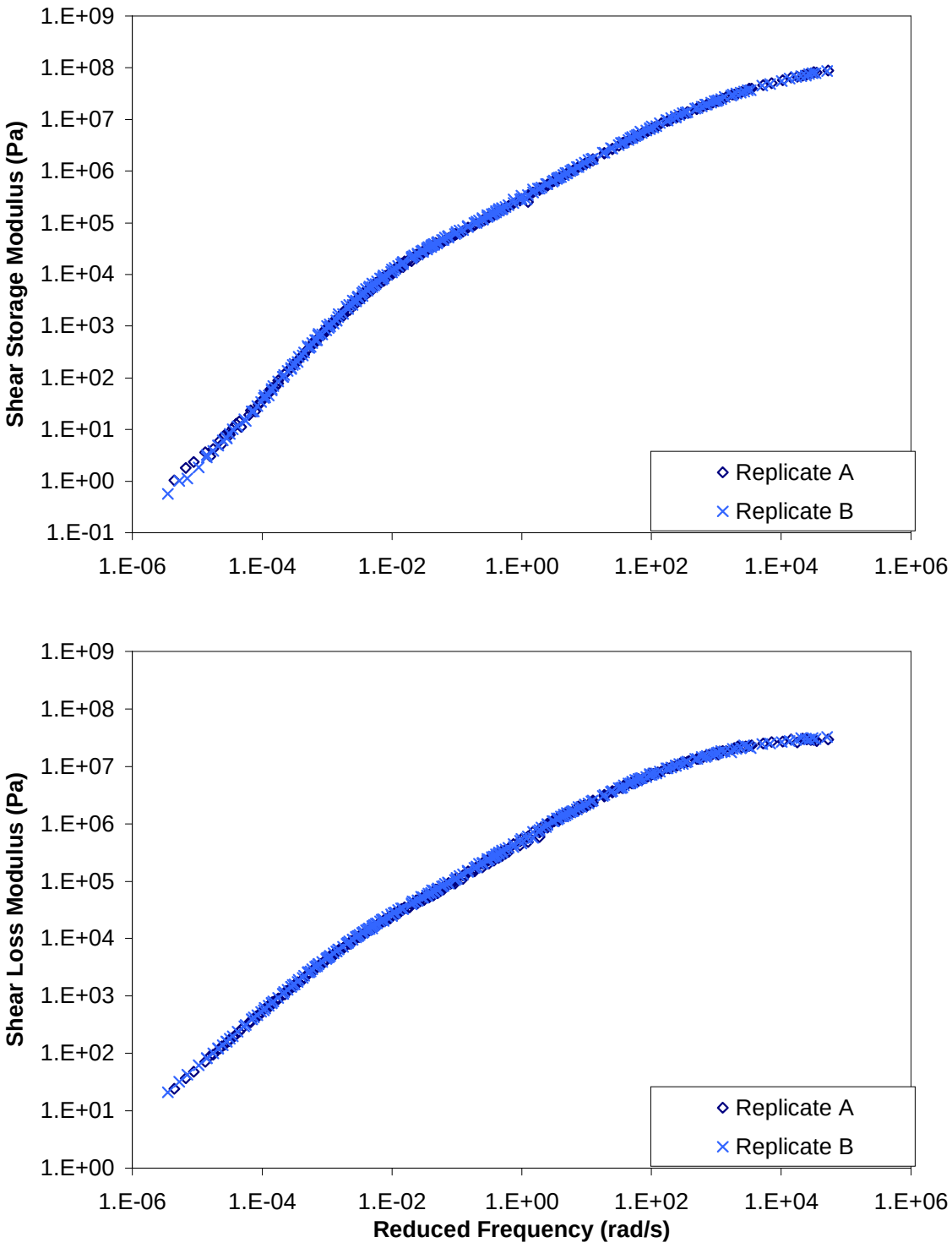


Figure A.7 Storage and loss shear moduli mastercurves for specimen AUG5.

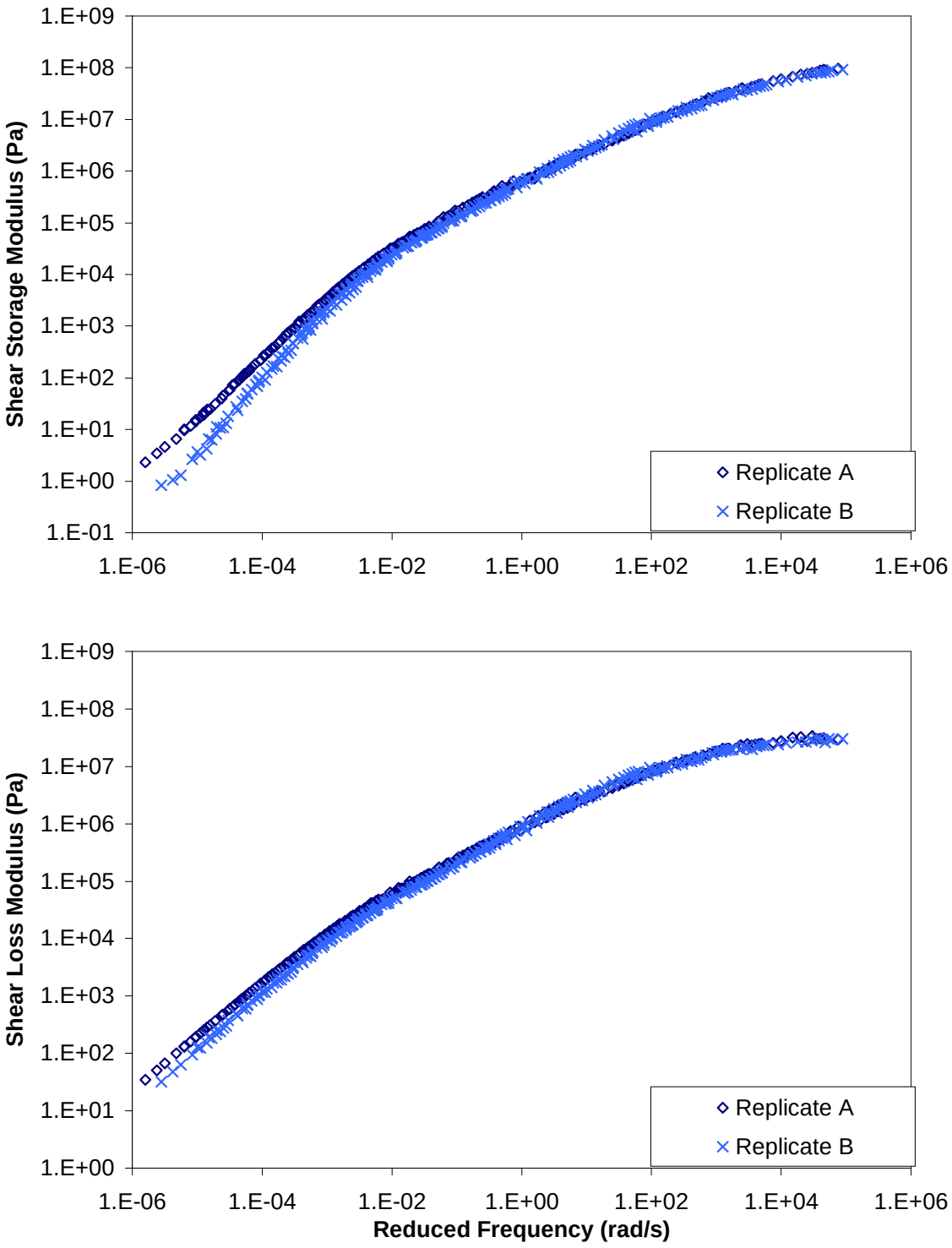


Figure A.8 Storage and loss shear moduli mastercurves for specimen ARG5.

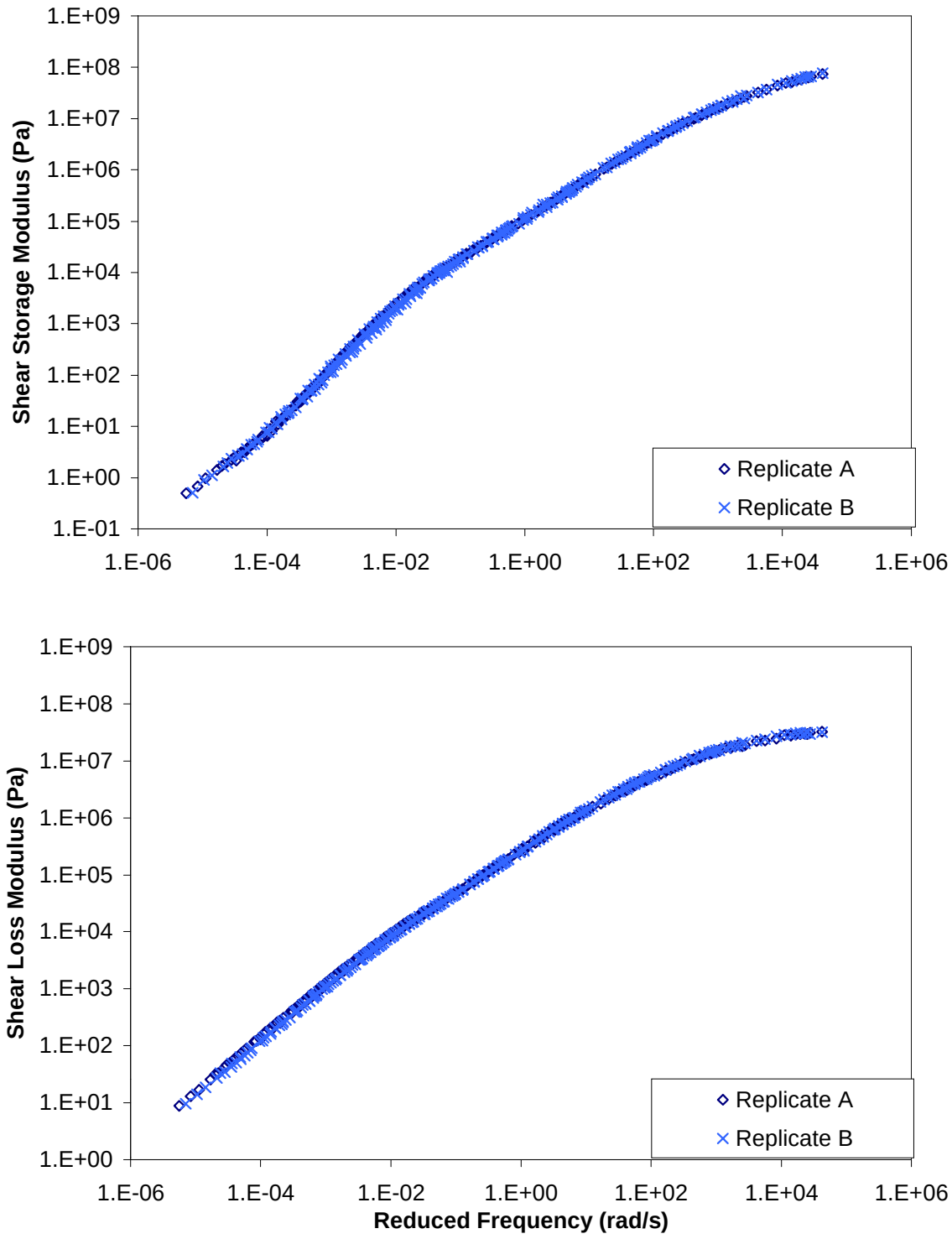


Figure A.9 Storage and loss shear moduli mastercurves for specimen AUN3.

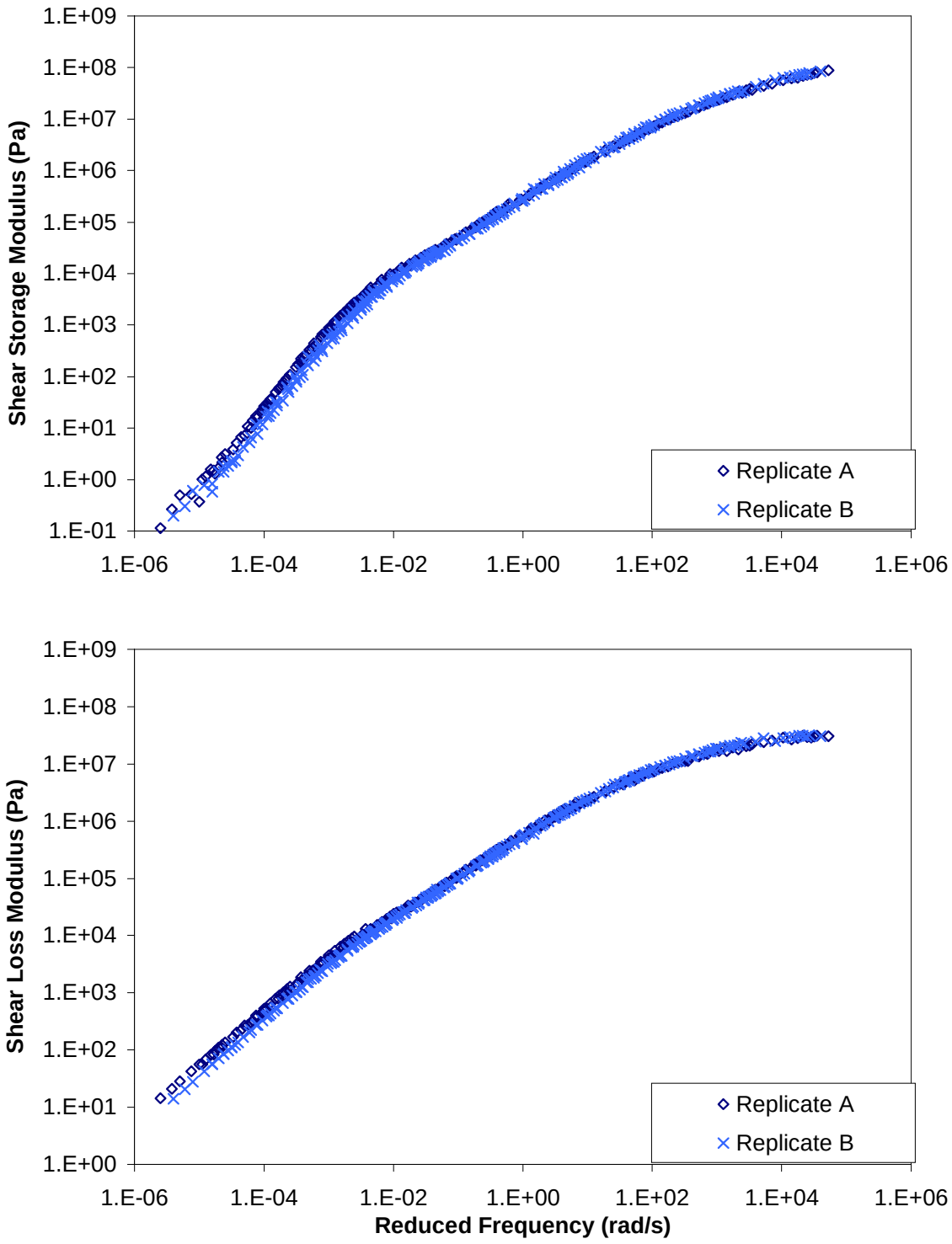


Figure A.10 Storage and loss shear moduli mastercurves for specimen ARN3.

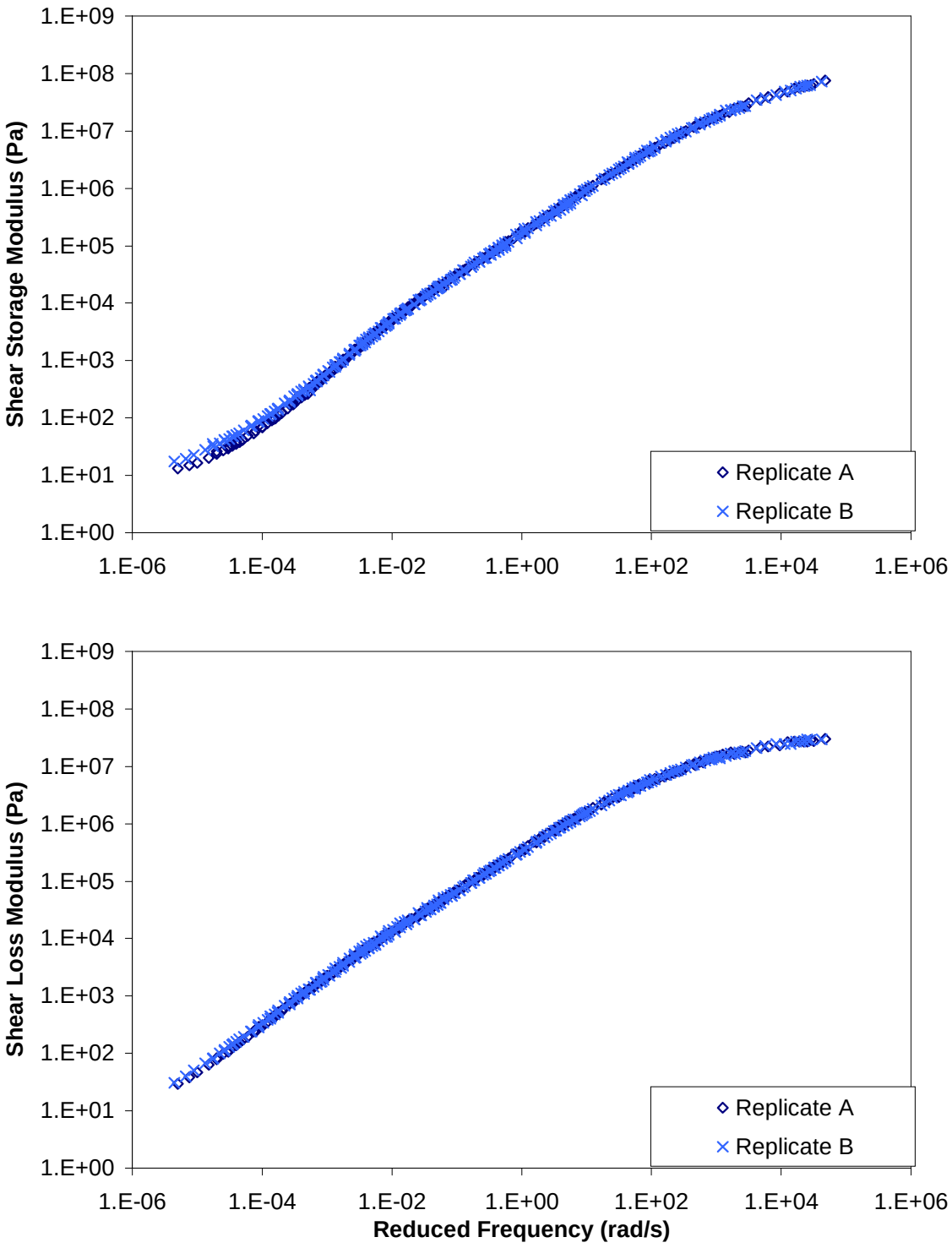


Figure A.11 Storage and loss shear moduli mastercurves for specimen AUN4.

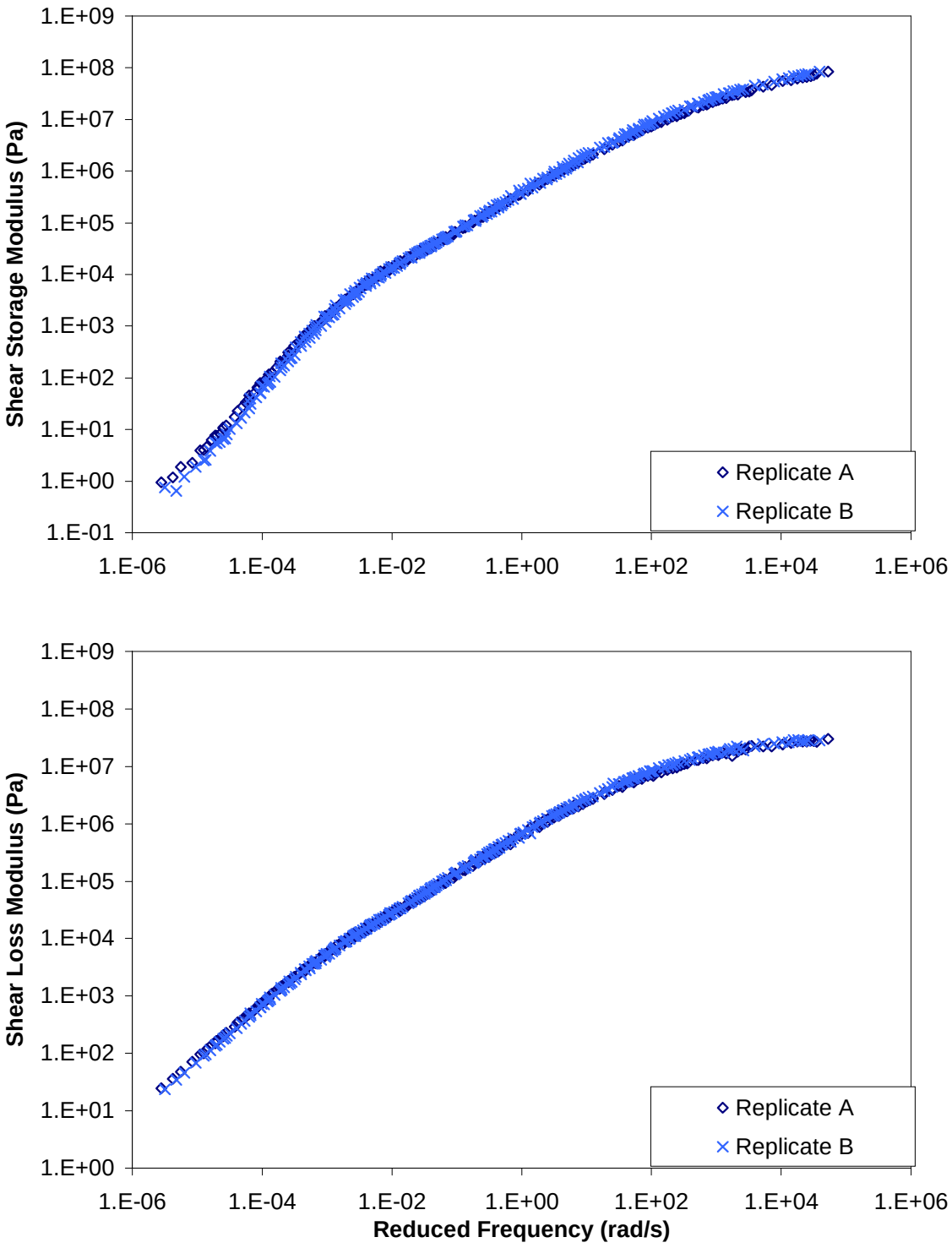


Figure A.12 Storage and loss shear moduli mastercurves for specimen ARN4.

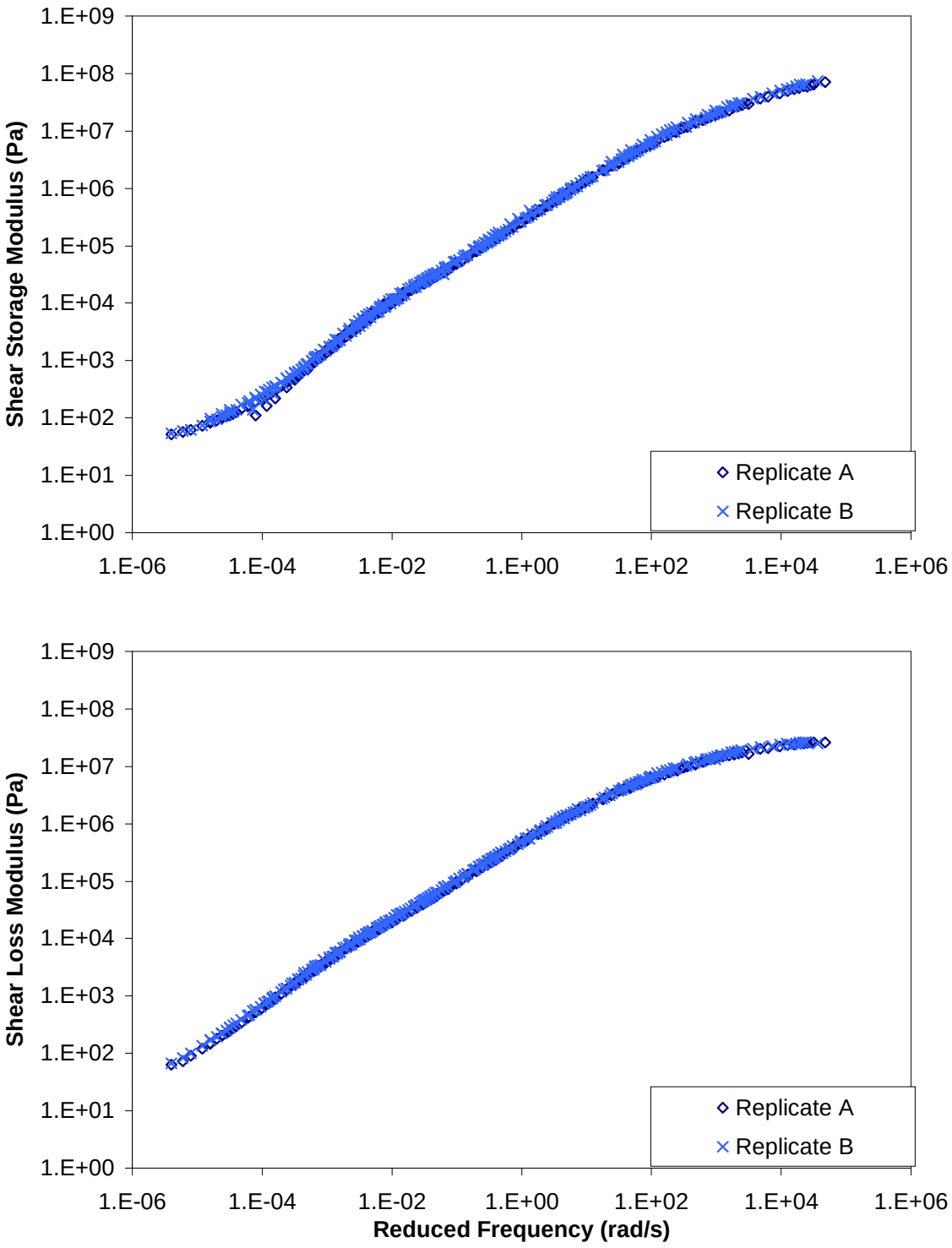


Figure A.13 Storage and loss shear moduli mastercurves for specimen AUN5.

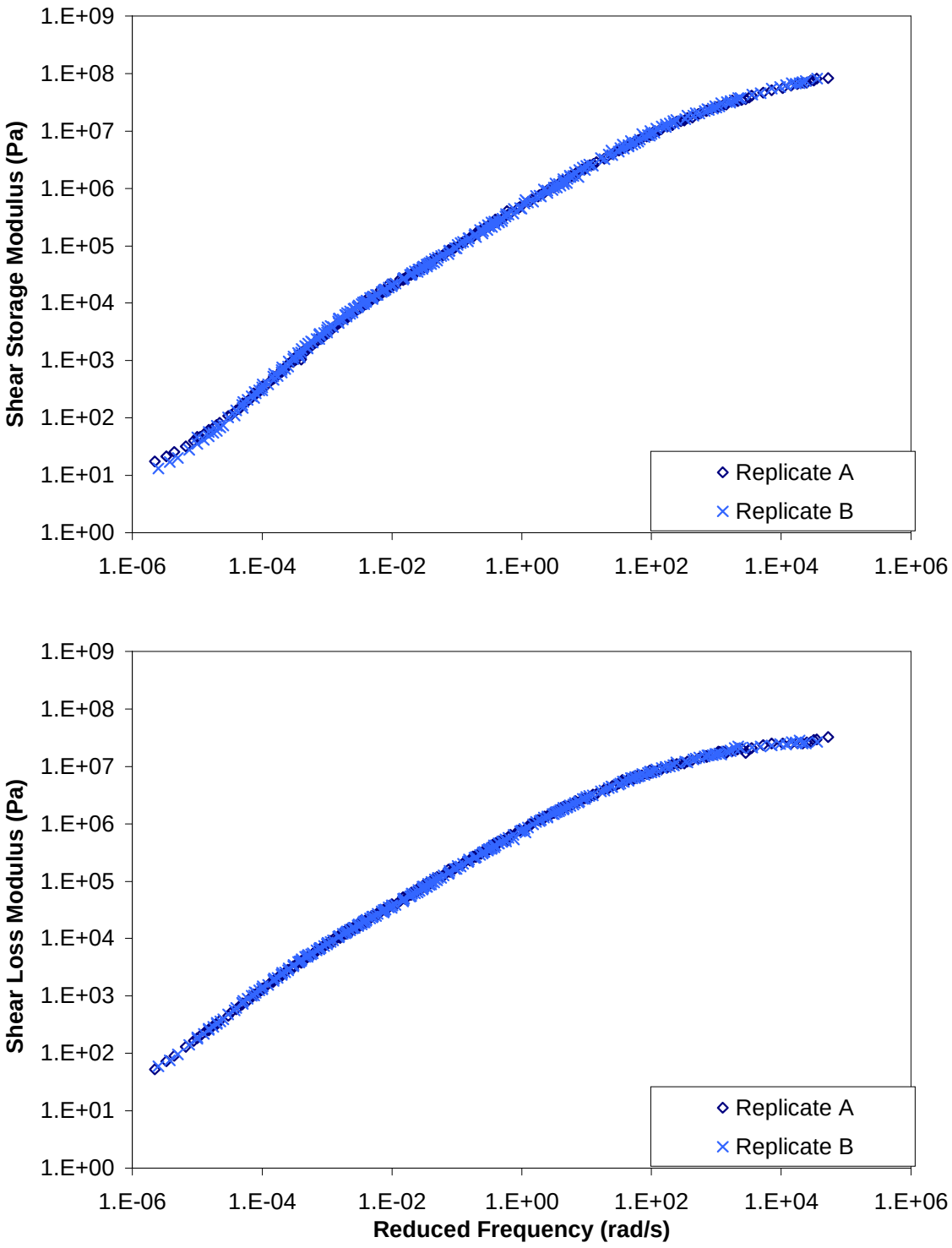


Figure A.14 Storage and loss shear moduli mastercurves for specimen ARN5.

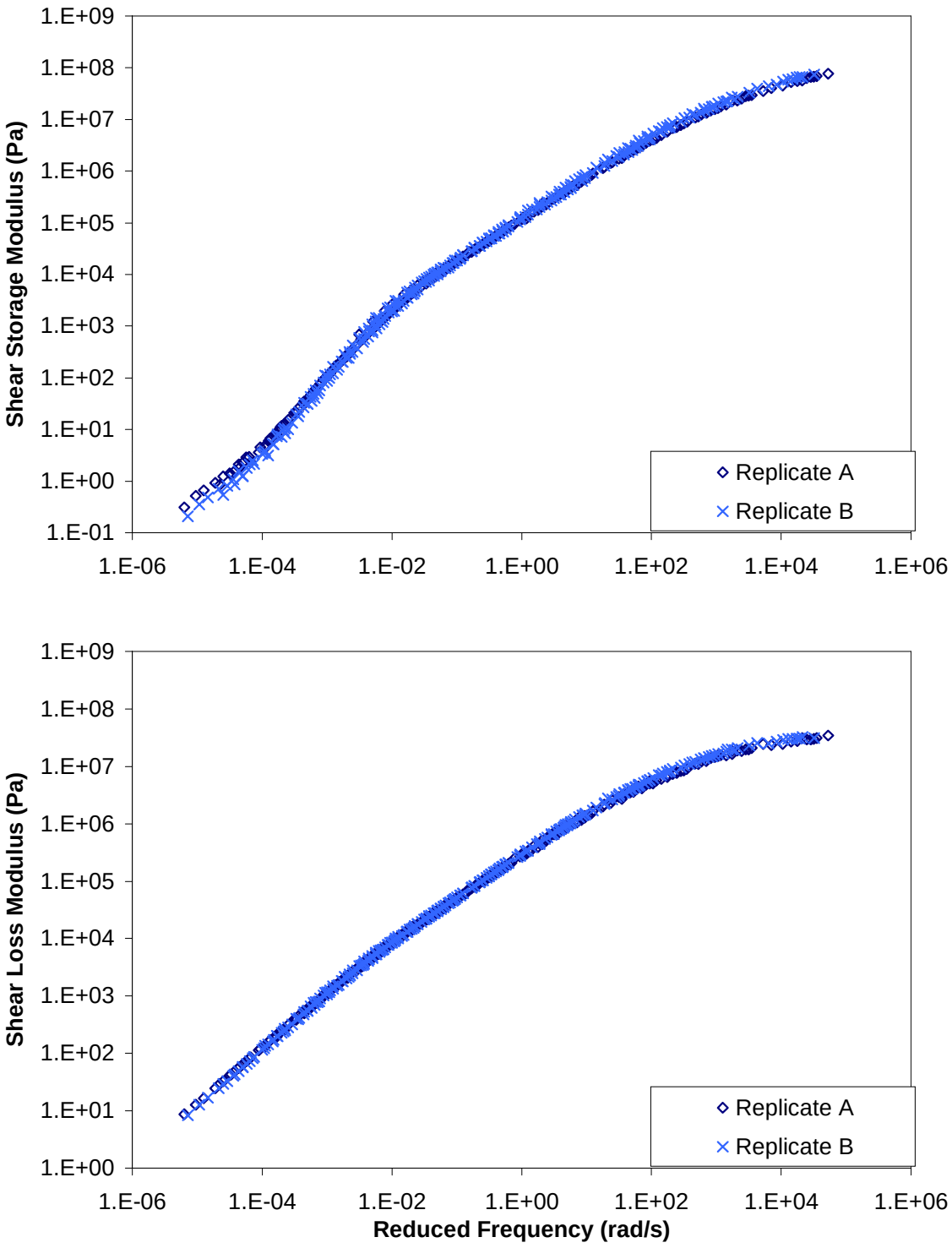


Figure A.15 Storage and loss shear moduli mastercurves for specimen AUS3.

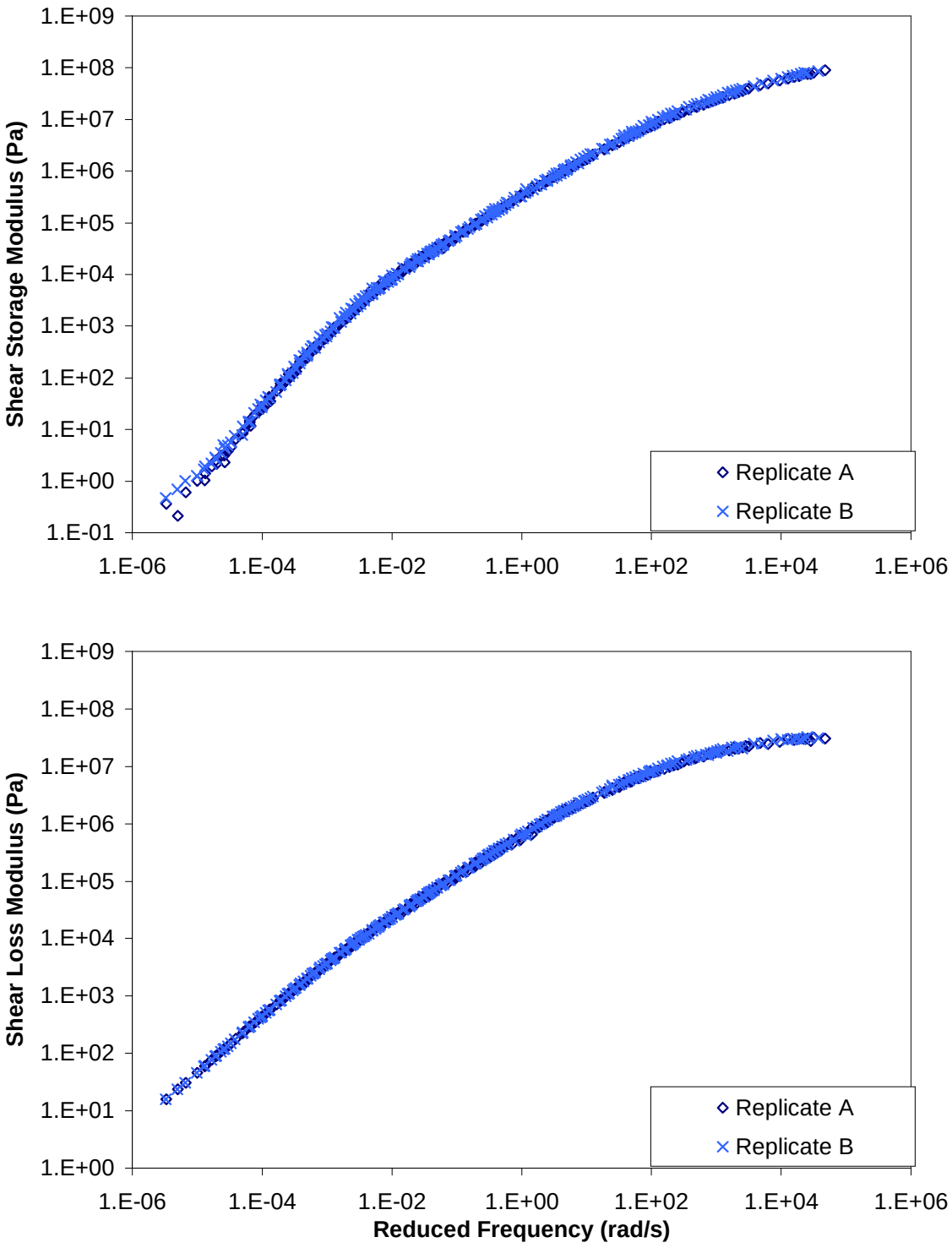


Figure A.16 Storage and loss shear moduli mastercurves for specimen ARS3.

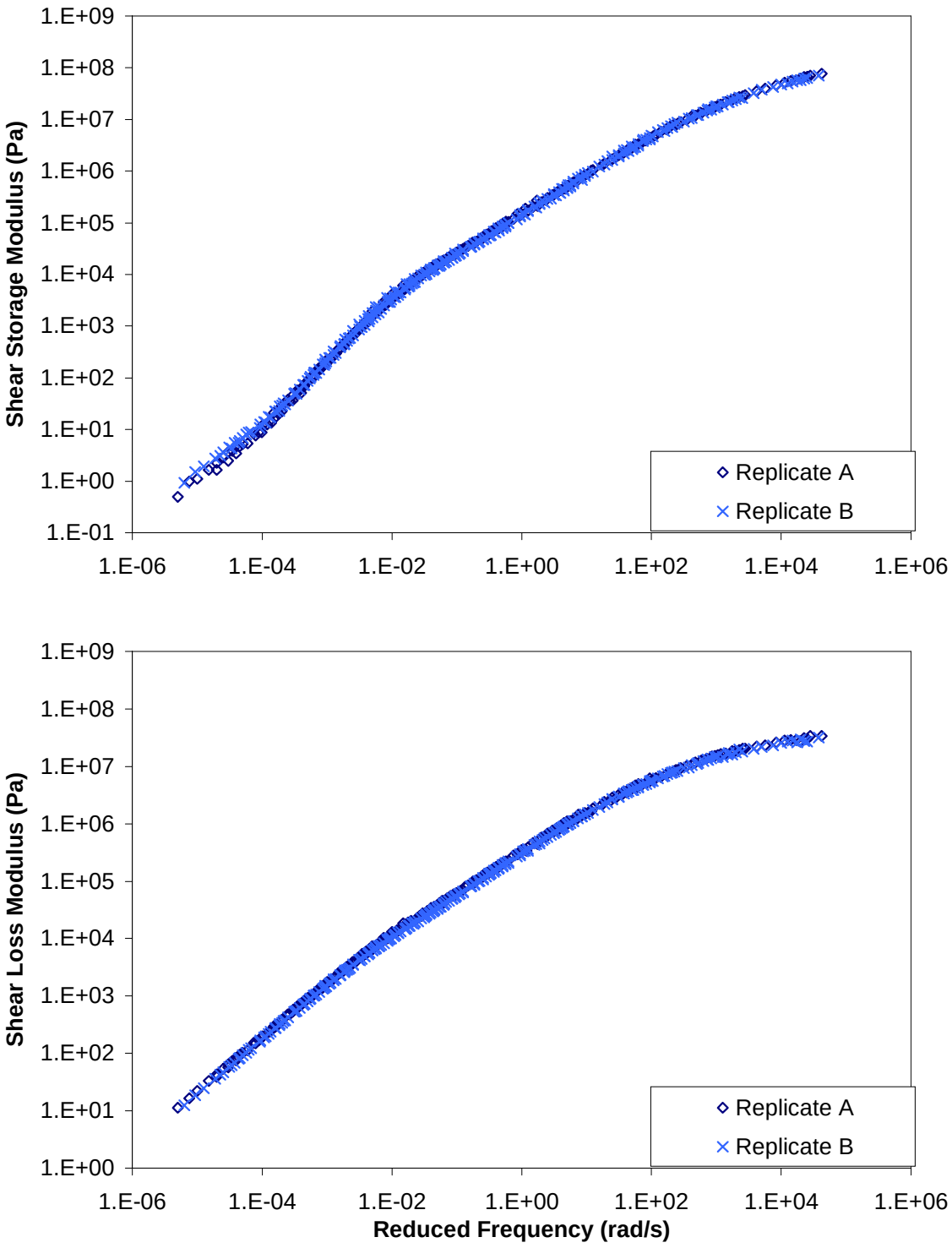


Figure A.17 Storage and loss shear moduli mastercurves for specimen AUS4.

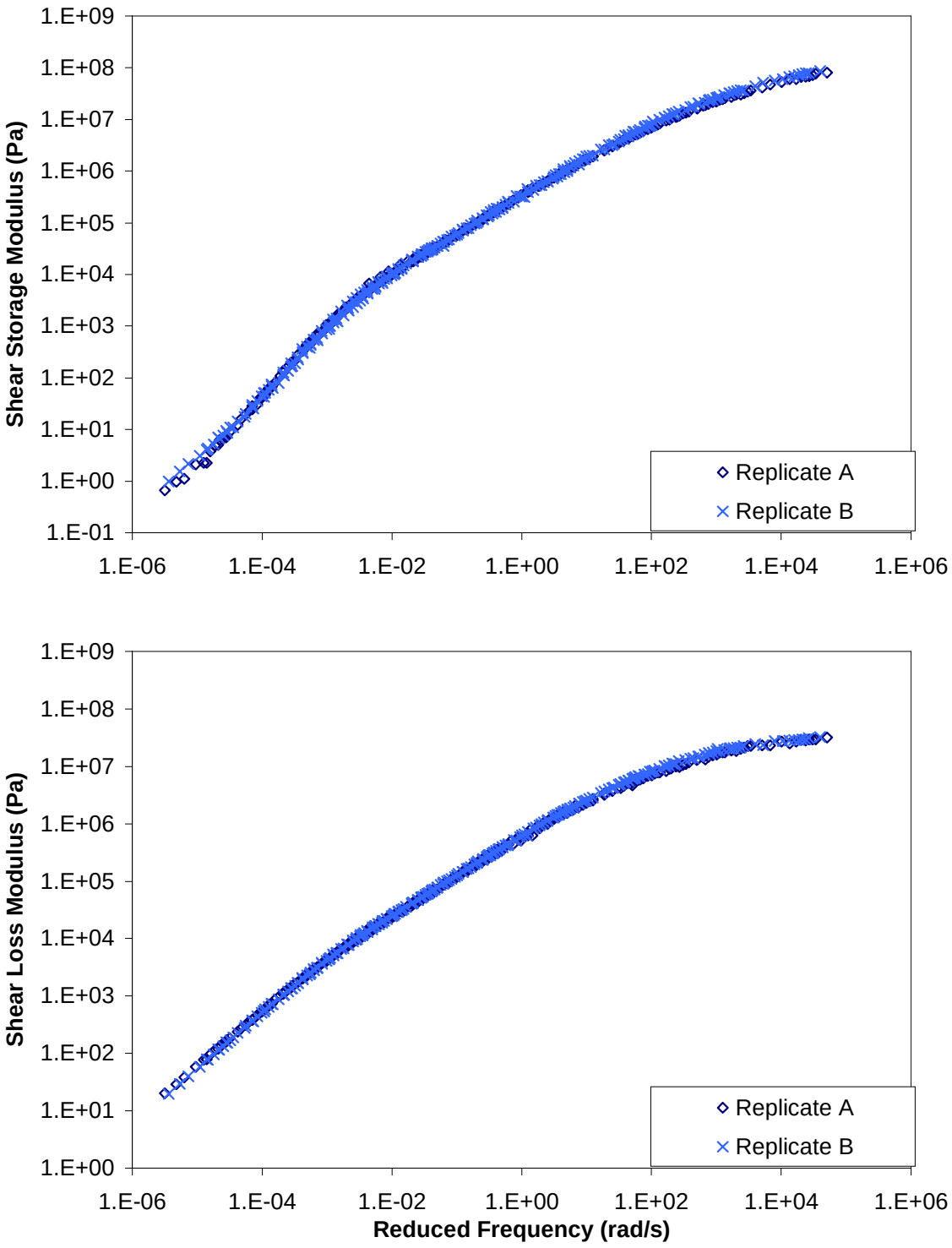


Figure A.18 Storage and loss shear moduli mastercurves for specimen ARS4.

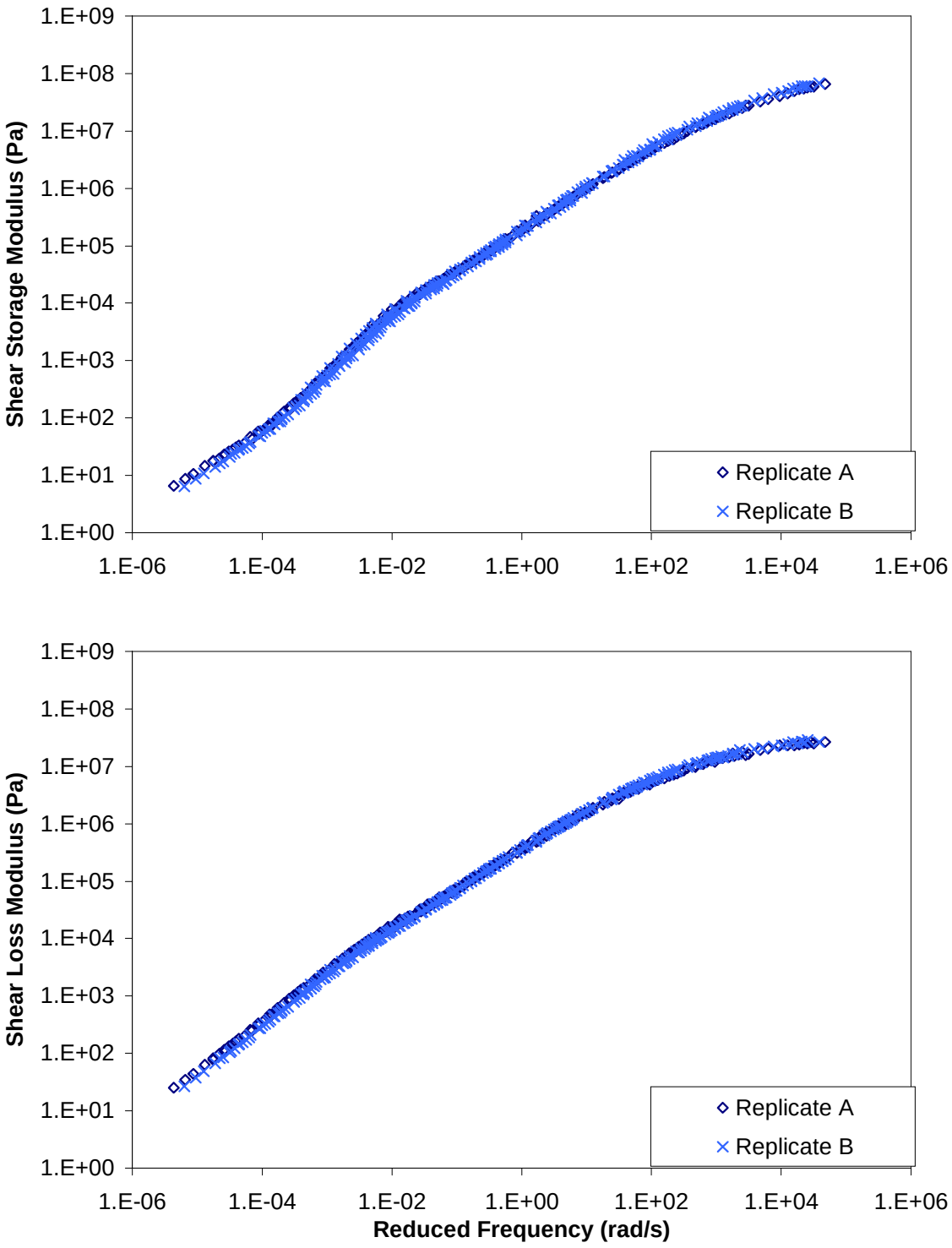


Figure A.19 Storage and loss shear moduli mastercurves for specimen AUS5.

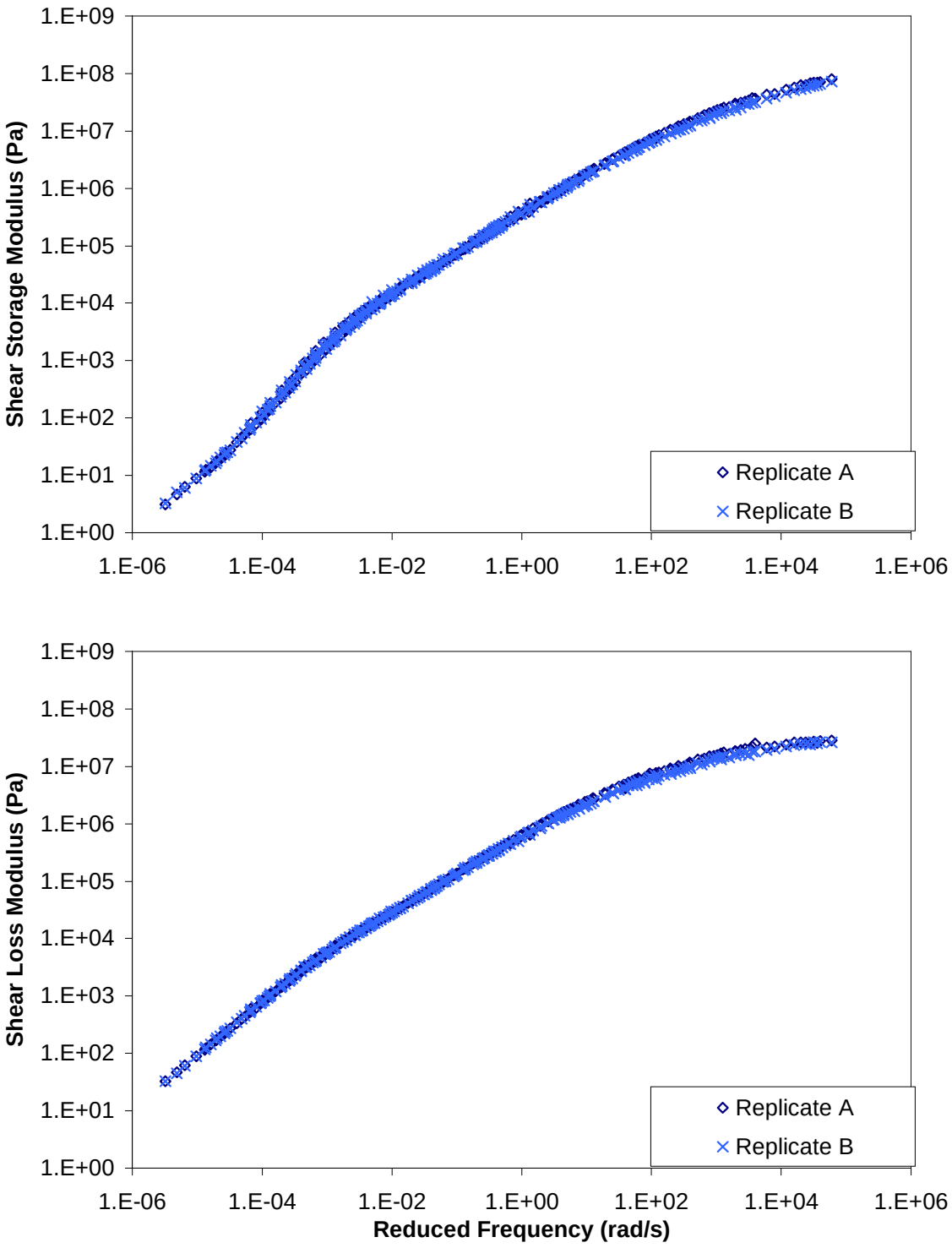


Figure A.20 Storage and loss shear moduli mastercurves for specimen ARS5.

# APPENDIX B

- This appendix includes the shift factors used in construction of storage and loss shear moduli mastercurves for all original specimens.

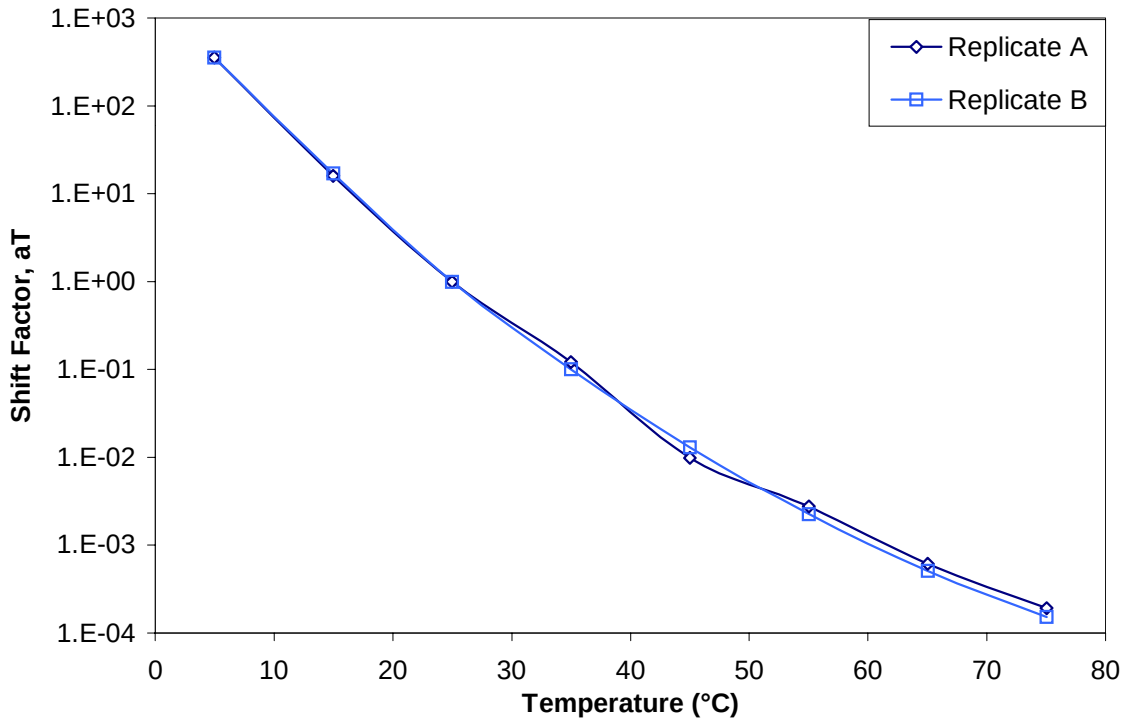


Figure B.1 Shift factors for original specimen AU00.

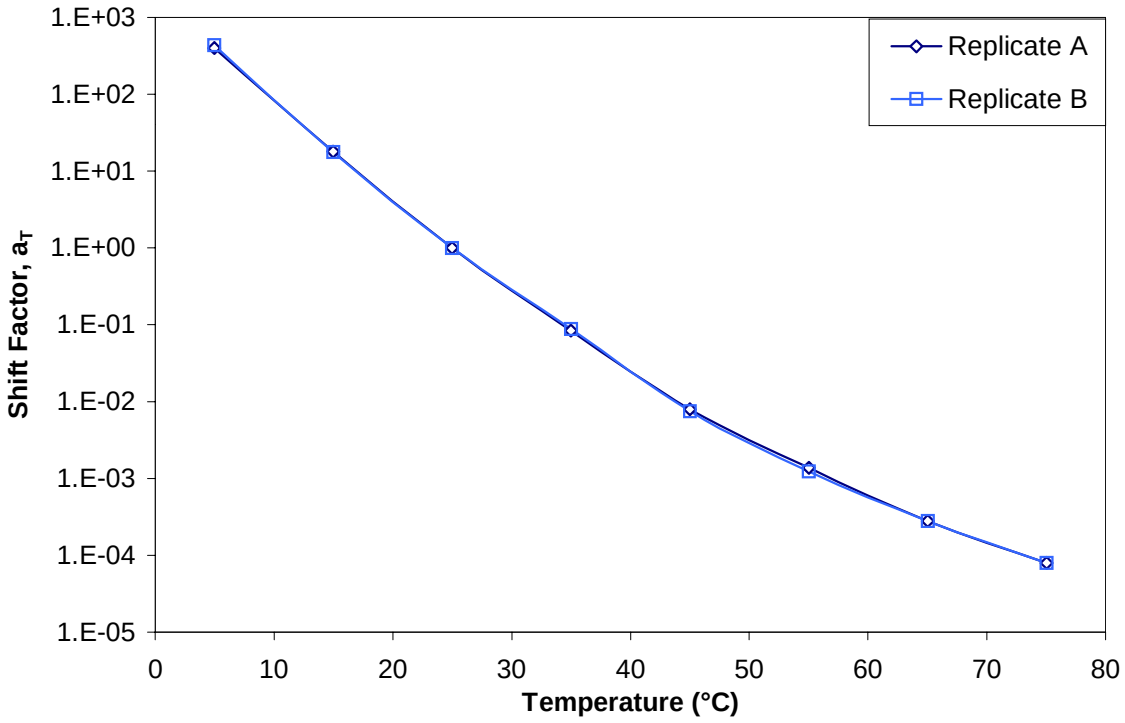


Figure B.2 Shift factors for original specimen AR00.

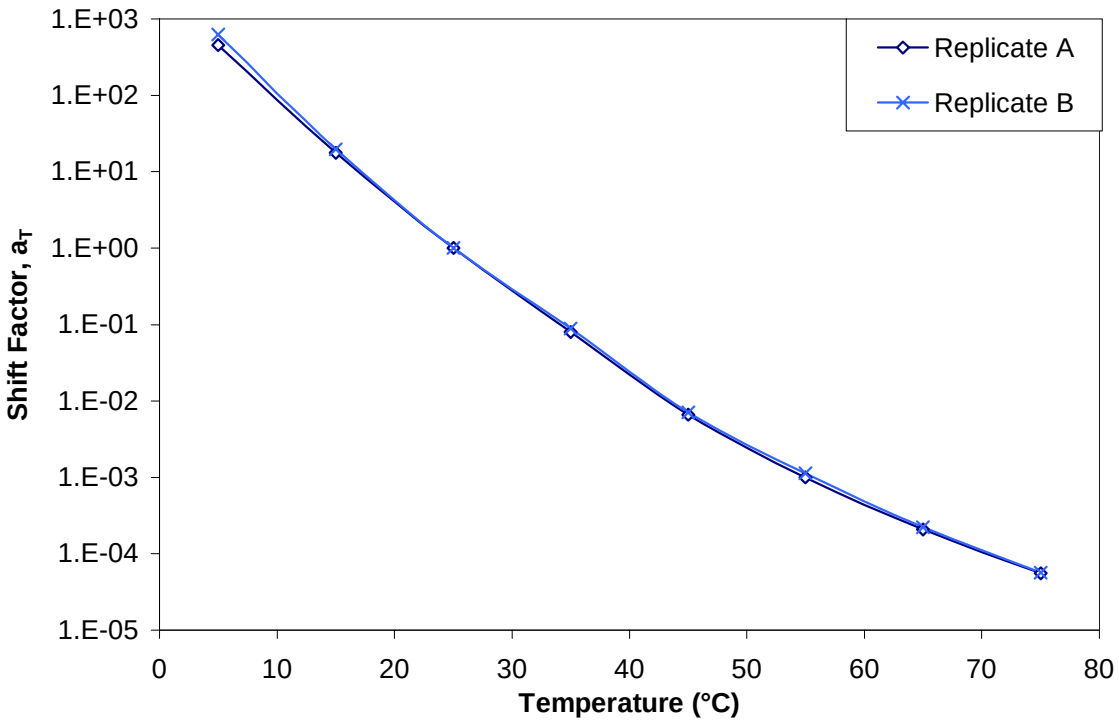


Figure B.3 Shift factors for original specimen AUG3.

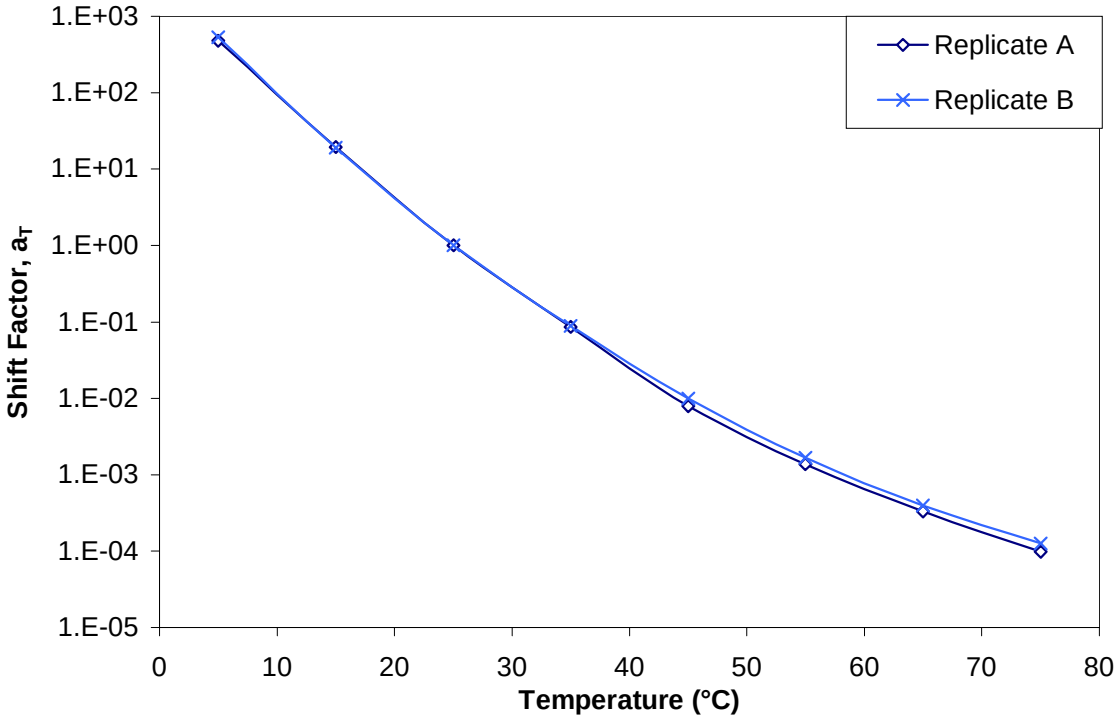


Figure B.4 Shift factors for original specimen ARG3.

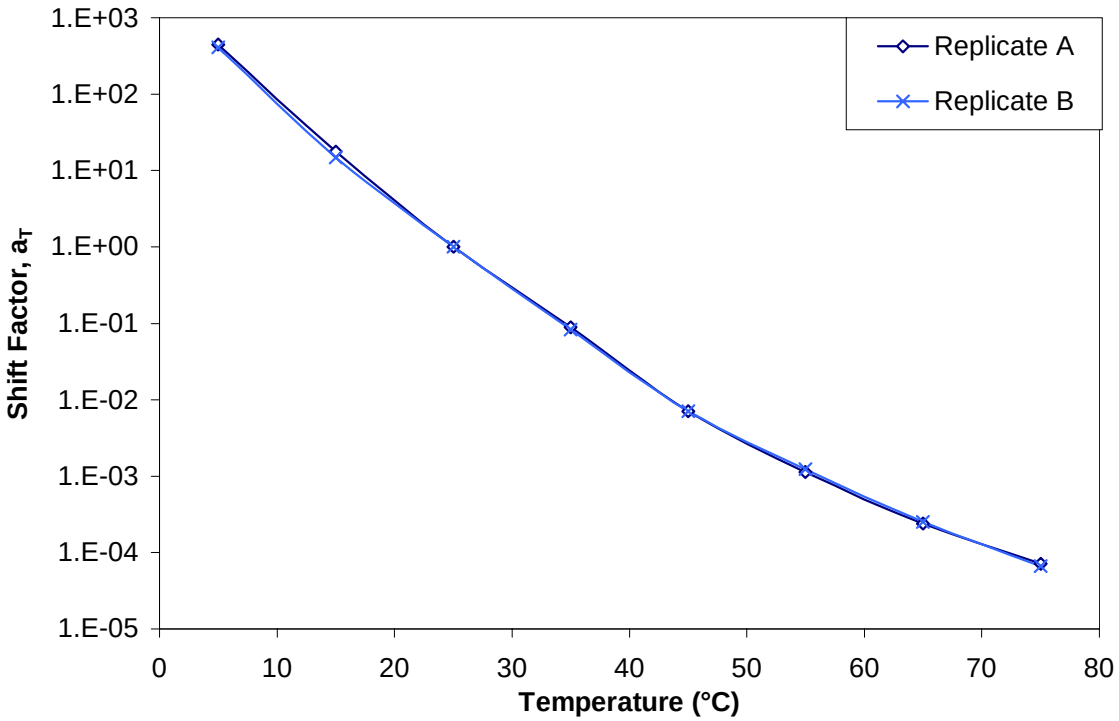


Figure B.5 Shift factors for original specimen AUG4.

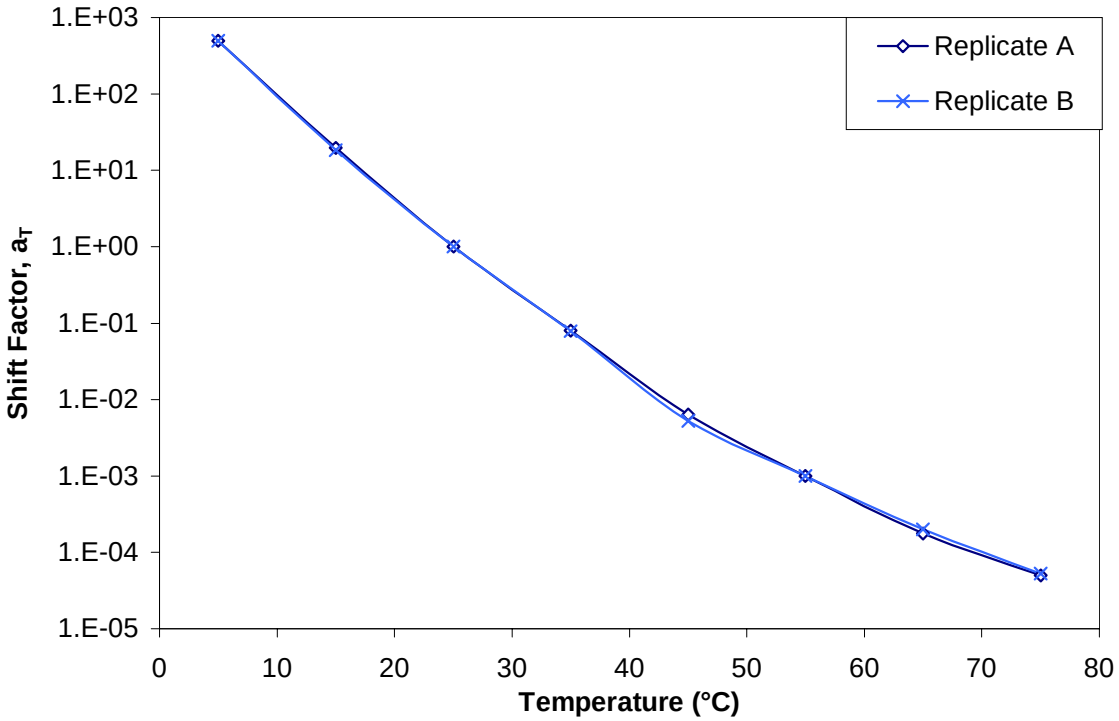


Figure B.6 Shift factors for original specimen ARG4.

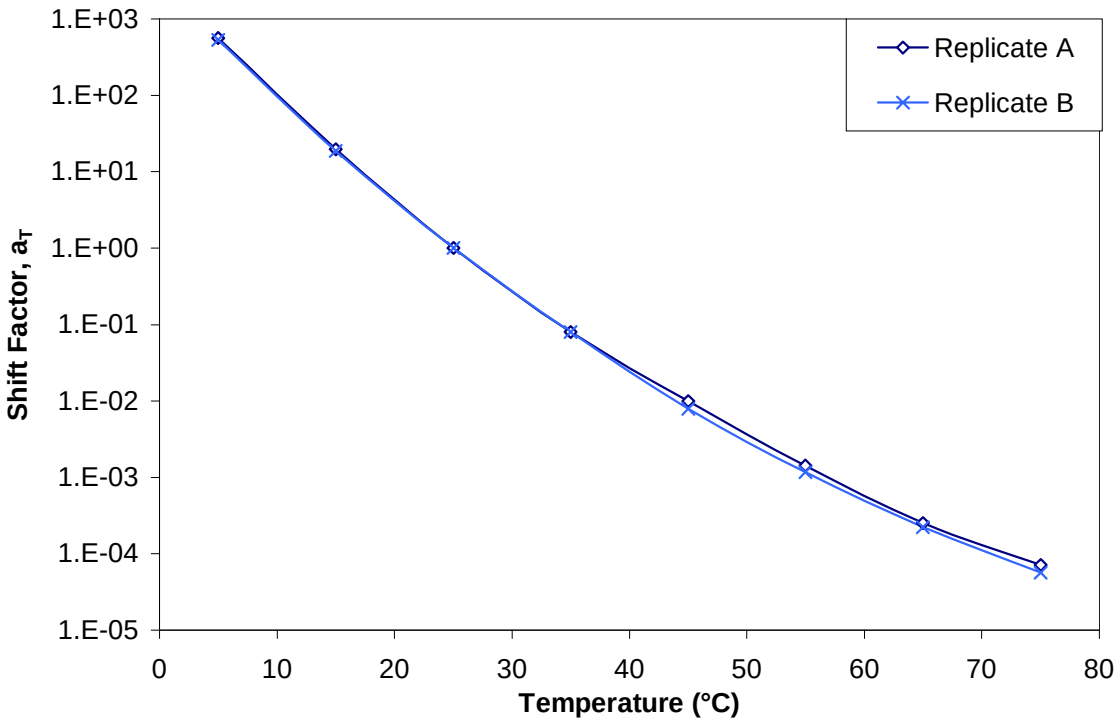


Figure B.7 Shift factors for original specimen AUG5.

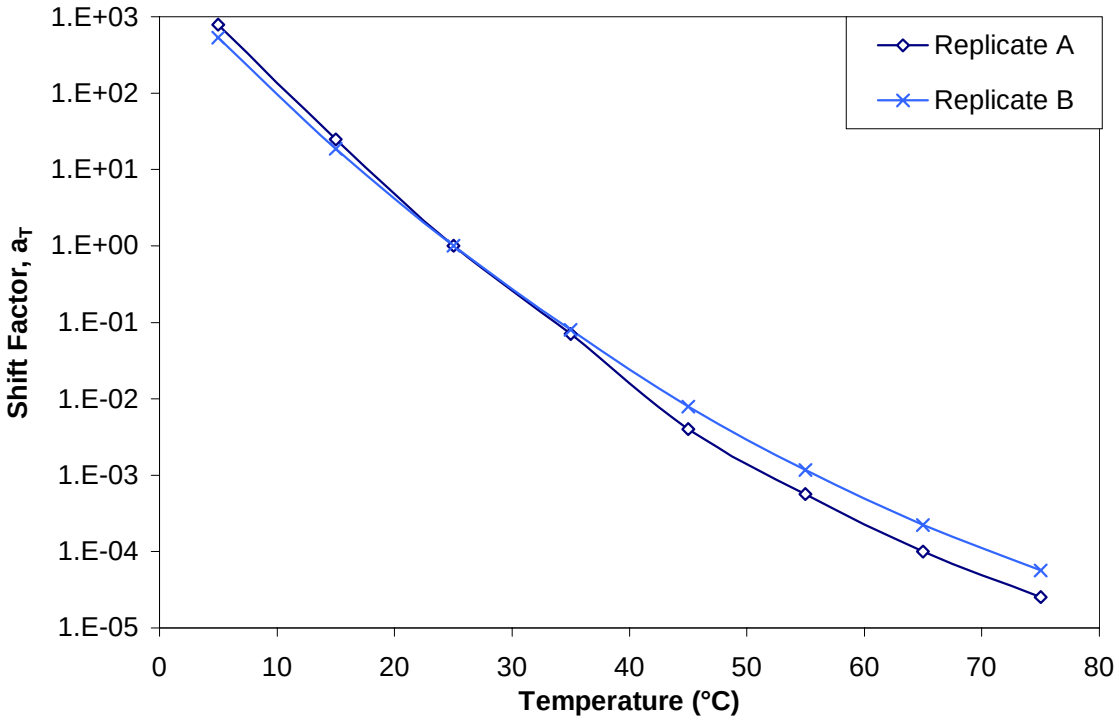


Figure B.8 Shift factors for original specimen ARG5.

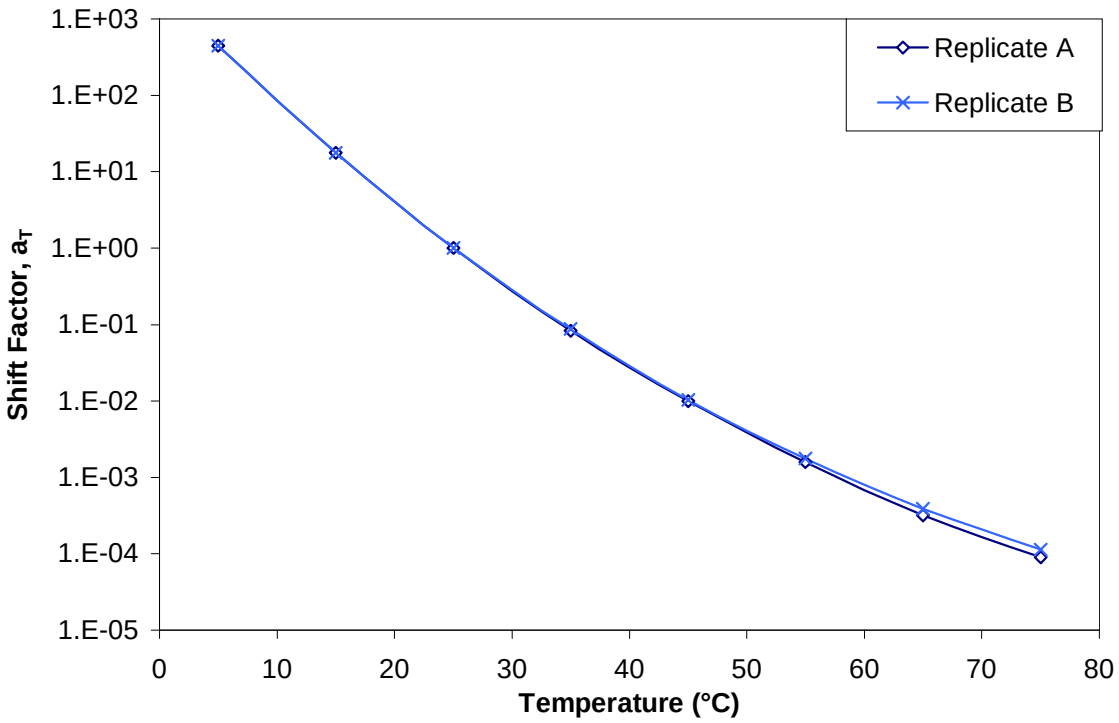


Figure B.9 Shift factors for original specimen AUN3.

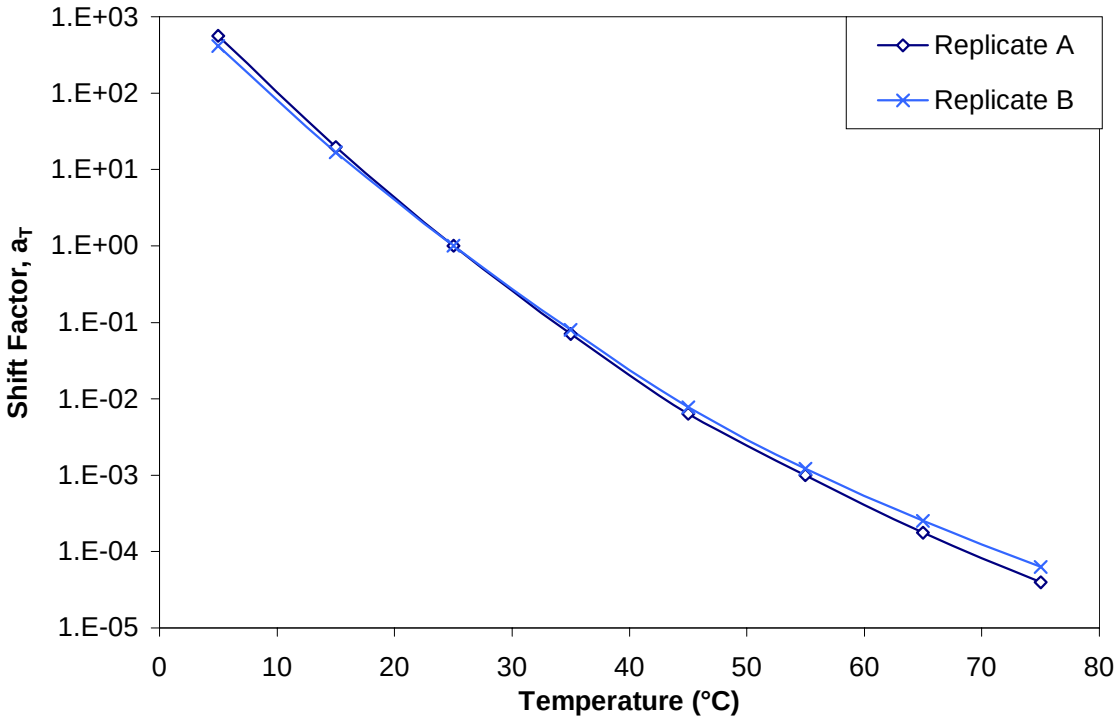


Figure B.10 Shift factors for original specimen ARN3.

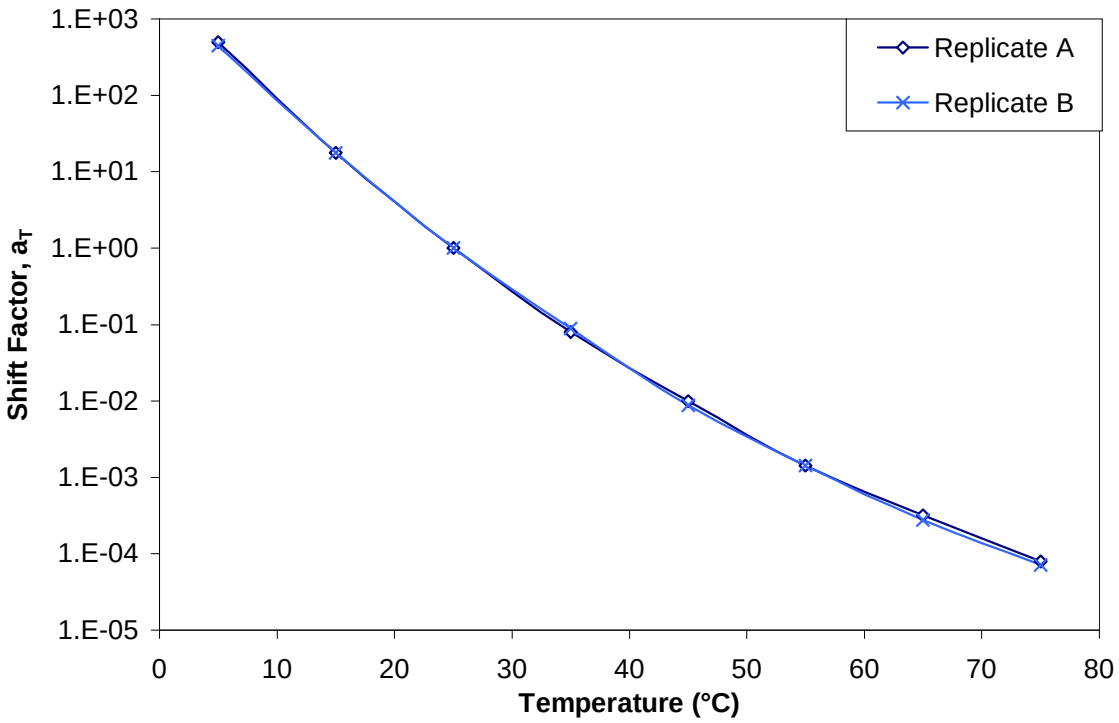


Figure B.11 Shift factors for original specimen AUN4.

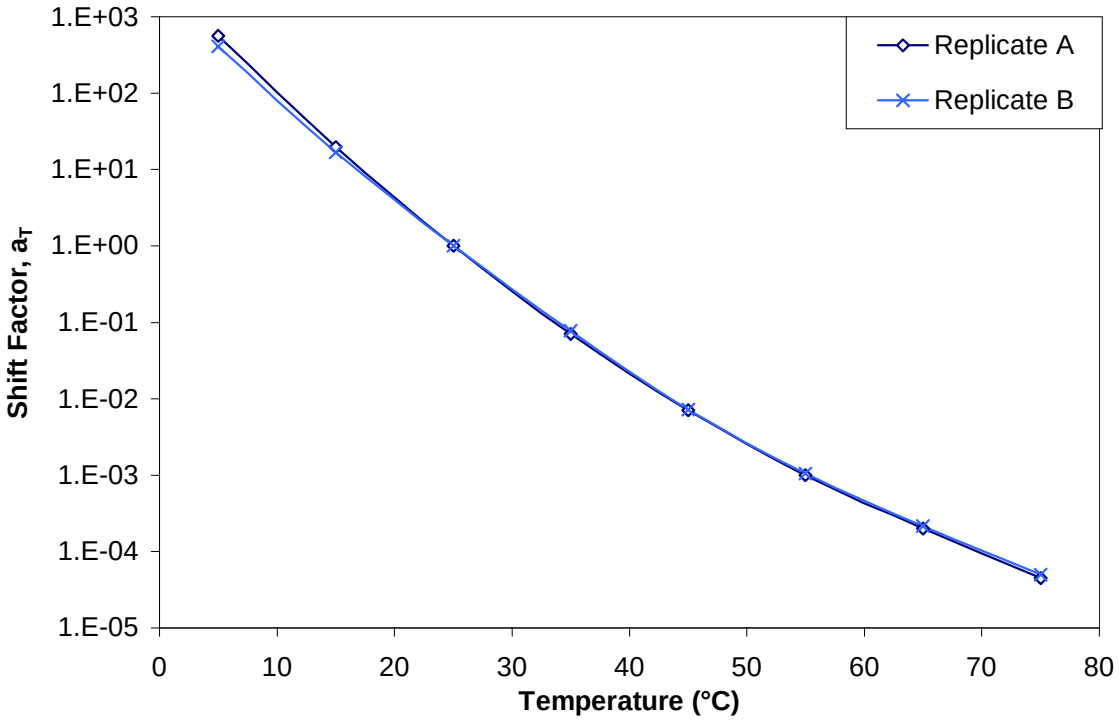


Figure B.12 Shift factors for original specimen ARN4.

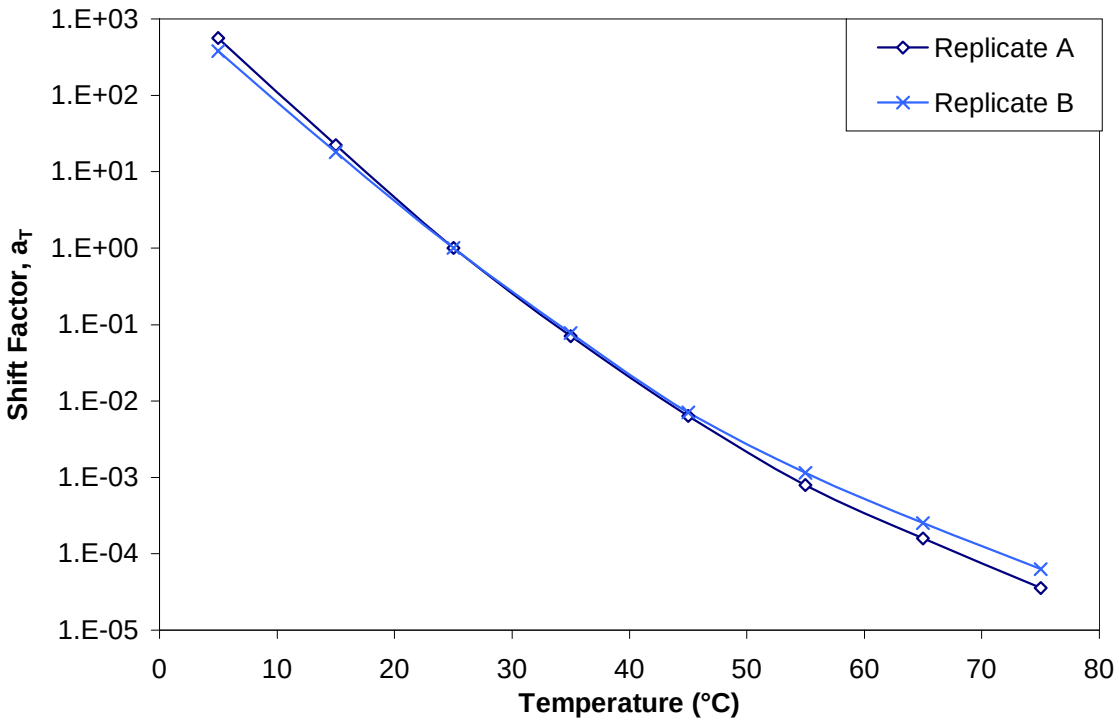


Figure B.13 Shift factors for original specimen AUN5.

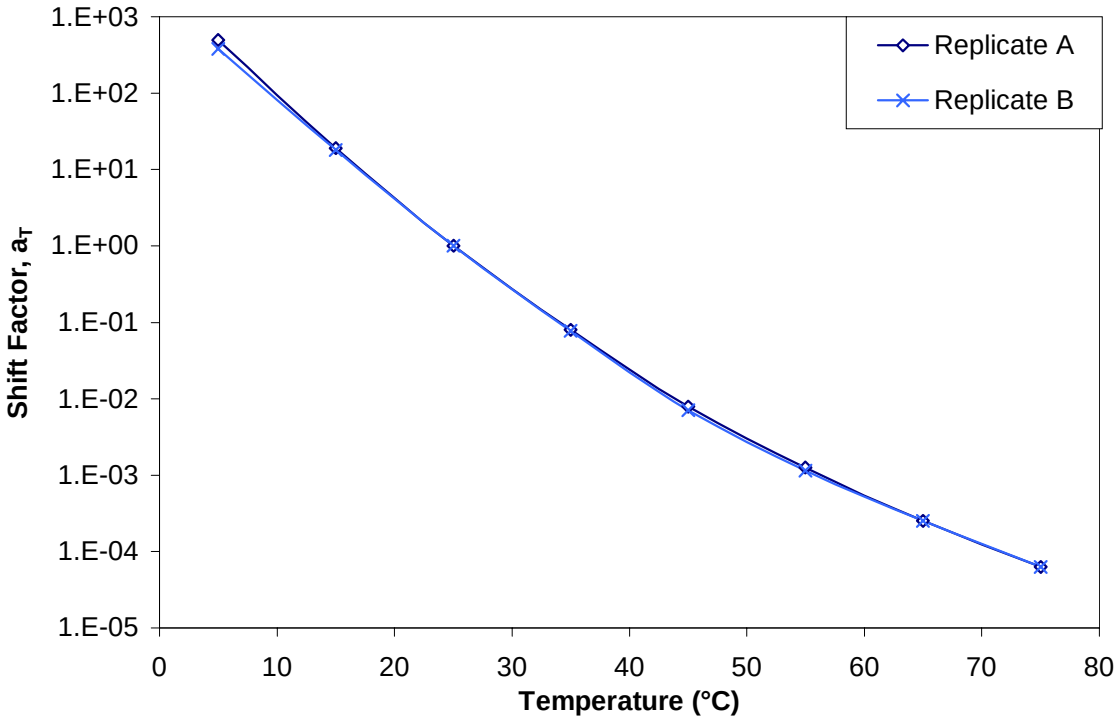


Figure B.14 Shift factors for original specimen ARN5.

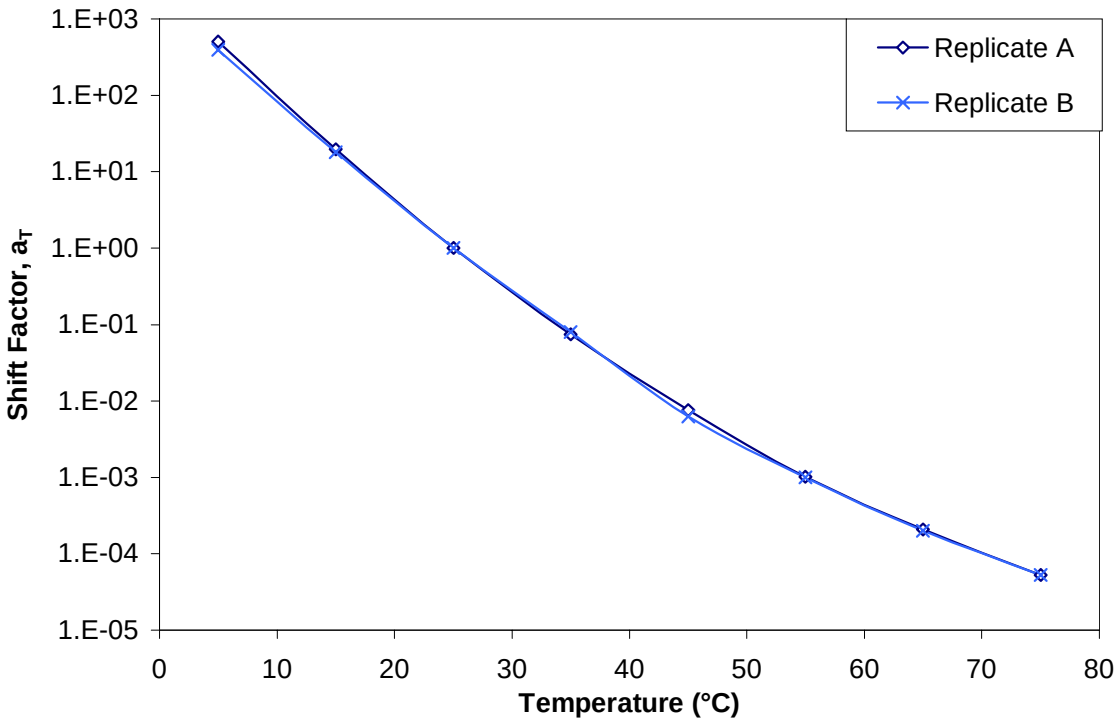


Figure B.15 Shift factors for original specimen AUS3.

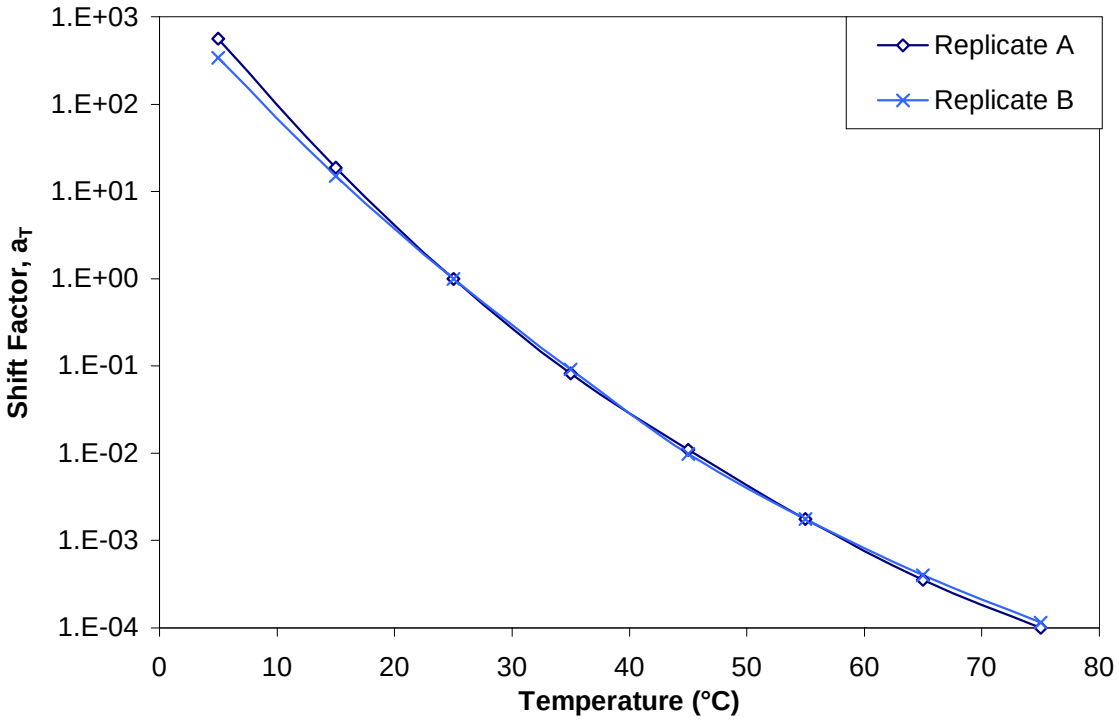


Figure B.16 Shift factors for original specimen ARS3.

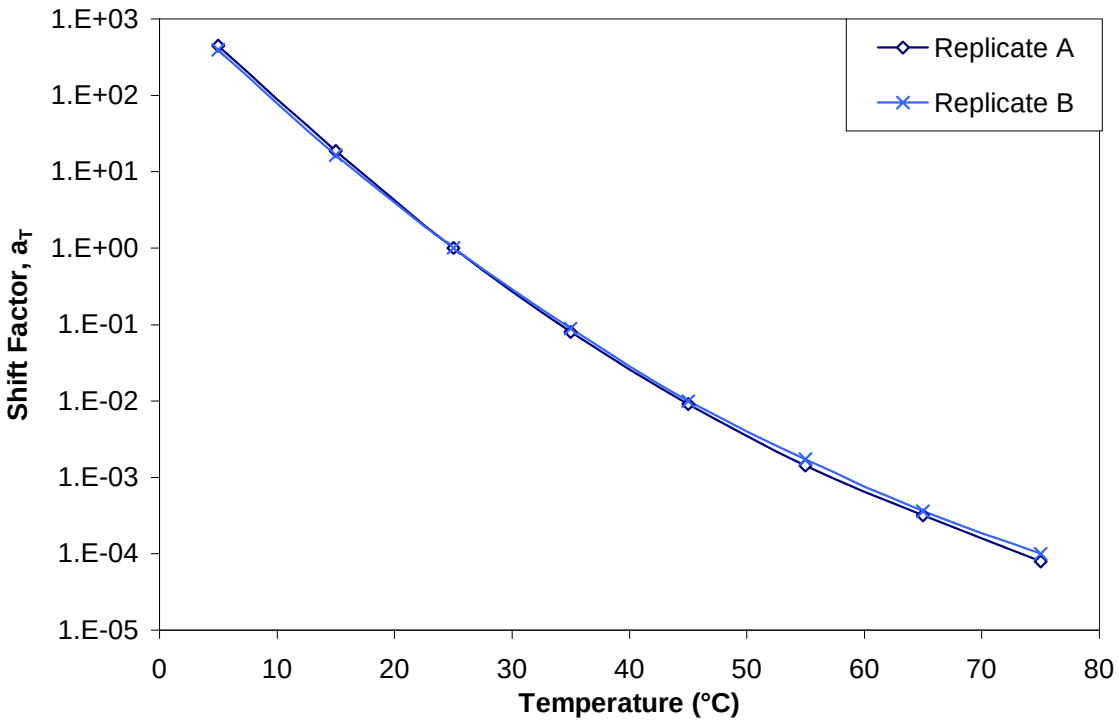


Figure B.17 Shift factors for original specimen AUS4.

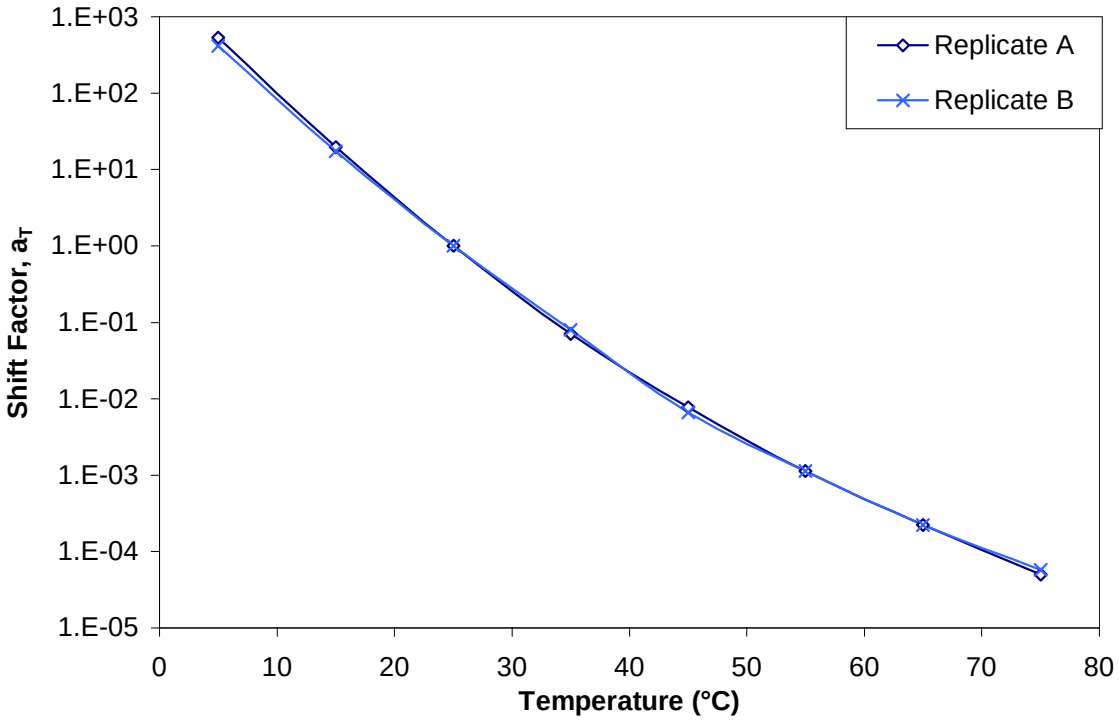


Figure B.18 Shift factors for original specimen ARS4.

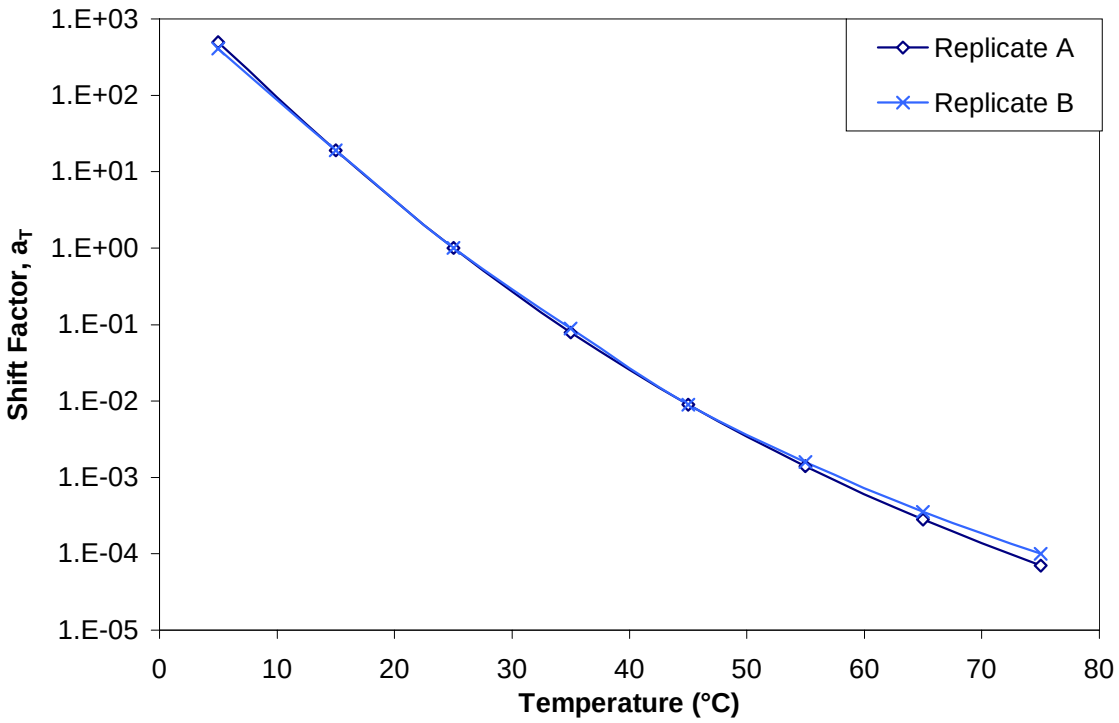


Figure B.19 Shift factors for original specimen AUS5.

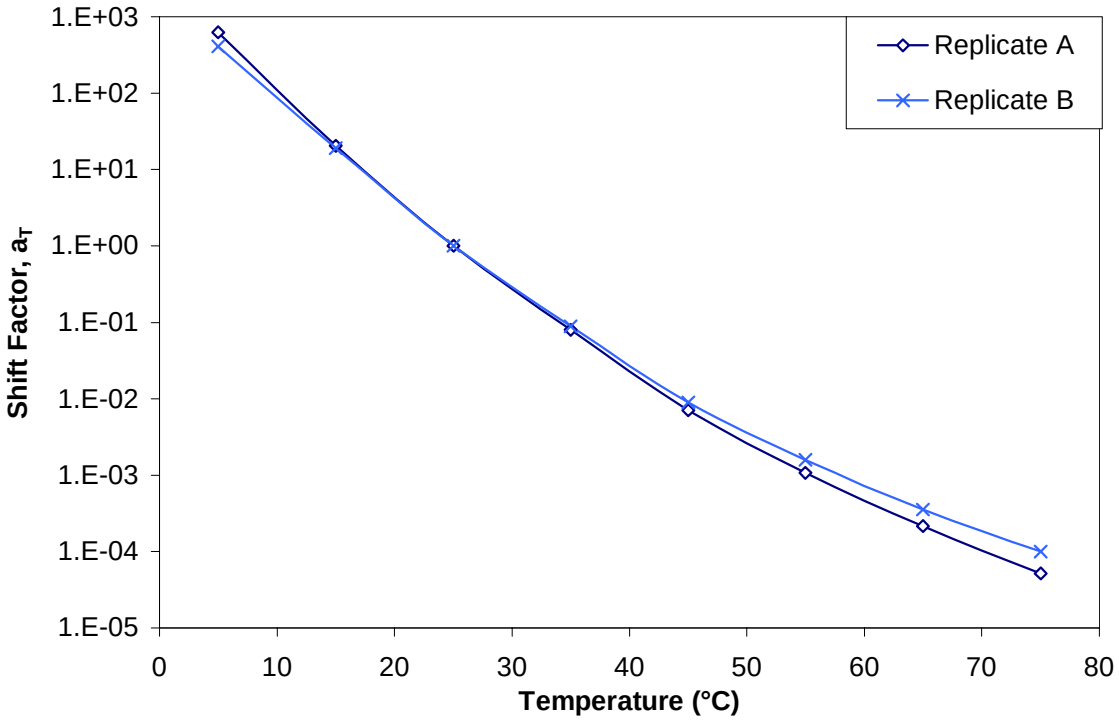


Figure B.20 Shift factors for original specimen ARS5.

# APPENDIX C

- This appendix includes the storage and loss shear modulus mastercurves for all stored specimens.

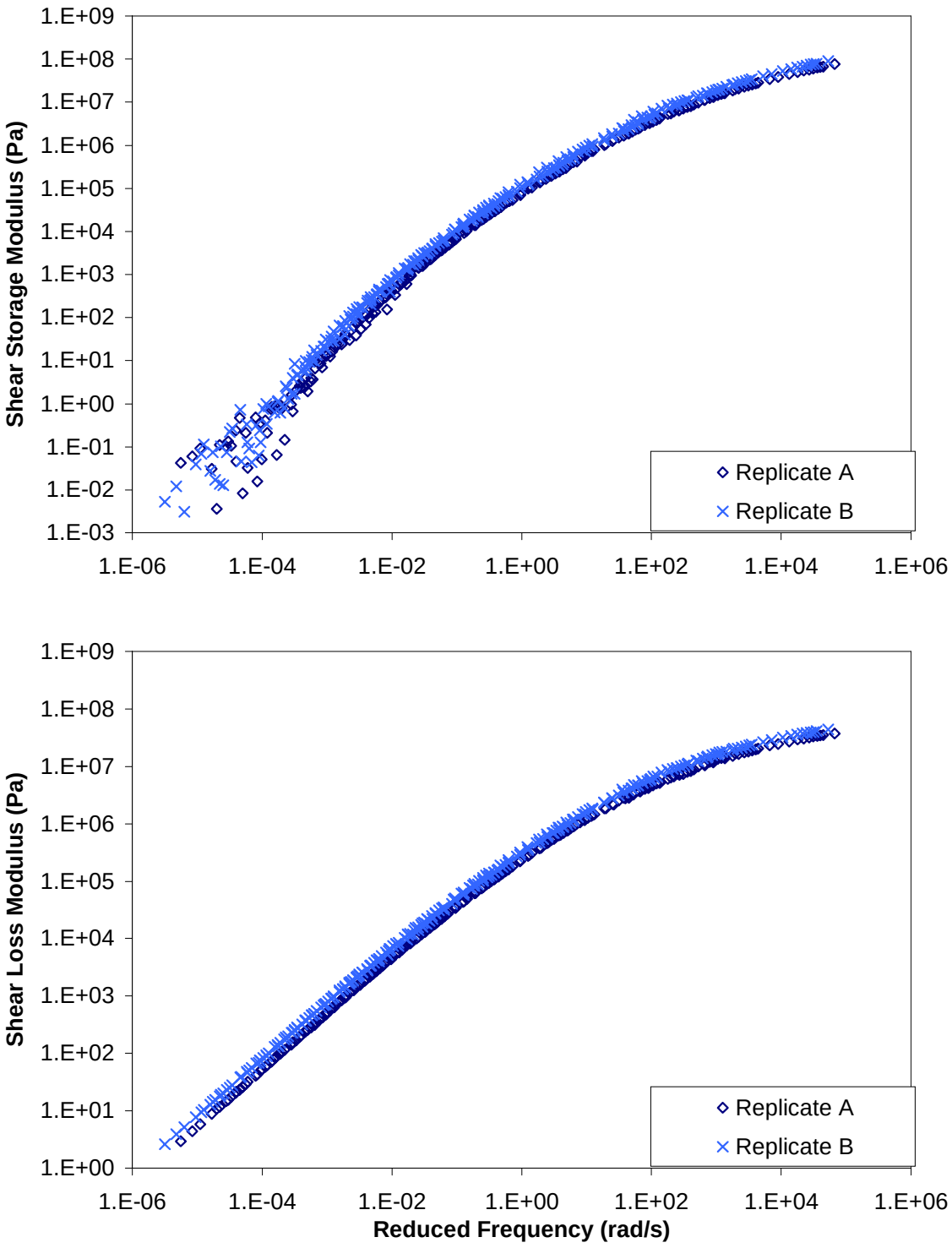


Figure C.1 Storage and loss shear moduli mastercurves for specimen AU00.

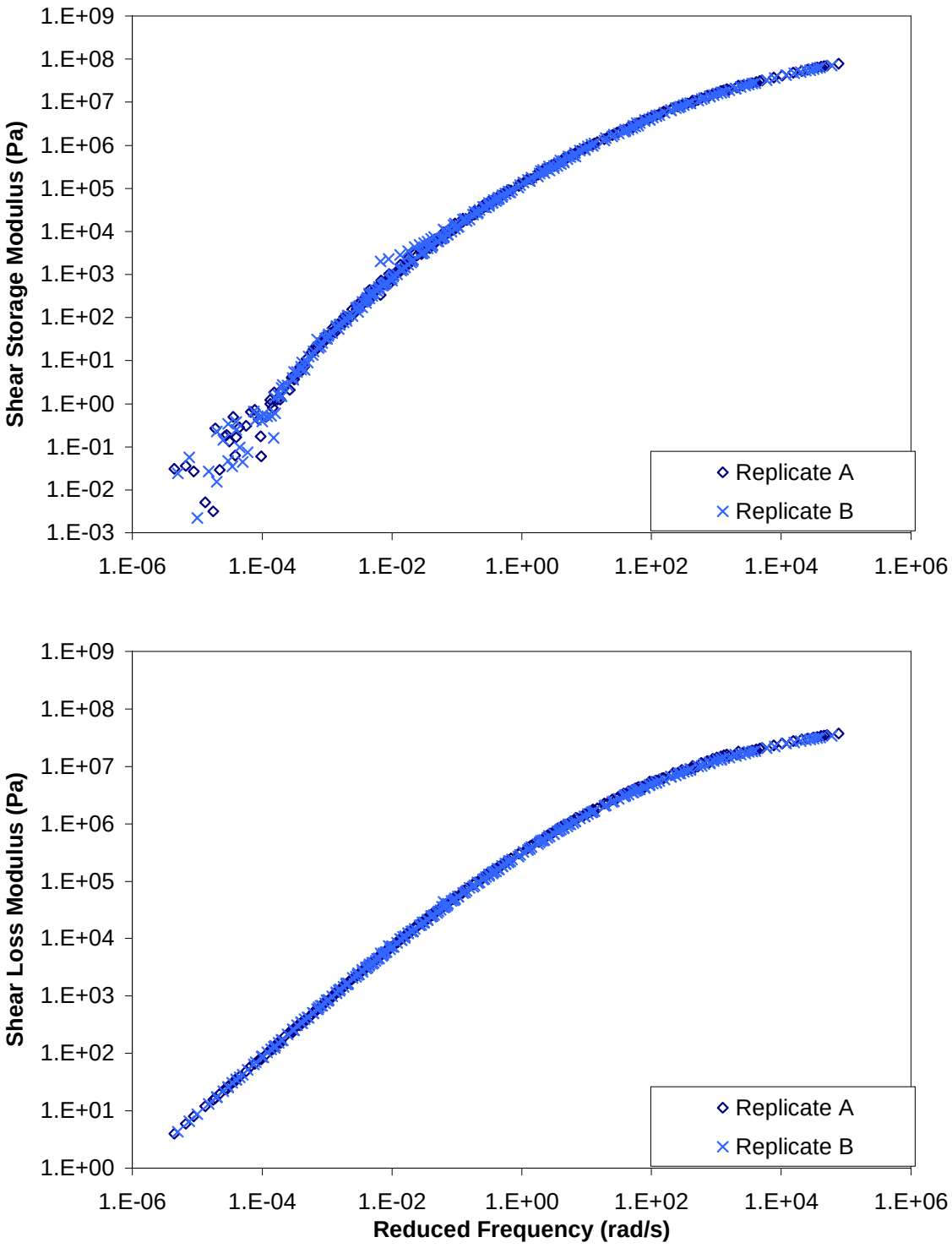


Figure C.2 Storage and loss shear moduli mastercurves for specimen AR00.

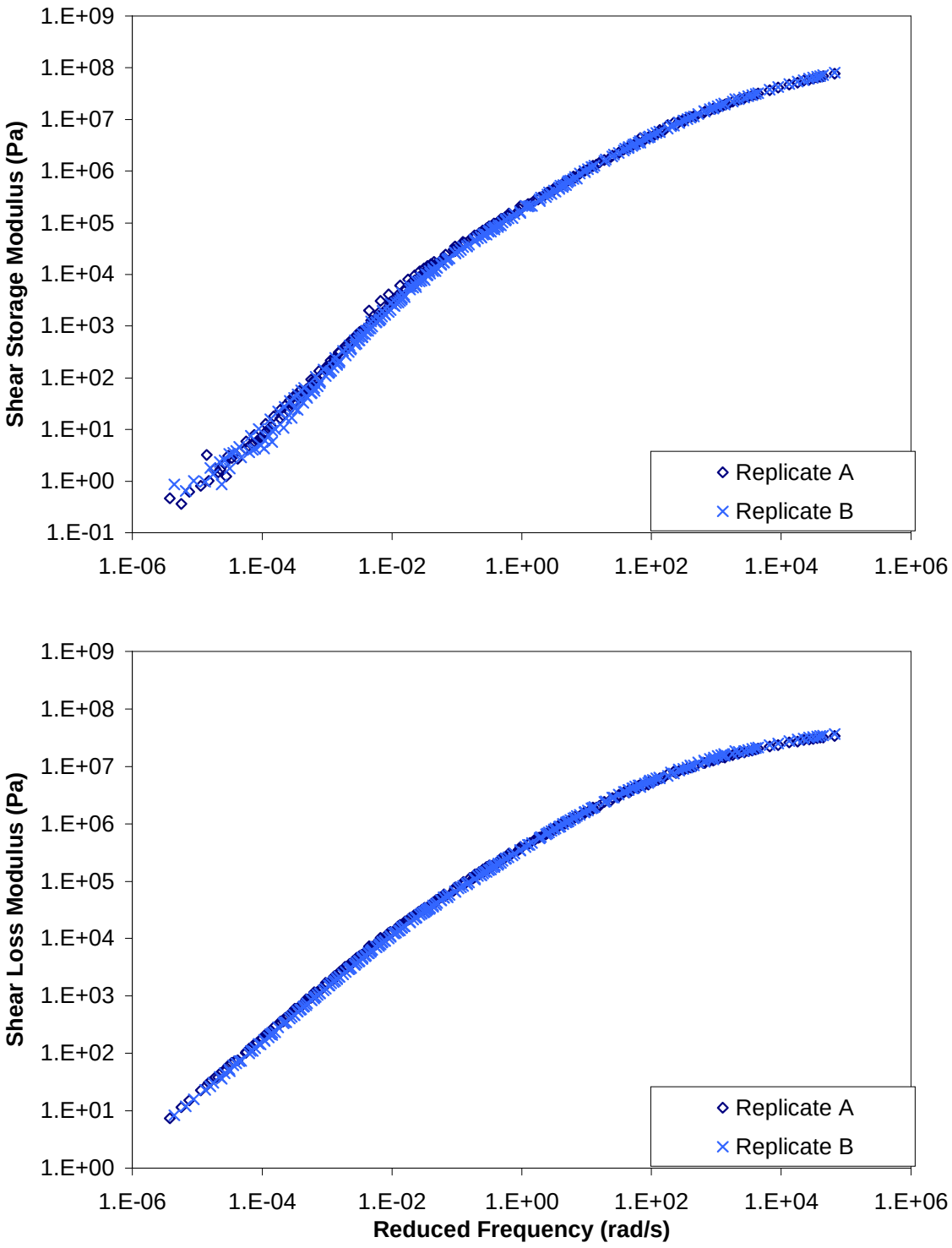


Figure C.3 Storage and loss shear moduli mastercurves for specimen AUG3.

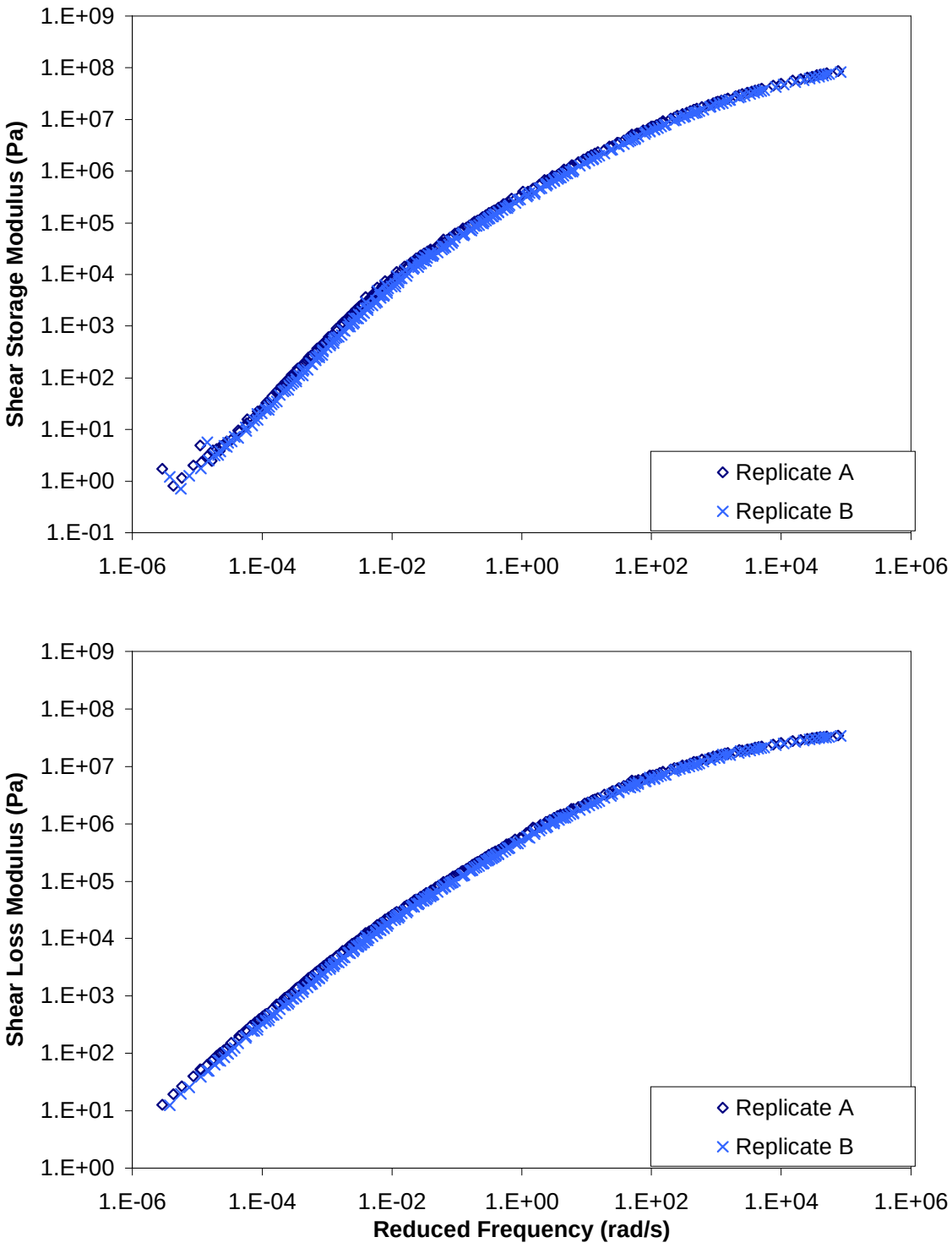


Figure C.4 Storage and loss shear moduli mastercurves for specimen ARG3.

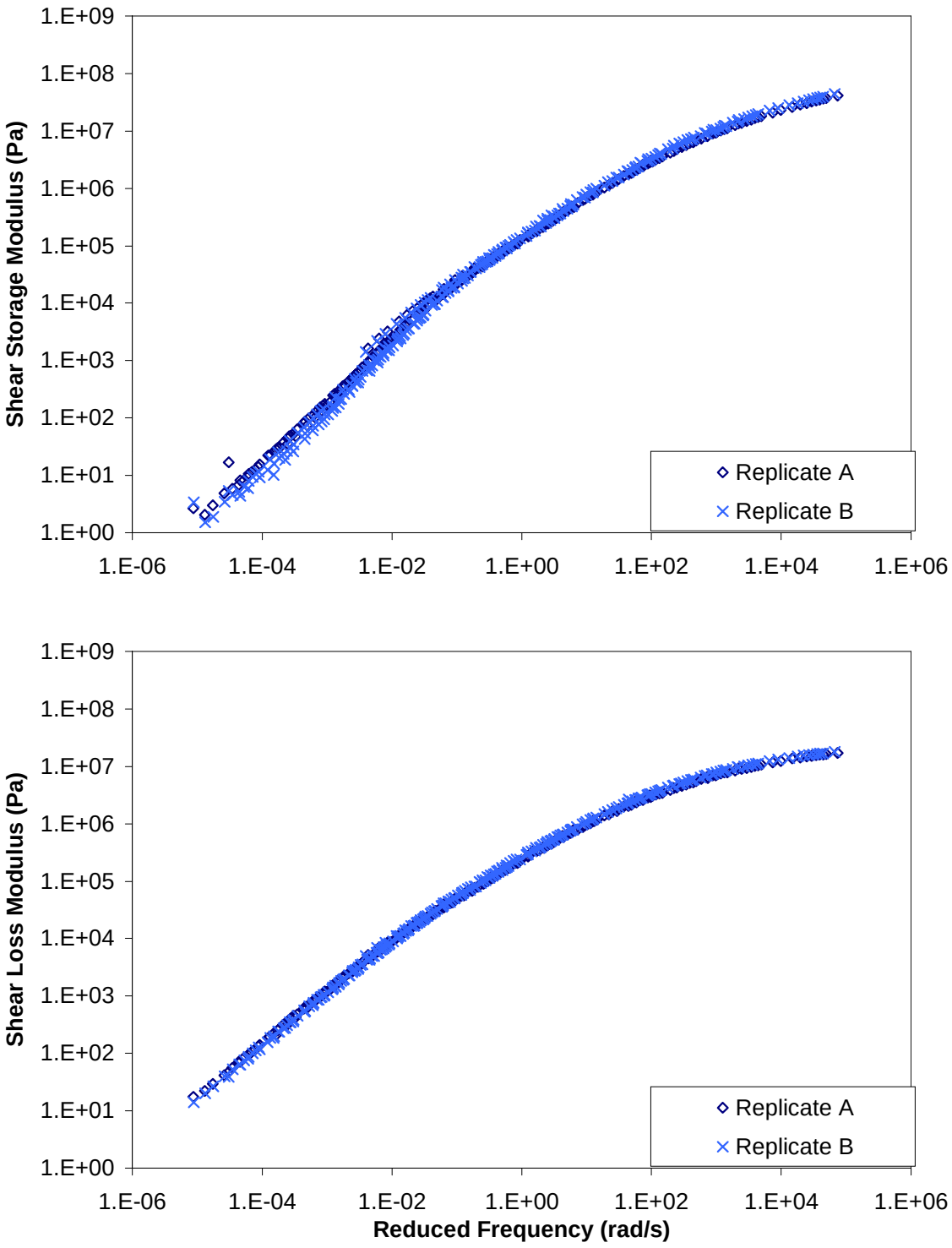


Figure C.5 Storage and loss shear moduli mastercurves for specimen AUG4.

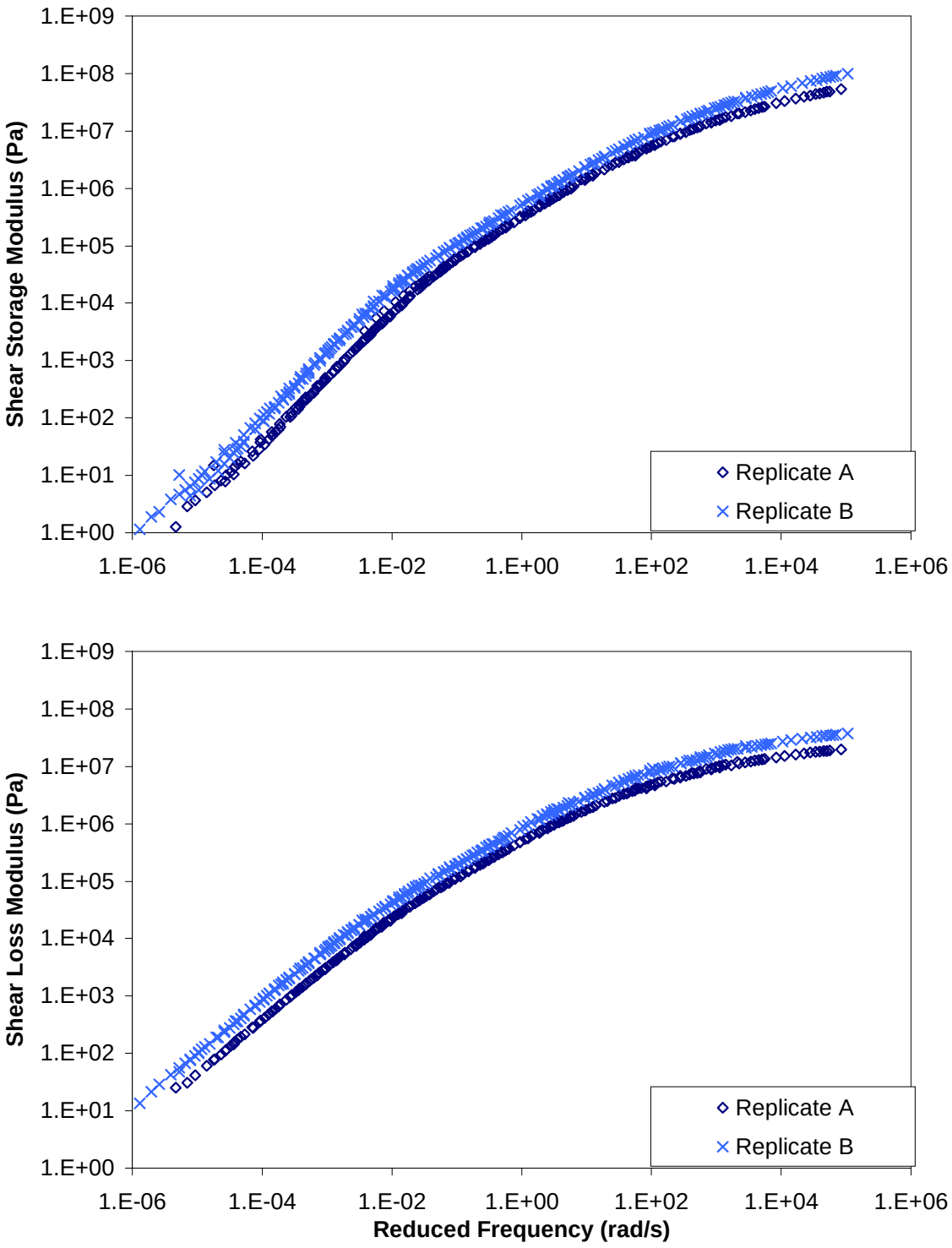


Figure C.6 Storage and loss shear moduli mastercurves for specimen ARG4.

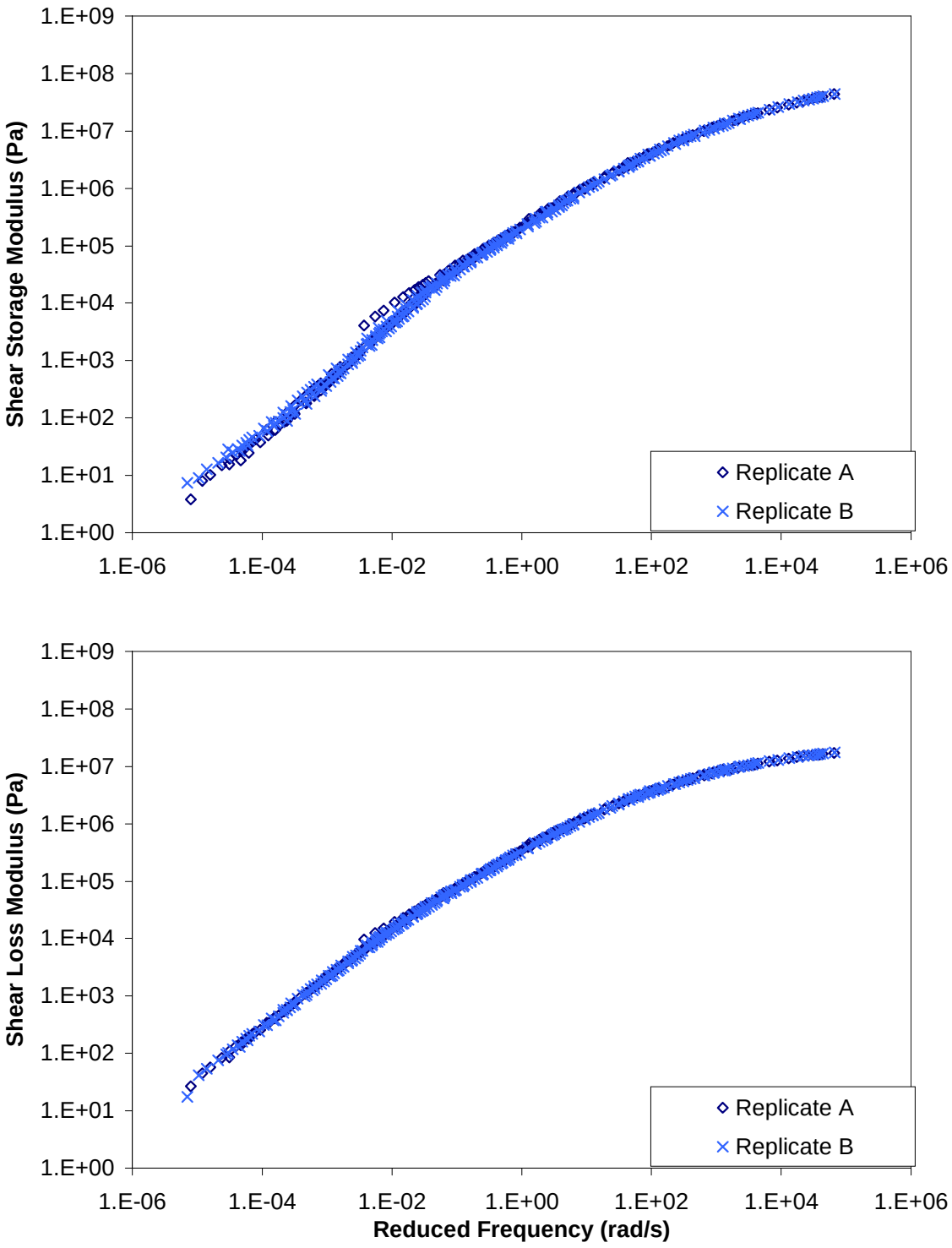


Figure C.7 Storage and loss shear moduli mastercurves for specimen AUG5.

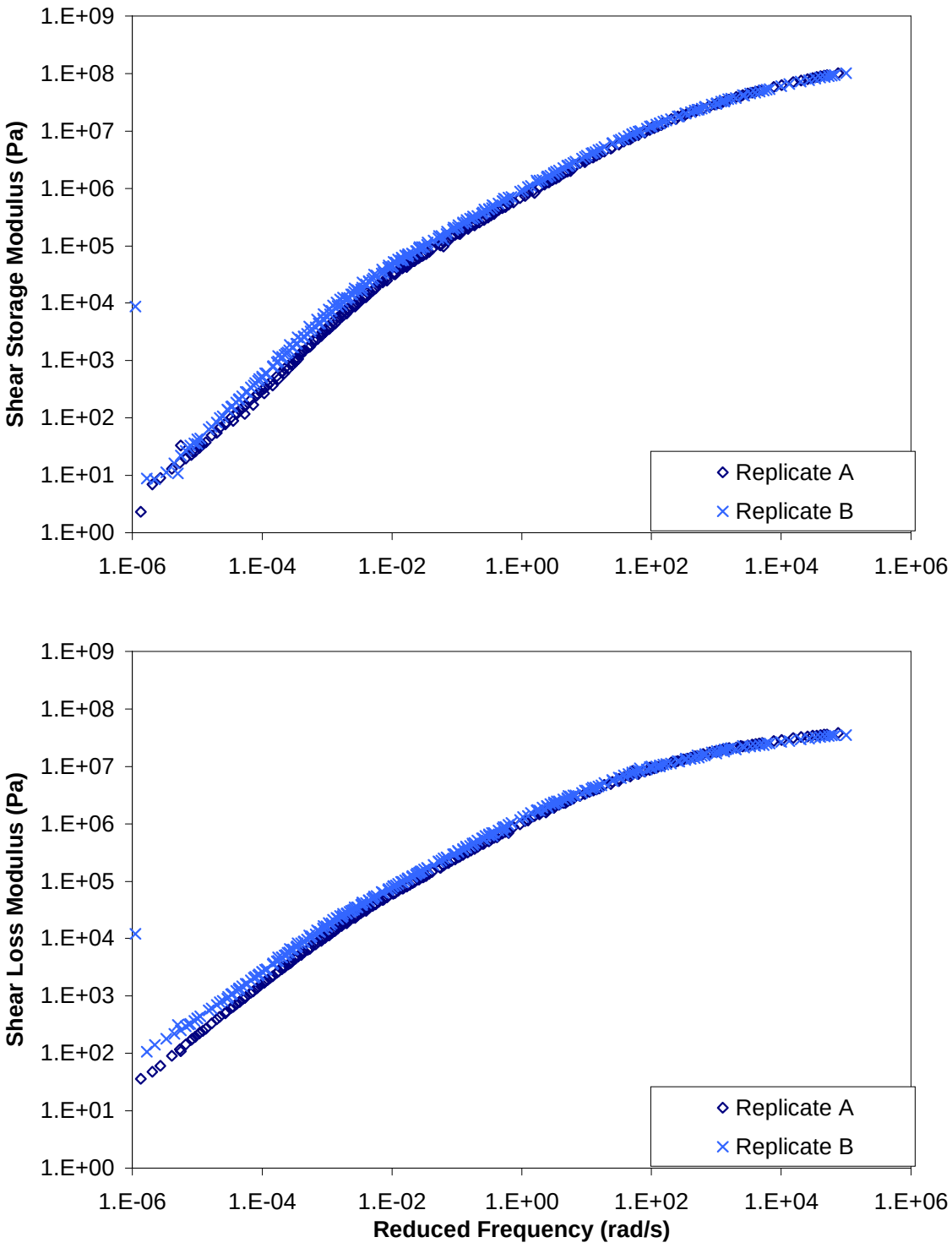


Figure C.8 Storage and loss shear moduli mastercurves for specimen ARG5.

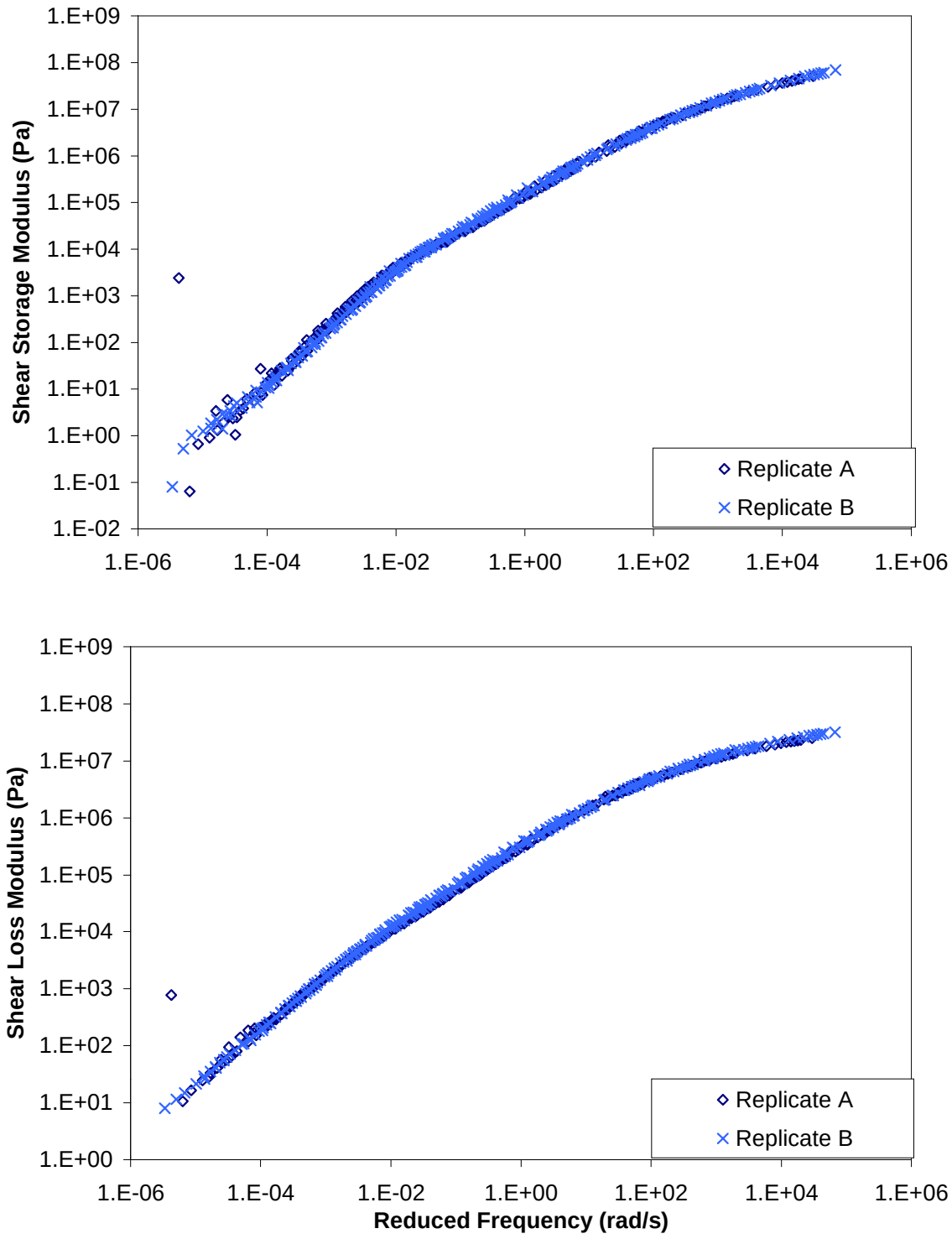


Figure C.9 Storage and loss shear moduli mastercurves for specimen AUN3.

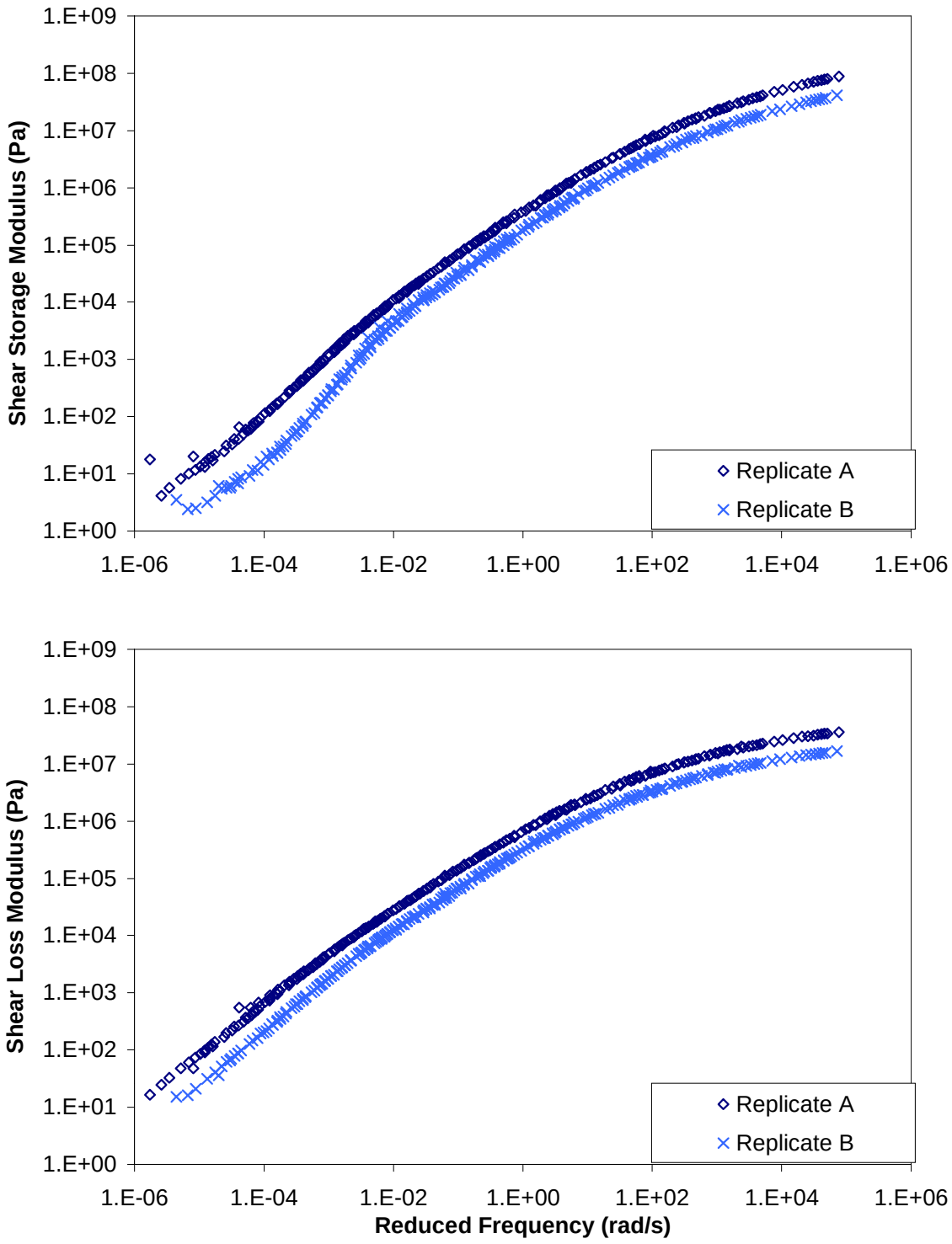


Figure C.10 Storage and loss shear moduli mastercurves for specimen ARN3.

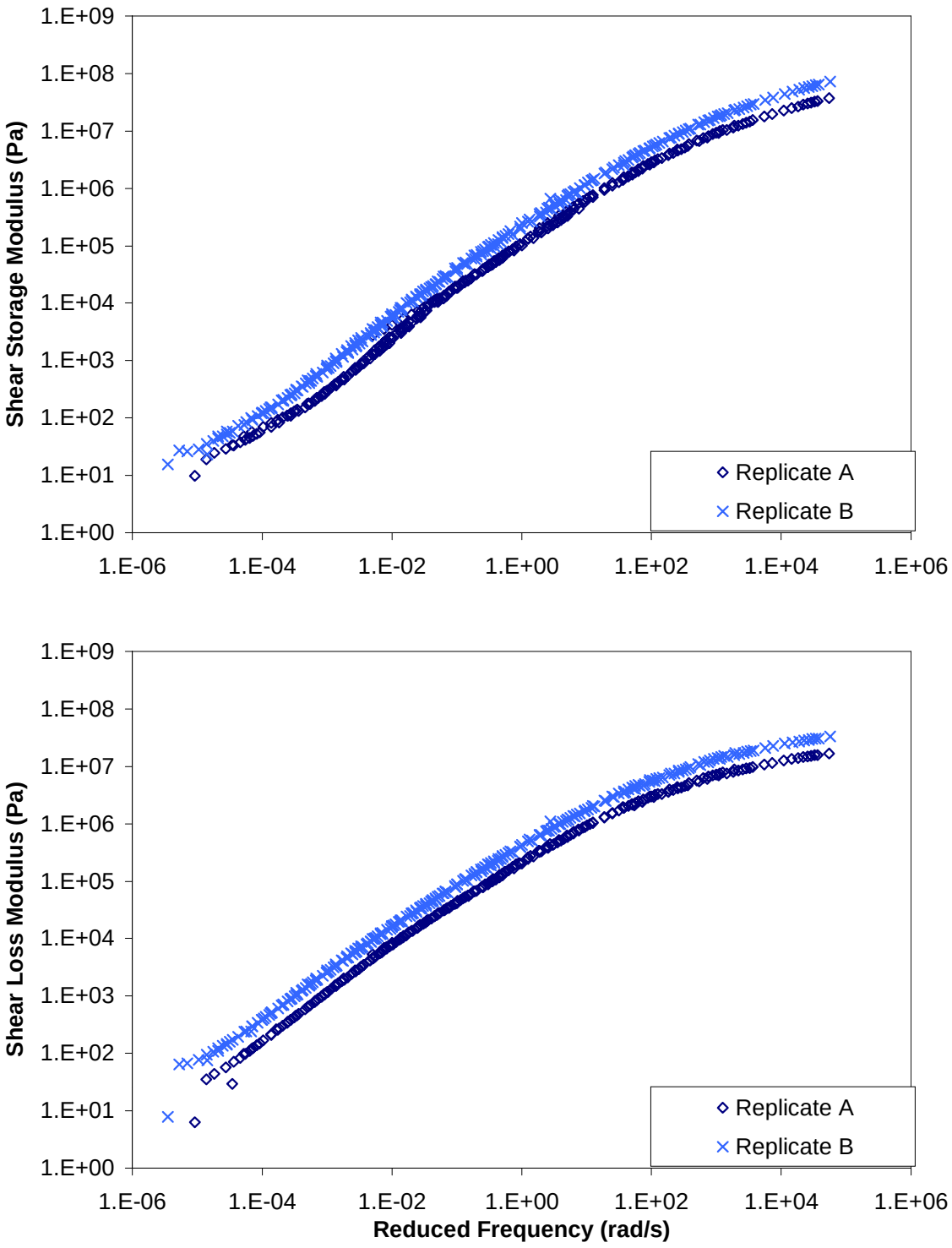


Figure C.11 Storage and loss shear moduli mastercurves for specimen AUN4.

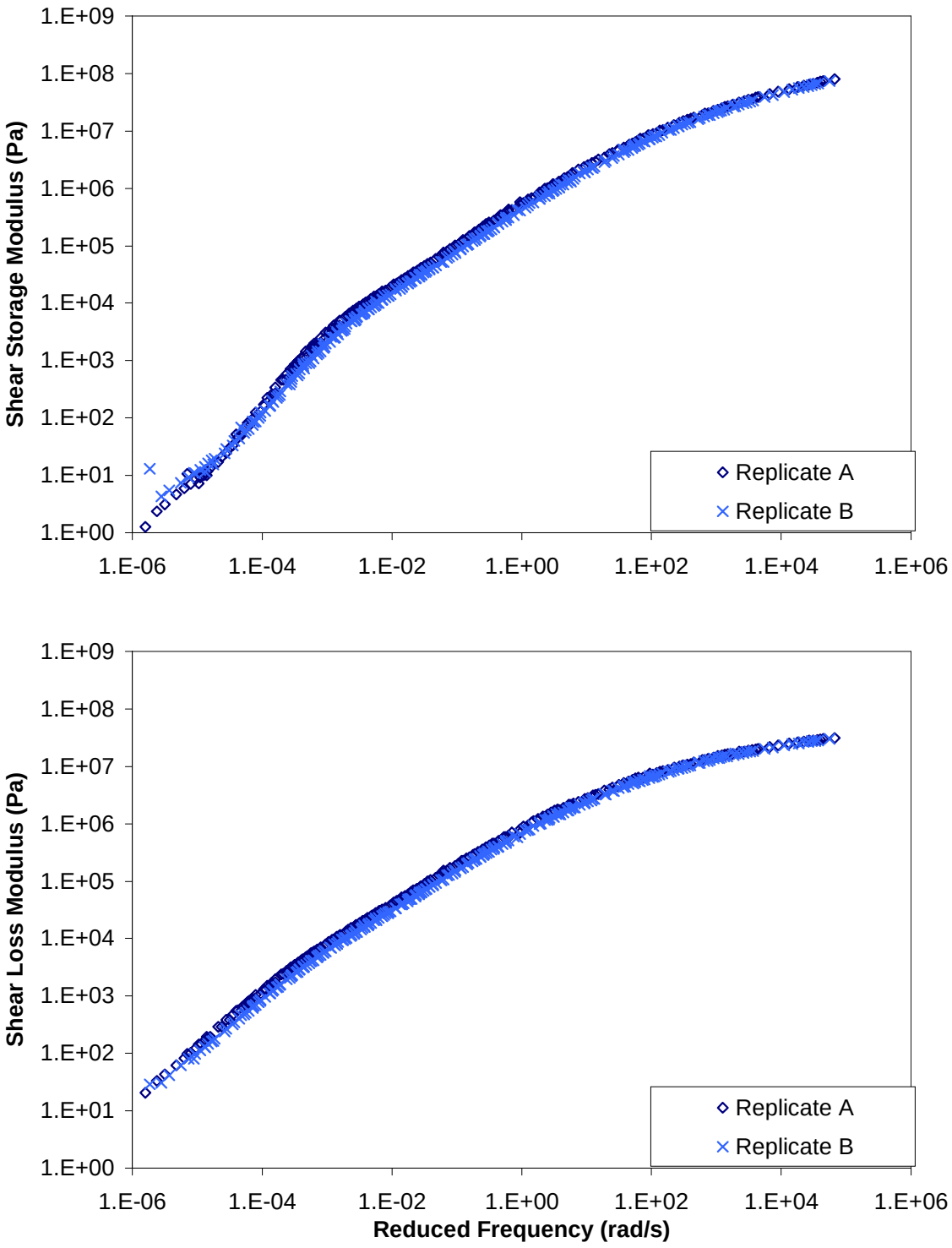


Figure C.12 Storage and loss shear moduli mastercurves for specimen ARN4.

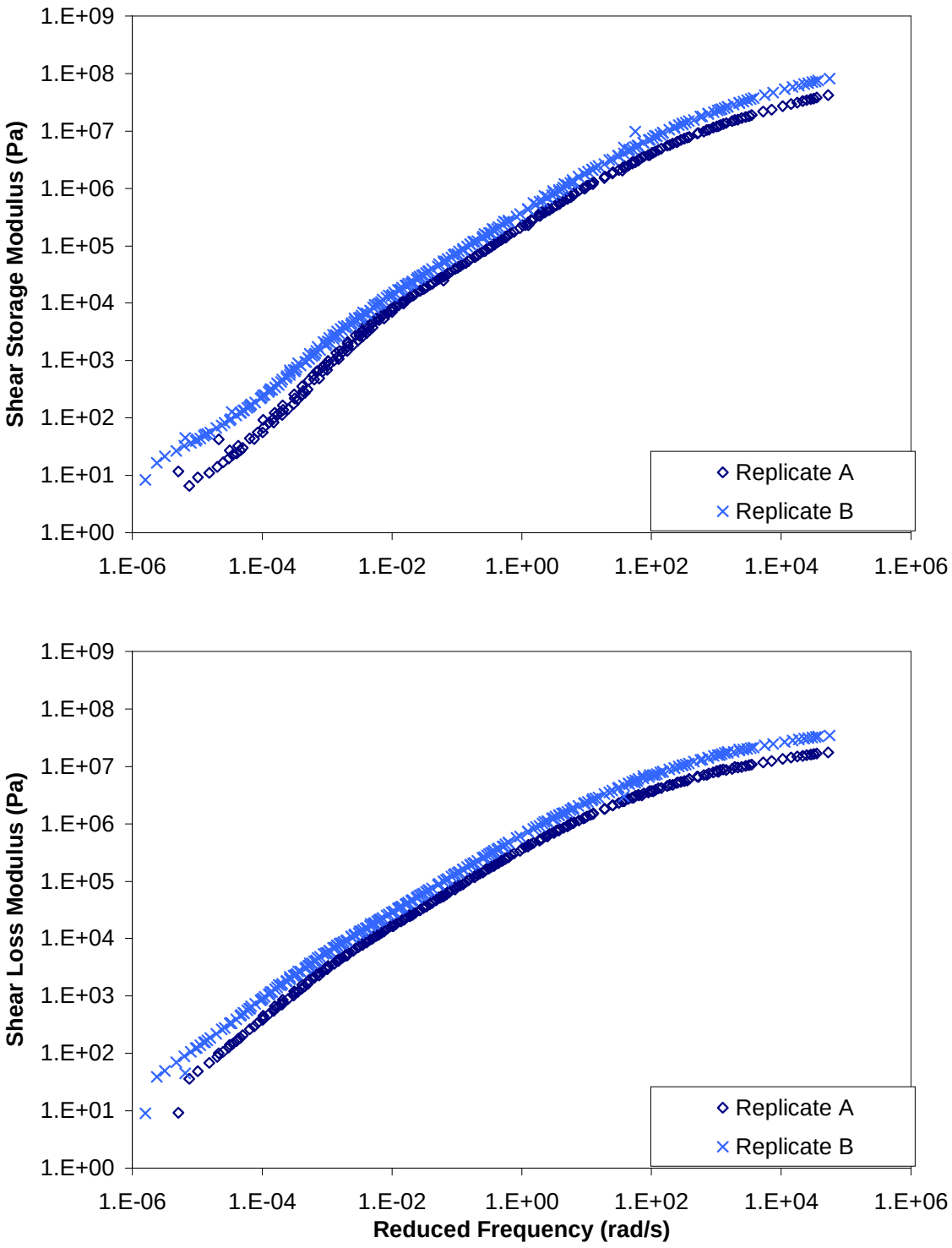


Figure C.13 Storage and loss shear moduli mastercurves for specimen AUN5.

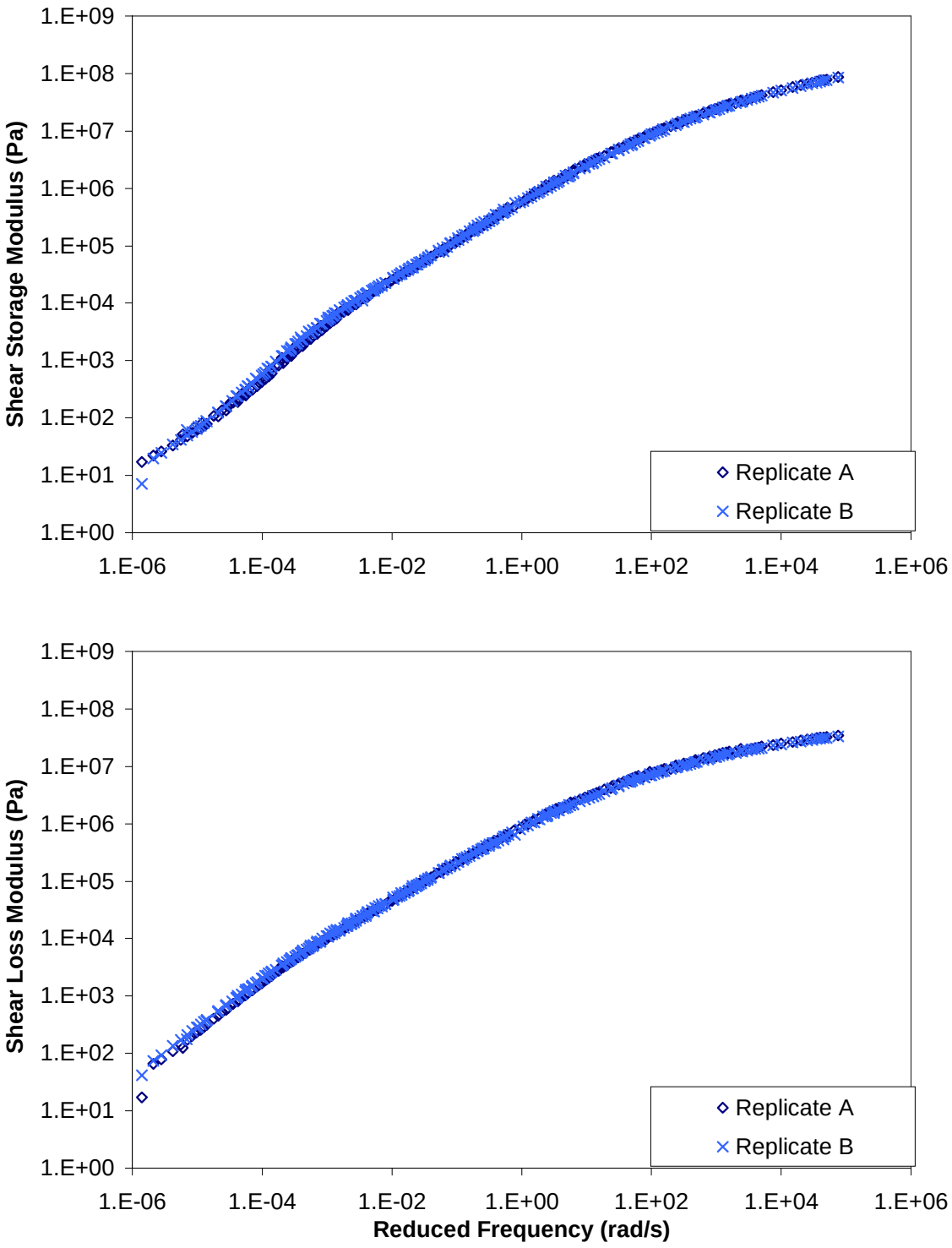


Figure C.14 Storage and loss shear moduli mastercurves for specimen ARN5.

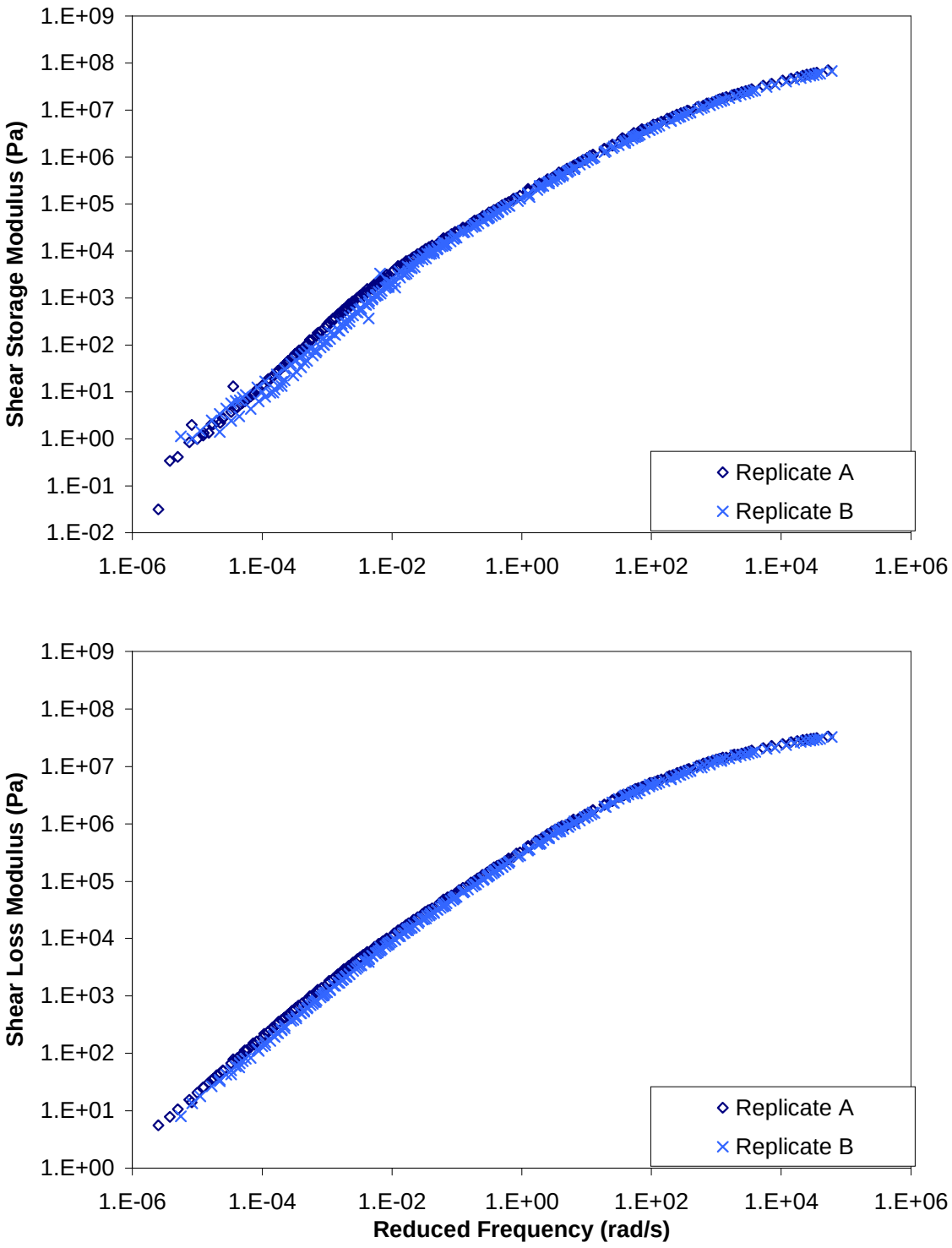


Figure C.15 Storage and loss shear moduli mastercurves for specimen AUS3.

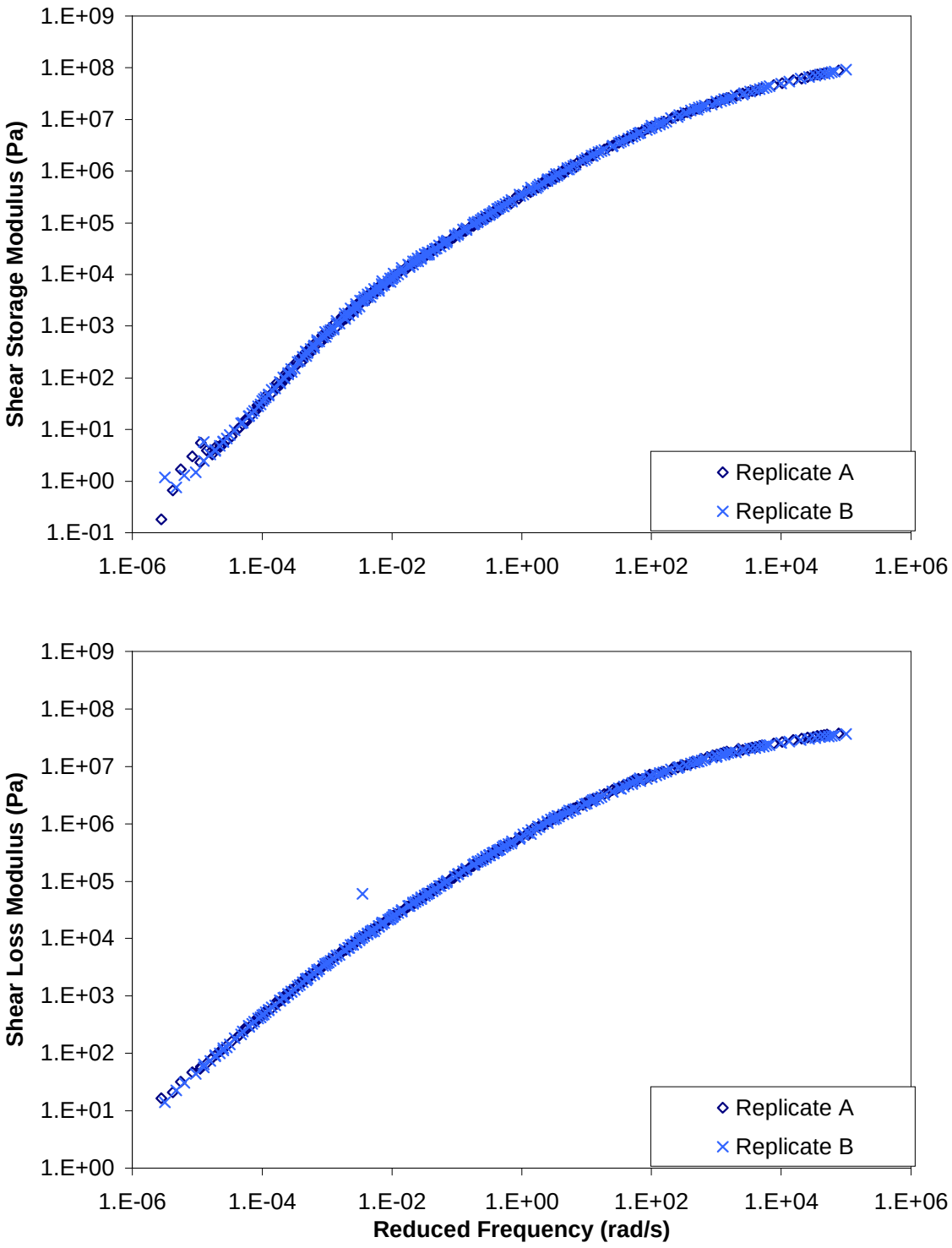


Figure C.16 Storage and loss shear moduli mastercurves for specimen ARS3.

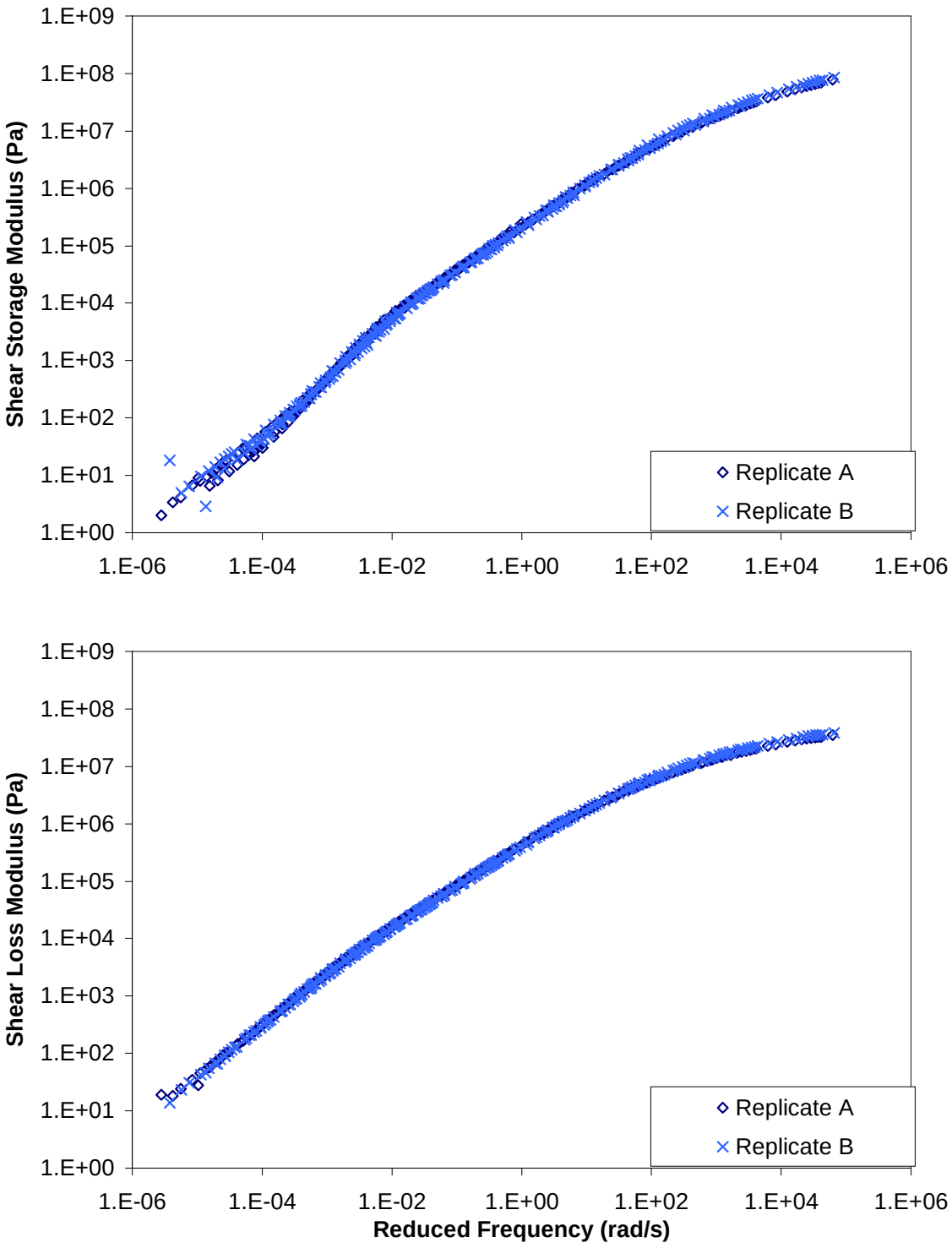


Figure C.17 Storage and loss shear moduli mastercurves for specimen AUS4.

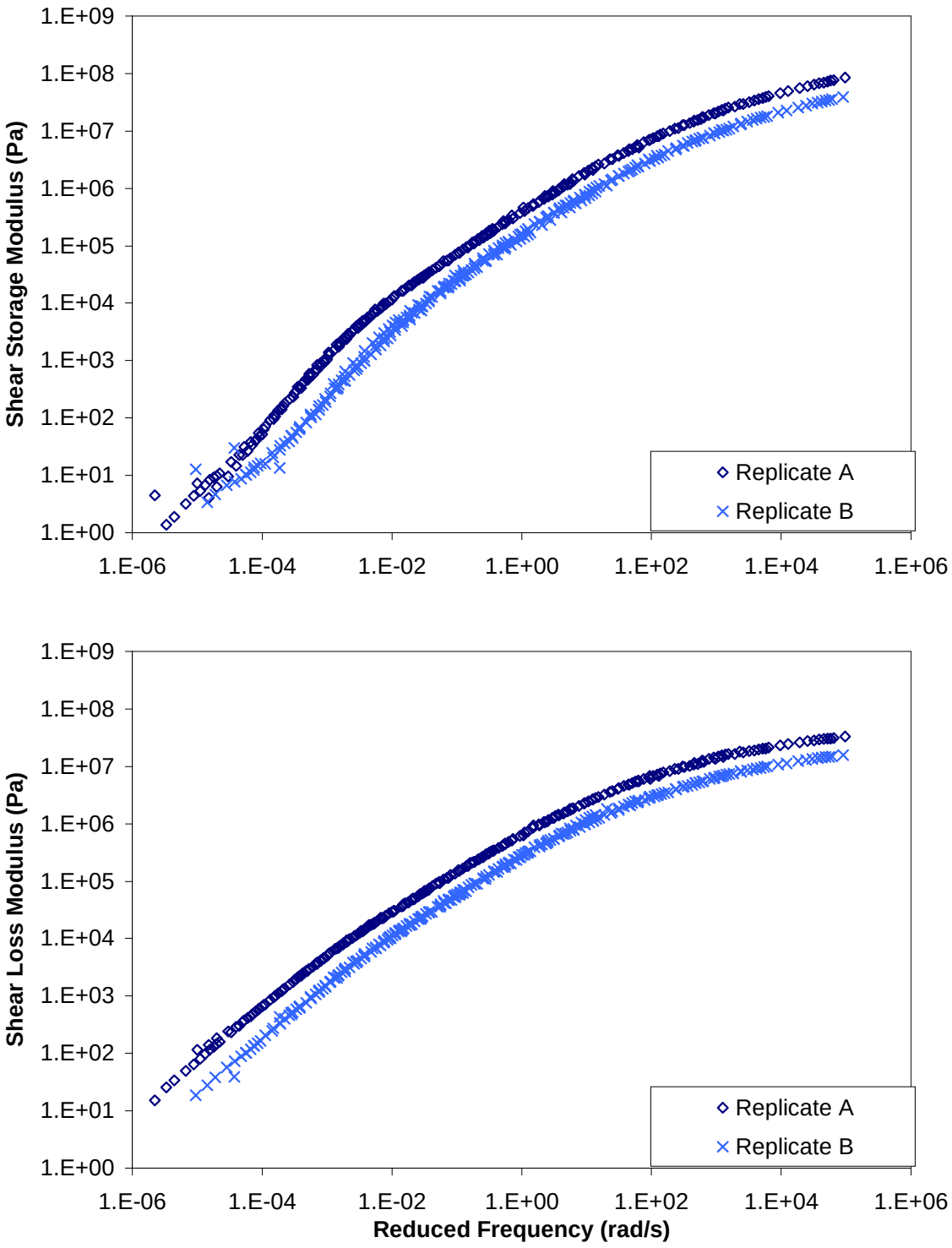


Figure C.18 Storage and loss shear moduli mastercurves for specimen ARS4.

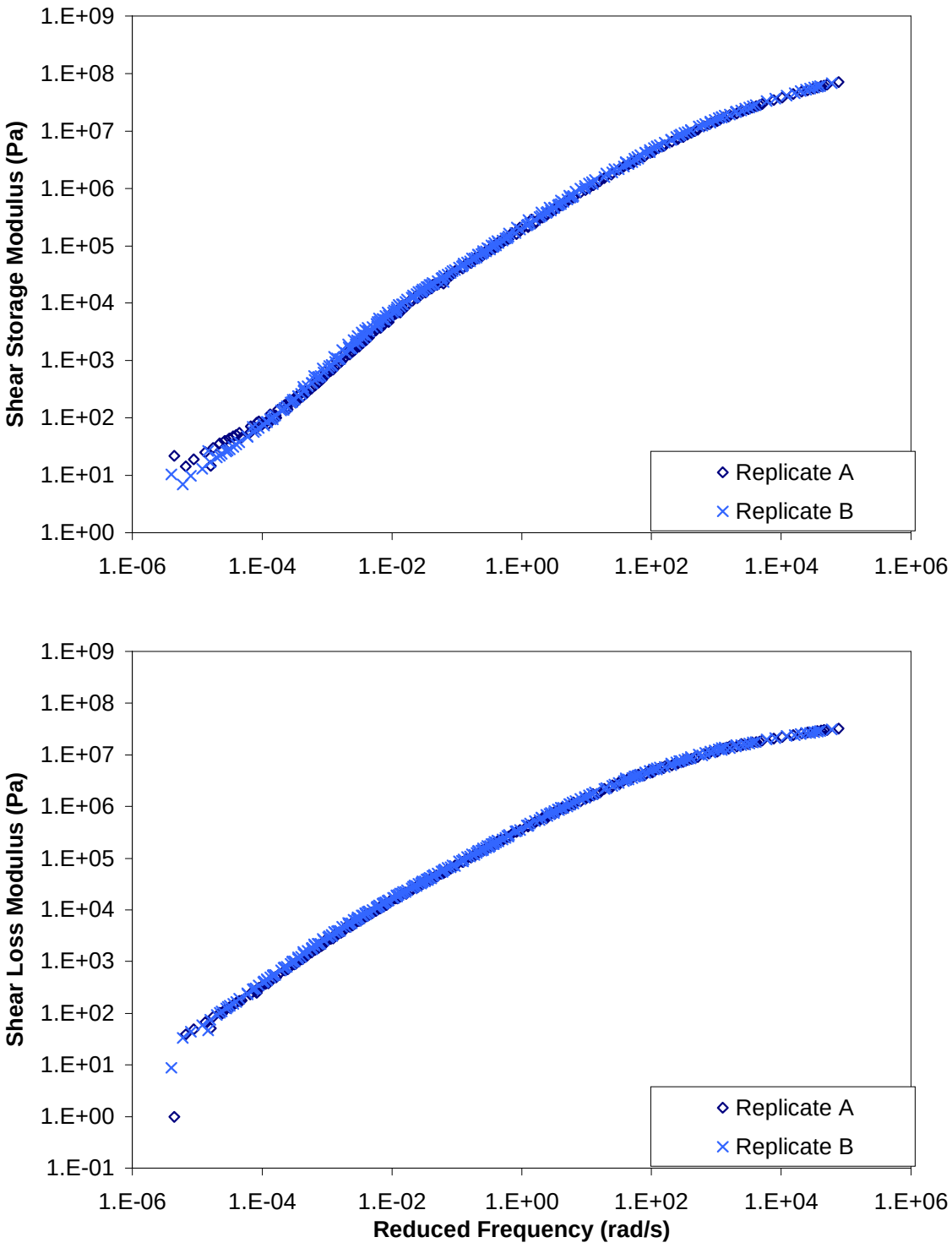


Figure C.19 Storage and loss shear moduli mastercurves for specimen AUS5.

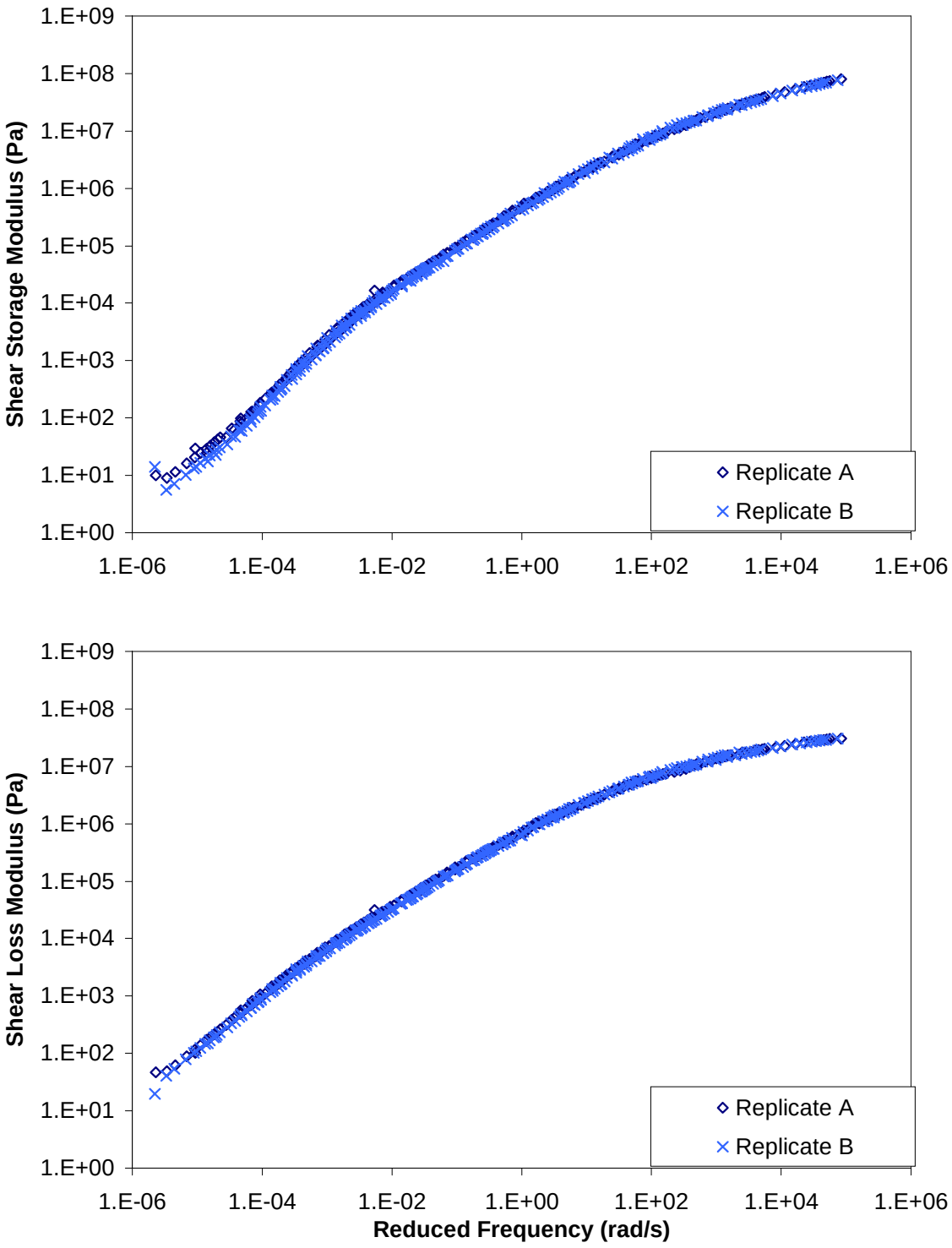


Figure C.20 Storage and loss shear moduli mastercurves for specimen ARS5.

# APPENDIX D

- This appendix includes the shift factors used in construction of storage and loss shear moduli mastercurves for all stored specimens.

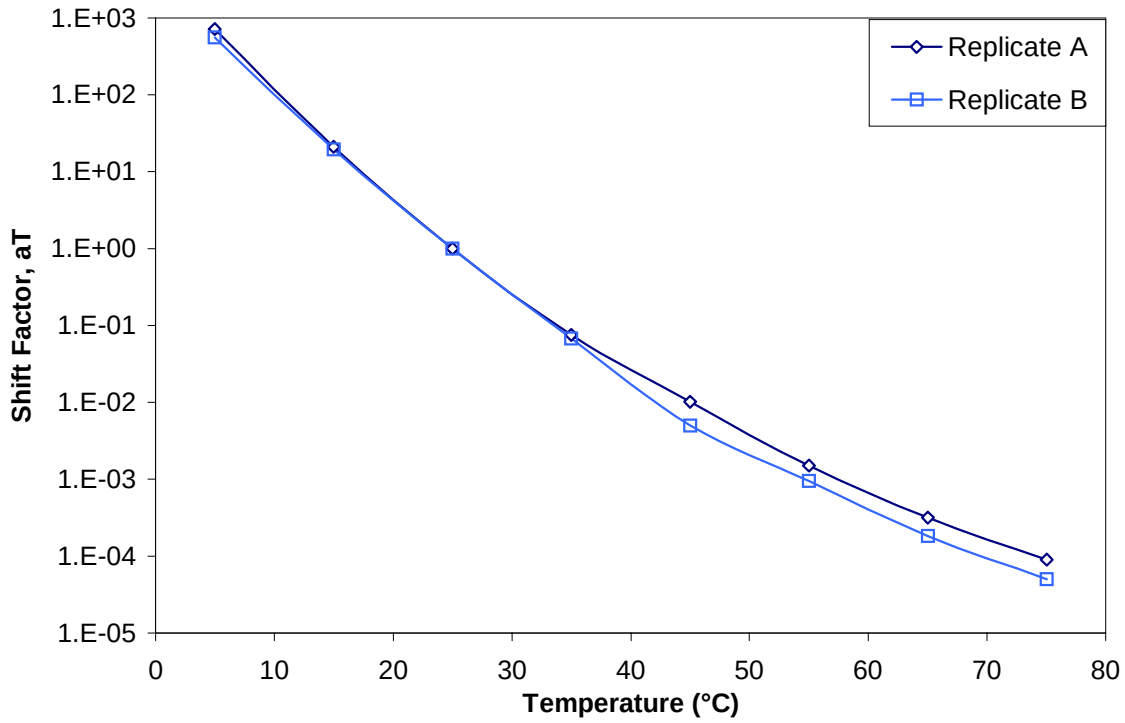


Figure D.1 Shift factors for stored specimen AU00.

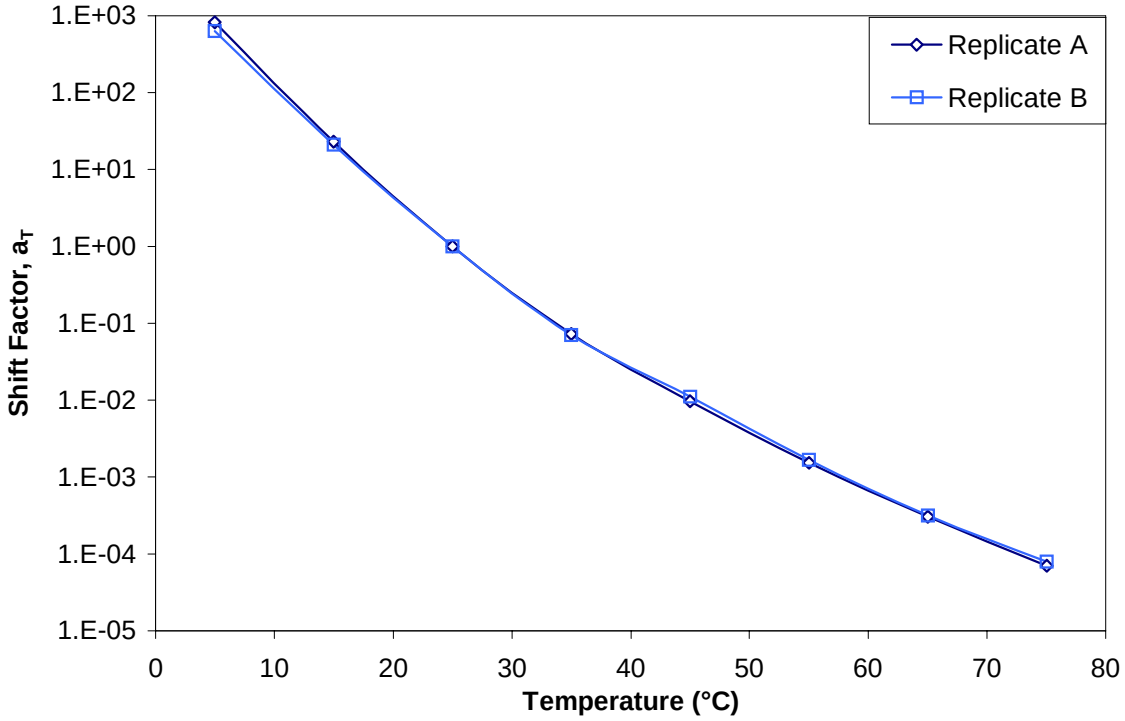


Figure D.2 Shift factors for stored specimen AR00.

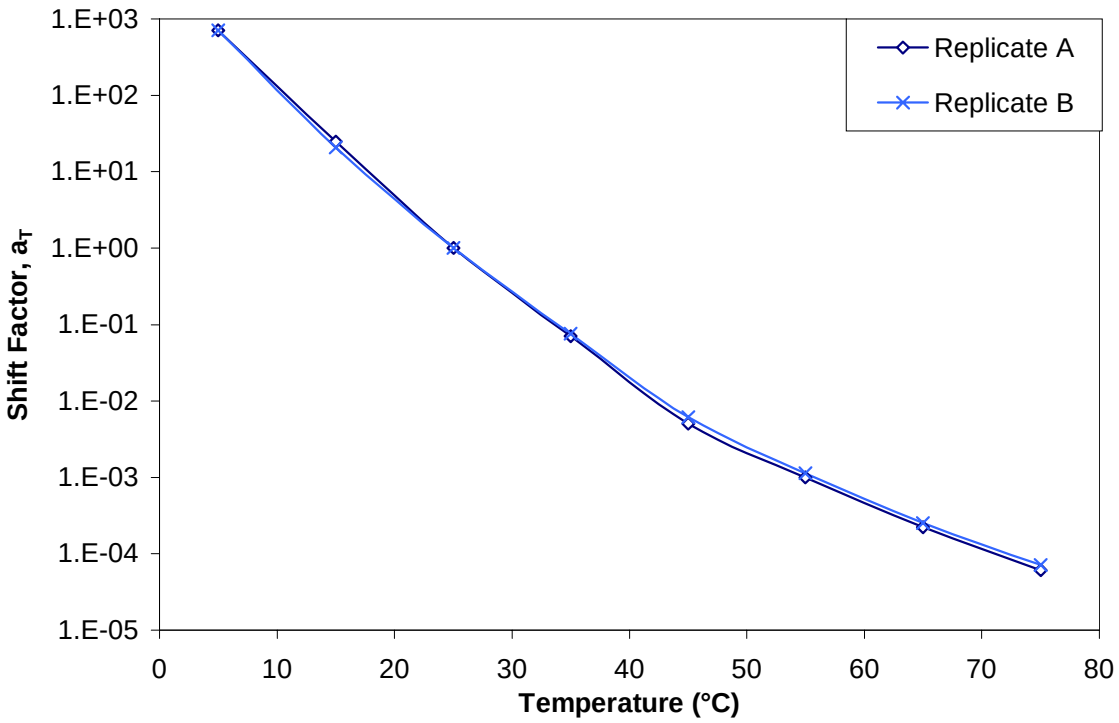


Figure D.3 Shift factors for stored specimen AUG3.

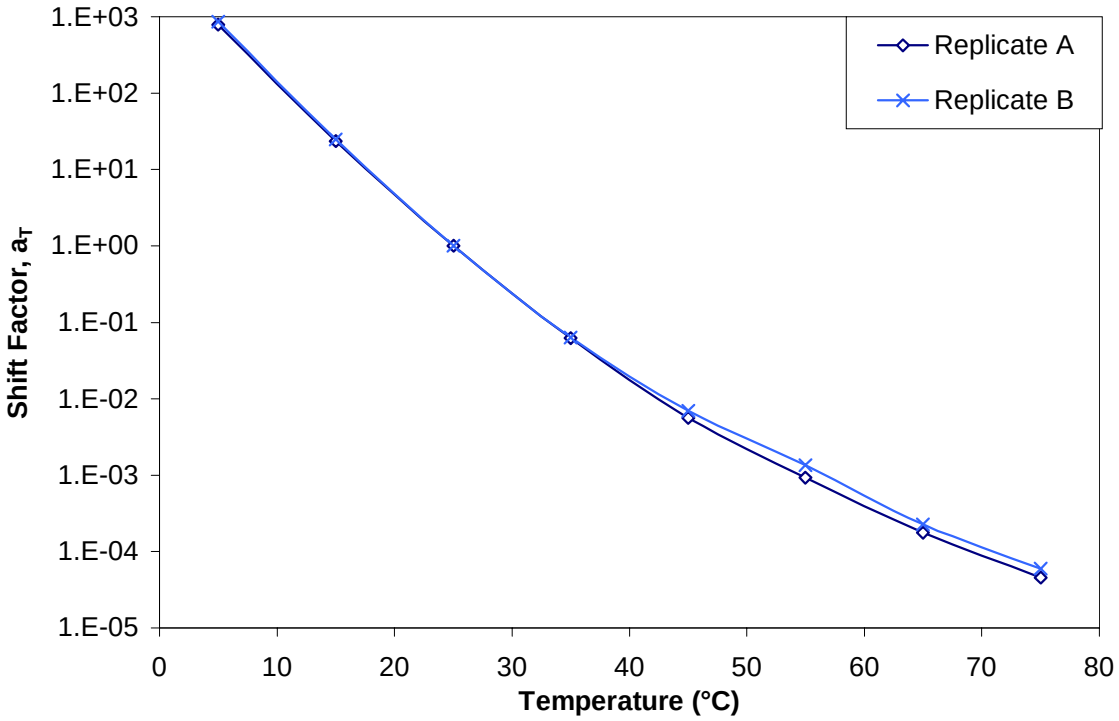


Figure D.4 Shift factors for stored specimen ARG3.

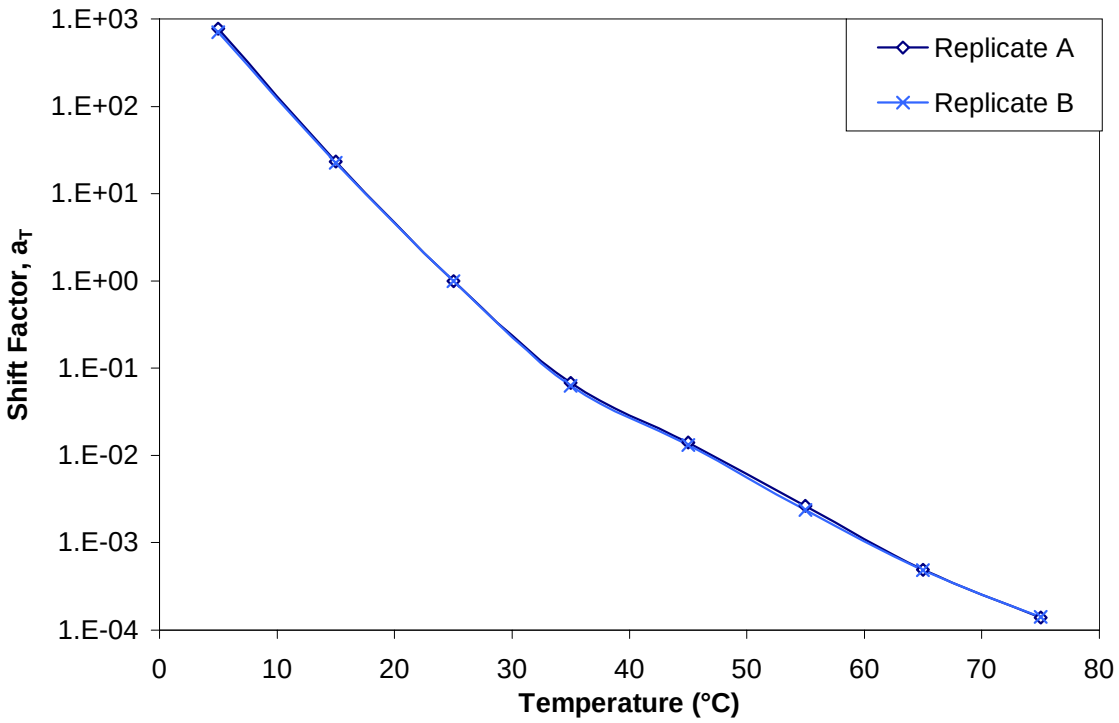


Figure D.5 Shift factors for stored specimen AUG4.

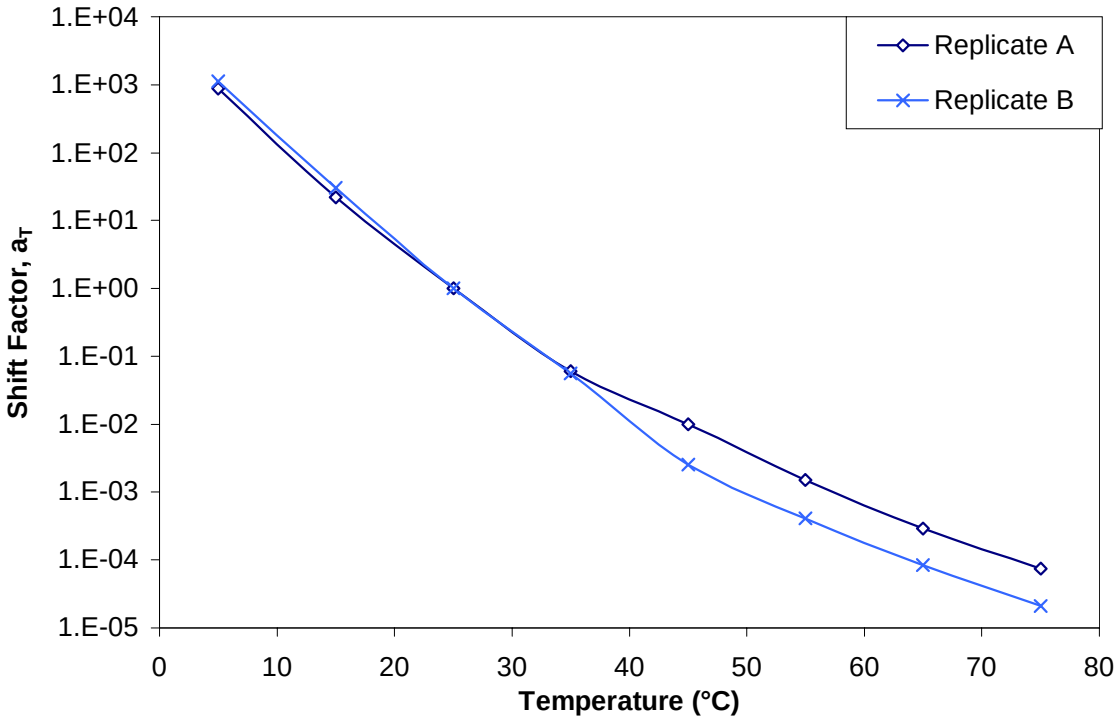


Figure D.6 Shift factors for stored specimen ARG4.

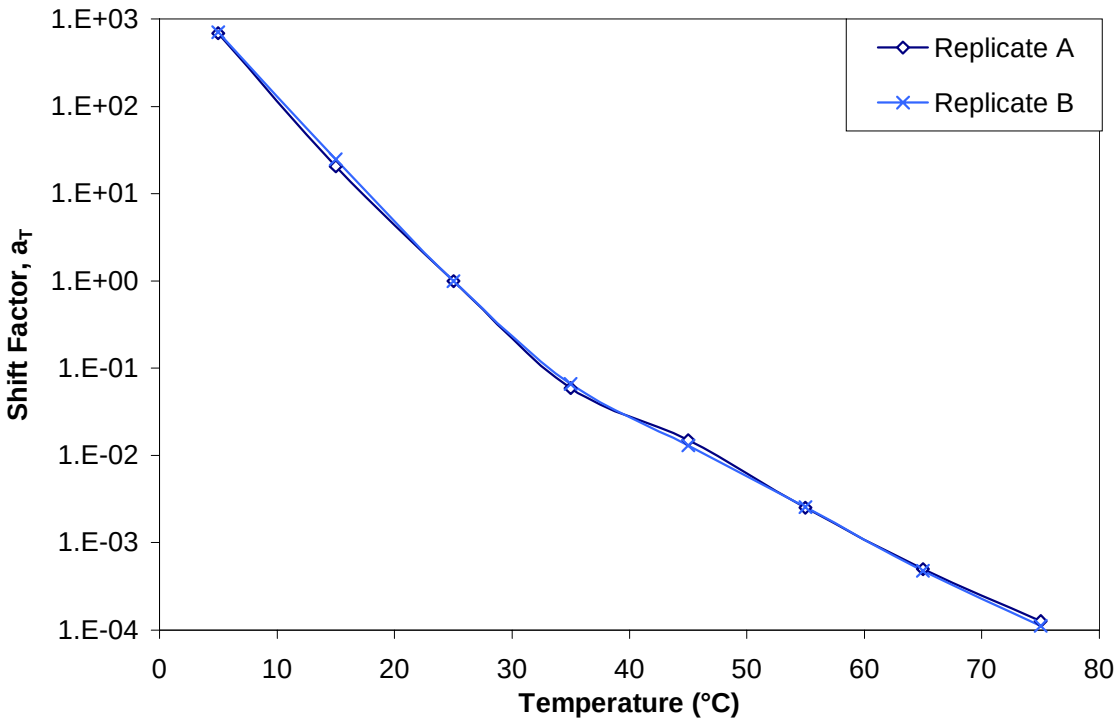


Figure D.7 Shift factors for stored specimen AUG5.

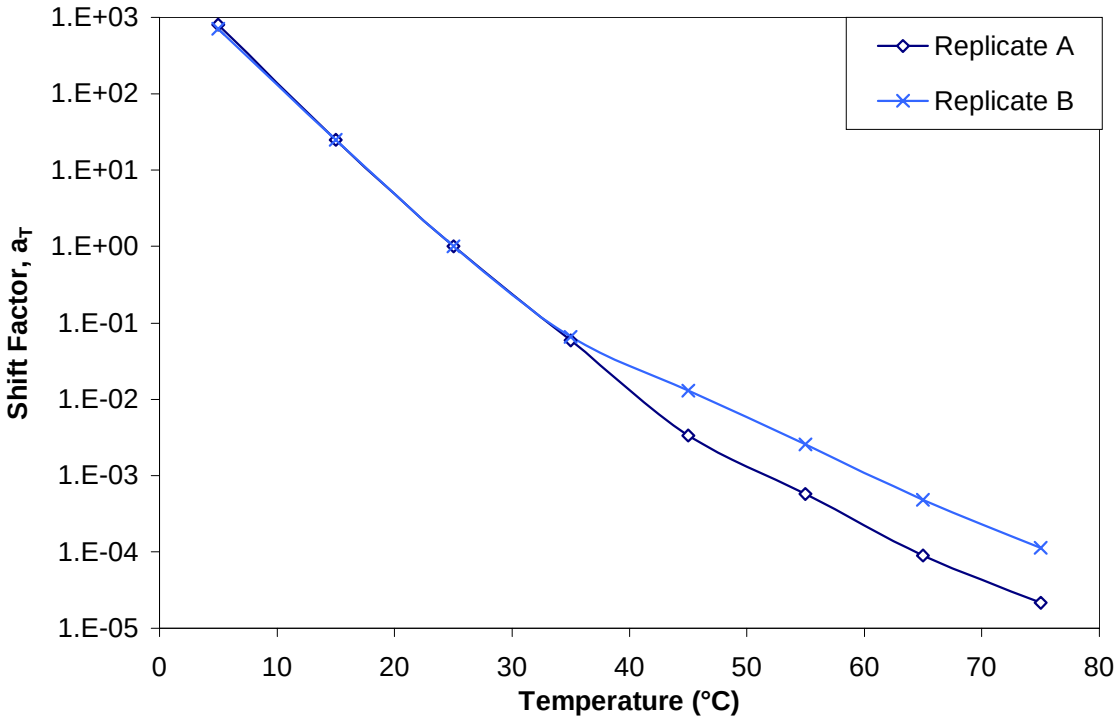


Figure D.8 Shift factors for stored specimen ARG5.

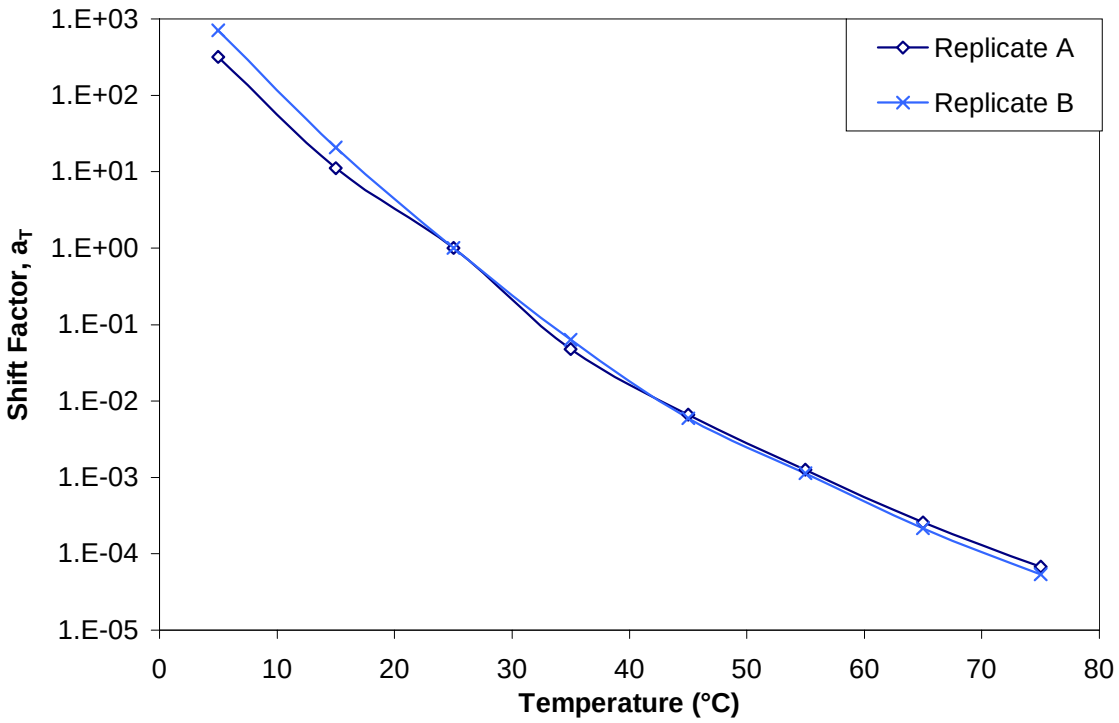


Figure D.9 Shift factors for stored specimen AUN3.

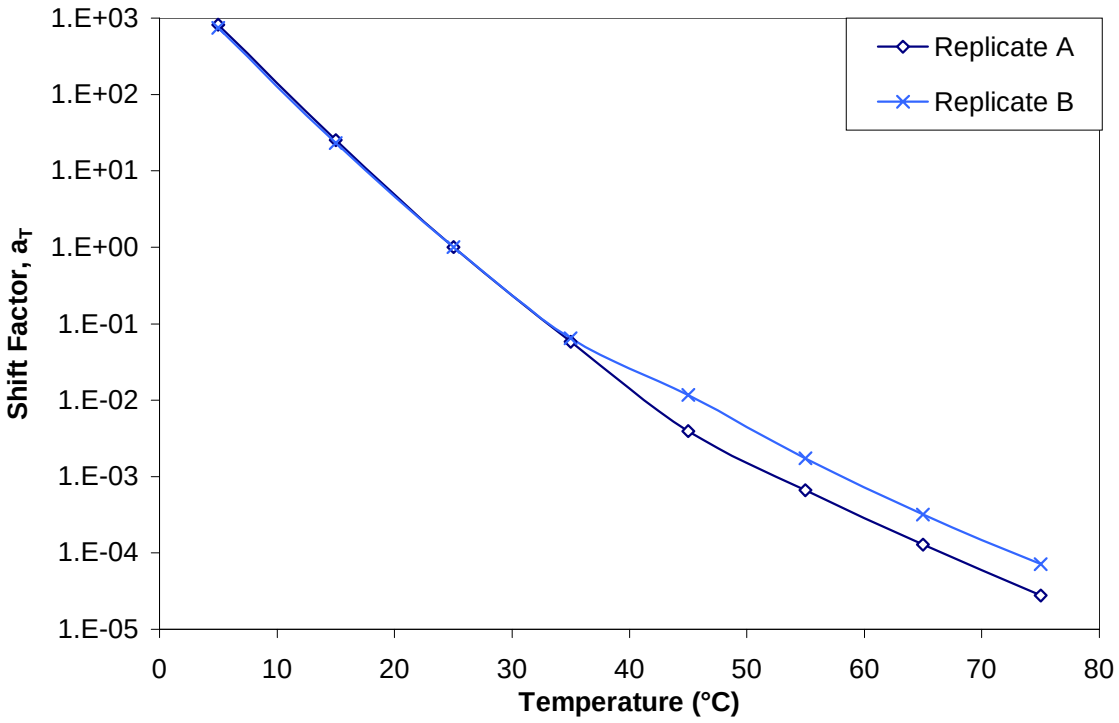


Figure D.10 Shift factors for stored specimen ARN3.

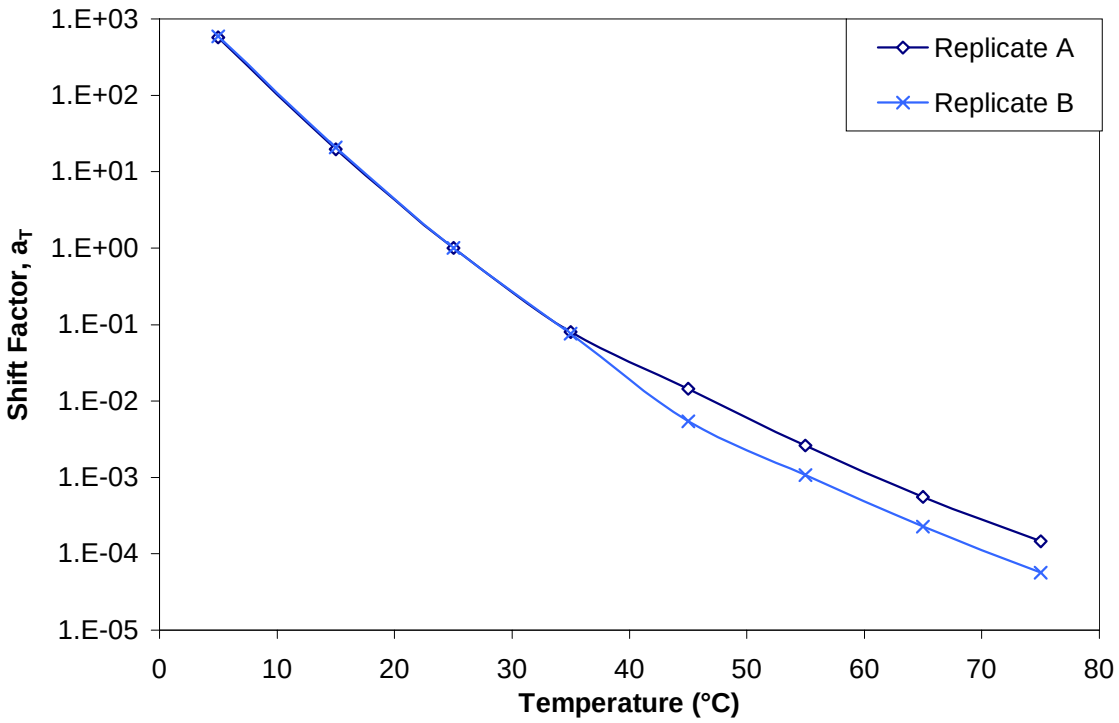


Figure D.11 Shift factors for stored specimen AUN4.

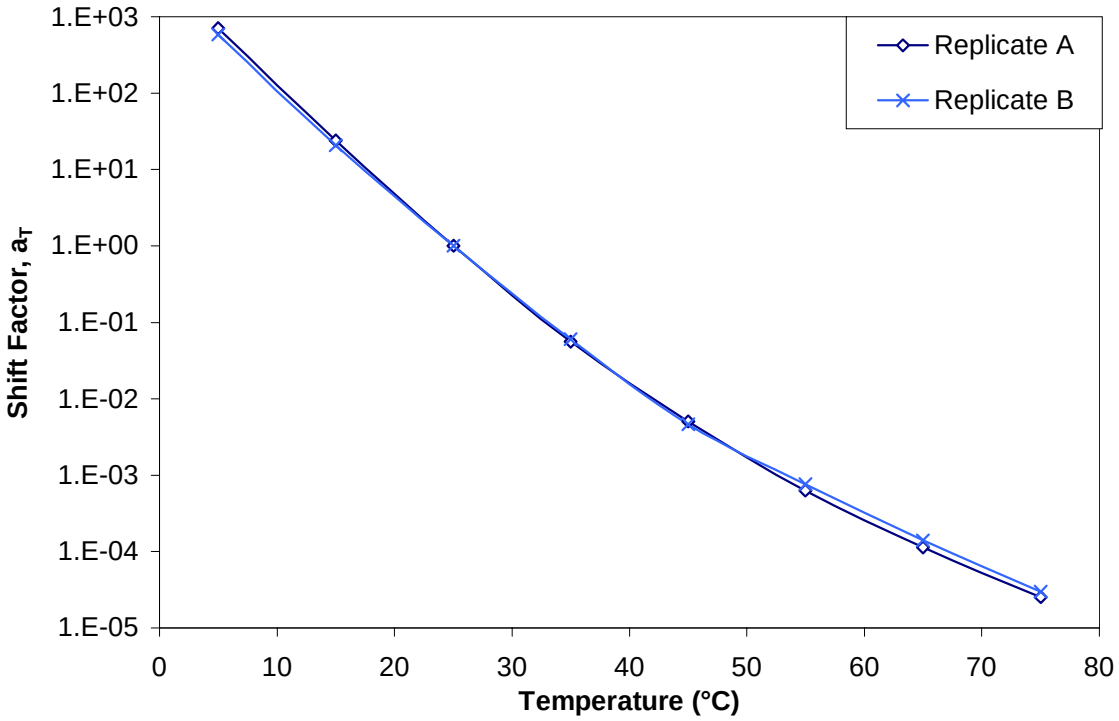


Figure D.12 Shift factors for stored specimen ARN4.

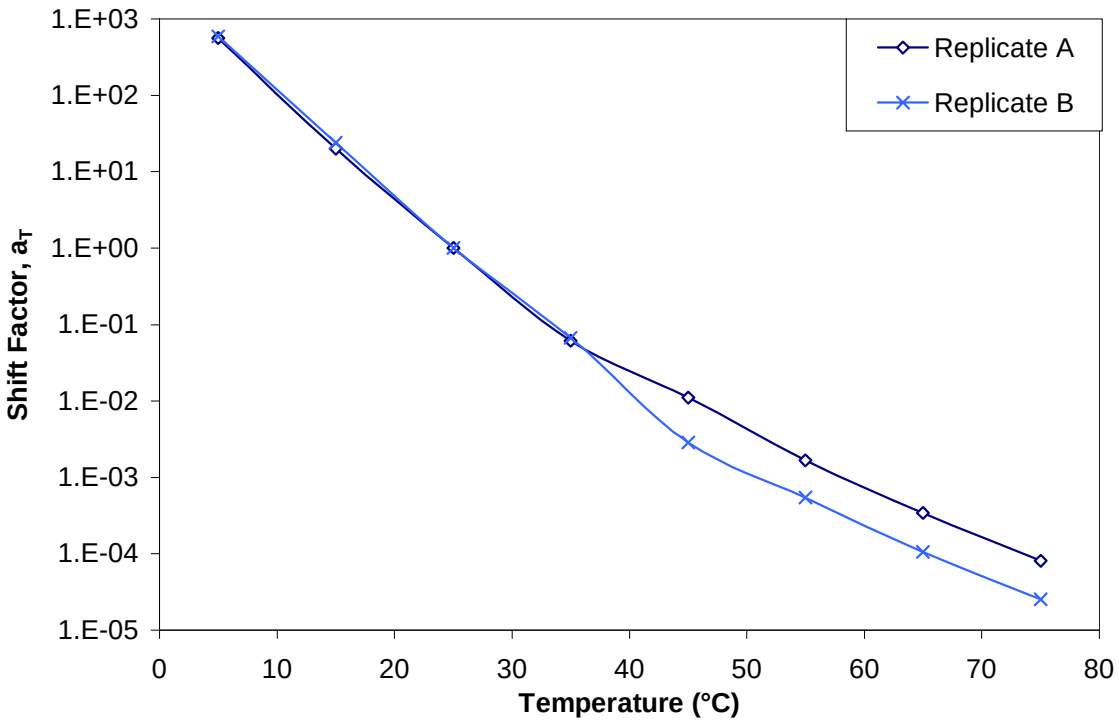


Figure D.13 Shift factors for stored specimen AUN5.

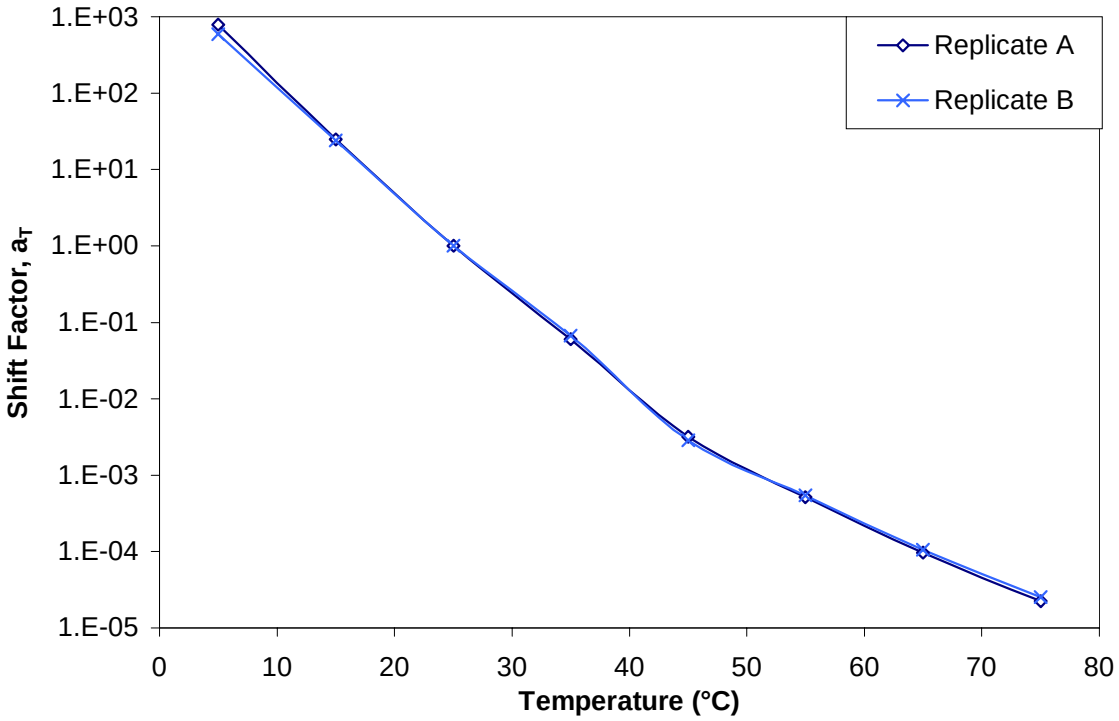


Figure D.14 Shift factors for stored specimen ARN5.

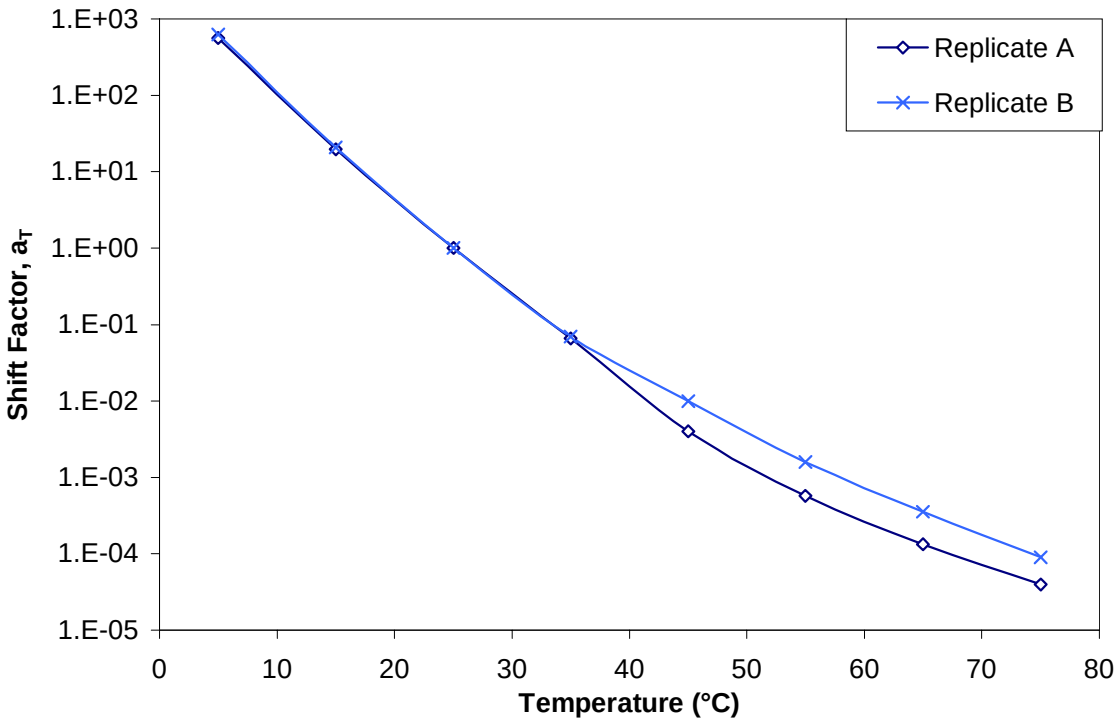


Figure D.15 Shift factors for stored specimen AUS3.

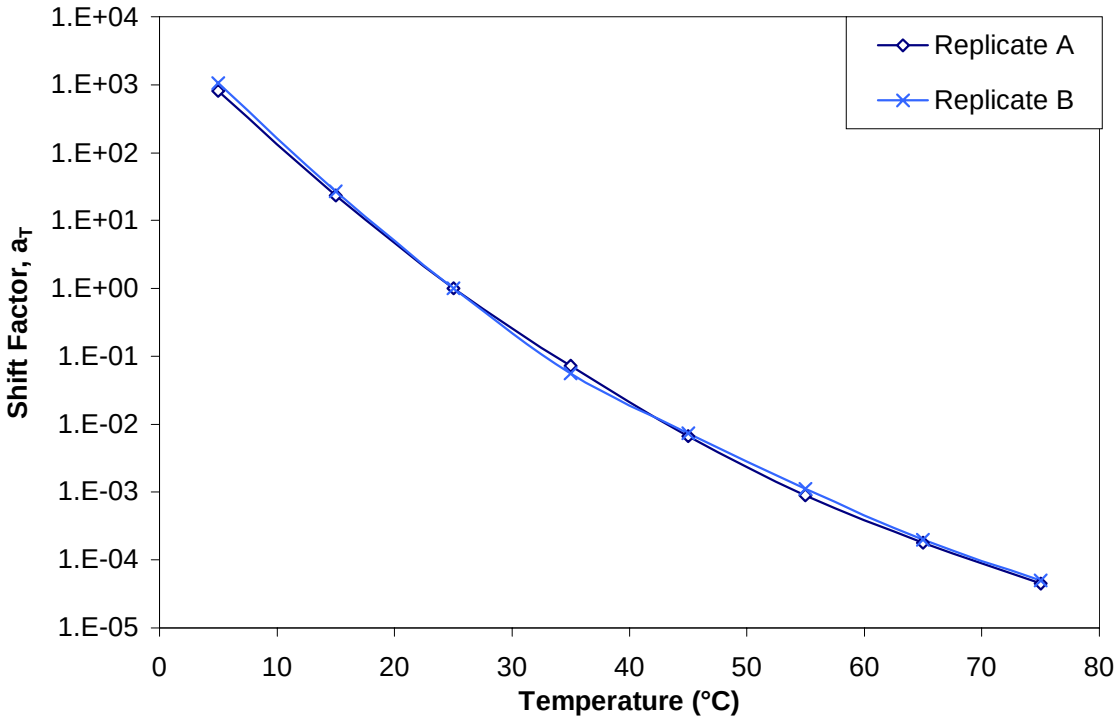


Figure D.16 Shift factors for stored specimen ARS3.

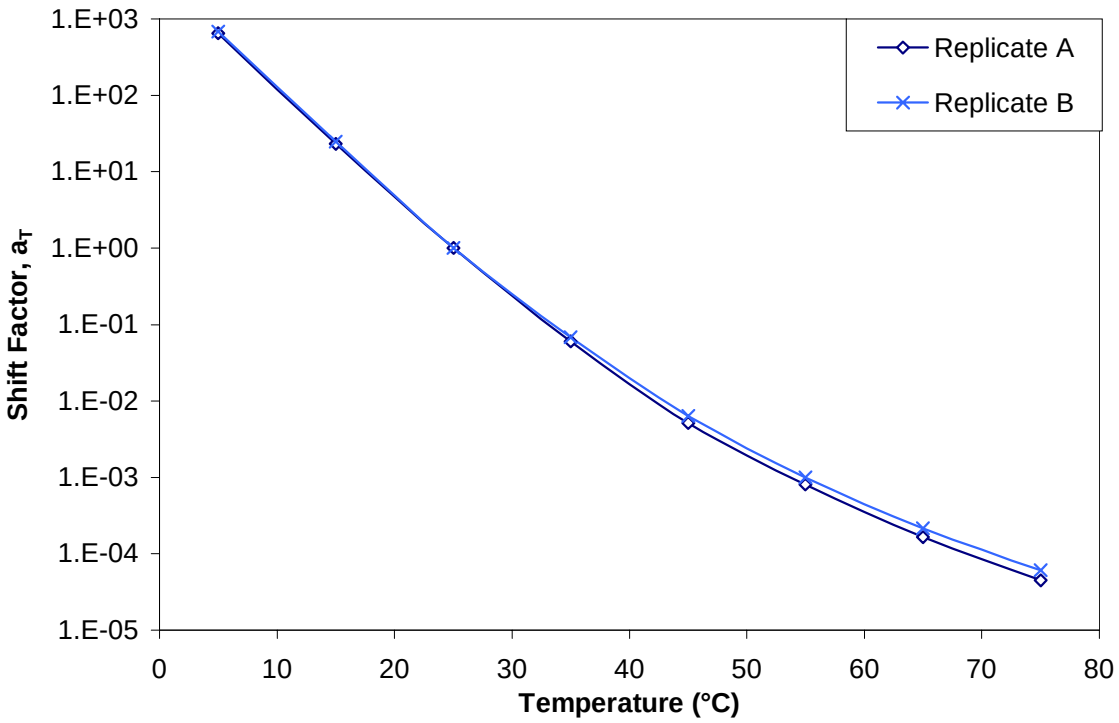


Figure D.17 Shift factors for stored specimen AUS4.

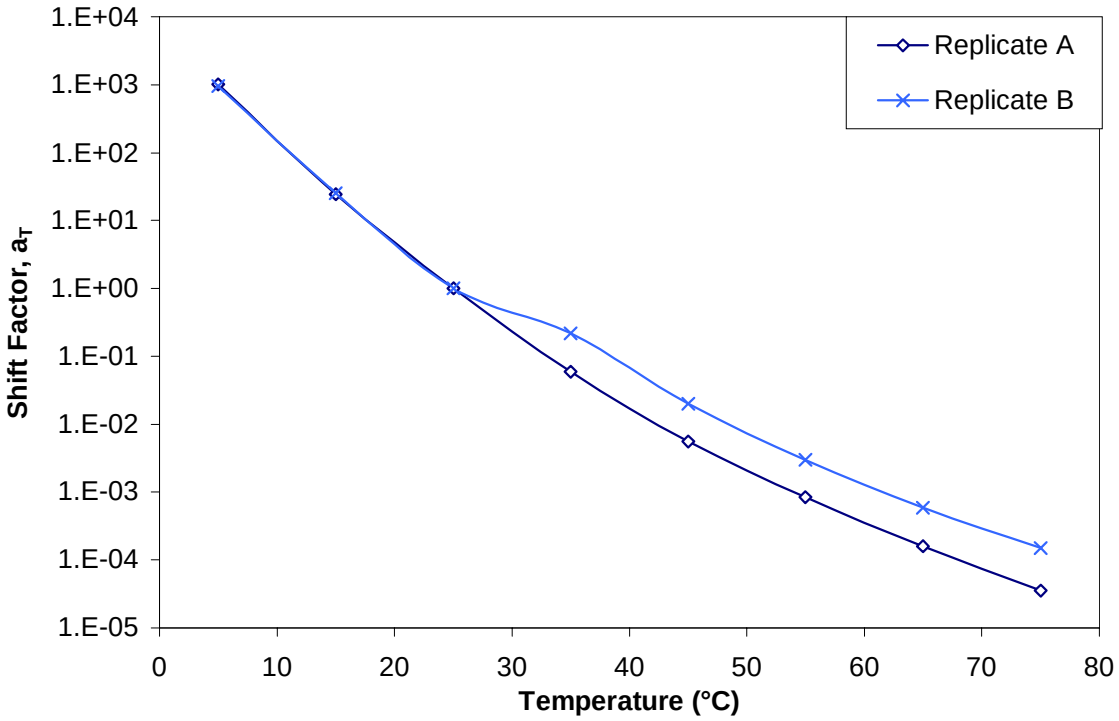


Figure D.18 Shift factors for stored specimen ARS4.

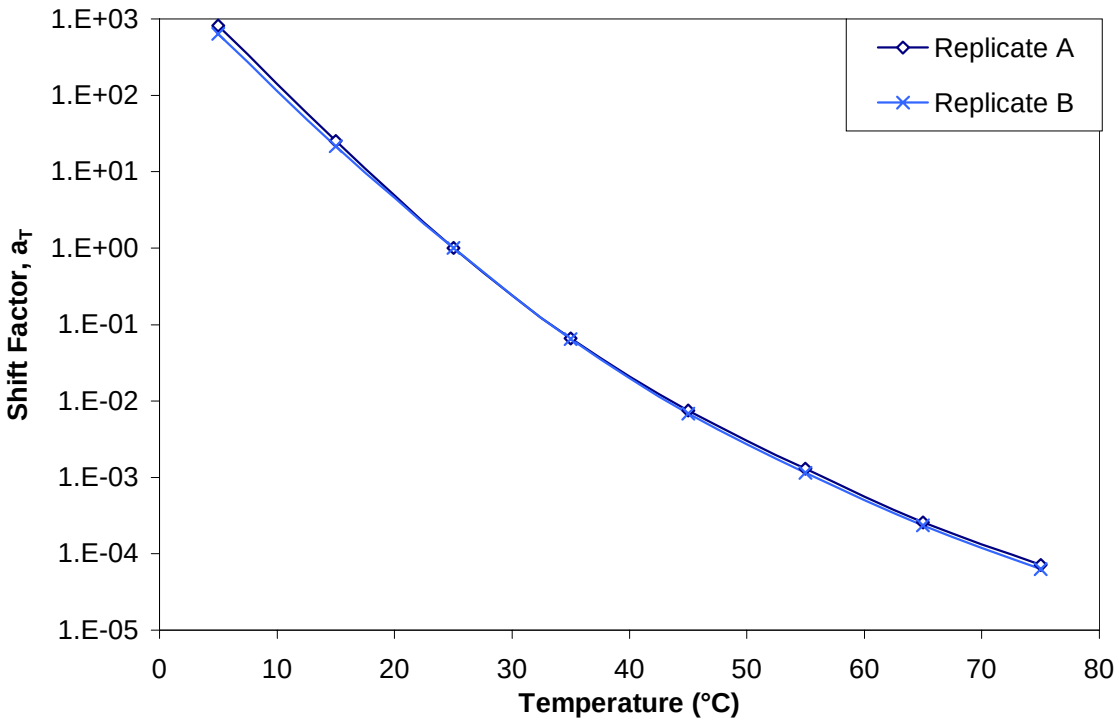


Figure D.19 Shift factors for stored spescimen AUS5.

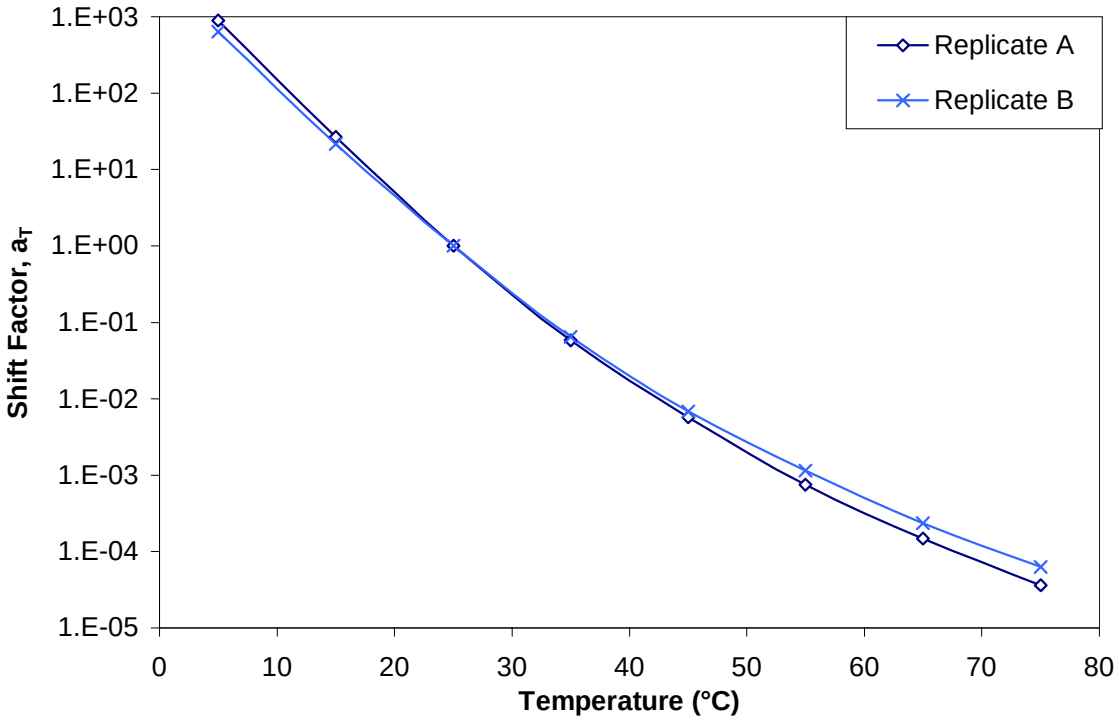


Figure D.20 Shift factors for stored specimen ARS5.

# APPENDIX E

- This appendix includes the comparison of original and stored storage and loss shear moduli mastercurves for all specimens.

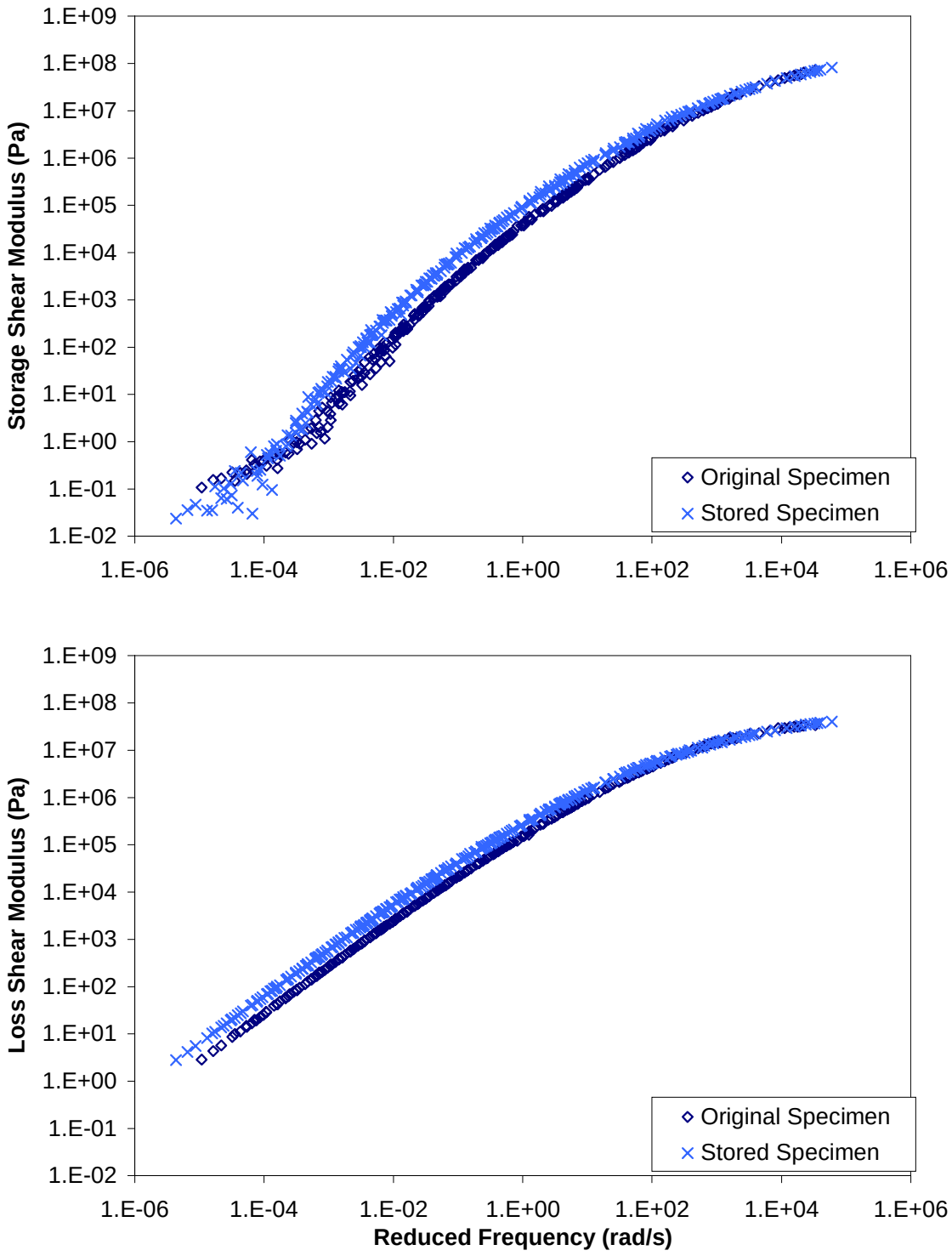


Figure E.1 Comparison of storage and loss shear mastercurves for specimen AU00.

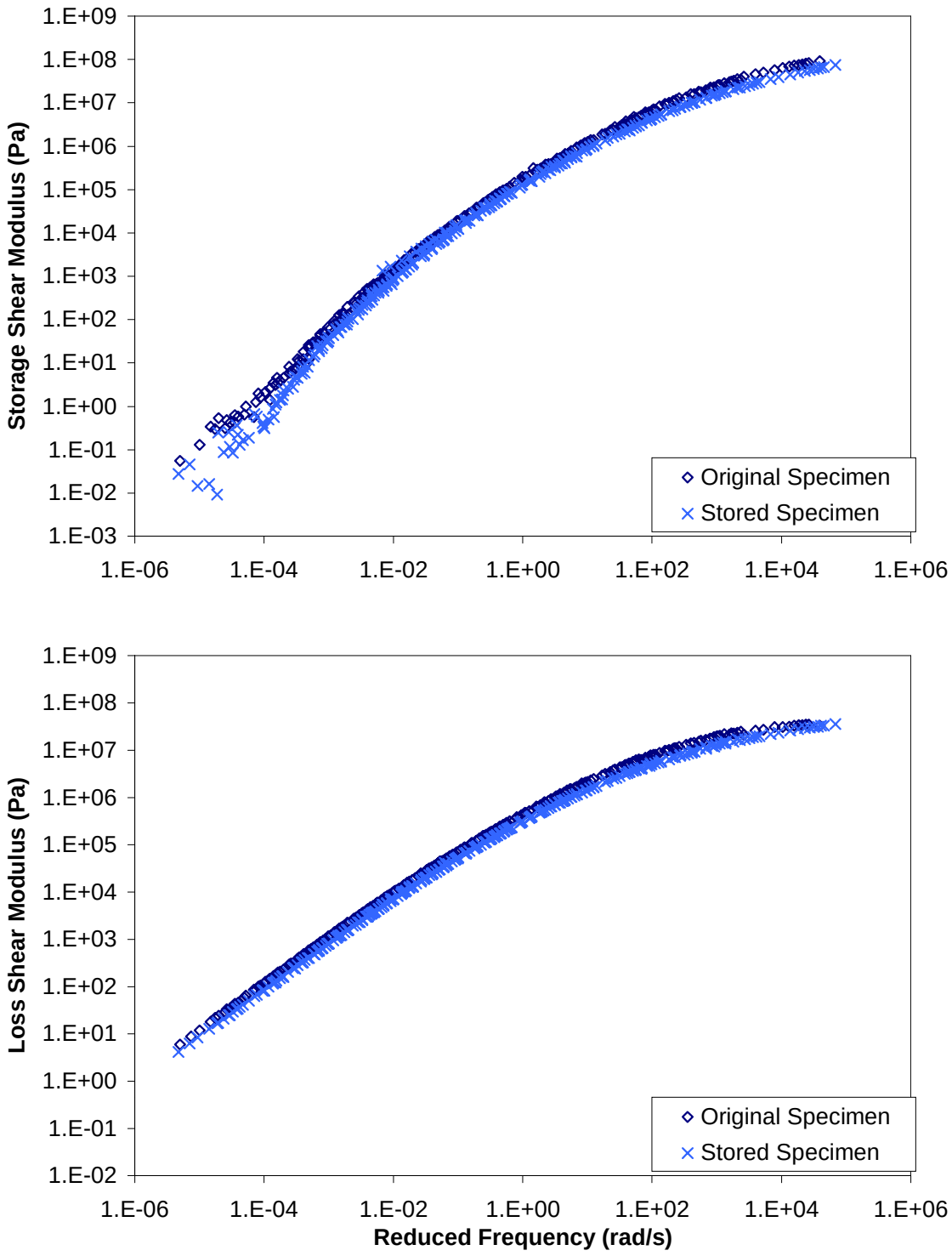


Figure E.2 Comparison of storage and loss shear mastercurves for specimen AR00.

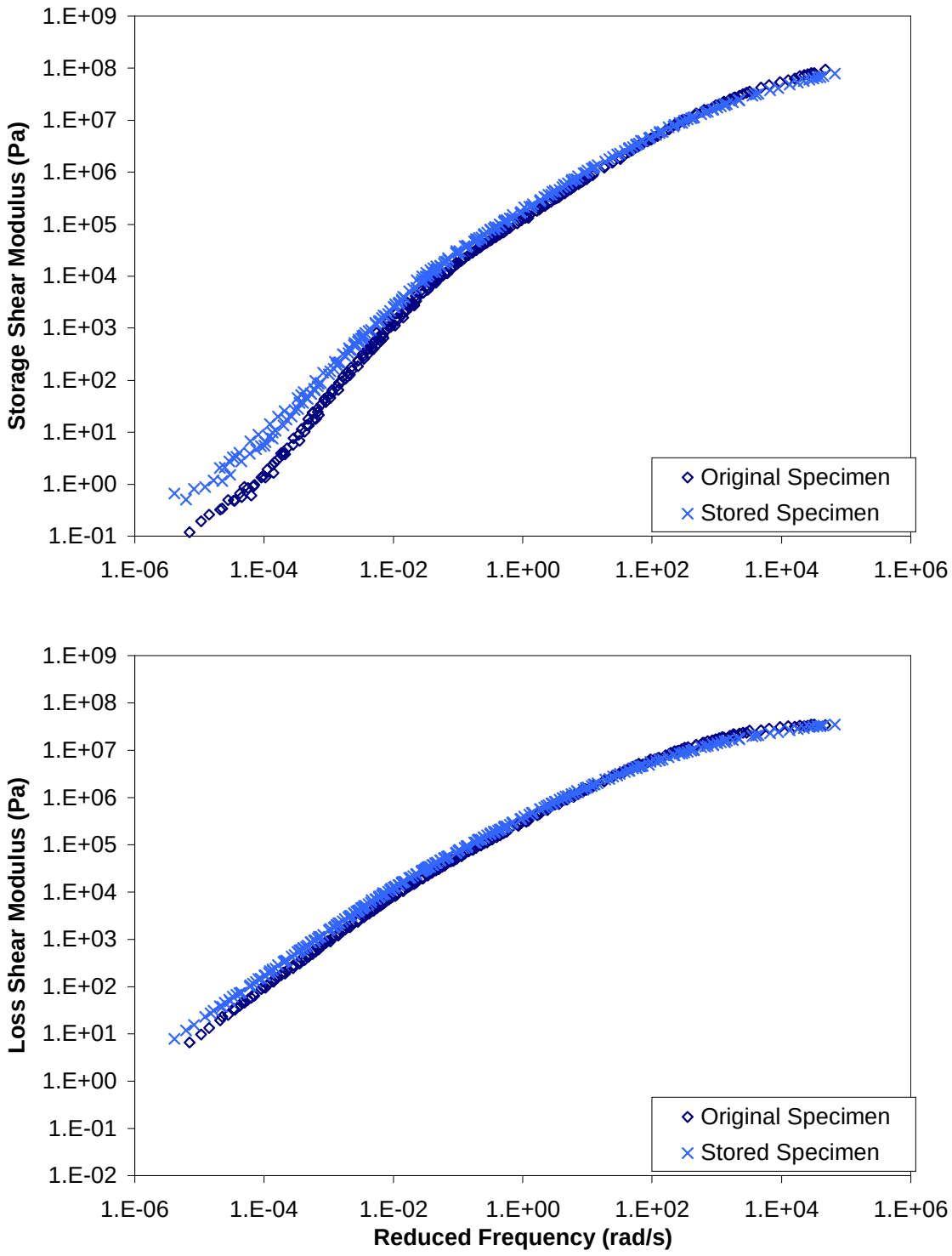


Figure E.3 Comparison of storage and loss shear mastercurves for specimen AUG3.

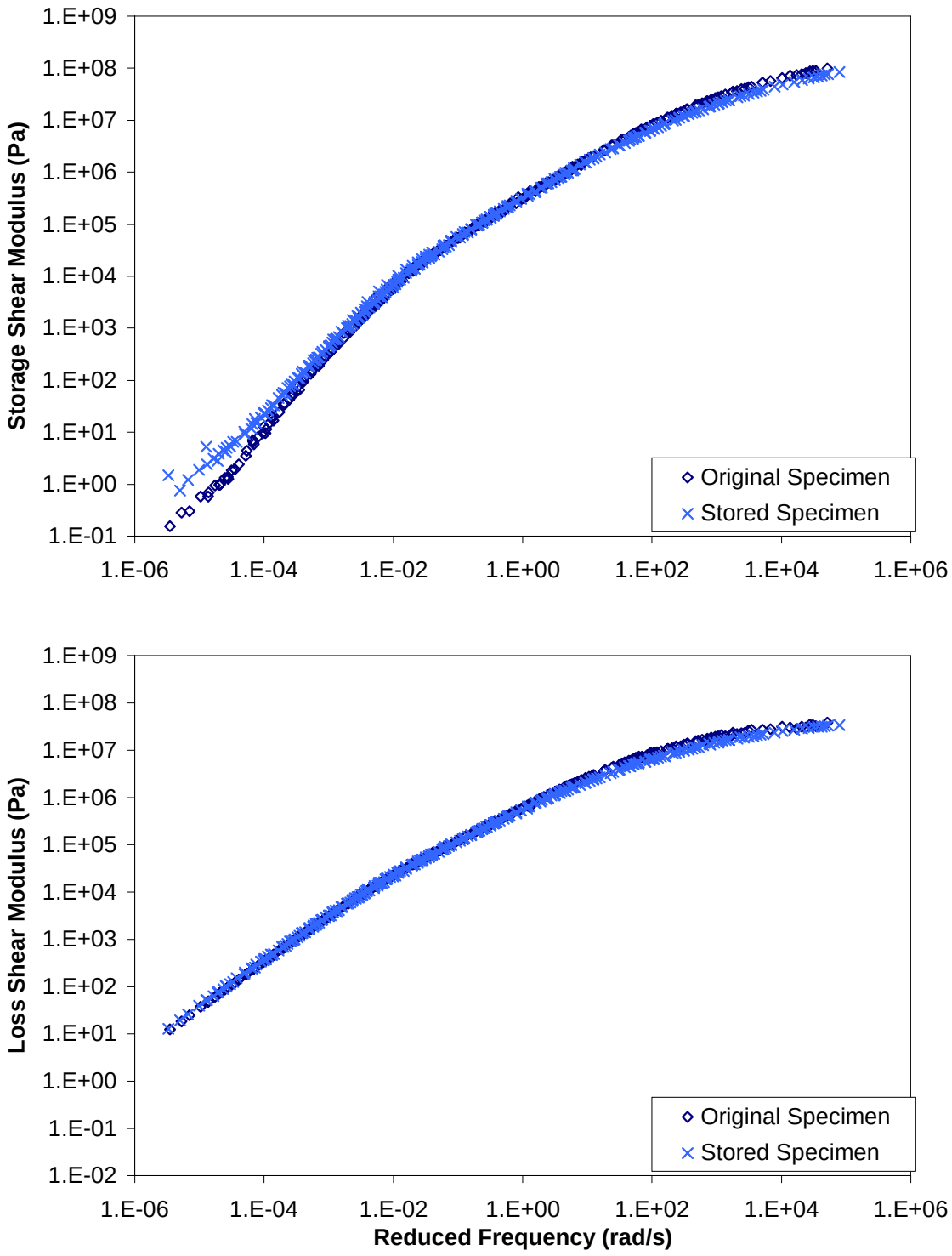


Figure E.4 Comparison of storage and loss shear mastercurves for specimen ARG3.

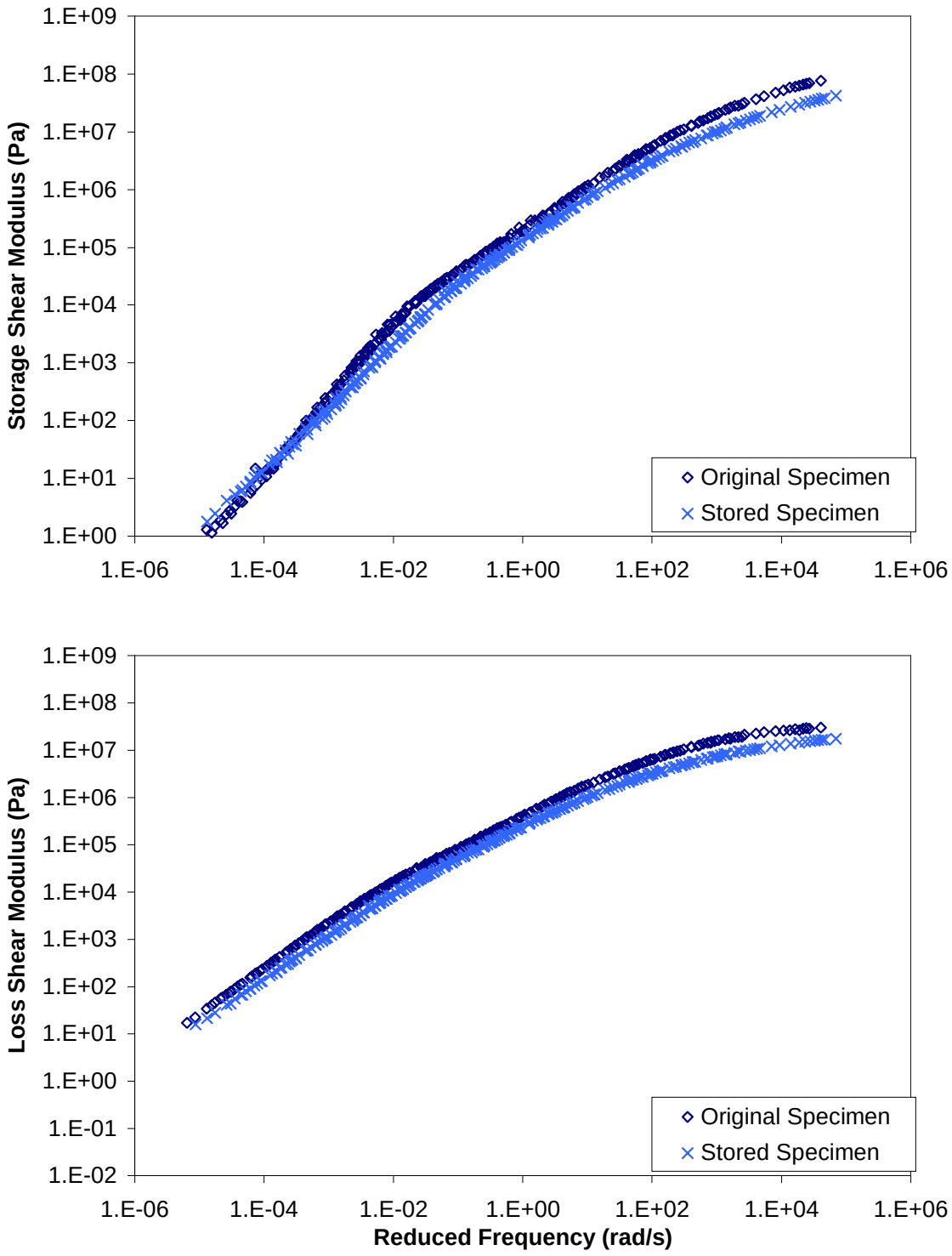


Figure E.5 Comparison of storage and loss shear mastercurves for specimen AUG4.

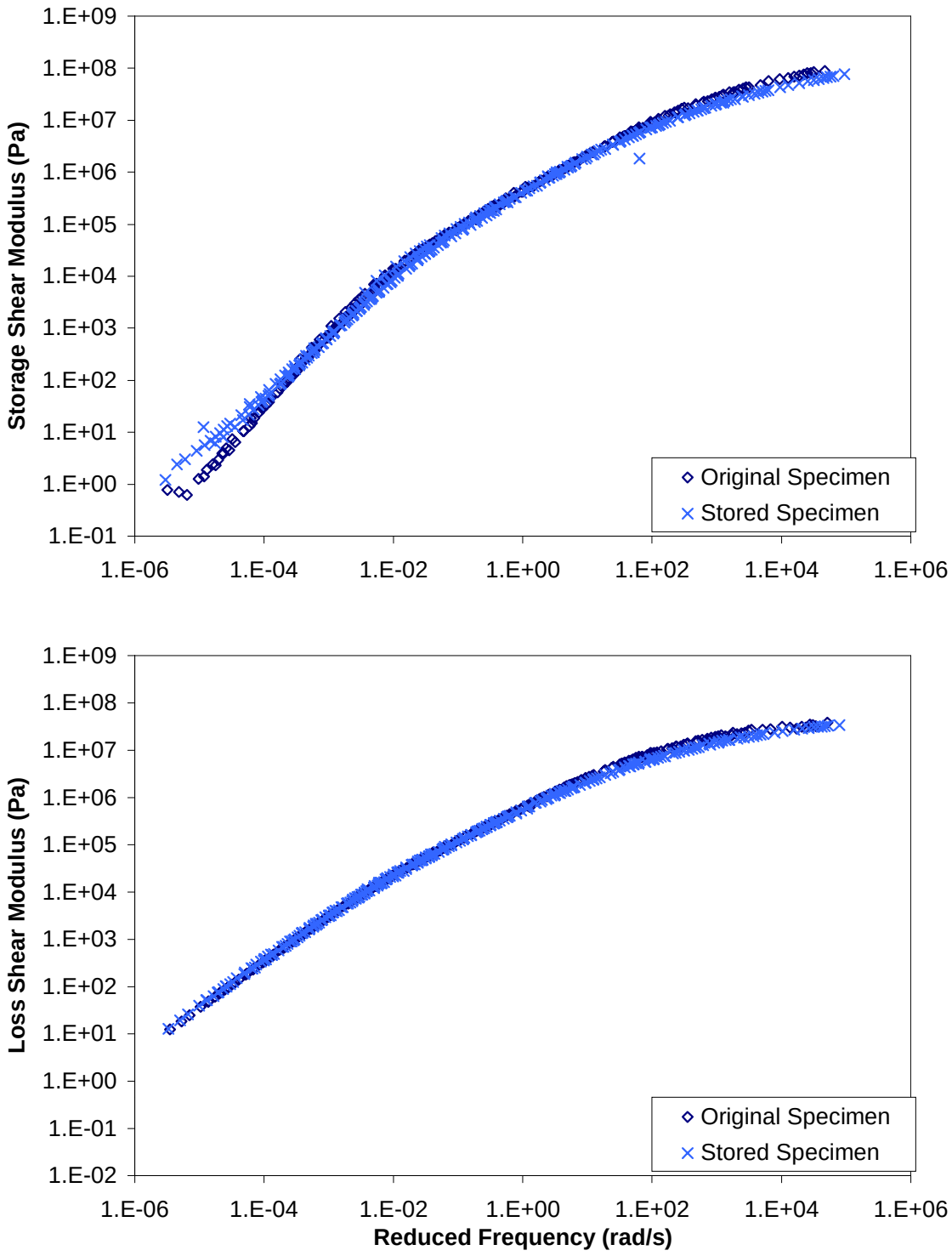


Figure E.6 Comparison of storage and loss shear mastercurves for specimen ARG4.

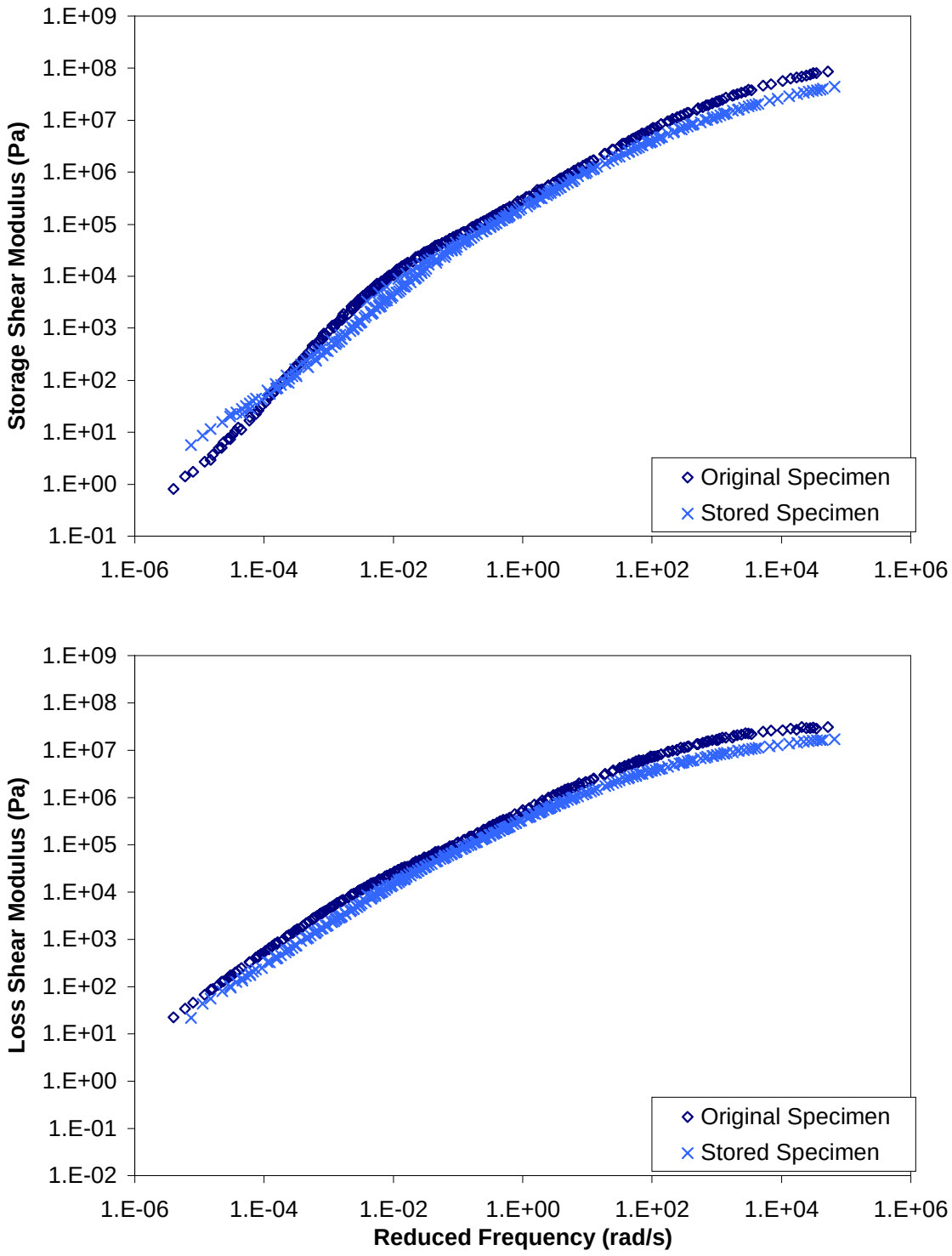


Figure E.7 Comparison of storage and loss shear mastercurves for specimen AUG5.

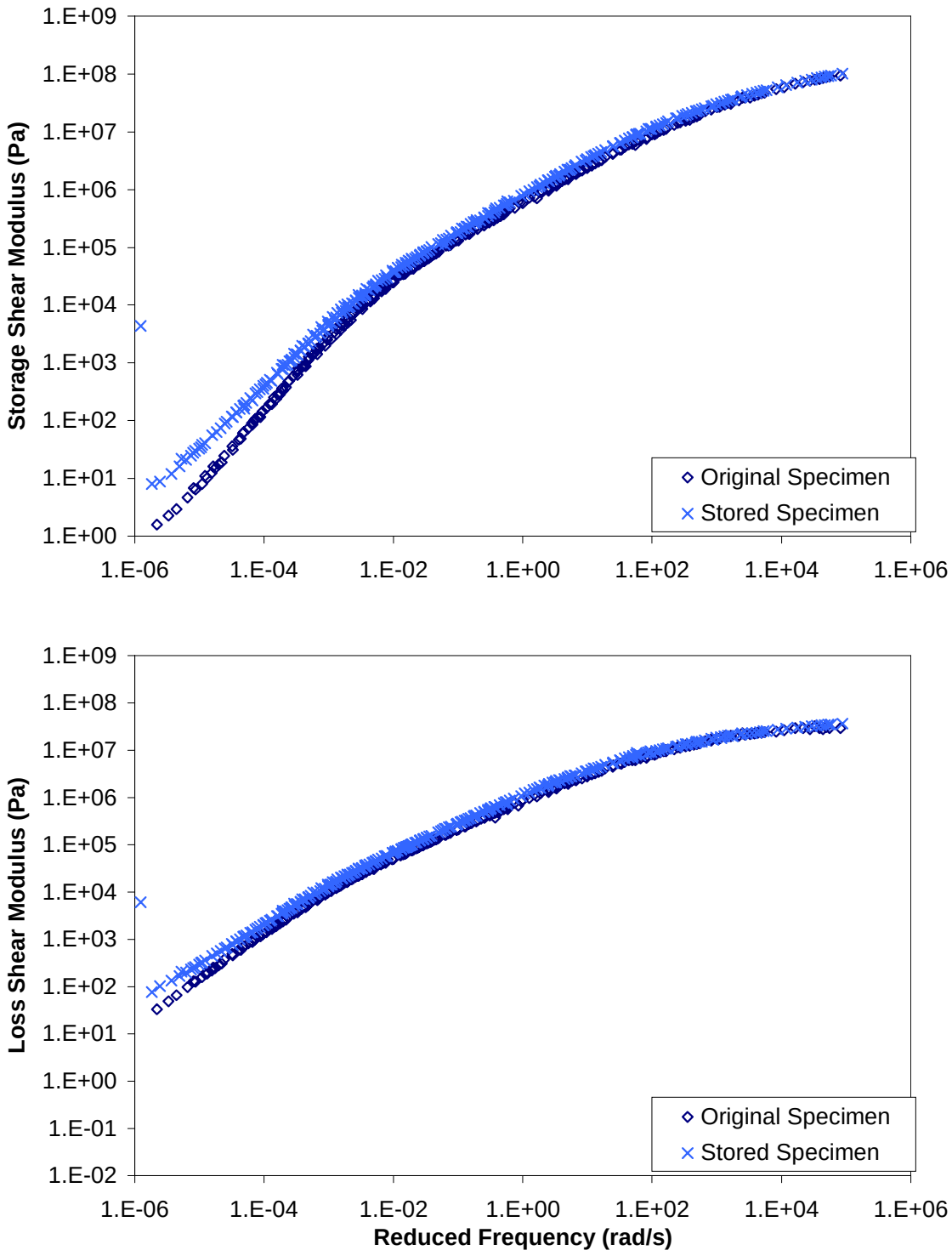


Figure E.8 Comparison of storage and loss shear mastercurves for specimen ARG5.

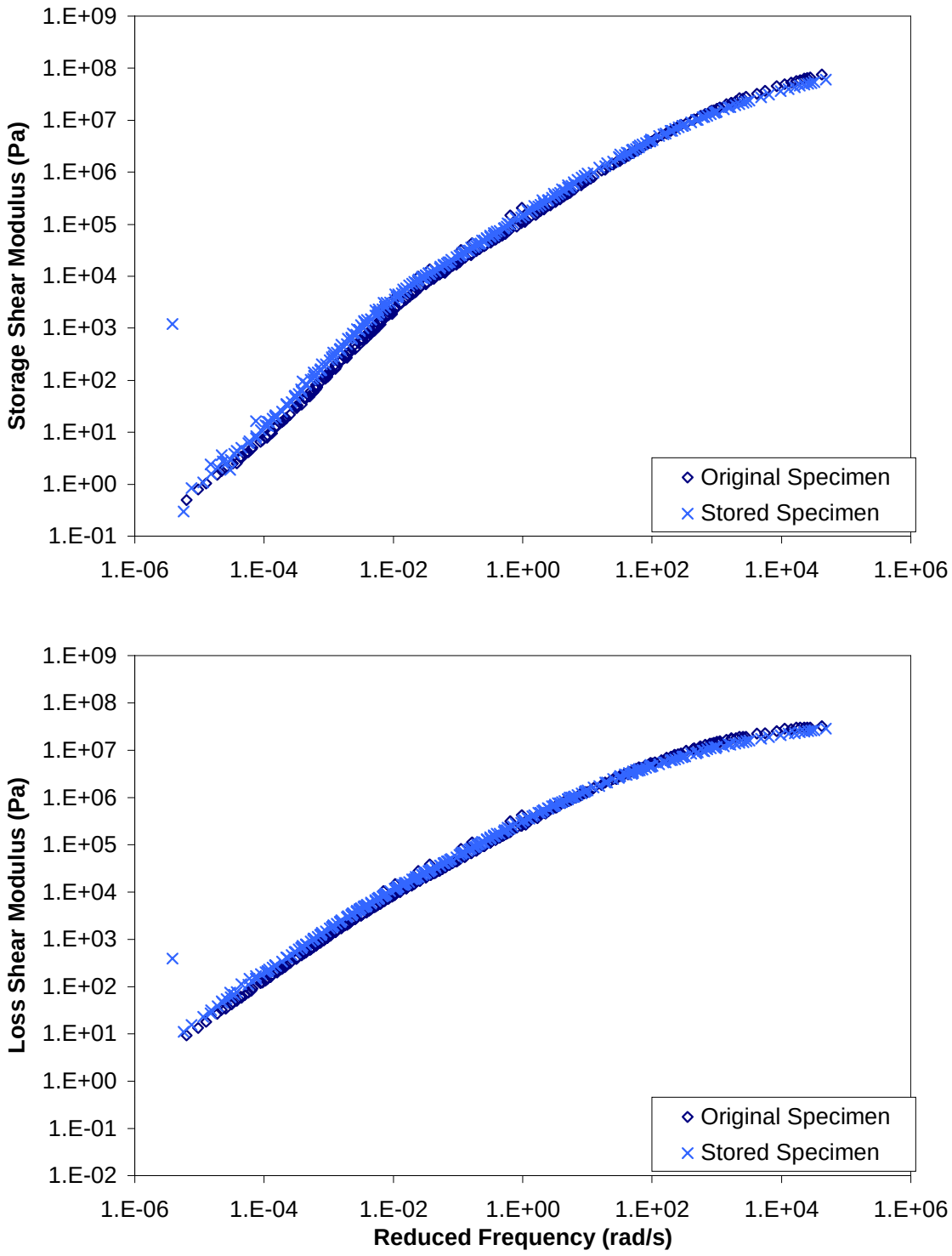


Figure E.9 Comparison of storage and loss shear mastercurves for specimen AUN3.

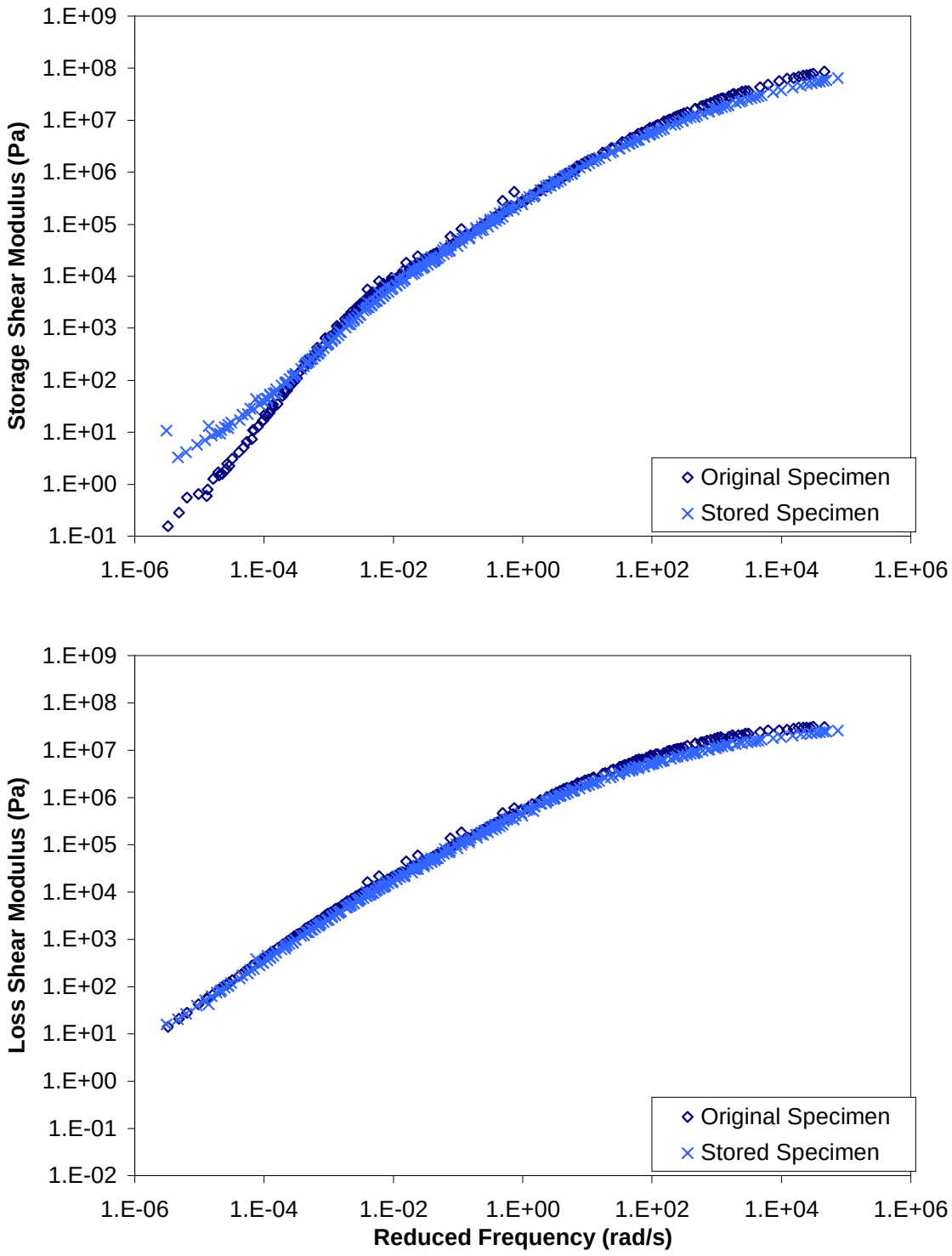


Figure E.10 Comparison of storage and loss shear mastercurves for specimen ARN3.

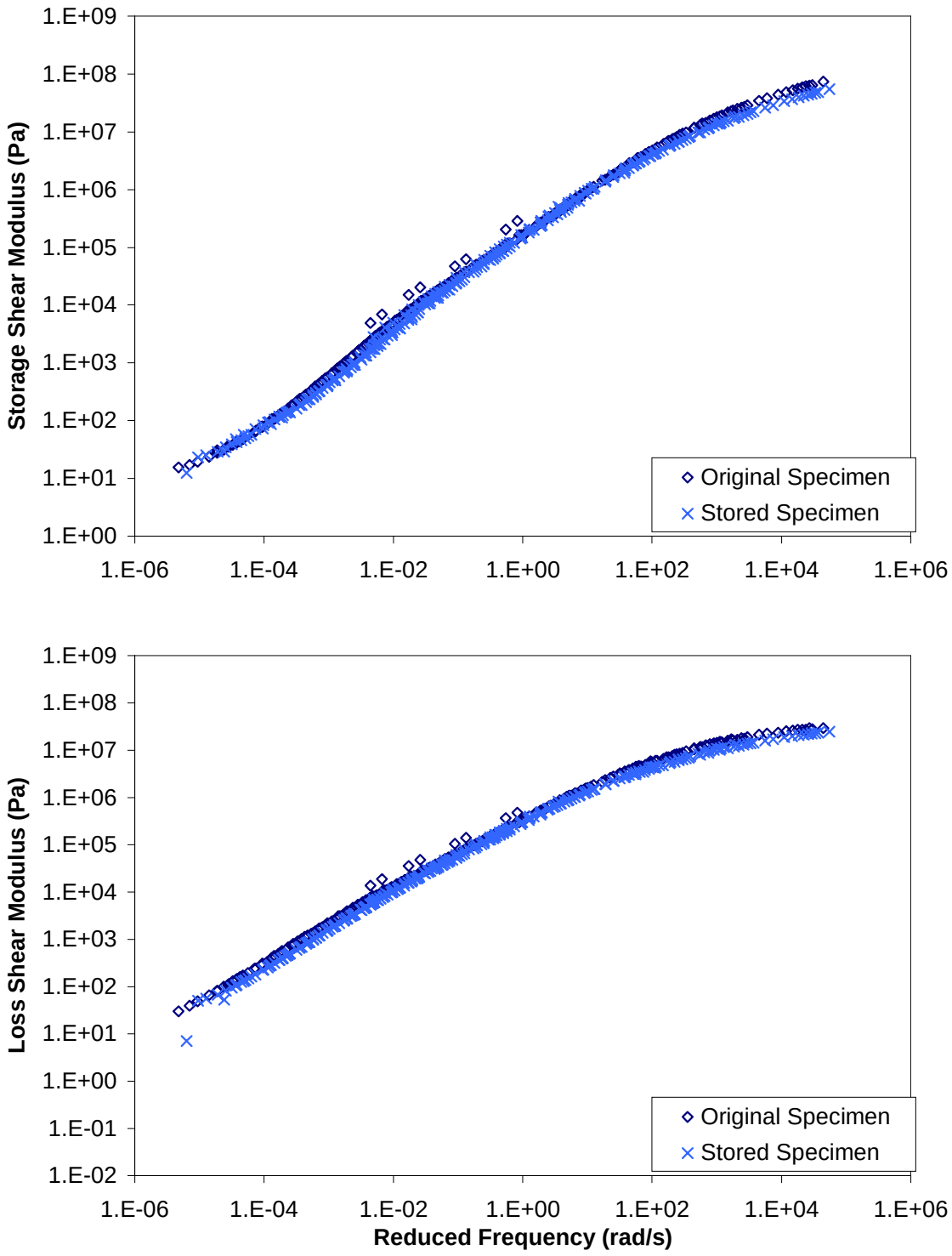


Figure E.11 Comparison of storage and loss shear mastercurves for specimen AUN4.

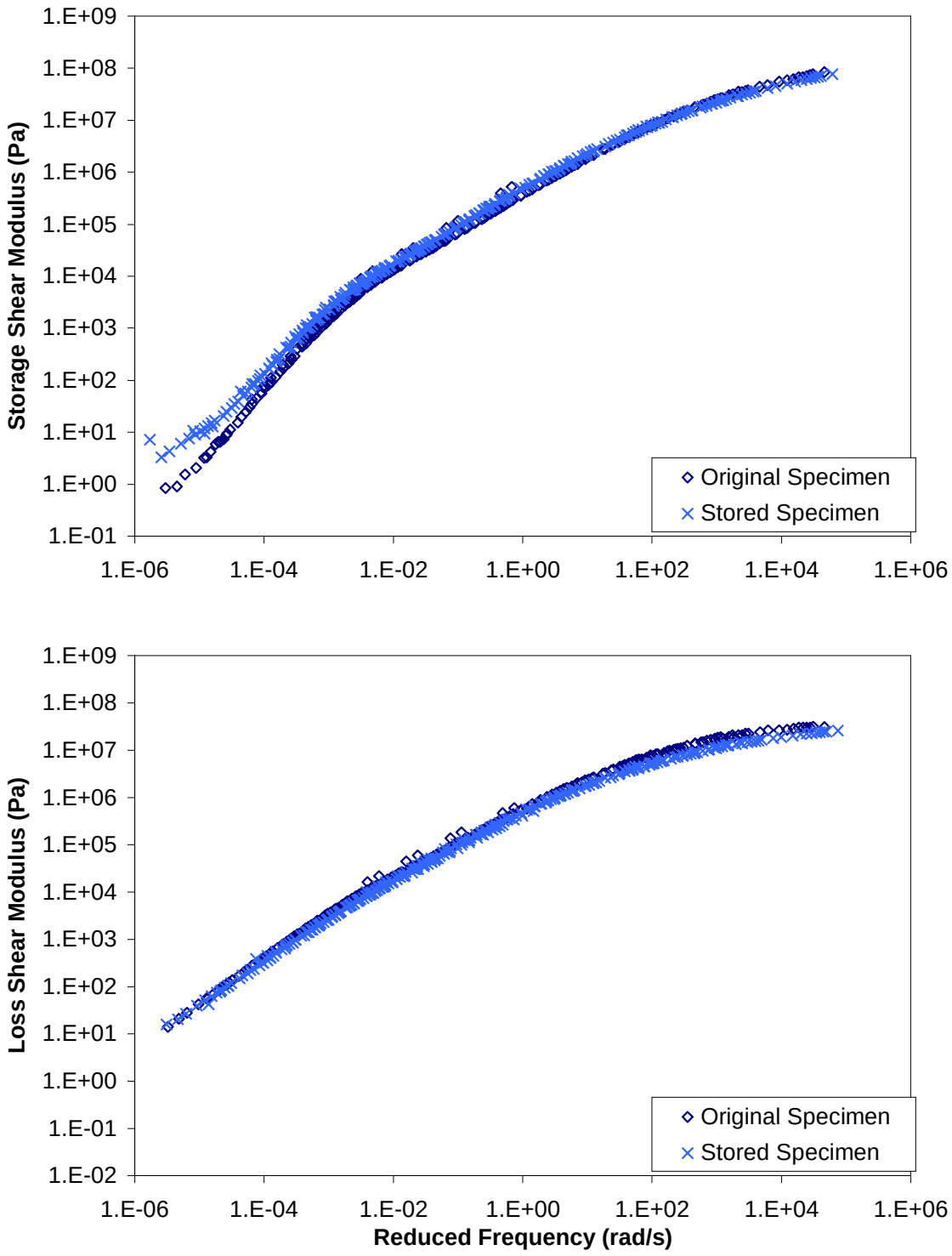


Figure E.12 Comparison of storage and loss shear mastercurves for specimen ARN4.

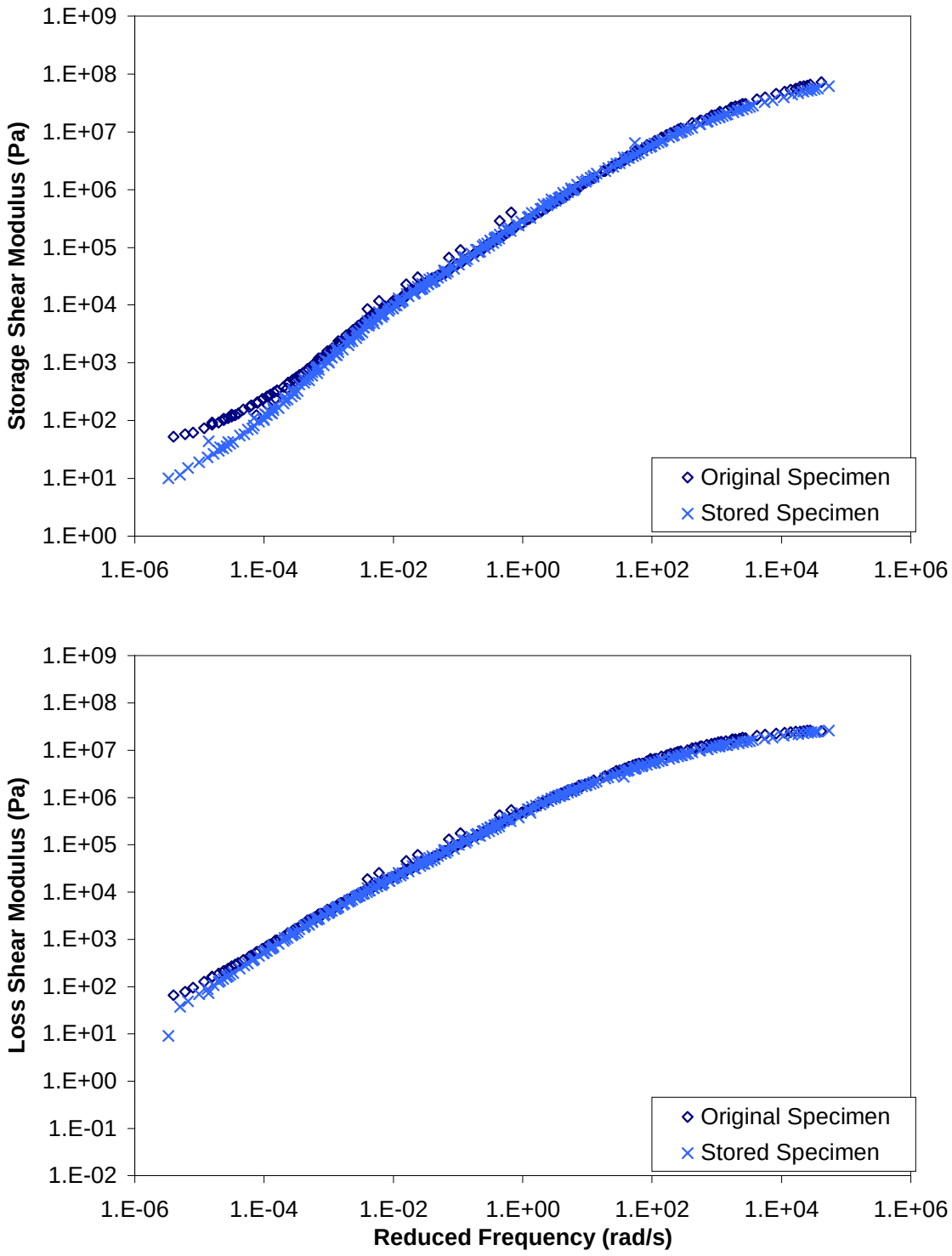


Figure E.13 Comparison of storage and loss shear mastercurves for specimen AUN5.

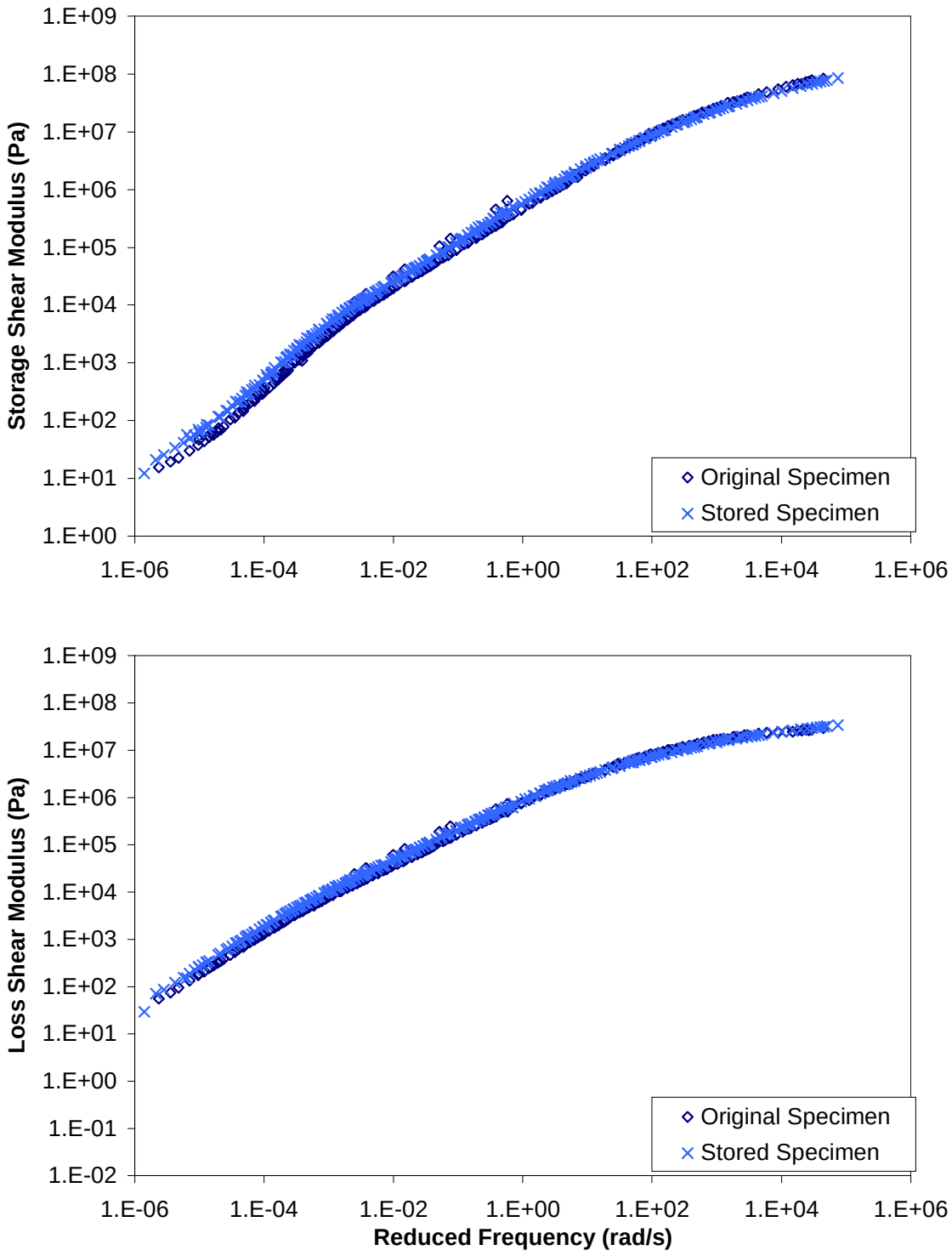


Figure E.14 Comparison of storage and loss shear mastercurves for specimen ARN5.

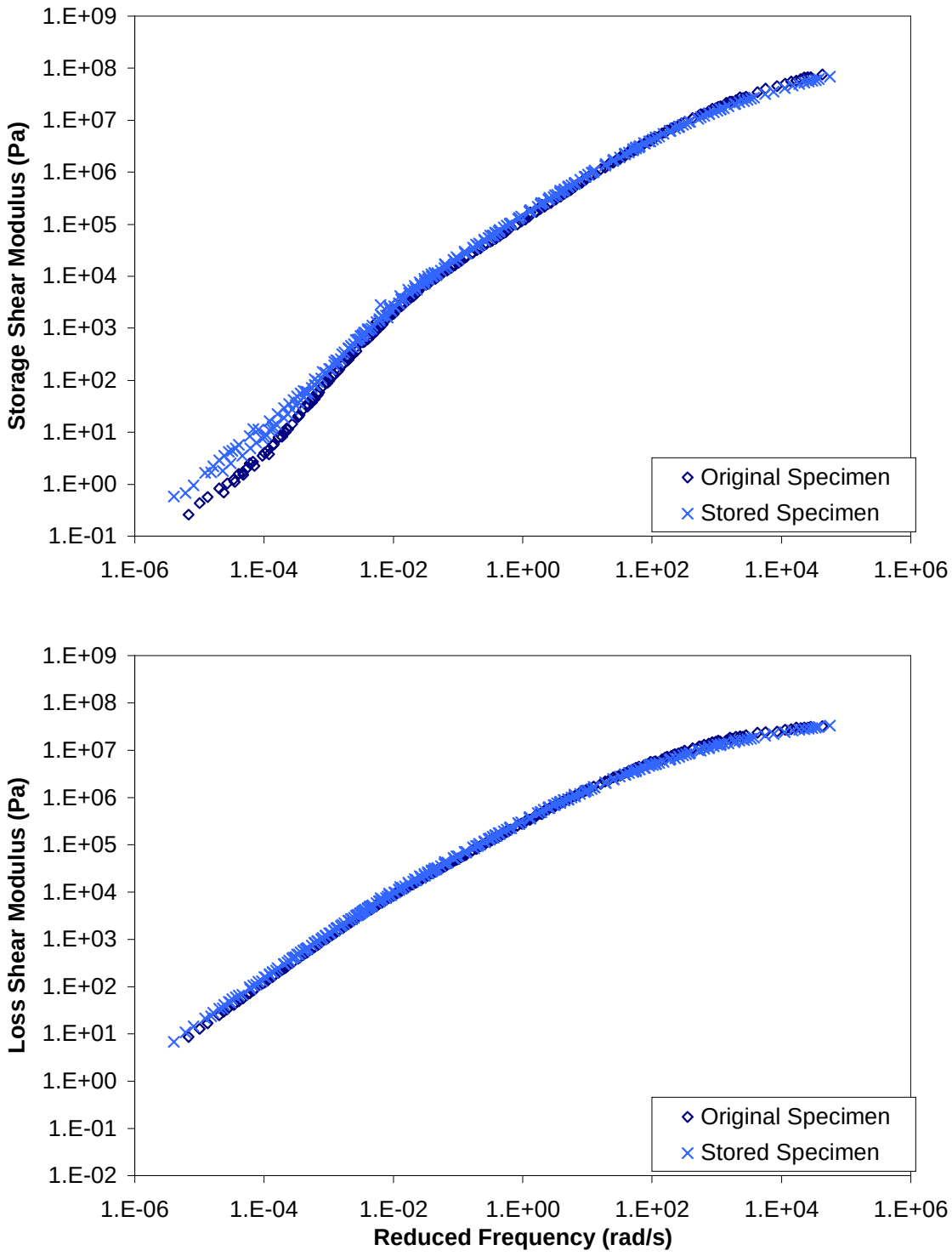


Figure E.15 Comparison of storage and loss shear mastercurves for specimen AUS3.

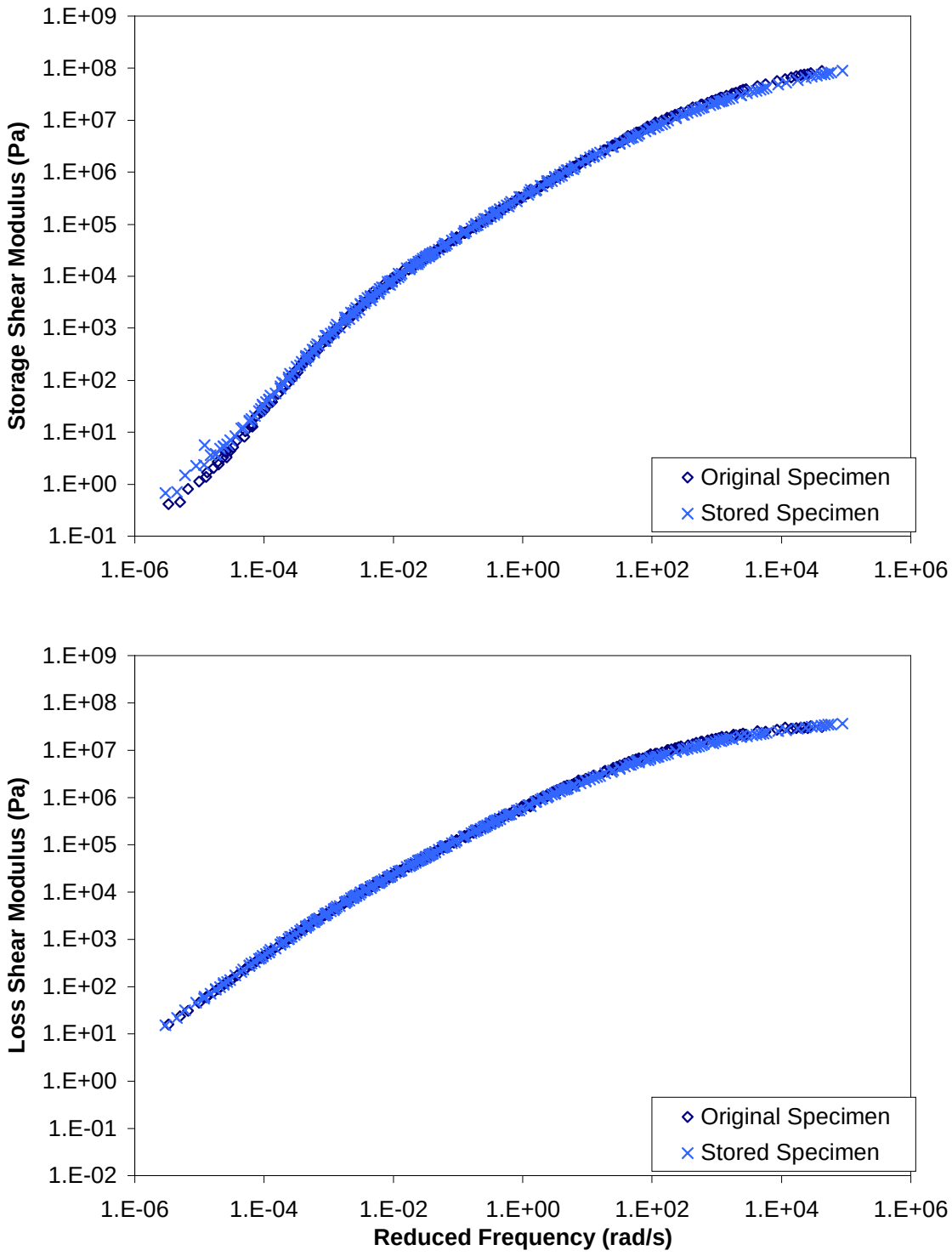


Figure E.16 Comparison of storage and loss shear mastercurves for specimen ARS3.

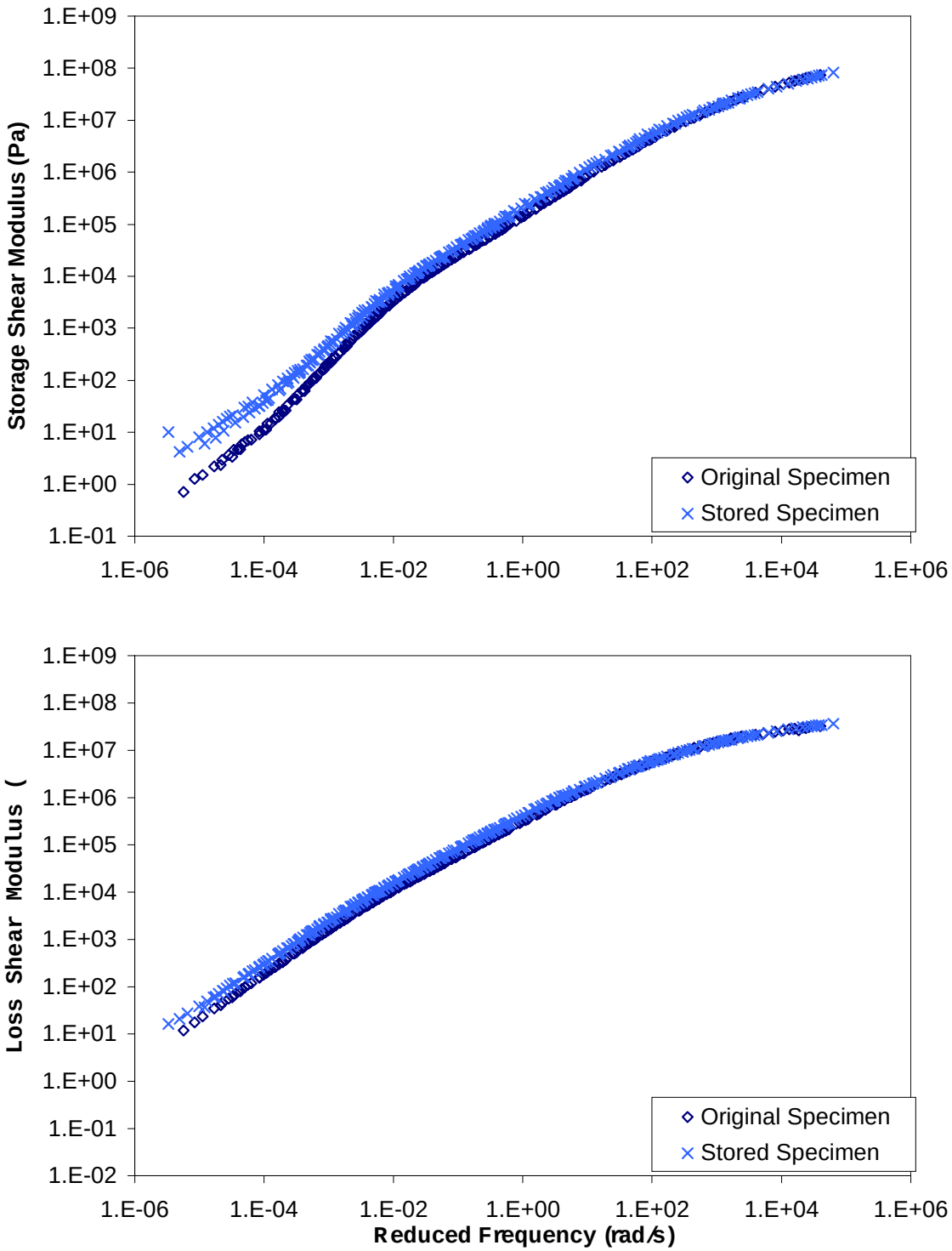


Figure E.17 Comparison of storage and loss shear mastercurves for specimen AUS4.

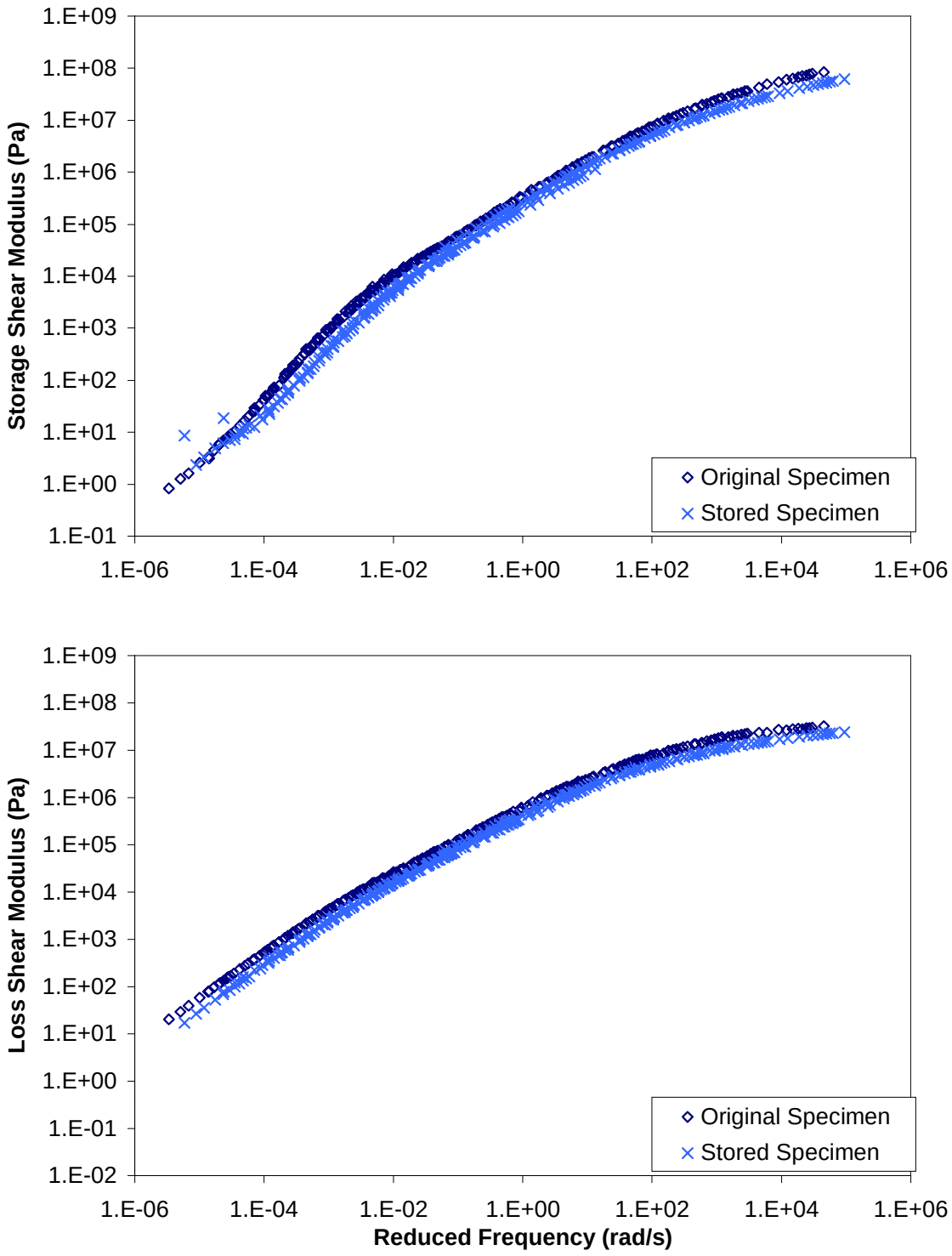


Figure E.18 Comparison of storage and loss shear mastercurves for specimen ARS4.

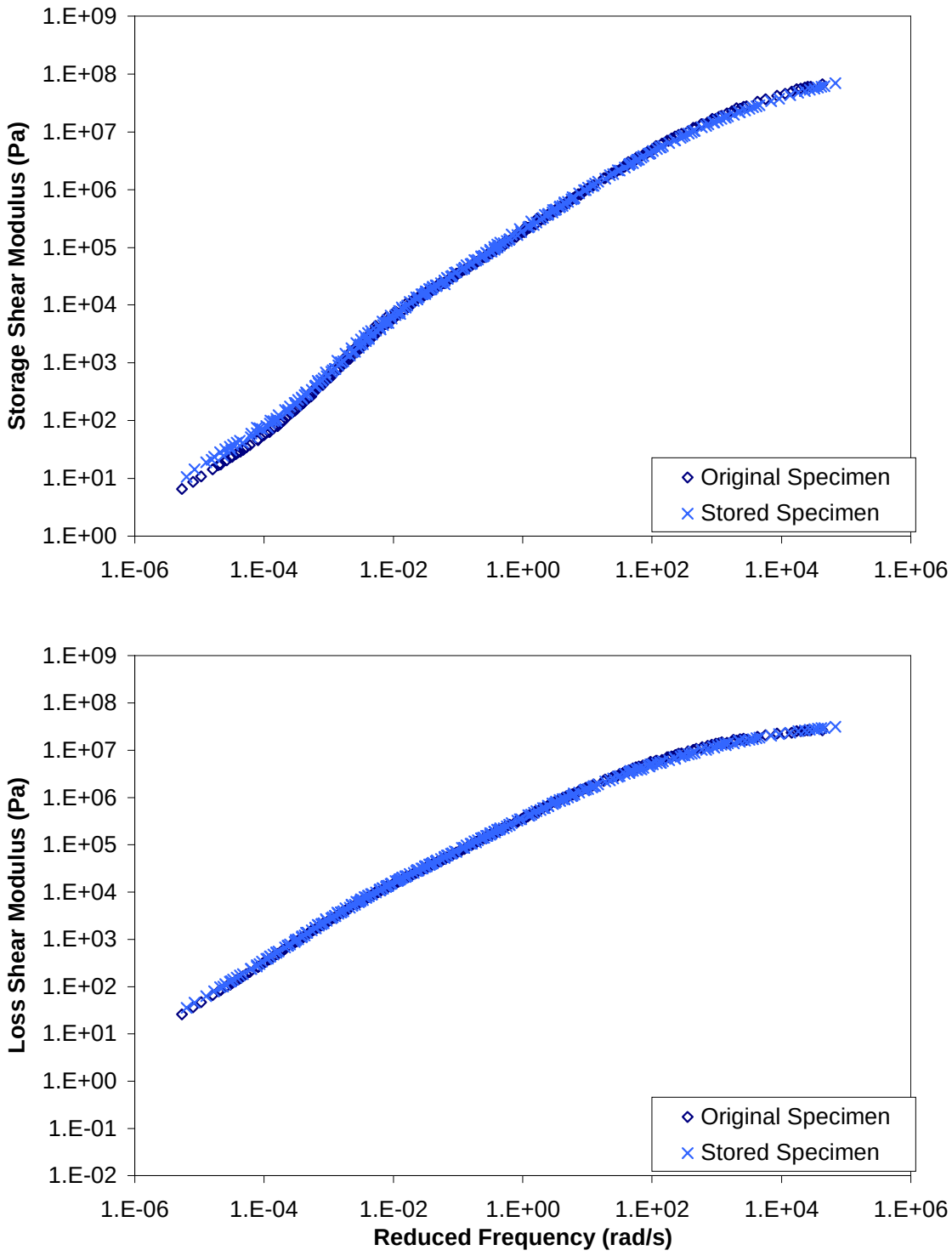


Figure E.19 Comparison of storage and loss shear mastercurves for specimen AUS5.

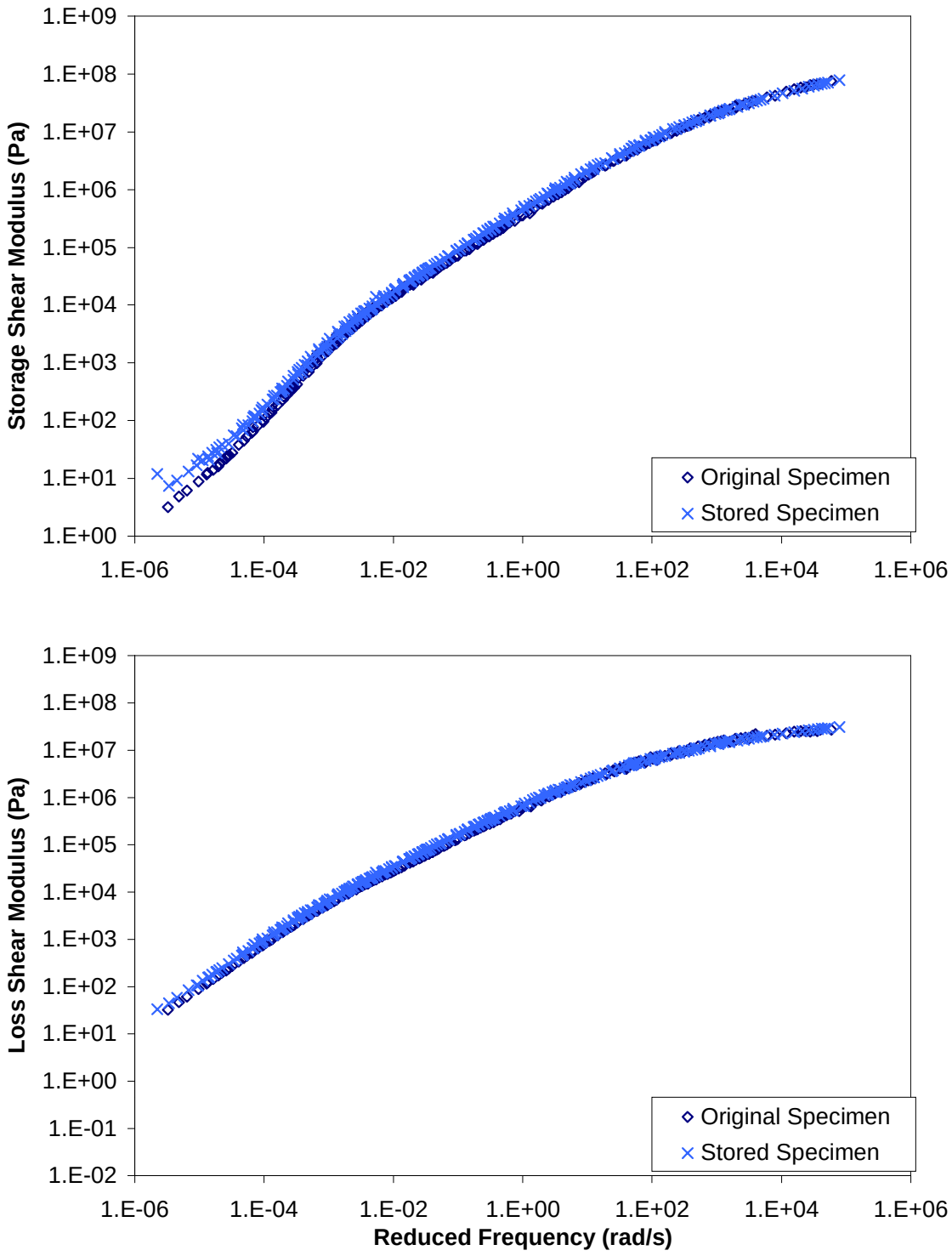


Figure E.20 Comparison of storage and loss shear mastercurves for specimen ARS5.

# APPENDIX F

- This appendix includes representations of the graphical method of determining model parameters for the Christensen-Anderson model for original specimens.

a)

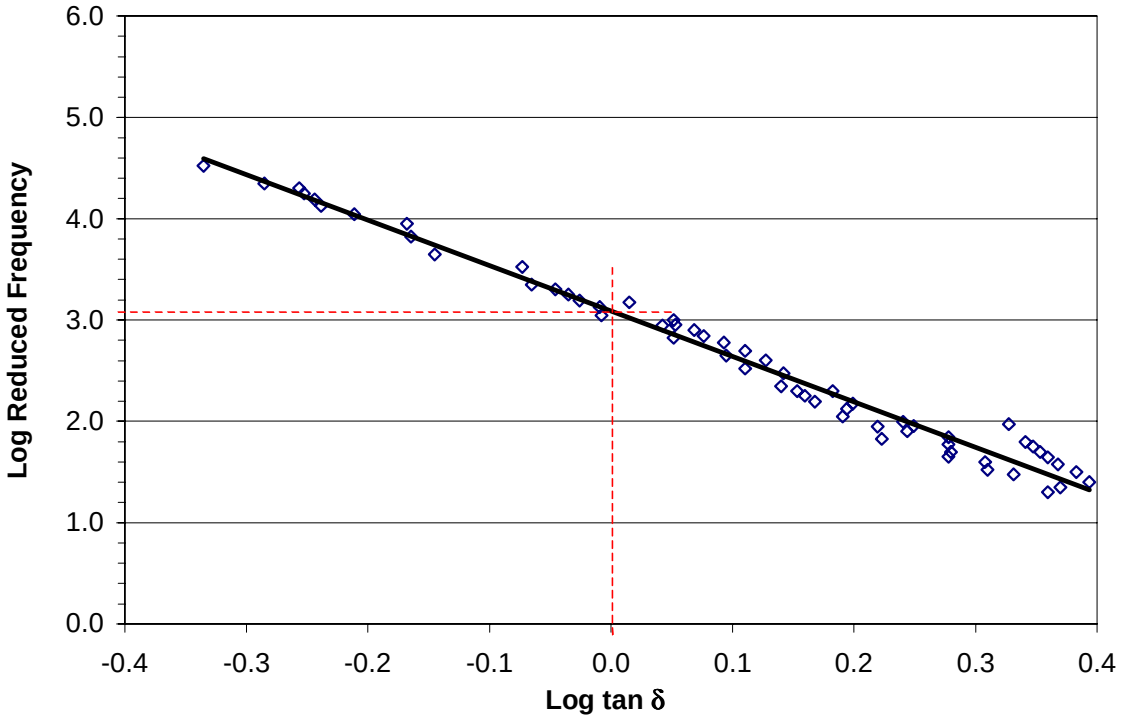


b)

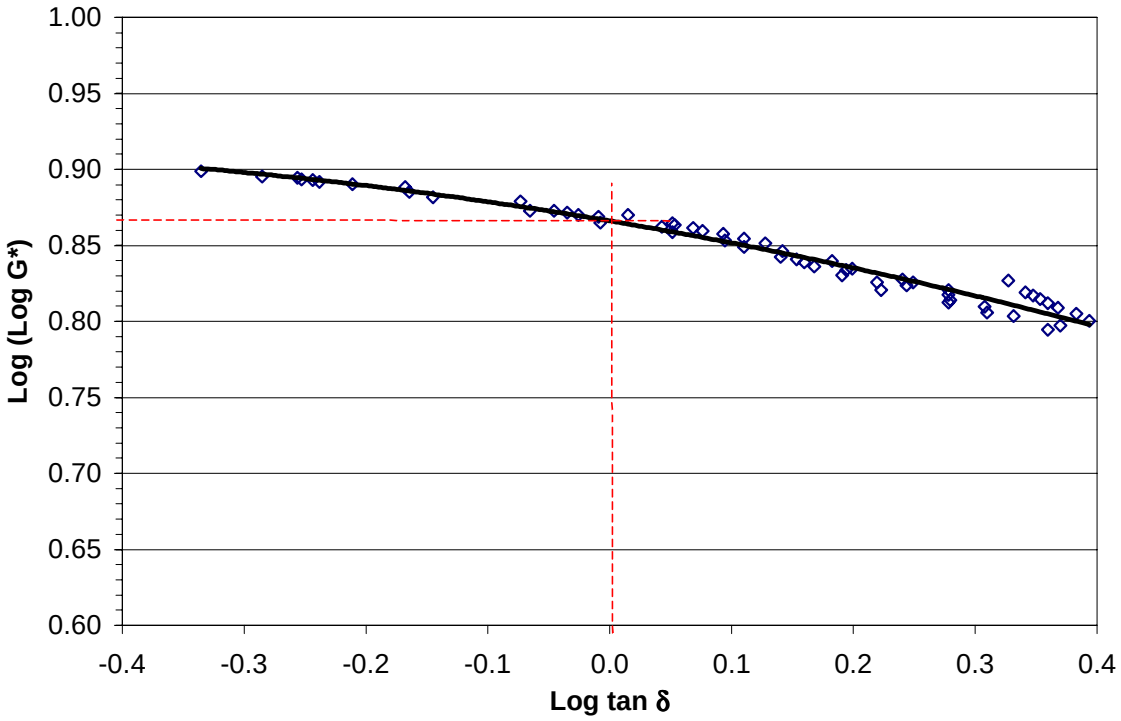


Figure F.1 Method of graphical determination of Christensen - Anderson model parameters: a) crossover frequency and b) rheological index for original specimen AU00.

a)

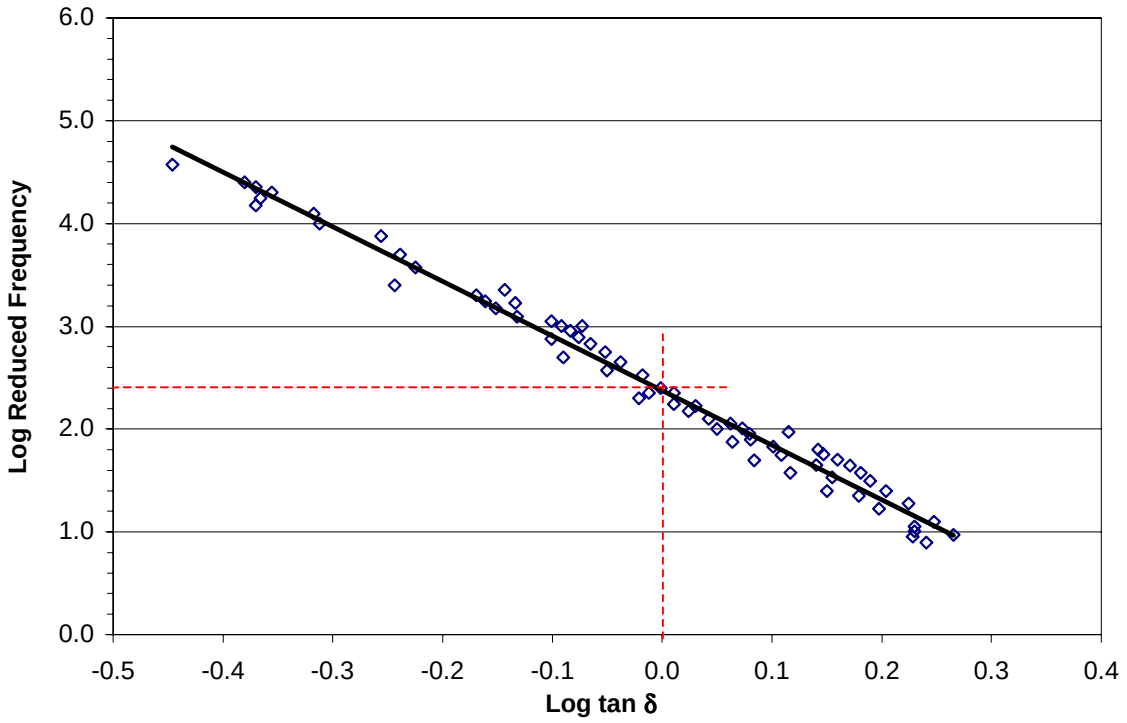


b)

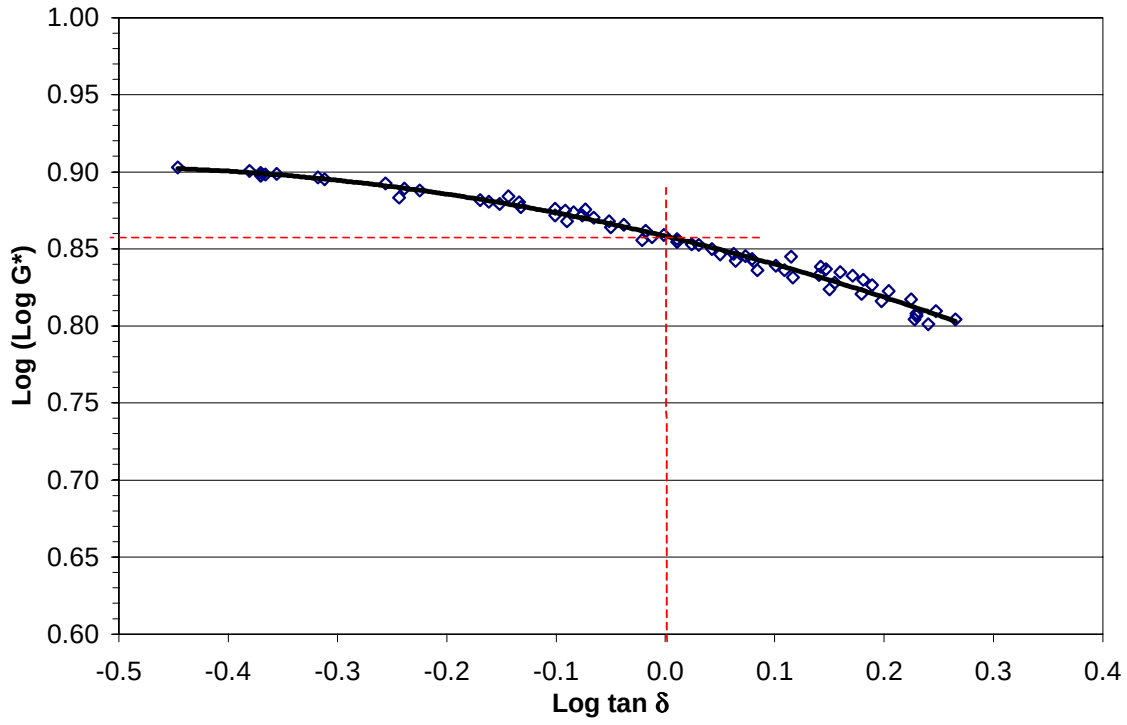


Figure F.2 Method of graphical determination of Christensen - Anderson model parameters: a) crossover frequency and b) rheological index for original specimen AR00.

a)

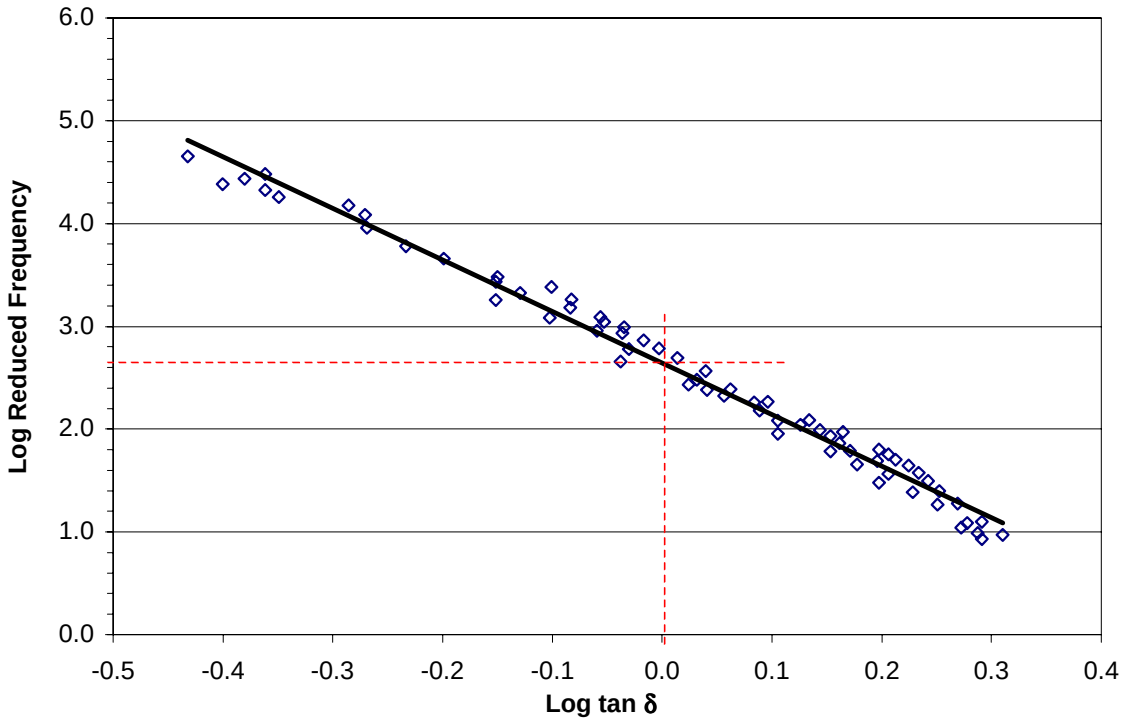


b)

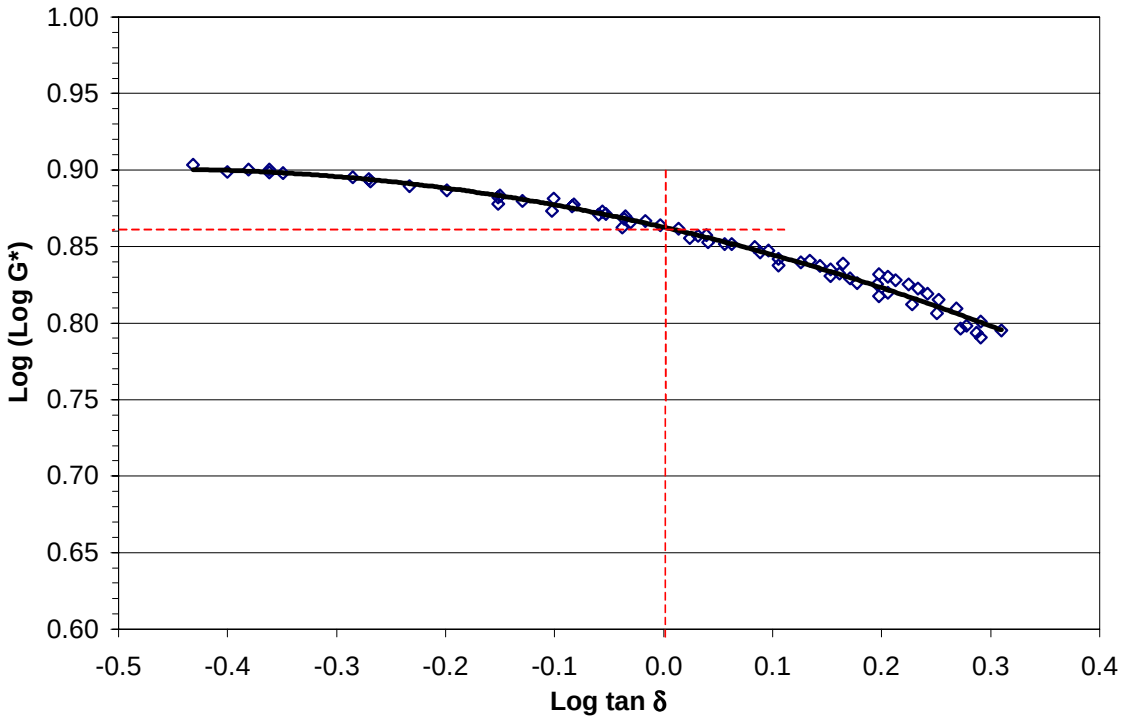


Figure F.3 Method of graphical determination of Christensen - Anderson model parameters: a) crossover frequency and b) rheological index for original specimen AUG3.

a)

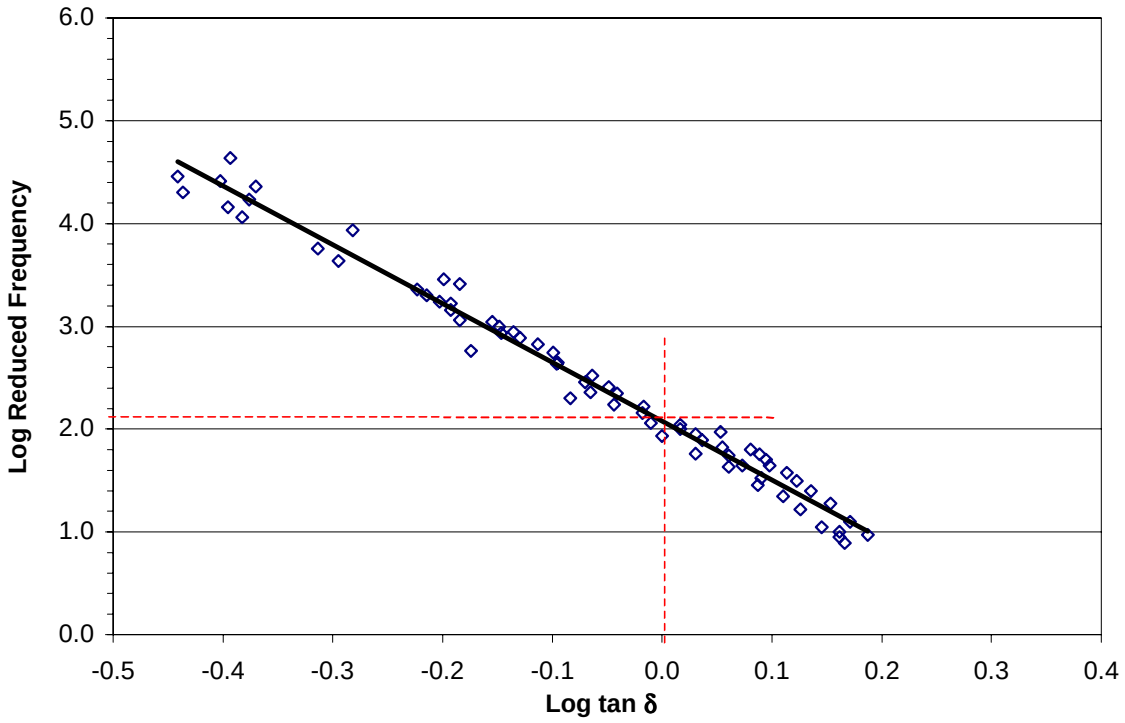


b)

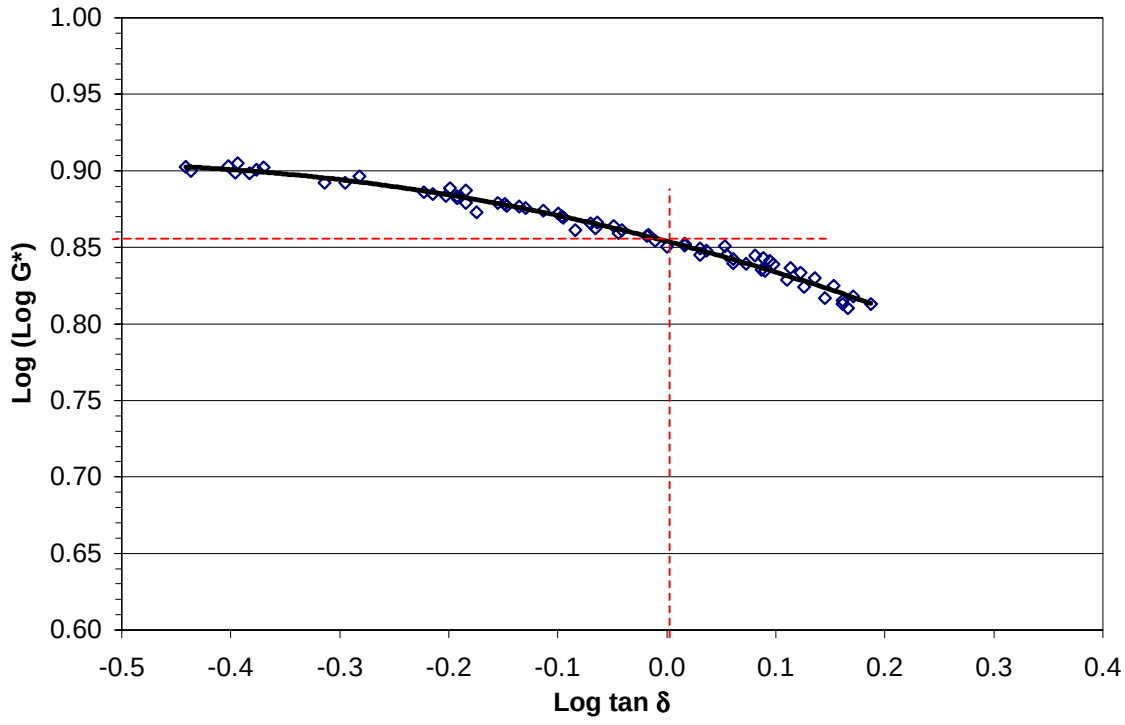


Figure F.4 Method of graphical determination of Christensen - Anderson model parameters: a) crossover frequency and b) rheological index for original specimen ARG3.

a)

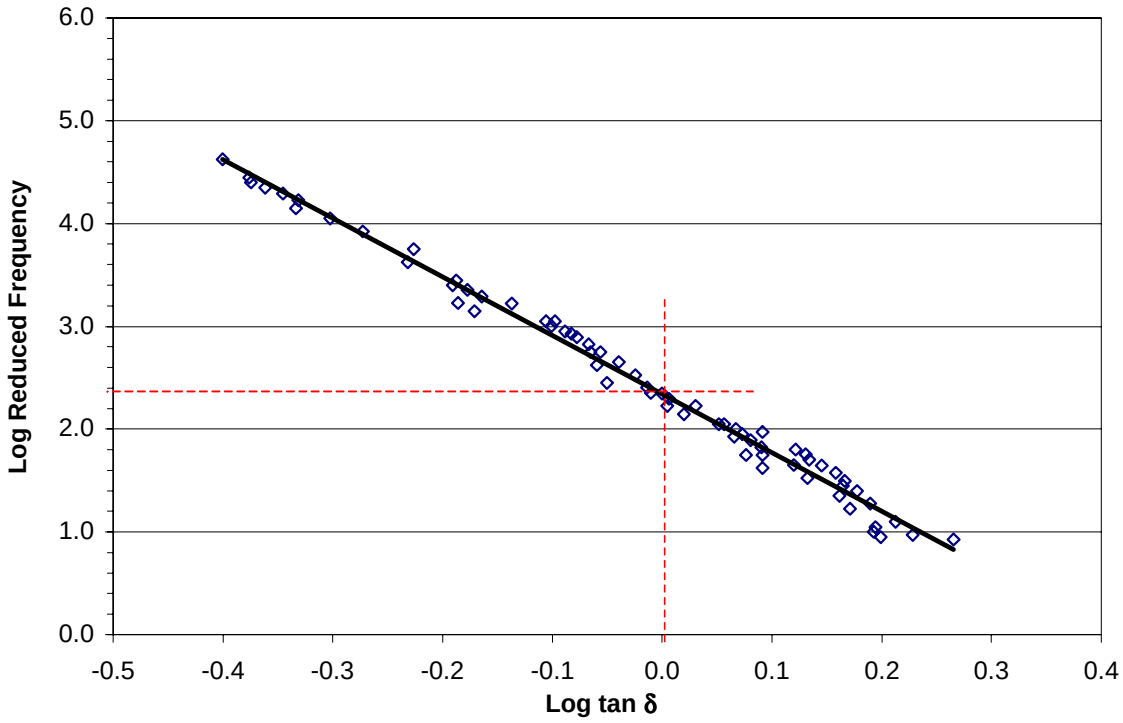


b)

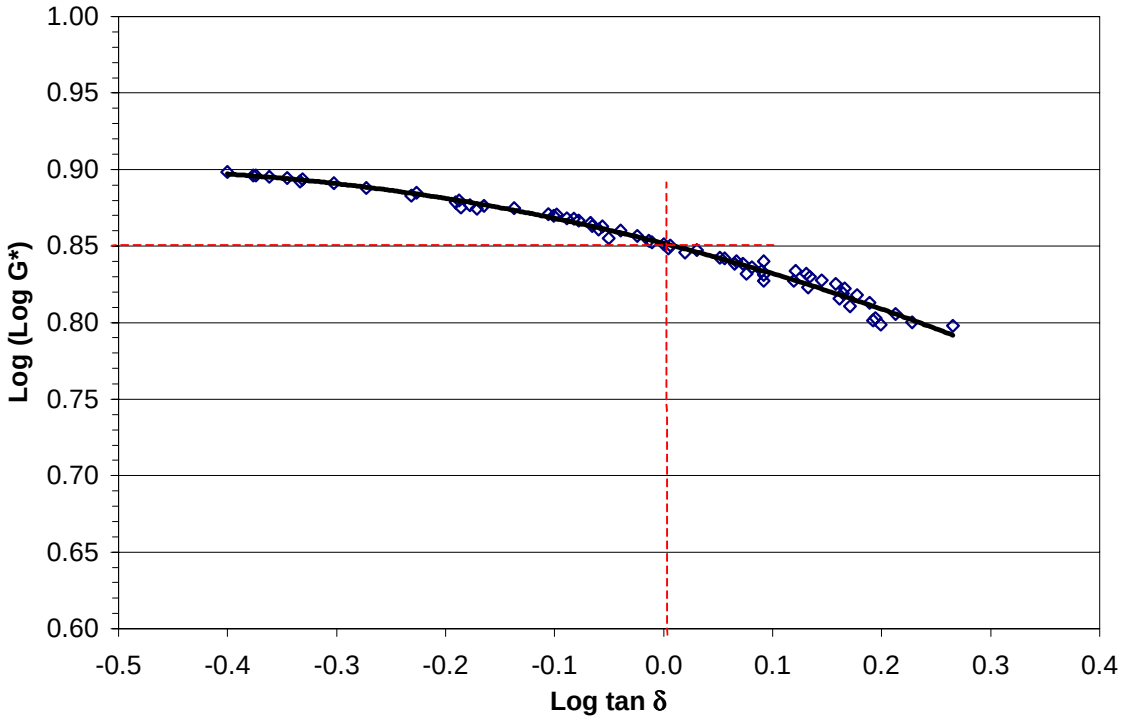


Figure F.5 Method of graphical determination of Christensen - Anderson model parameters: a) crossover frequency and b) rheological index for original specimen AUG4.

a)

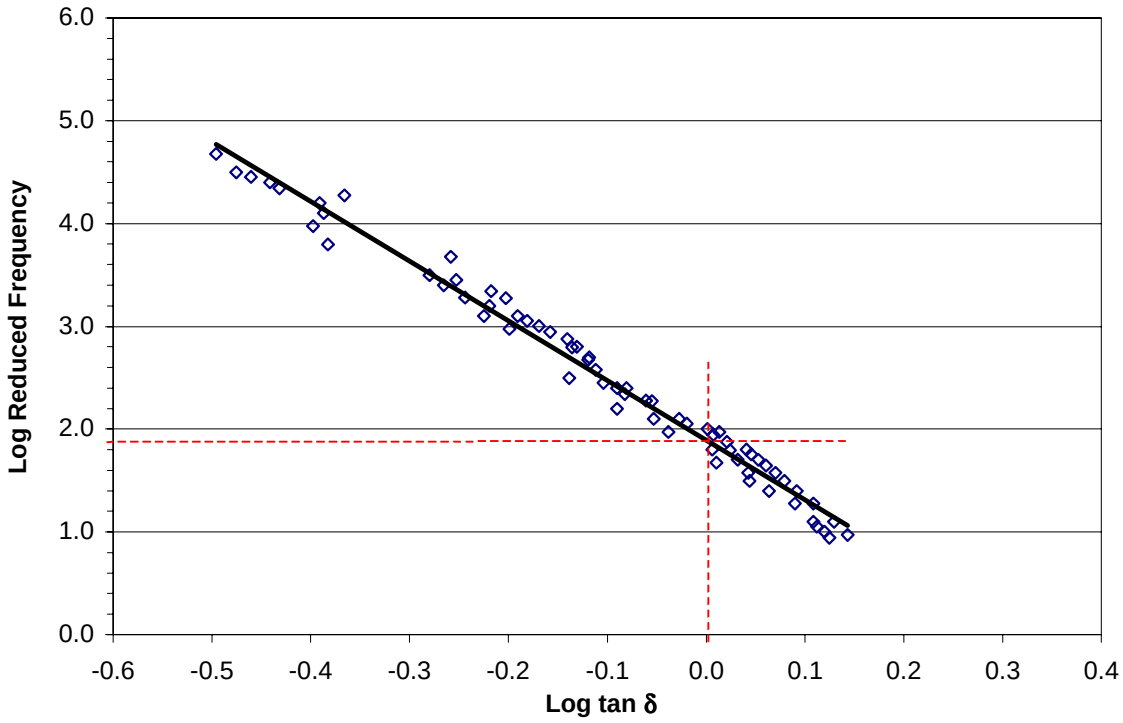


b)

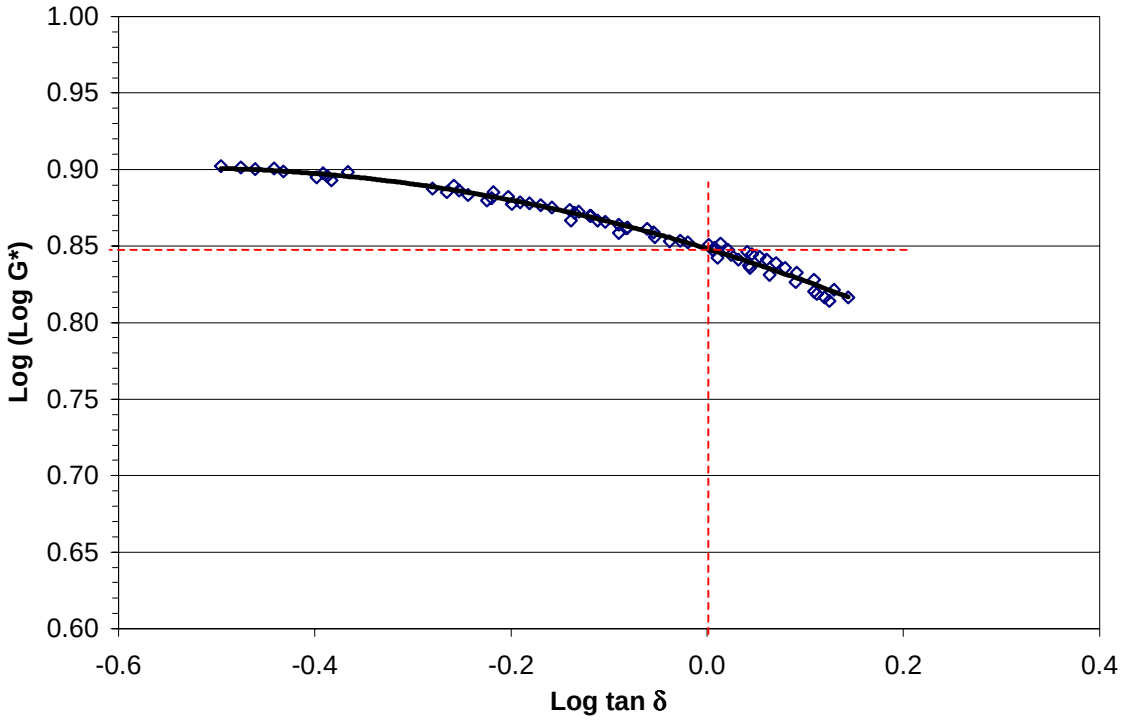


Figure F.6 Method of graphical determination of Christensen - Anderson model parameters: a) crossover frequency and b) rheological index for original specimen ARG4.

a)

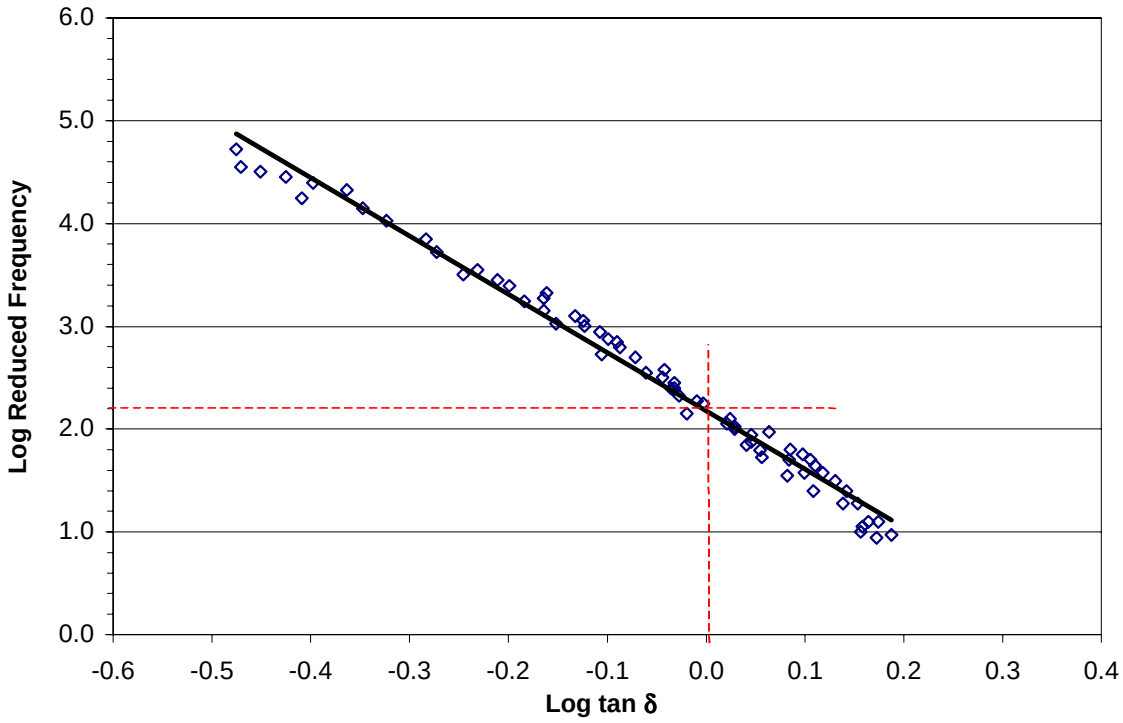


b)

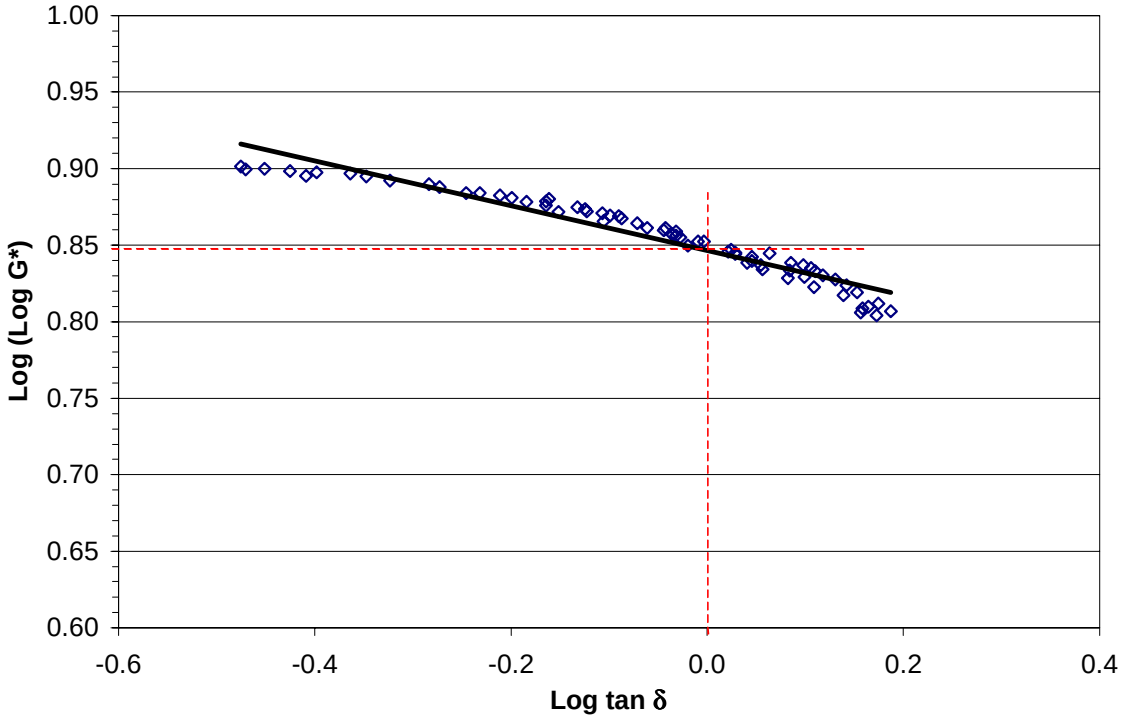


Figure F.7 Method of graphical determination of Christensen - Anderson model parameters: a) crossover frequency and b) rheological index for original specimen AUG5.

a)

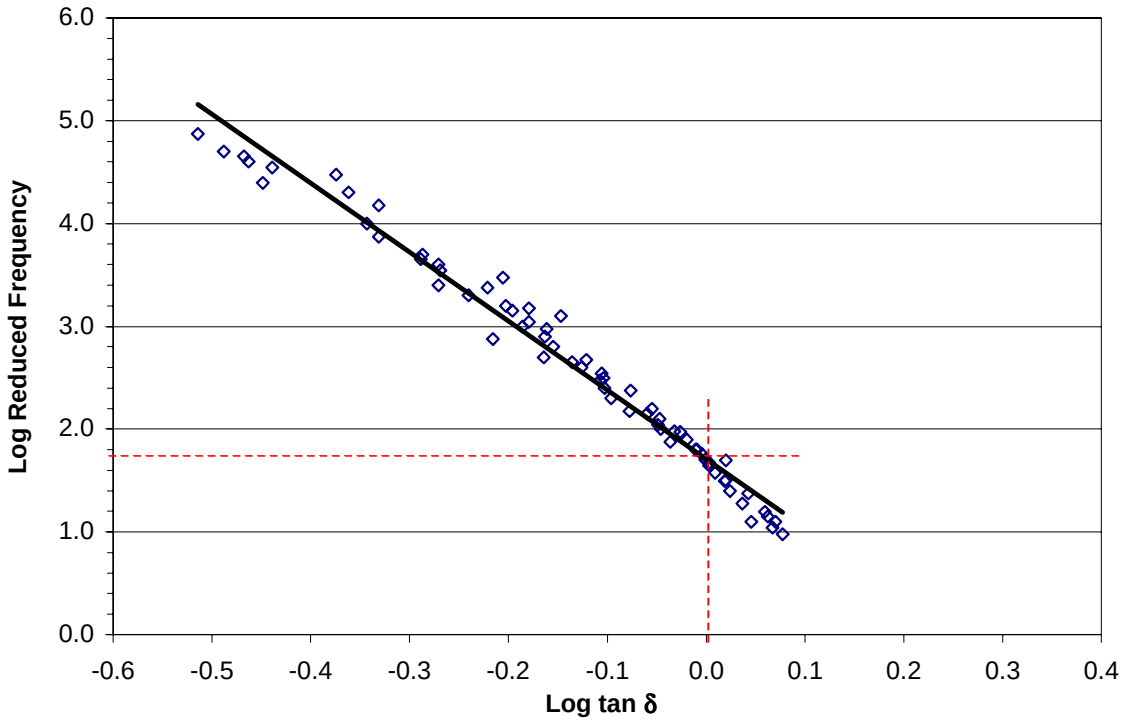


b)

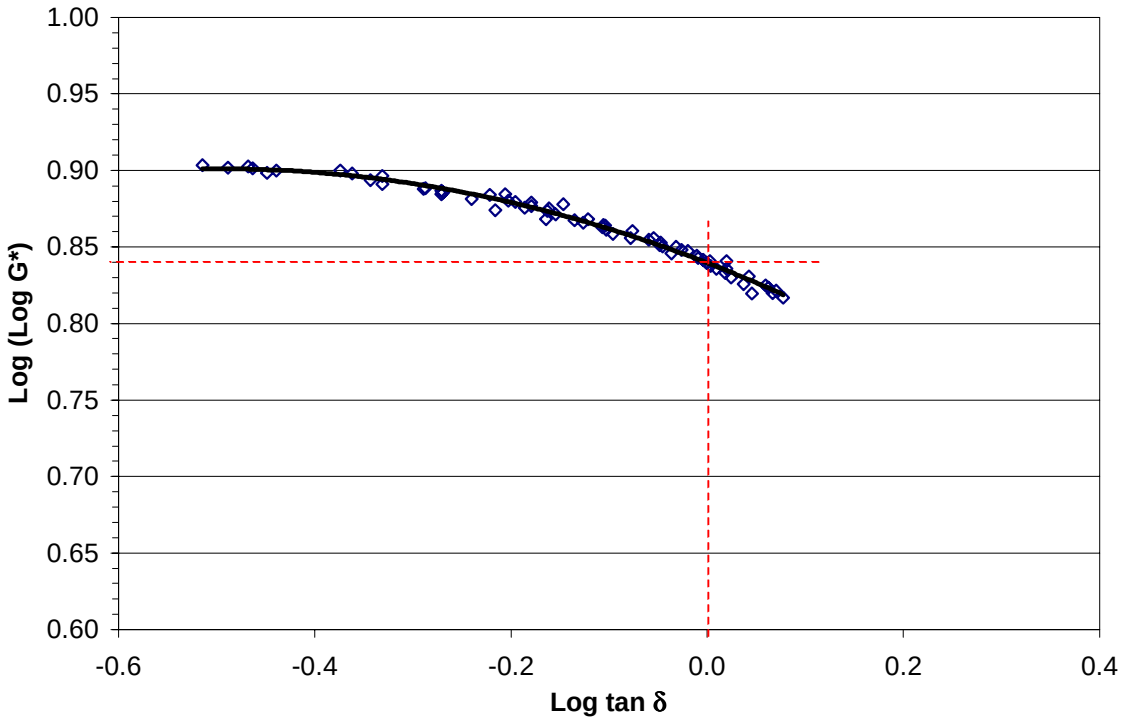


Figure F.8 Method of graphical determination of Christensen - Anderson model parameters: a) crossover frequency and b) rheological index for original specimen ARG5.

a)

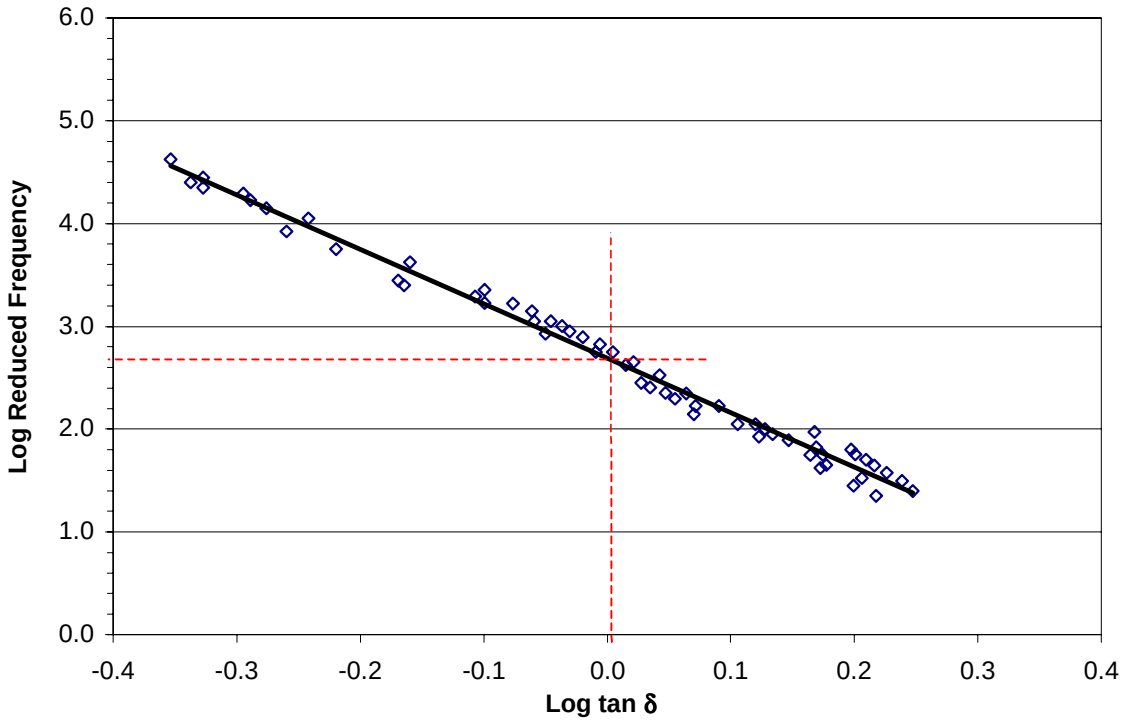


b)

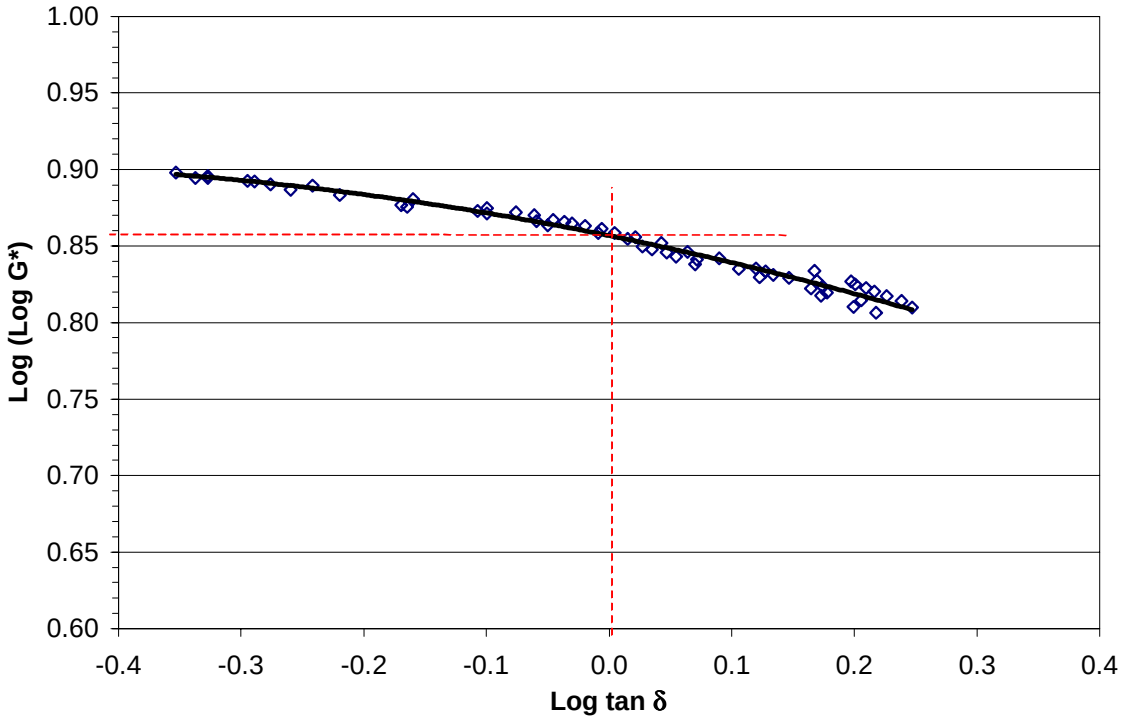


Figure F.9 Method of graphical determination of Christensen - Anderson model parameters: a) crossover frequency and b) rheological index for original specimen AUN3.

a)

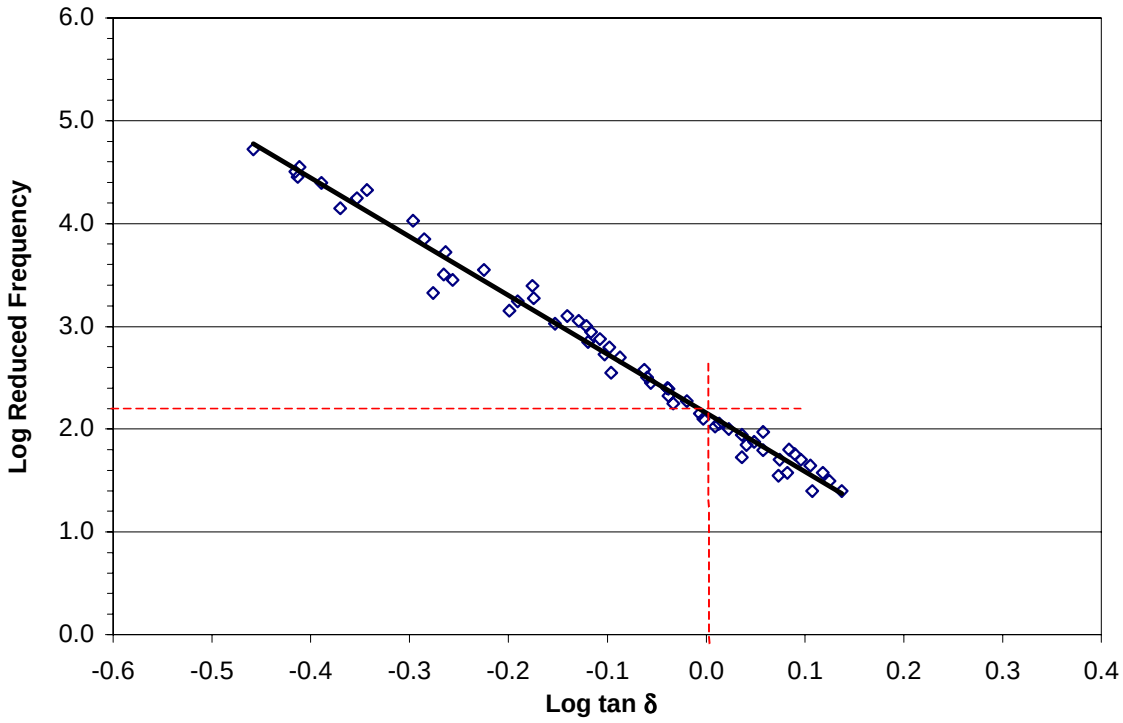


b)

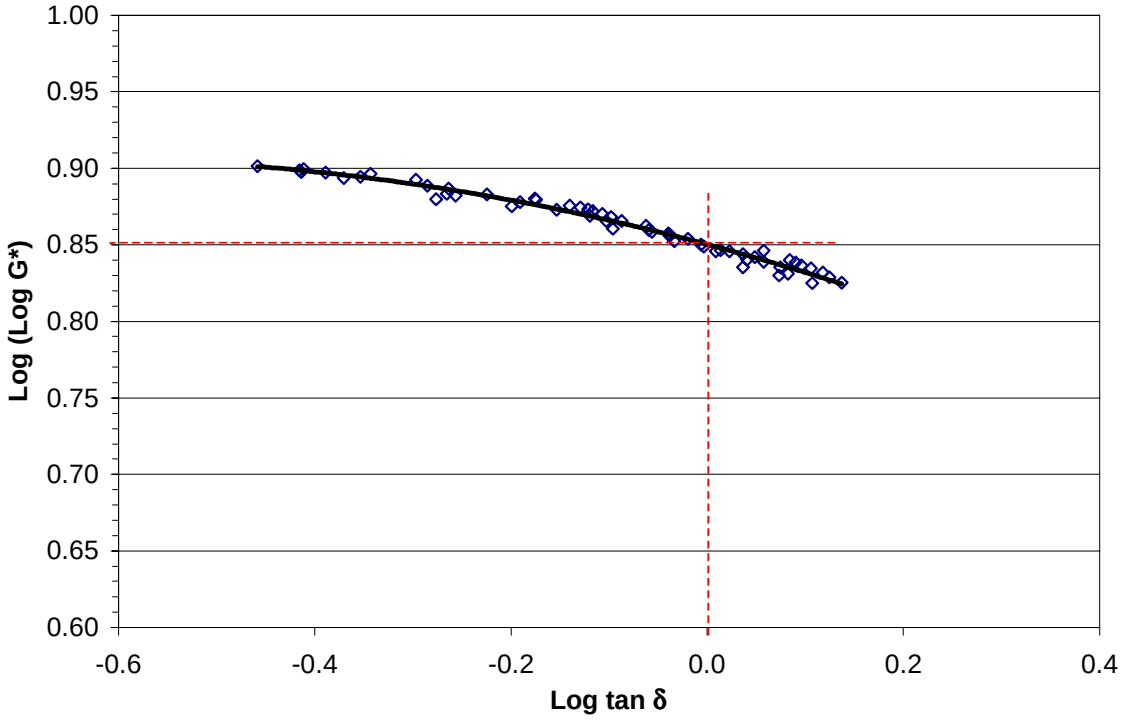


Figure F.10 Method of graphical determination of Christensen - Anderson model parameters: a) crossover frequency and b) rheological index for original specimen ARN3.

a)

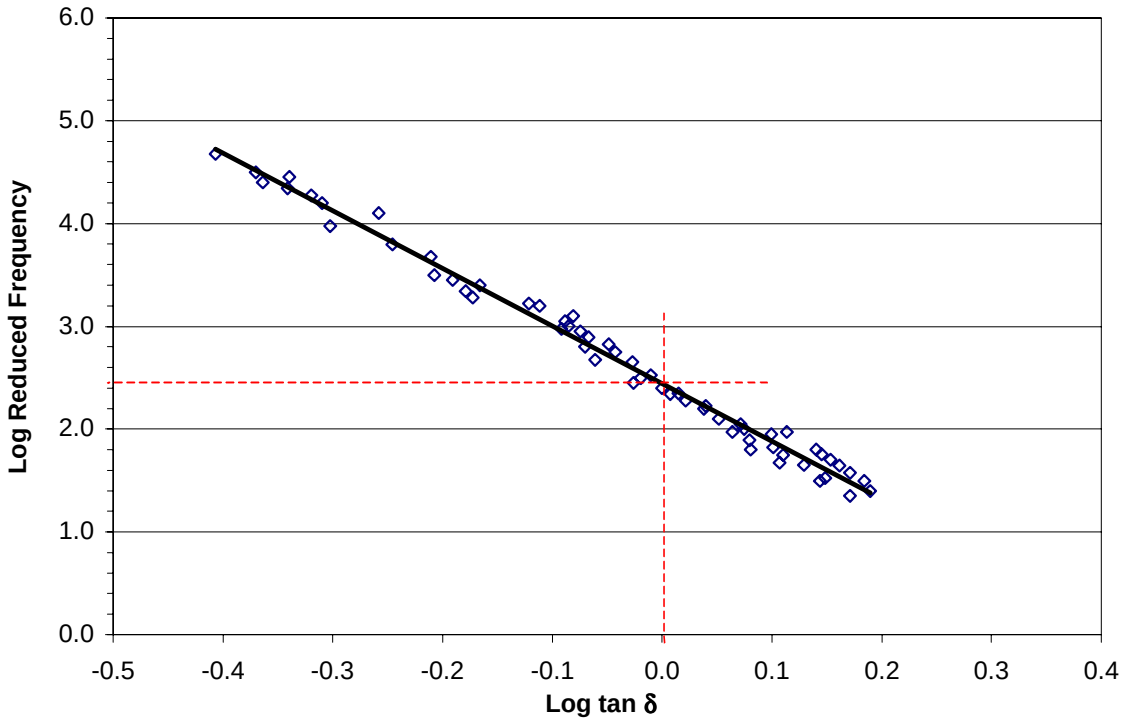


b)

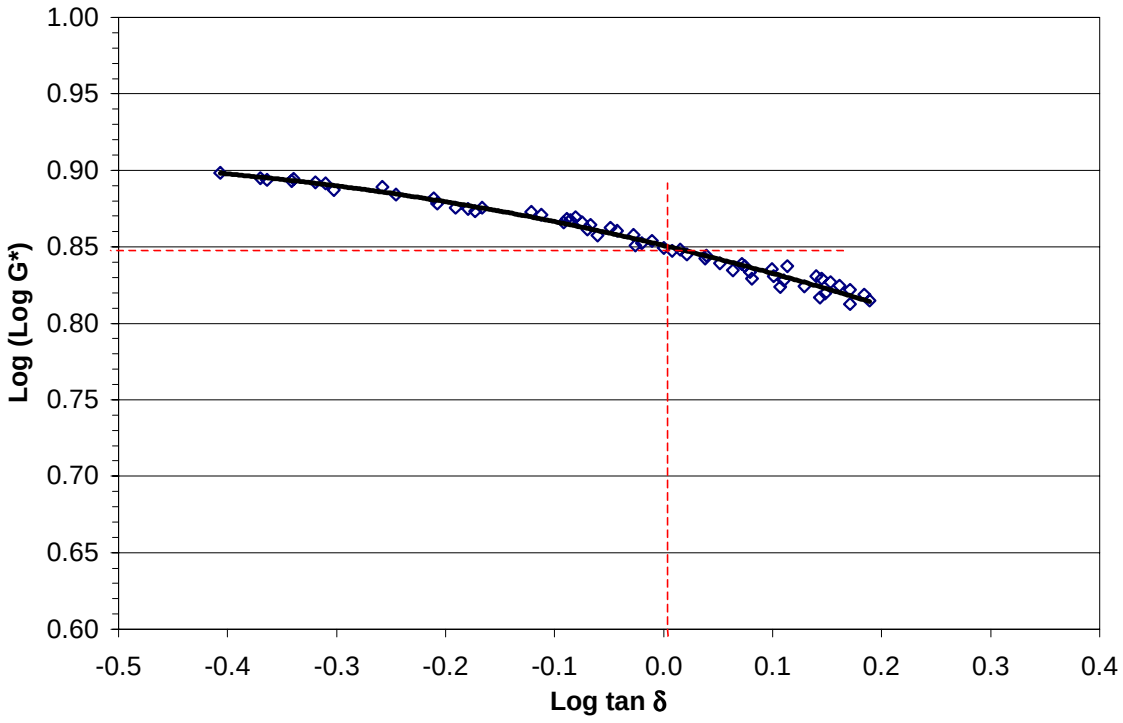


Figure F.11 Method of graphical determination of Christensen - Anderson model parameters: a) crossover frequency and b) rheological index for original specimen AUN4.

a)

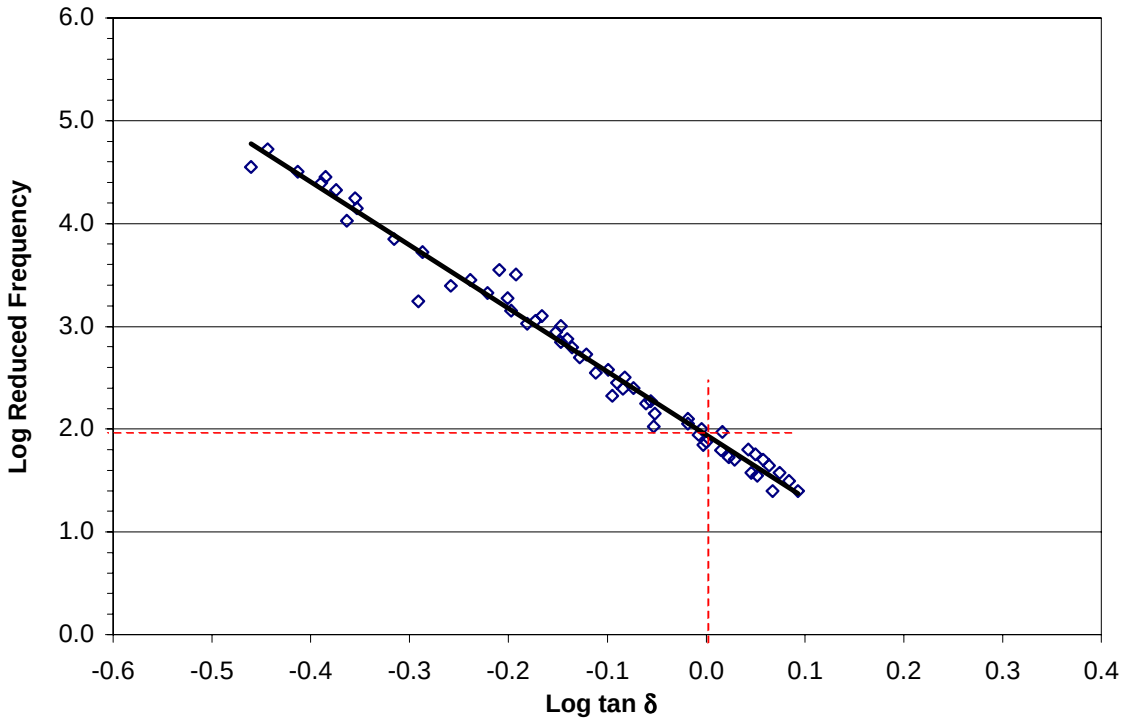


b)

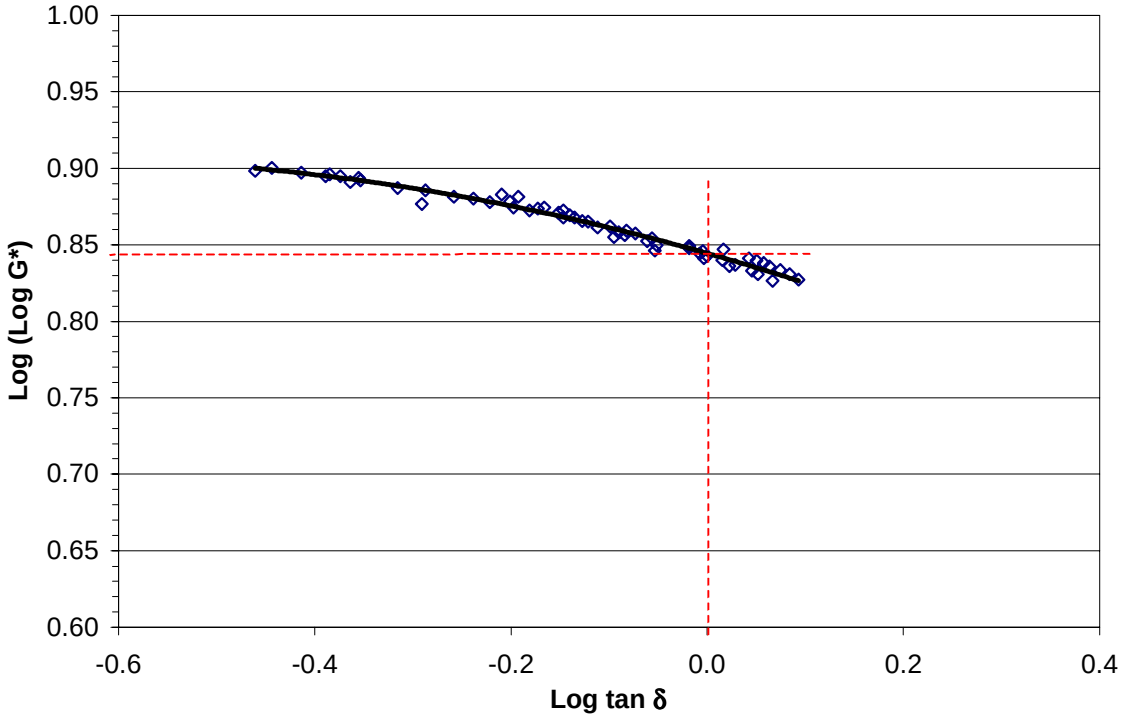


Figure F.12 Method of graphical determination of Christensen - Anderson model parameters: a) crossover frequency and b) rheological index for original specimen ARN4.

a)

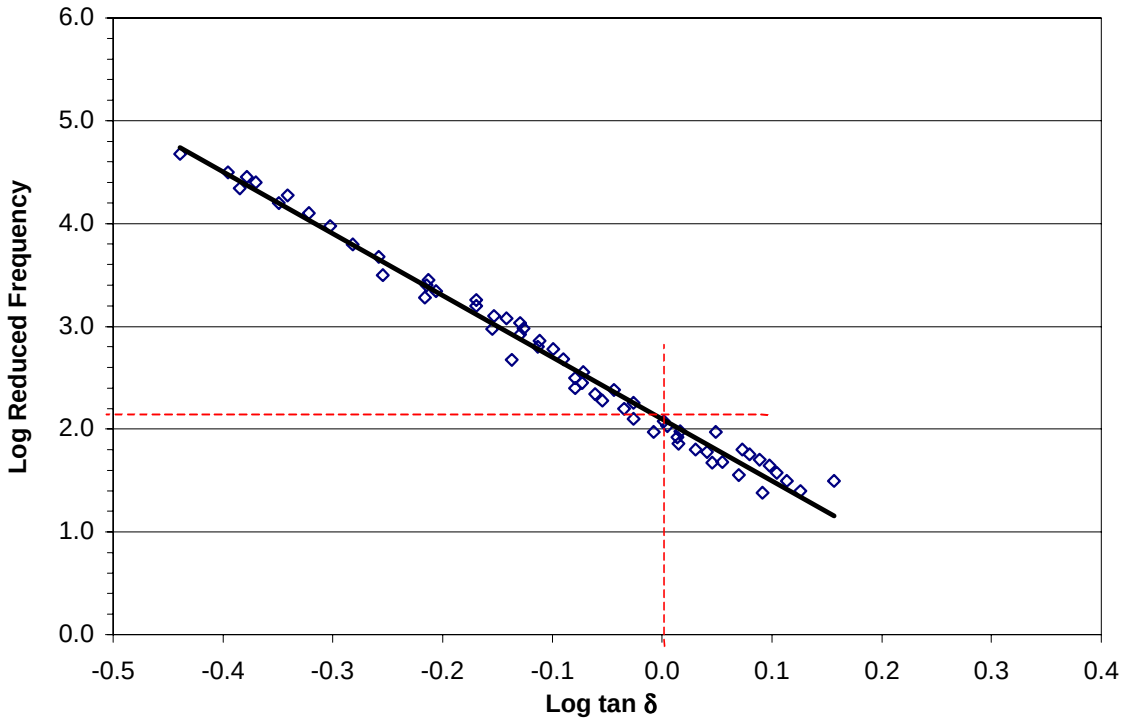


b)

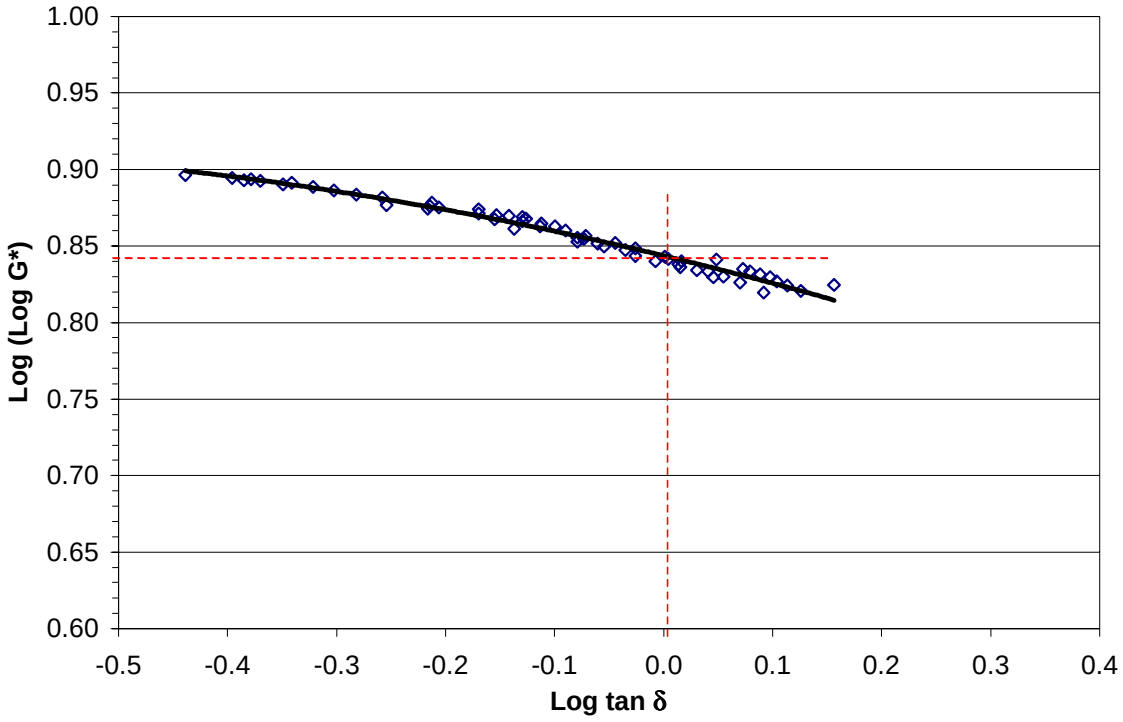


Figure F.13 Method of graphical determination of Christensen - Anderson model parameters: a) crossover frequency and b) rheological index for original specimen AUN5.

a)

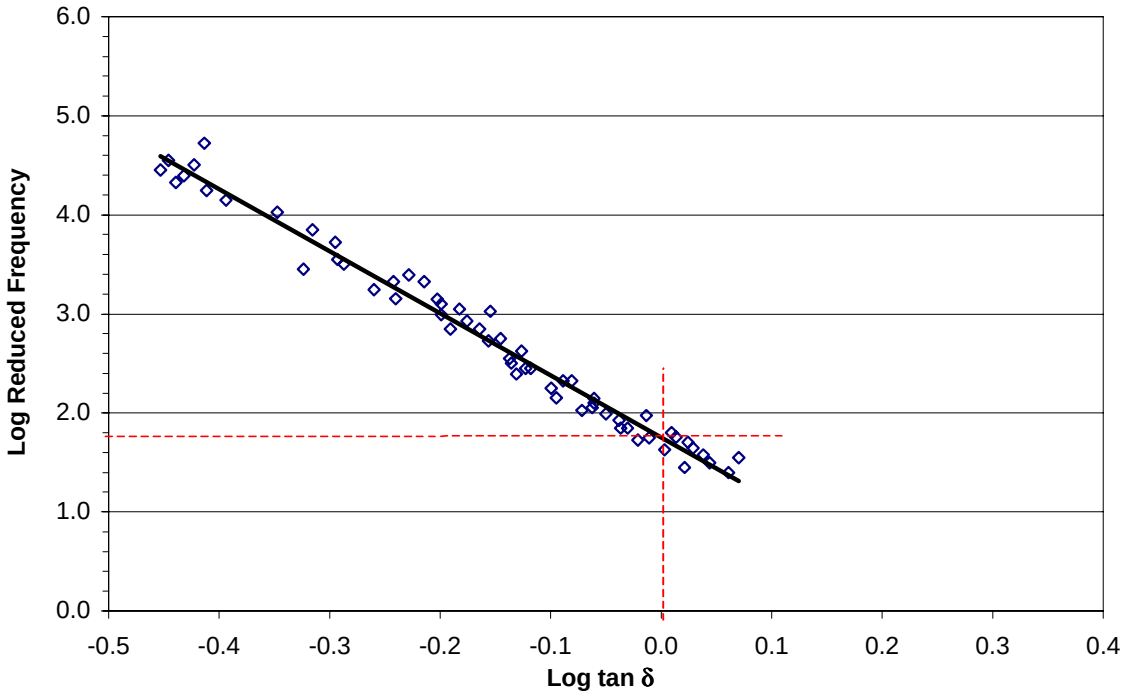


b)

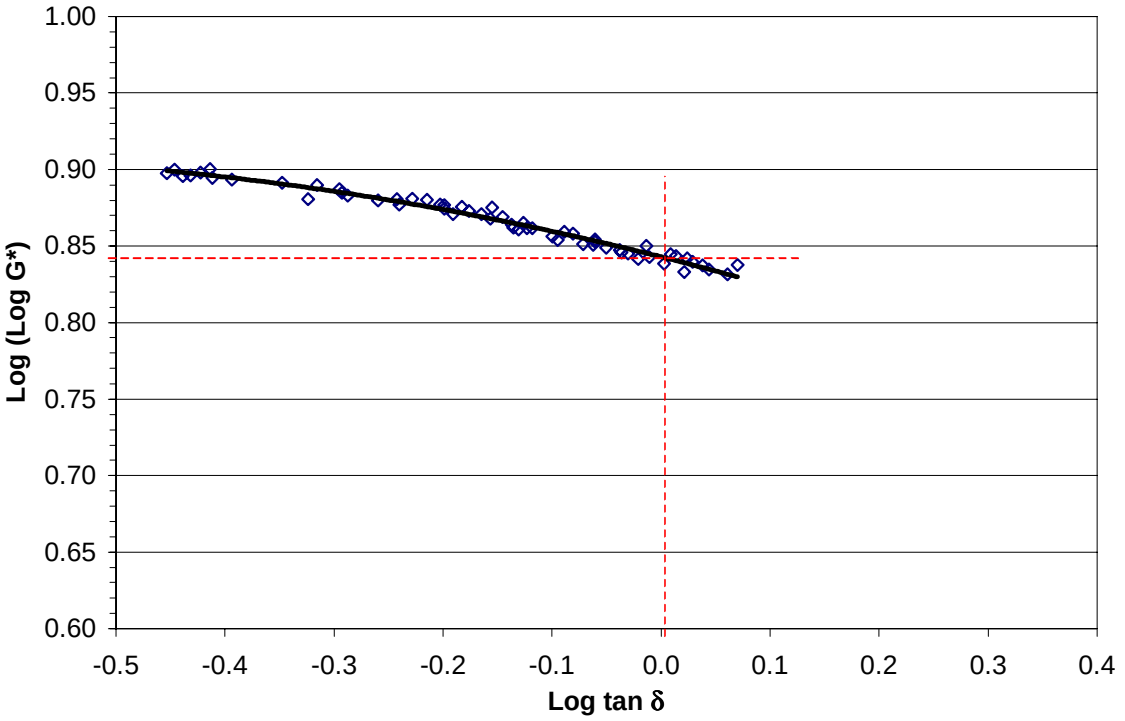


Figure F.14 Method of graphical determination of Christensen - Anderson model parameters: a) crossover frequency and b) rheological index for original specimen ARN5.

a)

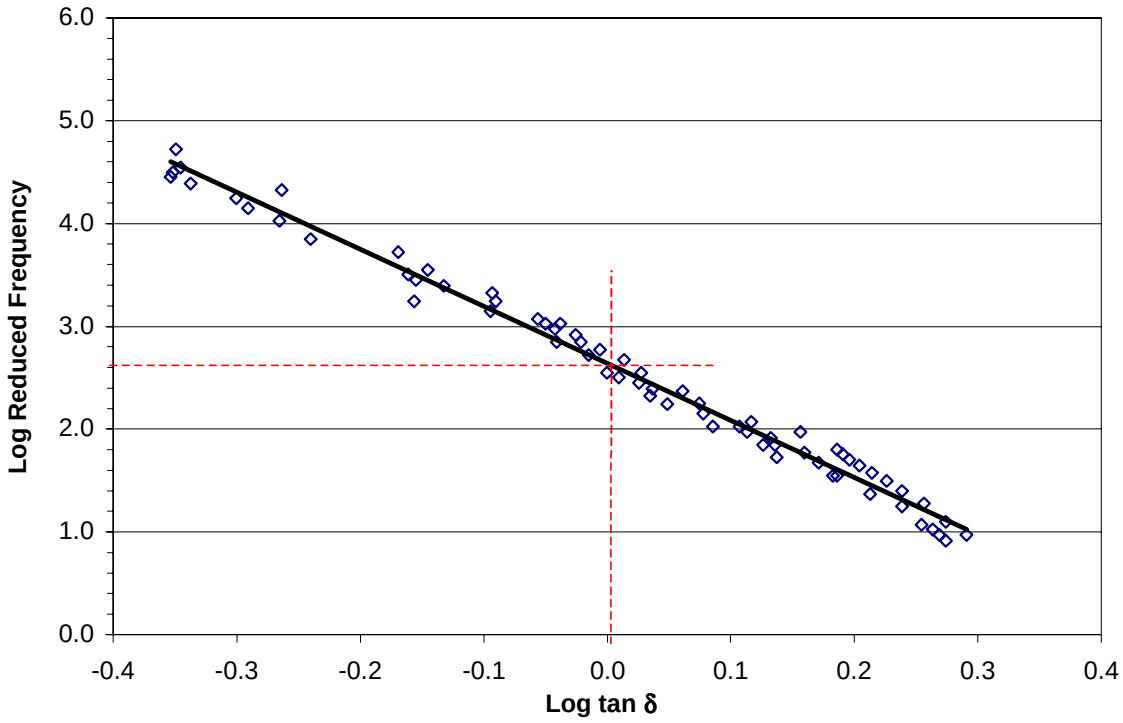


b)

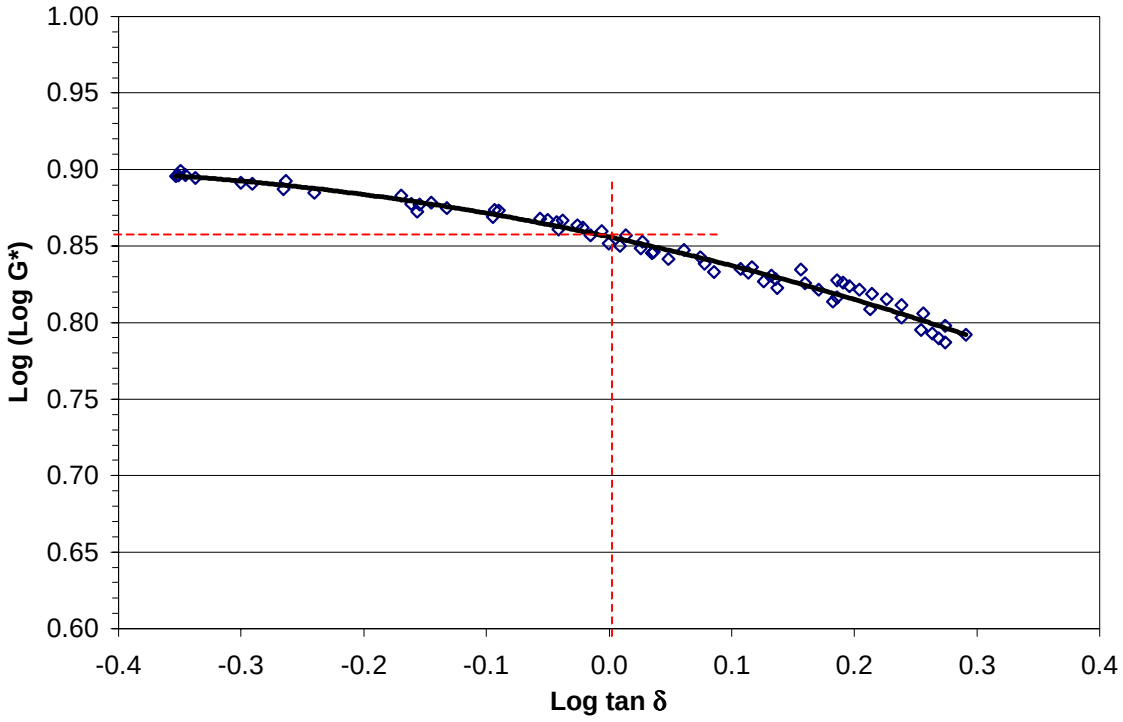


Figure F.15 Method of graphical determination of Christensen - Anderson model parameters: a) crossover frequency and b) rheological index for original specimen AUS3.

a)

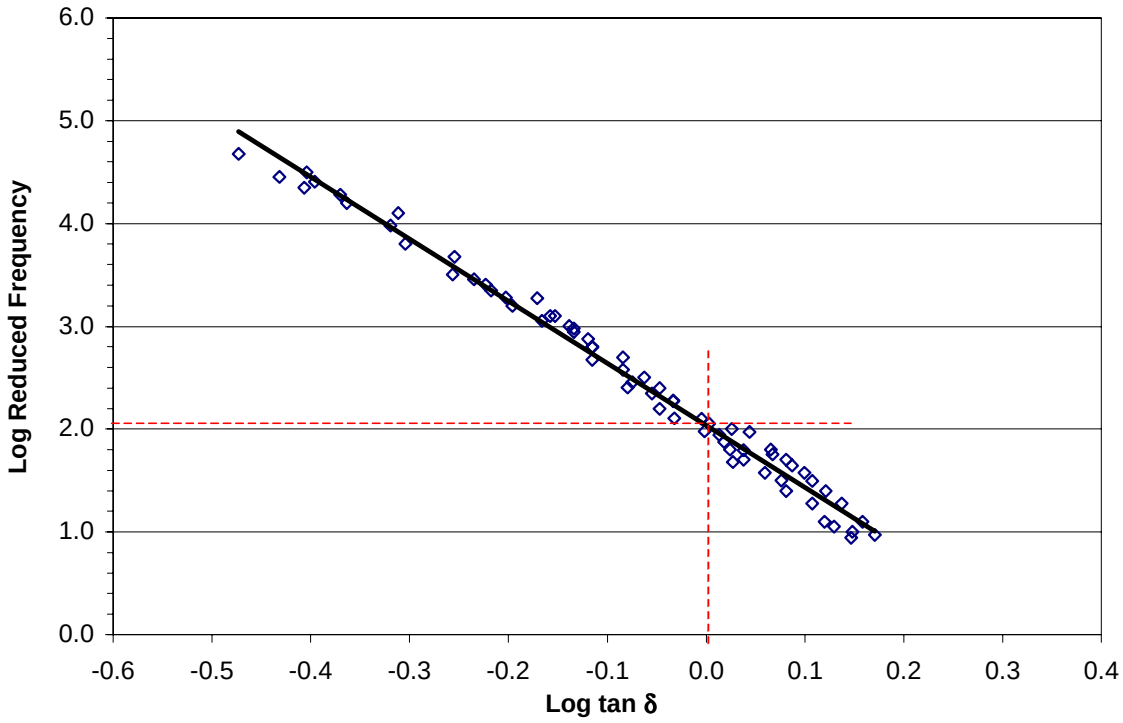


b)

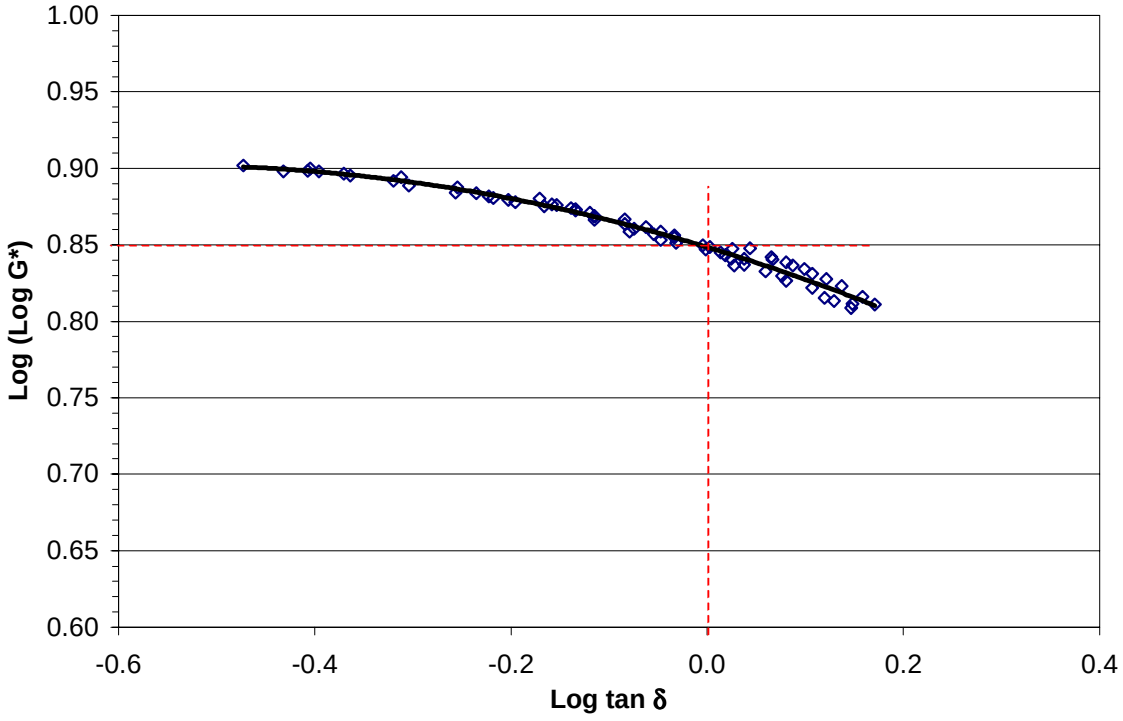


Figure F.16 Method of graphical determination of Christensen - Anderson model parameters: a) crossover frequency and b) rheological index for original specimen ARS3.

a)

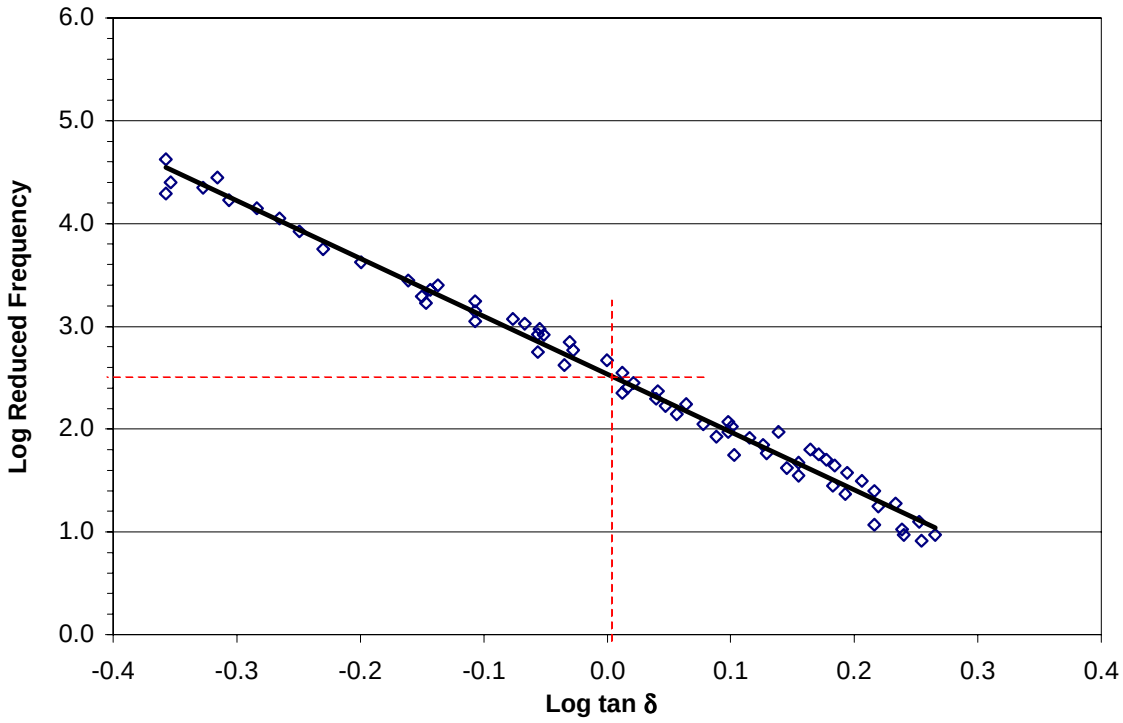


b)

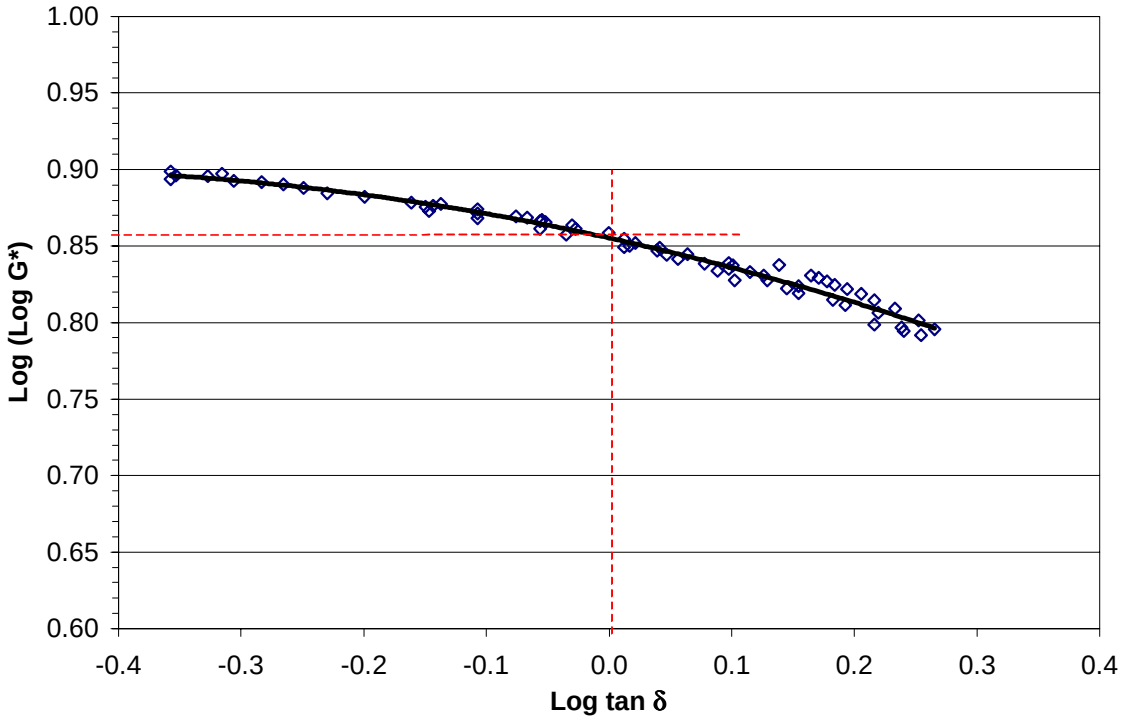


Figure F.17 Method of graphical determination of Christensen - Anderson model parameters: a) crossover frequency and b) rheological index for original specimen AUS4.

a)

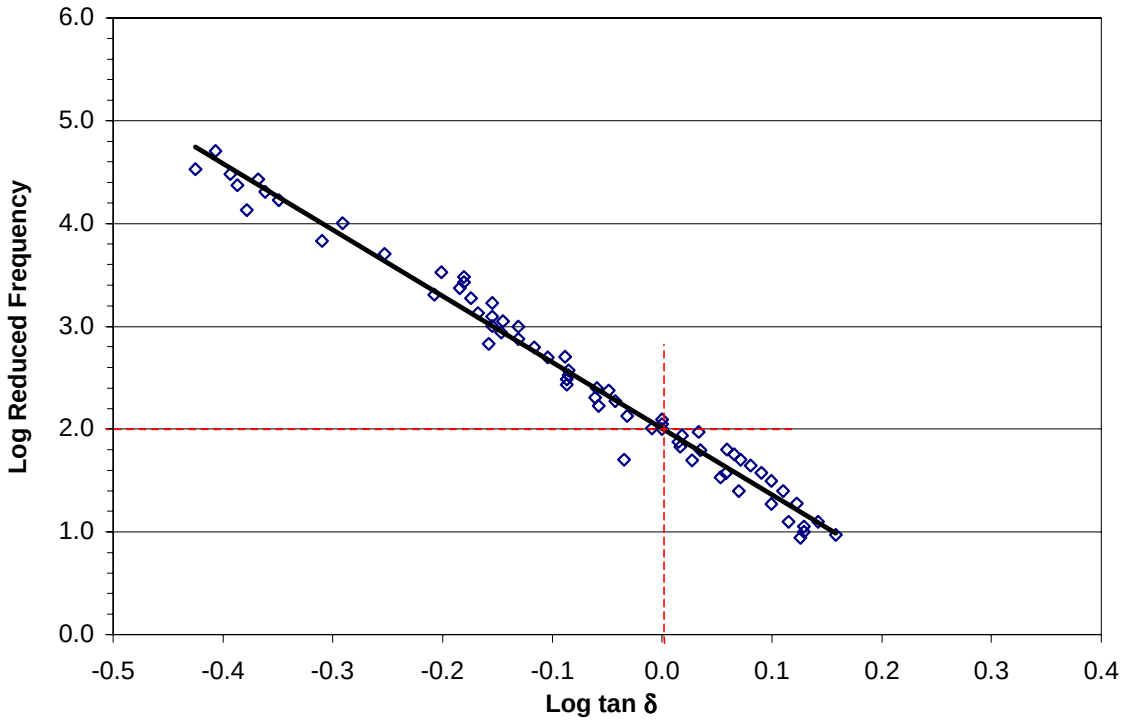


b)

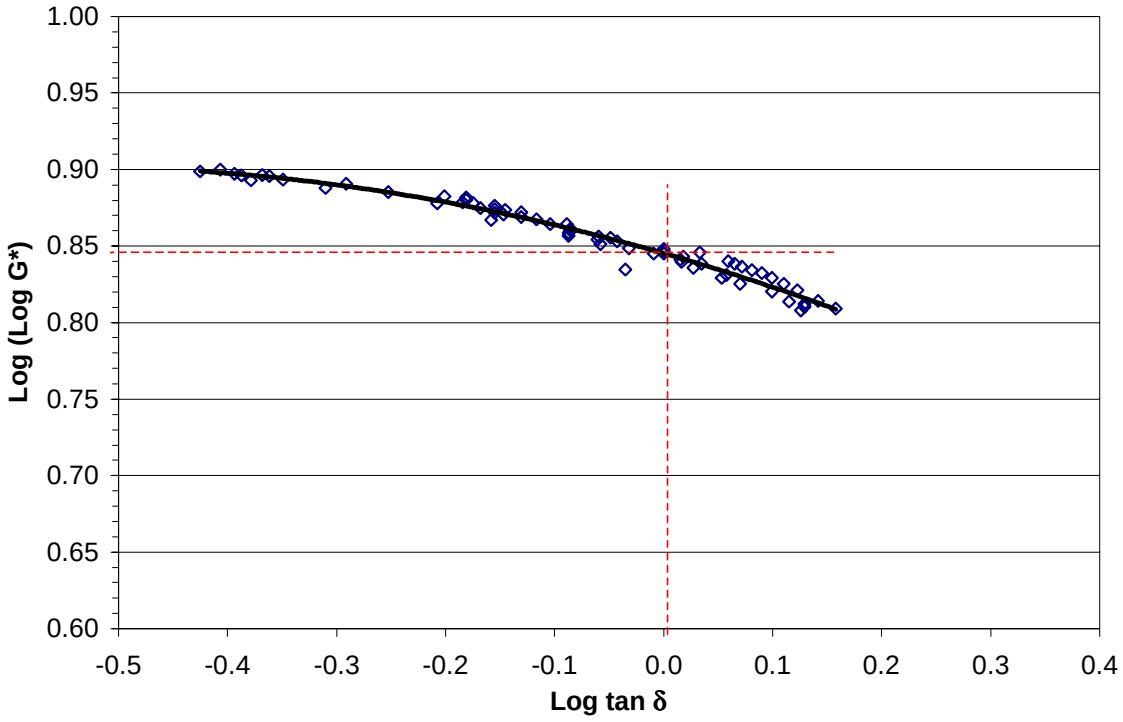


Figure F.18 Method of graphical determination of Christensen - Anderson model parameters: a) crossover frequency and b) rheological index for original specimen ARS4.

a)

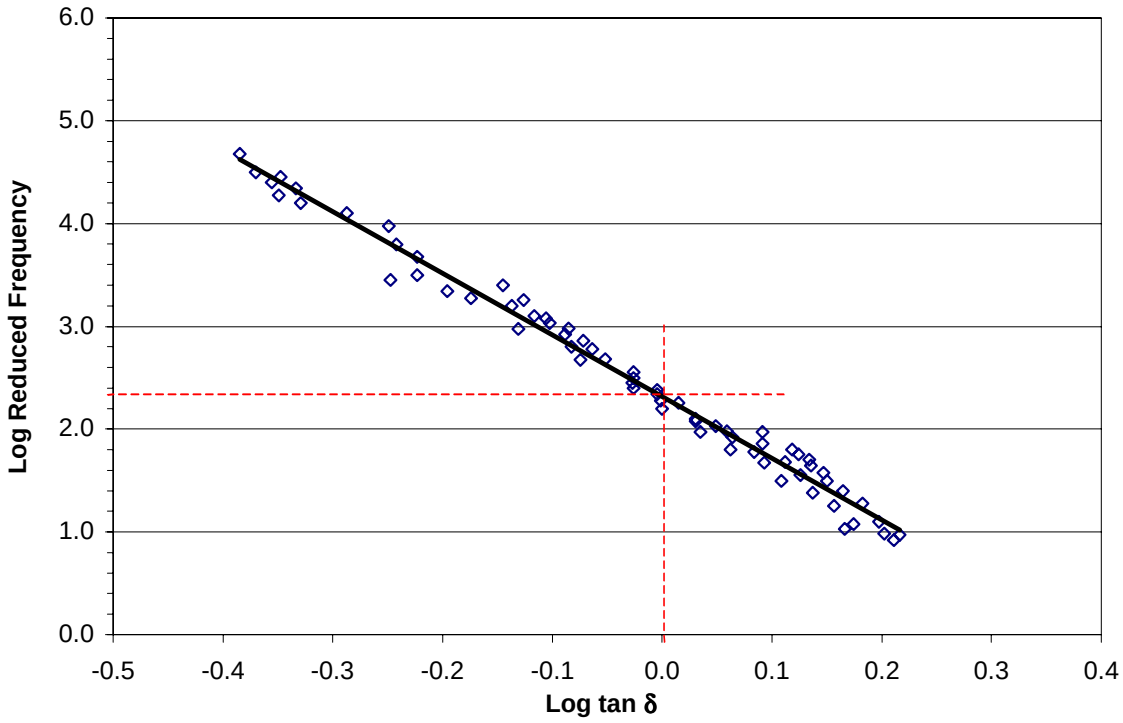


b)

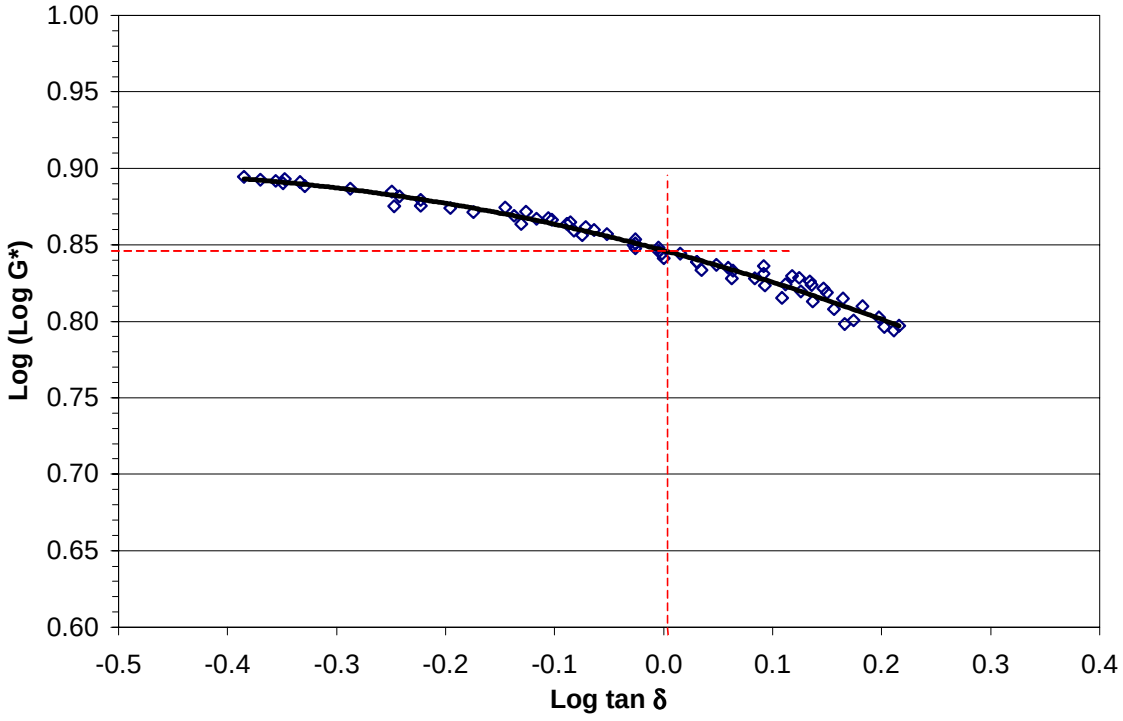


Figure F.19 Method of graphical determination of Christensen - Anderson model parameters: a) crossover frequency and b) rheological index for original specimen AUS5.

a)

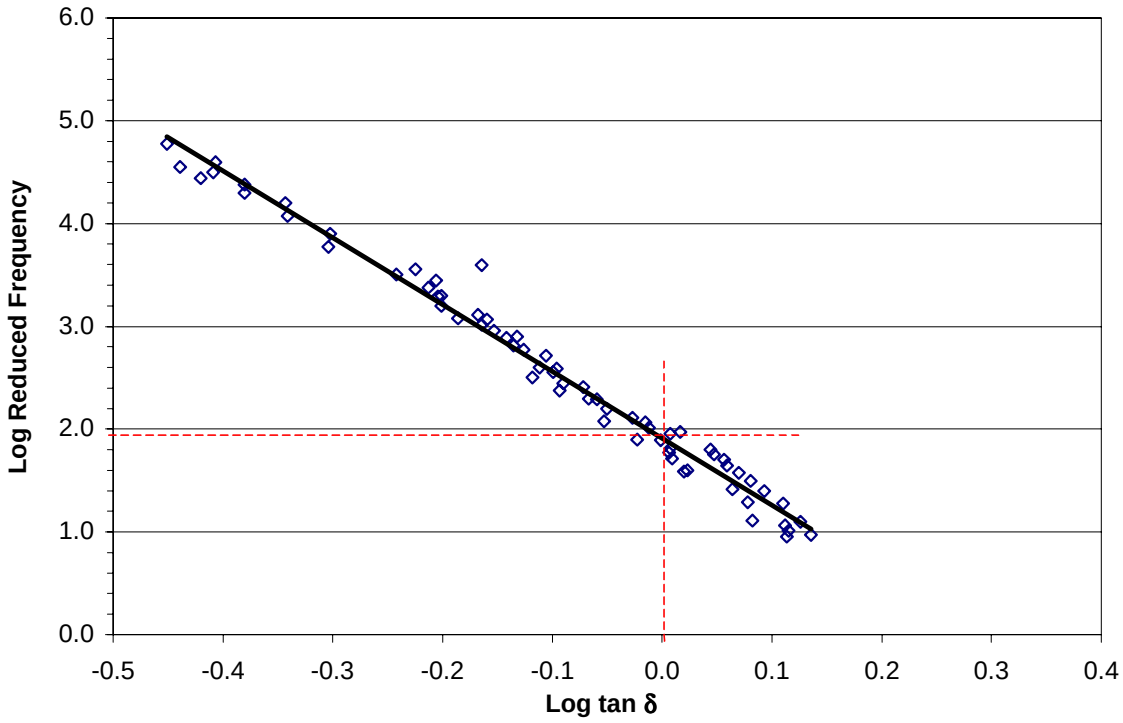


b)

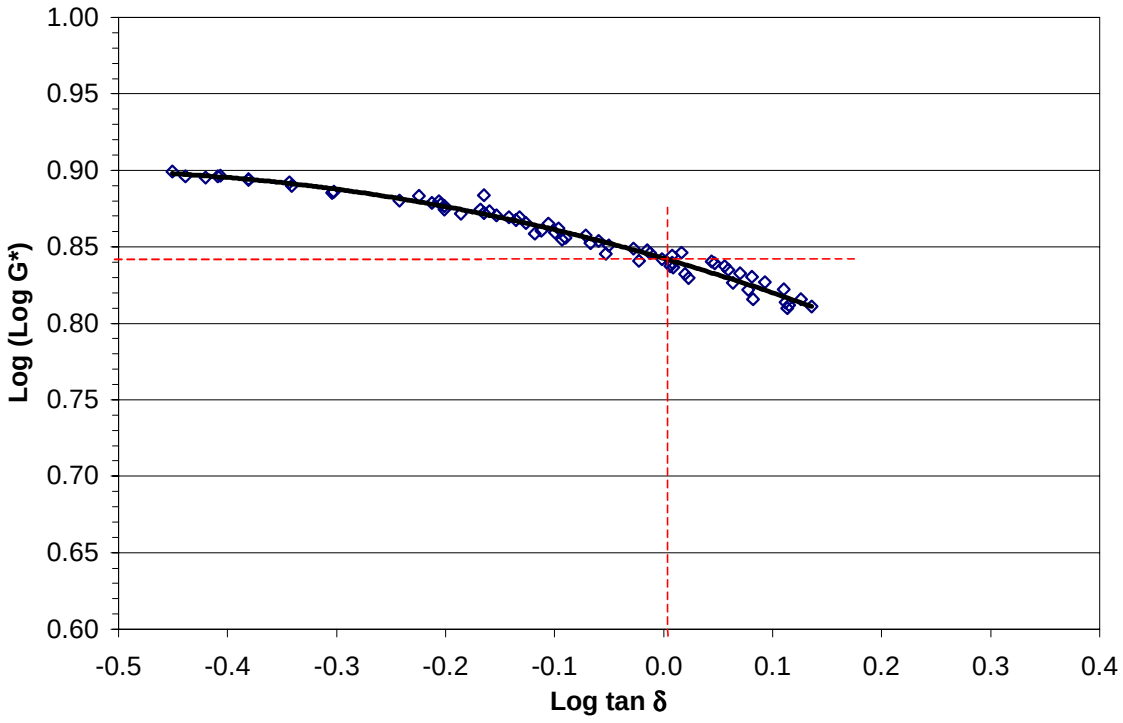


Figure F.20 Method of graphical determination of Christensen - Anderson model parameters: a) crossover frequency and b) rheological index for original specimen ARS5.

# APPENDIX G

- This appendix includes representations of the graphical method of determining model parameters for the Christensen-Anderson model for stored specimens.

a)

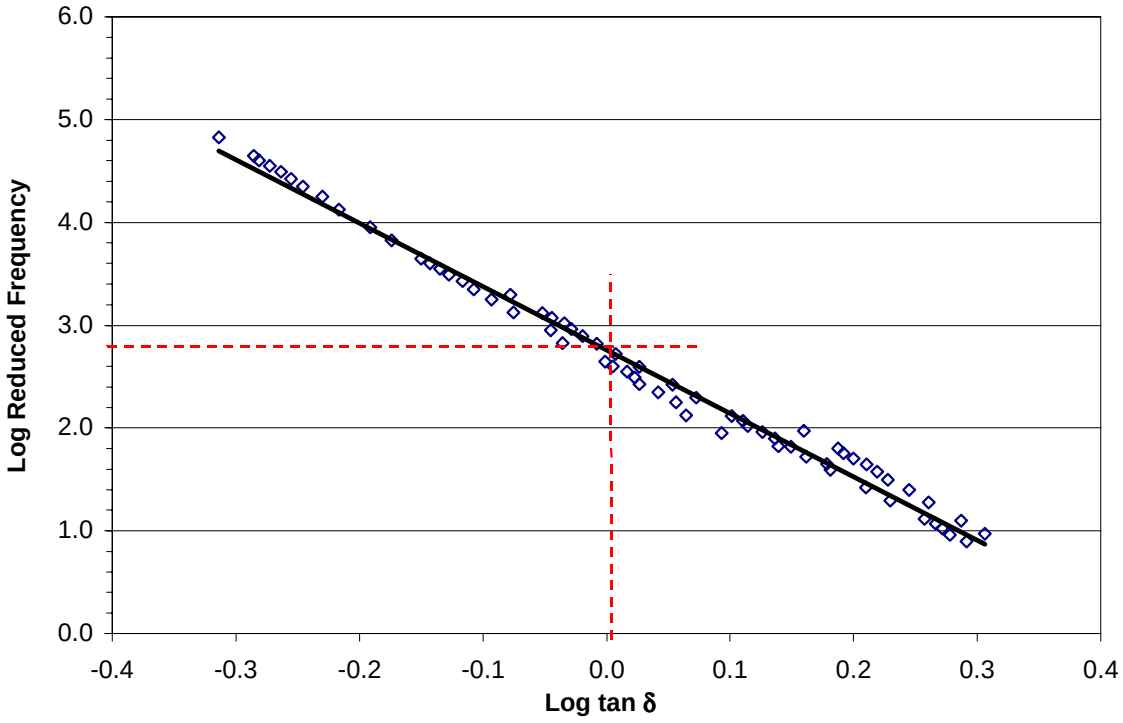


b)

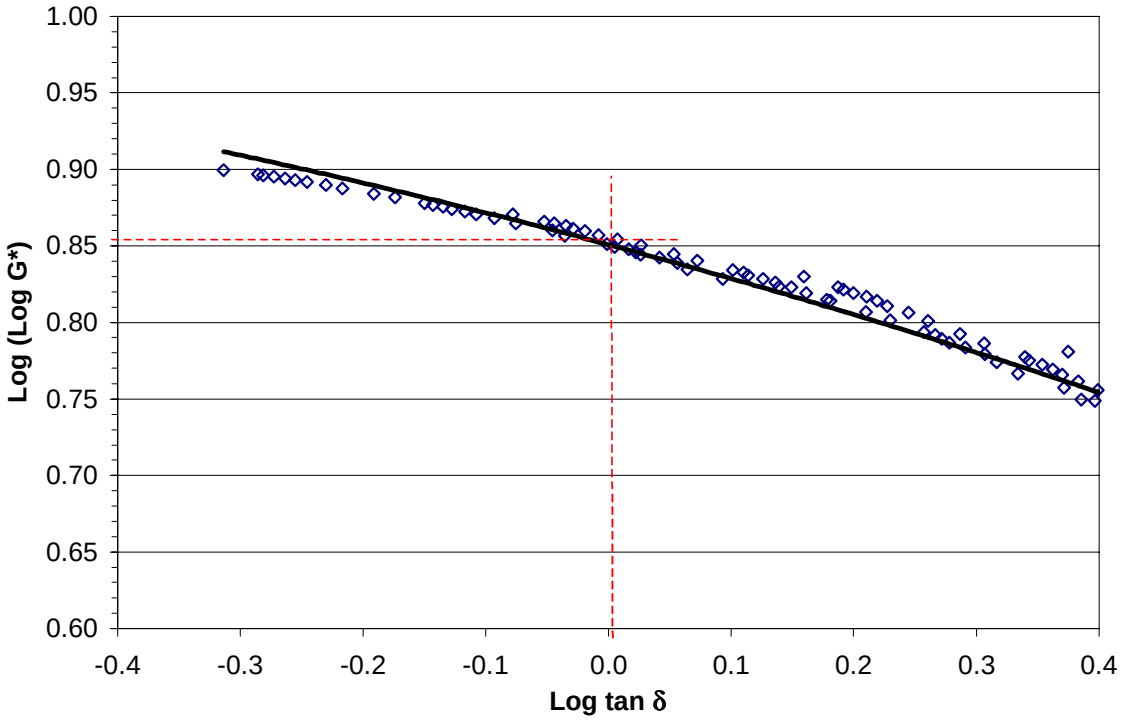


Figure G.1 Method of graphical determination of Christensen - Anderson model parameters: a) crossover frequency and b) rheological index for stored specimen AU00.

a)

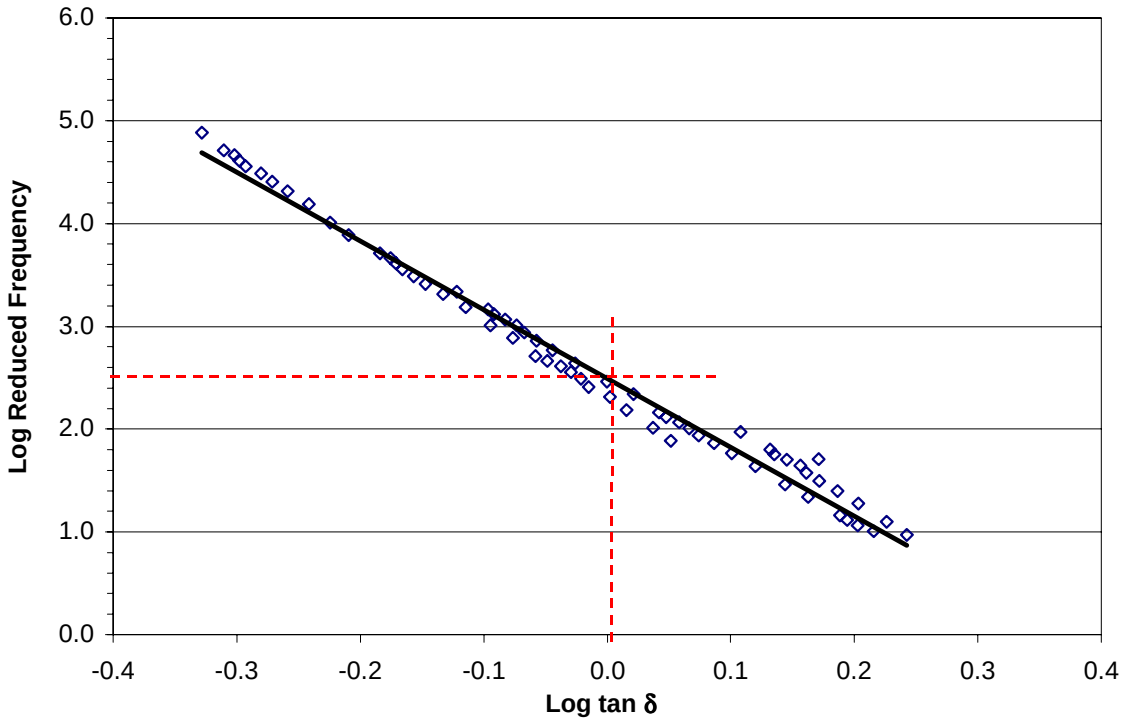


b)

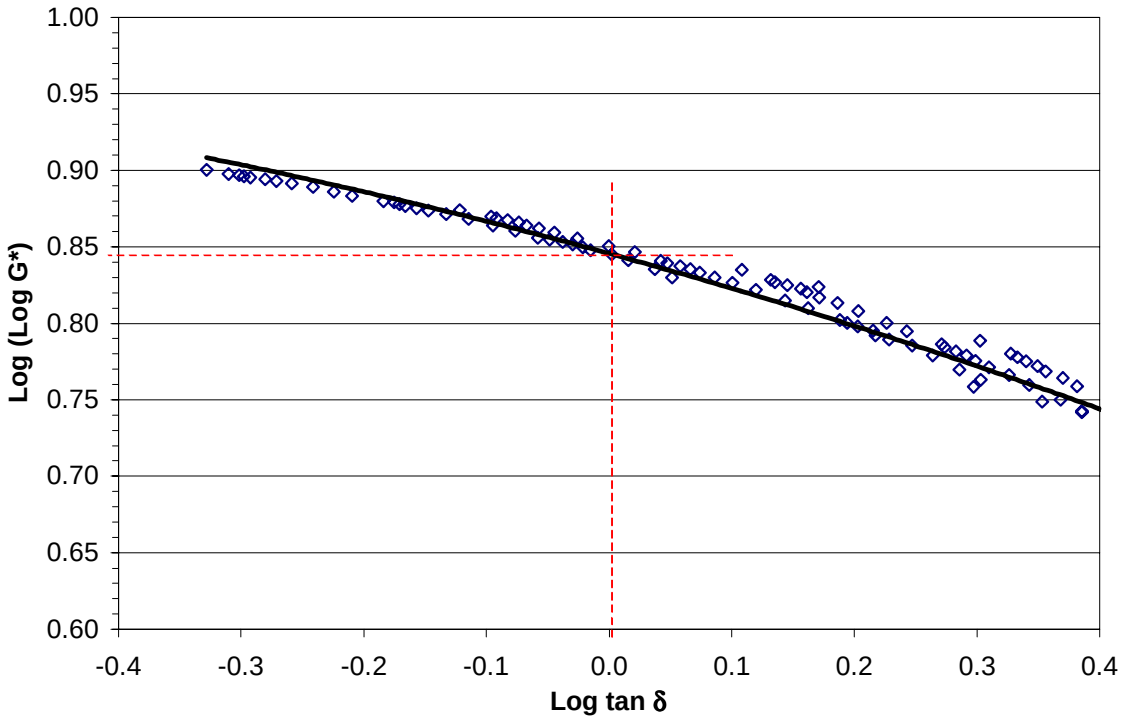


Figure G.2 Method of graphical determination of Christensen - Anderson model parameters: a) crossover frequency and b) rheological index for stored specimen AR00.

a)

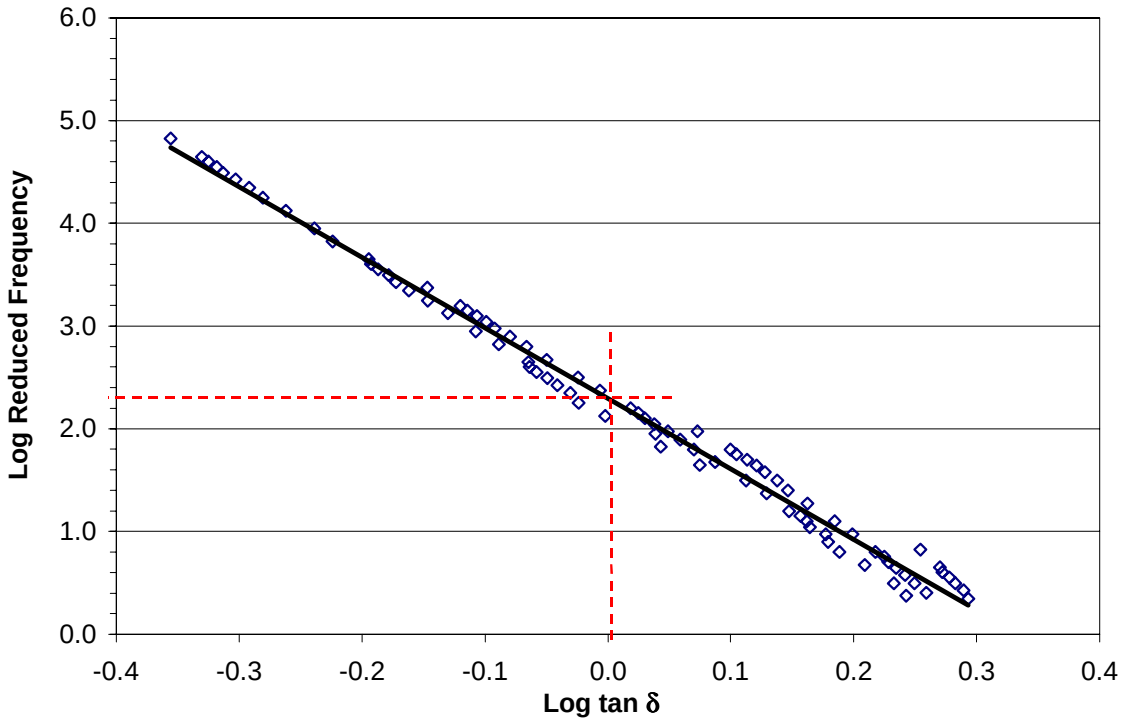


b)

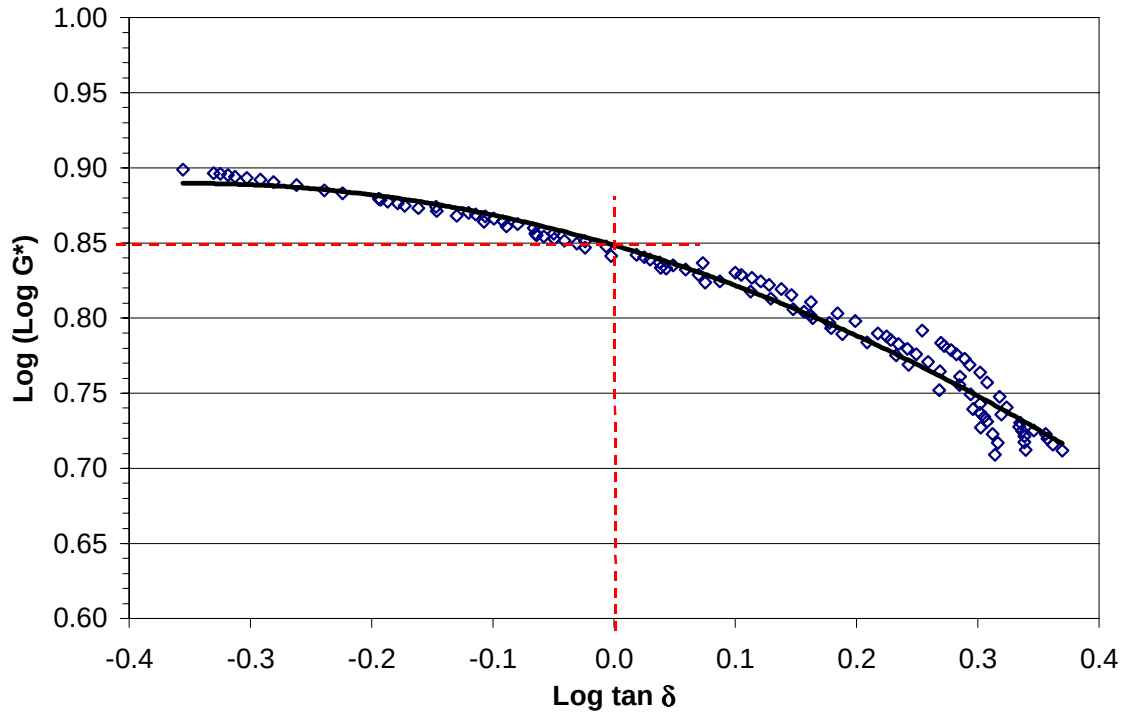


Figure G.3 Method of graphical determination of Christensen - Anderson model parameters: a) crossover frequency and b) rheological index for stored specimen AUG3.

a)

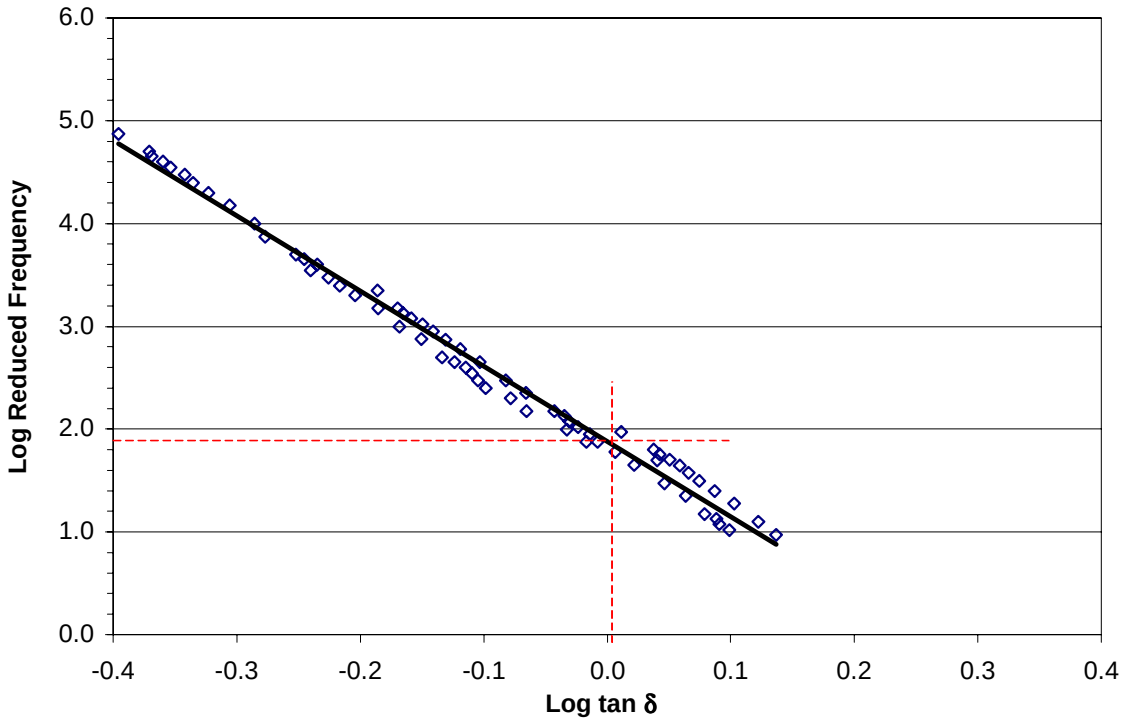


b)

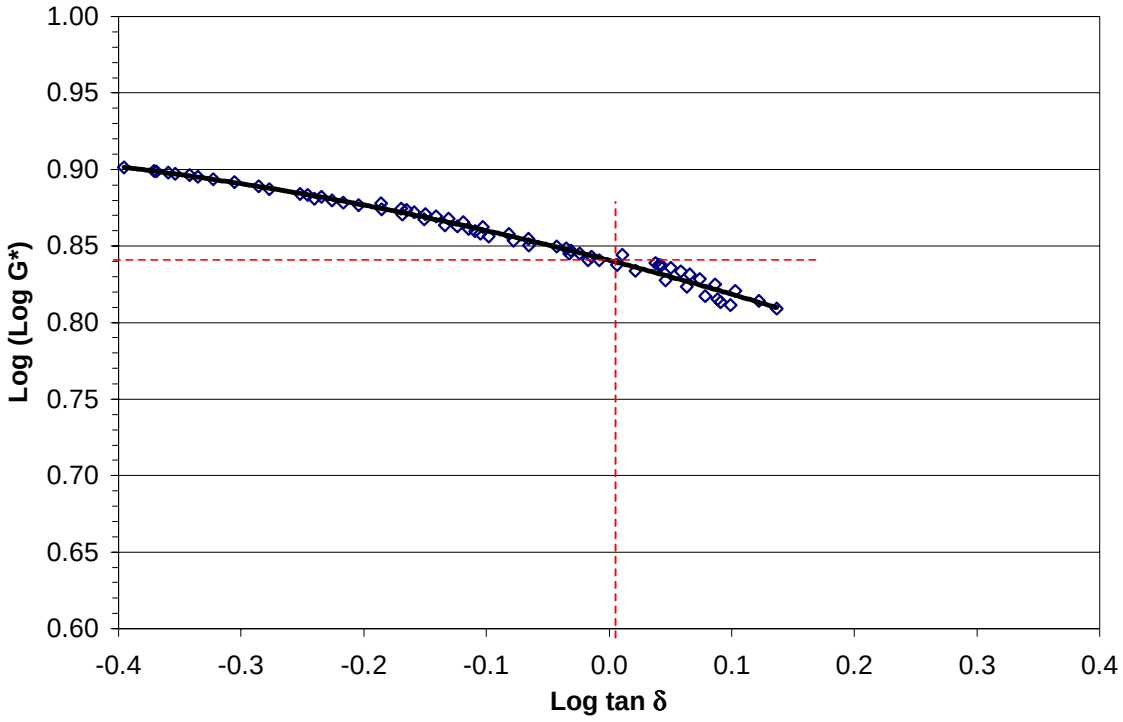


Figure G.4 Method of graphical determination of Christensen - Anderson model parameters: a) crossover frequency and b) rheological index for stored specimen ARG3.

a)

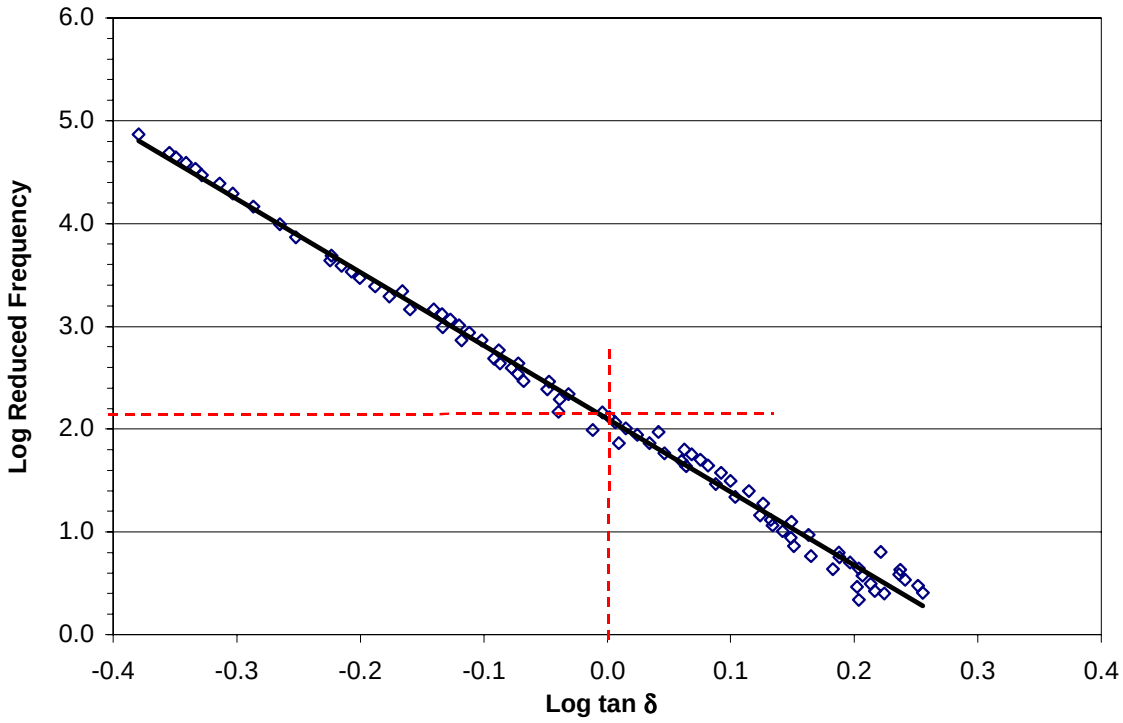


b)

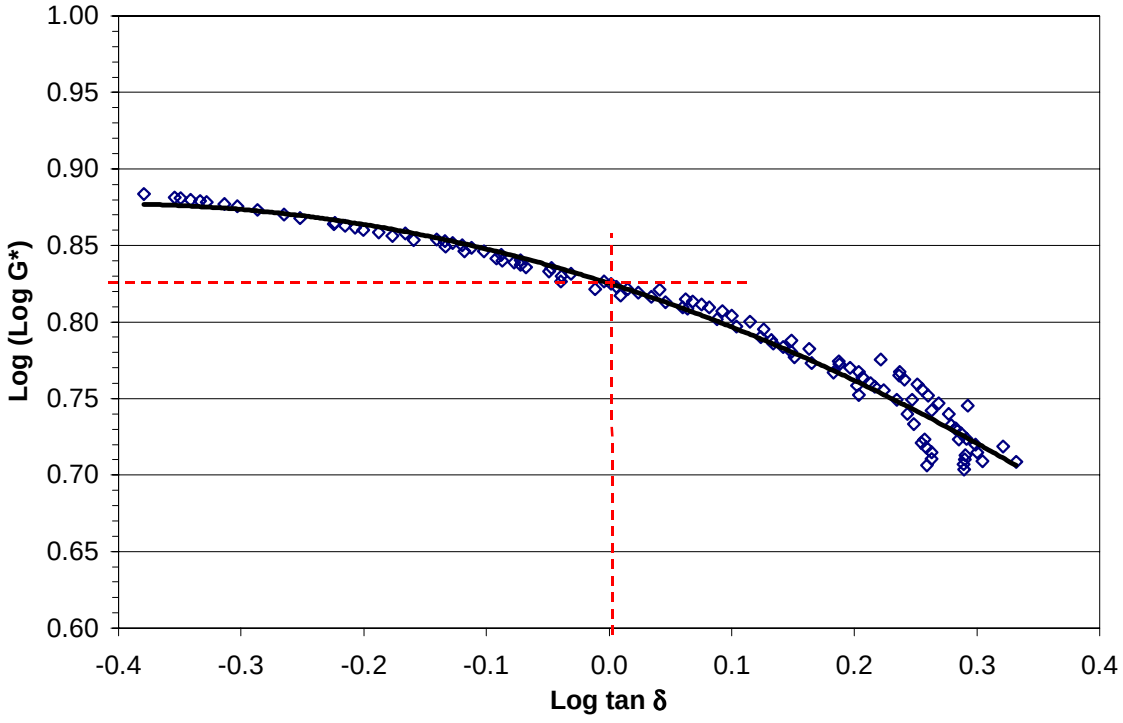


Figure G.5 Method of graphical determination of Christensen - Anderson model parameters: a) crossover frequency and b) rheological index for stored specimen AUG4.

a)

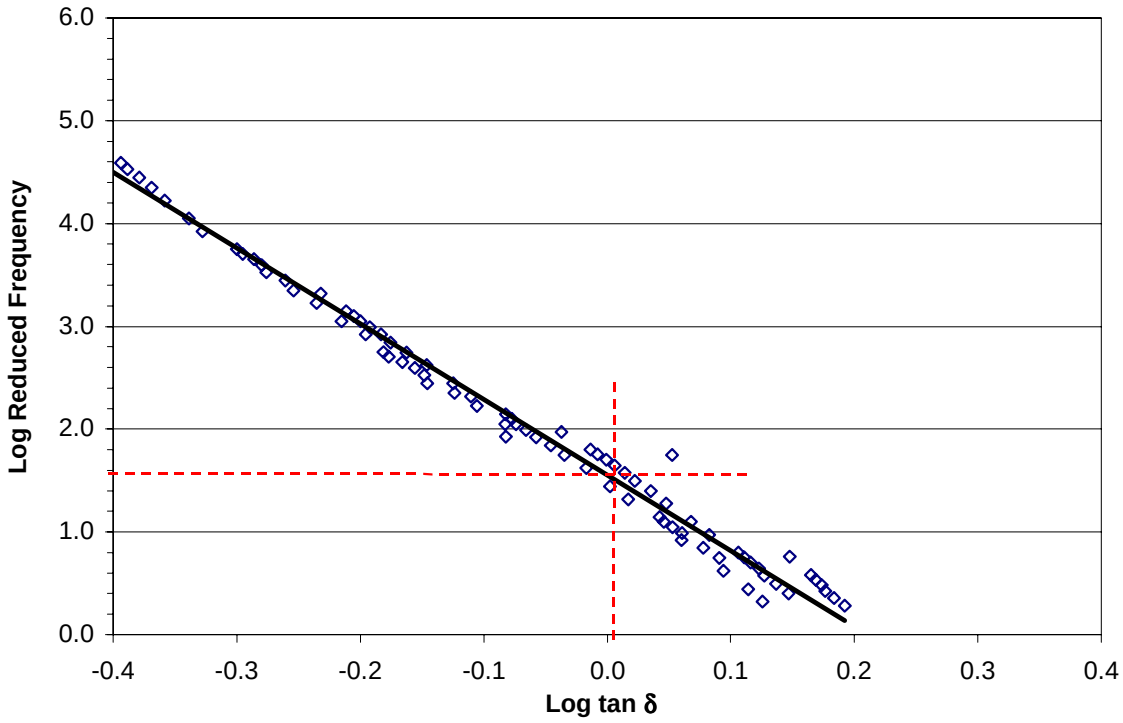


b)

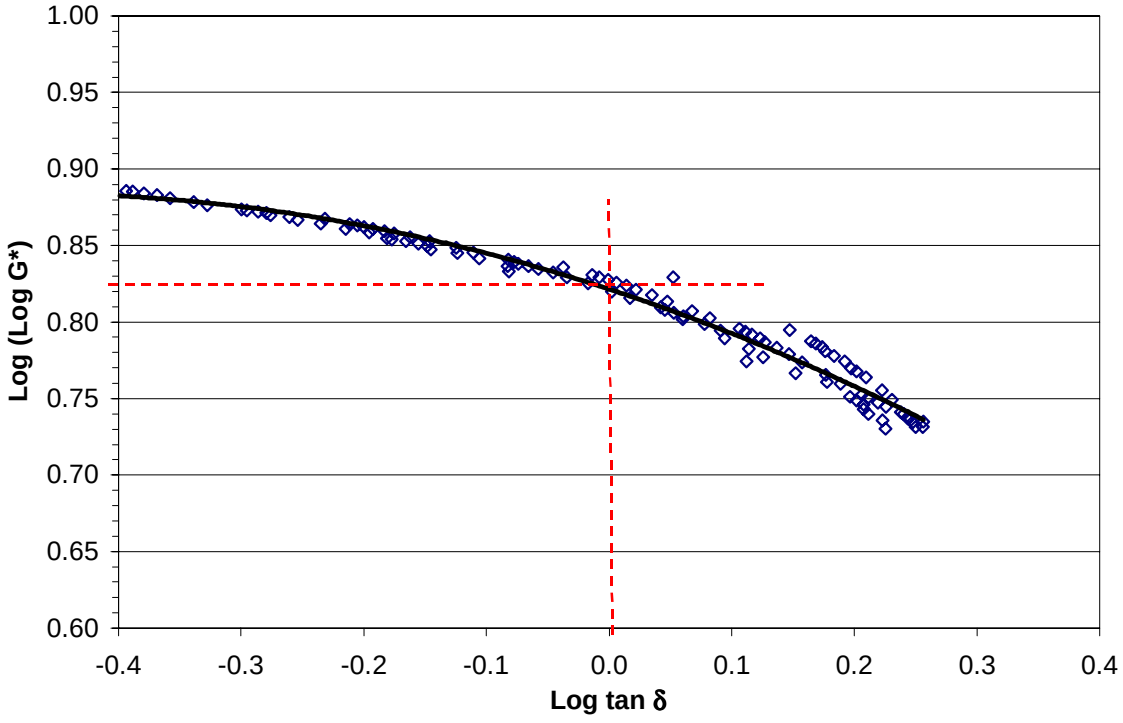


Figure G.6 Method of graphical determination of Christensen - Anderson model parameters: a) crossover frequency and b) rheological index for stored specimen ARG4.

a)

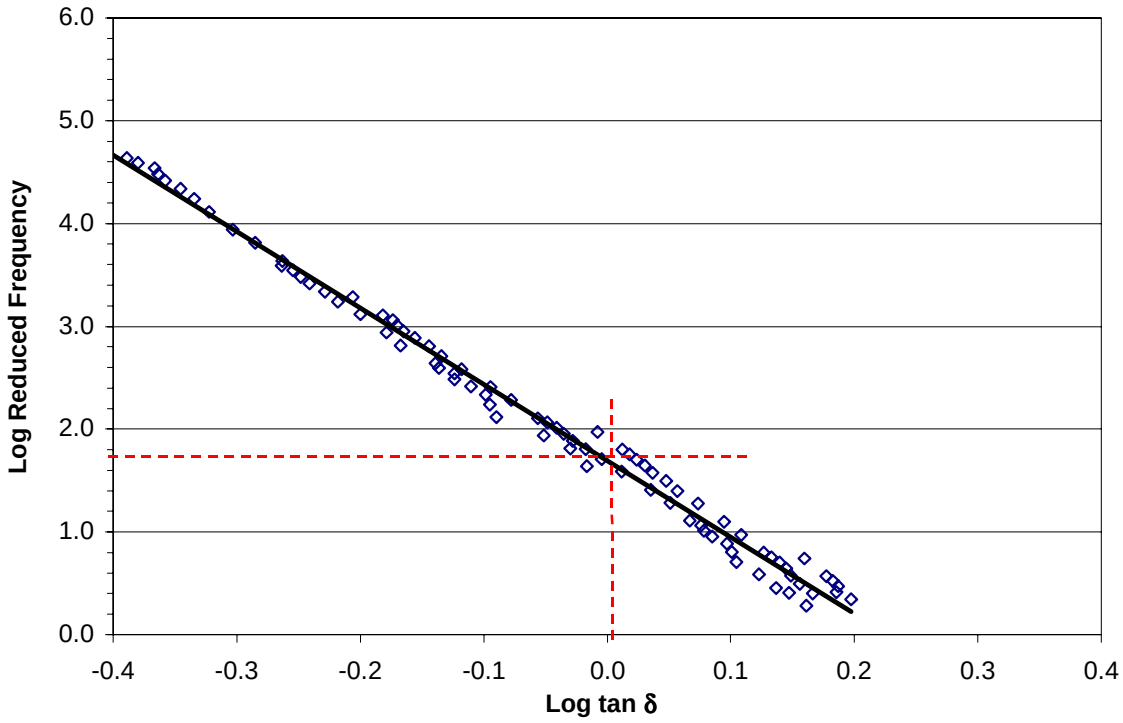


b)

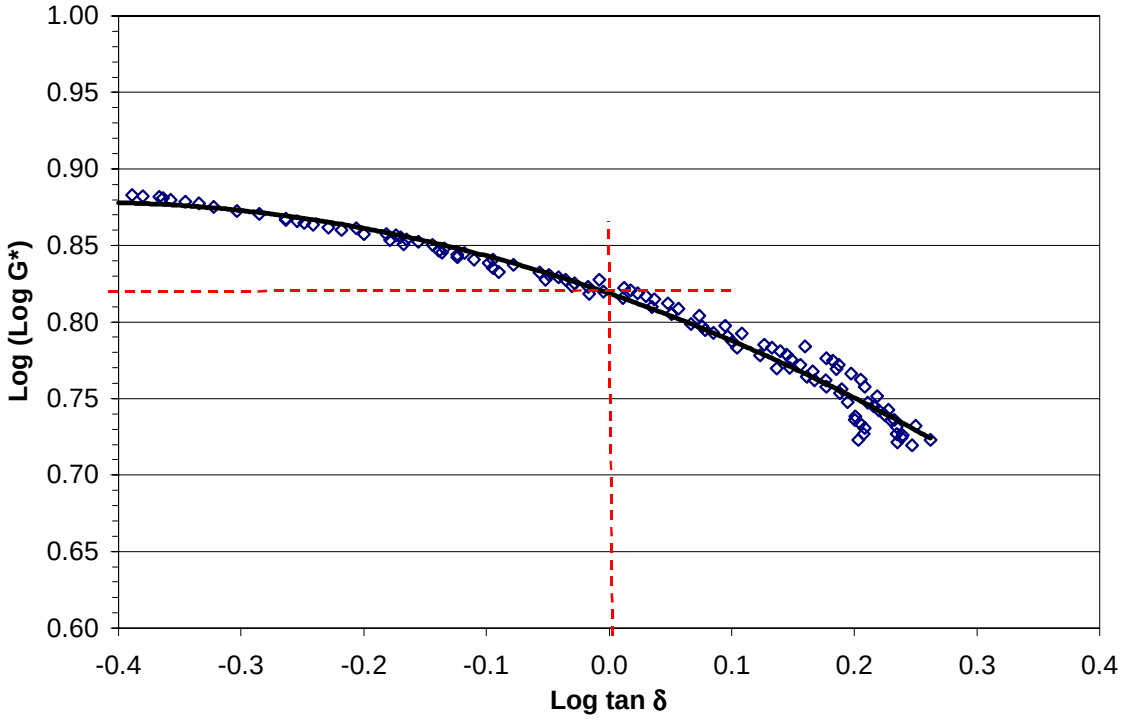


Figure G.7 Method of graphical determination of Christensen - Anderson model parameters: a) crossover frequency and b) rheological index for stored specimen AUG5.

a)

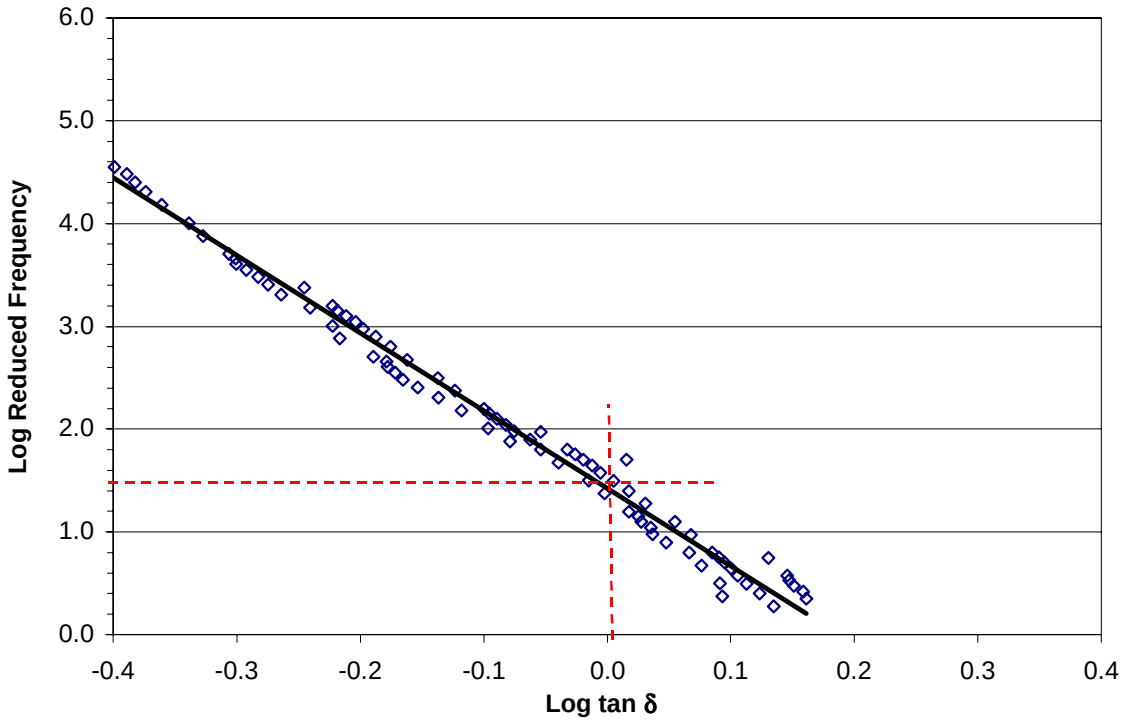


b)

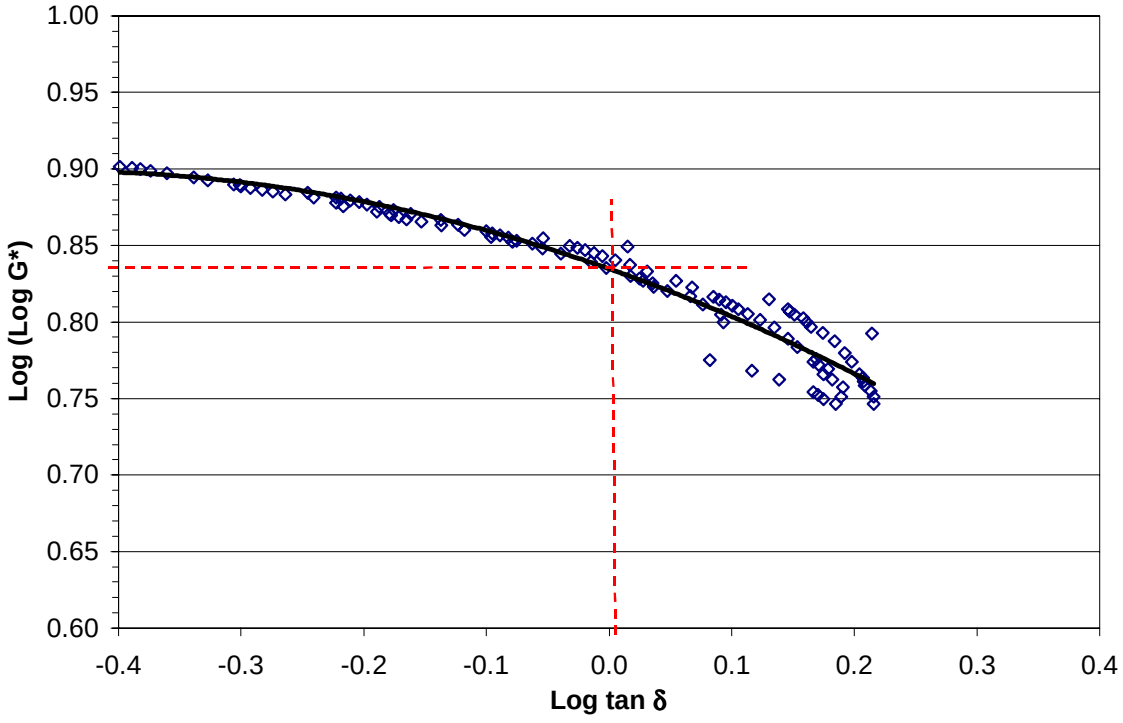


Figure G.8 Method of graphical determination of Christensen - Anderson model parameters: a) crossover frequency and b) rheological index for stored specimen ARG5.

a)

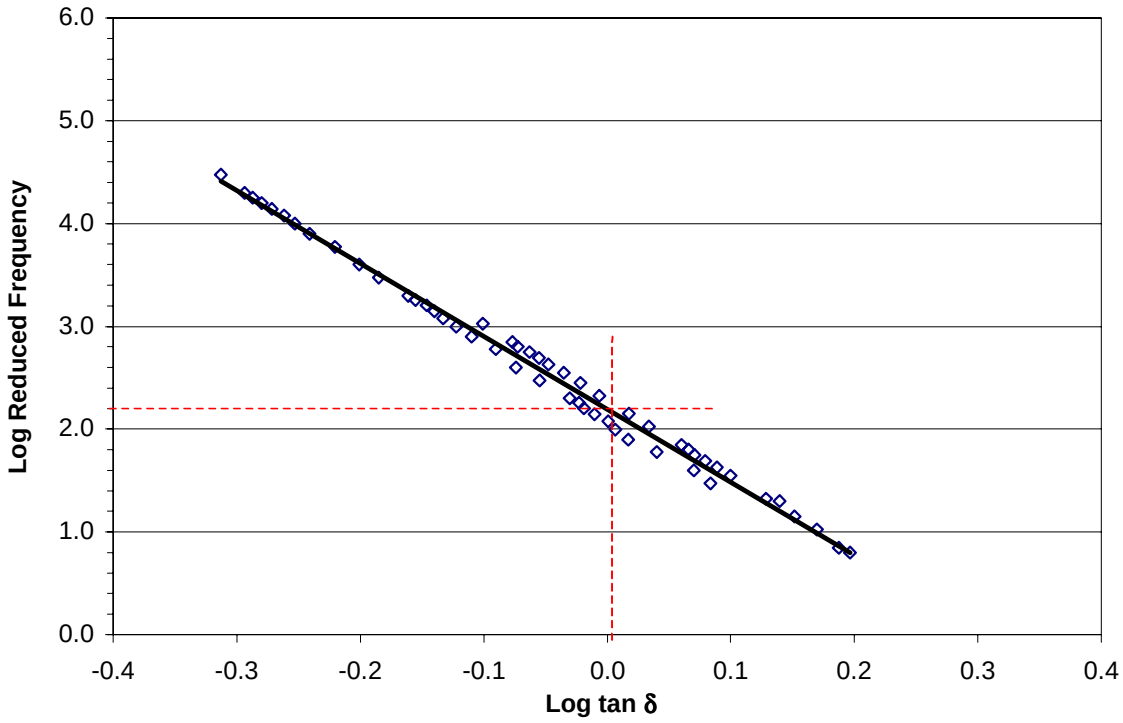


b)

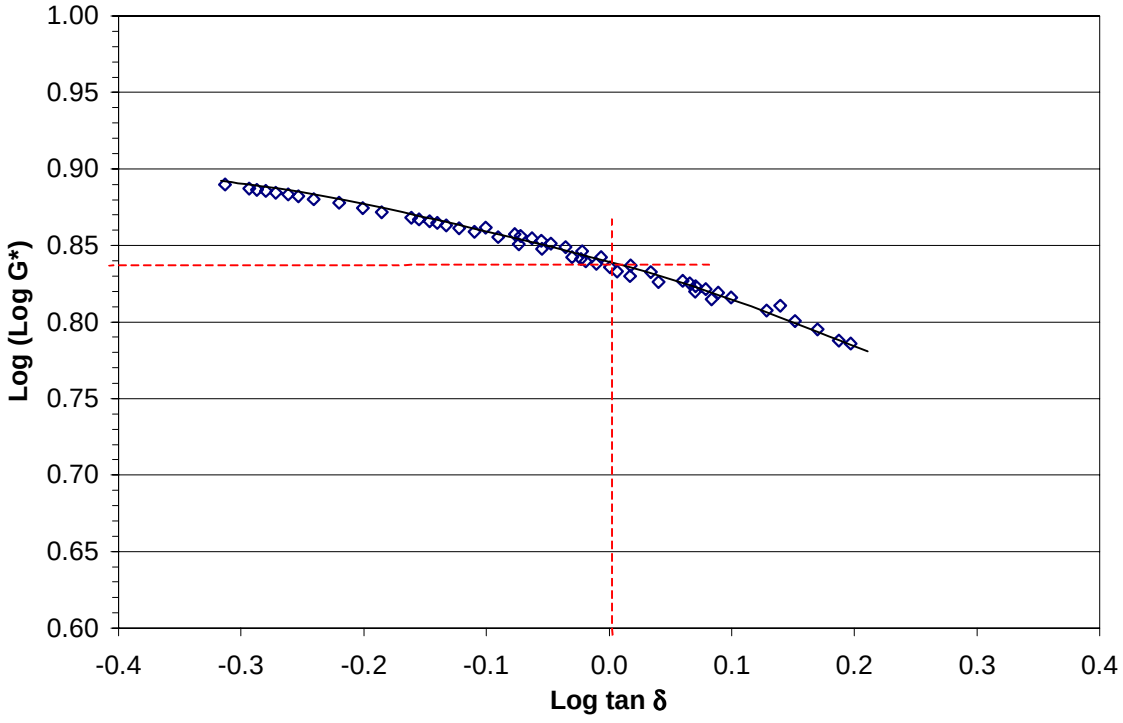


Figure G.9 Method of graphical determination of Christensen - Anderson model parameters: a) crossover frequency and b) rheological index for stored specimen AUN3.

a)

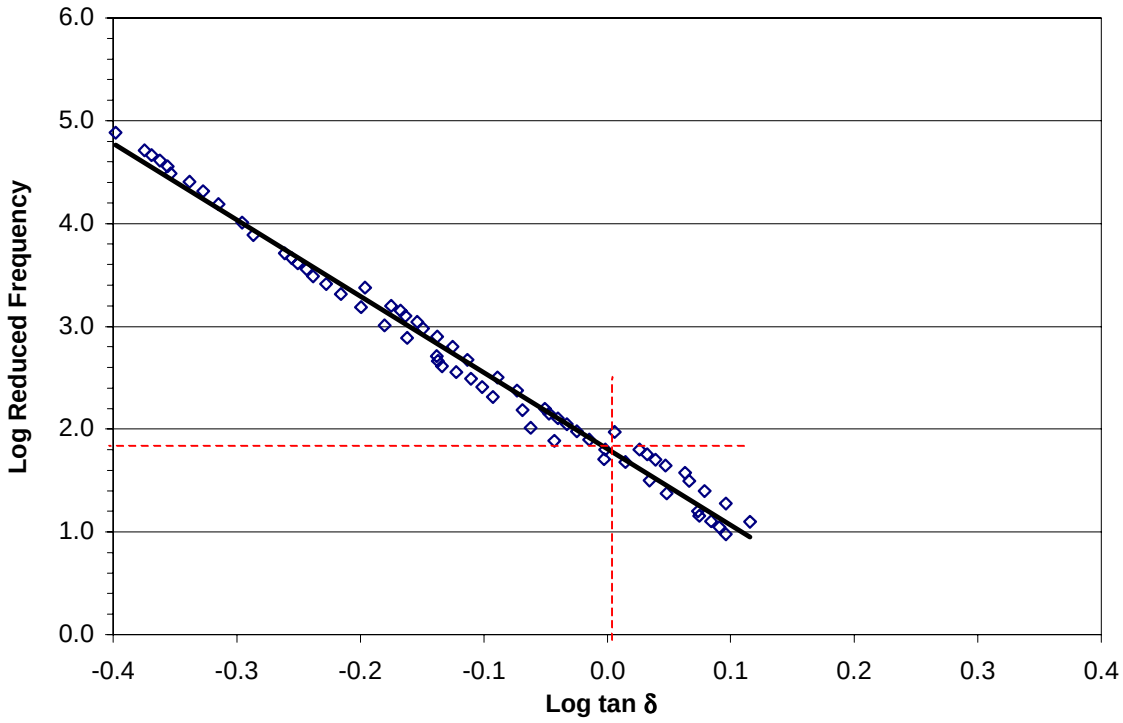


b)

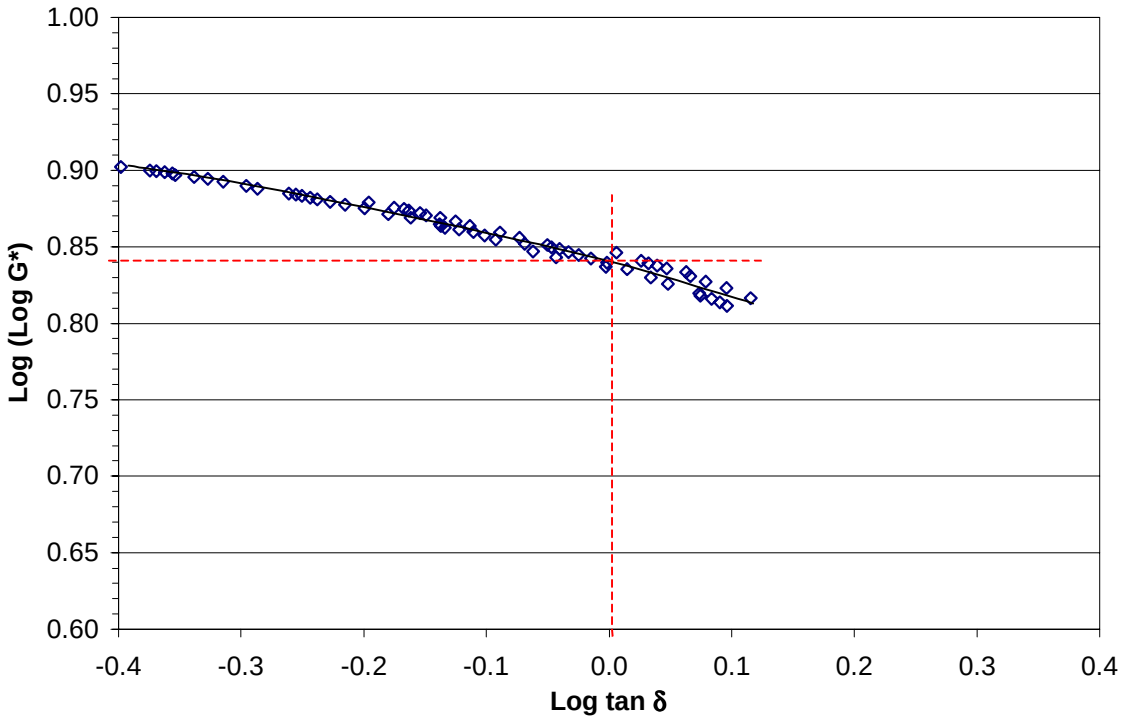


Figure G.10 Method of graphical determination of Christensen - Anderson model parameters: a) crossover frequency and b) rheological index for stored specimen ARN3.

a)

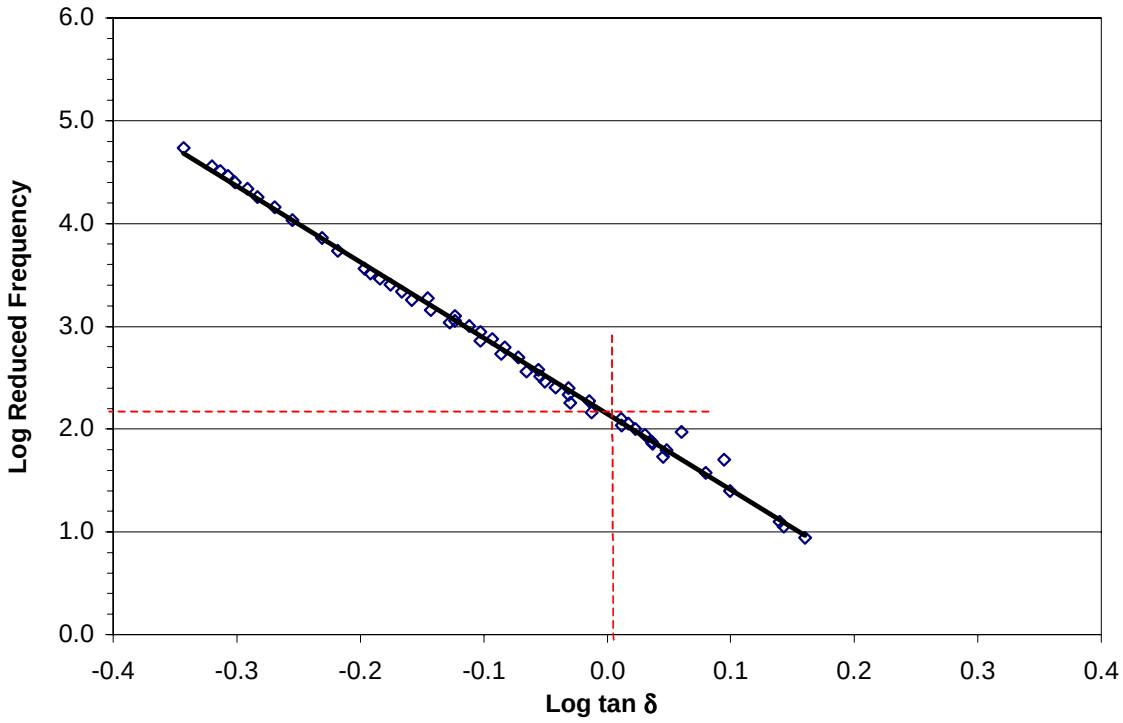


b)

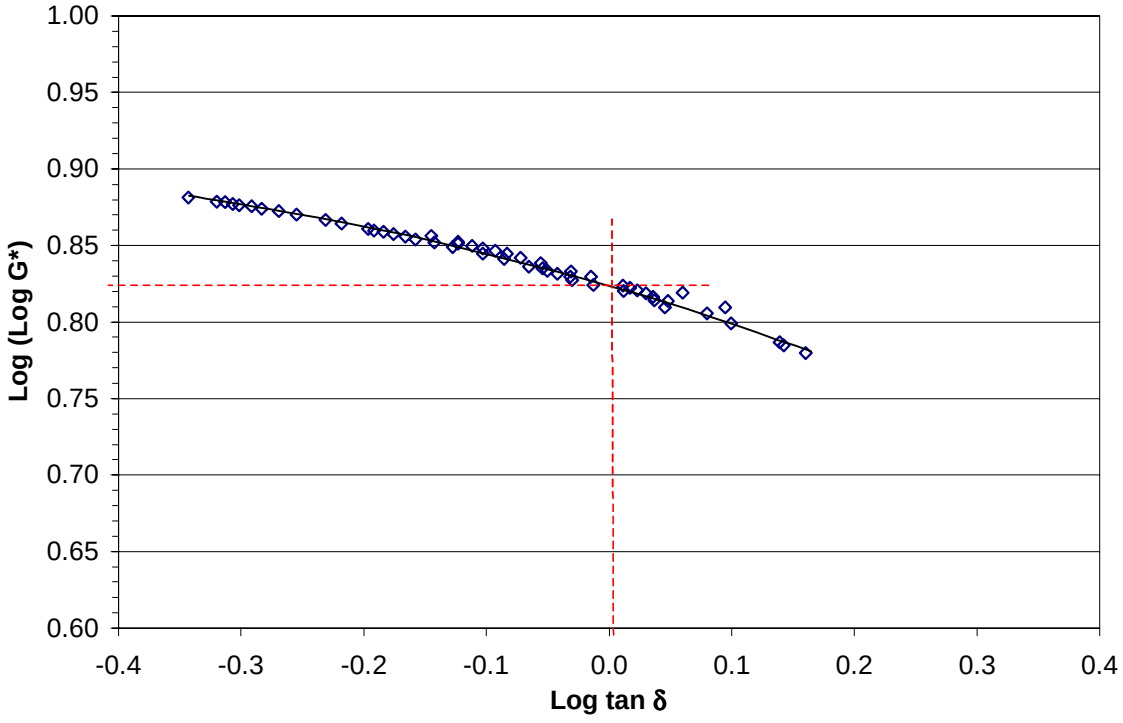


Figure G.11 Method of graphical determination of Christensen - Anderson model parameters: a) crossover frequency and b) rheological index for stored specimen AUN4.

a)

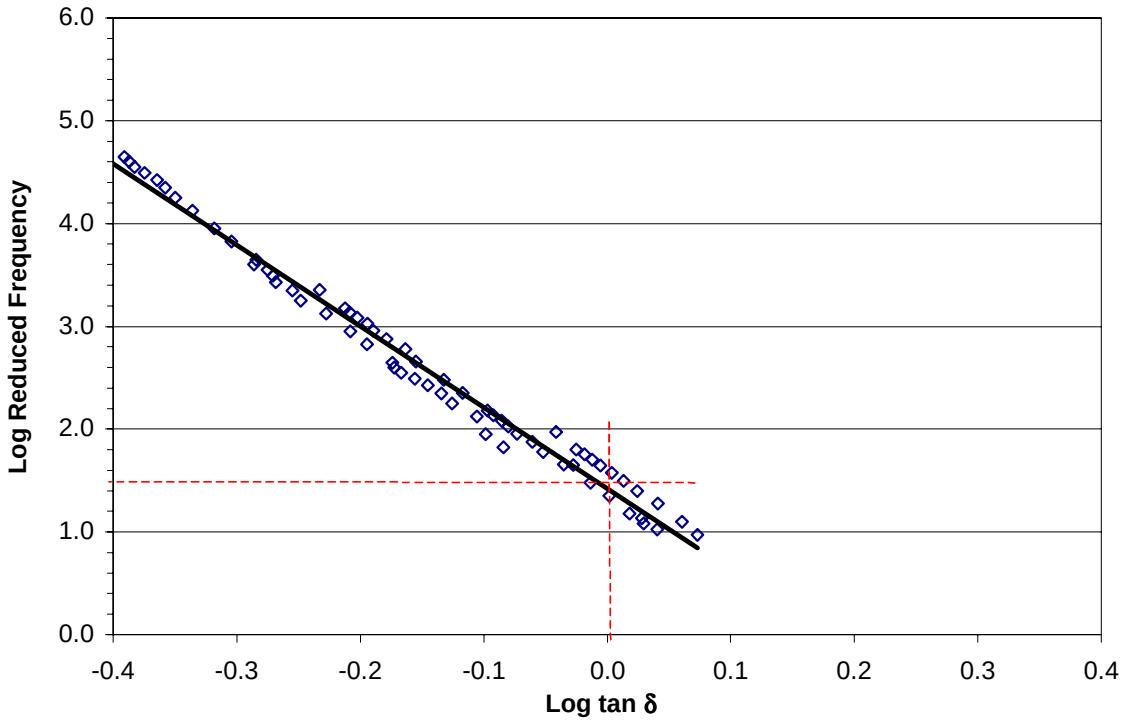


b)

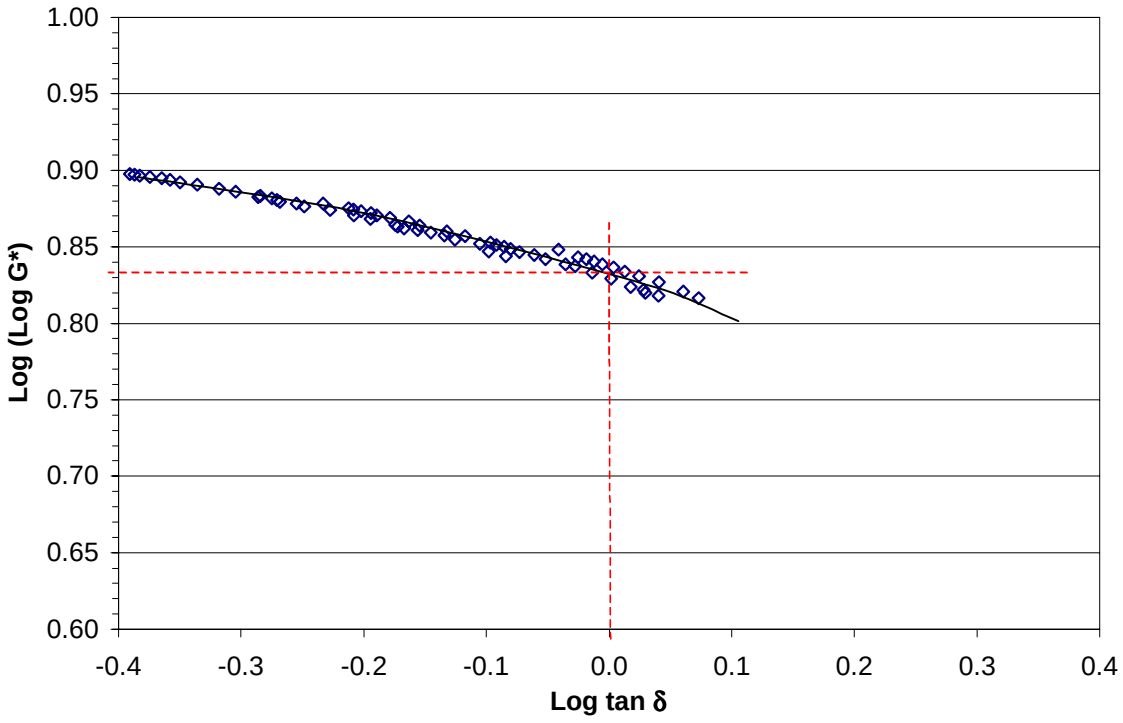


Figure G.12 Method of graphical determination of Christensen - Anderson model parameters: a) crossover frequency and b) rheological index for stored specimen ARN4.

a)

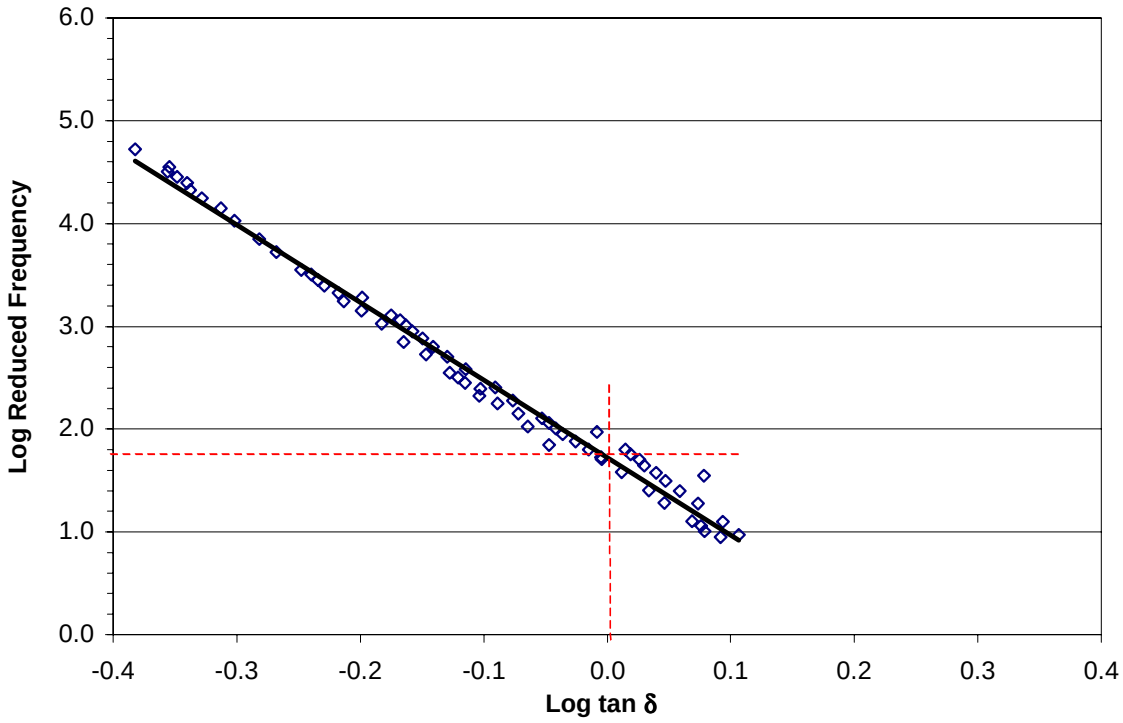


b)

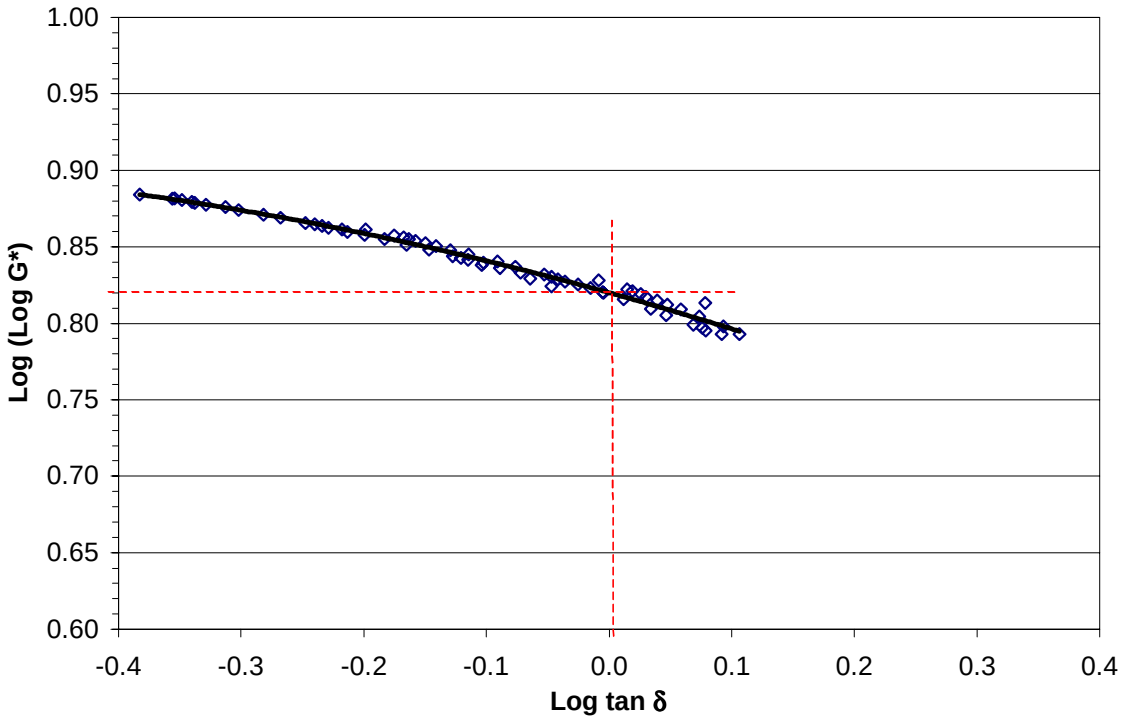


Figure G.13 Method of graphical determination of Christensen - Anderson model parameters: a) crossover frequency and b) rheological index for stored specimen AUN5.

a)

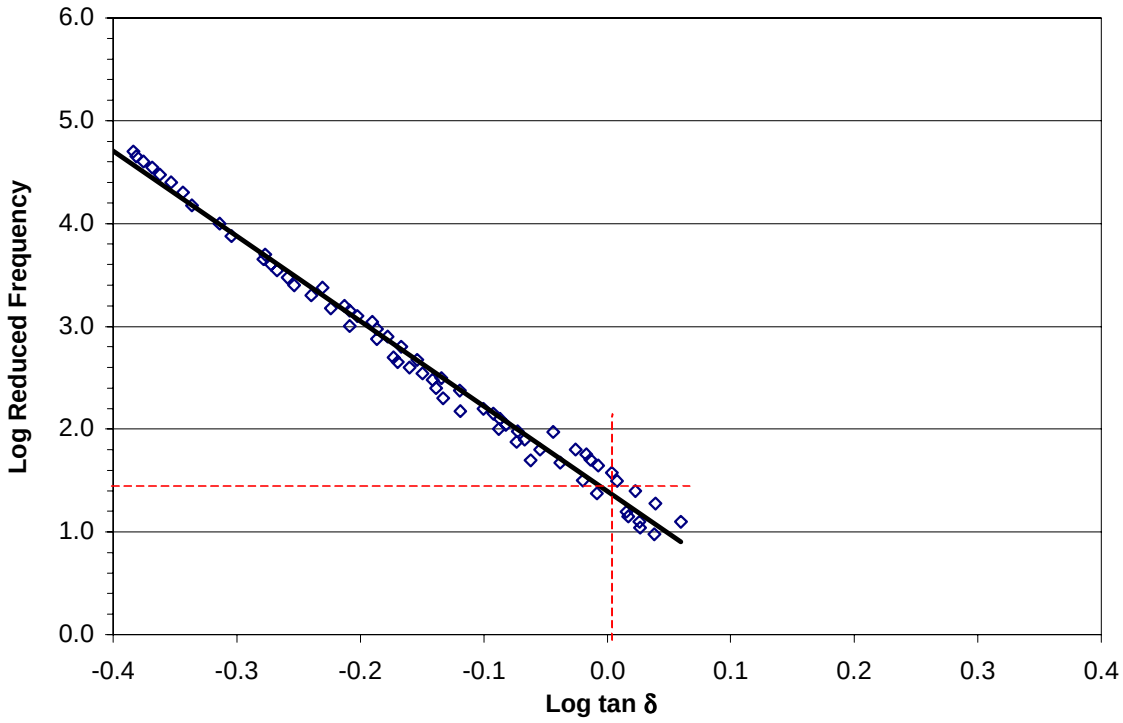


b)

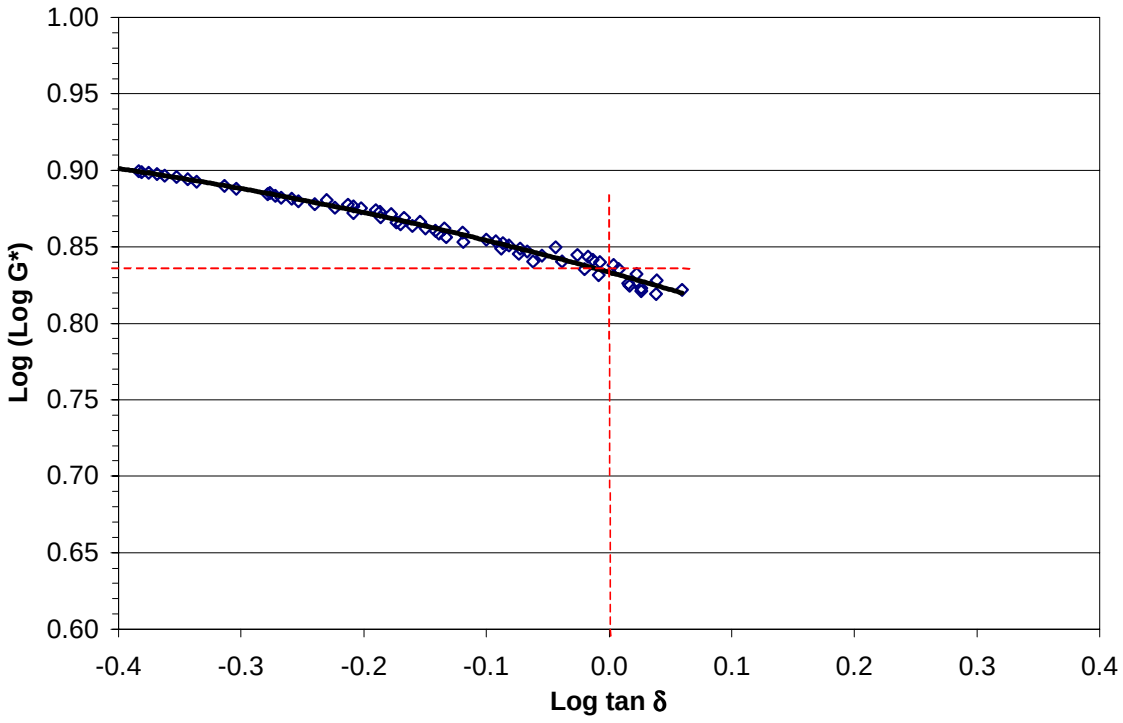


Figure G.14 Method of graphical determination of Christensen - Anderson model parameters: a) crossover frequency and b) rheological index for stored specimen ARN5.

a)

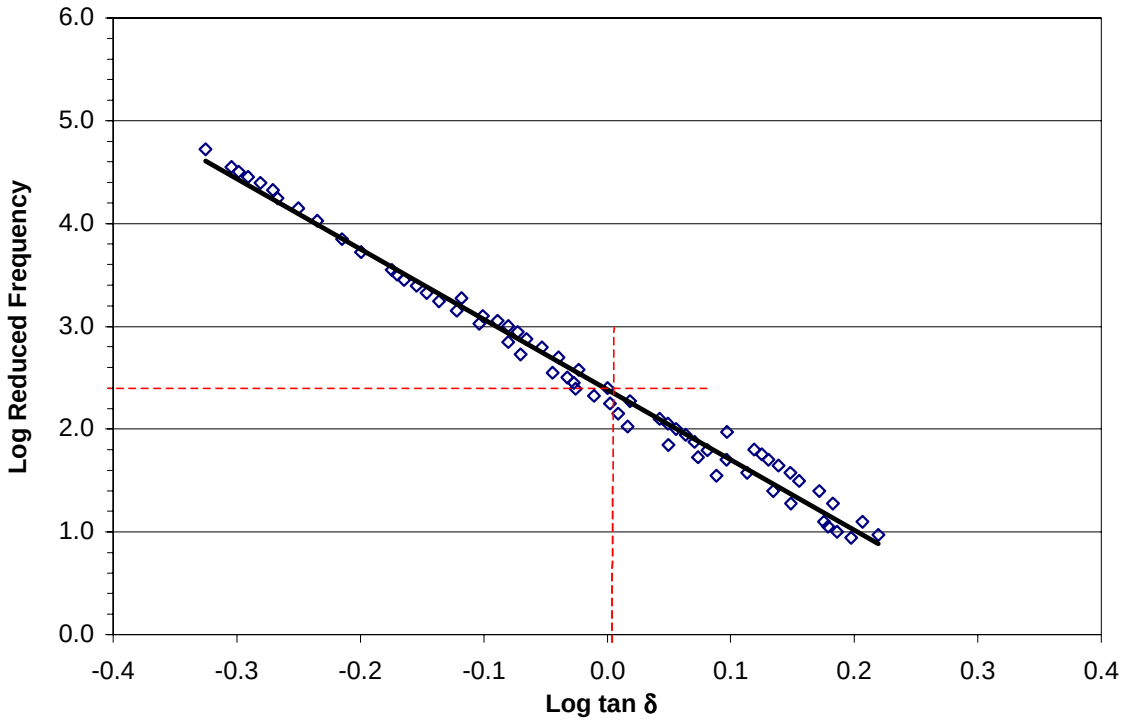


b)

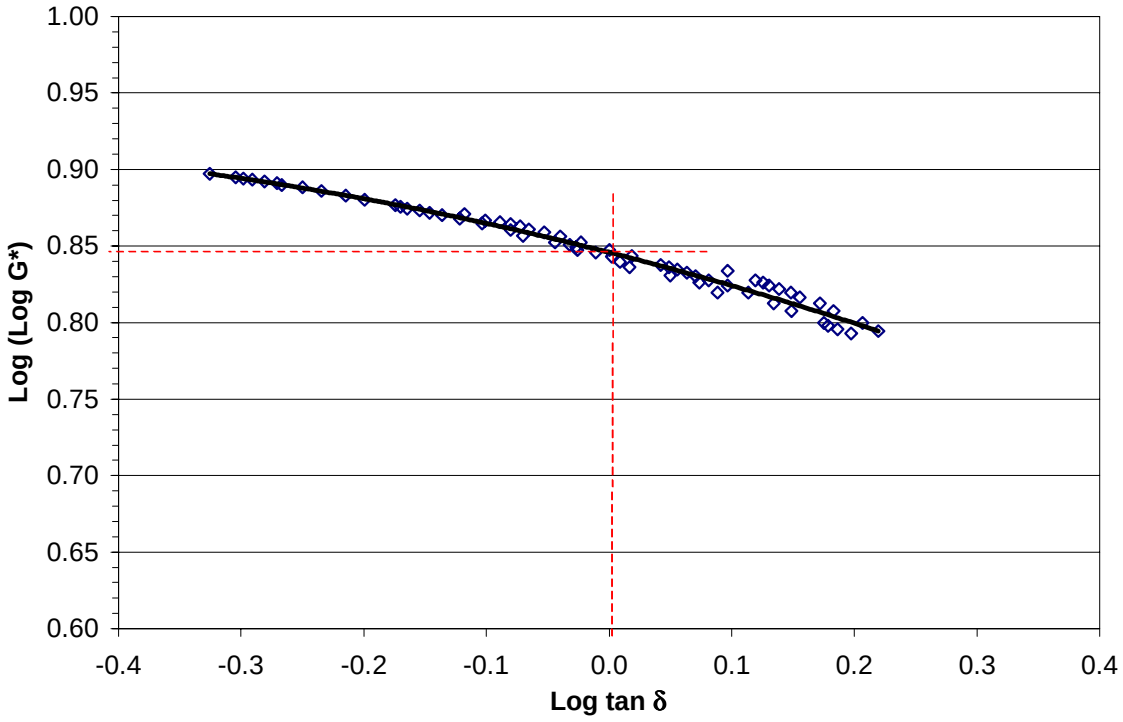


Figure G.15 Method of graphical determination of Christensen - Anderson model parameters: a) crossover frequency and b) rheological index for stored specimen AUS3.

a)

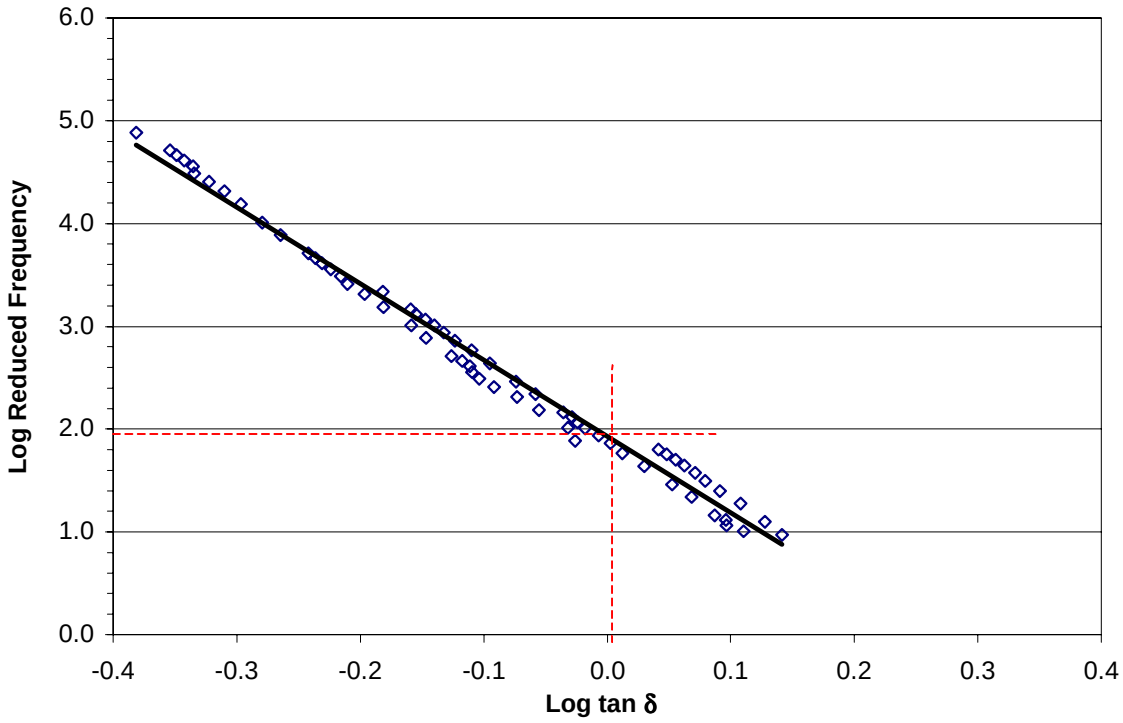


b)

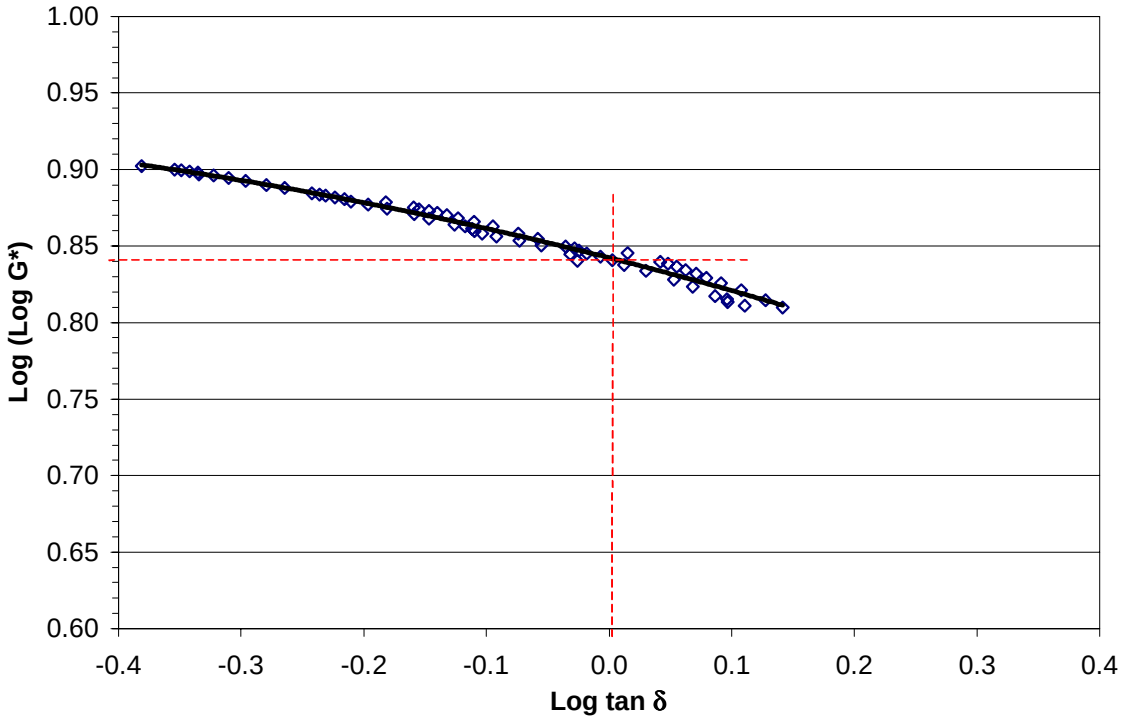


Figure G.16 Method of graphical determination of Christensen - Anderson model parameters: a) crossover frequency and b) rheological index for stored specimen ARS3.

a)

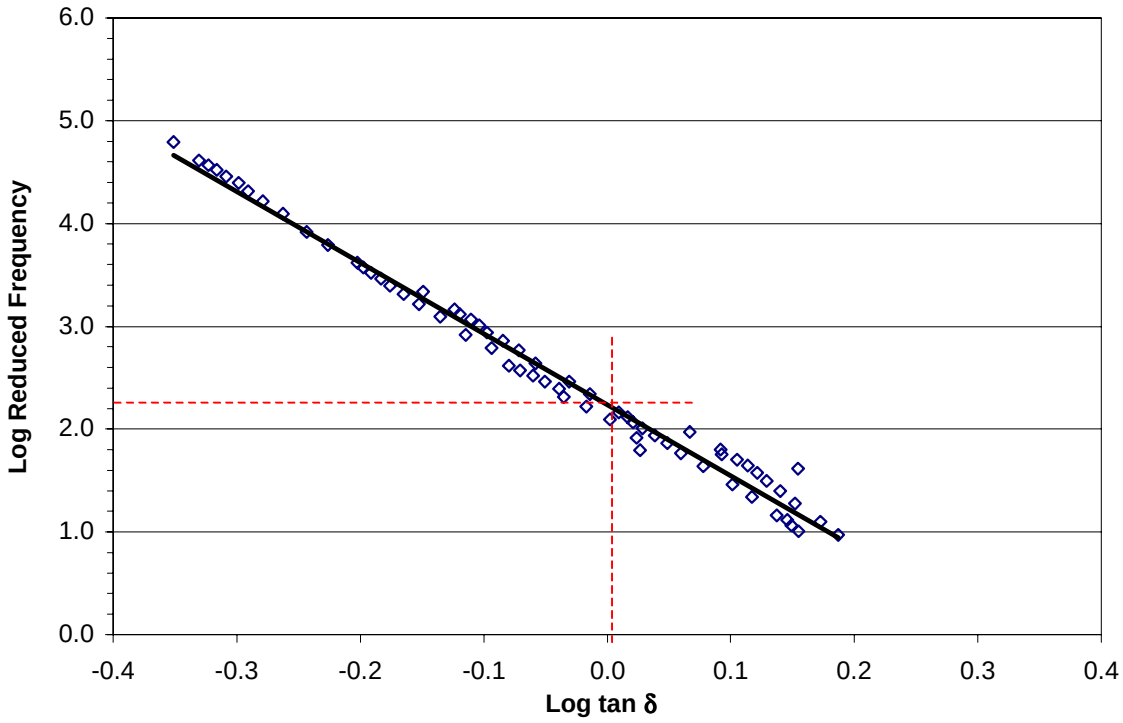


b)

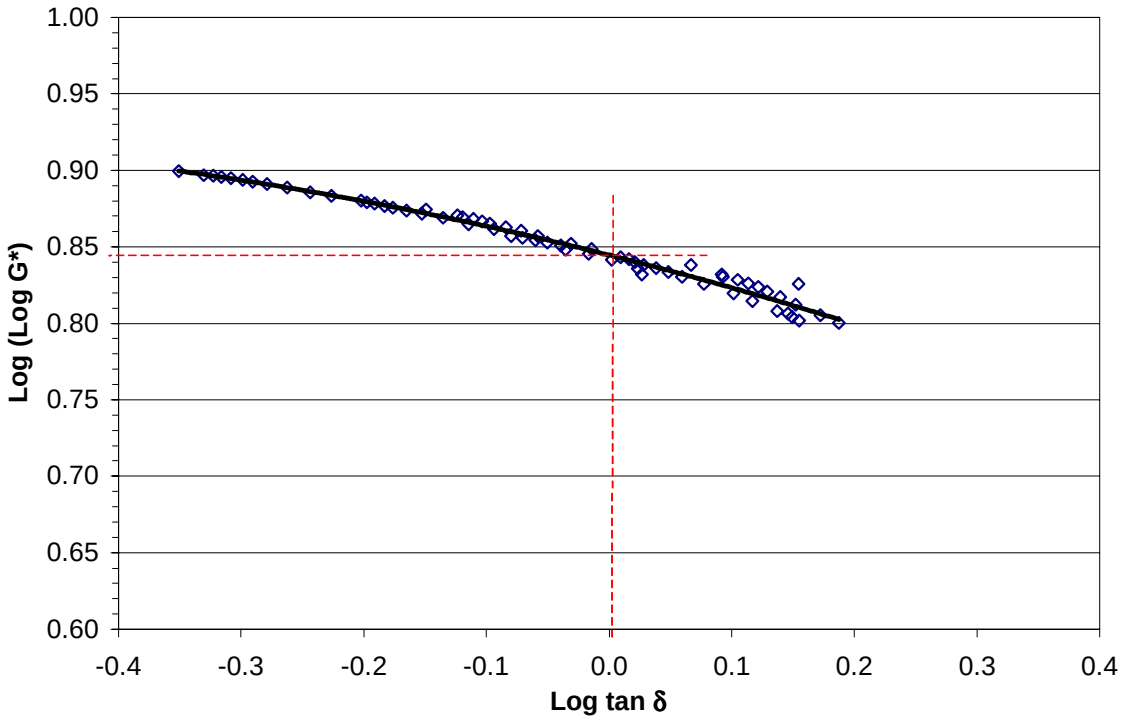


Figure G.17 Method of graphical determination of Christensen - Anderson model parameters: a) crossover frequency and b) rheological index for stored specimen AUS4.

a)

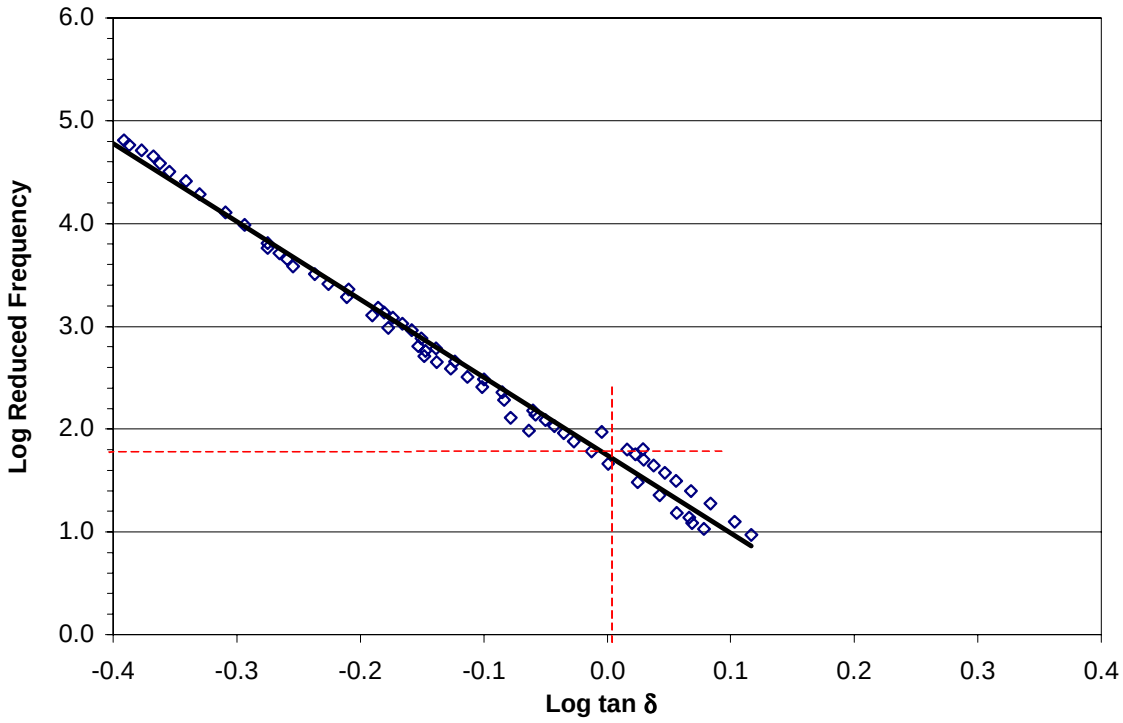


b)

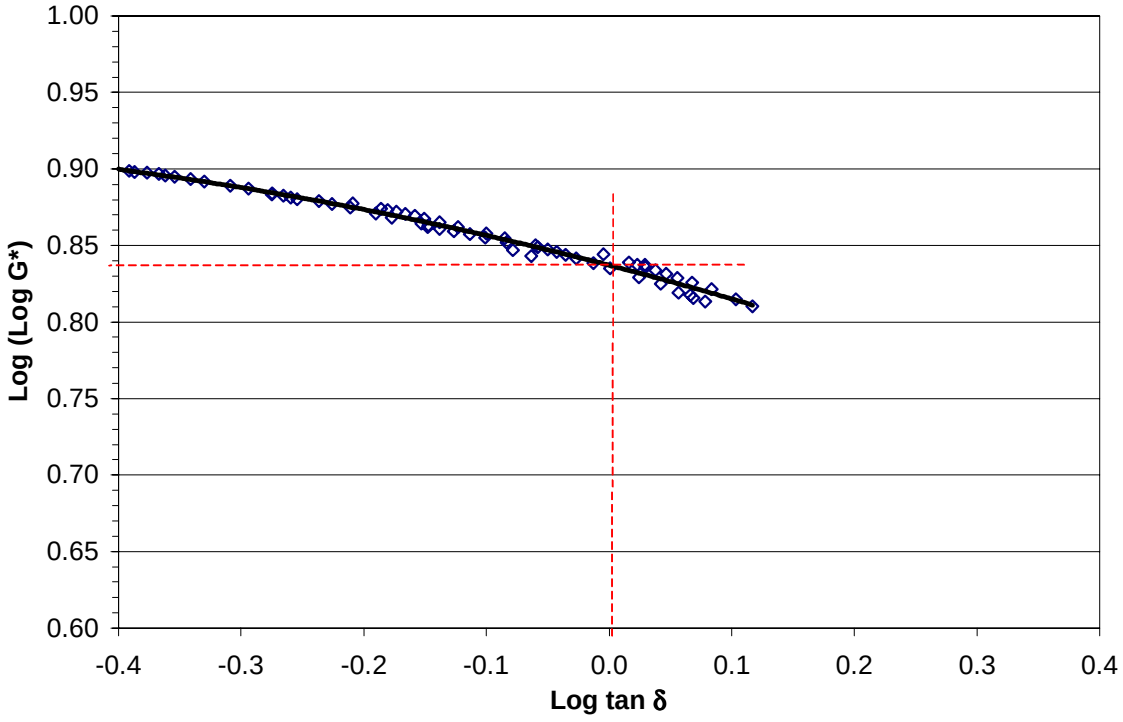


Figure G.18 Method of graphical determination of Christensen - Anderson model parameters: a) crossover frequency and b) rheological index for stored specimen ARS4.

a)

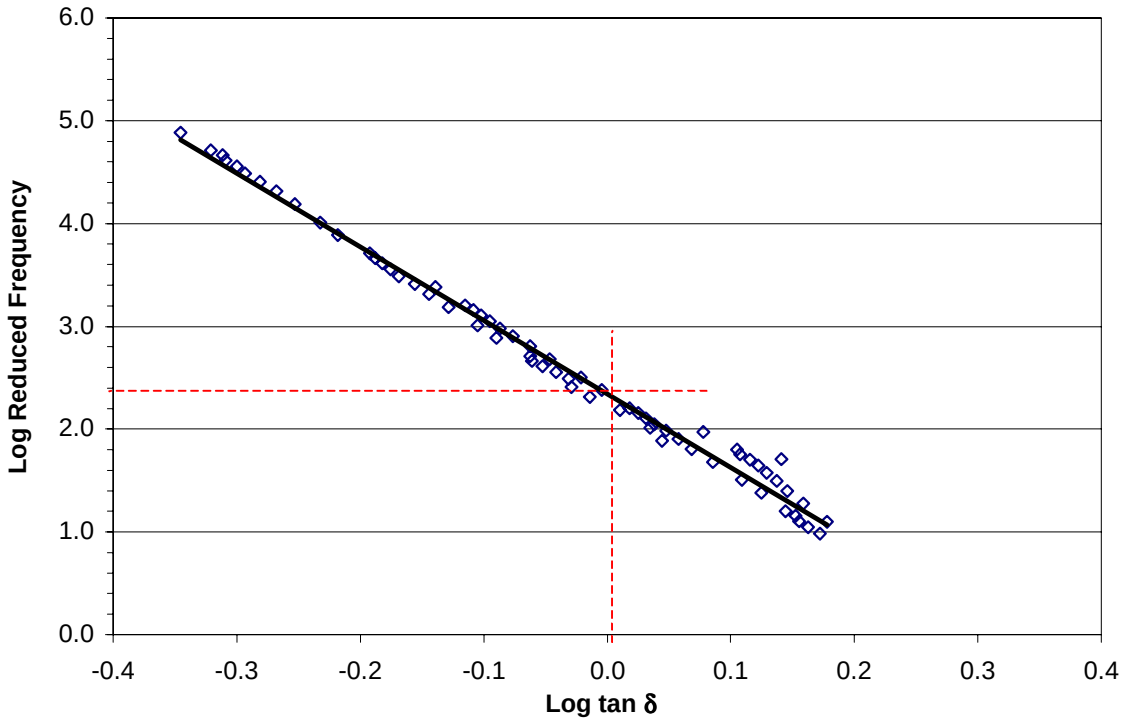


b)

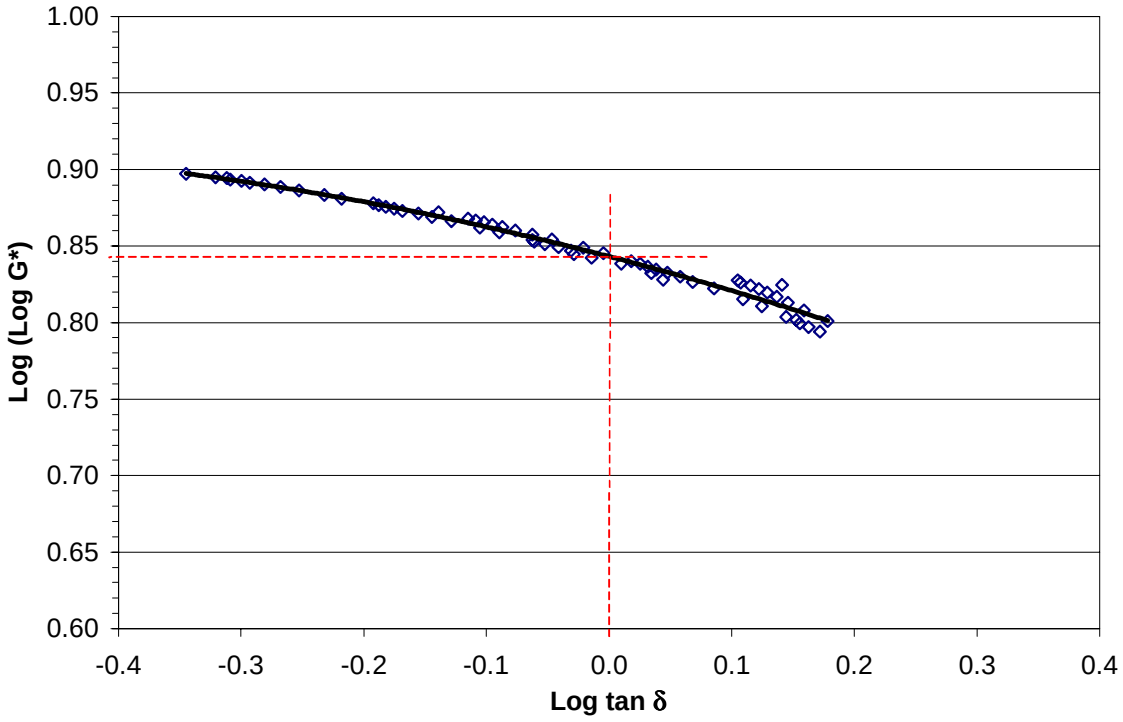


Figure G.19 Method of graphical determination of Christensen - Anderson model parameters: a) crossover frequency and b) rheological index for stored specimen AUS5.

a)

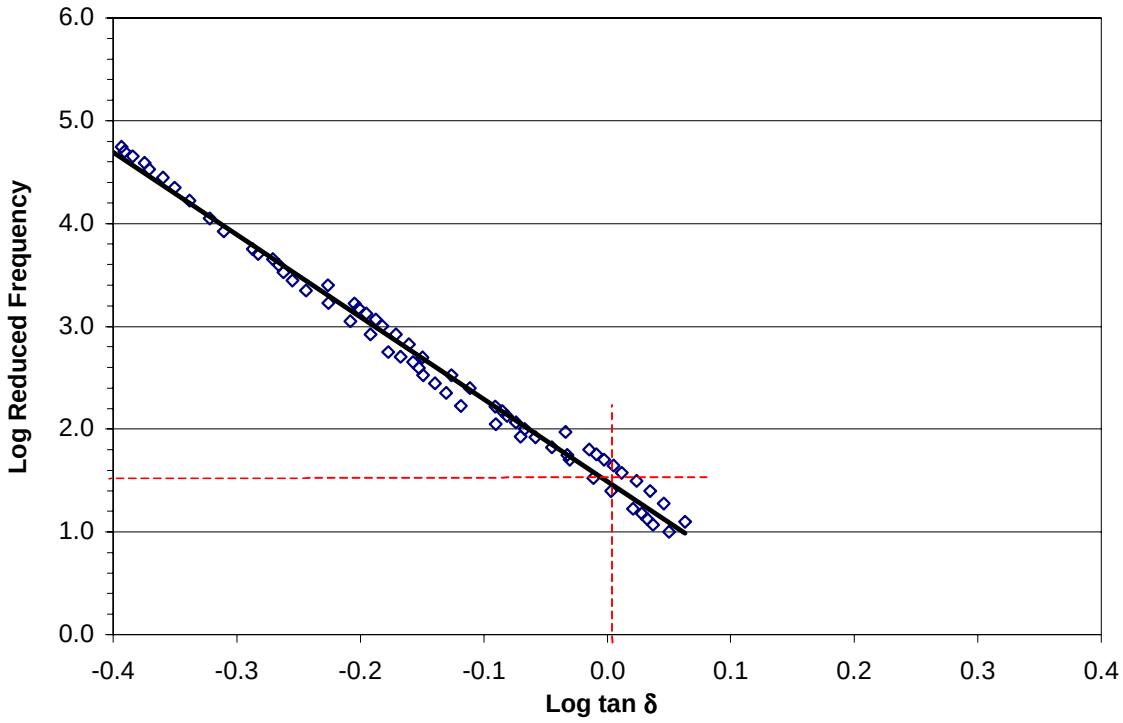


b)

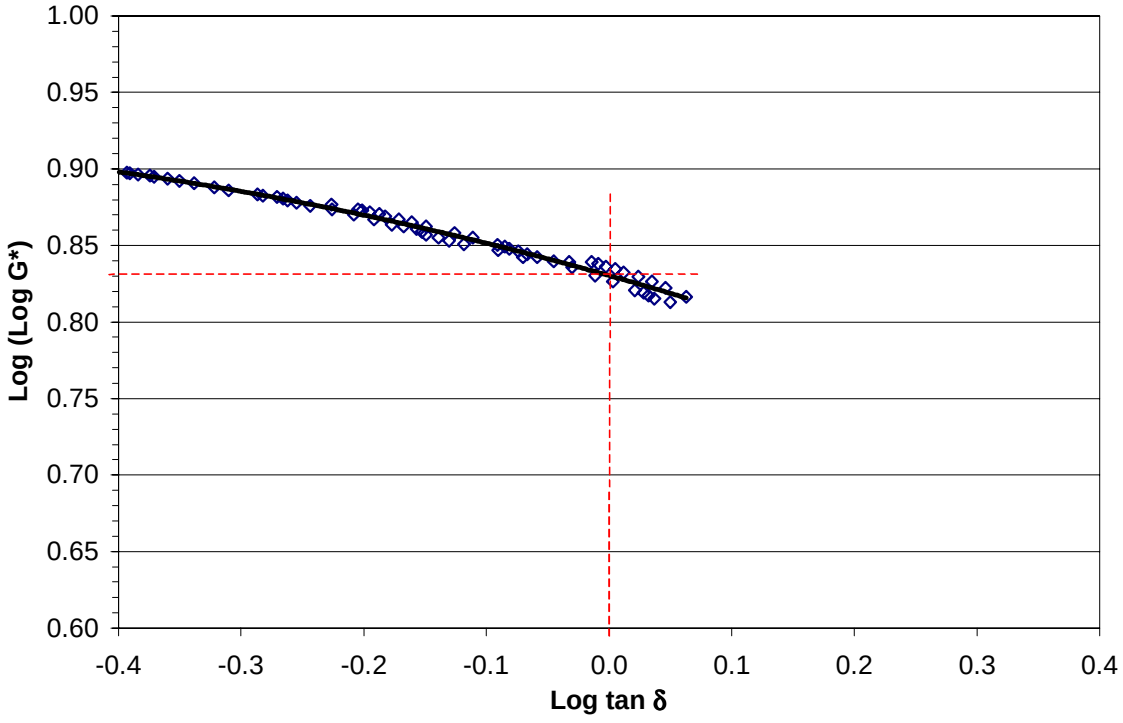


Figure G.20 Method of graphical determination of Christensen - Anderson model parameters: a) crossover frequency and b) rheological index for stored specimen ARS5.

# APPENDIX H

- This appendix includes the SAS input and output for original specimen AUG3 used in the non-linear regression of parameters for the shear complex moduli and phase angle equations proposed in the Christensen-Anderson model.

**SAS input for original specimen AUG3 determination of parameters for shear complex modulus model proposed by Christensen and Anderson**

```
options nodate pageno=1;
data mod;
input freq Gstar;
cards;
0.0000061    6.29E+00
0.0000092    9.49E+00
0.0000123    1.27E+01
0.0000184    1.84E+01
0.0000206    2.17E+01
0.0000246    2.41E+01
0.0000307    3.04E+01
0.0000308    3.16E+01
0.0000368    3.69E+01
0.0000411    4.24E+01
0.0000430    4.31E+01
0.0000491    4.92E+01
0.0000553    5.46E+01
0.0000614    6.06E+01
0.0000617    6.28E+01
0.0000822    8.26E+01
0.0000863    9.46E+01
0.0000921    8.93E+01
0.0001028    1.02E+02
0.0001228    1.20E+02
0.0001233    1.22E+02
0.0001295    1.40E+02
0.0001439    1.45E+02
0.0001645    1.65E+02
0.0001726    1.87E+02
0.0001842    1.77E+02
0.0001850    1.88E+02
```

| | |
|---|---|
| 0.0002056 | 2.07E+02 |
| 0.0002456 | 2.34E+02 |
| 0.0002589 | 2.78E+02 |
| 0.0003070 | 2.94E+02 |
| 0.0003083 | 3.09E+02 |
| 0.0003452 | 3.71E+02 |
| 0.0003683 | 3.50E+02 |
| 0.0004111 | 4.13E+02 |
| 0.0004297 | 4.12E+02 |
| 0.0004315 | 4.63E+02 |
| 0.0004911 | 4.66E+02 |
| 0.0004991 | 5.21E+02 |
| 0.0005179 | 5.52E+02 |
| 0.0005525 | 5.21E+02 |
| 0.0006042 | 6.42E+02 |
| 0.0006139 | 5.79E+02 |
| 0.0006167 | 6.14E+02 |
| 0.0006905 | 7.28E+02 |
| 0.0007486 | 7.68E+02 |
| 0.0007768 | 8.16E+02 |
| 0.0008223 | 8.12E+02 |
| 0.0008631 | 8.98E+02 |
| 0.0009209 | 8.75E+02 |
| 0.0009982 | 1.02E+03 |
| 0.0010278 | 1.01E+03 |
| 0.0012278 | 1.16E+03 |
| 0.0012334 | 1.20E+03 |
| 0.0012946 | 1.32E+03 |
| 0.0014389 | 1.40E+03 |
| 0.0014973 | 1.50E+03 |
| 0.0016445 | 1.59E+03 |
| 0.0017262 | 1.75E+03 |
| 0.0018417 | 1.72E+03 |
| 0.0018501 | 1.78E+03 |

| | |
|---|---|
| 0.0019964 | 1.97E+03 |
| 0.0020556 | 1.98E+03 |
| 0.0024557 | 2.27E+03 |
| 0.0024955 | 2.44E+03 |
| 0.0025893 | 2.57E+03 |
| 0.0029945 | 2.91E+03 |
| 0.0030696 | 2.80E+03 |
| 0.0030835 | 2.93E+03 |
| 0.0034524 | 3.36E+03 |
| 0.0034936 | 3.33E+03 |
| 0.0036835 | 3.32E+03 |
| 0.0039927 | 3.78E+03 |
| 0.0041113 | 3.82E+03 |
| 0.0042974 | 3.82E+03 |
| 0.0043155 | 4.15E+03 |
| 0.0044918 | 4.20E+03 |
| 0.0049113 | 4.33E+03 |
| 0.0049909 | 4.63E+03 |
| 0.0051786 | 4.90E+03 |
| 0.0053719 | 5.26E+03 |
| 0.0055252 | 4.90E+03 |
| 0.0060417 | 5.66E+03 |
| 0.0061392 | 5.40E+03 |
| 0.0061669 | 5.56E+03 |
| 0.0069048 | 6.37E+03 |
| 0.0074864 | 6.69E+03 |
| 0.0077679 | 7.10E+03 |
| 0.0080579 | 7.60E+03 |
| 0.0082226 | 7.29E+03 |
| 0.0086309 | 7.79E+03 |
| 0.0092087 | 7.89E+03 |
| 0.0099818 | 8.66E+03 |
| 0.0102782 | 8.94E+03 |
| 0.0107439 | 9.88E+03 |

| | |
|---|---|
| 0.0122783 | 1.02E+04 |
| 0.0123338 | 1.05E+04 |
| 0.0129464 | 1.12E+04 |
| 0.0143895 | 1.21E+04 |
| 0.0149727 | 1.24E+04 |
| 0.0161158 | 1.41E+04 |
| 0.0164451 | 1.36E+04 |
| 0.0172619 | 1.44E+04 |
| 0.0184175 | 1.46E+04 |
| 0.0185007 | 1.51E+04 |
| 0.0199636 | 1.60E+04 |
| 0.0205564 | 1.65E+04 |
| 0.0214877 | 1.80E+04 |
| 0.0249546 | 1.93E+04 |
| 0.0258928 | 2.05E+04 |
| 0.0268596 | 2.16E+04 |
| 0.0299455 | 2.24E+04 |
| 0.0308346 | 2.36E+04 |
| 0.0322316 | 2.52E+04 |
| 0.0345238 | 2.62E+04 |
| 0.0349364 | 2.54E+04 |
| 0.0376035 | 2.85E+04 |
| 0.0399273 | 2.87E+04 |
| 0.0411128 | 2.99E+04 |
| 0.0429754 | 3.16E+04 |
| 0.0431547 | 3.16E+04 |
| 0.0449182 | 3.15E+04 |
| 0.0483474 | 3.48E+04 |
| 0.0499091 | 3.42E+04 |
| 0.0517857 | 3.67E+04 |
| 0.0537193 | 3.77E+04 |
| 0.0604166 | 4.15E+04 |
| 0.0616691 | 4.19E+04 |
| 0.0628319 | 3.97E+04 |

| | |
|---|---|
| 0.0690476 | 4.66E+04 |
| 0.0748637 | 4.72E+04 |
| 0.0776785 | 5.13E+04 |
| 0.0805789 | 5.22E+04 |
| 0.0863095 | 5.54E+04 |
| 0.0942478 | 5.50E+04 |
| 0.0998182 | 5.89E+04 |
| 0.1074386 | 6.47E+04 |
| 0.1256637 | 7.04E+04 |
| 0.1294642 | 7.66E+04 |
| 0.1497273 | 8.09E+04 |
| 0.1611578 | 8.83E+04 |
| 0.1726190 | 9.60E+04 |
| 0.1884956 | 9.44E+04 |
| 0.1996365 | 1.01E+05 |
| 0.2148771 | 1.10E+05 |
| 0.2495456 | 1.20E+05 |
| 0.2513274 | 1.16E+05 |
| 0.2589284 | 1.30E+05 |
| 0.2685964 | 1.32E+05 |
| 0.2994547 | 1.37E+05 |
| 0.3141593 | 1.40E+05 |
| 0.3223157 | 1.51E+05 |
| 0.3493638 | 1.54E+05 |
| 0.3760350 | 1.68E+05 |
| 0.3769911 | 1.60E+05 |
| 0.3992729 | 1.70E+05 |
| 0.4297543 | 1.86E+05 |
| 0.4398230 | 1.80E+05 |
| 0.4491820 | 1.88E+05 |
| 0.4834735 | 2.05E+05 |
| 0.4990911 | 2.02E+05 |
| 0.5026548 | 2.01E+05 |
| 0.5371928 | 2.23E+05 |

| | |
|---|---|
| 0.5654867 | 2.21E+05 |
| 0.6283185 | 2.41E+05 |
| 0.7486367 | 2.74E+05 |
| 0.8057892 | 3.02E+05 |
| 0.9424778 | 3.26E+05 |
| 0.9981823 | 3.36E+05 |
| 1.0743857 | 3.75E+05 |
| 1.2244388 | 3.55E+05 |
| 1.2566371 | 4.04E+05 |
| 1.4972734 | 4.58E+05 |
| 1.6115785 | 5.09E+05 |
| 1.8366582 | 4.88E+05 |
| 1.8849556 | 5.48E+05 |
| 2.1487713 | 6.34E+05 |
| 2.4488776 | 6.08E+05 |
| 2.5132741 | 6.79E+05 |
| 2.6859641 | 7.49E+05 |
| 3.1415927 | 7.91E+05 |
| 3.2231570 | 8.56E+05 |
| 3.6733163 | 8.00E+05 |
| 3.7603498 | 9.55E+05 |
| 3.7699112 | 9.06E+05 |
| 4.2975426 | 1.06E+06 |
| 4.3982297 | 1.01E+06 |
| 4.8347355 | 1.16E+06 |
| 4.8977551 | 1.00E+06 |
| 5.0265482 | 1.12E+06 |
| 5.3719283 | 1.24E+06 |
| 5.6548668 | 1.21E+06 |
| 6.1221939 | 1.17E+06 |
| 6.2831853 | 1.31E+06 |
| 7.3466327 | 1.35E+06 |
| 8.0578924 | 1.65E+06 |
| 8.5710715 | 1.50E+06 |

| | |
|---|---|
| 9.4247780 | 1.74E+06 |
| 9.7955103 | 1.64E+06 |
| 11.0199490 | 1.81E+06 |
| 12.2443878 | 1.92E+06 |
| 12.5663706 | 2.12E+06 |
| 18.3665817 | 2.53E+06 |
| 18.8495559 | 2.80E+06 |
| 24.4887757 | 3.07E+06 |
| 25.1327412 | 3.41E+06 |
| 30.1994984 | 3.74E+06 |
| 31.4159265 | 3.94E+06 |
| 36.7331635 | 4.04E+06 |
| 37.6991118 | 4.43E+06 |
| 43.9822972 | 4.88E+06 |
| 45.2992477 | 5.00E+06 |
| 48.9775513 | 4.85E+06 |
| 50.2654825 | 5.35E+06 |
| 56.5486678 | 5.80E+06 |
| 60.3989969 | 5.94E+06 |
| 61.2219392 | 5.60E+06 |
| 62.8318531 | 6.18E+06 |
| 73.4663270 | 6.28E+06 |
| 85.7107148 | 6.90E+06 |
| 90.5984953 | 7.60E+06 |
| 94.2477796 | 7.97E+06 |
| 97.9551027 | 7.48E+06 |
| 110.1994905 | 8.20E+06 |
| 120.7979938 | 8.94E+06 |
| 122.4438783 | 8.53E+06 |
| 150.9974922 | 1.04E+07 |
| 181.1969906 | 1.19E+07 |
| 183.6658175 | 1.08E+07 |
| 211.3964891 | 1.27E+07 |
| 241.5959875 | 1.34E+07 |

244.8877567 1.28E+07
271.7954860 1.47E+07
301.9949844 1.56E+07
367.3316350 1.59E+07
452.9924766 1.92E+07
489.7755133 1.86E+07
603.9899688 2.21E+07
612.2193916 2.06E+07
734.6632700 2.27E+07
857.1071483 2.43E+07
905.9849532 2.68E+07
979.5510266 2.57E+07
1101.9949049 2.73E+07
1207.9799376 2.94E+07
1224.4387833 2.89E+07
1509.9749220 3.34E+07
1811.9699064 3.52E+07
1836.6581749 3.47E+07
2113.9648908 3.84E+07
2415.9598752 4.06E+07
2717.9548595 4.21E+07
3019.9498439 4.43E+07
4529.9247659 5.07E+07
6039.8996879 5.70E+07
9059.8495318 6.43E+07
12079.7993758 6.83E+07
15099.7492197 7.22E+07
18119.6990636 8.05E+07
21139.6489076 8.25E+07
24159.5987515 8.38E+07
27179.5485954 8.87E+07
30199.4984394 8.88E+07
45299.2476591 1.02E+08
;

```
proc nlin data=mod method=marquardt;
parms wc=300 R=0.99 Gg=1000000000;
model Gstar=Gg*(1+(wc/freq)**(log10(2)/R))**(-R/log10(2));
run;
```

**SAS output for original specimen AUG3 determination of parameters for shear complex modulus model proposed by Christensen and Anderson**

Non-Linear Least Squares Iterative Phase

Dependent Variable GSTAR Method: Marquardt

| Iter | WC | R | GG | Sum of Squares |
|---|---|---|---|---|
| 0 | 300.000000 | 0.990000 | 1000000000 | 1.92385128E18 |
| 1 | 283.883654 | 1.147377 | 460185243 | 8.31631047E16 |
| 2 | 335.252527 | 1.214806 | 316973114 | 1.7155279E15 |
| 3 | 450.450560 | 1.193747 | 298805354 | 7.69680222E13 |
| 4 | 504.677992 | 1.173808 | 292315674 | 3.95649615E13 |
| 5 | 509.707896 | 1.172246 | 291742625 | 3.92024271E13 |
| 6 | 509.773926 | 1.172201 | 291723558 | 3.9202406E13 |
| 7 | 509.775194 | 1.172200 | 291722880 | 3.9202406E13 |

NOTE: Convergence criterion met.

Non-Linear Least Squares Summary Statistics Dependent Variable GSTAR

| Source | DF | Sum of Squares | Mean Square |
|---|---|---|---|
| Regression | 3 | 8.56834505E16 | 2.85611502E16 |
| Residual | 261 | 3.9202406E13 | 150200789225 |
| Uncorrected Total | 264 | 8.57226529E16 | |
| (Corrected Total) | 263 | 7.52128899E16 | |

| Parameter | Estimate | Asymptotic Std. Error | Asymptotic 95 % Confidence Interval | |
|---|---|---|---|---|
| | | | Lower | Upper |
| WC | 509.8 | 20.4468 | 469.51 | 550.04 |
| R | 1.2 | 0.0217 | 1.13 | 1.21 |
| GG | 291722880.0 | 9586524.1229 | 272845859.28 | 310599900.77 |

Asymptotic Correlation Matrix

| Corr | WC | R | GG |
|---|---|---|---|
| WC | 1 | -0.911775958 | -0.83367586 |
| R | -0.911775958 | 1 | 0.9863253172 |
| GG | -0.83367586 | 0.9863253172 | 1 |

**SAS input for original specimen AUG3 determination of parameters for phase angle model proposed by Christensen and Anderson**

```
options nodate pageno=1;
data phase;
input freq delta;
datalines;
0.0000061    88.50
0.0000092    88.40
0.0000123    88.60
0.0000184    88.90
0.0000206    89.80
0.0000246    88.70
0.0000307    89.00
0.0000308    89.40
0.0000368    88.90
0.0000411    89.40
0.0000430    88.80
0.0000491    89.10
0.0000553    89.00
0.0000614    89.20
0.0000617    89.20
0.0000822    89.10
0.0000863    89.30
0.0000921    89.00
0.0001028    89.00
0.0001228    89.40
0.0001233    89.20
0.0001295    89.00
0.0001439    88.80
0.0001645    88.80
0.0001726    89.20
```

| | |
|---|---|
| 0.0001842 | 88.90 |
| 0.0001850 | 88.80 |
| 0.0002056 | 88.80 |
| 0.0002456 | 88.90 |
| 0.0002589 | 88.70 |
| 0.0003070 | 89.00 |
| 0.0003083 | 88.60 |
| 0.0003452 | 88.30 |
| 0.0003683 | 88.60 |
| 0.0004111 | 88.20 |
| 0.0004297 | 88.40 |
| 0.0004315 | 88.00 |
| 0.0004911 | 88.10 |
| 0.0004991 | 87.70 |
| 0.0005179 | 87.70 |
| 0.0005525 | 88.30 |
| 0.0006042 | 87.60 |
| 0.0006139 | 87.90 |
| 0.0006167 | 88.10 |
| 0.0006905 | 87.30 |
| 0.0007486 | 87.10 |
| 0.0007768 | 87.30 |
| 0.0008223 | 87.50 |
| 0.0008631 | 87.10 |
| 0.0009209 | 87.30 |
| 0.0009982 | 86.60 |
| 0.0010278 | 86.90 |
| 0.0012278 | 87.10 |
| 0.0012334 | 86.60 |
| 0.0012946 | 86.50 |
| 0.0014389 | 86.20 |
| 0.0014973 | 86.00 |
| 0.0016445 | 86.40 |
| 0.0017262 | 85.80 |

| | |
|---|---|
| 0.0018417 | 86.30 |
| 0.0018501 | 86.10 |
| 0.0019964 | 85.30 |
| 0.0020556 | 85.90 |
| 0.0024557 | 85.60 |
| 0.0024955 | 84.80 |
| 0.0025893 | 84.80 |
| 0.0029945 | 84.20 |
| 0.0030696 | 85.20 |
| 0.0030835 | 85.00 |
| 0.0034524 | 84.10 |
| 0.0034936 | 83.90 |
| 0.0036835 | 84.80 |
| 0.0039927 | 83.60 |
| 0.0041113 | 84.30 |
| 0.0042974 | 84.50 |
| 0.0043155 | 83.50 |
| 0.0044918 | 83.10 |
| 0.0049113 | 84.20 |
| 0.0049909 | 82.80 |
| 0.0051786 | 82.90 |
| 0.0053719 | 81.00 |
| 0.0055252 | 84.10 |
| 0.0060417 | 82.30 |
| 0.0061392 | 84.00 |
| 0.0061669 | 83.10 |
| 0.0069048 | 82.30 |
| 0.0074864 | 81.40 |
| 0.0077679 | 82.00 |
| 0.0080579 | 79.30 |
| 0.0082226 | 82.30 |
| 0.0086309 | 81.40 |
| 0.0092087 | 82.40 |
| 0.0099818 | 80.40 |

| | |
|---|---|
| 0.0102782 | 81.40 |
| 0.0107439 | 78.20 |
| 0.0122783 | 81.80 |
| 0.0123338 | 80.70 |
| 0.0129464 | 79.90 |
| 0.0143895 | 80.20 |
| 0.0149727 | 78.70 |
| 0.0161158 | 77.00 |
| 0.0164451 | 80.00 |
| 0.0172619 | 79.00 |
| 0.0184175 | 80.20 |
| 0.0185007 | 79.30 |
| 0.0199636 | 77.80 |
| 0.0205564 | 78.90 |
| 0.0214877 | 75.70 |
| 0.0249546 | 76.40 |
| 0.0258928 | 77.40 |
| 0.0268596 | 74.90 |
| 0.0299455 | 75.80 |
| 0.0308346 | 77.40 |
| 0.0322316 | 74.60 |
| 0.0345238 | 75.90 |
| 0.0349364 | 75.30 |
| 0.0376035 | 73.80 |
| 0.0399273 | 74.80 |
| 0.0411128 | 76.60 |
| 0.0429754 | 73.80 |
| 0.0431547 | 75.00 |
| 0.0449182 | 74.20 |
| 0.0483474 | 73.10 |
| 0.0499091 | 73.40 |
| 0.0517857 | 74.20 |
| 0.0537193 | 72.70 |
| 0.0604166 | 73.70 |

| | |
|---|---|
| 0.0616691 | 75.10 |
| 0.0628319 | 70.90 |
| 0.0690476 | 73.30 |
| 0.0748637 | 72.10 |
| 0.0776785 | 72.90 |
| 0.0805789 | 72.00 |
| 0.0863095 | 72.40 |
| 0.0942478 | 70.50 |
| 0.0998182 | 70.90 |
| 0.1074386 | 71.40 |
| 0.1256637 | 70.70 |
| 0.1294642 | 71.10 |
| 0.1497273 | 70.00 |
| 0.1611578 | 70.70 |
| 0.1726190 | 70.40 |
| 0.1884956 | 69.60 |
| 0.1996365 | 69.30 |
| 0.2148771 | 70.40 |
| 0.2495456 | 68.70 |
| 0.2513274 | 68.90 |
| 0.2589284 | 69.60 |
| 0.2685964 | 70.40 |
| 0.2994547 | 68.00 |
| 0.3141593 | 70.00 |
| 0.3223157 | 69.80 |
| 0.3493638 | 67.90 |
| 0.3760350 | 69.80 |
| 0.3769911 | 68.90 |
| 0.3992729 | 67.60 |
| 0.4297543 | 69.10 |
| 0.4398230 | 68.90 |
| 0.4491820 | 67.10 |
| 0.4834735 | 69.40 |
| 0.4990911 | 67.00 |

| | |
|---|---|
| 0.5026548 | 68.70 |
| 0.5371928 | 69.40 |
| 0.5654867 | 68.40 |
| 0.6283185 | 68.70 |
| 0.7486367 | 65.70 |
| 0.8057892 | 69.30 |
| 0.9424778 | 68.10 |
| 0.9981823 | 64.90 |
| 1.0743857 | 69.00 |
| 1.2244388 | 67.60 |
| 1.2566371 | 67.80 |
| 1.4972734 | 64.60 |
| 1.6115785 | 68.40 |
| 1.8366582 | 66.90 |
| 1.8849556 | 67.10 |
| 2.1487713 | 68.30 |
| 2.4488776 | 65.50 |
| 2.5132741 | 66.70 |
| 2.6859641 | 67.90 |
| 3.1415927 | 66.50 |
| 3.2231570 | 67.80 |
| 3.6733163 | 66.10 |
| 3.7603498 | 67.30 |
| 3.7699112 | 65.90 |
| 4.2975426 | 67.30 |
| 4.3982297 | 65.60 |
| 4.8347355 | 67.10 |
| 4.8977551 | 64.80 |
| 5.0265482 | 65.70 |
| 5.3719283 | 67.00 |
| 5.6548668 | 65.00 |
| 6.1221939 | 64.30 |
| 6.2831853 | 64.90 |
| 7.3466327 | 64.10 |

| | | |
|---|---|---|
| 8.0578924 | 65.90 | |
| 8.5710715 | 62.90 | |
| 9.4247780 | 63.90 | |
| 9.7955103 | 62.70 | |
| 11.0199490 | 61.90 | |
| 12.2443878 | 62.20 | |
| 12.5663706 | 62.90 | |
| 18.3665817 | 60.70 | |
| 18.8495559 | 61.70 | |
| 24.4887757 | 59.40 | |
| 25.1327412 | 60.80 | |
| 30.1994984 | 57.60 | |
| 31.4159265 | 60.20 | |
| 36.7331635 | 58.10 | |
| 37.6991118 | 59.70 | |
| 43.9822972 | 59.20 | |
| 45.2992477 | 56.40 | |
| 48.9775513 | 57.50 | |
| 50.2654825 | 58.50 | |
| 56.5486678 | 58.10 | |
| 60.3989969 | 54.90 | |
| 61.2219392 | 56.00 | |
| 62.8318531 | 57.60 | |
| 73.4663270 | 55.40 | |
| 85.7107148 | 54.90 | |
| 90.5984953 | 51.90 | |
| 94.2477796 | 55.60 | |
| 97.9551027 | 54.30 | |
| 110.1994905 | | 53.20 |
| 120.7979938 | | 51.90 |
| 122.4438783 | | 53.70 |
| 150.9974922 | | 50.80 |
| 181.1969906 | | 50.50 |
| 183.6658175 | | 51.30 |

| | |
|---|---|
| 211.3964891 | 48.70 |
| 241.5959875 | 47.70 |
| 244.8877567 | 49.10 |
| 271.7954860 | 46.60 |
| 301.9949844 | 47.10 |
| 367.3316350 | 47.60 |
| 452.9924766 | 42.50 |
| 489.7755133 | 45.90 |
| 603.9899688 | 43.00 |
| 612.2193916 | 44.80 |
| 734.6632700 | 43.90 |
| 857.1071483 | 42.60 |
| 905.9849532 | 41.10 |
| 979.5510266 | 42.70 |
| 1101.9949049 | 41.50 |
| 1207.9799376 | 38.30 |
| 1224.4387833 | 41.30 |
| 1509.9749220 | 39.50 |
| 1811.9699064 | 35.20 |
| 1836.6581749 | 39.60 |
| 2113.9648908 | 36.60 |
| 2415.9598752 | 38.40 |
| 2717.9548595 | 35.20 |
| 3019.9498439 | 35.30 |
| 4529.9247659 | 32.30 |
| 6039.8996879 | 30.30 |
| 9059.8495318 | 28.30 |
| 12079.7993758 | 28.20 |
| 15099.7492197 | 27.40 |
| 18119.6990636 | 24.10 |
| 21139.6489076 | 23.50 |
| 24159.5987515 | 21.70 |
| 27179.5485954 | 22.60 |
| 30199.4984394 | 23.50 |

```
45299.2476591          20.30
;
run;

proc nlin data=phase method=marquardt;
parms wc=447 R=1.72;
model delta=(90)/(1+(freq/wc)**(log10(2)/R));

run;
```

**SAS output for original specimen AUG3 determination of parameters for phase angle model proposed by Christensen and Anderson**

Non-Linear Least Squares Iterative Phase

Dependent Variable DELTA Method: Marquardt

| Iter | WC | R | Sum of Squares |
|---|---|---|---|
| 0 | 447.000000 | 1.720000 | 3526.967329 |
| 1 | 382.628256 | 1.443891 | 2126.564263 |
| 2 | 401.171525 | 1.473797 | 2109.937064 |
| 3 | 399.901097 | 1.472097 | 2109.887228 |
| 4 | 400.021229 | 1.472216 | 2109.886982 |
| 5 | 400.012926 | 1.472207 | 2109.886981 |

NOTE: Convergence criterion met.

Non-Linear Least Squares Summary Statistics Dependent Variable DELTA

| Source | DF | Sum of Squares | Mean Square |
|---|---|---|---|
| Regression | 2 | 1379472.3730 | 689736.1865 |
| Residual | 262 | 2109.8870 | 8.0530 |
| Uncorrected Total | 264 | 1381582.2600 | |
| (Corrected Total) | 263 | 74704.3617 | |

| Parameter | Estimate | Asymptotic Std. Error | Asymptotic 95 % Confidence Interval | |
|---|---|---|---|---|
| | | | Lower | Upper |
| WC | 400.0129256 | 30.258317160 | 340.43171252 | 459.59413867 |
| R | 1.4722074 | 0.020973600 | 1.43090862 | 1.51350625 |

Asymptotic Correlation Matrix

| Corr | WC | R |
|---|---|---|
| WC | 1 | 0.6064335177 |
| R | 0.6064335177 | 1 |

# APPENDIX I

- This appendix includes the SAS input and output for original specimen AUG3 used in the non-linear regression of parameters for the storage and loss shear moduli equations proposed in the Gahvari model.

**SAS input for original specimen AUG3 determination of parameters for storage shear modulus model proposed by Gahvari**

```
options nodate pageno=1;
data;
input x y;
datalines;
30.1994984      2.00E+06
45.2992477      2.77E+06
60.3989969      3.42E+06
90.5984953      4.69E+06
120.7979938     5.52E+06
150.9974922     6.60E+06
181.1969906     7.55E+06
211.3964891     8.41E+06
241.5959875     9.05E+06
271.7954860     1.01E+07
301.9949844     1.06E+07
452.9924766     1.41E+07
603.9899688     1.61E+07
905.9849532     2.02E+07
1207.9799376    2.31E+07
1509.9749220    2.58E+07
1811.9699064    2.88E+07
2113.9648908    3.08E+07
2415.9598752    3.18E+07
2717.9548595    3.44E+07
3019.9498439    3.61E+07
4529.9247659    4.29E+07
6039.8996879    4.92E+07
9059.8495318    5.66E+07
12079.7993758   6.02E+07
15099.7492197   6.41E+07
18119.6990636   7.35E+07
```

21139.6489076 7.57E+07
24159.5987515 7.78E+07
27179.5485954 8.19E+07
30199.4984394 8.14E+07
45299.2476591 9.58E+07
1.2244388 1.35E+05
1.8366582 1.91E+05
2.4488776 2.52E+05
3.6733163 3.24E+05
4.8977551 4.27E+05
6.1221939 5.05E+05
7.3466327 5.89E+05
8.5710715 6.82E+05
9.7955103 7.52E+05
11.0199490 8.52E+05
12.2443878 8.96E+05
18.3665817 1.24E+06
24.4887757 1.56E+06
36.7331635 2.14E+06
48.9775513 2.60E+06
61.2219392 3.13E+06
73.4663270 3.56E+06
85.7107148 3.97E+06
97.9551027 4.37E+06
110.1994905 4.91E+06
122.4438783 5.05E+06
183.6658175 6.78E+06
244.8877567 8.39E+06
367.3316350 1.07E+07
489.7755133 1.29E+07
612.2193916 1.46E+07
734.6632700 1.63E+07
857.1071483 1.79E+07
979.5510266 1.89E+07

| | |
|---|---|
| 1101.9949049 | 2.05E+07 |
| 1224.4387833 | 2.17E+07 |
| 1836.6581749 | 2.68E+07 |
| 0.0628319 | 1.30E+04 |
| 0.0942478 | 1.84E+04 |
| 0.1256637 | 2.32E+04 |
| 0.1884956 | 3.30E+04 |
| 0.2513274 | 4.19E+04 |
| 0.3141593 | 4.80E+04 |
| 0.3769911 | 5.78E+04 |
| 0.4398230 | 6.50E+04 |
| 0.5026548 | 7.30E+04 |
| 0.5654867 | 8.15E+04 |
| 0.6283185 | 8.74E+04 |
| 0.9424778 | 1.22E+05 |
| 1.2566371 | 1.53E+05 |
| 1.8849556 | 2.13E+05 |
| 2.5132741 | 2.69E+05 |
| 3.1415927 | 3.15E+05 |
| 3.7699112 | 3.70E+05 |
| 4.3982297 | 4.18E+05 |
| 5.0265482 | 4.61E+05 |
| 5.6548668 | 5.13E+05 |
| 6.2831853 | 5.54E+05 |
| 9.4247780 | 7.67E+05 |
| 12.5663706 | 9.68E+05 |
| 18.8495559 | 1.33E+06 |
| 25.1327412 | 1.66E+06 |
| 31.4159265 | 1.96E+06 |
| 37.6991118 | 2.24E+06 |
| 43.9822972 | 2.50E+06 |
| 50.2654825 | 2.79E+06 |
| 56.5486678 | 3.07E+06 |
| 62.8318531 | 3.31E+06 |

| | |
|---|---|
| 94.2477796 | 4.50E+06 |
| 0.0053719 | 8.21E+02 |
| 0.0080579 | 1.41E+03 |
| 0.0107439 | 2.01E+03 |
| 0.0161158 | 3.17E+03 |
| 0.0214877 | 4.43E+03 |
| 0.0268596 | 5.61E+03 |
| 0.0322316 | 6.70E+03 |
| 0.0376035 | 7.95E+03 |
| 0.0429754 | 8.79E+03 |
| 0.0483474 | 1.01E+04 |
| 0.0537193 | 1.12E+04 |
| 0.0805789 | 1.62E+04 |
| 0.1074386 | 2.07E+04 |
| 0.1611578 | 2.91E+04 |
| 0.2148771 | 3.68E+04 |
| 0.2685964 | 4.42E+04 |
| 0.3223157 | 5.20E+04 |
| 0.3760350 | 5.81E+04 |
| 0.4297543 | 6.65E+04 |
| 0.4834735 | 7.22E+04 |
| 0.5371928 | 7.84E+04 |
| 0.8057892 | 1.07E+05 |
| 1.0743857 | 1.34E+05 |
| 1.6115785 | 1.87E+05 |
| 2.1487713 | 2.34E+05 |
| 2.6859641 | 2.81E+05 |
| 3.2231570 | 3.24E+05 |
| 3.7603498 | 3.69E+05 |
| 4.2975426 | 4.08E+05 |
| 4.8347355 | 4.51E+05 |
| 5.3719283 | 4.84E+05 |
| 8.0578924 | 6.75E+05 |
| 0.0004991 | 2.05E+01 |

| | |
|---|---|
| 0.0007486 | 3.88E+01 |
| 0.0009982 | 6.10E+01 |
| 0.0014973 | 1.05E+02 |
| 0.0019964 | 1.61E+02 |
| 0.0024955 | 2.22E+02 |
| 0.0029945 | 2.93E+02 |
| 0.0034936 | 3.57E+02 |
| 0.0039927 | 4.22E+02 |
| 0.0044918 | 5.07E+02 |
| 0.0049909 | 5.77E+02 |
| 0.0074864 | 1.00E+03 |
| 0.0099818 | 1.44E+03 |
| 0.0149727 | 2.42E+03 |
| 0.0199636 | 3.38E+03 |
| 0.0249546 | 4.56E+03 |
| 0.0299455 | 5.51E+03 |
| 0.0349364 | 6.44E+03 |
| 0.0399273 | 7.51E+03 |
| 0.0449182 | 8.59E+03 |
| 0.0499091 | 9.73E+03 |
| 0.0748637 | 1.45E+04 |
| 0.0998182 | 1.92E+04 |
| 0.1497273 | 2.77E+04 |
| 0.1996365 | 3.57E+04 |
| 0.2495456 | 4.37E+04 |
| 0.2994547 | 5.15E+04 |
| 0.3493638 | 5.81E+04 |
| 0.3992729 | 6.50E+04 |
| 0.4491820 | 7.33E+04 |
| 0.4990911 | 7.87E+04 |
| 0.7486367 | 1.13E+05 |
| 0.9981823 | 1.43E+05 |
| 1.4972734 | 1.97E+05 |
| 0.0000863 | 1.17E+00 |

| | |
|---|---|
| 0.0001295 | 2.42E+00 |
| 0.0001726 | 2.76E+00 |
| 0.0002589 | 6.32E+00 |
| 0.0003452 | 1.09E+01 |
| 0.0004315 | 1.58E+01 |
| 0.0005179 | 2.23E+01 |
| 0.0006042 | 2.71E+01 |
| 0.0006905 | 3.45E+01 |
| 0.0007768 | 3.83E+01 |
| 0.0008631 | 4.47E+01 |
| 0.0012946 | 8.12E+01 |
| 0.0017262 | 1.29E+02 |
| 0.0025893 | 2.34E+02 |
| 0.0034524 | 3.47E+02 |
| 0.0043155 | 4.72E+02 |
| 0.0051786 | 6.07E+02 |
| 0.0060417 | 7.59E+02 |
| 0.0069048 | 8.58E+02 |
| 0.0077679 | 9.87E+02 |
| 0.0086309 | 1.16E+03 |
| 0.0129464 | 1.97E+03 |
| 0.0172619 | 2.76E+03 |
| 0.0258928 | 4.47E+03 |
| 0.0345238 | 6.36E+03 |
| 0.0431547 | 8.18E+03 |
| 0.0517857 | 9.95E+03 |
| 0.0604166 | 1.16E+04 |
| 0.0690476 | 1.34E+04 |
| 0.0776785 | 1.51E+04 |
| 0.0863095 | 1.67E+04 |
| 0.1294642 | 2.47E+04 |
| 0.1726190 | 3.21E+04 |
| 0.2589284 | 4.55E+04 |
| 0.0000206 | 7.38E-02 |

| | |
|---|---|
| 0.0000308 | 3.33E-01 |
| 0.0000411 | 4.48E-01 |
| 0.0000617 | 8.64E-01 |
| 0.0000822 | 1.25E+00 |
| 0.0001028 | 1.77E+00 |
| 0.0001233 | 1.65E+00 |
| 0.0001439 | 2.92E+00 |
| 0.0001645 | 3.34E+00 |
| 0.0001850 | 3.90E+00 |
| 0.0002056 | 4.19E+00 |
| 0.0003083 | 7.61E+00 |
| 0.0004111 | 1.32E+01 |
| 0.0006167 | 2.00E+01 |
| 0.0008223 | 3.55E+01 |
| 0.0010278 | 5.41E+01 |
| 0.0012334 | 7.23E+01 |
| 0.0014389 | 9.14E+01 |
| 0.0016445 | 1.01E+02 |
| 0.0018501 | 1.22E+02 |
| 0.0020556 | 1.43E+02 |
| 0.0030835 | 2.56E+02 |
| 0.0041113 | 3.78E+02 |
| 0.0061669 | 6.70E+02 |
| 0.0082226 | 9.78E+02 |
| 0.0102782 | 1.34E+03 |
| 0.0123338 | 1.70E+03 |
| 0.0143895 | 2.06E+03 |
| 0.0164451 | 2.37E+03 |
| 0.0185007 | 2.82E+03 |
| 0.0205564 | 3.17E+03 |
| 0.0308346 | 5.14E+03 |
| 0.0411128 | 6.94E+03 |
| 0.0616691 | 1.07E+04 |
| 0.0000614 | 8.54E-01 |

```
0.0000921	1.49E+00
0.0001228	1.29E+00
0.0001842	3.55E+00
0.0002456	4.66E+00
0.0003070	5.12E+00
0.0003683	8.44E+00
0.0004297	1.15E+01
0.0004911	1.52E+01
0.0005525	1.59E+01
0.0006139	2.16E+01
0.0009209	4.08E+01
0.0012278	5.87E+01
0.0018417	1.12E+02
0.0024557	1.72E+02
0.0030696	2.34E+02
0.0036835	2.99E+02
0.0042974	3.69E+02
0.0049113	4.37E+02
0.0055252	5.06E+02
0.0061392	5.68E+02
0.0092087	1.04E+03
0.0122783	1.46E+03
0.0184175	2.49E+03
;
run;

proc nlin method=dud;
parms p=0.2 l=3 loggg=10;
x1=log10(x);
y1=log10(y);
model y1=loggg*(1-exp(-p*(x1+l)));
run;
```

**SAS output for original specimen AUG3 determination of parameters for storage shear modulus model proposed by Gahvari**

Non-Linear Least Squares DUD Initialization Dependent Variable Y1

| DUD | P | L | LOGGG | Sum of Squares |
|---|---|---|---|---|
| -4 | 0.200000 | 3.000000 | 10.000000 | 372.225956 |
| -3 | 0.220000 | 3.000000 | 10.000000 | 347.350316 |
| -2 | 0.200000 | 3.300000 | 10.000000 | 159.975043 |
| -1 | 0.200000 | 3.000000 | 11.000000 | 345.682063 |

Non-Linear Least Squares Iterative Phase Dependent Variable Y1 Method:DUD

| Iter | P | L | LOGGG | Sum of Squares |
|---|---|---|---|---|
| 0 | 0.200000 | 3.300000 | 10.000000 | 159.975043 |
| 1 | 0.176192 | 3.901714 | 10.191711 | 9.874392 |
| 2 | 0.168454 | 4.086803 | 10.373486 | 1.529849 |
| 3 | 0.168070 | 4.102284 | 10.394371 | 1.469341 |
| 4 | 0.168483 | 4.098090 | 10.380703 | 1.467849 |
| 5 | 0.167433 | 4.100805 | 10.419671 | 1.466114 |
| 6 | 0.167463 | 4.100229 | 10.418530 | 1.466028 |
| 7 | 0.167462 | 4.100234 | 10.418545 | 1.466028 |
| 8 | 0.167461 | 4.100247 | 10.418547 | 1.466028 |
| 9 | 0.167457 | 4.100253 | 10.418708 | 1.466028 |
| 10 | 0.167457 | 4.100252 | 10.418710 | 1.466028 |

NOTE: Convergence criterion met.

Non-Linear Least Squares Summary Statistics Dependent Variable Y1

| Source | DF | Sum of Squares | Mean Square |
|---|---|---|---|
| Regression | 3 | 5768.4925192 | 1922.8308397 |
| Residual | 251 | 1.4660278 | 0.0058407 |
| Uncorrected Total | 254 | 5769.9585471 | |
| (Corrected Total) | 253 | 1230.0230832 | |

| Parameter | Estimate | Asymptotic Std. Error | Asymptotic 95 % Confidence Interval | |
|---|---|---|---|---|
| | | | Lower | Upper |
| P | 0.16745681 | 0.00197935155 | 0.163558501 | 0.171355110 |
| L | 4.10025243 | 0.00818964811 | 4.084123037 | 4.116381825 |
| LOGGG | 10.41870964 | 0.06938617139 | 10.282054579 | 10.555364707 |

Asymptotic Correlation Matrix

| Corr | P | L | LOGGG |
|---|---|---|---|
| P | 1 | -0.686406049 | -0.978455216 |
| L | -0.686406049 | 1 | 0.569293201 |
| LOGGG | -0.978455216 | 0.5692932005 | 1 |

**SAS input for original specimen AUG3 determination of parameters for loss shear modulus model proposed by Gahvari**

```
options nodate pageno=1;
data loss;
input x y;
datalines;
30.1994984      3.16E+06
45.2992477      4.17E+06
60.3989969      4.86E+06
90.5984953      5.98E+06
120.7979938     7.04E+06
150.9974922     8.09E+06
181.1969906     9.15E+06
211.3964891     9.58E+06
241.5959875     9.94E+06
271.7954860     1.07E+07
301.9949844     1.14E+07
452.9924766     1.29E+07
603.9899688     1.51E+07
905.9849532     1.76E+07
1207.9799376    1.82E+07
1509.9749220    2.13E+07
1811.9699064    2.03E+07
2113.9648908    2.29E+07
2415.9598752    2.52E+07
2717.9548595    2.43E+07
3019.9498439    2.56E+07
4529.9247659    2.71E+07
6039.8996879    2.88E+07
9059.8495318    3.05E+07
12079.7993758   3.23E+07
15099.7492197   3.32E+07
```

| | |
|---|---|
| 18119.6990636 | 3.28E+07 |
| 21139.6489076 | 3.29E+07 |
| 24159.5987515 | 3.10E+07 |
| 27179.5485954 | 3.41E+07 |
| 30199.4984394 | 3.55E+07 |
| 45299.2476591 | 3.55E+07 |
| 1.2244388 | 3.28E+05 |
| 1.8366582 | 4.49E+05 |
| 2.4488776 | 5.53E+05 |
| 3.6733163 | 7.32E+05 |
| 4.8977551 | 9.09E+05 |
| 6.1221939 | 1.05E+06 |
| 7.3466327 | 1.21E+06 |
| 8.5710715 | 1.33E+06 |
| 9.7955103 | 1.46E+06 |
| 11.0199490 | 1.60E+06 |
| 12.2443878 | 1.70E+06 |
| 18.3665817 | 2.21E+06 |
| 24.4887757 | 2.64E+06 |
| 36.7331635 | 3.43E+06 |
| 48.9775513 | 4.09E+06 |
| 61.2219392 | 4.65E+06 |
| 73.4663270 | 5.17E+06 |
| 85.7107148 | 5.64E+06 |
| 97.9551027 | 6.07E+06 |
| 110.1994905 | 6.57E+06 |
| 122.4438783 | 6.88E+06 |
| 183.6658175 | 8.45E+06 |
| 244.8877567 | 9.69E+06 |
| 367.3316350 | 1.17E+07 |
| 489.7755133 | 1.33E+07 |
| 612.2193916 | 1.45E+07 |
| 734.6632700 | 1.57E+07 |
| 857.1071483 | 1.64E+07 |

| | |
|---|---|
| 979.5510266 | 1.74E+07 |
| 1101.9949049 | 1.81E+07 |
| 1224.4387833 | 1.91E+07 |
| 1836.6581749 | 2.21E+07 |
| 0.0628319 | 3.75E+04 |
| 0.0942478 | 5.18E+04 |
| 0.1256637 | 6.65E+04 |
| 0.1884956 | 8.85E+04 |
| 0.2513274 | 1.08E+05 |
| 0.3141593 | 1.32E+05 |
| 0.3769911 | 1.49E+05 |
| 0.4398230 | 1.68E+05 |
| 0.5026548 | 1.87E+05 |
| 0.5654867 | 2.06E+05 |
| 0.6283185 | 2.24E+05 |
| 0.9424778 | 3.03E+05 |
| 1.2566371 | 3.74E+05 |
| 1.8849556 | 5.05E+05 |
| 2.5132741 | 6.23E+05 |
| 3.1415927 | 7.25E+05 |
| 3.7699112 | 8.27E+05 |
| 4.3982297 | 9.23E+05 |
| 5.0265482 | 1.02E+06 |
| 5.6548668 | 1.10E+06 |
| 6.2831853 | 1.18E+06 |
| 9.4247780 | 1.57E+06 |
| 12.5663706 | 1.89E+06 |
| 18.8495559 | 2.47E+06 |
| 25.1327412 | 2.97E+06 |
| 31.4159265 | 3.42E+06 |
| 37.6991118 | 3.83E+06 |
| 43.9822972 | 4.19E+06 |
| 50.2654825 | 4.56E+06 |
| 56.5486678 | 4.92E+06 |

| | |
|---|---|
| 62.8318531 | 5.22E+06 |
| 94.2477796 | 6.58E+06 |
| 0.0053719 | 5.19E+03 |
| 0.0080579 | 7.47E+03 |
| 0.0107439 | 9.67E+03 |
| 0.0161158 | 1.37E+04 |
| 0.0214877 | 1.74E+04 |
| 0.0268596 | 2.09E+04 |
| 0.0322316 | 2.43E+04 |
| 0.0376035 | 2.74E+04 |
| 0.0429754 | 3.03E+04 |
| 0.0483474 | 3.33E+04 |
| 0.0537193 | 3.60E+04 |
| 0.0805789 | 4.97E+04 |
| 0.1074386 | 6.13E+04 |
| 0.1611578 | 8.33E+04 |
| 0.2148771 | 1.04E+05 |
| 0.2685964 | 1.24E+05 |
| 0.3223157 | 1.41E+05 |
| 0.3760350 | 1.58E+05 |
| 0.4297543 | 1.74E+05 |
| 0.4834735 | 1.92E+05 |
| 0.5371928 | 2.09E+05 |
| 0.8057892 | 2.82E+05 |
| 1.0743857 | 3.50E+05 |
| 1.6115785 | 4.74E+05 |
| 2.1487713 | 5.89E+05 |
| 2.6859641 | 6.94E+05 |
| 3.2231570 | 7.93E+05 |
| 3.7603498 | 8.81E+05 |
| 4.2975426 | 9.75E+05 |
| 4.8347355 | 1.07E+06 |
| 5.3719283 | 1.14E+06 |
| 8.0578924 | 1.51E+06 |

| | |
|---|---|
| 0.0004991 | 5.21E+02 |
| 0.0007486 | 7.68E+02 |
| 0.0009982 | 1.02E+03 |
| 0.0014973 | 1.49E+03 |
| 0.0019964 | 1.96E+03 |
| 0.0024955 | 2.43E+03 |
| 0.0029945 | 2.90E+03 |
| 0.0034936 | 3.32E+03 |
| 0.0039927 | 3.76E+03 |
| 0.0044918 | 4.17E+03 |
| 0.0049909 | 4.59E+03 |
| 0.0074864 | 6.61E+03 |
| 0.0099818 | 8.54E+03 |
| 0.0149727 | 1.22E+04 |
| 0.0199636 | 1.56E+04 |
| 0.0249546 | 1.88E+04 |
| 0.0299455 | 2.18E+04 |
| 0.0349364 | 2.46E+04 |
| 0.0399273 | 2.77E+04 |
| 0.0449182 | 3.03E+04 |
| 0.0499091 | 3.27E+04 |
| 0.0748637 | 4.50E+04 |
| 0.0998182 | 5.57E+04 |
| 0.1497273 | 7.60E+04 |
| 0.1996365 | 9.44E+04 |
| 0.2495456 | 1.12E+05 |
| 0.2994547 | 1.27E+05 |
| 0.3493638 | 1.43E+05 |
| 0.3992729 | 1.57E+05 |
| 0.4491820 | 1.73E+05 |
| 0.4990911 | 1.86E+05 |
| 0.7486367 | 2.50E+05 |
| 0.9981823 | 3.04E+05 |
| 1.4972734 | 4.14E+05 |

| | |
|---|---|
| 0.0000863 | 9.46E+01 |
| 0.0001295 | 1.40E+02 |
| 0.0001726 | 1.87E+02 |
| 0.0002589 | 2.78E+02 |
| 0.0003452 | 3.71E+02 |
| 0.0004315 | 4.63E+02 |
| 0.0005179 | 5.51E+02 |
| 0.0006042 | 6.41E+02 |
| 0.0006905 | 7.27E+02 |
| 0.0007768 | 8.15E+02 |
| 0.0008631 | 8.97E+02 |
| 0.0012946 | 1.32E+03 |
| 0.0017262 | 1.75E+03 |
| 0.0025893 | 2.56E+03 |
| 0.0034524 | 3.34E+03 |
| 0.0043155 | 4.12E+03 |
| 0.0051786 | 4.86E+03 |
| 0.0060417 | 5.61E+03 |
| 0.0069048 | 6.32E+03 |
| 0.0077679 | 7.03E+03 |
| 0.0086309 | 7.71E+03 |
| 0.0129464 | 1.10E+04 |
| 0.0172619 | 1.42E+04 |
| 0.0258928 | 2.00E+04 |
| 0.0345238 | 2.54E+04 |
| 0.0431547 | 3.05E+04 |
| 0.0517857 | 3.53E+04 |
| 0.0604166 | 3.98E+04 |
| 0.0690476 | 4.46E+04 |
| 0.0776785 | 4.91E+04 |
| 0.0863095 | 5.28E+04 |
| 0.1294642 | 7.24E+04 |
| 0.1726190 | 9.04E+04 |
| 0.2589284 | 1.22E+05 |

| | |
|---|---|
| 0.0000206 | 2.17E+01 |
| 0.0000308 | 3.16E+01 |
| 0.0000411 | 4.24E+01 |
| 0.0000617 | 6.28E+01 |
| 0.0000822 | 8.25E+01 |
| 0.0001028 | 1.02E+02 |
| 0.0001233 | 1.22E+02 |
| 0.0001439 | 1.45E+02 |
| 0.0001645 | 1.65E+02 |
| 0.0001850 | 1.88E+02 |
| 0.0002056 | 2.07E+02 |
| 0.0003083 | 3.09E+02 |
| 0.0004111 | 4.13E+02 |
| 0.0006167 | 6.14E+02 |
| 0.0008223 | 8.11E+02 |
| 0.0010278 | 1.01E+03 |
| 0.0012334 | 1.20E+03 |
| 0.0014389 | 1.39E+03 |
| 0.0016445 | 1.59E+03 |
| 0.0018501 | 1.78E+03 |
| 0.0020556 | 1.97E+03 |
| 0.0030835 | 2.92E+03 |
| 0.0041113 | 3.80E+03 |
| 0.0061669 | 5.52E+03 |
| 0.0082226 | 7.22E+03 |
| 0.0102782 | 8.84E+03 |
| 0.0123338 | 1.04E+04 |
| 0.0143895 | 1.19E+04 |
| 0.0164451 | 1.34E+04 |
| 0.0185007 | 1.49E+04 |
| 0.0205564 | 1.62E+04 |
| 0.0308346 | 2.31E+04 |
| 0.0411128 | 2.91E+04 |
| 0.0616691 | 4.05E+04 |

| | |
|---|---|
| 0.0000061 | 6.29E+00 |
| 0.0000092 | 9.49E+00 |
| 0.0000123 | 1.27E+01 |
| 0.0000184 | 1.84E+01 |
| 0.0000246 | 2.41E+01 |
| 0.0000307 | 3.04E+01 |
| 0.0000368 | 3.69E+01 |
| 0.0000430 | 4.31E+01 |
| 0.0000491 | 4.92E+01 |
| 0.0000553 | 5.46E+01 |
| 0.0000614 | 6.06E+01 |
| 0.0000921 | 8.93E+01 |
| 0.0001228 | 1.20E+02 |
| 0.0001842 | 1.77E+02 |
| 0.0002456 | 2.34E+02 |
| 0.0003070 | 2.93E+02 |
| 0.0003683 | 3.50E+02 |
| 0.0004297 | 4.12E+02 |
| 0.0004911 | 4.66E+02 |
| 0.0005525 | 5.20E+02 |
| 0.0006139 | 5.78E+02 |
| 0.0009209 | 8.74E+02 |
| 0.0012278 | 1.16E+03 |
| 0.0018417 | 1.72E+03 |
| 0.0024557 | 2.27E+03 |
| 0.0030696 | 2.79E+03 |
| 0.0036835 | 3.30E+03 |
| 0.0042974 | 3.80E+03 |
| 0.0049113 | 4.31E+03 |
| 0.0055252 | 4.87E+03 |
| 0.0061392 | 5.37E+03 |
| 0.0092087 | 7.82E+03 |
| 0.0122783 | 1.01E+04 |
| 0.0184175 | 1.44E+04 |

```
;
run;

proc nlin data=loss method=dud;
parms d=4 logomd=4 loggmax=7.5;
x1=log10(x);
y1=log10(y);
model y1=loggmax+d-sqrt((x1-logomd)**2+d**2);
run;
```

**SAS output for original specimen AUG3 determination of parameters for loss shear modulus model proposed by Gahvari**

Non-Linear Least Squares DUD Initialization Dependent Variable Y1

| DUD | D | LOGOMD | LOGGMAX | Sum of Squares |
|---|---|---|---|---|
| -4 | 4.000000 | 4.000000 | 7.500000 | 35.098918 |
| -3 | 4.400000 | 4.000000 | 7.500000 | 68.022783 |
| -2 | 4.000000 | 4.400000 | 7.500000 | 2.023036 |
| -1 | 4.000000 | 4.000000 | 8.250000 | 317.329402 |

Non-Linear Least Squares Iterative Phase Dependent Variable Y1 Method:DUD

| Iter | D | LOGOMD | LOGGMAX | Sum of Squares |
|---|---|---|---|---|
| 0 | 4.000000 | 4.400000 | 7.500000 | 2.023036 |
| 1 | 3.622526 | 4.282028 | 7.480812 | 0.814900 |
| 2 | 3.596040 | 4.253138 | 7.472081 | 0.792431 |
| 3 | 3.605163 | 4.251263 | 7.483135 | 0.732663 |
| 4 | 3.614687 | 4.255002 | 7.481206 | 0.731770 |
| 5 | 3.620420 | 4.257742 | 7.480834 | 0.731699 |
| 6 | 3.619284 | 4.256658 | 7.480472 | 0.731698 |
| 7 | 3.619415 | 4.256928 | 7.480595 | 0.731698 |
| 8 | 3.619474 | 4.256940 | 7.480604 | 0.731698 |
| 9 | 3.619413 | 4.256915 | 7.480616 | 0.731698 |
| 10 | 3.619451 | 4.256940 | 7.480619 | 0.731698 |

NOTE: Convergence criterion met.

Non-Linear Least Squares Summary Statistics Dependent Variable Y1

| Source | DF | Sum of Squares | Mean Square |
|---|---|---|---|
| Regression | 3 | 6711.4909090 | 2237.1636363 |
| Residual | 261 | 0.7316976 | 0.0028034 |
| Uncorrected Total | 264 | 6712.2226066 | |
| (Corrected Total) | 263 | 808.4902623 | |

| Parameter | Estimate | Asymptotic Std. Error | Asymptotic 95 % Confidence Interval | |
|---|---|---|---|---|
| | | | Lower | Upper |
| D | 3.619450794 | 0.05139891025 | 3.5182401487 | 3.7206614398 |
| LOGOMD | 4.256939701 | 0.04157024828 | 4.1750828751 | 4.3387965275 |
| LOGGMAX | 7.480618546 | 0.01409987052 | 7.4528542029 | 7.5083828898 |

Asymptotic Correlation Matrix

| Corr | D | LOGOMD | LOGGMAX |
|---|---|---|---|
| D | 1 | 0.9383492058 | 0.6253538365 |
| LOGOMD | 0.9383492058 | 1 | 0.8444529198 |
| LOGGMAX | 0.6253538365 | 0.8444529198 | 1 |

# APPENDIX J

- This appendix includes the SAS input and output for original specimen AUG3 used in the non-linear regression of parameters for the shear complex moduli and phase angle equations proposed in the Marasteanu-Anderson model.

**SAS input for original specimen AUG3 determination of parameters for shear complex modulus model proposed by Marasteanu and Anderson**

```
options nodate pageno=1;
data mod;
input freq Gstar;
cards;
0.0000061     6.29E+00
0.0000092     9.49E+00
0.0000123     1.27E+01
0.0000184     1.84E+01
0.0000206     2.17E+01
0.0000246     2.41E+01
0.0000307     3.04E+01
0.0000308     3.16E+01
0.0000368     3.69E+01
0.0000411     4.24E+01
0.0000430     4.31E+01
0.0000491     4.92E+01
0.0000553     5.46E+01
0.0000614     6.06E+01
0.0000617     6.28E+01
0.0000822     8.26E+01
0.0000863     9.46E+01
0.0000921     8.93E+01
0.0001028     1.02E+02
0.0001228     1.20E+02
0.0001233     1.22E+02
0.0001295     1.40E+02
0.0001439     1.45E+02
0.0001645     1.65E+02
```

| | |
|---|---|
| 0.0001726 | 1.87E+02 |
| 0.0001842 | 1.77E+02 |
| 0.0001850 | 1.88E+02 |
| 0.0002056 | 2.07E+02 |
| 0.0002456 | 2.34E+02 |
| 0.0002589 | 2.78E+02 |
| 0.0003070 | 2.94E+02 |
| 0.0003083 | 3.09E+02 |
| 0.0003452 | 3.71E+02 |
| 0.0003683 | 3.50E+02 |
| 0.0004111 | 4.13E+02 |
| 0.0004297 | 4.12E+02 |
| 0.0004315 | 4.63E+02 |
| 0.0004911 | 4.66E+02 |
| 0.0004991 | 5.21E+02 |
| 0.0005179 | 5.52E+02 |
| 0.0005525 | 5.21E+02 |
| 0.0006042 | 6.42E+02 |
| 0.0006139 | 5.79E+02 |
| 0.0006167 | 6.14E+02 |
| 0.0006905 | 7.28E+02 |
| 0.0007486 | 7.68E+02 |
| 0.0007768 | 8.16E+02 |
| 0.0008223 | 8.12E+02 |
| 0.0008631 | 8.98E+02 |
| 0.0009209 | 8.75E+02 |
| 0.0009982 | 1.02E+03 |
| 0.0010278 | 1.01E+03 |
| 0.0012278 | 1.16E+03 |
| 0.0012334 | 1.20E+03 |
| 0.0012946 | 1.32E+03 |
| 0.0014389 | 1.40E+03 |
| 0.0014973 | 1.50E+03 |
| 0.0016445 | 1.59E+03 |

| | |
|---|---|
| 0.0017262 | 1.75E+03 |
| 0.0018417 | 1.72E+03 |
| 0.0018501 | 1.78E+03 |
| 0.0019964 | 1.97E+03 |
| 0.0020556 | 1.98E+03 |
| 0.0024557 | 2.27E+03 |
| 0.0024955 | 2.44E+03 |
| 0.0025893 | 2.57E+03 |
| 0.0029945 | 2.91E+03 |
| 0.0030696 | 2.80E+03 |
| 0.0030835 | 2.93E+03 |
| 0.0034524 | 3.36E+03 |
| 0.0034936 | 3.33E+03 |
| 0.0036835 | 3.32E+03 |
| 0.0039927 | 3.78E+03 |
| 0.0041113 | 3.82E+03 |
| 0.0042974 | 3.82E+03 |
| 0.0043155 | 4.15E+03 |
| 0.0044918 | 4.20E+03 |
| 0.0049113 | 4.33E+03 |
| 0.0049909 | 4.63E+03 |
| 0.0051786 | 4.90E+03 |
| 0.0053719 | 5.26E+03 |
| 0.0055252 | 4.90E+03 |
| 0.0060417 | 5.66E+03 |
| 0.0061392 | 5.40E+03 |
| 0.0061669 | 5.56E+03 |
| 0.0069048 | 6.37E+03 |
| 0.0074864 | 6.69E+03 |
| 0.0077679 | 7.10E+03 |
| 0.0080579 | 7.60E+03 |
| 0.0082226 | 7.29E+03 |
| 0.0086309 | 7.79E+03 |
| 0.0092087 | 7.89E+03 |

| | |
|---|---|
| 0.0099818 | 8.66E+03 |
| 0.0102782 | 8.94E+03 |
| 0.0107439 | 9.88E+03 |
| 0.0122783 | 1.02E+04 |
| 0.0123338 | 1.05E+04 |
| 0.0129464 | 1.12E+04 |
| 0.0143895 | 1.21E+04 |
| 0.0149727 | 1.24E+04 |
| 0.0161158 | 1.41E+04 |
| 0.0164451 | 1.36E+04 |
| 0.0172619 | 1.44E+04 |
| 0.0184175 | 1.46E+04 |
| 0.0185007 | 1.51E+04 |
| 0.0199636 | 1.60E+04 |
| 0.0205564 | 1.65E+04 |
| 0.0214877 | 1.80E+04 |
| 0.0249546 | 1.93E+04 |
| 0.0258928 | 2.05E+04 |
| 0.0268596 | 2.16E+04 |
| 0.0299455 | 2.24E+04 |
| 0.0308346 | 2.36E+04 |
| 0.0322316 | 2.52E+04 |
| 0.0345238 | 2.62E+04 |
| 0.0349364 | 2.54E+04 |
| 0.0376035 | 2.85E+04 |
| 0.0399273 | 2.87E+04 |
| 0.0411128 | 2.99E+04 |
| 0.0429754 | 3.16E+04 |
| 0.0431547 | 3.16E+04 |
| 0.0449182 | 3.15E+04 |
| 0.0483474 | 3.48E+04 |
| 0.0499091 | 3.42E+04 |
| 0.0517857 | 3.67E+04 |
| 0.0537193 | 3.77E+04 |

| | |
|---|---|
| 0.0604166 | 4.15E+04 |
| 0.0616691 | 4.19E+04 |
| 0.0628319 | 3.97E+04 |
| 0.0690476 | 4.66E+04 |
| 0.0748637 | 4.72E+04 |
| 0.0776785 | 5.13E+04 |
| 0.0805789 | 5.22E+04 |
| 0.0863095 | 5.54E+04 |
| 0.0942478 | 5.50E+04 |
| 0.0998182 | 5.89E+04 |
| 0.1074386 | 6.47E+04 |
| 0.1256637 | 7.04E+04 |
| 0.1294642 | 7.66E+04 |
| 0.1497273 | 8.09E+04 |
| 0.1611578 | 8.83E+04 |
| 0.1726190 | 9.60E+04 |
| 0.1884956 | 9.44E+04 |
| 0.1996365 | 1.01E+05 |
| 0.2148771 | 1.10E+05 |
| 0.2495456 | 1.20E+05 |
| 0.2513274 | 1.16E+05 |
| 0.2589284 | 1.30E+05 |
| 0.2685964 | 1.32E+05 |
| 0.2994547 | 1.37E+05 |
| 0.3141593 | 1.40E+05 |
| 0.3223157 | 1.51E+05 |
| 0.3493638 | 1.54E+05 |
| 0.3760350 | 1.68E+05 |
| 0.3769911 | 1.60E+05 |
| 0.3992729 | 1.70E+05 |
| 0.4297543 | 1.86E+05 |
| 0.4398230 | 1.80E+05 |
| 0.4491820 | 1.88E+05 |
| 0.4834735 | 2.05E+05 |

| | |
|---|---|
| 0.4990911 | 2.02E+05 |
| 0.5026548 | 2.01E+05 |
| 0.5371928 | 2.23E+05 |
| 0.5654867 | 2.21E+05 |
| 0.6283185 | 2.41E+05 |
| 0.7486367 | 2.74E+05 |
| 0.8057892 | 3.02E+05 |
| 0.9424778 | 3.26E+05 |
| 0.9981823 | 3.36E+05 |
| 1.0743857 | 3.75E+05 |
| 1.2244388 | 3.55E+05 |
| 1.2566371 | 4.04E+05 |
| 1.4972734 | 4.58E+05 |
| 1.6115785 | 5.09E+05 |
| 1.8366582 | 4.88E+05 |
| 1.8849556 | 5.48E+05 |
| 2.1487713 | 6.34E+05 |
| 2.4488776 | 6.08E+05 |
| 2.5132741 | 6.79E+05 |
| 2.6859641 | 7.49E+05 |
| 3.1415927 | 7.91E+05 |
| 3.2231570 | 8.56E+05 |
| 3.6733163 | 8.00E+05 |
| 3.7603498 | 9.55E+05 |
| 3.7699112 | 9.06E+05 |
| 4.2975426 | 1.06E+06 |
| 4.3982297 | 1.01E+06 |
| 4.8347355 | 1.16E+06 |
| 4.8977551 | 1.00E+06 |
| 5.0265482 | 1.12E+06 |
| 5.3719283 | 1.24E+06 |
| 5.6548668 | 1.21E+06 |
| 6.1221939 | 1.17E+06 |
| 6.2831853 | 1.31E+06 |

| | |
|---|---|
| 7.3466327 | 1.35E+06 |
| 8.0578924 | 1.65E+06 |
| 8.5710715 | 1.50E+06 |
| 9.4247780 | 1.74E+06 |
| 9.7955103 | 1.64E+06 |
| 11.0199490 | 1.81E+06 |
| 12.2443878 | 1.92E+06 |
| 12.5663706 | 2.12E+06 |
| 18.3665817 | 2.53E+06 |
| 18.8495559 | 2.80E+06 |
| 24.4887757 | 3.07E+06 |
| 25.1327412 | 3.41E+06 |
| 30.1994984 | 3.74E+06 |
| 31.4159265 | 3.94E+06 |
| 36.7331635 | 4.04E+06 |
| 37.6991118 | 4.43E+06 |
| 43.9822972 | 4.88E+06 |
| 45.2992477 | 5.00E+06 |
| 48.9775513 | 4.85E+06 |
| 50.2654825 | 5.35E+06 |
| 56.5486678 | 5.80E+06 |
| 60.3989969 | 5.94E+06 |
| 61.2219392 | 5.60E+06 |
| 62.8318531 | 6.18E+06 |
| 73.4663270 | 6.28E+06 |
| 85.7107148 | 6.90E+06 |
| 90.5984953 | 7.60E+06 |
| 94.2477796 | 7.97E+06 |
| 97.9551027 | 7.48E+06 |
| 110.1994905 | 8.20E+06 |
| 120.7979938 | 8.94E+06 |
| 122.4438783 | 8.53E+06 |
| 150.9974922 | 1.04E+07 |
| 181.1969906 | 1.19E+07 |

| | |
|---|---|
| 183.6658175 | 1.08E+07 |
| 211.3964891 | 1.27E+07 |
| 241.5959875 | 1.34E+07 |
| 244.8877567 | 1.28E+07 |
| 271.7954860 | 1.47E+07 |
| 301.9949844 | 1.56E+07 |
| 367.3316350 | 1.59E+07 |
| 452.9924766 | 1.92E+07 |
| 489.7755133 | 1.86E+07 |
| 603.9899688 | 2.21E+07 |
| 612.2193916 | 2.06E+07 |
| 734.6632700 | 2.27E+07 |
| 857.1071483 | 2.43E+07 |
| 905.9849532 | 2.68E+07 |
| 979.5510266 | 2.57E+07 |
| 1101.9949049 | 2.73E+07 |
| 1207.9799376 | 2.94E+07 |
| 1224.4387833 | 2.89E+07 |
| 1509.9749220 | 3.34E+07 |
| 1811.9699064 | 3.52E+07 |
| 1836.6581749 | 3.47E+07 |
| 2113.9648908 | 3.84E+07 |
| 2415.9598752 | 4.06E+07 |
| 2717.9548595 | 4.21E+07 |
| 3019.9498439 | 4.43E+07 |
| 4529.9247659 | 5.07E+07 |
| 6039.8996879 | 5.70E+07 |
| 9059.8495318 | 6.43E+07 |
| 12079.7993758 | 6.83E+07 |
| 15099.7492197 | 7.22E+07 |
| 18119.6990636 | 8.05E+07 |
| 21139.6489076 | 8.25E+07 |
| 24159.5987515 | 8.38E+07 |
| 27179.5485954 | 8.87E+07 |

```
30199.4984394        8.88E+07
45299.2476591        1.02E+08
;
proc nlin data=mod method=marquardt;
parms wc=300 v=0.30 w=1 Gg=1000000000;
model Gstar=Gg*(1+(wc/freq)**v)**(-w/v);
```

**run;**

**SAS output for original specimen AUG3 determination of parameters for shear complex modulus model proposed by Marasteanu and Anderson**

Non-Linear Least Squares Iterative Phase

Dependent Variable GSTAR Method: Marquardt

| Iter | WC | V | W | GG | Sum of Squares |
|---|---|---|---|---|---|
| 0 | 300.000000 | 0.300000 | 1.000000 | 1000000000 | 1.80908821E18 |
| 1 | 331.420248 | 0.252853 | 0.967424 | 473841999 | 6.64555392E16 |
| 2 | 352.433076 | 0.240012 | 0.991734 | 333430963 | 9.81087007E14 |
| 3 | 368.676554 | 0.245898 | 1.031596 | 307939115 | 4.03551452E13 |
| 4 | 422.740458 | 0.252230 | 1.022555 | 297224882 | 3.92603063E13 |
| 5 | 455.547493 | 0.254113 | 1.013869 | 295048247 | 3.92513282E13 |
| 6 | 471.538832 | 0.254920 | 1.009798 | 294041994 | 3.92042879E13 |
| 7 | 478.539840 | 0.255271 | 1.007998 | 293603884 | 3.92019258E13 |
| 8 | 481.595079 | 0.255426 | 1.007205 | 293411573 | 3.92018316E13 |
| 9 | 482.939547 | 0.255494 | 1.006855 | 293326714 | 3.92018249E13 |
| 10 | 483.533130 | 0.255524 | 1.006700 | 293289207 | 3.9201824E13 |
| 11 | 483.795509 | 0.255537 | 1.006631 | 293272620 | 3.92018239E13 |

NOTE: Convergence criterion met.

Non-Linear Least Squares Summary Statistics Dependent Variable GSTAR

| Source | DF | Sum of Squares | Mean Square |
|---|---|---|---|
| Regression | 4 | 8.56834511E16 | 2.14208628E16 |
| Residual | 260 | 3.92018239E13 | 150776245604 |
| Uncorrected Total | 264 | 8.57226529E16 | |
| (Corrected Total) | 263 | 7.52128899E16 | |

| Parameter | Estimate | Asymptotic Std. Error | Asymptotic 95 % Confidence Interval Lower | Upper |
|---|---|---|---|---|
| WC | 483.8 | 423.012 | -349.18 | 1316.77 |
| V | 0.3 | 0.022 | 0.21 | 0.30 |
| W | 1.0 | 0.111 | 0.79 | 1.22 |
| GG | 293272620.2 | 27574352.610 | 238974426.62 | 347570813.74 |

Asymptotic Correlation Matrix

| Corr | WC | V | W | GG |
|---|---|---|---|---|
| WC | 1 | 0.9839490846 | -0.998900522 | -0.94911901 |
| V | 0.9839490846 | 1 | -0.975601734 | -0.989529931 |
| W | -0.998900522 | -0.975601734 | 1 | 0.9363485795 |
| GG | -0.94911901 | -0.989529931 | 0.9363485795 | 1 |

**SAS input for original specimen AUG3 determination of parameters for phase angle model proposed by Marasteanu and Anderson**

```
options nodate pageno=1;
data phase;
input freq delta;
cards;
0.0000061    88.50
0.0000092    88.40
0.0000123    88.60
0.0000184    88.90
0.0000206    89.80
0.0000246    88.70
0.0000307    89.00
0.0000308    89.40
0.0000368    88.90
0.0000411    89.40
0.0000430    88.80
0.0000491    89.10
0.0000553    89.00
0.0000614    89.20
0.0000617    89.20
0.0000822    89.10
0.0000863    89.30
0.0000921    89.00
0.0001028    89.00
0.0001228    89.40
0.0001233    89.20
0.0001295    89.00
0.0001439    88.80
0.0001645    88.80
0.0001726    89.20
0.0001842    88.90
```

| | |
|---|---|
| 0.0001850 | 88.80 |
| 0.0002056 | 88.80 |
| 0.0002456 | 88.90 |
| 0.0002589 | 88.70 |
| 0.0003070 | 89.00 |
| 0.0003083 | 88.60 |
| 0.0003452 | 88.30 |
| 0.0003683 | 88.60 |
| 0.0004111 | 88.20 |
| 0.0004297 | 88.40 |
| 0.0004315 | 88.00 |
| 0.0004911 | 88.10 |
| 0.0004991 | 87.70 |
| 0.0005179 | 87.70 |
| 0.0005525 | 88.30 |
| 0.0006042 | 87.60 |
| 0.0006139 | 87.90 |
| 0.0006167 | 88.10 |
| 0.0006905 | 87.30 |
| 0.0007486 | 87.10 |
| 0.0007768 | 87.30 |
| 0.0008223 | 87.50 |
| 0.0008631 | 87.10 |
| 0.0009209 | 87.30 |
| 0.0009982 | 86.60 |
| 0.0010278 | 86.90 |
| 0.0012278 | 87.10 |
| 0.0012334 | 86.60 |
| 0.0012946 | 86.50 |
| 0.0014389 | 86.20 |
| 0.0014973 | 86.00 |
| 0.0016445 | 86.40 |
| 0.0017262 | 85.80 |
| 0.0018417 | 86.30 |

| | |
|---|---|
| 0.0018501 | 86.10 |
| 0.0019964 | 85.30 |
| 0.0020556 | 85.90 |
| 0.0024557 | 85.60 |
| 0.0024955 | 84.80 |
| 0.0025893 | 84.80 |
| 0.0029945 | 84.20 |
| 0.0030696 | 85.20 |
| 0.0030835 | 85.00 |
| 0.0034524 | 84.10 |
| 0.0034936 | 83.90 |
| 0.0036835 | 84.80 |
| 0.0039927 | 83.60 |
| 0.0041113 | 84.30 |
| 0.0042974 | 84.50 |
| 0.0043155 | 83.50 |
| 0.0044918 | 83.10 |
| 0.0049113 | 84.20 |
| 0.0049909 | 82.80 |
| 0.0051786 | 82.90 |
| 0.0053719 | 81.00 |
| 0.0055252 | 84.10 |
| 0.0060417 | 82.30 |
| 0.0061392 | 84.00 |
| 0.0061669 | 83.10 |
| 0.0069048 | 82.30 |
| 0.0074864 | 81.40 |
| 0.0077679 | 82.00 |
| 0.0080579 | 79.30 |
| 0.0082226 | 82.30 |
| 0.0086309 | 81.40 |
| 0.0092087 | 82.40 |
| 0.0099818 | 80.40 |
| 0.0102782 | 81.40 |

| | |
|---|---|
| 0.0107439 | 78.20 |
| 0.0122783 | 81.80 |
| 0.0123338 | 80.70 |
| 0.0129464 | 79.90 |
| 0.0143895 | 80.20 |
| 0.0149727 | 78.70 |
| 0.0161158 | 77.00 |
| 0.0164451 | 80.00 |
| 0.0172619 | 79.00 |
| 0.0184175 | 80.20 |
| 0.0185007 | 79.30 |
| 0.0199636 | 77.80 |
| 0.0205564 | 78.90 |
| 0.0214877 | 75.70 |
| 0.0249546 | 76.40 |
| 0.0258928 | 77.40 |
| 0.0268596 | 74.90 |
| 0.0299455 | 75.80 |
| 0.0308346 | 77.40 |
| 0.0322316 | 74.60 |
| 0.0345238 | 75.90 |
| 0.0349364 | 75.30 |
| 0.0376035 | 73.80 |
| 0.0399273 | 74.80 |
| 0.0411128 | 76.60 |
| 0.0429754 | 73.80 |
| 0.0431547 | 75.00 |
| 0.0449182 | 74.20 |
| 0.0483474 | 73.10 |
| 0.0499091 | 73.40 |
| 0.0517857 | 74.20 |
| 0.0537193 | 72.70 |
| 0.0604166 | 73.70 |
| 0.0616691 | 75.10 |

| | |
|---|---|
| 0.0628319 | 70.90 |
| 0.0690476 | 73.30 |
| 0.0748637 | 72.10 |
| 0.0776785 | 72.90 |
| 0.0805789 | 72.00 |
| 0.0863095 | 72.40 |
| 0.0942478 | 70.50 |
| 0.0998182 | 70.90 |
| 0.1074386 | 71.40 |
| 0.1256637 | 70.70 |
| 0.1294642 | 71.10 |
| 0.1497273 | 70.00 |
| 0.1611578 | 70.70 |
| 0.1726190 | 70.40 |
| 0.1884956 | 69.60 |
| 0.1996365 | 69.30 |
| 0.2148771 | 70.40 |
| 0.2495456 | 68.70 |
| 0.2513274 | 68.90 |
| 0.2589284 | 69.60 |
| 0.2685964 | 70.40 |
| 0.2994547 | 68.00 |
| 0.3141593 | 70.00 |
| 0.3223157 | 69.80 |
| 0.3493638 | 67.90 |
| 0.3760350 | 69.80 |
| 0.3769911 | 68.90 |
| 0.3992729 | 67.60 |
| 0.4297543 | 69.10 |
| 0.4398230 | 68.90 |
| 0.4491820 | 67.10 |
| 0.4834735 | 69.40 |
| 0.4990911 | 67.00 |
| 0.5026548 | 68.70 |

| | |
|---|---|
| 0.5371928 | 69.40 |
| 0.5654867 | 68.40 |
| 0.6283185 | 68.70 |
| 0.7486367 | 65.70 |
| 0.8057892 | 69.30 |
| 0.9424778 | 68.10 |
| 0.9981823 | 64.90 |
| 1.0743857 | 69.00 |
| 1.2244388 | 67.60 |
| 1.2566371 | 67.80 |
| 1.4972734 | 64.60 |
| 1.6115785 | 68.40 |
| 1.8366582 | 66.90 |
| 1.8849556 | 67.10 |
| 2.1487713 | 68.30 |
| 2.4488776 | 65.50 |
| 2.5132741 | 66.70 |
| 2.6859641 | 67.90 |
| 3.1415927 | 66.50 |
| 3.2231570 | 67.80 |
| 3.6733163 | 66.10 |
| 3.7603498 | 67.30 |
| 3.7699112 | 65.90 |
| 4.2975426 | 67.30 |
| 4.3982297 | 65.60 |
| 4.8347355 | 67.10 |
| 4.8977551 | 64.80 |
| 5.0265482 | 65.70 |
| 5.3719283 | 67.00 |
| 5.6548668 | 65.00 |
| 6.1221939 | 64.30 |
| 6.2831853 | 64.90 |
| 7.3466327 | 64.10 |
| 8.0578924 | 65.90 |

| | |
|---|---|
| 8.5710715 | 62.90 |
| 9.4247780 | 63.90 |
| 9.7955103 | 62.70 |
| 11.0199490 | 61.90 |
| 12.2443878 | 62.20 |
| 12.5663706 | 62.90 |
| 18.3665817 | 60.70 |
| 18.8495559 | 61.70 |
| 24.4887757 | 59.40 |
| 25.1327412 | 60.80 |
| 30.1994984 | 57.60 |
| 31.4159265 | 60.20 |
| 36.7331635 | 58.10 |
| 37.6991118 | 59.70 |
| 43.9822972 | 59.20 |
| 45.2992477 | 56.40 |
| 48.9775513 | 57.50 |
| 50.2654825 | 58.50 |
| 56.5486678 | 58.10 |
| 60.3989969 | 54.90 |
| 61.2219392 | 56.00 |
| 62.8318531 | 57.60 |
| 73.4663270 | 55.40 |
| 85.7107148 | 54.90 |
| 90.5984953 | 51.90 |
| 94.2477796 | 55.60 |
| 97.9551027 | 54.30 |
| 110.1994905 | 53.20 |
| 120.7979938 | 51.90 |
| 122.4438783 | 53.70 |
| 150.9974922 | 50.80 |
| 181.1969906 | 50.50 |
| 183.6658175 | 51.30 |
| 211.3964891 | 48.70 |

| | |
|---|---|
| 241.5959875 | 47.70 |
| 244.8877567 | 49.10 |
| 271.7954860 | 46.60 |
| 301.9949844 | 47.10 |
| 367.3316350 | 47.60 |
| 452.9924766 | 42.50 |
| 489.7755133 | 45.90 |
| 603.9899688 | 43.00 |
| 612.2193916 | 44.80 |
| 734.6632700 | 43.90 |
| 857.1071483 | 42.60 |
| 905.9849532 | 41.10 |
| 979.5510266 | 42.70 |
| 1101.9949049 | 41.50 |
| 1207.9799376 | 38.30 |
| 1224.4387833 | 41.30 |
| 1509.9749220 | 39.50 |
| 1811.9699064 | 35.20 |
| 1836.6581749 | 39.60 |
| 2113.9648908 | 36.60 |
| 2415.9598752 | 38.40 |
| 2717.9548595 | 35.20 |
| 3019.9498439 | 35.30 |
| 4529.9247659 | 32.30 |
| 6039.8996879 | 30.30 |
| 9059.8495318 | 28.30 |
| 12079.7993758 | 28.20 |
| 15099.7492197 | 27.40 |
| 18119.6990636 | 24.10 |
| 21139.6489076 | 23.50 |
| 24159.5987515 | 21.70 |
| 27179.5485954 | 22.60 |
| 30199.4984394 | 23.50 |
| 45299.2476591 | 20.30 |

;

```
proc nlin data=phase method=marquardt;
parms wc=300 v=.30 w=1;
model delta=(90*w)/(1+(freq/wc)**v);
run;
```

**SAS output for original specimen AUG3 determination of parameters for phase angle model proposed by Marasteanu and Anderson**

Non-Linear Least Squares Iterative Phase

Dependent Variable DELTA Method: Marquardt

| Iter | WC | V | W | Sum of Squares |
|---|---|---|---|---|
| 0 | 300.000000 | 0.300000 | 1.000000 | 9115.801278 |
| 1 | 396.054422 | 0.182466 | 0.994143 | 3472.678131 |
| 2 | 199.929623 | 0.177360 | 1.049240 | 1929.313846 |
| 3 | 228.958759 | 0.175017 | 1.055299 | 1821.731646 |
| 4 | 231.931052 | 0.175442 | 1.054696 | 1821.439658 |
| 5 | 232.248228 | 0.175494 | 1.054585 | 1821.438391 |
| 6 | 232.284336 | 0.175500 | 1.054573 | 1821.438375 |

NOTE: Convergence criterion met.

Non-Linear Least Squares Summary Statistics Dependent Variable DELTA

| Source | DF | Sum of Squares | Mean Square |
|---|---|---|---|
| Regression | 3 | 1379760.8216 | 459920.2739 |
| Residual | 261 | 1821.4384 | 6.9787 |
| Uncorrected Total | 264 | 1381582.2600 | |
| (Corrected Total) | 263 | 74704.3617 | |

| Parameter | Estimate Std. | Asymptotic Error | Asymptotic 95 % Confidence Interval | |
|---|---|---|---|---|
| | | | Lower | Upper |
| WC | 232.2843364 | 28.000804220 | 177.14738001 | 287.42129273 |
| V | 0.1755002 | 0.004783772 | 0.16608036 | 0.18492001 |
| W | 1.0545726 | 0.009426753 | 1.03601020 | 1.07313502 |

Asymptotic Correlation Matrix

| Corr | WC | V | W |
|---|---|---|---|
| WC | 1 | 0.5507908841 | -0.803917526 |
| V | 0.5507908841 | 1 | -0.89258289 |
| W | -0.803917526 | -0.89258289 | 1 |

# APPENDIX K

- This appendix includes the graphs of response of the original data versus the responses predicted by the Christensen-Anderson (C-A) graphically determined parameter, Christensen-Anderson (C-A) regressed parameter, Marasteanu-Anderson (M-A), and Gahvari models.

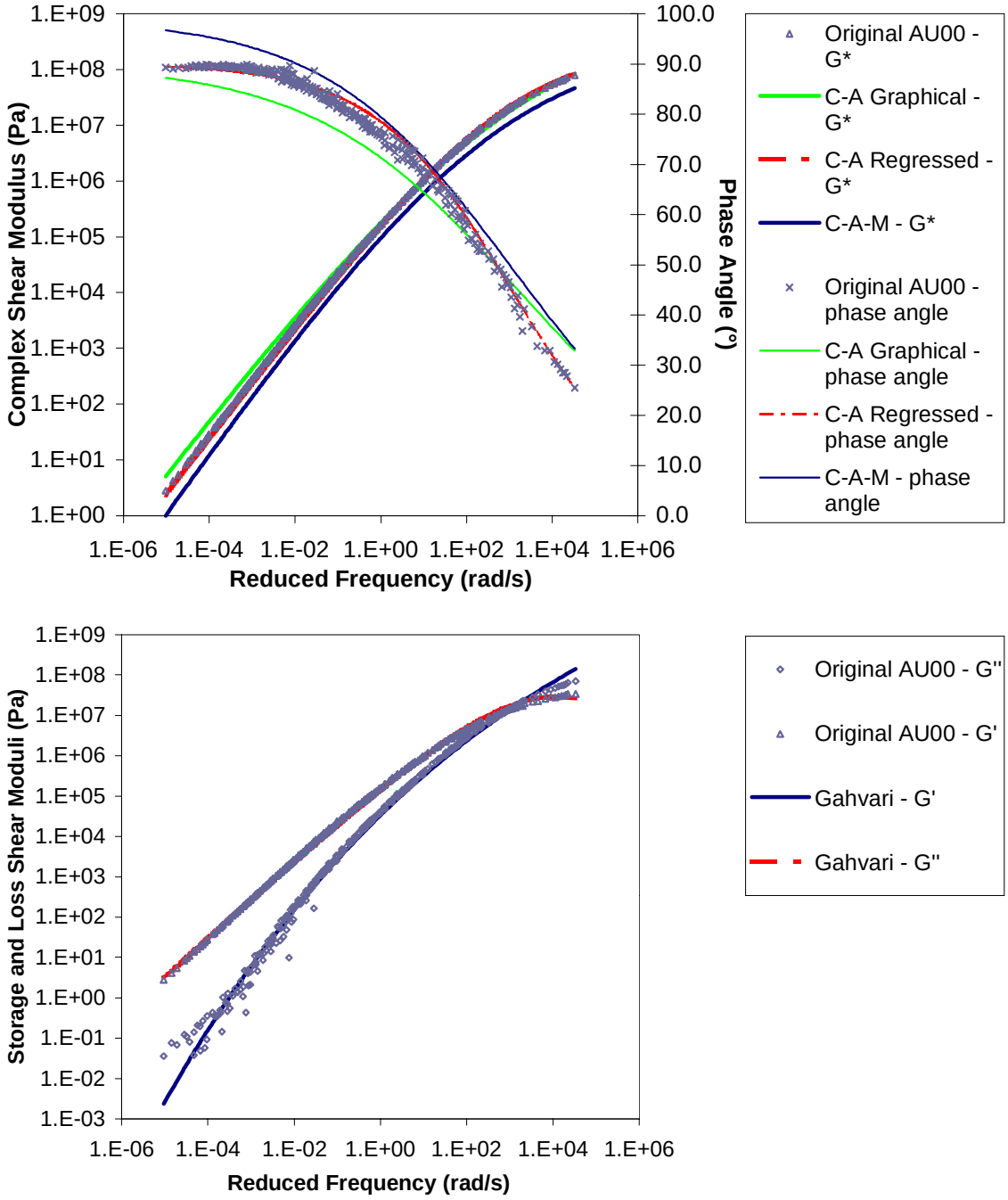


Figure K.1 Graphs of original specimen AU00 response versus responses predicted by the Christensen-Anderson (C-A) graphically determined parameter, Christensen-Anderson (C-A) regressed parameter, Marasteanu-Anderson (M-A), and Gahvari models.

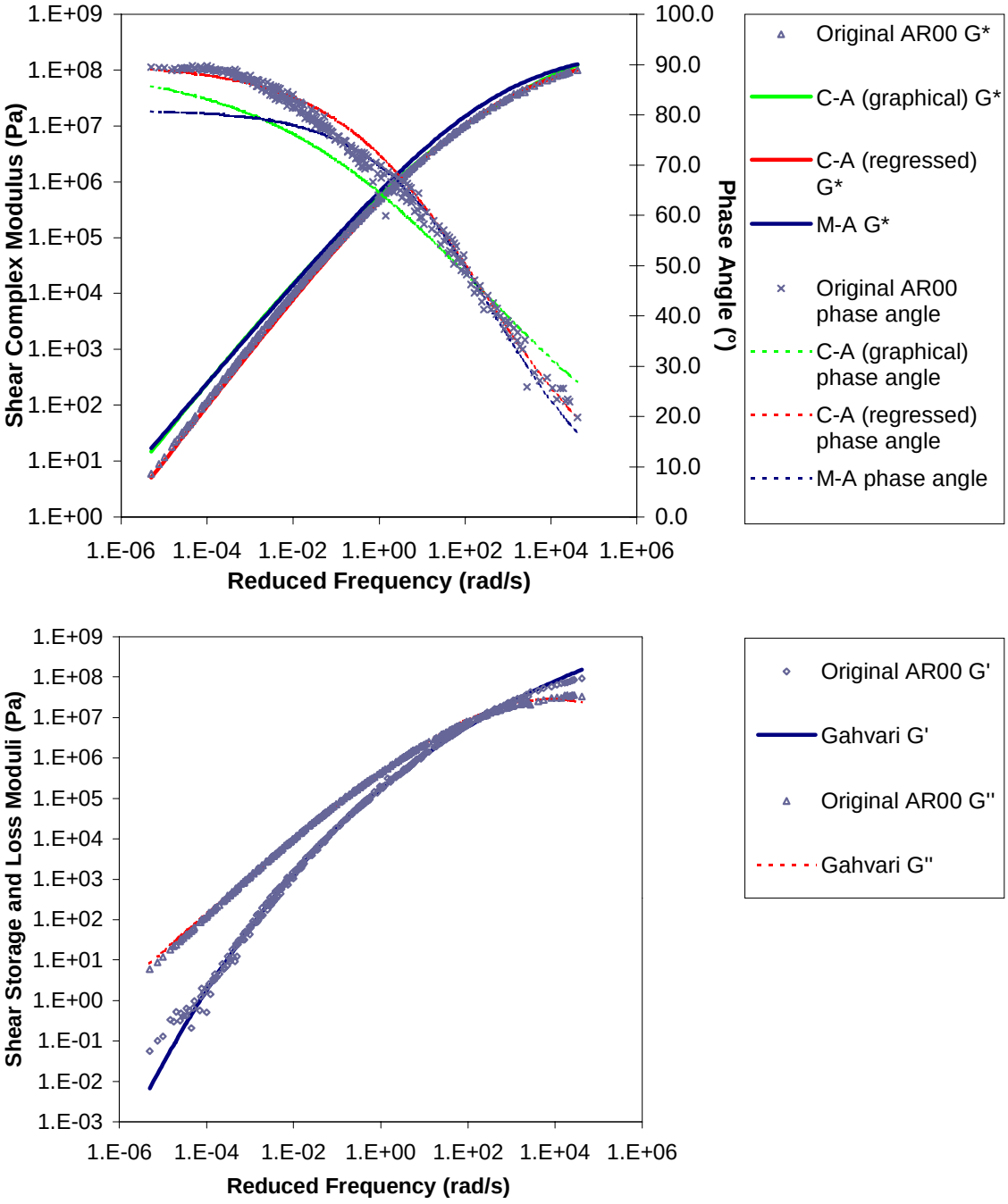


Figure K.2 Graphs of original specimen AR00 response versus responses predicted by the Christensen-Anderson (C-A) graphically determined parameter, Christensen-Anderson (C-A) regressed parameter, Marasteanu-Anderson (M-A), and Gahvari models.

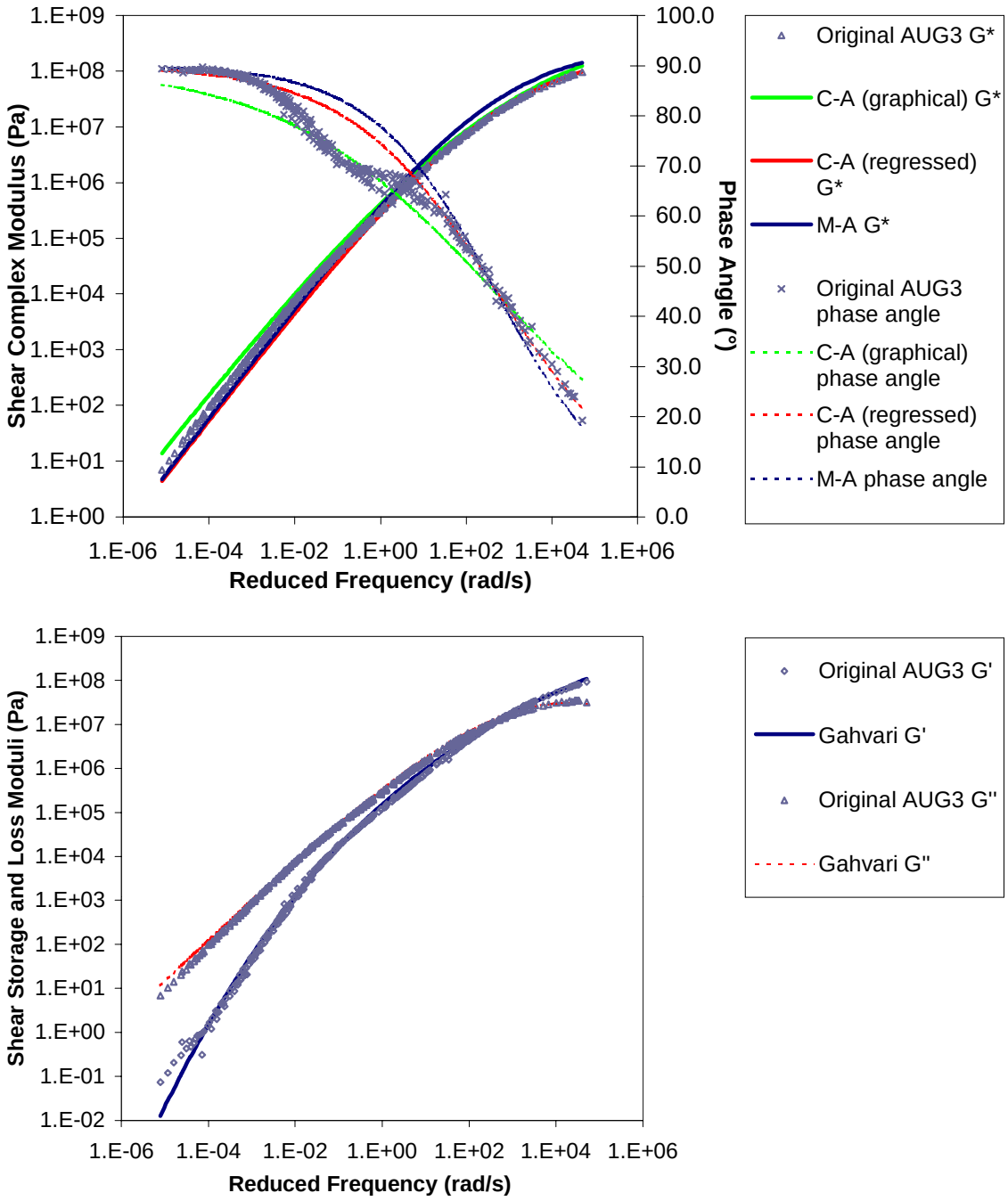


Figure K.3 Graphs of original specimen AUG3 response versus responses predicted by the Christensen-Anderson (C-A) graphically determined parameter, Christensen-Anderson (C-A) regressed parameter, Marasteanu-Anderson (M-A), and Gahvari models.

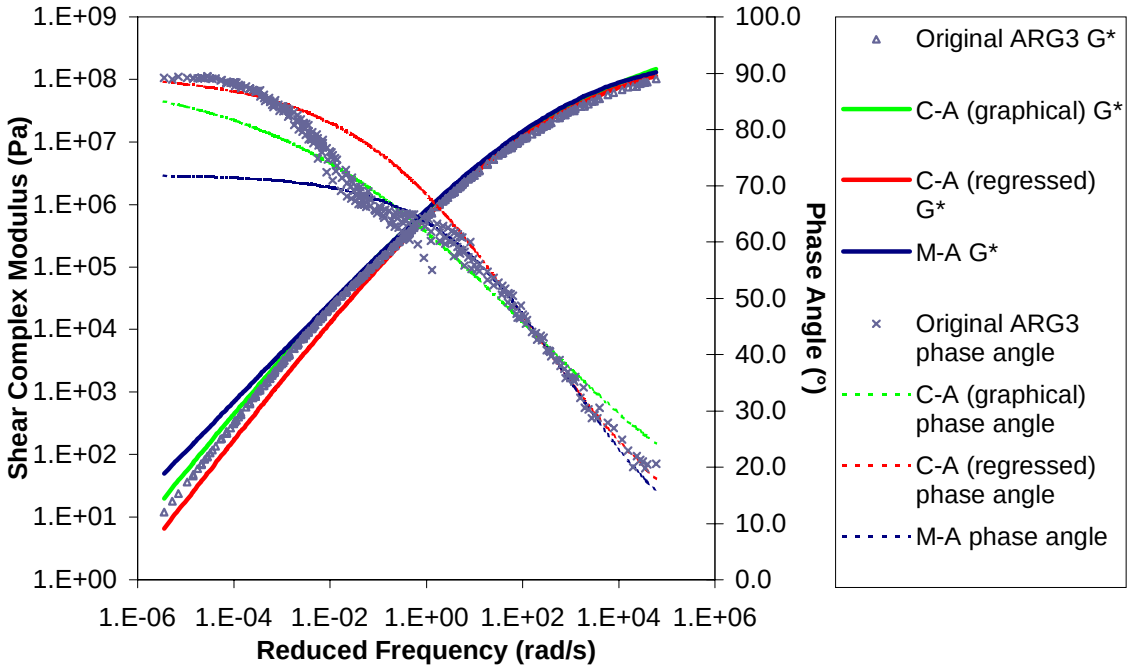


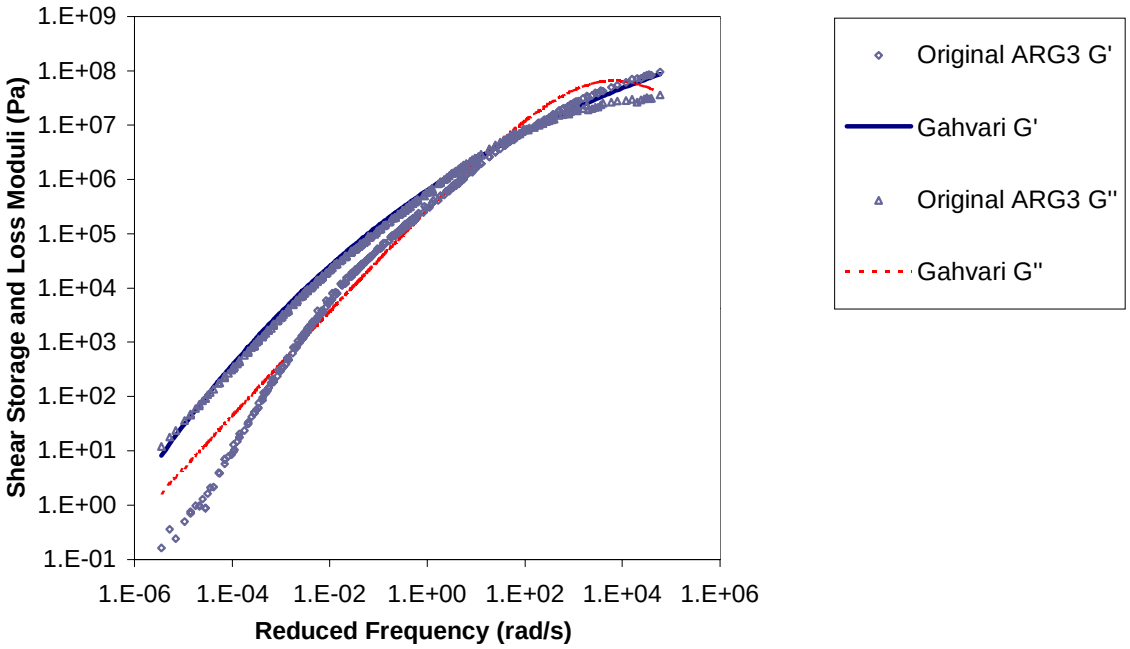


Figure K.4 Graphs of original specimen ARG3 response versus responses predicted by the Christensen-Anderson (C-A) graphically determined parameter, Christensen-Anderson (C-A) regressed parameter, Marasteanu-Anderson (M-A), and Gahvari models.

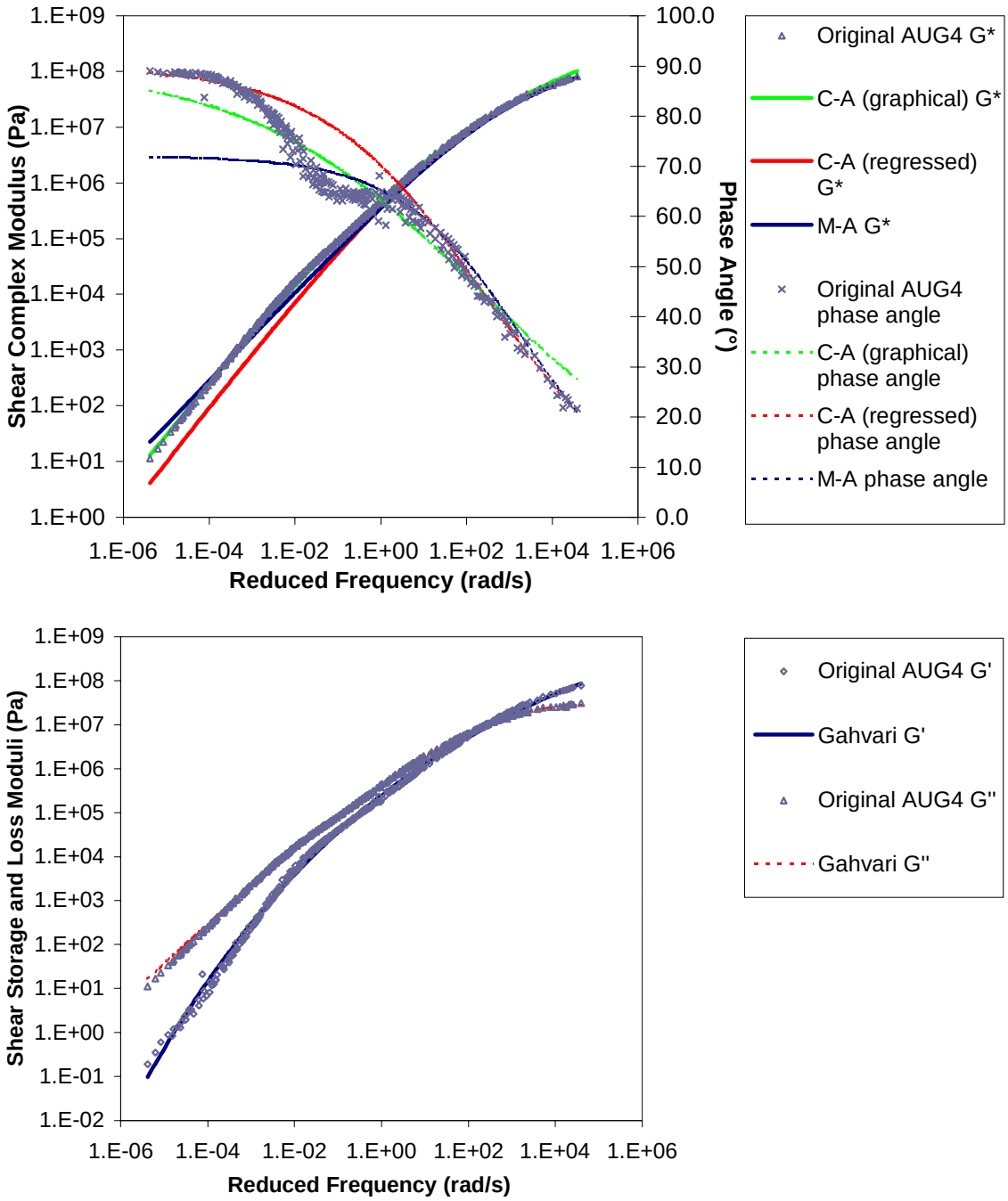


Figure K.5 Graphs of original specimen Aug4 response versus responses predicted by the Christensen-Anderson (C-A) graphically determined parameter, Christensen-Anderson (C-A) regressed parameter, Marasteanu-Anderson (M-A), and Gahvari models.

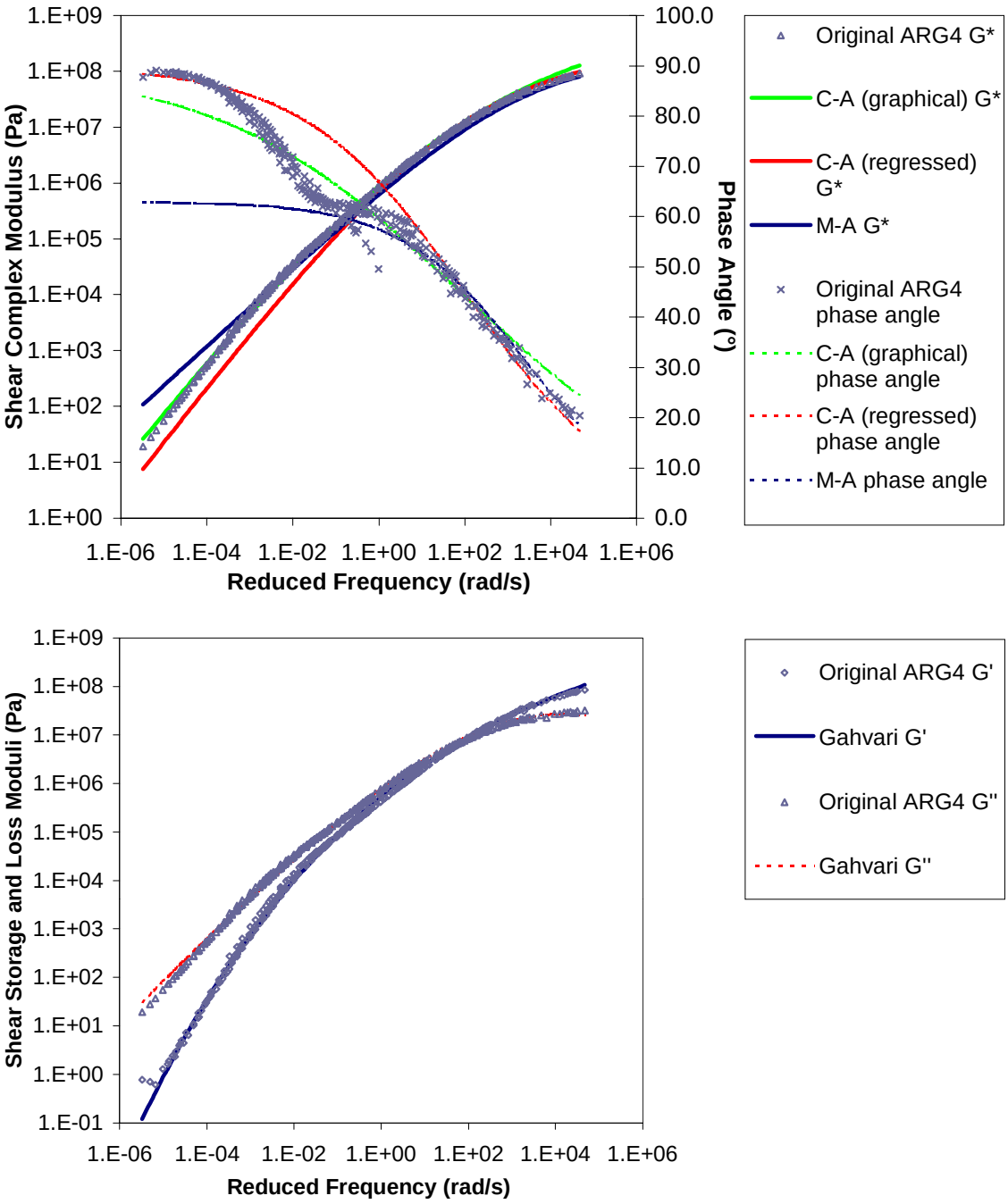


Figure K.6 Graphs of original specimen ARG4 response versus responses predicted by the Christensen-Anderson (C-A) graphically determined parameter, Christensen-Anderson (C-A) regressed parameter, Marasteanu-Anderson (M-A), and Gahvari models.

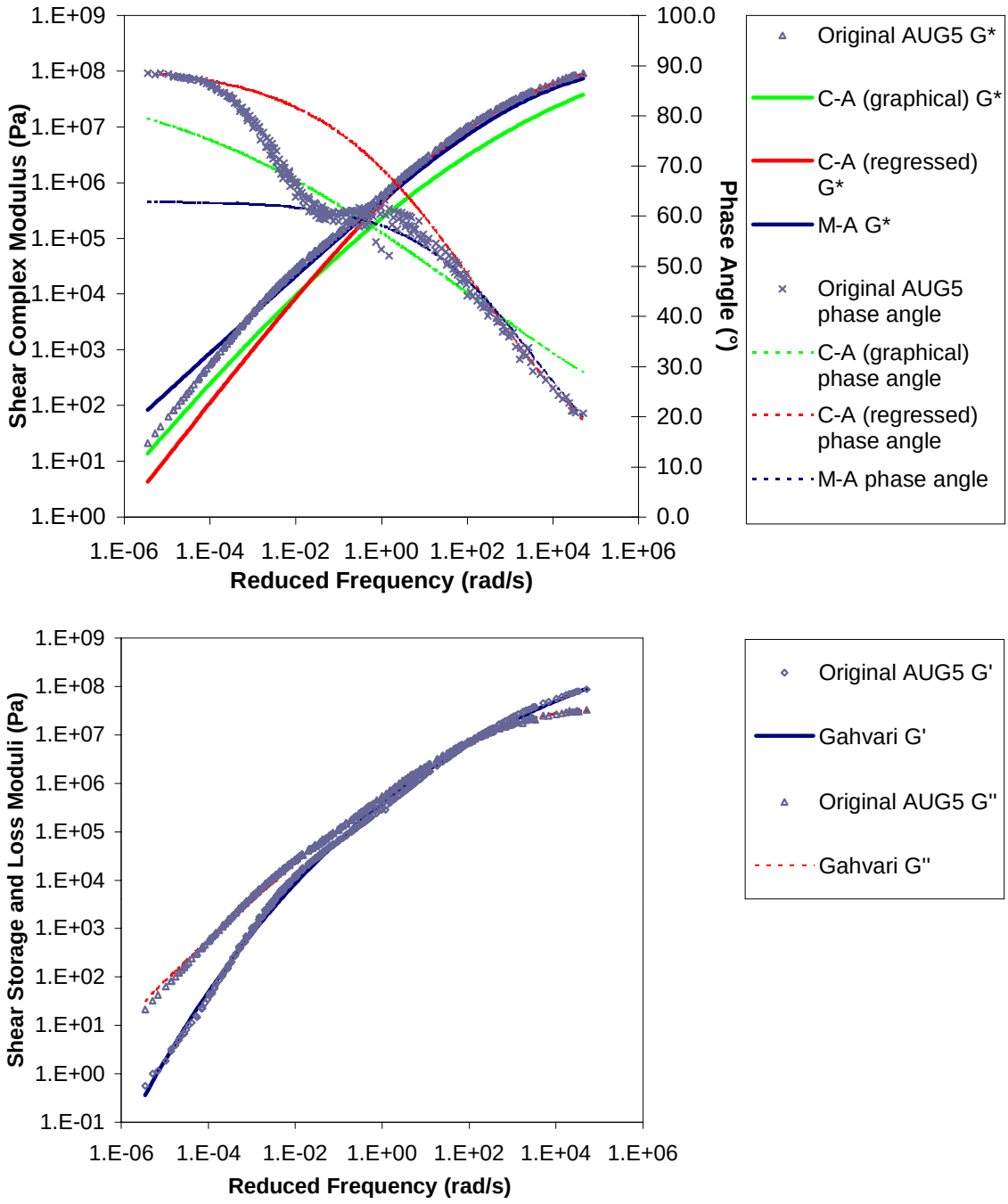


Figure K.7 Graphs of original specimen AUG5 response versus responses predicted by the Christensen-Anderson (C-A) graphically determined parameter, Christensen-Anderson (C-A) regressed parameter, Marasteanu-Anderson (M-A), and Gahvari models.

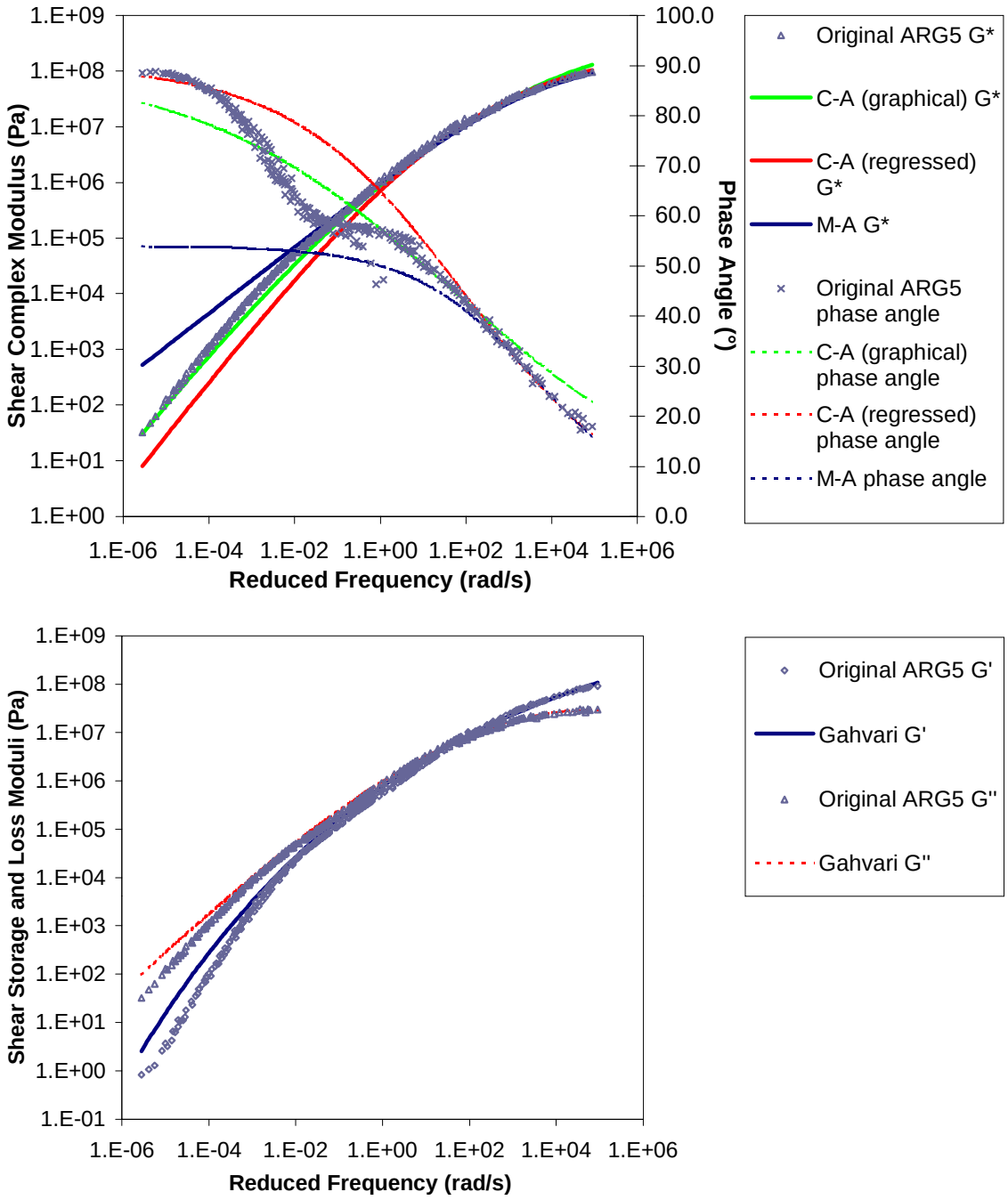


Figure K.8 Graphs of original specimen ARG5 response versus responses predicted by the Christensen-Anderson (C-A) graphically determined parameter, Christensen-Anderson (C-A) regressed parameter, Marasteanu-Anderson (M-A), and Gahvari models.

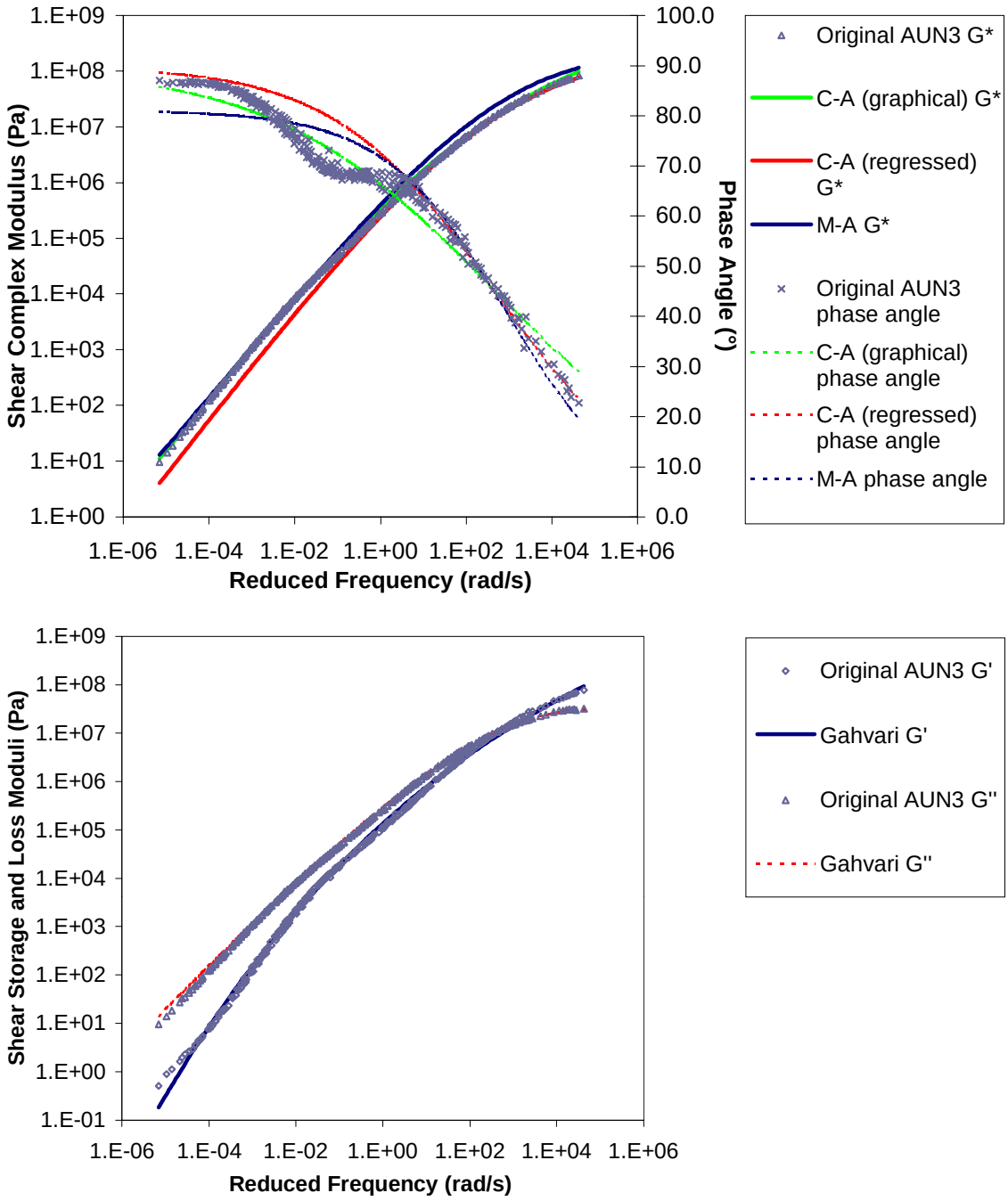


Figure K.9 Graphs of original specimen AUN3 response versus responses predicted by the Christensen-Anderson (C-A) graphically determined parameter, Christensen-Anderson (C-A) regressed parameter, Marasteanu-Anderson (M-A), and Gahvari models.

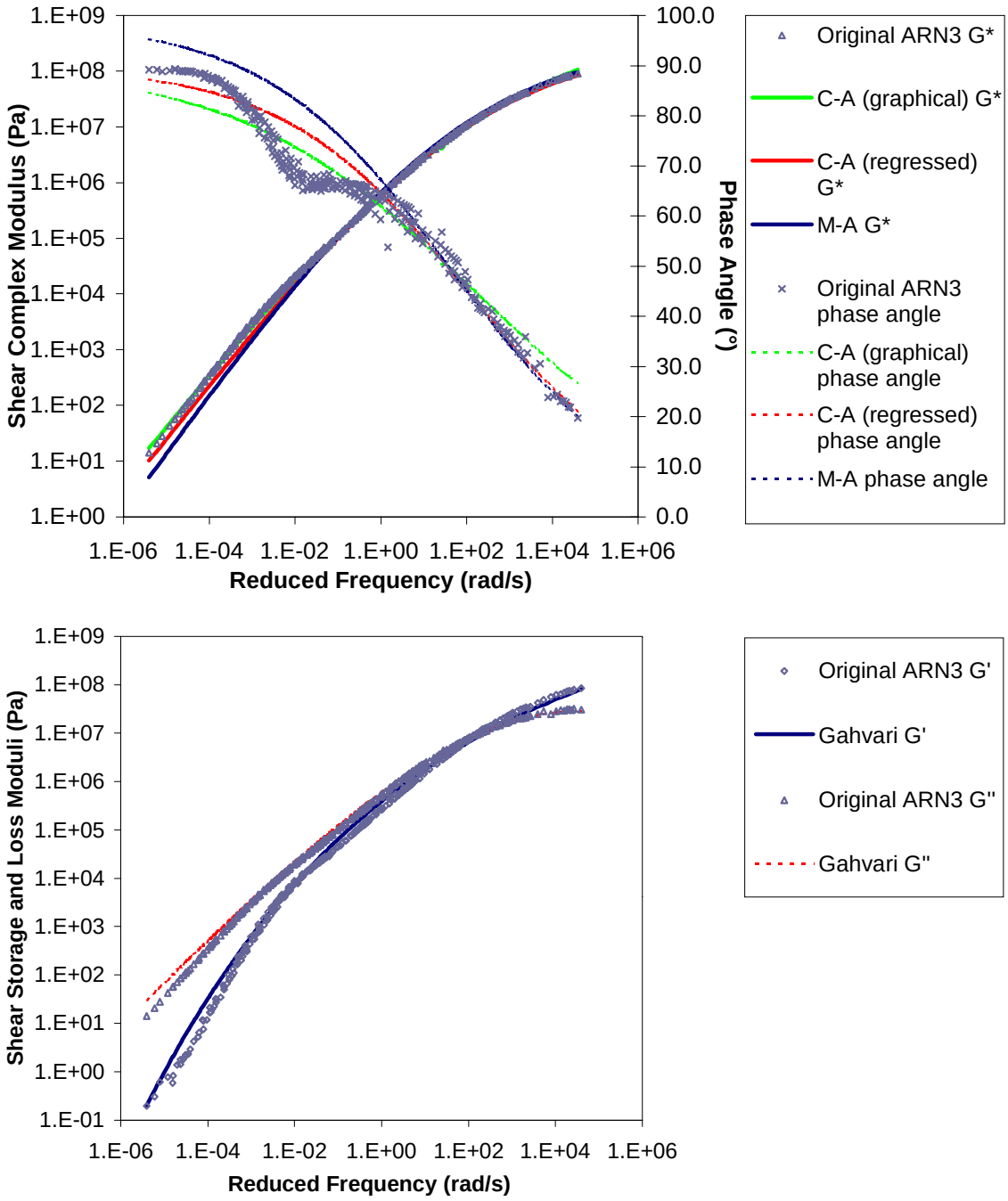


Figure K.10 Graphs of original specimen ARN3 response versus responses predicted by the Christensen-Anderson (C-A) graphically determined parameter, Christensen-Anderson (C-A) regressed parameter, Marasteanu-Anderson (M-A), and Gahvari models.

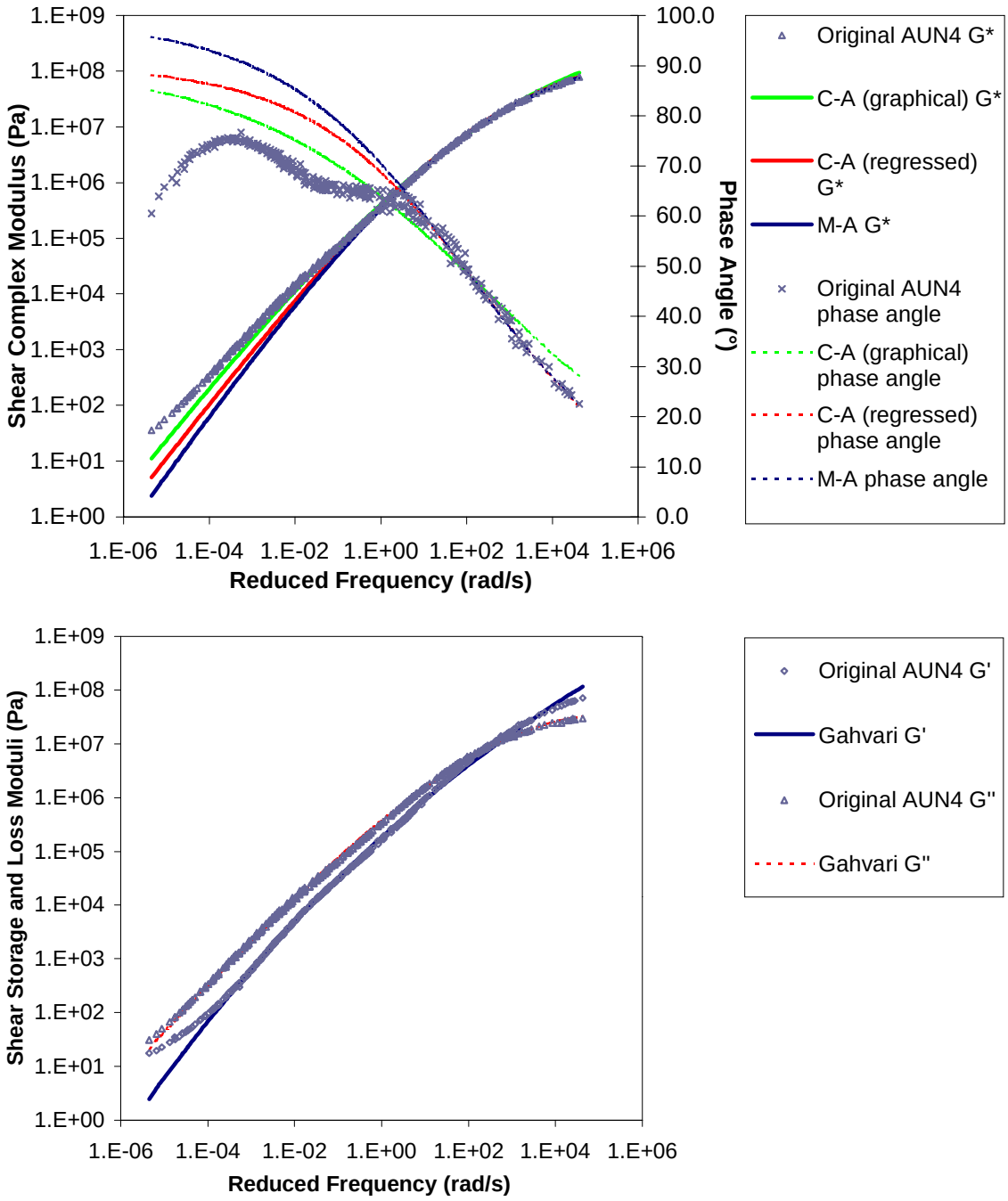


Figure K.11 Graphs of original specimen AUN4 response versus responses predicted by the Christensen-Anderson (C-A) graphically determined parameter, Christensen-Anderson (C-A) regressed parameter, Marasteanu-Anderson (M-A), and Gahvari models.

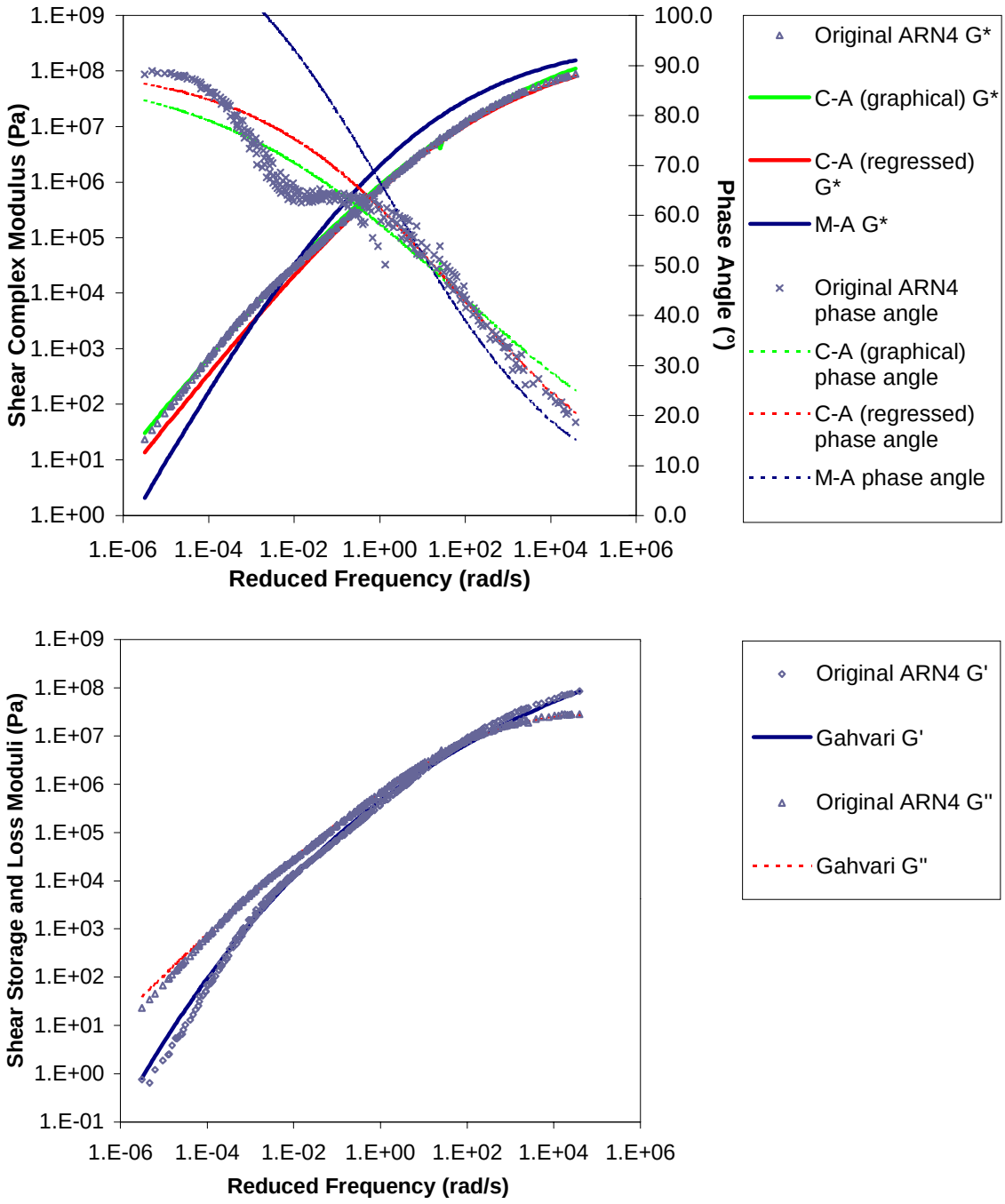


Figure K.12 Graphs of original specimen ARN4 response versus responses predicted by the Christensen-Anderson (C-A) graphically determined parameter, Christensen-Anderson (C-A) regressed parameter, Marasteanu-Anderson (M-A), and Gahvari models.

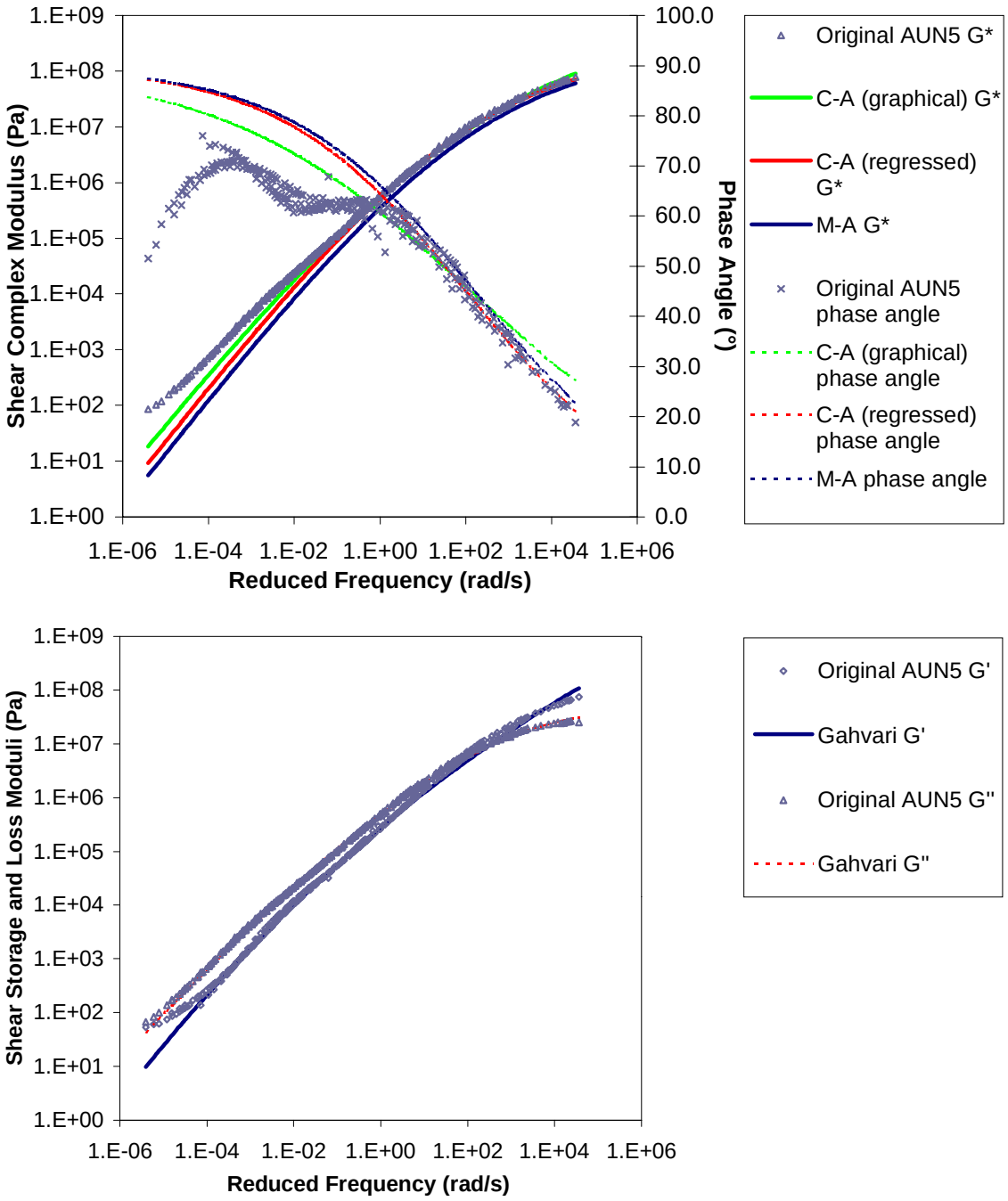


Figure K.13 Graphs of original specimen AUN5 response versus responses predicted by the Christensen-Anderson (C-A) graphically determined parameter, Christensen-Anderson (C-A) regressed parameter, Marasteanu-Anderson (M-A), and Gahvari models.

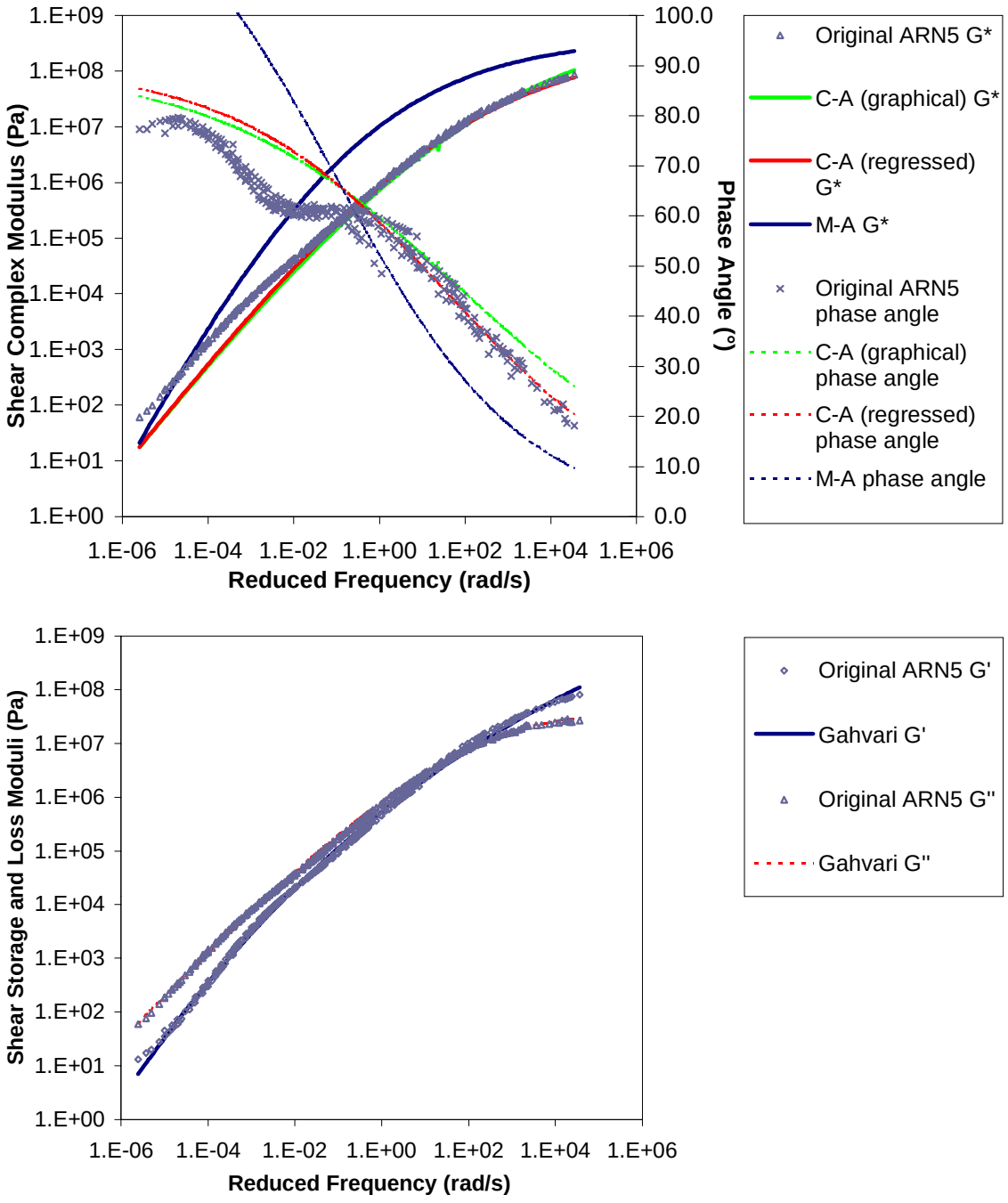


Figure K.14 Graphs of original specimen ARN5 response versus responses predicted by the Christensen-Anderson (C-A) graphically determined parameter, Christensen-Anderson (C-A) regressed parameter, Marasteanu-Anderson (M-A), and Gahvari models.

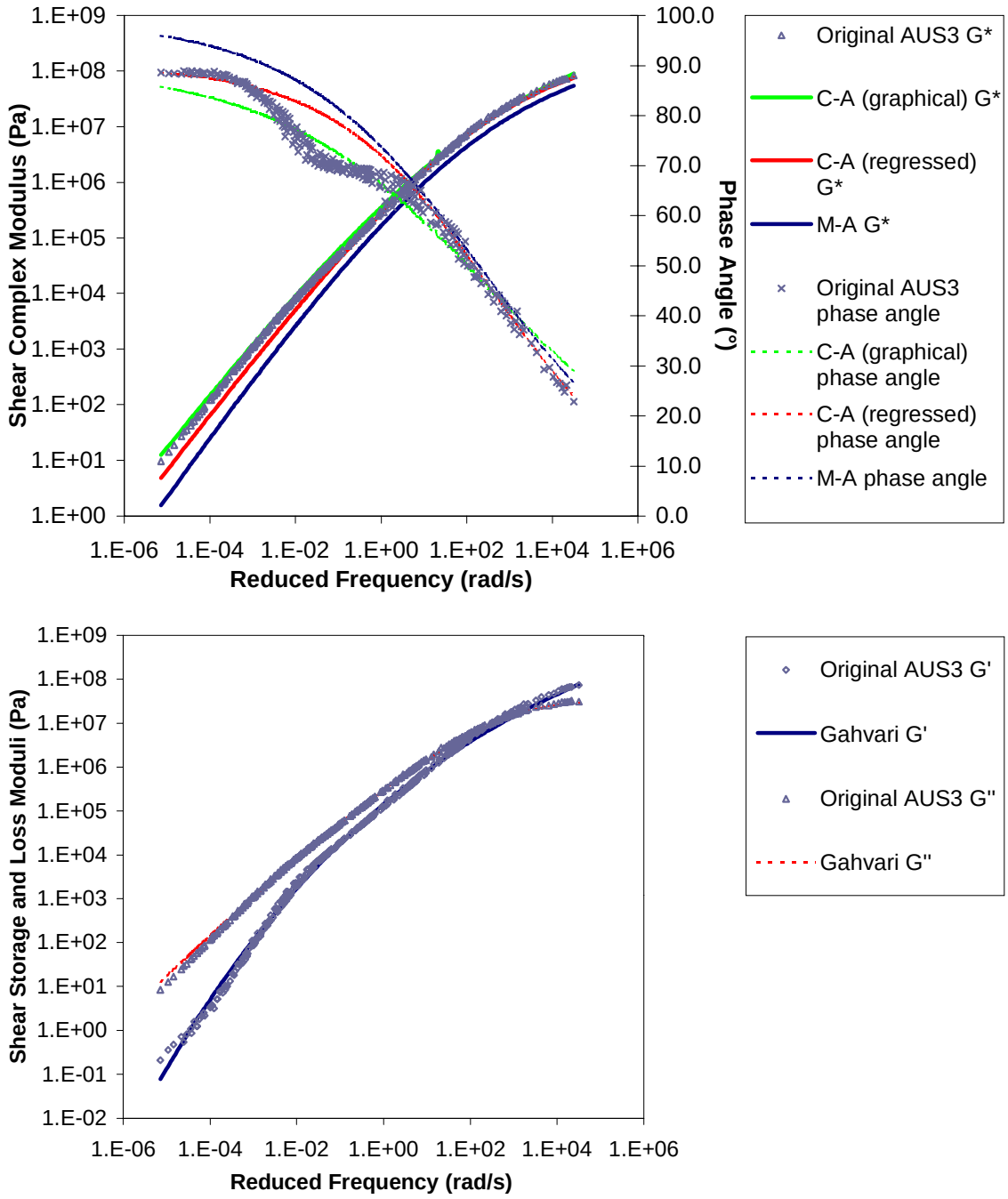


Figure K.15 Graphs of original specimen AUS3 response versus responses predicted by the Christensen-Anderson (C-A) graphically determined parameter, Christensen-Anderson (C-A) regressed parameter, Marasteanu-Anderson (M-A), and Gahvari models.

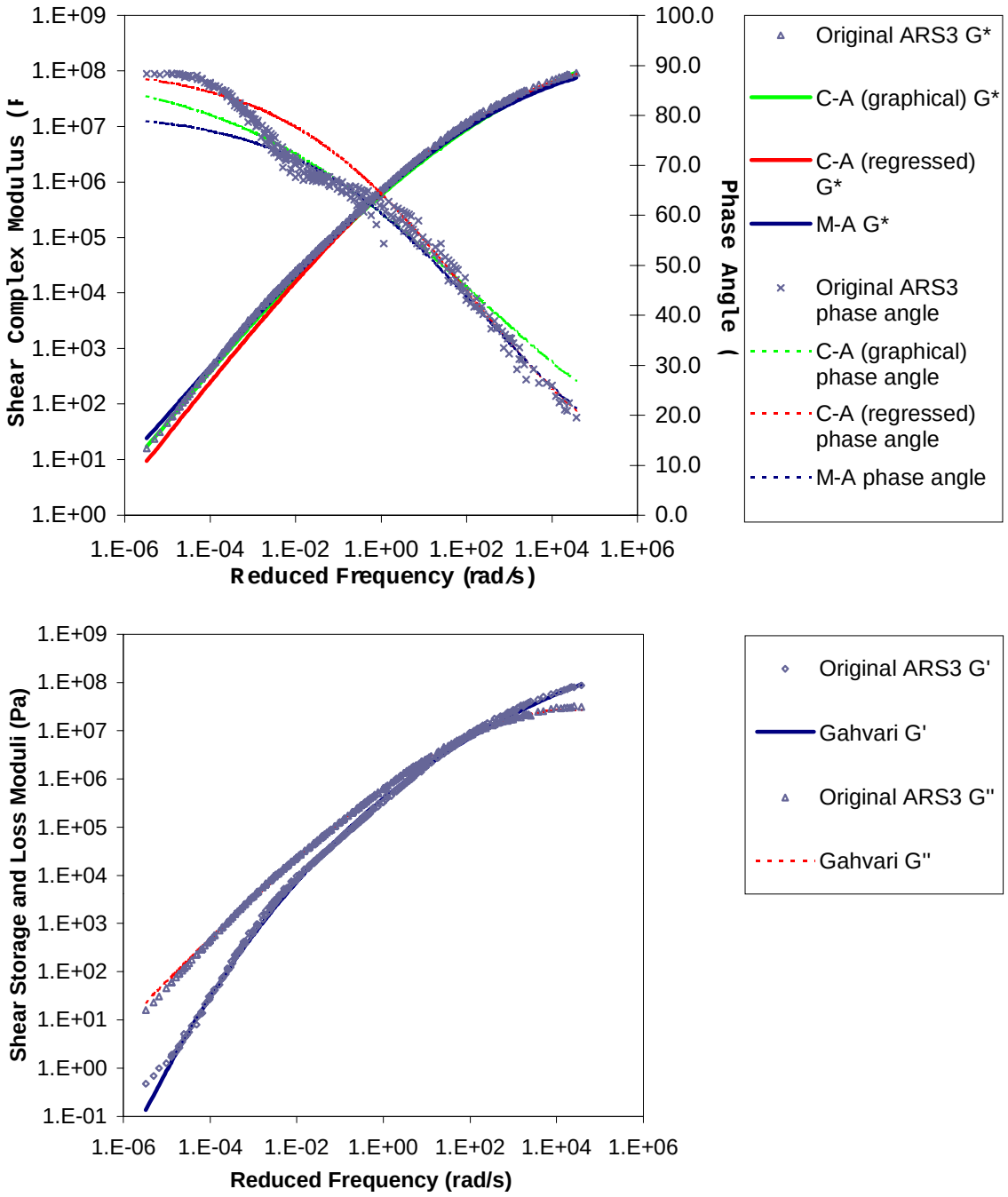


Figure K.16 Graphs of original specimen ARS3 response versus responses predicted by the Christensen-Anderson (C-A) graphically determined parameter, Christensen-Anderson (C-A) regressed parameter, Marasteanu-Anderson (M-A), and Gahvari models.

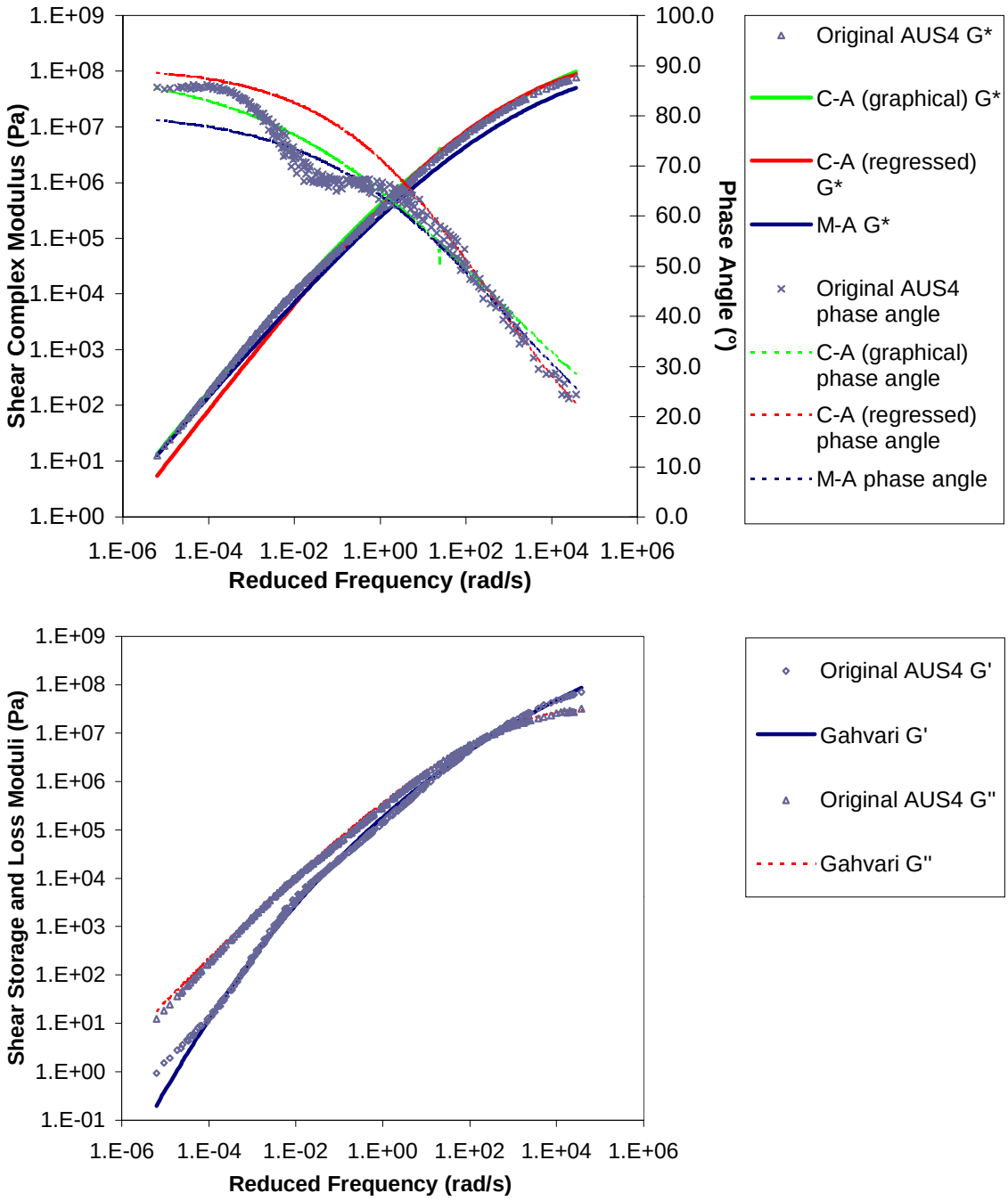


Figure K.17 Graphs of original specimen AUS4 response versus responses predicted by the Christensen-Anderson (C-A) graphically determined parameter, Christensen-Anderson (C-A) regressed parameter, Marasteanu-Anderson (M-A), and Gahvari models.

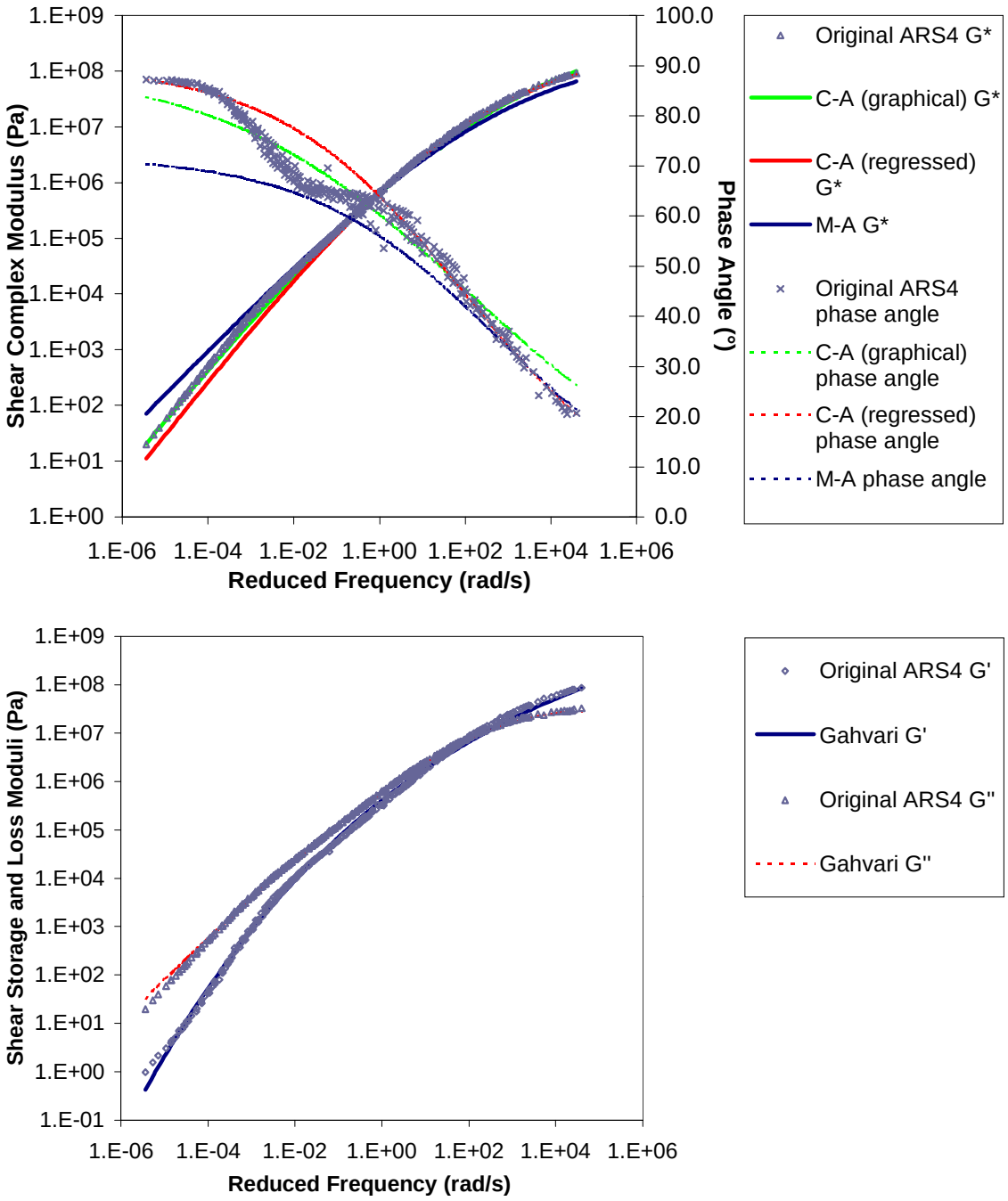


Figure K.18 Graphs of original specimen ARS4 response versus responses predicted by the Christensen-Anderson (C-A) graphically determined parameter, Christensen-Anderson (C-A) regressed parameter, Marasteanu-Anderson (M-A), and Gahvari models.

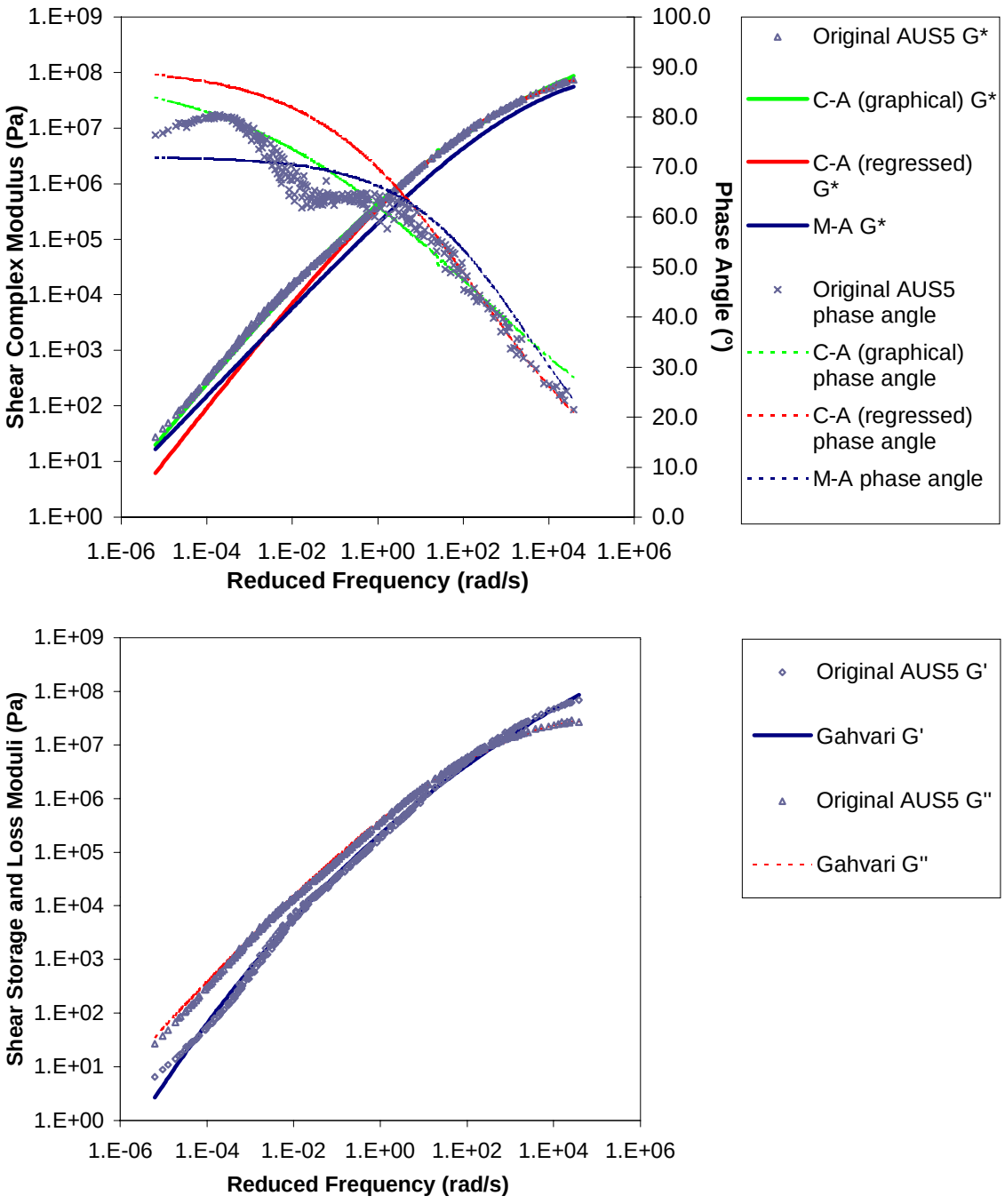


Figure K.19 Graphs of original specimen AUS5 response versus responses predicted by the Christensen-Anderson (C-A) graphically determined parameter, Christensen-Anderson (C-A) regressed parameter, Marasteanu-Anderson (M-A), and Gahvari models.

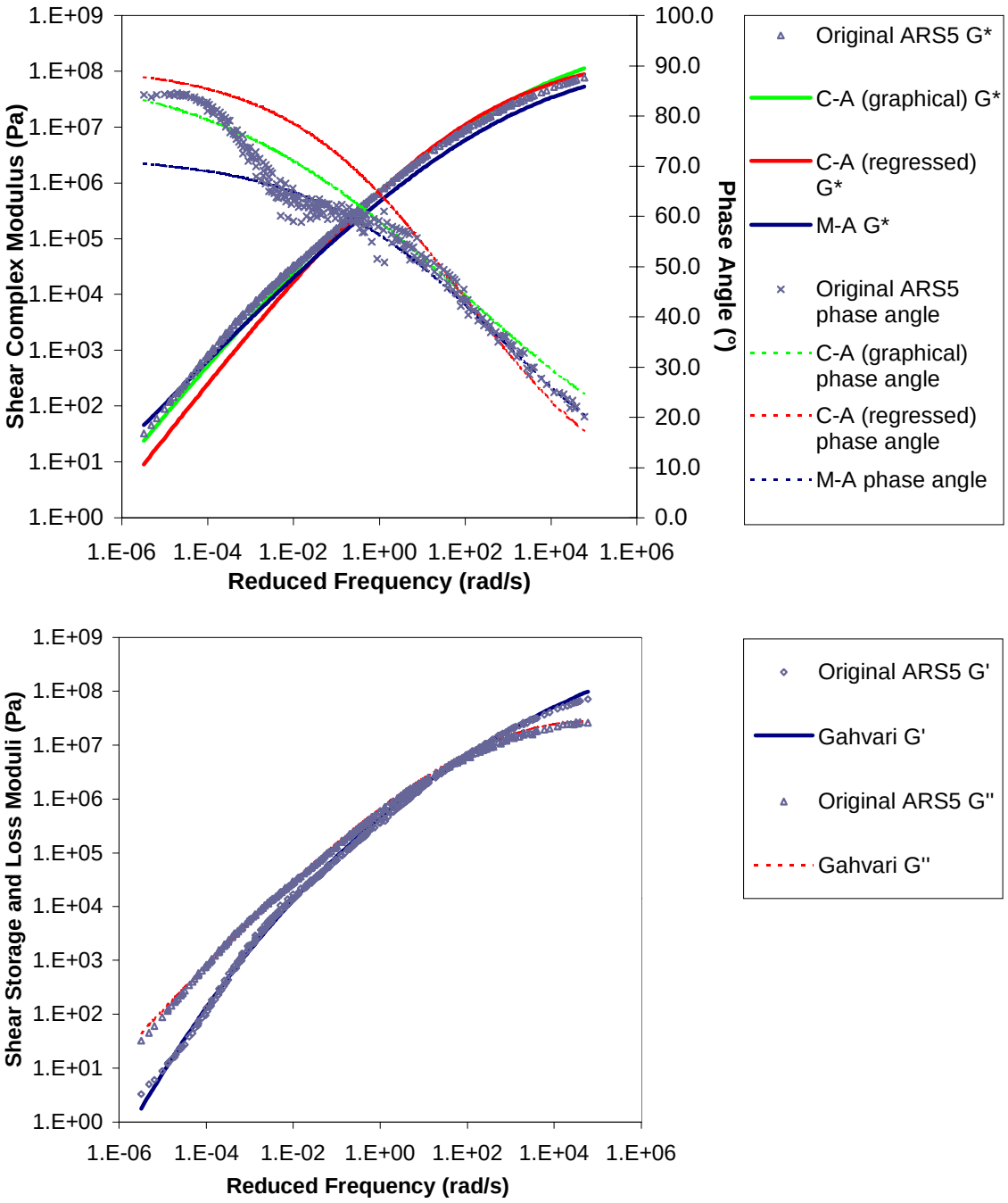


Figure K.20 Graphs of original specimen ARS5 response versus responses predicted by the Christensen-Anderson (C-A) graphically determined parameter, Christensen-Anderson (C-A) regressed parameter, Marasteanu-Anderson (M-A), and Gahvari models.

# APPENDIX L

- This appendix includes the graphs of response of the stored data versus the responses predicted by the Christensen-Anderson (C-A) graphically determined parameter, Christensen-Anderson (C-A) regressed parameter, Marasteanu-Anderson (M-A), and Gahvari models.

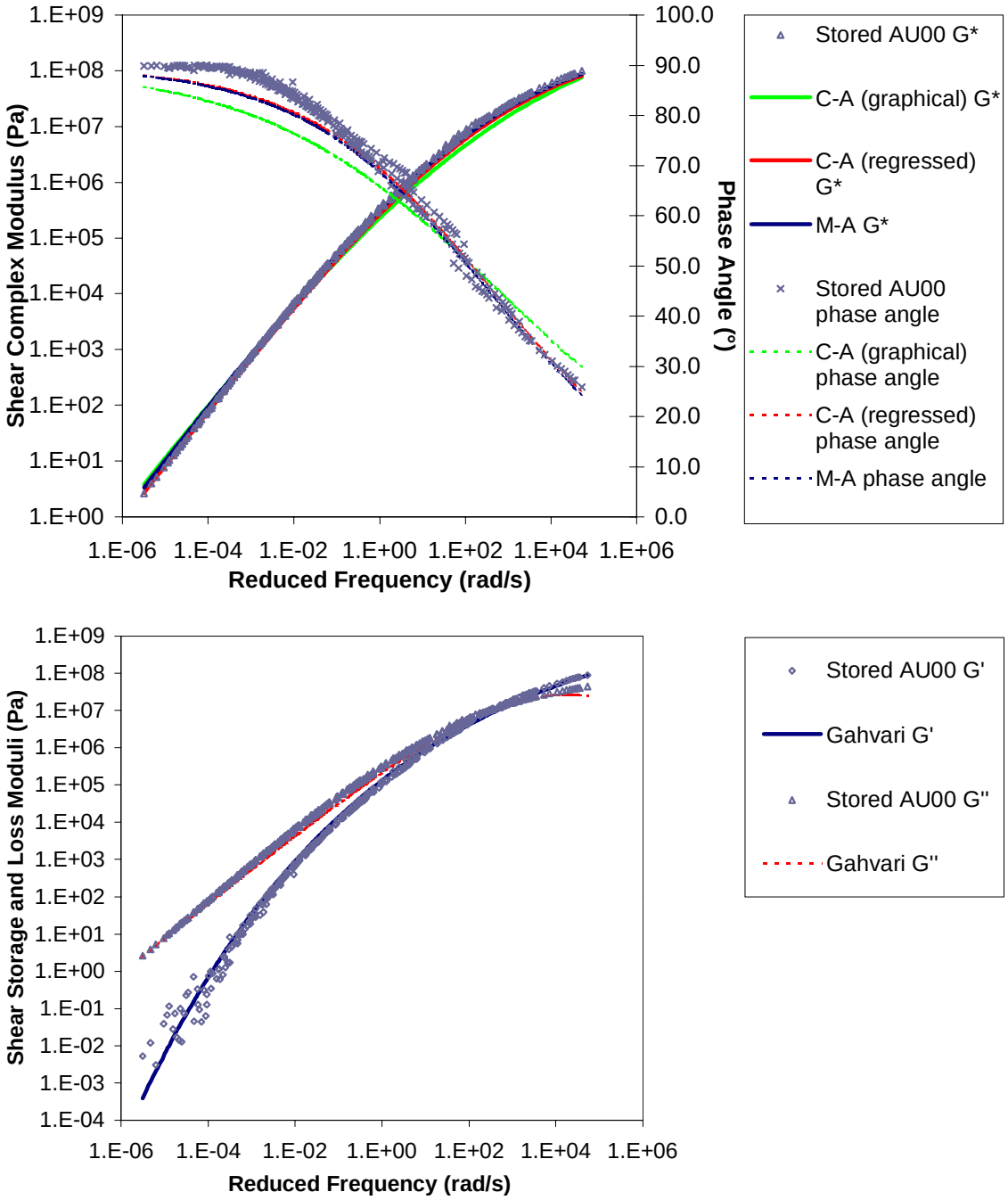


Figure L.1 Graphs of stored specimen AU00 response versus responses predicted by the Christensen-Anderson (C-A) graphically determined parameter, Christensen-Anderson (C-A) regressed parameter, Marasteanu-Anderson (M-A), and Gahvari models.

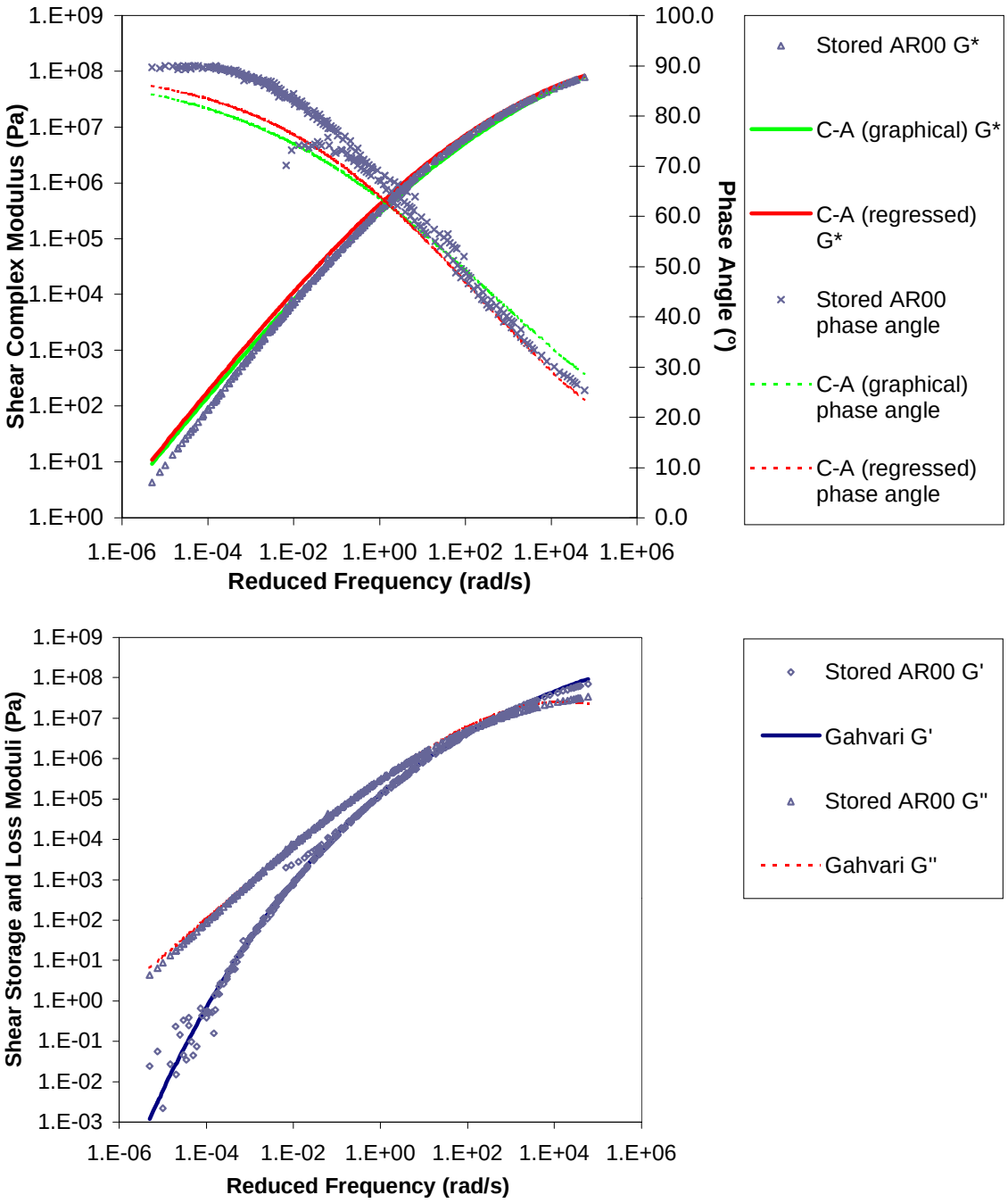


Figure L.2 Graphs of stored specimen AR00 response versus responses predicted by the Christensen-Anderson (C-A) graphically determined parameter, Christensen-Anderson (C-A) regressed parameter, Marasteanu-Anderson (M-A), and Gahvari models.

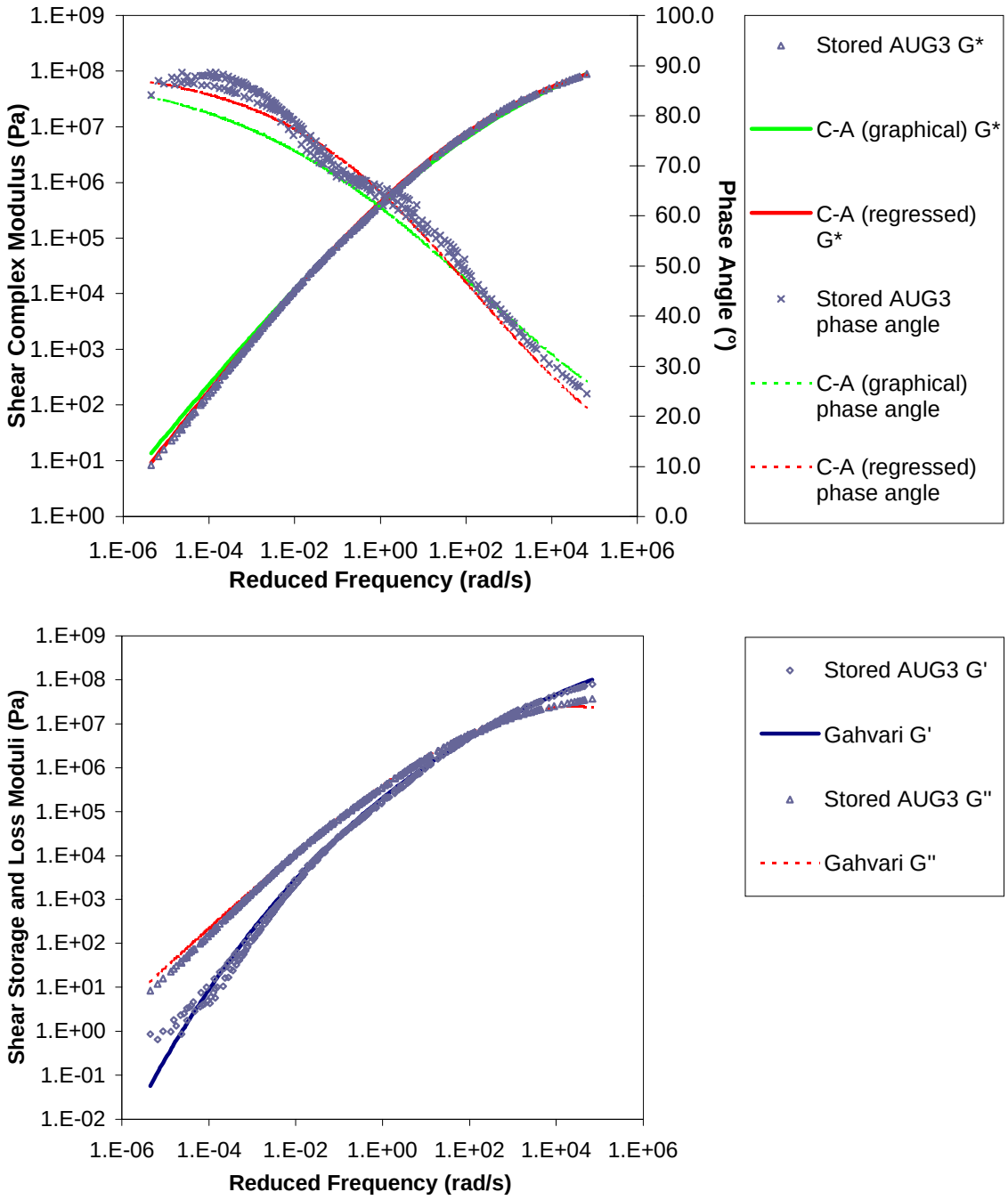


Figure L.3 Graphs of stored specimen AUG3 response versus responses predicted by the Christensen-Anderson (C-A) graphically determined parameter, Christensen-Anderson (C-A) regressed parameter, Marasteanu-Anderson (M-A), and Gahvari models.

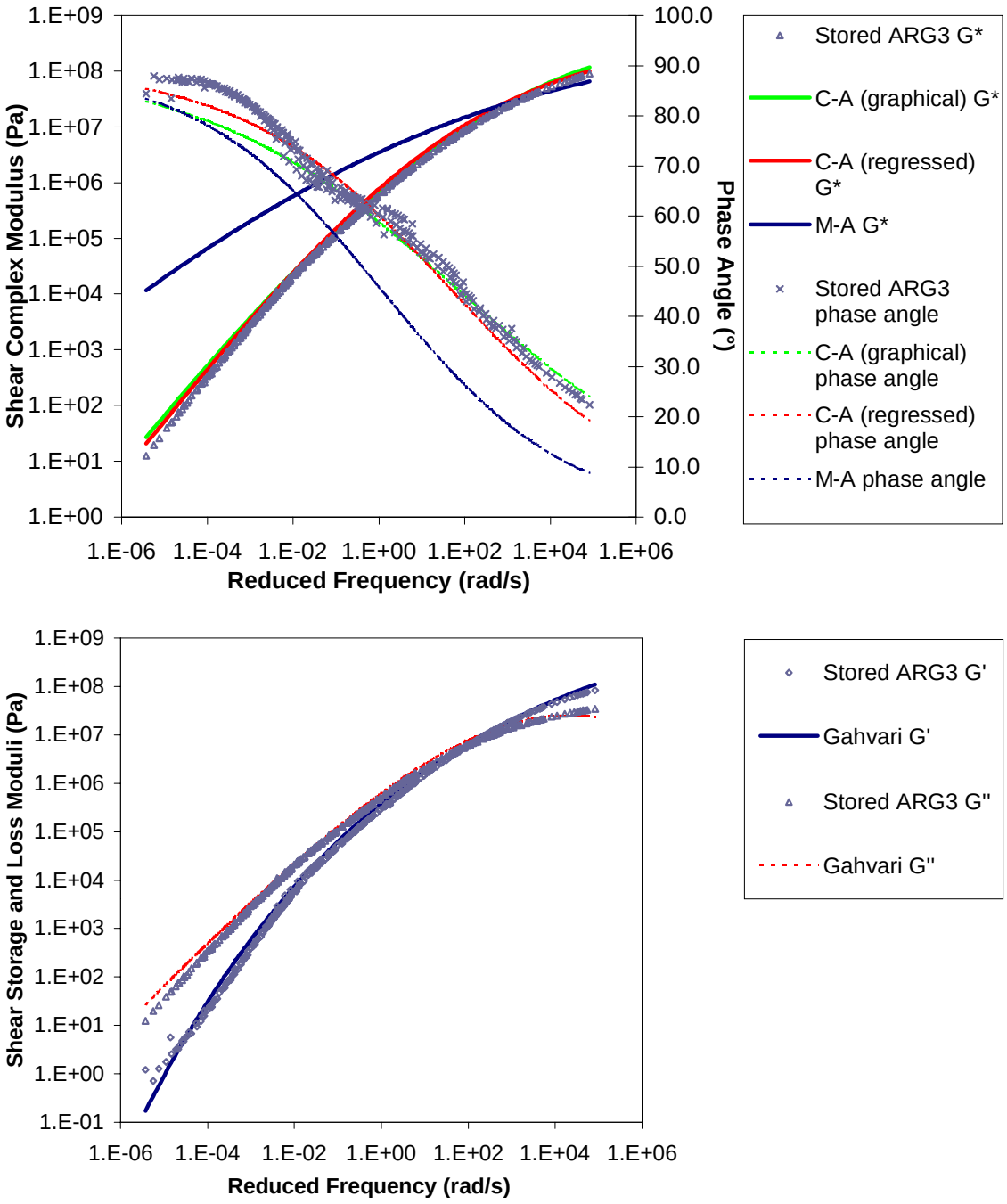


Figure L.4 Graphs of stored specimen ARG3 response versus responses predicted by the Christensen-Anderson (C-A) graphically determined parameter, Christensen-Anderson (C-A) regressed parameter, Marasteanu-Anderson (M-A), and Gahvari models.

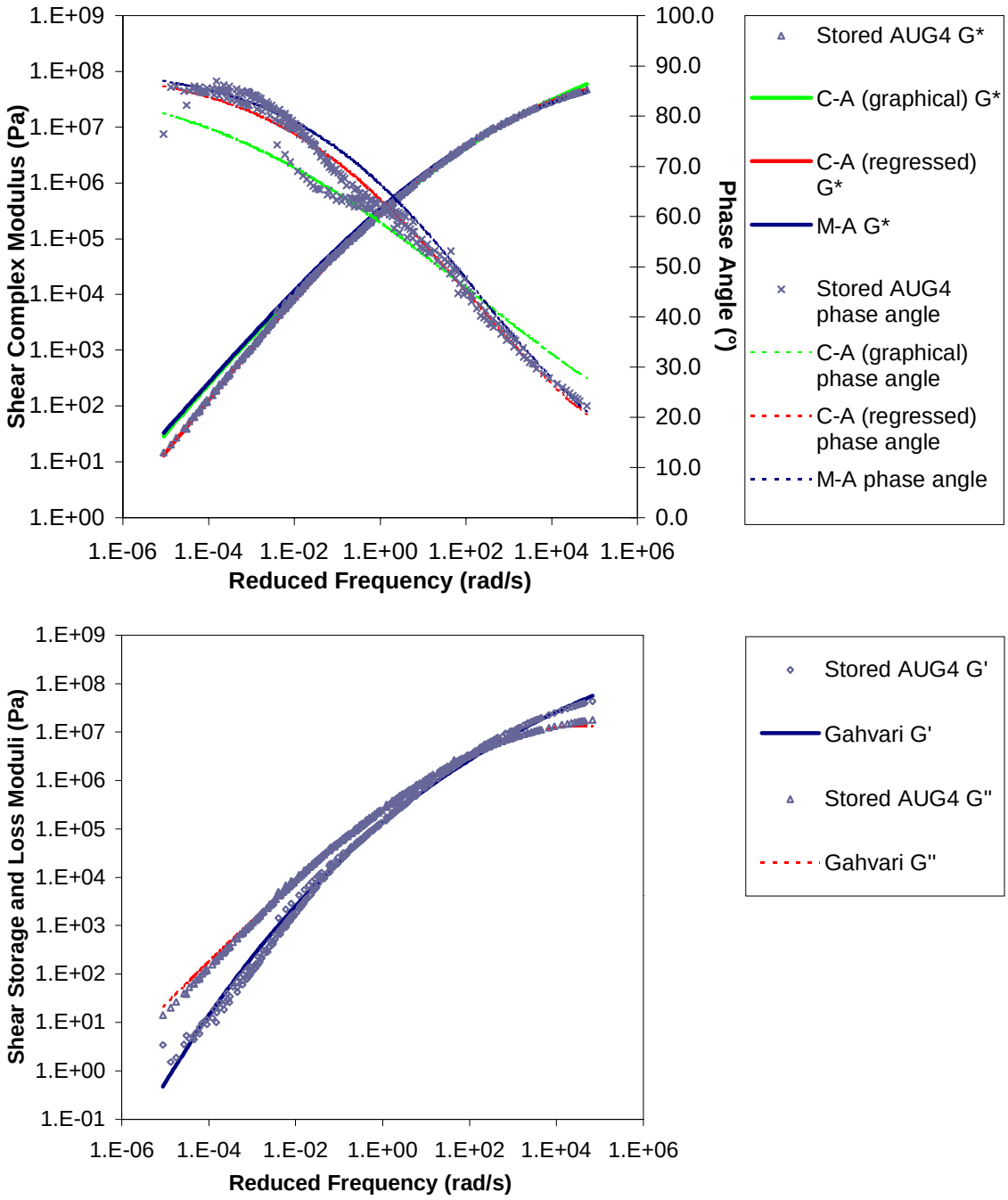


Figure L.5 Graphs of stored specimen AUG4 response versus responses predicted by the Christensen-Anderson (C-A) graphically determined parameter, Christensen-Anderson (C-A) regressed parameter, Marasteanu-Anderson (M-A), and Gahvari models.

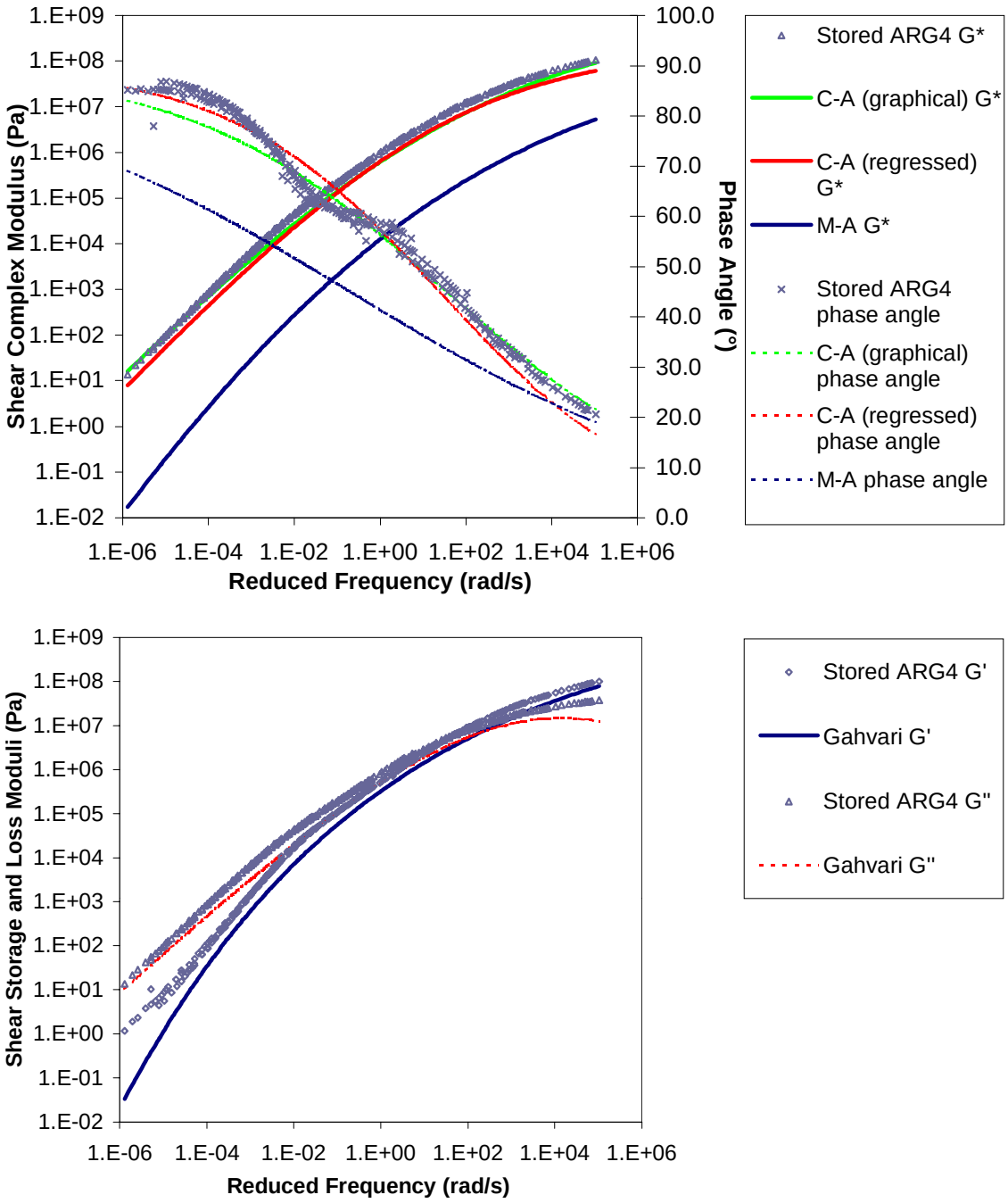


Figure L.6 Graphs of stored specimen ARG4 response versus responses predicted by the Christensen-Anderson (C-A) graphically determined parameter, Christensen-Anderson (C-A) regressed parameter, Marasteanu-Anderson (M-A), and Gahvari models.

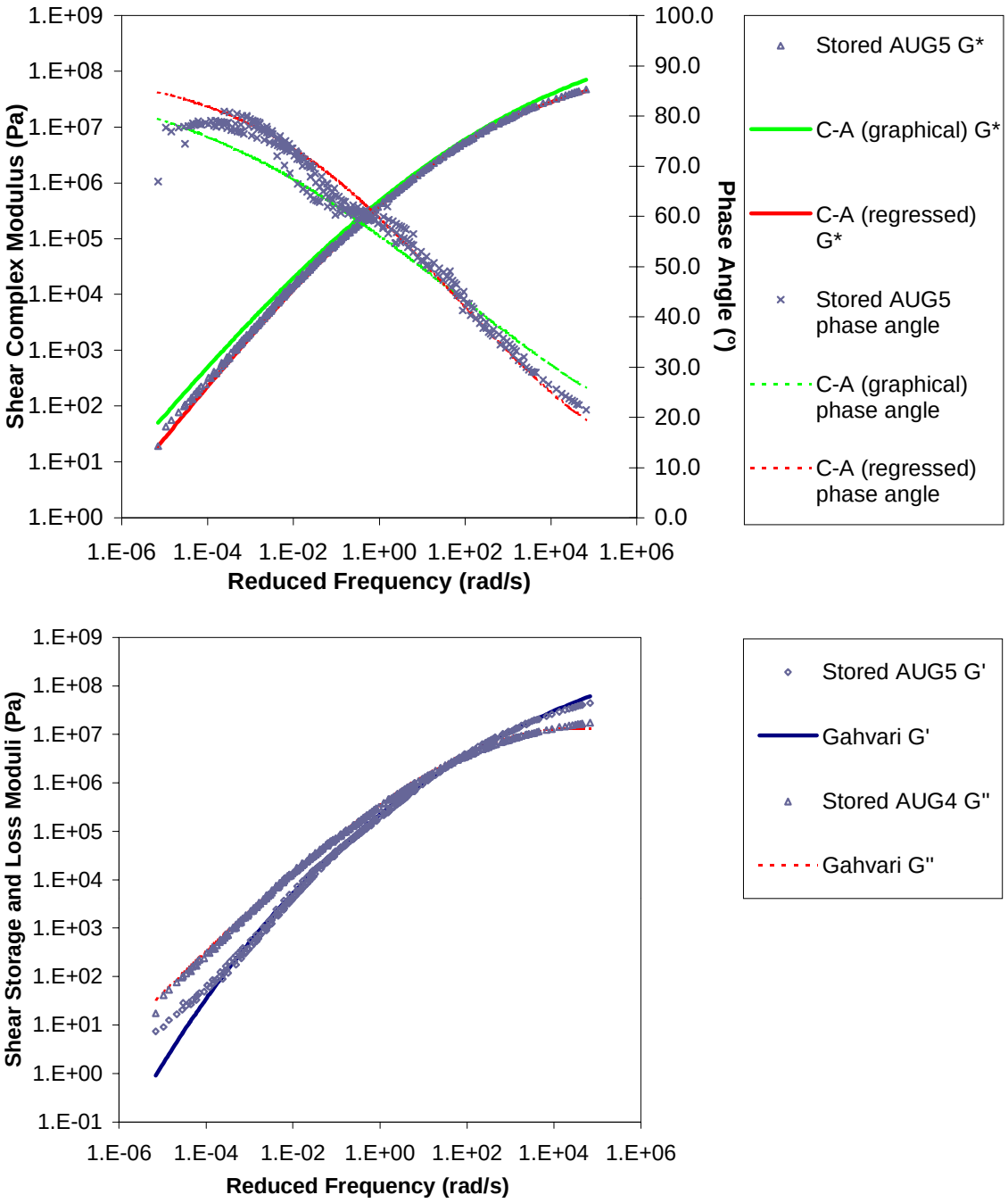


Figure L.7 Graphs of stored specimen AUG5 response versus responses predicted by the Christensen-Anderson (C-A) graphically determined parameter, Christensen-Anderson (C-A) regressed parameter, Marasteanu-Anderson (M-A), and Gahvari models.

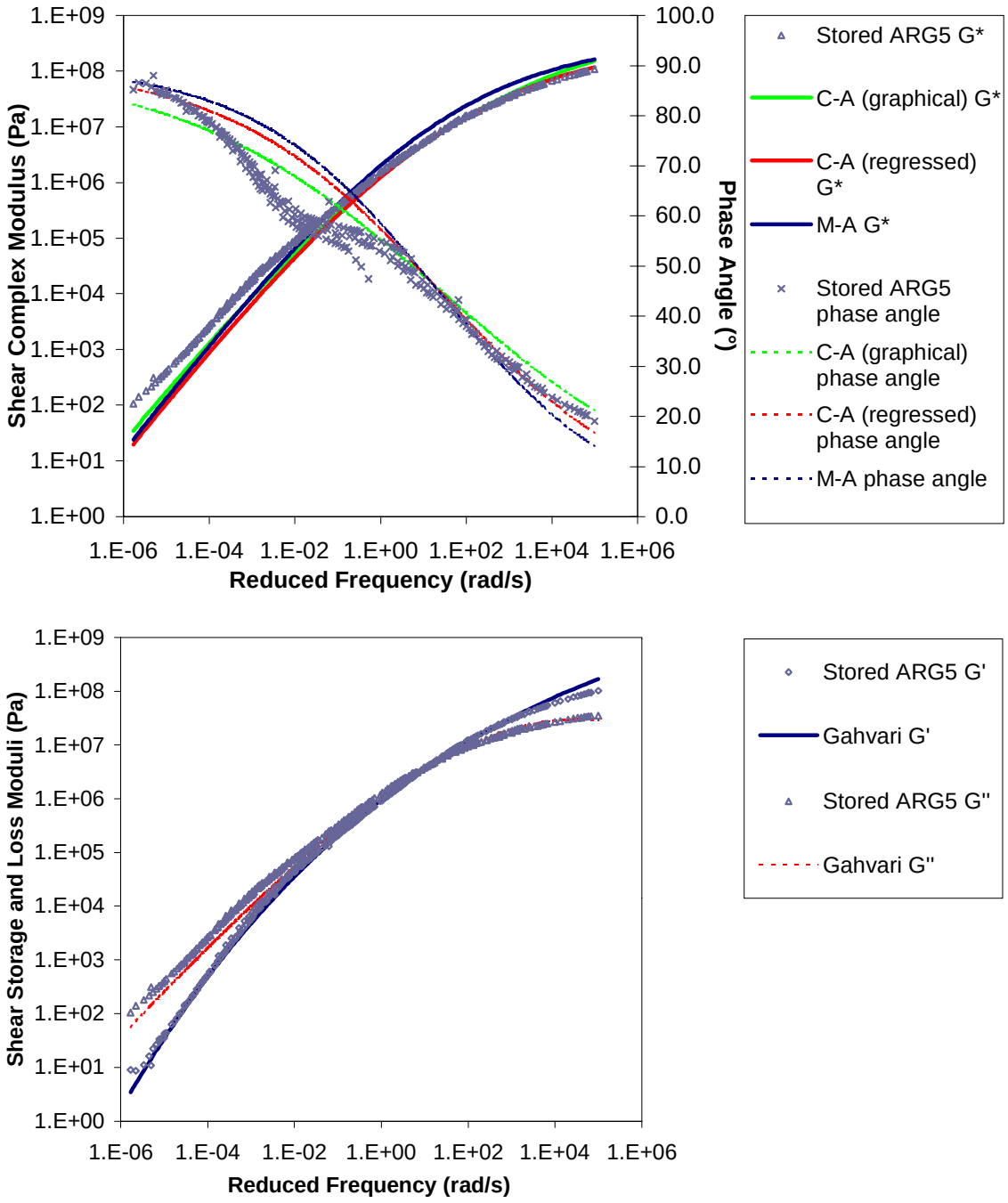


Figure L.8 Graphs of stored specimen ARG5 response versus responses predicted by the Christensen-Anderson (C-A) graphically determined parameter, Christensen-Anderson (C-A) regressed parameter, Marasteanu-Anderson (M-A), and Gahvari models.

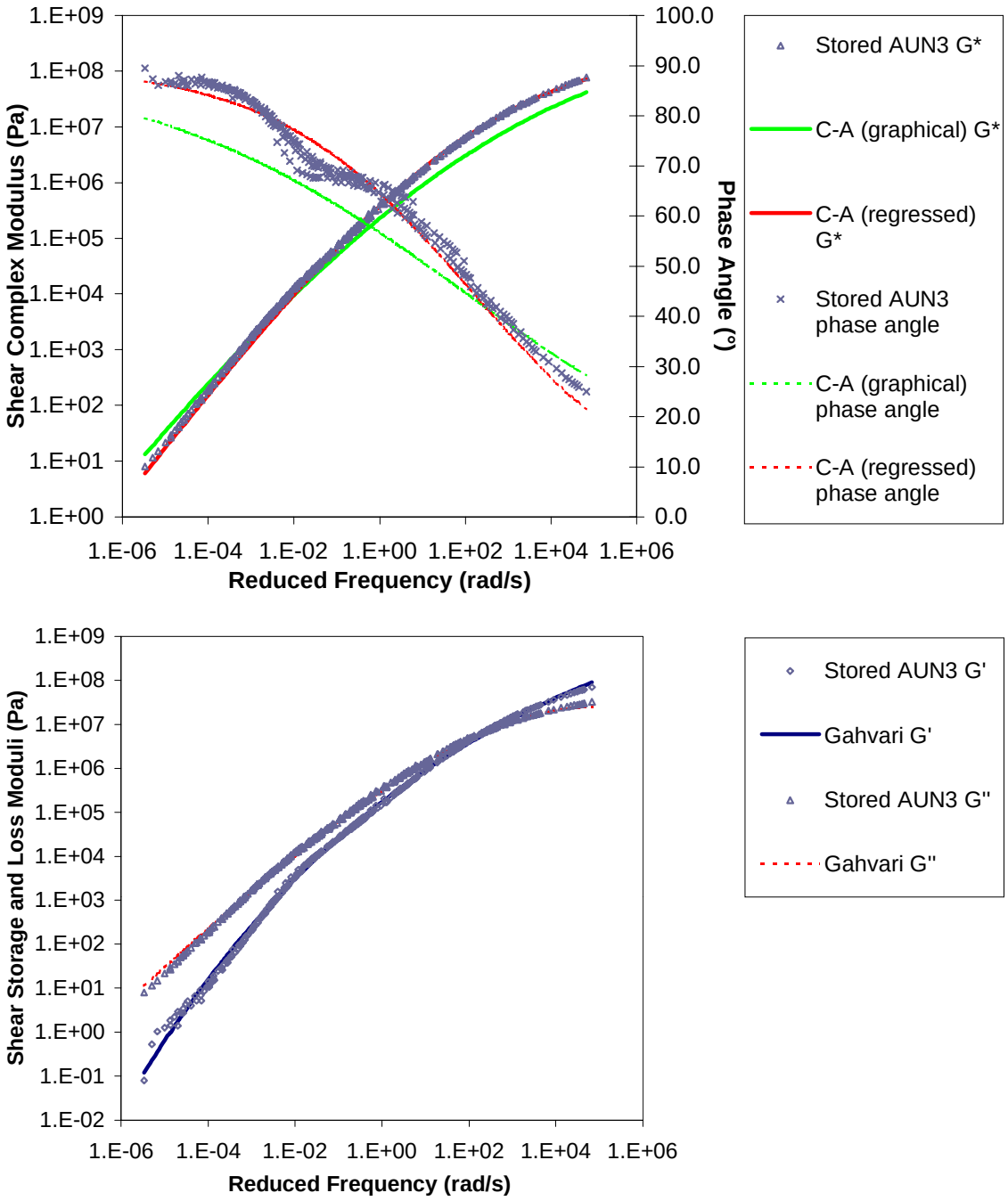


Figure L.9 Graphs of stored specimen AUN3 response versus responses predicted by the Christensen-Anderson (C-A) graphically determined parameter, Christensen-Anderson (C-A) regressed parameter, Marasteanu-Anderson (M-A), and Gahvari models.

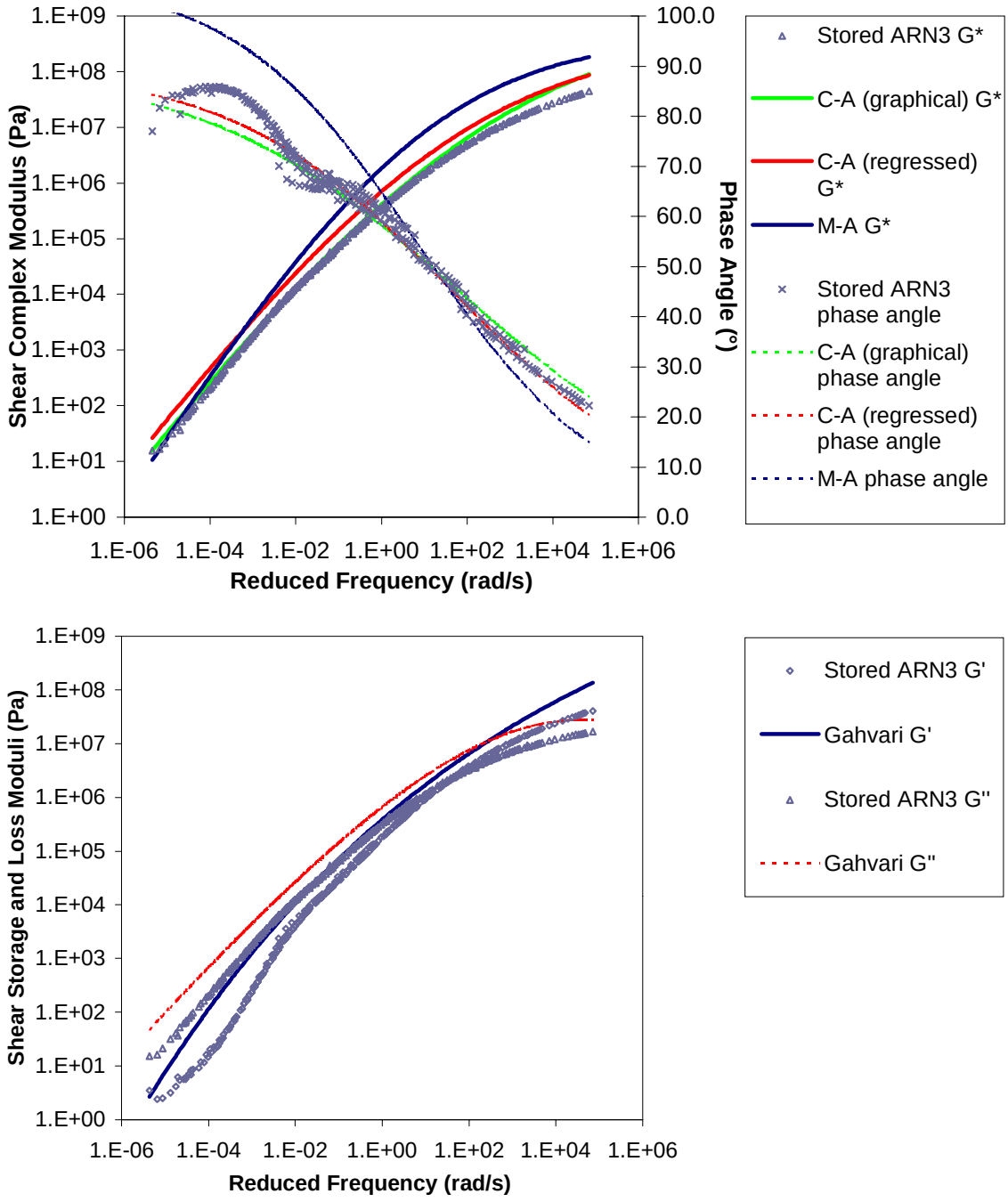


Figure L.10 Graphs of stored specimen ARN3 response versus responses predicted by the Christensen-Anderson (C-A) graphically determined parameter, Christensen-Anderson (C-A) regressed parameter, Marasteanu-Anderson (M-A), and Gahvari models.

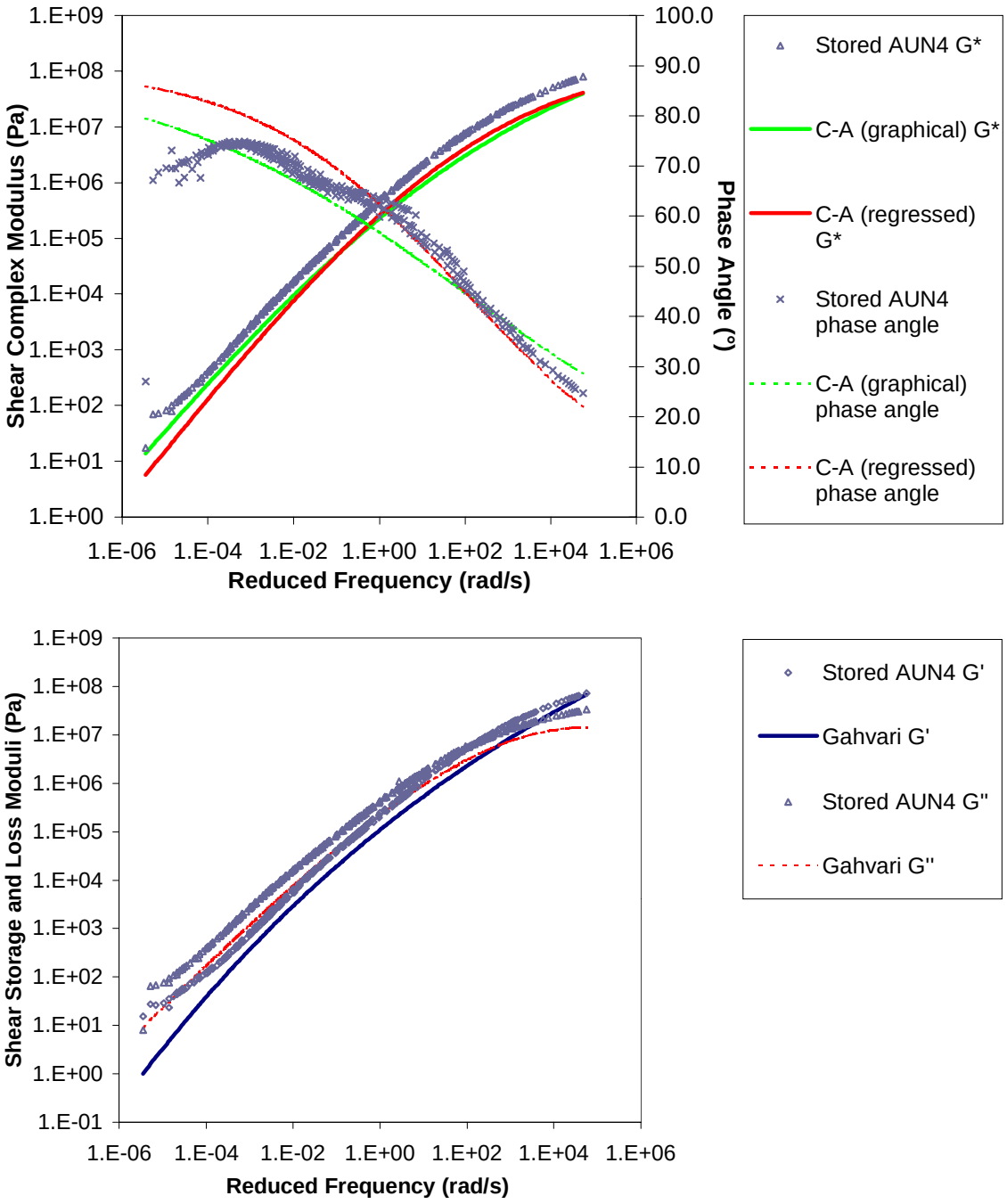


Figure L.11 Graphs of stored specimen AUN4 response versus responses predicted by the Christensen-Anderson (C-A) graphically determined parameter, Christensen-Anderson (C-A) regressed parameter, Marasteanu-Anderson (M-A), and Gahvari models.

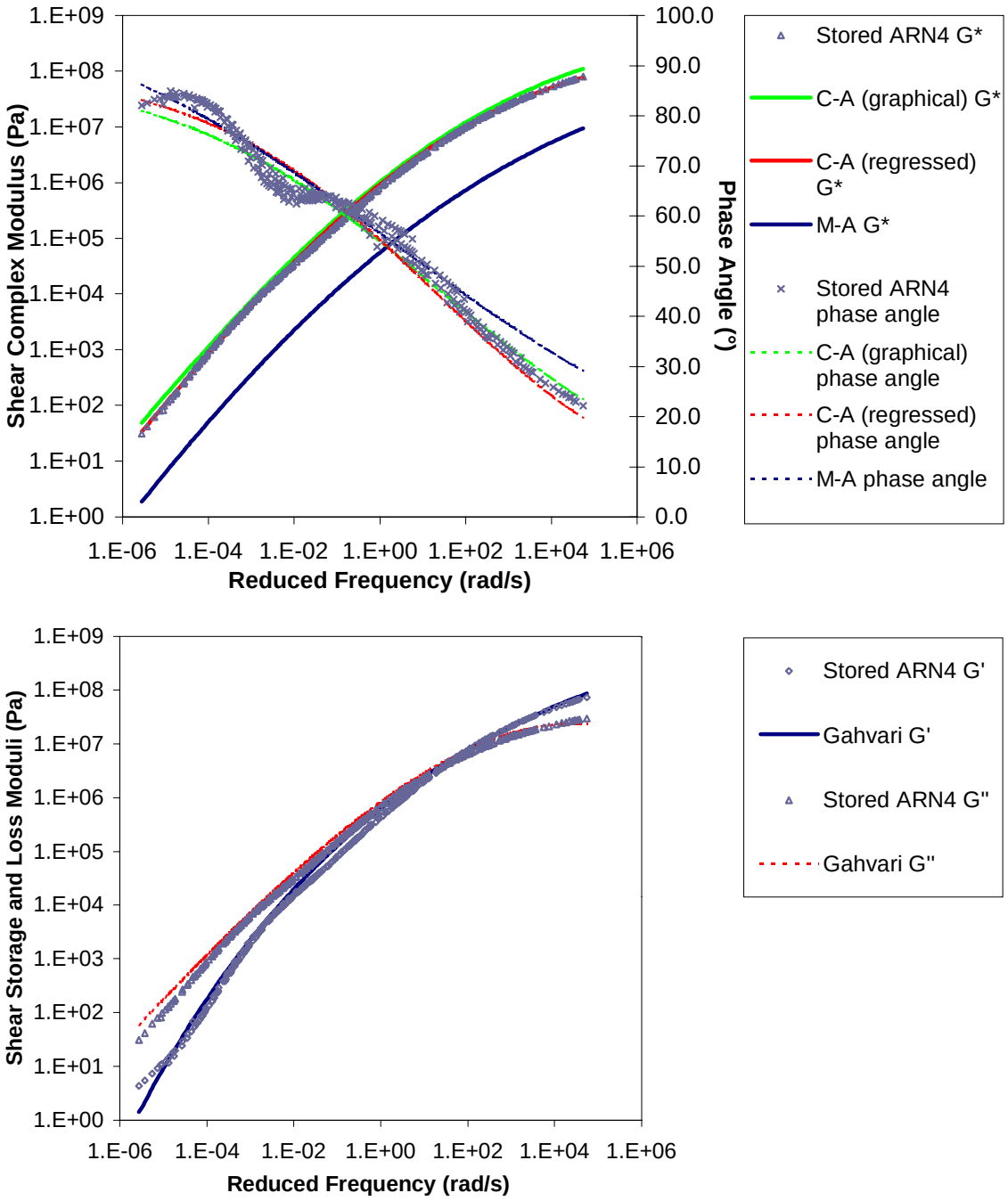


Figure L.12 Graphs of stored specimen ARN4 response versus responses predicted by the Christensen-Anderson (C-A) graphically determined parameter, Christensen-Anderson (C-A) regressed parameter, Marasteanu-Anderson (M-A), and Gahvari models.

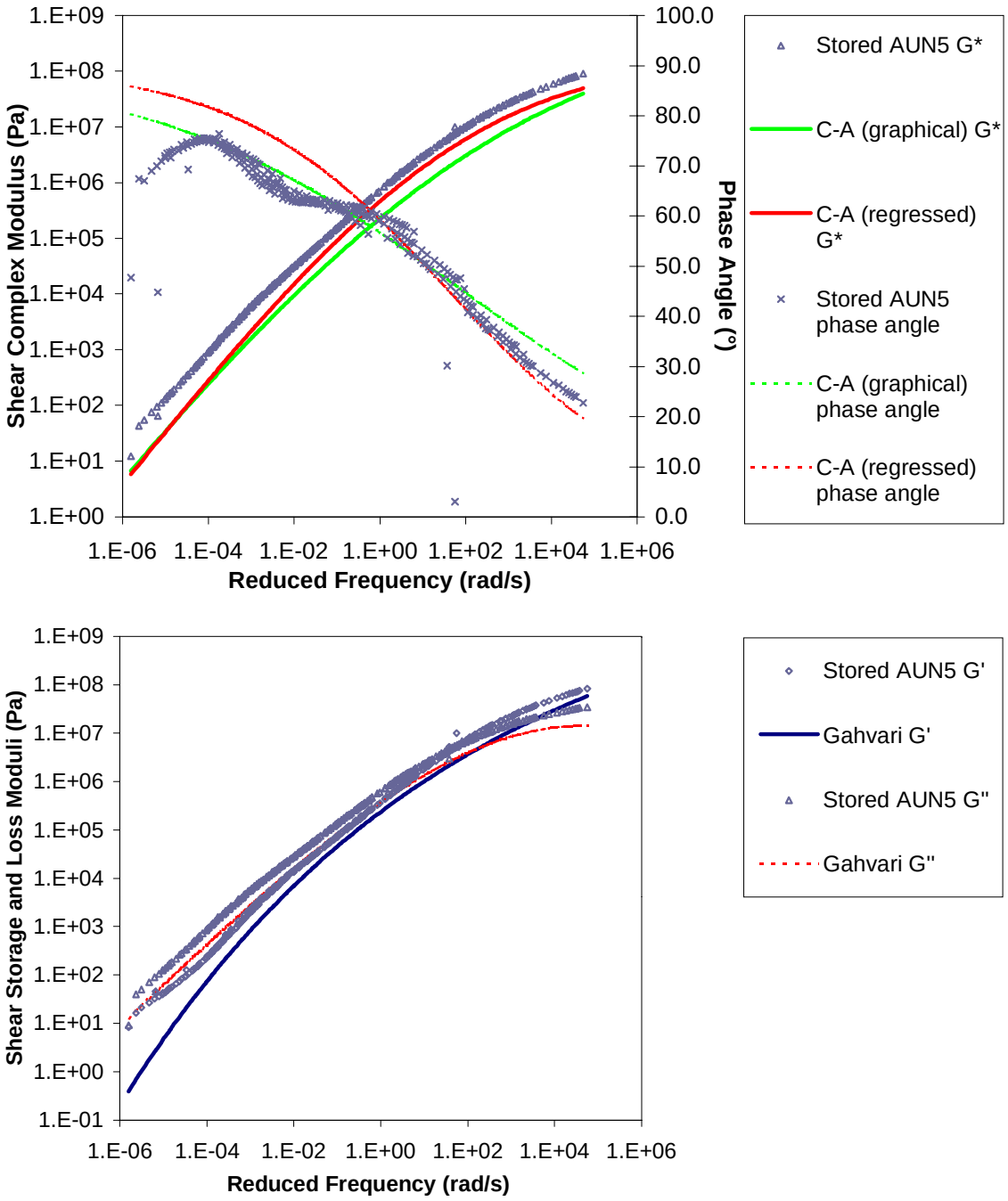


Figure L.13 Graphs of stored specimen AUN5 response versus responses predicted by the Christensen-Anderson (C-A) graphically determined parameter, Christensen-Anderson (C-A) regressed parameter, Marasteanu-Anderson (M-A), and Gahvari models.

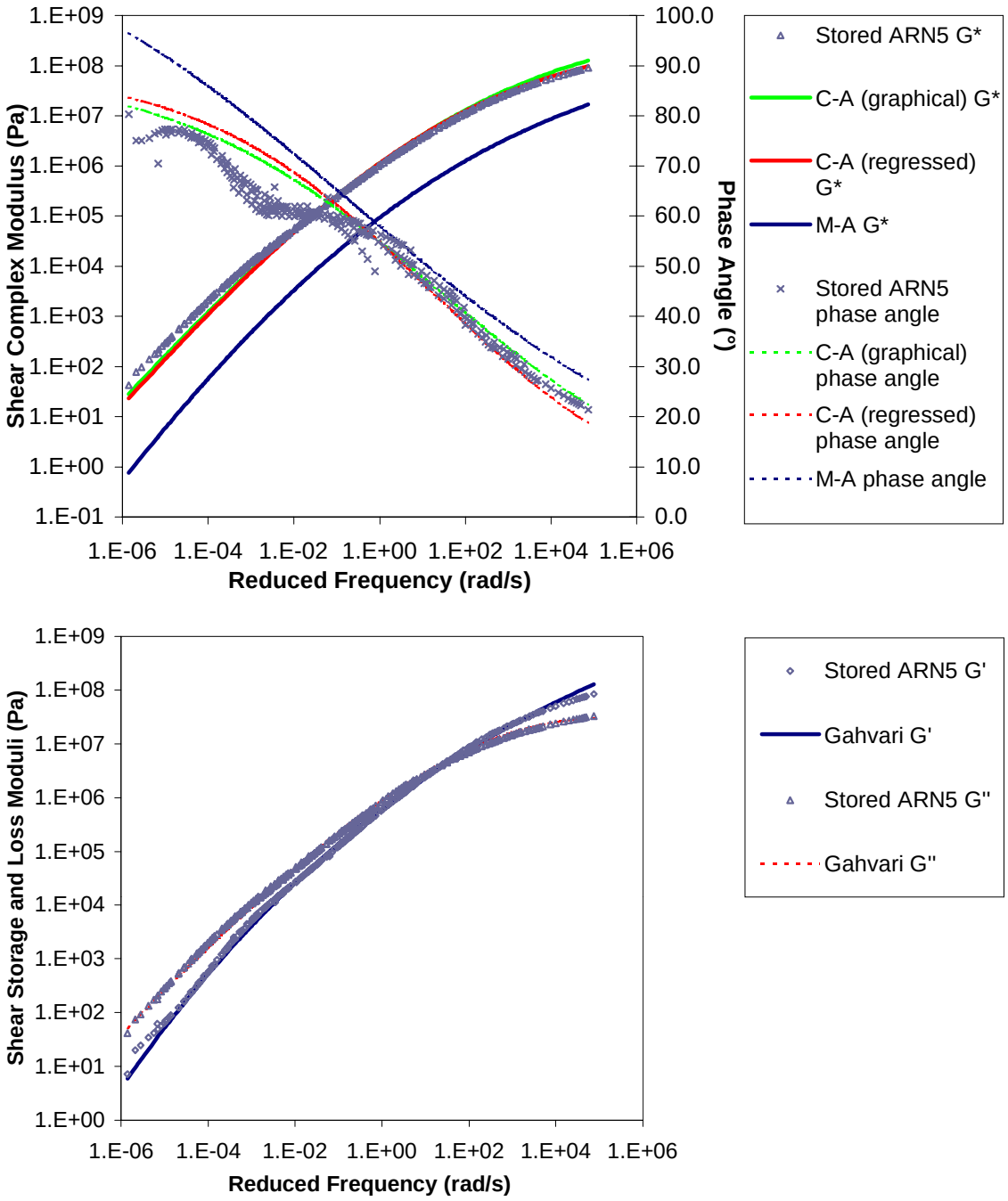


Figure L.14 Graphs of stored specimen ARN5 response versus responses predicted by the Christensen-Anderson (C-A) graphically determined parameter, Christensen-Anderson (C-A) regressed parameter, Marasteanu-Anderson (M-A), and Gahvari models.

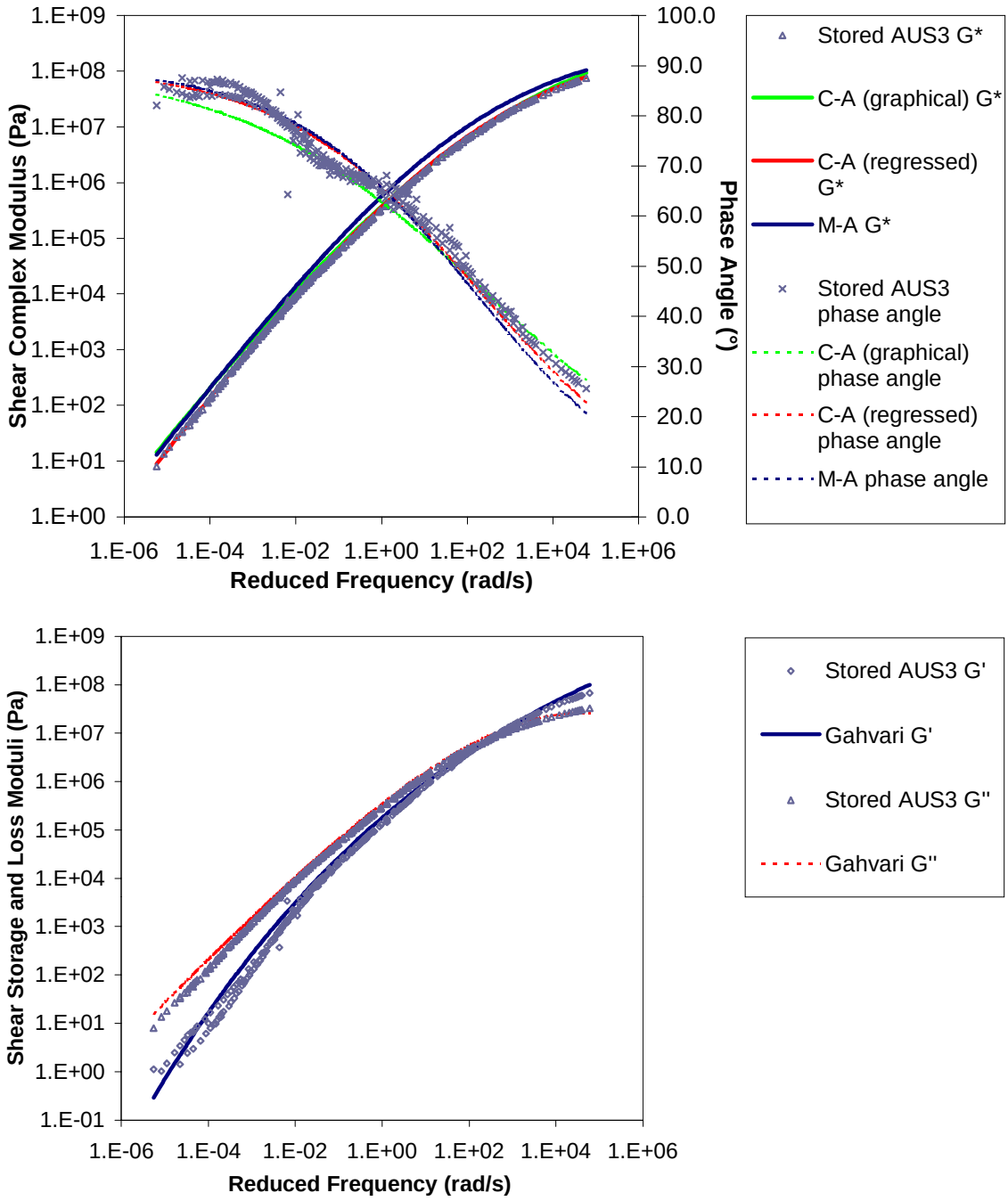


Figure L.15 Graphs of stored specimen AUS3 response versus responses predicted by the Christensen-Anderson (C-A) graphically determined parameter, Christensen-Anderson (C-A) regressed parameter, Marasteanu-Anderson (M-A), and Gahvari models.

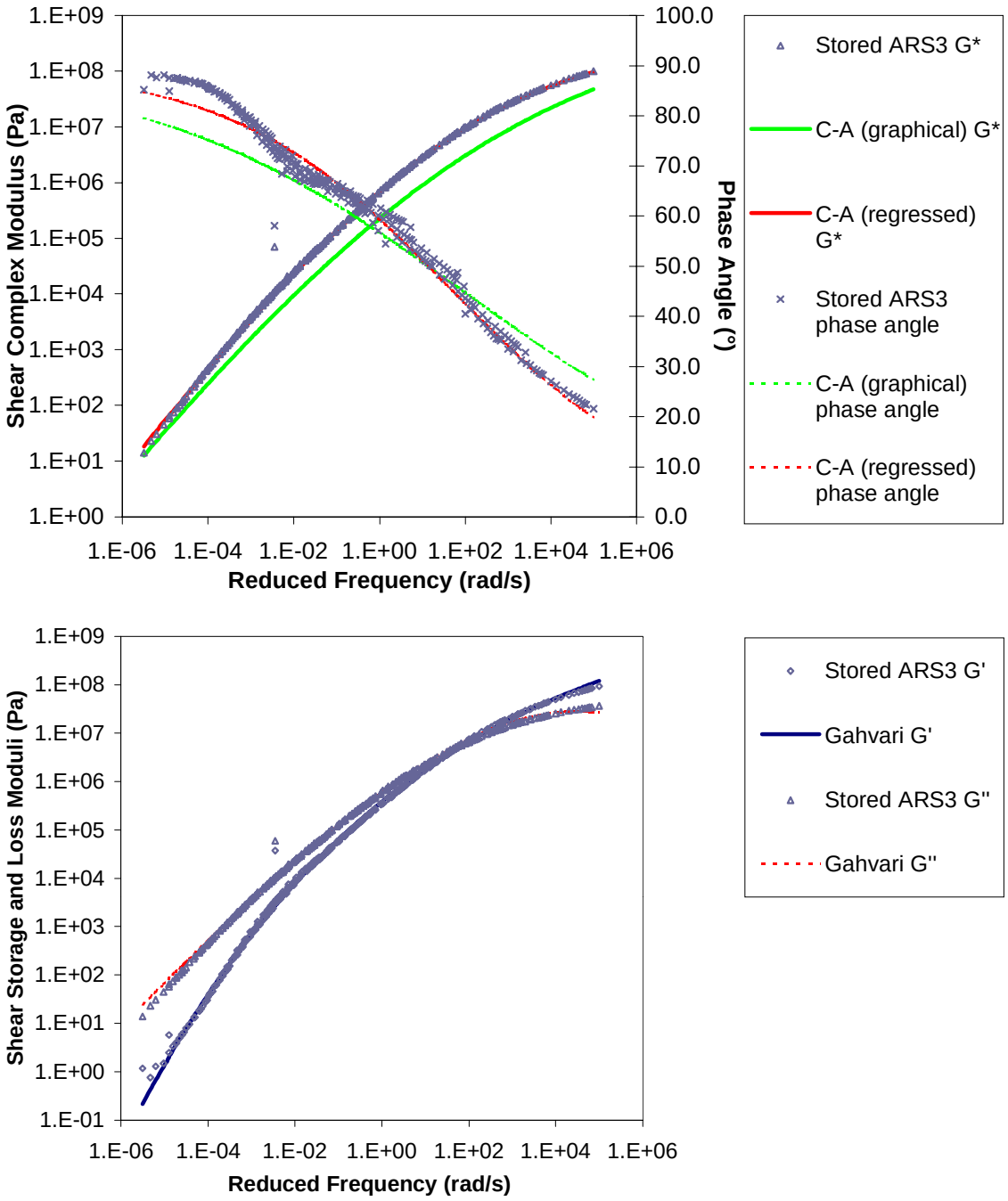


Figure L.16 Graphs of stored specimen ARS3 response versus responses predicted by the Christensen-Anderson (C-A) graphically determined parameter, Christensen-Anderson (C-A) regressed parameter, Marasteanu-Anderson (M-A), and Gahvari models.

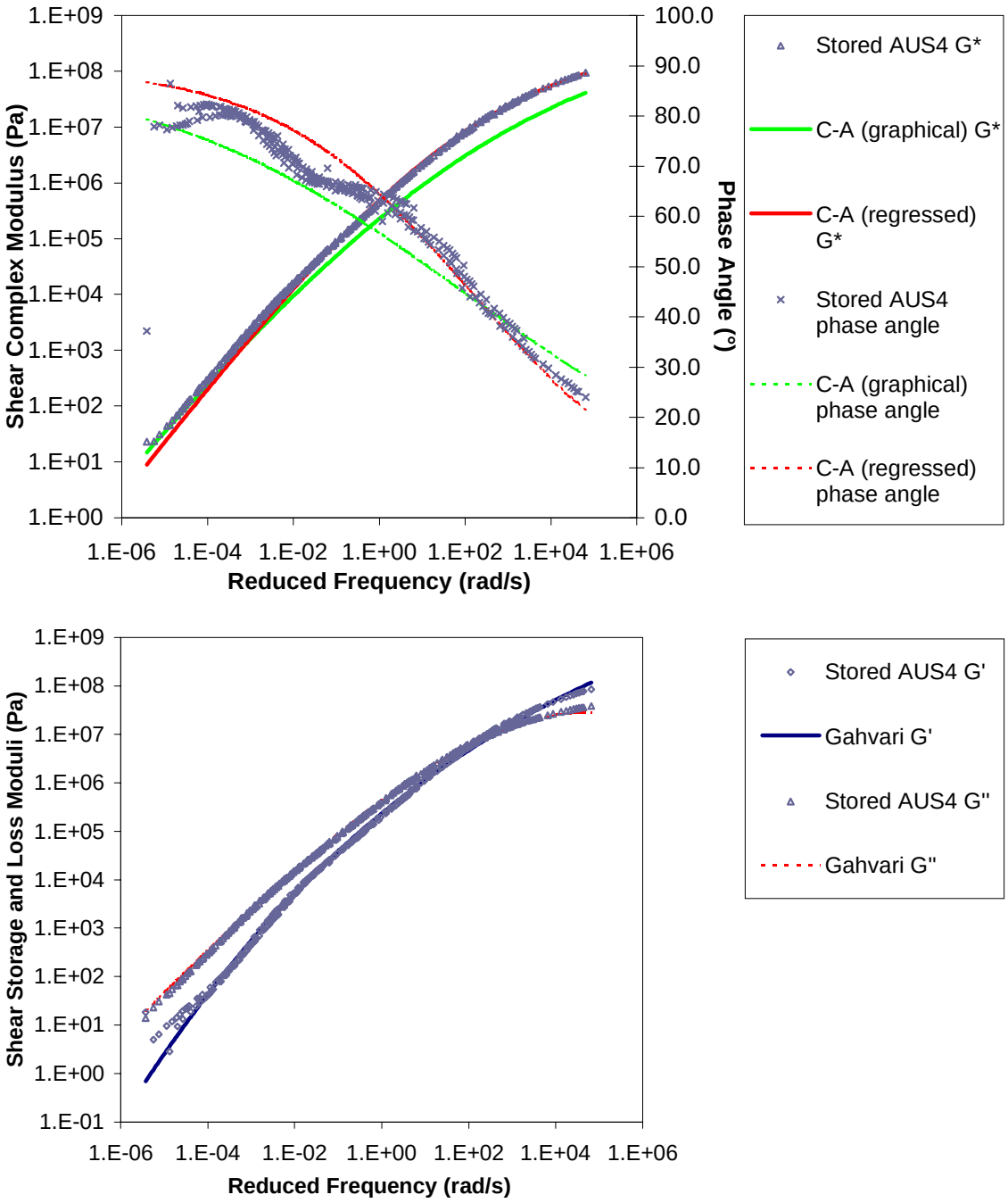


Figure L.17 Graphs of stored specimen AUS4 response versus responses predicted by the Christensen-Anderson (C-A) graphically determined parameter, Christensen-Anderson (C-A) regressed parameter, Marasteanu-Anderson (M-A), and Gahvari models.

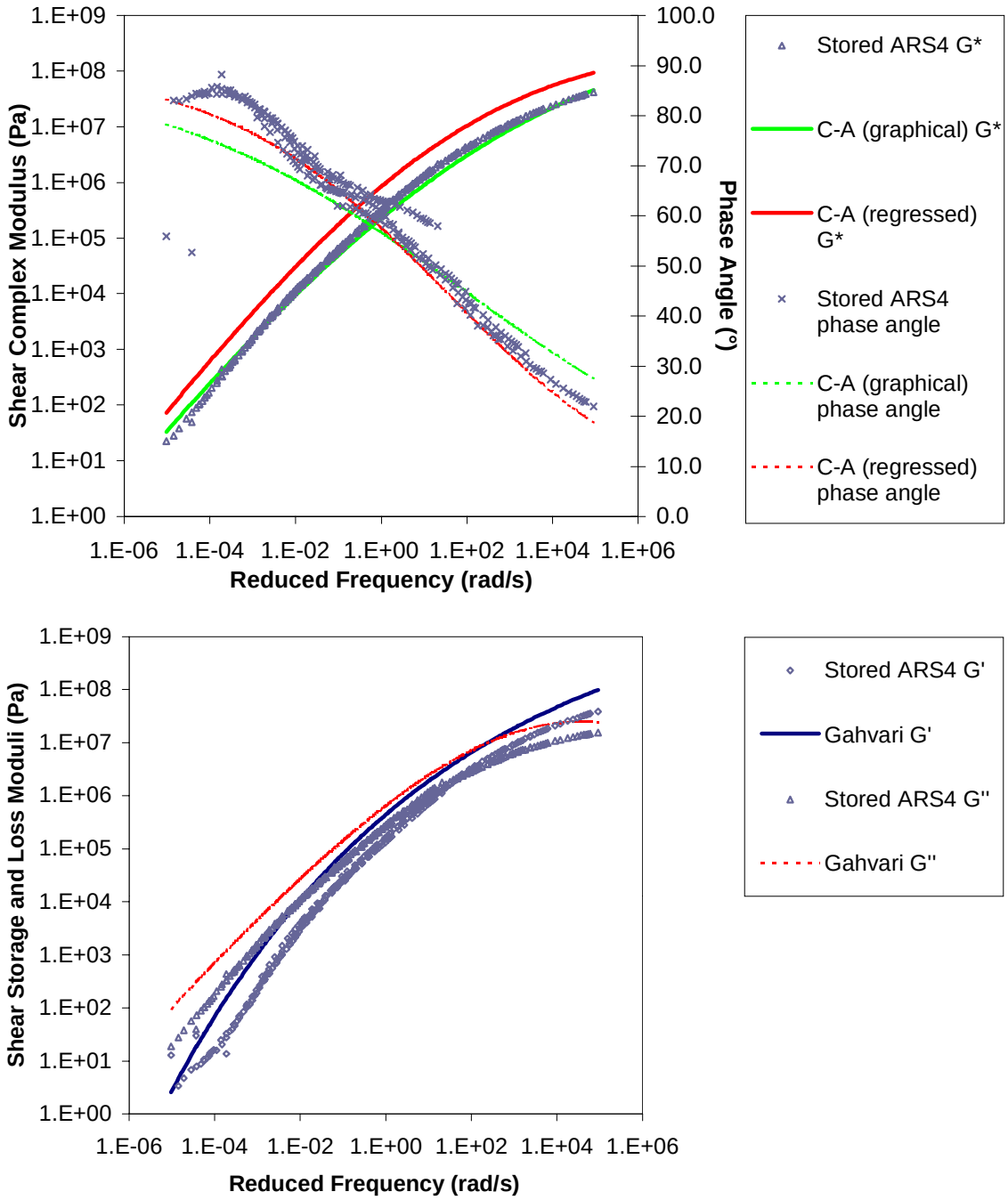


Figure L.18 Graphs of stored specimen ARS4 response versus responses predicted by the Christensen-Anderson (C-A) graphically determined parameter, Christensen-Anderson (C-A) regressed parameter, Marasteanu-Anderson (M-A), and Gahvari models.

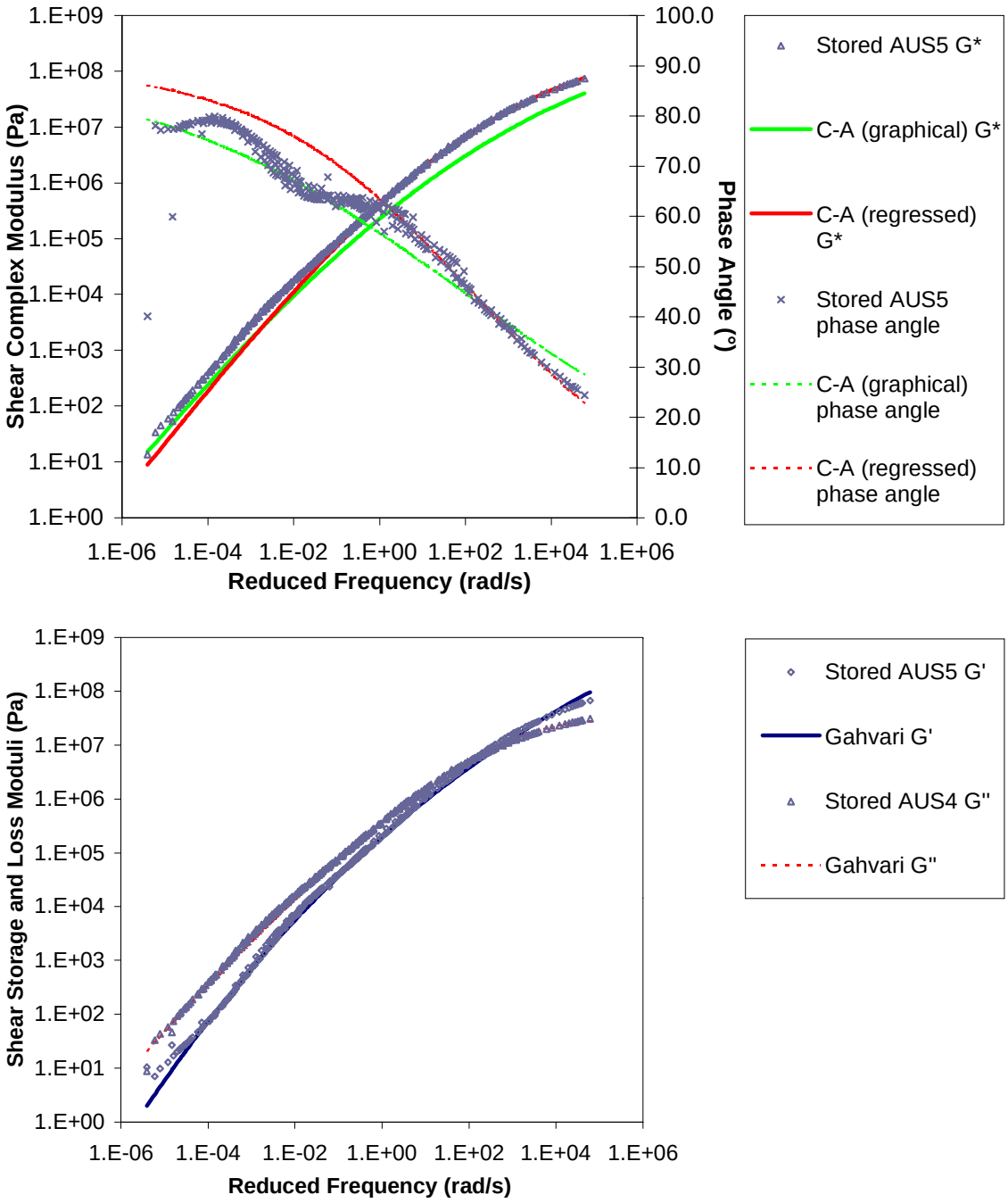


Figure L.19 Graphs of stored specimen AUS5 response versus responses predicted by the Christensen-Anderson (C-A) graphically determined parameter, Christensen-Anderson (C-A) regressed parameter, Marasteanu-Anderson (M-A), and Gahvari models.

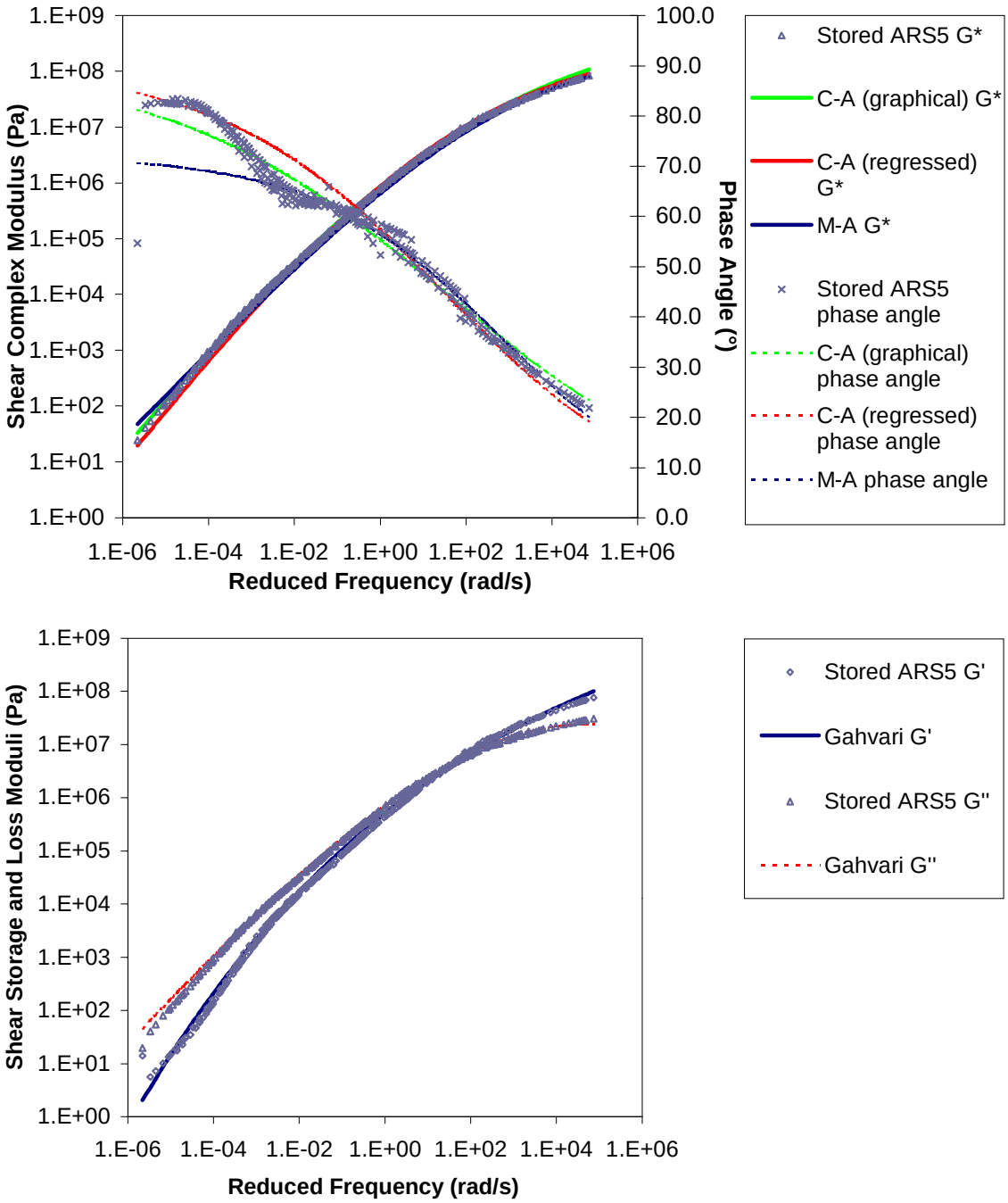


Figure L.20 Graphs of stored specimen ARS5 response versus responses predicted by the Christensen-Anderson (C-A) graphically determined parameter, Christensen-Anderson (C-A) regressed parameter, Marasteanu-Anderson (M-A), and Gahvari models.

# VITA

## Stacey D. Reubush

The author was born on August 5, 1975 in Staunton, Virginia. She completed her high school education at Riverheads High School in Greenville, Virginia in 1993. She received her Bachelor of Science degree in Civil Engineering from the Virginia Polytechnic Institute and State University in May 1997. She joined the Masters Program at Virginia Tech in August 1997. During her study, she was a teaching and research assistant in the Transportation Infrastructure and Systems Engineering program in the Department of Civil and Environmental Engineering where she taught a Civil Engineering Materials laboratory and conducted research in the area of evaluation of polymer-modified asphalt binders.